COMPARISON OF WIND AND WAVE SOURCES FOR TURKISH COASTS

A THESIS SUBMITTED TO
THE GRADUATE SCHOOL OF NATURAL AND APPLIED SCIENCES
OF
MIDDLE EAST TECHNICAL UNIVERSITY

BY

MUSTAFA ESEN

IN PARTIAL FULFILLMENT OF THE REQUIREMENTS
FOR
THE DEGREE OF DOCTOR OF PHILOSOPHY
IN
CIVIL ENGINEERING

SEPTEMBER 2014

Approval of the thesis:

COMPARISON OF WIND AND WAVE SOURCES FOR TURKISH COASTS

submitted by **MUSTAFA ESEN** in partial fulfillment of the requirements for the degree of **Doctor of Philosophy in Civil Engineering Department, Middle East Technical University** by,

Prof. Dr. Canan Özgen ______________
Dean, Graduate School of **Natural and Applied Sciences**

Prof. Dr. Ahmet Cevdet Yalçıner ______________
Head of Department, **Civil Engineering**

Prof. Dr. Ayşen Ergin ______________
Supervisor, **Civil Engineering Dept., METU**

Examining Committee Members:

Prof. Dr. Can Elmar Balas ______________
Civil Engineering Dept., Gazi University

Prof. Dr. Ayşen Ergin ______________
Civil Engineering Dept., METU

Prof. Dr. İsmail Aydın ______________
Civil Engineering Dept., METU

Prof. Dr. Ahmet Cevdet Yalçıner ______________
Civil Engineering Dept., METU

Assoc. Prof. Dr. Utku Kanoğlu ______________
Engineering Sciences Dept., METU

Date: 05.09.2014

I hereby declare that all information in this document has been obtained and presented in accordance with academic rules and ethical conduct. I also declare that, as required by these rules and conduct, I have fully cited and referenced all material and results that are not original to this work.

Name, Last Name : Mustafa Esen

Signature :

ABSTRACT

COMPARISON OF WIND AND WAVE SOURCES FOR TURKISH COASTS

Esen, Mustafa

Ph.D., Department of Civil Engineering

Supervisor: Prof. Dr. Ayşen Ergin

September 2014, 422 pages

Hourly wind measurements are the most important and commonly used data to estimate wave climate for Turkish coasts. There are several data sources, available for coastal engineers in Turkey, among which hourly wind measurements of Turkish coastal meteorological stations (TCMSs) are the most easily obtained and used data. However, due to several features and factors, the overall performance of TCMSs' representability for onshore winds is low. Therefore, a need arises to search and use alternative wind data sources.

ECMWF which provides 6 hourly wind data under various data sets is planned to be used, but at first the accuracy of ECMWF wind data is investigated. For this, ECMWF wind data is compared with land-based in-situ wind measurements at Sinop region, after the land-based wind data is carried to the same environment and elevation of ECWMF wind data. By smoothing the in-situ wind fields and increasing the data set with obtaining hourly wind data with linear connection of successive 6 hourly ECMWF winds, the wind changes are divided into certain groups and by looking into their correlations with the corresponding ECMWF wind data four different modification methods are achieved. At next stage, ECMWF wind speeds are modified by these four methods and the modifications which give the best correlations with in-situ wind are determined.

In the final stage, these modification methods are applied to certain storms during which in-situ wave measurements are available. Using the modified ECMWF wind speeds, wave estimations are performed with a numerical model and the resulting wave heights are compared to in-situ wave heights. In addition, in order to have an idea about possible use of these modification methods for other coastal regions, a storm, during which wave measurements are available, is chosen at Hopa, Black Sea coast of Turkey.

Keywords: Coastal Meteorological Stations, ECMWF, In-Situ Wind Measurements

ÖZ

TÜRKİYE KIYILARI İÇİN RÜZGAR VE DALGA KAYNAKLARININ KARŞILAŞTIRILMASI

Esen, Mustafa
Doktora, İnşaat Mühendisliği Bölümü
Tez Yöneticisi: Prof. Dr.Ayşen Ergin
Eylül 2014, 422 sayfa

Saatlik rüzgar ölçümleri, Türkiye kıyılarındaki dalga iklimini tahmin etmek için kullanılan en önemli ve yaygın veridir. Türkiye'deki kıyı mühendisleri için ulaşılabilir çeşitli veri kaynakları arasından TürkiyeKıyı Meteoroloji İstasyonları'nın (TKMİ'nin) saatlik rüzgar ölçümleri en kolay ulaşılan ve en çok kullanılan veridir. Ancak, çeşitli fiziksel unsurlar ve faktörler nedeniyle, TKMİ'lerin denizden esen rüzgarlar için temsil edilebilirlik genel performansı düşüktür. Bu nedenle, yeni rüzgar verisi kaynaklarının araştırılması ve kullanılması için gereksinim belirmiştir.

Bu amaçla, çeşitli veri tabanları altında rüzgar verisi sağlayan ECMWF'in(Avrupa Orta Mesafe Hava Tahmin Merkezi'nin) kullanılması planlanmıştır. Ancak, ilk olarak ECMWF rüzgar verisinin hassasiyeti ve kullanılabilirliği incelenmiştir. Bu doğrultuda, ECMWF rüzgar verisi, Sinop'ta karada gerçekleştirilen saha rüzgar ölçümlerinin denizel ortamda ortalama su seviyesine göre 10 m yüksekliğe taşınması ile elde edilen rüzgarlarlakarşılaştırılmıştır.

Saha rüzgar ölçümlerinin düzlenmesi, veri tabanının, ardışık 6 saat aralıklı ECMWF rüzgarlarının lineer birleştirilmesi yoluyla elde edilen saatlik ECMWF rüzgar verileri ile artırılması, rüzgar hızlarının ve rüzgar hızı değişimlerinin boyutlarına göre çeşitli

gruplara ayrılması ile saha rüzgar ölçümleri ile ECMWF rüzgar verisi arasında dört farklı modifikasyon yöntemi geliştirilmiştir. Bir sonraki aşamada ise, ECMWF rüzgar hızları bu dört metod kullanılarak modife edilmiş ve saha ölçümleri ile modife edilmiş ECMWF rüzgar verisi arasında en iyi korrelasyonu veren modifikasyon metodları belirlenmiştir.

En son aşamada, seçilen metodlar kullanılarak, saha dalga ölçümlerinin olduğu zaman dilimi içerisinde kalan çeşitli fırtınalardaki rüzgar hızları modife edilmiştir. Seçilen bir numerik model ile modife rüzgar hızlarından dalga tahminleri gerçekleştirilmiştir ve elde edilen dalga yükseklikleri saha dalga ölçümleri ile karşılaştırılmıştır. Ek olarak, belirlenen bu modifikasyon metodlarının başka kıyı alanları için de kullanılabilirliğinin anlaşılabilmesi için, saha dalga ölçümlerinin olduğu bir başka lokasyon, Hopa, daha belirlenmiş ve saha ölçümlerine denk gelen zaman dilimi içerisinde gözlemlenen çeşitli fırtınalar ele alınarak, modife edilmiş rüzgar hızları kullanılarak tahmin edilen dalga özellikleri incelenmiştir.

Anhahtar Kelimeler: Kıyı Meteoroloji İstasyonları, ECMWF, Rüzgar Ölçümleri

To my beloved family and Prof. Dr. Ayşen Ergin…

ACKNOWLEDGEMENTS

I would like to express my deepest gratitude to Prof. Dr. Ayşen Ergin for not only supervising this thesis study but also encouraging me at each step of my studies as well as enlightening my life by showing how to be a good researcher and a good person. I am forever indebted to her indescribable contributions to my academic, professional and personal life. Being the last PhD student of a legend would be one of the unforgettable memories and successes of my life.

I would like to extend my sincere thanks to Prof. Dr. Ahmet Cevdet Yalçıner and Dr. Işıkhan Güler. They always encouraged me and guided me at different steps of my thesis as well as on other research studies. Their experience and guidance made it easier to withstand every difficulty.

It is absolutely fantastic to be a friend, roommate and colleague of Dr. Cüneyt Baykal who provided his unlimited help throughout this thesis study whenever needed. Without his valuable suggestions, fruitful outcomes of our brainstorm sessions and intense discussions, it would not be possible to finish this thesis study.

I would like to extend my sincere thanks and appreciations to Assistant Prof. Dr. Gülizar Özyurt Tarakcioğlu, who provided her valuable ideas and suggestions with great enthusiasm and encouragement.

It would not be possible to finish this thesis without the support of a great friend, Dr. Hülya Karakuş Cihan who not only helped me with her golden suggestions but also by being a great colleague sharing the great burden of professional life.

I would like to express my sincere thanks to Erdinç Söğüt for his great help at work as well as encouragement during this study.

I would like to add Çağıl Kirezci to the list of many people who contributed to this thesis study with his valuable support and help.

I would like to thank Prof. Dr. Erdal Özhan and MEDCOAST for providing data of NATO-TU Waves Project to be used in this thesis study.

It is a pleasure to be a part of Coastal and Ocean Engineering Division and to share some of the great moments of my life with each and every member of its family. I would like to thank Dr. Ceren Özer Sözdinler, Gökhan Güler, Çağdaş Bilici, Koray Kaan Özdemir, Işıl İnsel, Ayşe Karancı, Aykut Ayça, Kemal Cihan Şimşek, Miran Dzabic and Yaprak Onat for the support and joyous times we shared through the years.

I would like to express my sincere thanks to our lab staff Arif Kayışlı, Yusuf Korkut and Nuray Sefa.

Finally, I would like to thank my family, Vahap Esen, Sultan Esen, and Engin Esen for the spectacular gift of life they provided me with and the inexpressible love they bestowed on me without which I would not achieve this great honor.

TABLE OF CONTENTS

LIST OF FIGURES

FIGURES

LIST OF TABLES

TABLES

ABBREVIATIONS

AMS	Automatic Meteorological Station
CMS	Coastal Meteorological Station
E	East
ECMWF	European Centre for Medium-Range Wave Forecasts
ENE	East North East
EPS	Ensemble Prediction System
ERA	ECMWF Re-Analysis
ESE	East South East
MSL	Mean Sea Level
N	North
NE	North East
NIH	Nocturnal Inversion Height
NNE	North North East
NNW	North North West
NW	North West
PBL	Planetary Boundary Layer
S	South
SE	South East
SSE	South South East
SSW	South South West
SW	South West
TCMS	Turkish Coastal Meteorological Station
UTC	Current Local Time
W	West
WAM	WAve Model
WNW	West North West

WSW	West South West

NOMENCLATURE

A	Coefficient of Linear Conversion
B	Coefficient of Linear Conversion
E10	ECMWF Wind Speed at 10 m Elevation above MSL
E10L	Hourly ECMWF Wind Speeds at 10 m Elevation above MSL Obtained by Linearly Connecting 6 Hourly ECMWF Wind Speeds
E10m	Modified ECMWF Wind Speed at 10 m Elevation above MSL
E10m1	Modified ECMWF Wind Speed at 10 m Elevation above MSL by Method 1
E10m2	Modified ECMWF Wind Speed at 10 m Elevation above MSL by Method 2
E10m3	Modified ECMWF Wind Speed at 10 m Elevation above MSL by Method 3
E10m4	Modified ECMWF Wind Speed at 10 m Elevation above MSL by Method 4
E10Spline	Hourly ECMWF Wind Speeds at 10 m Elevation above MSL Obtained by Connecting 6 Hourly ECMWF Wind Speeds by Spline Method
E100	ECMWF Wind Speed at 100 m Elevation above MSL
F	Fetch Distance
F_E	Effective Fetch Distance
H_S	Significant Wave Height
k	Von Karman's Constant
L16	Land-Based In-Situ Wind Measurements at 16 m Elevation above the Reference Land Elevation

L25	Land-Based In-Situ Wind Measurements at 25 m Elevation above the Reference Land Elevation
L60	Land-Based In-Situ Wind Measurements at 60 m Elevation above the Reference Land Elevation
$S10_{ave}$	Average of 5 Consecutive In-Situ Wind Speeds Carried to 10 m Elevation above MSL
$S10_S$	Smoothed In-Situ Wind Speeds Carried to 10 m Elevation above MSL
S60	In-Situ Wind Speeds Carried to 60 m Elevation above MSL
U	Wind Speed
U_{10}	Wind Speed at 10 m Elevation
U_{10N}	Wind Speed at 10 m Elevation for Neutrally Stable Air
U_{60}	Wind Speed at 60 m Elevation
U_B	Wind Speed Measured at the Buoy
U_H	Wind Speed at Elevation H
U_L	Over-Land Wind Speed
U_{land}	Wind Speed on Land
U_M	Wind Speed at 10 m Elevation Obtained from Atmospheric Model
U_M^C	Corrected Wind Speed of the Atmospheric Model
U_{sea}	Wind Speed on Sea
U_Z	Wind Speed at Elevation Z
U_W	Over-Lake Wind Speed
U_*	Friction Velocity
Z	Elevation Z
Z_H	Elevation H
Z_0	Surface Roughness
α	Hellman Exponent
β	Exponent in Relationship between H and U

β_0	Coefficient
β_1	Coefficient
β_i	Measurement Error for U_B
ε_i	Measurement Error for U_M
ΔT	Air-Water Temperature Difference
$\Delta\Theta$	Clockwise Angle between Over-Land and Over-Lake Winds

CHAPTER 1

INTRODUCTION

Wind and wave sources to be used as input data for coastal engineering applications all around the world as well as in Turkey have been one of the key triggering and initiating points in design approach. Without good, long and reliable wind or wave data, there would not be a reliable and representative starting point for a design stage. The reliability issue of the wind data to be used as input should be given the upmost priority to come up with both economically and technically optimum design.

In Turkey, hourly wind measurements of coastal meteorological stations of Turkish State Meteorological Service, located in the coastal regions all around Turkey, have been the main preferred wind data input for prediction of design wave data for a very long time. Although, the aforementioned wind data and wind sources have been in use for a quite long time, the reliability and representability of the related wind data for their specific locations have never been put to issue or very limited research have been performed to reveal these issues.

Over the years, after each similar application to obtain design wave data for different locations in Turkey, it is found that there is a big reliability and representability problem for the hourly wind measurements of coastal meteorological stations (CMSs) for Turkish coasts. This problem varies from location to location. This is the starting point of this study in which it is mainly aimed to have general idea about the performance of hourly wind measurements of CMSs, to find an alternative source, which is ECMWF, that can be used instead of CMSs, to understand the general performance of ECMWF wind data by performing site specific comparisons and to develop a method to modify ECMWF wind data so that representative wind and wave data can be obtained.

In Chapter 2, which may be subdivided into three sections, firstly, previous studies on differences between land and sea based wind measurements and the land-sea conversion methods are summarized. Secondly, general information about ECMWF and its products will be given and in the last part, comparative studies between ECMWF and in-situ wind and wave measurements performed in the literature especially for similar basins with Turkish coasts are specified.

In Chapter 3, overall overview of TCMSs in terms of their representability of onshore winds around their regions is performed. In this overview, the main focus is given to general findings about wind roses, wind histograms as well as the locations at which TCMSs are situated.

In Chapter 4, the land-based in-situ wind measurements performed in Sinop, Turkey are analyzed by comparing the wind measurements at three different elevations. From these analyses, identical vertical profile for this location, together with the decision on in-situ wind data of which elevation to be used for the following studies will be done.

In Chapter 5, a spatial study is performed for the aim of deciding which ECMWF grid point to use for comparative studies. In this chapter, the grid points are classified into groups in terms of their similarities in wind roses and percentages.

In Chapter 6, firstly land-based in-situ wind measurements are carried to wind data at 10 m elevation above MSL by conversions on both horizontal and vertical planes. In order to increase the number of data, hourly ECMWF wind data is obtained by applying a simple method and in order to resemble the trends of both wind fields to have better correlations with lower range, the in-situ wind fields are smoothed. These are performed for all of the 29 chosen continuous data sets. Since, it is visually observed that the correlations differ according to the wind speed change trends, the data sets are subdivided into several groups and for each group correlation coefficients are obtained. For the modification of ECMWF wind data, four methods that are based on these correlations are introduced. The general performance of these methods is evaluated and two methods that have the best representability of in-situ wind fields are chosen for the following wave studies.

In Chapter 7, using the modified ECMWF wind data for certain storms in the past during which in-situ wave measurements are available, wave estimations are performed by using a numerical model, W61. Since this is only performed for Sinop, the overall performance of the modification methods are hard to evaluate, thus an additional case study is performed for Hopa, Turkey considering one storm again during which in-situ wave measurements are available.

In Chapter 8, the main focus, procedure and findings of this study are summarized together with the recommendations for future studies.

CHAPTER 2

LITERATURE SURVEY

2.1. Horizontal (Onshore-Offshore) and Vertical Wind Data Conversion Methods

In this doctorate study, onshore (land-based) in-situ wind measurements have been used to obtain wind and wave climate. Therefore, it is necessary to perform extensive research regarding similar studies and to mention their findings and important points. In this part of the literature survey, firstly details of the studies on onshore-offshore wind conversions will be mentioned. This will be followed by general information about ECMWF (European Medium Range Weather Forecasts) and their products together with general structure of atmospheric and ocean models that are in use in ECMWF. Finally, several studies that use ECMWF wind and wave data will be reviewed and their outcomes will be specified to enlighten the studies in the upcoming chapters of this thesis.

There are numerous studies and publications on horizontal and vertical wind profiles on land and sea and respective conversions. In this section, the focus is given to major publications which will be specified in the following parts of this section. In Sections 2.1.1 to 2.1.5, discussions regarding wind profiles on land and sea and respective approaches and equations will be given in detail.

Basic definitions defining the problem on horizontal and vertical wond profiles on land and sea are given in Coastal Engineering Manual (CEM, 2008) where the idealized wind profile in a spatially homogeneous marine area is defined in three layers. The lowest part is called “constant shear layer” where there is limited or no Coriolis effect resulting in almost no directional changes in winds. The other two layers above are called “Ekman layer” and “Geostrophic Level” (CEM, 2008).

Two potential local effects that may be regarded as important concerning coastal areas are orography and sea breezes. The blocking effect for winds perpendicular to a land barrier can be regarded as blocked when U/h is below 0.1 and unblocked when U/h is above 0.1. U and h in this relation is defined as wind speed (m/s) and land barrier height (m) (CEM, 2008). Moreover, it is defined that the extent of sea breeze is around 10 to 20 km with wind speeds less than 10 m/s in CEM (2008).

In CEM (2008), winds close to marine surface are defined to follow a logarithmic structure that may be defined as;

$$U_z = \frac{U_*}{k} ln\left(\frac{z}{z_0}\right) \qquad [2.1]$$

where U_z, U_*, k, z and z_0 are called wind speed at height z above the surface, friction velocity, von Karman's constant, height above the surface and roughness height of the surface, respectively. This approach may also be considered in the vertical conversion of the wind speeds. However, since this approach involves too many parameters and several assumptions for this approach are needed to be used, it is not considered in this thesis study.

Demirbilek et al (1993) specifies that one of the critical parameters influencing the wave growth is the air-sea temperature difference. For most of the cases, this information lacks thus 10 m wind speeds under neutral stability conditions ($\Delta T=0$) are considered in wave estimations from winds. Demirbilek et al (1993) mentions that the use of 10 m wind speeds are adequate for wave heights smaller than 3 m, whereas, for wave heights between 3 m and 10 m, 20 m wind speeds are more appropriate for use. Since no conversion methods are given in Demirbilek et al. (1993) concerning land and sea wind profiles, sea and land based wind profiles and conversions are only confined to below given approaches.

2.1.1. Hsu (1981)

Hsu (1981) used simultaneous offshore and onshore wind measurements at several stations all around the world. Offshore wind data were obtained from NOAA buoys, research platforms and merchant ships. For wind speeds ranging from 5 m/s to 6 m/s, Hsu's (1981) study show that, on average, the onshore mean wind speeds are around %63 of the offshore mean wind speeds. Hsu (1981) provides information that only the stations within the beach area measuring the wind speeds above both internal boundary layer (IBL) and the nocturnal inversion height (NIH) represent offshore conditions.

Internal Boundary Layer (IBL) is a layer within the atmosphere bounded below by the surface, and above by a more or less sharp discontinuity in some atmospheric property. Internal boundary layers are associated with the horizontal advection of air across a discontinuity in some property of the surface (i.e. aerodynamic roughness length or surface heat flux) and can be viewed as layers in which the atmosphere is adjusting to new surface properties (www.termwiki.com). On clear, calm nights, radiational cooling results in a temperature increase with height. This is known as nocturnal inversion height (NIH) (global.brittanica.com).

Hsu (1981) developed a formula to convert the measured wind speeds from onshore to offshore;

$$U_{sea} = 3U_{land}^{2/3} \qquad [2.2]$$

The above given formula is valid for onshore wind speeds within the range 2 m/s ≤ U_{land} ≤ 10 m/s. According to Hsu (1981), this approach is an average estimation applicable for many geographic regions as well as various climatic conditions. In Hsu's (1981) approach, there is no specification regarding the wind direction conversion or difference between onshore and offshore wind directions. Hsu's study (1981) also showed that more inland the meteorological station is, more difference between offshore and onshore wind measurements are observed.

In case, there is elevation difference between onshore and offshore wind measurements, corrections should be made on vertical plane. In Hsu's study (1981), this vertical plane correction was performed using power law wind distribution in the planetary boundary layer (PBL) as given by Davenport (1965). The power law formula is given below (Davenport, 1965):

$$(\frac{U}{U_H}) = (\frac{Z}{Z_H})^P \quad [2.3]$$

In the above given formula, U is the wind speed at height Z, U_H and Z_H are the velocity within and above the atmospheric PBL, respectively, and P is an exponent that depends on the atmospheric stability and surface roughness, Z_o. This P value is also called Hellman exponent and sometimes shown as α.

Atmospheric stability can be defined as a measure of the atmosphere's tendency to encourage or deter vertical motion, and vertical motion is directly correlated to different types of weather systems and their severity.

The P value in power law approach differs in accordance with the terrain type. Several representative P values for several terrains may be seen in the below given Figure 2.1 (Hsu, 1981).

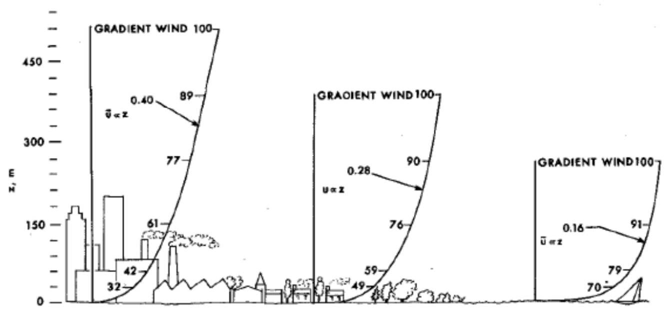

Figure 2.1: The P values in the power law approach over different terrains (Hsu, 1981)

In addition to Hsu's (1981) statements on vertical conversion of wind speeds, a similar approach is used for determination of wind speeds at various heights in vertical plane in wind turbine engineering. As for P (α) value, which is also called Hellman exponent, several values for various conditions are used since this exponent depends on the coastal location, terrain shape and stability of air. These values are given in Table 2.1.

As air passes from land to sea or from sea to land, it readjusts to new boundary conditions. This adjustment is not immediately achieved throughout the depth of the air layer but is generated at the surface and diffuses upward. The layer of air whose properties have been affected by the new surface is referred to as an internal boundary layer (IBL) and its depth grows with increasing distance, or fetch, downwind from the shoreline (Hsu, 1981).

Table 2.1: Several values of Hellman exponent for various conditions and terrains (Kaltschmitt, et. al., 2007)

Location	Hellmann exponent (α)
Unstable air above open water surface	0.06
Neutral air above open water surface	0.10
Unstable air above flat open coast	0.11
Neutral air above flat open coast	0.16
Stable air above open water surface	0.27
Unstable air above human inhabited areas	0.27
Neutral air above human inhabited areas	0.34
Stable air above flat open coast	0.40
Stable air above human inhabited areas	0.60

2.1.2. Hsu (1984)

Based on various simultaneous onshore (U_{land}) and offshore (U_{sea}) wind speed measurements in many different areas around the world and under many different wind conditions, it is found by Hsu (1984) that the below given formulas can be used for operational use:

$$U_{sea} = 3.93U_{land}^{1/2} \qquad U_{land} < 10 \text{ m/s} \qquad [2.4]$$

$$U_{sea} = 1.24U_{land} \qquad U_{land} \geq 10 \text{ m/s} \qquad [2.5]$$

Hsu (1984) states that onshore and offshore wind speed differences have long been known to exist. In most of the cases, due to lack of offshore wind measurements, marine meteorologists and coastal engineers are traditionally required to forecast offshore winds using onshore winds. However, as simultaneous onshore and offshore observations do not always exist, systematic studies such as simple comparisons between these two environments usually lack (Hsu, 1984). Hsu's study (1984) aims to provide simple formulas for operational use for such conversions between onshore and offshore. Hsu (1984) improved the formulas originally proposed in Hsu (1981) and extended the data to cover conditions ranging between breezes and hurricanes. It should be noted that Hsu (1984) did not include atmospheric mesoscale systems (i.e. low-level jets under special conditions, land-breeze and sea-breeze systems and coastal fronts during the winter season).

As can be seen from Figure 2.2 (Hsu, 1984), there is large scatter in data points even though mesoscale systems were not included. This large scatter is based on different physics involved. Hsu (1984) indicates that the aforementioned formulas are useful as first approximation for onshore-offshore wind conversions and can be useful over low-relief (<0.5-1 km in height) and open coasts.

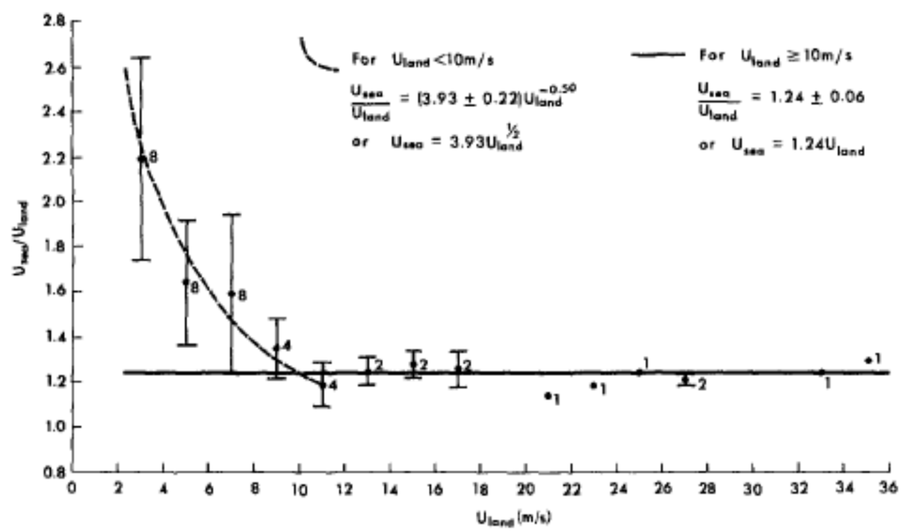

Figure 2.2: Ratio of U_{sea}/U_{land} as a function of U_{land} (Hsu, 1984)

2.1.3. Hsu (1986)

Hsu (1986) mentions that since a low-level jet may prevail over a coastal region near the surface, particularly in the offshore regions, U_{sea} may not be equal to zero when U_{land} is zero. In other words, when onshore conditions are calm, it is not necessary that offshore winds are also calm. This is because strong pressure gradient and baroclinic effect exist across the coastal zone resulting in sea breezes during the day and land breezes or low-level jets during the night (Hsu, 1986). Therefore, the use of a formula linearly relating U_{sea} and U_{land}, can be of practical use for onshore-offshore wind speed conversions. This linear relation may be written in such form:

$$U_{sea} = A + BU_{land} \qquad [2.6]$$

In addition to linear conversion approach between onshore and offshore wind speed conversions, it is necessary to look into directional differences between simultaneous onshore and offshore wind measurements. Hsu (1986) summarized several previous studies in the literature together with his findings.

It was shown by Haltiner and Martin (1957) that the surface cross-isobar angle differences between onshore and offshore airflow can be 20°. According to Mazzarella (1985) the field accuracy for wind direction for common wind speeds is approximately 8°, and for gusts this value is 15°. In addition to these differences, several additional differences may occur due to frictional effects, instrumental errors and recorder inaccuracies which in addition to the aforementioned onshore-offshore airflow differences may cause 45° directional difference in winds (Hsu, 1986). In other words, for the same geostrophic wind across the coastal zone, the difference in wind direction between onshore and offshore may be as large as 45° (Hsu, 1986).

Hsu (1986) states that, a linear wind conversion maybe employed as long as the directional difference between onshore and offshore winds is smaller than 45°. This approach may be used for winds blowing from sea to land and from land to sea. It is also stated that this linear approach is applicable under various weather systems such as hurricanes, land and sea breezes and cannot be used for atmospheric fronts and squall lines across the coastal zone (Hsu, 1986). The above given information regarding under what conditions this linear approach may be used is also an implication that onshore wind data may be used to obtain offshore wind data since the above given conditions do not cover the transient weather systems, which usually do not last more than a day or two (Hsu, 1986).

Under the above stated conditions and assuming that ΔT is negligible the linear conversion formula was found by Hsu (1986) as;

$$U_{sea} = 1.62 + 1.17U_{land} \qquad [2.7]$$

In order to obtain the above given formula, the data used in Hsu (1981) and several additional wind data were considered. According to Hsu (1986), the results are an indication that Equation 2.6 may be used for operational use.

2.1.4. Schwing and Blanton (1984)

Schwing and Blanton (1984) used both onshore and offshore wind data to obtain wind driven currents along a coastal area in USA. It is stated that, the onshore station was at a height of 10 m and the offshore station was located 30 m above the sea surface. In this study, onshore wind data were not adjusted to the offshore conditions, meaning that onshore-offshore wind speed conversions were not performed. Schwing and Blanton (1984) also base their approach of not applying directional wind conversions to Weisberg and Pietrafesa's findings (1983). Weisberg and Pietrafesa (1983) specifies that it may be possible to correct onshore data to resemble offshore winds, but directional variability makes the problem complex and corrections may not apply during some seasons.

Schwing and Blanton (1984) observed that the variance in offshore wind speeds and directions were higher. In other words, the overall wind field ranges greatly for an offshore location. Schwing and Blanton (1984) also sorted the wind vectors into their alongshore and cross-shore components and observed that variance was greater in the alongshore than in the cross-shore direction.

In Schwing and Blanton's study (1984), it is found that the currents estimated from unadjusted onshore winds were significantly different from measured currents. As a result, Schwing and Blanton (1984) stated that onshore wind speeds must be corrected and directional adjustments are preferable to obtain accurate enough wind data.

2.1.5. Liu et al (1984)

Liu et al (1984) aimed to obtain wave data for Lake Michigan, USA. Continuous wind data were necessary to be used as input to the wave model. For this, nine US Coast Guard Stations around Lake Michigan were used. In these stations, wind speed and direction observations as well as air temperature are recorded with 2 hour time intervals.

Liu et al (1984) did not perform any corrections for winds blowing off the lake. However, for those winds blowing from land, an overall land-sea correction to the wind speed and wind direction was implemented using the below given formulas developed by Schwab (1978);

$$U_w = U_L\left(1.2 + \frac{1.85}{U_L}\right)\left[1 - \frac{\Delta T}{|\Delta T|}\left(\frac{|\Delta T|}{1920}\right)^{1/3}\right] \qquad [2.8]$$

$$\Delta\theta = (12.5 - 1.5\Delta T) - (0.38 - 0.03\Delta T)U_w \qquad [2.9]$$

In the above given formulas, U_w and U_L are over-lake and over-land wind speeds (m/s), respectively, ΔT is the air-water temperature difference (°C) with water temperature estimated from local climatology and assumed constant throughout the lake and Δθ is the clockwise angle between over-land and over-lake winds (°).

As mentioned above, equations 2.6 and 2.7 were developed by Schwab (1978), based on the graphs provided in Resio and Vincent (1977). These formulas had been successfully applied to modeling storm surge and current fluctuations in the Great Lakes, USA (Liu et al, 1984).

Liu et al (1984) uses atmospheric data by means of a model to obtain wind fields and wave heights for Lake Michigan. Then, he compares the modeled and measured wind speeds together with modeled wave heights and wave heights from Liu and Ross's (1980) study. The wind speeds comparisons indicate that with a root-mean-square difference of 1.2 m/s, these results are excellent. As for waves, the modeled and measured results substantially agree both in pattern and in magnitude and this does not always follow the prevailing wind. To achieve quantitative comparisons, the predicted wave heights are compared with measured wave heights at various points. Although there is indication of underestimation for higher wave heights and overestimation of lower wave heights by the model, the results are encouraging with a root-mean-square difference of 0.3 m (Liu et al., 1984).

2.2. ECMWF (European Centre for Medium Range Weather Forecasts)

In 1904, Vilhelm Bjerknes, who is a Norwegian hydro dynamist, suggested that the weather conditions could be quantitatively estimated as initial atmospheric conditions by application of a complete set of hydrodynamic and thermodynamic equations (Persson and Grazzini, 2007). The technological developments following the Second World War made Bjerknes's suggestion applicable and possible in terms of mathematical forecasts (Persson and Grazzini, 2007).

The first global model began operating in 1966 at NMC Washington, with a 300-km grid and six-layer vertical resolution (Persson and Grazzini, 2007). This was followed by, a program that was implemented by the Council of Ministers of the European Communities in October 1967 (Persson and Grazzini, 2007) which eventually resulted in signing of ECMWF convention in October 1973 by nineteen European countries.

2.2.1. ECMWF Forecasting System

The ECMWF forecasting system consists of five components (Persson and Grazzini, 2005):

- A general circulation model
- An ocean wave model
- A data assimilation system
- An ensemble forecast system which was initiated in 1992.
- A seasonal forecasting system started to operate in 1998
- A monthly forecasting system which was introduced in 2002

Overall information of the first two components of ECMWF forecasting system, the details of which are more important than other components in terms of the wind and wave data that are used in this study, are summarized in the below given parts.

The General Circulation Model:

Starting with 15 levels in vertical plane and horizontal resolution of 1.875° in latitude and longitude corresponding to roughly 200 km grid length on a circle, the model has been constantly improved as given in Table 2.2 (Persson and Grazzini, 2007).

Table 2.2: Evolution of ECMWF model resolution since 1985 (Persson and Grazzini, 2007)

Spectral Resolution	Vertical Levels	Year
106	19	1985
213	31	1991
319	50	1998
511	60	2000
799	91	2006
1279	91	2010

The Ocean Wave Model:

A global wave model as well as a limited area model for the North Atlantic and the European seas became operational in 1992 (Persson and Grazzini, 2007). In 1998, the wave model was integrated into the atmospheric model.

2.2.2. ECMWF Global Atmospheric Model

ECMWF general circulation model have three components (Persson and Grazzini, 2007):

- Dynamic
- Physical
- Coupled ocean wave

The model formulation can be summarized by six basic physical equations, the way the numerical computations are carried out and the time and space resolutions (Persson and Grazzini, 2007).

Two of these six equations are diagnostic indicating the static correlation between different parameters:

- Gas Law
- Hydrostatic Equation

The other four equations, which are prognostic,describe the dynamic changes of the horizontal and vertical wind components, temperature and water vapour contents of an air parcel, and the surface pressure (Persson and Grazzini, 2007):

- Equation of Continuity
- Equation of Motion
- Thermodynamic Equation
- Conservation of Moisture

The physical processes that can be represented in ECMWF models are shown in Figure 2.3. Several important details of ECMWF model and the input data to this model are given in the following parts.

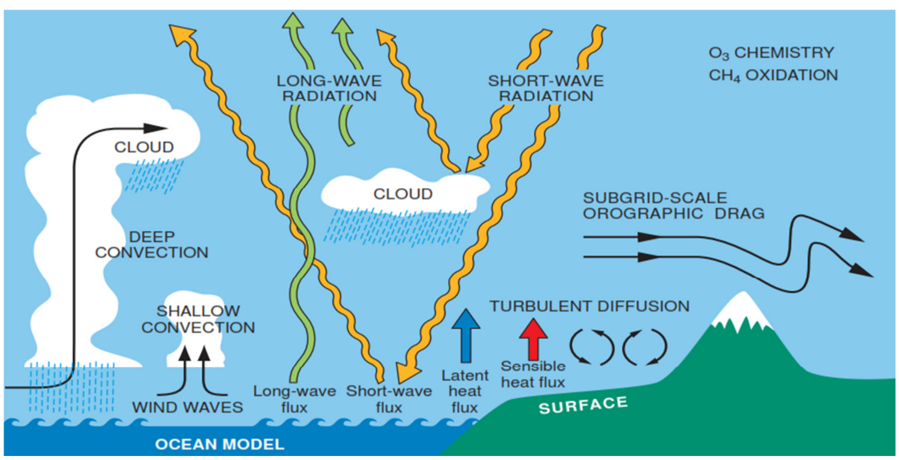

Figure 2.3: Main physical processes represented in the ECMWF model (Persson and Grazzini, 2007)

The Numerical Formulation and Scheme:

The numerical formulation of ECMWF global atmospheric model bases on a semi-Lagrangian numerical scheme. In this numerical scheme, at every time step the grid-points of the numerical mesh represent the arrival points of backward trajectories at the future time. The point reached during this back-tracking defines where an air parcel was at the beginning of the time-step. During the transport, the particle is subjected to various physical and dynamical forcing. Essentially, all prognostic variables are then found through interpolation (using values at the previous time-step for the interpolation grid) to this departure point (Persson and Grazzini, 2007).

Horizontal and Vertical Resolutions:

For representation of upper-air fields and for the computation of horizontal derivatives, a spectral method, which is based on a spherical harmonic representation, with roughly 25 km grid length, is used (Persson and Grazzini, 2007). The horizontal resolution is upgraded to approximately 16 km grid length in 2010.

The atmosphere is divided into 91 vertical layers which roughly correspond to 80 km. There are as many levels in the lowest 1.5 km of the model atmosphere as in the highest 45 km (Persson and Grazzini, 2007).

Time Resolution:

In the recently introduced model, the change of state of the atmospheric variables is described by the dynamic equations over 12 minute periods. This 12-minute forecast defines a new state from which another 12-minute forecast is made. The choice of 12 minutes has been made to obtain enough accuracy and to avoid numerical instabilities. In the Ensemble Prediction System (EPS), the temporal resolution is 30 minutes while in the monthly and seasonal forecast it is 1 hour (Persson and Grazzini, 2007).

Resolution at Earth's Surface:

In order to better represent the conditions at the surface and to achieve better model physics, it is preferred to use a grid point system instead of a spectral formulation. However, since the rapidly decreasing east-west distance between the grid points would easily favour numerical instabilities near the poles, implementation of a reduced Gaussian grid, which is almost regular in latitude, is preferred. A regular Gaussian grid is only applied in a band between 24°N and 24°S (Persson and Grazzini, 2007). The average distance between the reduced Gaussian grid points is about 19 in the new T_L1279 model.

The Model Orography:

The orographic information is originated from a data set which has a 1 km resolution and contains mean elevation values above MSL (mean sea level), the land fraction and the fractional cover of different vegetation types. This detailed data is upscaled to the coarser model resolutions. The resulting mean orography gives quite a realistic description over most of the land areas, but is insufficient in high mountain areas where the sub-grid orographic variability becomes important (Persson and Grazzini, 2007).

The Land-Sea Mask:

The land-sea mask is a field that contains the relative percentage of land and water area for every grid point. At the current status of the model, this land-sea mask number is not used to create a mix environment but only to divide the model surface into sea and land points, defined by a land-sea mask taking values between 0 (100% sea) to 1 (100% land). A grid point is defined as a land point if its value is greater than 0.5, indicating that more than 50% of the actual area within the grid-box is covered by land (Persson and Grazzini, 2007).

Planetary Boundary Layer (PBL):

The Planetary Boundary Layer (PBL) plays an important role for the whole atmosphere-earth system by means of exchange of momentum, heat and moisture.

Even with this fairly high resolution, the vertical gradients of temperature, wind, moisture etc. cannot be described very accurately. Thus, the large scale variables such as wind, temperature and specific humidity are used in the model with the assumption that the transports are proportional to the vertical gradients. At the earth's surface, the turbulent transports of momentum, heat and moisture are computed as a function of air-surface differences and surface characteristics (Persson and Grazzini, 2007).

The Ocean Wave Model:

The wave model used at ECMWF is WAM (WAve Model) which describes the rate of change of the wave spectrum due to advection, wind input, dissipation due to white capping and non-linear wave interactions. The model gives the distribution of wave energy over frequency and direction, and gives a complete specification of the sea state. Two versions of the WAM model are running at ECMWF: the global model and a limited area model.

The global model has an irregular latitude-longitude ($0.36° \times 0.36°$) grid with an average resolution of 40 km. The advection time step is 12 minutes, the same for the the wind input. The wave spectrum has 30 frequency bins and 24 directions (15° intervals) (Persson and Grazzini, 2007).

The limited area models ($0.25° \times 0.25°$) cover the North Atlantic, Norwegian Sea, North Sea, Baltic Sea, Mediterranean and the Black Sea. They have a resolution of 28 km. Shallow water effects are included and the advection and the source time steps are 10 minutes. Like the global model they have 30 frequency bins and 24 directions (Persson and Grazzini, 2007).

Wave Model Performance:

Starting with the introduction of the T511 model, verification of significant wave height and peak period against Northern Hemisphere buoy data has shown a good performance of wave analysis and forecasts. On the other hand, there may be underestimation of the wave forecasts near the coasts and in enclosed basins such as the Baltic and the Mediterranean Seas (Persson and Grazzini, 2007). Furthermore, in rapidly varying circumstances such as the ones that occur near fronts or at the peak of the storms, the limited resolution of the atmospheric and wave model may prevent a realistic representation of the sea state (Persson and Grazzini, 2007).

Swell propagation is handled by a simple scheme which gives rise to a smoothing of the wave field resulting in errors in the order of 10-20 cm in significant wave height (Persson and Grazzini, 2007).

Additionally, existance of many small islands in the Pacific cannot be resolved by the model. They block the propagation of wave energy (Persson and Grazzini, 2007).

Satellite Observations:

The quality, quantity and diversity of satellite observations have been significantly increased over the years. Some of these satellites are equipped with several instruments providing ECMWF with a total number of 28 data sources (Persson and Grazzini, 2007).

Although satellite data is slightly less accurate than conventional observations, they have a great advantage in terms of their broad geographical coverage. In addition, the use of satellite data ensures that the elusive small amplitude-large scale errors over the oceans are corrected for (Persson and Grazzini, 2007).

Quality Control of Observations:

A detailed quality control is applied to the observational data to ensure that only good quality data are used for the analysis. Several methods have been in use in ECMWF which can be categorized as;

- Thinning: To avoid flooding the system with unnecessary data, a thinning procedure,acting as a tool in removing redundant data or data with highly correlated errors, is applied. This process is usually applied to satellite data and sometimes to aircraft and buoy data(Persson and Grazzini, 2007).

- Blacklisting: Stations or platforms with biased or erratic observations are put on a blacklist that can be classified as permanent and temporary. The stations in permanently blacklisted platforms are either badly calibrated or equipped. Temporarily blacklisted platforms have been detected by daily or monthly monitoring to suffer from a sudden deterioration in quality (Persson and Grazzini, 2007).

The data assimilation system, acting as an automatic quality control, can still reject non-thinned or non-blacklisted data if they are climatologically unrealistic, appear as duplicates (or triplicates), or are very different from the first-guess field of the model or disagrees significantly with its neighbors (Persson and Grazzini, 2005).

Interpolation:

In addition to the aforementioned grid resolutions of ECMWF model, data can also be provided with finer resolutions such as 0.1°. As mentioned above the current model has a resolution of approximately 16 km which roughly corresponds to 0.2°. Interpolation is used to obtain data of grids with finer resolution.

Grid to grid interpolation is performed by bilinear interpolation, generating each point of the output grid from its four neighboring points in the input grid. The weights applied to the four input grid points are calculated by:

- performing a linear fit along each line of latitude,
- normalizing the two partial weights for each point,
- performing a linear fit in the north-south direction.

Vegetation and soil type fields as well as Wave 2D spectra use the nearest neighbor. The schematic view of the bilinear interpolation can be seen in Figure 2.4.

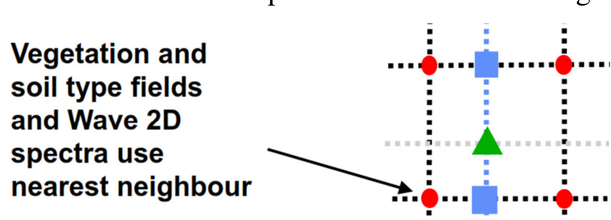

Figure 2.4: Bilinear Interpolation Scheme(Dando, 2013)

The interpolation scheme also handles quasi-regular Gaussian grid input fields. An output latitude line may be generated from two input latitude lines, one to the north and one to the south, which have different grid intervals. The schematic view of this method is shown in Figure 2.5.

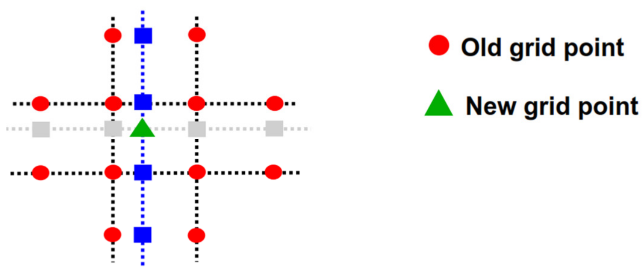

Figure 2.5: Interpolation Scheme for Quasi-Regular Gaussian Grids (Dando, 2013)

A Gaussian field cannot have lines of latitude at the poles. To generate a `line' of latitude points at the North or South Pole, the interpolation scheme performs a linear interpolation of points on the Gaussian grid line nearest to the pole and then puts these values into the output grid. For U and V wind component values, this provides grid points at the pole which have a directional value.

The processing does bilinear interpolation using four neighboring points. Neighbors are used if they have the same land/sea characteristic in the old land-sea mask as the new point in the new land-sea mask. If the four neighbors do not all have the same type, the nearest neighbor of matching type is used. If all four neighbors have different type from the new point, they are all used.

2.2.3. Archived Data

<u>Re-Analysis Data:</u>

The ECMWF re-analysis project is a meteorological reanalysis project. The first reanalysis product, ERA-15, generated re-analyses from December 1978 to February 1994 (approximately 15 years). The second product, ERA-40 began in 1957 and covers a period of 45 years up to 2002. ECMWF released ERA-Interim, which covers the period from 1979 to present (en.wikipedia.org). With re-analysis project, in addition to re-analyzing all the old data using a consistent system, much archived data that was not available to the original analyses is made available to the users (en.wikipedia.org).

The primary objectives of ERA-40 were to produce and promote the use of comprehensive set of global analyses describing the state of atmosphere, land and ocean wave conditions and to foster European and international research by making the observations, the analyses and the study reports widely available (Kallberg et al., 2007). The data sets of ERA-40 are based on quantities analyzed or computed within the ERA-40 data assimilation scheme or from forecasts based on these analyses. ERA-40 archive covers three main data sets: atmospheric daily, wave and atmospheric monthly means (www.ecmwf.int).

The ERA-15 archive contains global analyses and short range forecasts of all relevant weather parameters. The data sets are based on quantities analyzed or computed within the ERA-15 data assimilation scheme or from forecasts based on these analyses. There are four classes of data sets in ERA-15; basic 2.5° data sets, full resolution data sets, wave archive and monthly means. ERA-15 products can be summarized as:

- 6-hourly atmospheric fields on pressure levels
- 6-hourly surface fields
- Monthly averages of daily means
- Synoptic monthly averages at 0 UTC, 6 UTC, 12 UTC, 18 UTC

The basic data sets have data with a resolution of 2.5° x 2.5°. They are particularly suitable for users with limited data processing resources. The full resolution data sets provide access to most of the data from the ERA-15 atmospheric model archived at ECMWF. These archives have a higher space resolution, thus, they should only be used where high resolution is essential. This archive includes analysis, forecast accumulation and forecast data at surface, pressure levels and model levels. The wave archive contains analysis data from the ERA-15 wave model. The monthly means data sets contain data at the resolution of the data assimilation and forecast system used by ERA-15 (T106 for spectral fields and N80 for Gaussian fields). Data services associated with these data sets include the provision of interpolation to requested resolutions and representation forms

ERA-Interim project was initiated in 2006 to provide a bridge between ERA-40 and the next reanalysis project of ECMWF. The main objective of the project was to improve certain key aspects of ERA-40. ERA-Interim has the following spatial resolution:

- 60 levels in the vertical
- T255 spherical-harmonic representation for the basic dynamical fields
- A reduced Gaussian grid with approximate spatial resolution of 79 km spacing for surface and other grid-point fields.

The atmospheric model is coupled to an ocean wave model resolving 30 wave frequencies and 24 wave directions at the nodes of its reduced 1.0°x1.0° latitude/longitude grid. ERA-Interim products can be summarized as:

- 6-hourly atmospheric fields on model levels, pressure levels, potential temperature and potential vorticity
- 3-hourly surface fields and daily vertical integrals
- Monthly averages of daily means
- Synoptic monthly averages at 0 UTC, 6 UTC, 12 UTC, 18 UTC

For all re-analysis data sets, a full extraction, enabling users to obtain sub-areas of data with various resolutions, is provided. All data is delivered in GRIB format (www.ecmwf.int).

<u>Operational Data:</u>

The operational data archive is subdivided into eight classes of data sets (www.ecmwf.int):

- Atmospheric Model
- ECMWF/WCRP Level III-A Global Atmospheric (TOGA)

- Wave Model
- Ensemble Prediction System (EPS)-Atmospheric and Wave
- Atmospheric Model Monthly Means
- Wave Model Monthly Mean
- Monthly Forecasting System
- Seasonal Forecasting System

The operational data sets provide access to most of the data from the atmospheric model archived at ECMWF. These archives have a higher time and space resolution containing all parameters, thus they should only be used where high resolution is essential (www.ecmwf.int).

These data sets contain data at the resolution of the data assimilation and forecast system in operational use at ECMWF. Since the resolution and internal representation of the archive may vary according to changes in ECMWF's operational practice, data services associated with these data sets include the provision of interpolation to requested resolutions and representation forms (www.ecmwf.int).

This archive includes analysis, first-guess and forecast data on the surface, pressure levels and model levels (www.ecmwf.int).

2.3. Comparisons between ECMWF Data and In-Situ Measurements

In this part of the literature survey, comparative studies, in which ECMWF wind and wave data are compared with in-situ wind and wave measurements, are discussed. In this part, the main focus will be given to the comparisons for enclosed and semi-enclosed basins such as the Mediterranean and Black Seas. Additionally, several overall findings for the open seas and oceans will also be mentioned.

2.3.1. Cavaleri and Bertotti (2004)

Cavaleri and Berttoti (2004) used ECMWF meteorological model with different resolutions. Comparisons were performed between results of the different resolutions and between results and satellite/buoy data. It is found that wind speeds and wave heights were underestimated in enclosed basins (Cavaleri and Bertotti, 2004).

The findings indicate that as fetch decreases, errors tend to increase. Large errors are found at short fetches that are in the order of 100 km. The errors gradually decrease with the distance from the coast. The error is larger and more persistent for waves rather than winds. Increase in resolution leads to improvement of the results. Even though the results improve, even with the highest resolution which is about 25 km, the bias does not disappear (Cavaleri and Bertotti, 2004).

It is also found that the main reason behind wind speed underestimations is the slow development of the marine boundary layer. Moreover, implementation of envelope orography instead of mean orography, results in substantial increase of marine wind speeds closely influenced by land (Cavaleri and Bertotti, 2004). In a method where envelope orography is used, it is assumed that mountain passes and valleys are filled with stagnant air. This situation increases the average height if the model mountains and enhances the blocking effect.

The modeled surface wind fields over the oceans are generally good with small bias and small scatter index (Janssen et al. 2000, Abdalla et al. 2002). The bias and scatter index values are slightly larger in winter and smaller in summer. Even though the peak wind speeds are still underestimated at areas where strong gradients are observed, the overall performance of ECMWF wind data can be regarded satisfactory (Cavaleri and Bertotti, 2004).

On the other hand, the conditions are different for enclosed basins especially at locations where surface wind fields are affected by the presence of land. In these areas, the marine modeled surface wind speeds are underestimated almost for all cases. The bias strongly depends on the proximity of the land (Cavaleri and Bertotti, 1997). This situation is felt for relatively large distances so that the problem also appears in comparatively larger basins such as the Mediterranean Sea (Cavaleri and Bertotti, 2004).

Cavaleri and Bertotti (2004) states that a similar situation was also observed for waves in terms of small bias and scatter index in Abdalla et al. (2002). Moreover, in Pielke's study (2002), comparisons between ECMWF wave data and recorded wave data obtained from directional buoys along Italian coastline indicate that the underestimation is 30% on average. This underestimation exceeds 40% for local maxima. It is considered that the lack of resolution is the main reason behind underestimation in coastal areas (Pielke, 2002). This lack of resolution results in inadequate representation of the coastline in the model, as a result, it is natural to obtain poor quality winds and waves within the proximity of land (Cavaleri and Bertotti, 2004).

In Cavaleri and Bertotti's study (2004), it is focused on various separate events in the Mediterranean Sea and the model was implemented with different resolutions varying between 25 km and 190 km for each event. The results show that the increase in resolution induces increase in wind speeds at 10 m above MSL, U_{10}, and significant wave heights, H_s. The differences between results for each resolution tend to be larger for waves than winds. This is a naturally expected result given the sensitivity of waves to wind variations. Therefore, the bias is larger for H_s than U_{10} (Cavaleri and Bertotti, 2004).

In the oceans, both the wind and wave results are found to be very close to the correct values, which is actually the case. The situation in the Mediterranean Sea, which is an enclosed basin, is found to be quite different. As for the Mediterranean Sea case, every increase of resolution leads to a substantial increase of both U_{10} and H_s, and it is only with the highest resolutions that an asymptotic behavior is observed. This is an indication that the ECMWF wave and wind data are below the correct values (Cavaleri and Bertotti, 2004).

In Cavaleri and Bertotti's study (2004), ECMWF analysis results from 1992 to 1998, available at 6 hour intervals are used. The surface winds have been extracted with 0.5° grid resolution. There was considerable scatter, related to improperly modeled variability of the atmosphere (Abdalla and Cavaleri, 2002), but also to the varying capability of the model to reproduce the different meteorological situations. This resulted in suggestion of smoothing of the spatial distribution of the best-fitting slopes. Although this may hide some very local details, it provides a more reliable general pattern. In the three considered sub-basins, the underestimate of H_s reaches 50%, with lower values along the African coastline (between 10 and 20%). 50% underestimation in the northern part of the basin gradually decreases while moving towards the southern coasts (Cavaleri and Bertotti, 2004). This reflects two facts:

- the more complicated orography along the northern coastsin the Mediterranean Sea,
- dominant directions (between west and northeast) where the storms come from.

Moreover, it was found that as fetch increases, the modeled wind bias decreases. The same is also true for waves (Cavaleri and Bertotti, 2004). In the analysis, to minimize the consequences of model resolution on the description of the coastline or the effect of local winds not properly represented in the global meteorological model, cases with a fetch larger than 100 km and a wave height larger than 1 m were used. However, it is by now accepted (i.e. Komen et al. 1994, Janssen, 1998) that the error of waves is smaller than the error of the winds. It can be verified that the consistency of the wind and wave underestimates using the simple relationship $H_s \propto (U_{10})^{\beta}$ (Komen et al. 1994), where β varies between 1 for very short fetches and 2 for fully developed seas. In the Mediterranean Sea, using β=1.5 as a first-order approximation is assumed to be logical. Using this value, the percentage errors, E, may be found as $E_{Hs} = 1.5 \times E_{U10}$. This suggests a wind speed bias of about 20% at short fetches, decreasing with the distance from the coast. The findings of percentage errors of wind speeds and wave heights for short fetches are summarized in Table 2.3 (Cavaleri and Bertotti, 2004).

Table 2.3: Percentage errors for wind speeds and wave heights at short distances for different spectral resolution T (Cavaleri and Bertotti, 2004)

T	106	213	319	511	639	799
Wind	25	18	15	11	8	6
Waves	35	28	24	17	12	9

On the average, the wind error reaches very low values after 500 to 600 km, while for the waves this happens after 800 to 1000 km. This depends on the memory the waves have of the early stages of generation (Cavaleri and Bertotti, 2004).

2.3.2. Cavaleri and Bertotti (1997)

Checking the output of the ECMWF global model and the accuracy of the derived waves for the Mediterranean Sea, Cavaleri and Berttotti (1997) found that an underestimation of the significant wave heights, H_s, of between 20% and 30% are observed. The percent bias varies from place to place, as a function of the local orography, local basin dimensions, correct representation of the coastal details in the wave model grid and islands. An obvious example is the practical impossibility of properly representing the islands in the Aegean Sea. Therefore, as expected, the errors are larger in the smaller basins. The reasons for this are:

- Firstly, for a given resolution, the smaller the basin, the poorer its representation in the model. The smaller basins and the associated orography often lead to an increase of the local complexity of the fields.
- Secondly, for the small basins, any error in space and time in the ECMWF model leads to an immediate response and thus error in the wave.

In Cavaleri and Berttoti's study (1997), it is tried to come up with an empirical calibration in wind fields so that satisfactory results may be obtained. The study area is chosen as the Adriatic Sea. The Adriatic Sea is dominated by two winds, sirocco, blowing from southeast along the basin, and bora, a northeast wind. While sirocco often observed along the whole basin, bora is mostly confined to the northern section. Using the same wind source, global and limited area versions of WAM model are run (Cavaleri and Berttoti, 1997).

In a similar fashion, 11 more storms are also analyzed, practically considering all the possible stormy situations, in terms of intensity and the shape of the fields. The results show that the average underestimate of H_s is fixed at 50% with a variability of ±15%. Moreover, the mean direction at all of the stations does not show any substantial bias, which is an indication that the ECMWF wind directions are correct. Finally, the mean period T_m is largely underestimated at all the stations (Cavaleri and Berttoti, 1997).

One of the main problems faced during Cavaleri and Bertotti's studies (1997) is the lack of extensive wind data in the open sea. Therefore, a statistical relationship could not be achieved.

Rather than going through a long and tedious sequence of tests, Cavaleri and Bertotti (1997) speed up the procedure by assuming the empirical relationship $H \sim U^{\beta}$.With this approach, physical relationship between these two quantities is not expressed and the increase in wind speeds enhances corresponding wave heights. Additionally, no assumptions are made about β, which can vary from place to place. It is assumed that the enhancement factor is 1.5, with an approximation of 0.05. In a way this sounds like a crude solution because, whatever the reasons, one would expect the correction to vary from spot to spot and with the meteorological situation.

In Cavaleri and Bertotti's study (1997), the focus is given to the stormy events. It is expected to have results of overall quality decrease under calm conditions which are less important for wave modelers. Moreover, horizontal diffusion, which is used in meteorological models to maintain numerical stability by smoothing over the improperly resolved small-scale features, is also considered. It is hypothesized that the lack of data is overcome by locally smoothing the wind fields with consequent average decrease in wind speeds (Cavaleri and Berttoti, 1997).

2.3.3. Signell et al (2005)

Signell et al (2005) states that winds play a dominant role in the dynamics of semi-enclosed seas, where wind waves are well suited to show the quality of the driving surface winds derived from meteorological models. Particularly in a small basin, they are sensitive to changes in the driving winds. Wave data are typically more readily available because of the difficulties of making long-term wind measurements over the seas.

Signell et al (2005) remarks that, in the literature (i.e. Komen et al., 1994) it is accepted that, as a general rule, the wave model errors are smaller than those due to the wind. Therefore, when modeled and observed wave results are compared, the wave height errors can be used to identify deficiencies of the driving wind fields. The performance of oceanographic simulations, whether for research or operational forecasting, depends on the quality of the driving wind fields (Signell et al, 2005).

The purpose of Signell et al's study (2005) was to identify the wind field, which would produce the best wave results in the Adriatic Sea. Signell et al (2005) expects that the results can be applied to other semi-enclosed basins with similar characteristics.

Signell et al (2005)'s study describes an initial assessment of the quality of surface winds from these new limited area models, comparing the output of four operational or near-operational wind models for the Adriatic Sea and the derived modeled waves to observed data.

Signell et al. (2005) indicates that the effect of winds forcing on simulated oceanographic processes has been addressed in several recent studies such as Cavaleri and Bertotti's study (1997).Signell et al (2005) found that the ECMWF winds with 100 km resolution need to be enhanced by a factor of 1.50 in order to obtain modeled waves at three locations along the Italian coastline by simulating waves in the Adriatic using the WAM model.

Signell et al (2005) mentions a subsequent study performed by Cavaleri (2002) in which it is found that, if higher resolution ECMWF winds were used (i.e. 40 km resolution), the factor could be reduced to 1.35. Moreover, in consistent with this result, Wakelin and Proctor (2002) found that ECMWF winds underestimate the surge heights in the Adriatic Sea.

Signell et al (2005) concludes that one of the reasons why global meteorological models do not succeed in achieving high-quality surface winds in enclosed basins is the relatively coarse resolution with which the local geometry, in particular the orography that surrounds the basin, is described. This lack of resolution implies a spatial smoothing that removes fine resolution effects due to valleys, ridges and etc.

Moreover, Signell et al (2005) adds that the higher-resolution models show more realistic wind and wave magnitudes than the coarse ECMWF model. On average, ECMWF underestimates winds by 36%; higher-resolution models by 8% and 11%. Cavaleri et al. (2002) has derived calibration coefficients for the ECMWF winds and waves varying from point to point.

Signell et al (2005) concludes that even though their studies are performed in the Adriatic Sea, the results have a general validity for other semi-enclosed basins where the orography plays a substantial role. It is stated that ECMWF wind fields are the smoothest fields, and show an underestimate of wind speed that depends on the size of the basin and its orographic characteristics (Signell et al, 2005).

2.3.4. Soukissian and Voukouvalas (2013)

In Soukissian and Voukouvalas (2013), it is stated that an alternative method for evaluating wind resources is the reanalysis of surface sea winds. This re-analyses is produced by assimilating measured surface data into model-generated surface winds through dynamically and physically consistent way. The spatial resolution of the data is rather coarse describing only the large-scale features. To overcome this shortcoming, appropriate downscaling techniques are applied to achieve the desired fine scale fields. Regional atmospheric models are the well-known instrument of recalculating the coarse fields of meteorological parameters obtained from global models of atmospheric circulation. The main advantage of regional modeling is the high spatial resolution of results (Soukissian and Voukouvalas, 2013).

In Soukissian and Voukouvalas (2013) regarding wind measurements in the Aegean Sea, ERA-Interim data sets are used. ERA-Interim covers the period since 1979 up to date and the temporal resolution of the product is 6 hours (four analyses per day, at 00, 06, 12 and 18UTC). The spatial resolution is about 0.75° x 0.75°.

One of the objectives of this study is stated as development and application of a realistic regression model relating buoy wind measurements to gridded wind speed fields obtained from model simulations in order to better estimate offshore wind power potential. The analyzed wind data sources consist of:

- in-situ buoy wind measurements of POSEIDON marine monitoring network, at a height of 3 m above the sea surface,
- 10-km resolution model generated wind fields of ERA-Interimglobal re-analyses.

The spatial resolution of ERA-Interim global re-analysis is approximately 125 km and in the related studies, this has been dynamically downscaled with the POSEIDON non-hydrostatic limited area atmospheric model. For comparison purposes, buoy wind measurements were adjusted to 10 m reference level (Soukissian and Voukouvalas, 2013).

The buoy wind data consists of time series of wind speeds covering a 5-year long period between 2000 and 2004. Specifically, the analyzed time series are obtained from 4 buoys of the POSEIDON system. The buoy records exhibit various gaps, but even after applying the quality control the remaining number of records is still regarded as sufficient (Soukissian and Voukouvalas, 2013).

It is stated in Soukissian and Voukouvalas (2013) that, the correction from an observed wind speed U_z at a level z, to a wind speed U_{10} valid at 10m is necessary to enable the comparison with the gridded model data. In order to carry the wind speeds to 10m height, reference information specified by Thomas et al. (2005)'s assumption in which most of the world's oceans are considered as near-neutral stability.

In the studies, the wind speed at 10 m over the sea surface obtained from the atmospheric model, U_M, was analyzed and compared with the corresponding buoy wind speeds. It is found that the relevant differences regarding mean wind speeds are rather significant, changing between 3.7% and 24.81%, indicating that the model underestimates wind speeds (Soukissian and Voukouvalas, 2013).

For the wind data comparisons, the buoy locations are considered as reference positions. Therefore, the model wind data have been collocated with the buoy data by using a square distance weighted relation applied to the four closest neighboring points in space and in time keeping the common time frame same. It is found that, regarding the buoy wind speed data, the alteration of sampling period (from 3 h to 6 h) has a negligible effect on the basic statistics of the corresponding time series, leaving actually the main statistical parameters intact (Soukissian and Voukouvalas, 2013).

Moreover, it is concluded that the collocation procedure had negligible effects on the mean wind speeds obtained from model results, in which the relevant differences remain below 1% for three locations and around 5% for the other location. However, important changes are observed in the kurtosis and skewness parameters for all locations (Soukissian and Voukouvalas, 2013).

Additionally, as the mean values of the deviations between collocated wind speeds from buoy and model are positive, it is derived that the atmospheric model generally underestimates wind speeds. The overall correlation coefficients for four locations vary between 0.7 and 0.84.

Due to the negligible effects of the first collocation procedure on the main statistics, additional procedures are adopted in Soukissian and Voukouvalas(2013). It was decided to implement the homogenization-correction procedure for wind data obtained from the atmospheric model with reference to buoy wind data (Soukissian and Voukouvalas, 2013).

It is assumed that, U_B (buoy wind speeds) and U_M (model wind speeds) are variables measured with errors. Thus, a linear relation between these two random variables can be written in the following form (Soukissian and Voukouvalas, 2013);

$$U_M = \beta_0 + \beta_1 U_B + \varepsilon_i - \beta_1 \delta_i \quad [2.10]$$

In the above given formula, β_i, ε_i are the corresponding measurement errors of U_B and U_M. After estimating β_0 and β_1, the general form of the relation between U_B and U_M is re-arranged as;

$$U_M^c = A + BU_M \quad [2.11]$$

In this formula, U_M^C is regarded as the corrected wind speed of the atmospheric model, A and B are the calibration parameters for the atmospheric model. It is found that, while "A" value ranges between -1.15 and -0.48, "B" value ranges between 1.32 and 1.58 for four buoy locations (Soukissian and Voukouvalas, 2013).

Comparisons between wind speed histograms corresponding to the atmospheric model results before and after the correction procedures can be summarized as (Soukissian and Voukouvalas, 2013);

- The histograms obtained from U_M have distinct differences from the histograms obtained from U_B.
- The histograms obtained from U_M^C resemble much like the histograms obtained from U_B.
- The statistics after the correction procedures are very close to the main statistics of buoy wind speeds.

CHAPTER 3

TURKISH COASTAL METEOROLOGICAL STATIONS

As stated in Chapter 1, in this thesis study, firstly, the overall performance of Turkish Coastal Meteorological Stations (TCMSs) have been researched in terms of wind roses and wind histograms. It is expected that these reference studies would give indications of overall and individual quality and level of representativeness of wind measurements performed by TCMSs.

This chapter is structured in the following steps;

- General information about how the measurements are made and which equipment types are used in TCMSs.
- General information about coordinates and locations of TCMSs.
- Wind roses obtained from TCMS wind measurements.
- General evaluation and discussion on the overall performance of TCMSs.

3.1. General Information about Equipment and Wind Measurements in TCMSs

The wind measurements are generally performed with four different types of equipment as given below (www.dmi.gov.tr);

- Fixed anemometer which directly measures the wind speed and direction
- Manual anemometer which can be used by the user by only handling it on the air and has the advantage to be mobile.
- Mechanical anemograph which measures the wind direction, hourly mean speeds and the fluctuations in wind speeds by recording the changes in wind speeds and directions.

In Figure 3.1, examples of fixed and manual anemometers used at TCMSs are shown. There is no such example for the mechanical anemograph (www.dmi.gov.tr).

To control, check and calibrate the aforementioned equipment, wind turbines such as shown in Figure 3.2, are used. However, there is no information regarding how often these checks and calibrations are being performed for each TCMS (www.dmi.gov.tr).

Figure 3.1: Examples of Fixed Anemometer (right) and Manual Anemometer (left) (www.dmi.gov.tr)

Figure 3.2: Example of a Wind Turbine (www.dmi.gov.tr)

The aforementioned equipment is used in climatic and sometimes installed to synoptic meteorological station. As for automatic meteorological stations which are becoming more and more common around Turkish coasts, different observation techniques and equipment are installed.

Automatic meteorological stations (AMSs) have sensors that are sensitive to changes meteorological parameters and can measure these changes. Moreover, the main processor that converts the engineering units (i.e. volt, frequencies, etc.) into meteorological units, the observation units that displays this information in the monitors and communication system that transfers the meteorological codes to the main weather centers are also installed in these stations (www.dmi.gov.tr).

In addition to the data measurement and transfer, AMSs also store this data in certain formats, obtaining graphs using the measured data and getting graphical outputs so that there won't be any data loss (www.dmi.gov.tr).

AMSs consist of following units;

- Censors and censor interfaces,
- Data gathering unit,
- Supervisory control and process unit,
- Display unit,
- Communication interfaces,
- Power supply units,

AMSs have several advantages over climatic and synoptic meteorological stations that can be summarized as (www.dmi.gov.tr);

- More standardization in measurements.
- Continuous measurement of parameters both day and night.
- Achieving more reliable and accurate results.
- Ease in display of meteorological measurements.
- Local and remote access to data archive,
- Not affected by environmental conditions,

Equipment in AMSs consists of wind speed and direction sensors, temperature and humidity sensors, precipitation and rain gauge, pressure sensor, pyranometer and tracker. Among this equipment, general information on wind speed and wind sensors which is directly related to the thesis study is mentioned here.

Automatic Meteorological Stations (AMS):

Wind speed sensor measures the wind speeds at the top of a 10 m high pole. Wind speed sensor has three buckets that works according to the number of returns. The optical numerator within the sensor counts the number of returns of the sensor shaft per unit time. The directional numbers are given in clockwise directions with respect to N which is regarded as 0°. General schematic view of an AMS is shown in Figure 3.3 (www.dmi.gov.tr).

A bucket anemometer is used for wind speed measurements in AMSs. The bucket turns with wind impact and the wind speed is calculated according to the number of turns within a unit period of time. Different methods are used to calculate the number of turns, but the most commonly used methods are photodiode and switch methods. Bucket shaft is connected to a disc and there is a LED or a magnet on one side of the slot within the disk and on the other side of the slot a photodiode or a switch exists. As disc turns, photodiode or switch creates pulses and the number of pulses that is created indicates the related wind speeds (www.dmi.gov.tr). In Figure 3.4, a typical wind speed and direction sensor is shown and in Figure 3.5, the general schematic view of the aforementioned described system can be observed.

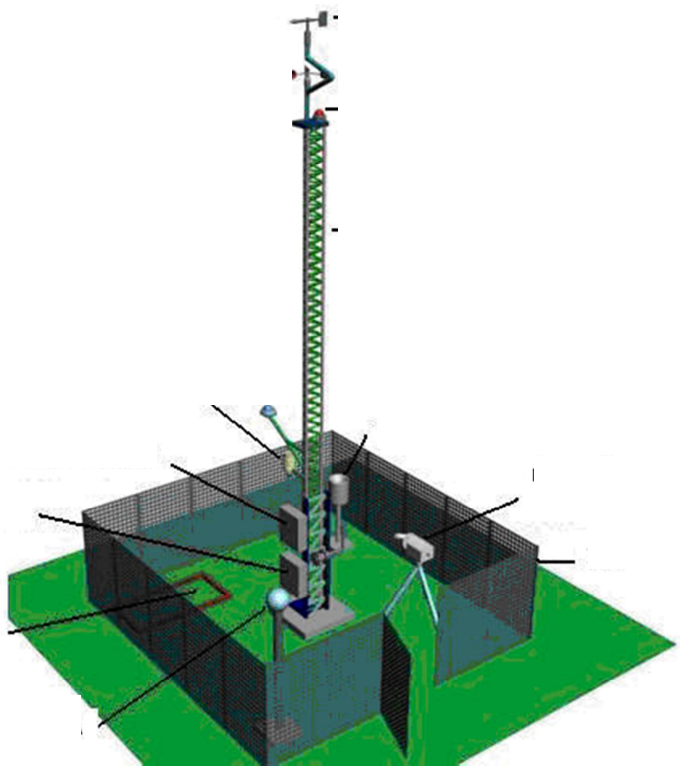

Figure 3.3: General Schematic View of AMS (www.dmi.gov.tr)

Figure 3.4: A Typical Bucket Anemometer (www.dmi.gov.tr)

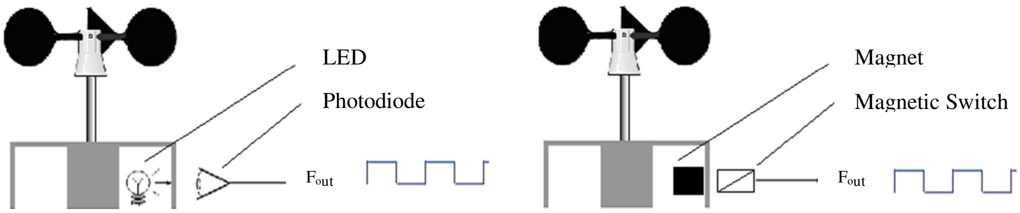

Figure 3.5: General Schematic View of Wind Speed Measurement System (www.dmi.gov.tr)

The wind direction is measured with the help of a specific apparatus. Placing the apparatus facing N which is the starting point and denoted as 0°, the wind direction is obtained by measuring the relative position of the equipment with respect to its initial position. The angular position is determined by three methods:

- Potentiometer method: In this method, the mobile part of the potentiometer is connected to the shaft and the initial resistance of the potentiometer is zero. As equipment turns, the determined resistance is measured and the wind direction is obtained.
- Magnetic switch method: A disc is connected to the shaft of the equipment. There are 36 magnetic switches around the disc. The switch on the opposite side of the magnet gives signal and the wind direction corresponding to that signal is determined.
- Photodiode method: A dics is connected to the shaft of the equipment. There are six different slots at different elevations and there are six LED and photodiodes, underneath and on top of the disc, respectively. The photodiodes creates pulses according to the position of the disc and these pulses are encoded as 6 bytes. The wind direction is calculated with respect to the the relativity of the bytes with respect to 1 or 0. This is regarded as the most sophisticated measurement method.

A typical schematic view of the wind direction apparatus is given in Figure 3.6.

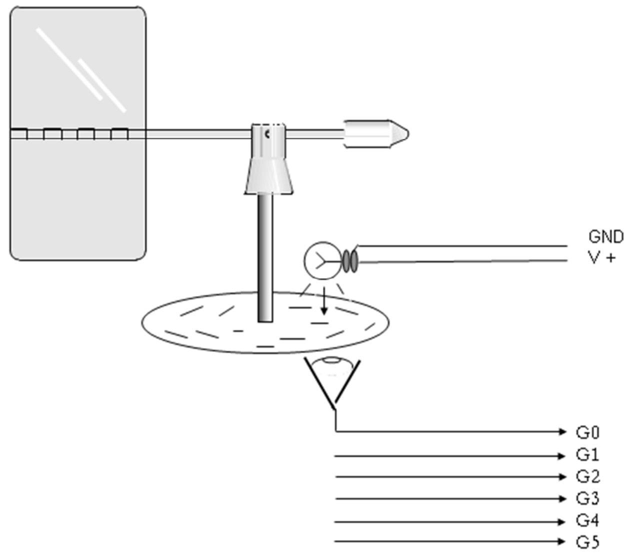

Figure 3.6: A Typical Schematic View of Wind Direction Apparatus (www.dmi.gov.tr)

3.2. General Information about TCMSs

In the second part of Chapter 3, general information about TCMSs in terms of coordinates, elevations and etc. will be listed and their locations are discussed. As a first step, Table 3.1, Table 3.2, Table 3.3 and Table 3.4, which gives detailed information about TCMSs are prepared separately for the Black Sea, the Marmara Sea, the Aegean Sea and the Mediterranean Sea. The boundary between Aegean Sea and Mediterranean Sea is chosen as somewhere between Marmaris and Dalaman.

There are 26, 26, 27 and 25 CMSs respectively at Black Sea, Marmara Sea, Aegean Sea and Mediterranean Sea coasts, counting up to a total of 104 TCMSs. The locations of all of the TCMSs are given in Figure 3.7. The locations of TCMSs at the Black Sea, the Marmara Sea, Aegean Sea and Mediterranean Seas are shown separately in Figure 3.8 to 3.11.

Table 3.1: Details of CMSs around Turkish Black Sea (www.dmi.gov.tr)

Name	Coordinates	Elevation (m)	Distance to Coastline (km)
Hopa	41.41°N – 41.43°E	33	0.3
Pazar	41.18°N – 40.90°E	78	0.8
Rize	42.04°N – 40.50°E	3	0.1
Trabzon Havl.	41.00°N – 39.78°E	39	0.5
Akçaabat	41.03°N – 35.56°E	3	0
Giresun	40.52°N – 38.39°E	38	0.2
Ordu	40.98°N – 37.89°E	5	0.2
Fatsa	41.04°N – 37.49°E	2	0.1
Ünye	41.14°N – 37.29°E	16	0.1
Çarsamba Havl.	41.26°N – 36.56°E	7	2.2
Samsun Bölge	41.34°N – 36.25°E	4	0.2
Alaçam	41.63°N – 35.64°E	7	0.9
Sinop	42.03°N – 35.15°E	32	0.1
Sinop Havl.	41.55°N – 35.92°E	7	0.6
Çatalzeytin	41.95°N – 34.22°E	75	0.1
Bozkurt	41.96°N – 34.00°E	167	2.4
İnebolu	41.98°N – 33.76°E	64	0.1
Cide	41.88°N – 32.95°E	36	0.1
Amasra	41.75°N – 32.38°E	73	0.1
Zonguldak	41.45°N – 31.78°E	135	0.6
Karadeniz Ereğli	41.27°N – 31.43°E	19	1.0
Akçakoca	41.09°N – 31.14°E	10	0.1
Karasu	41.11°N – 30.69°E	4	0.1
Şile	41.17°N – 29.60°E	83	0.4
Kumköy-Kilyos	41.25°N – 29.04°E	38	0.1
Kıyıköy	41.64°N – 28.09°E	-	0.3

Table 3.2: Details of CMSs around Turkish Marmara Sea (www.dmi.gov.tr)

Name	Coordinates	Elevation (m)	Distance to Coastline (km)
Göztepe	40.97°N – 29.06°E	16	0.6
Göztepe Marmara	40.99°N – 29.05°E	41	2
Büyükada	40.85°N – 29.12°E	236	0.5
İstanbul Bölge	40.91°N – 29.16°E	18	1.6
Pendik	40.89°N – 29.24°E	46	2
Gebze	40.82°N – 29.43°E	130	5.9
Kocaeli	40.77°N – 29.92°E	74	0.6
Gölcük	40.73°N – 29.81°E	18	0.2
Altınova	40.70°N – 29.51°E	20	3.7
Yalova Havl.	40.68°N – 29.37°E	13	0.7
Yalova	40.66°N – 29.28°E	4	0.2
Çınarcık	40.64°N – 29.11°E	16	0.1
Armutlu	40.52°N – 28.82°E	70	0.9
Gemlik	40.44°N – 29.15°E	10	0.4
Bandırma	40.33°N – 28.00°E	63	3.5
Bandırma Havl.	40.32°N – 27.97°E	42	3.2
Erdek	40.40°N – 27.79°E	2	0.1
Çanakkale	40.14°N – 26.40°E	6	0
Çanakkale Havl.	40.14°N – 26.43°E	8	2.1
Şarköy	40.61°N – 27.12°E	-	0.1
Tekirdağ	40.96°N – 27.50°E	4	0
Kamiloba	41.05°N – 28.42°E	54	0.6
Büyükçekmece	41.02°N – 28.58°E	-	0.2
Florya	40.98°N – 28.79°E	37	0.4
Atatürk Havl.	40.98°N – 28.82°E	33	3
İst. Deniz Bil. Enst.	41.02°N – 28.96°E	10	1.6

Table 3.3: Details of CMSs around Turkish Aegean Sea (www.dmi.gov.tr)

Name	Coordinates	Elevation (m)	Distance to Coastline (km)
Enez	40.72°N – 26.08°E	-	2.5
Gökçeada	40.19°N – 25.91°E	19	5.1
Gökçeada Havl.	40.20°N – 25.88°E	19	2.9
Bozcaada	39.83°N – 26.07°E	30	0.2
Ayvalık	39.31°N – 26.69°E	4	6.8
Burhaniye	39.50°N – 26.98°E	20	6.5
Edremit	39.59°N – 27.02°E	21	3.7
Balıkesir Kocaseyit Havl.	39.56°N – 27.03°E	19	0.1
Dikili	39.07°N – 26.89°E	3	0
Aliağa	38.79°N – 26.97°E	27	1.3
Foça Toprak Su	38.69°N – 26.74°E	37	0.2
Kakliç Havl.	38.51°N – 26.98°E	5	6.4
Çigli Havl.	38.51°N – 27.01°E	5	9.6
İzmir Bölge	38.39°N – 27.08°E	29	0.6
Urla	38.36°N – 26.83°E	60	0.6
Karaburun	38.64°N – 26.51°E	150	0.9
Çeşme	38.30°N – 26.37°E	5	0.5
Seferihisar	38.20°N – 26.84°E	22	4.2
Gümüldere (Özdere)	38.07°N – 26.00°E	70	0.9
Kuşadası	37.86°N – 27.27°E	25	0.6
Didim	37.37°N – 27.26°E	44	2.9
Turgutreis Marina	37.00°N – 27.26°E	6	3
Bodrum	37.03°N – 27.02°E	26	0.2
Ören	37.03°N – 27.97°E	1	0.5
Datça	36.71°N – 27.69°E	28	0.1
Marmaris	36.84°N – 26.84°E	16	0.5

Table 3.4: Details of CMSs around Turkish Mediterranean Sea (www.dmi.gov.tr)

Name	Coordinates	Elevation (m)	Distance to Coastline (km)
Dalaman	36.77°N – 28.80°E	9	9.1
Dalaman Havl.	36.73°N – 28.79°E	5	4.5
Fethiye	36.63°N – 29.12°E	3	0.7
Kaş	36.20°N – 29.65°E	153	0.6
Kale (Demre)	36.24°N – 29.98°E	25	2.3
Finike	36.30°N – 30.15°E	2	0.4
Kumluca	36.36°N – 30.30°E	60	5.8
Kemer	36.59°N – 30.57°E	10	1.1
Antalya Bölge	36.89°N – 30.68°E	47	0.3
Antalya Havl.	36.91°N – 30.80°E	64	6.7
Belek	36.86°N – 31.06°E	6	1.3
Manavgat	36.79°N – 31.44°E	38	4.2
Alanya	36.55°N – 31.98°E	6	0.4
Gazipaşa	36.27°N – 32.30°E	21	2.2
Gazipaşa Havl.	36.30°N – 32.30°E	32	2.7
Anamur	36.07°N – 32.86°E	2	0.1
Aydıncık	36.15°N – 33.30°E	200	1.6
Silifke	36.38°N – 33.94°E	10	9.5
Erdemli	36.63°N – 34.34°E	7	0.3
Mersin	36.78°N – 34.60°E	7	0.1
Karataş	36.57°N – 35.39°E	22	0.2
Yumurtalık	36.77°N – 35.79°E	34	0.3
Dörtyol	36.82°N – 36.20°E	29	1.9
İskenderun	36.59°N – 36.15°E	4	0.4
Samandağ	36.08°N – 35.95°E	4	0.4

Figure 3.7: TCMS Locations (Google Earth, 2014)

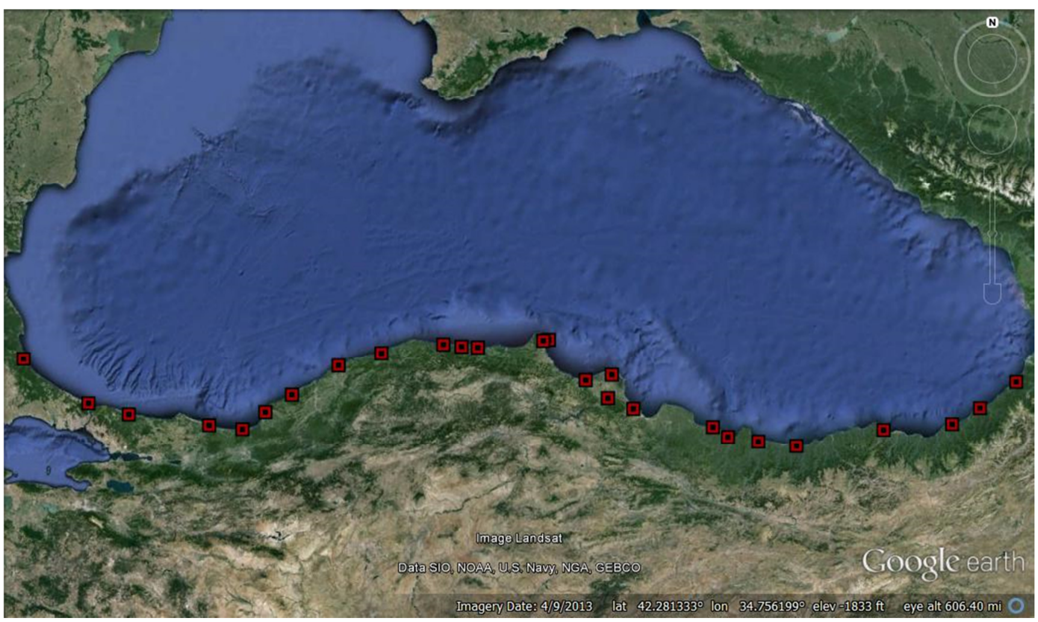

Figure 3.8: CMS Locations around the Black Sea coast of Turkey (Google Earth, 2014)

Figure 3.9: CMS Locations around the Marmara Sea coast of Turkey (Google Earth, 2014)

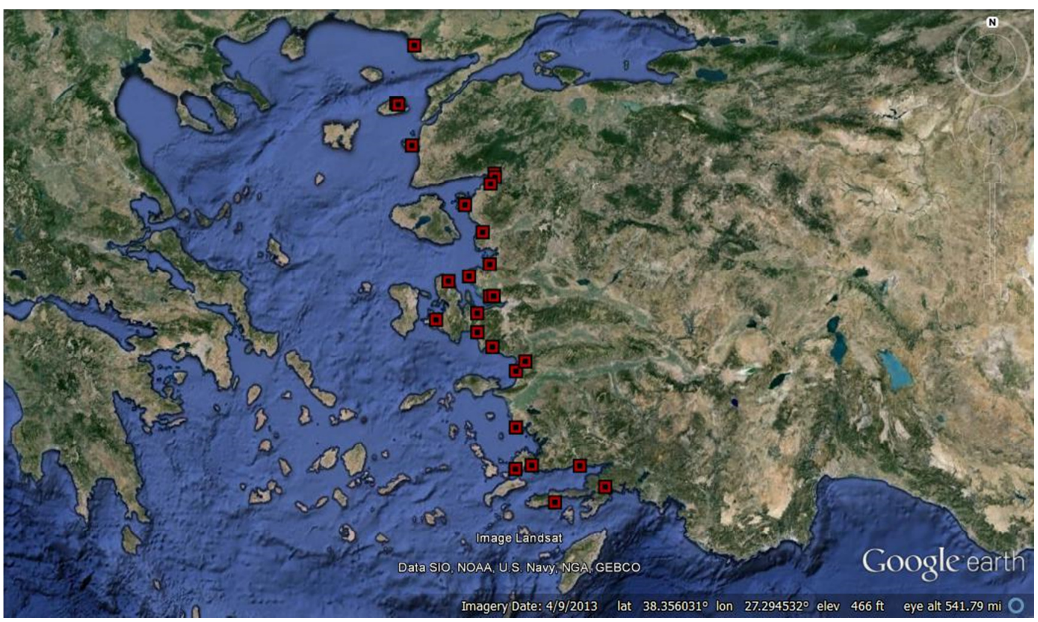

Figure 3.10: CMS Locations around the Aegean Sea coast of Turkey (Google Earth, 2014)

Figure 3.11: CMS Locations around the Mediterranean Sea coast of Turkey (Google Earth, 2014)

The locations of TCMSs play key role in measurement quality of TCMSs. It is extremely important that TCMSs should be at an open coastal area, preferably away from blocking effects such as urbanization, forestation, very high hills and mountains and etc. so that their measurements may represent coastal wind conditions. In short, the use of highly blocked or obstructed TCMSs should be avoided and utmost care should be given to these TCMSs. Up to date, there has been very limited studies regarding the quality and representability of TCMS wind measurements. The first aim in this part of the thesis is to look into TCMS locations to have an overall idea whether they are placed at favorable locations.. For this aim, TCMS locations for four seas around Turkey are taken separately as in the following sections starting with the Black Sea coast.

3.2.1. CMSs around the Black Sea Coast

The CMSs around Turkish Black Sea coasts are given in Figure 3.12 to 3.23. Following each figure, the conditions around TCMSs will be discussed regarding the issues mentioned above.

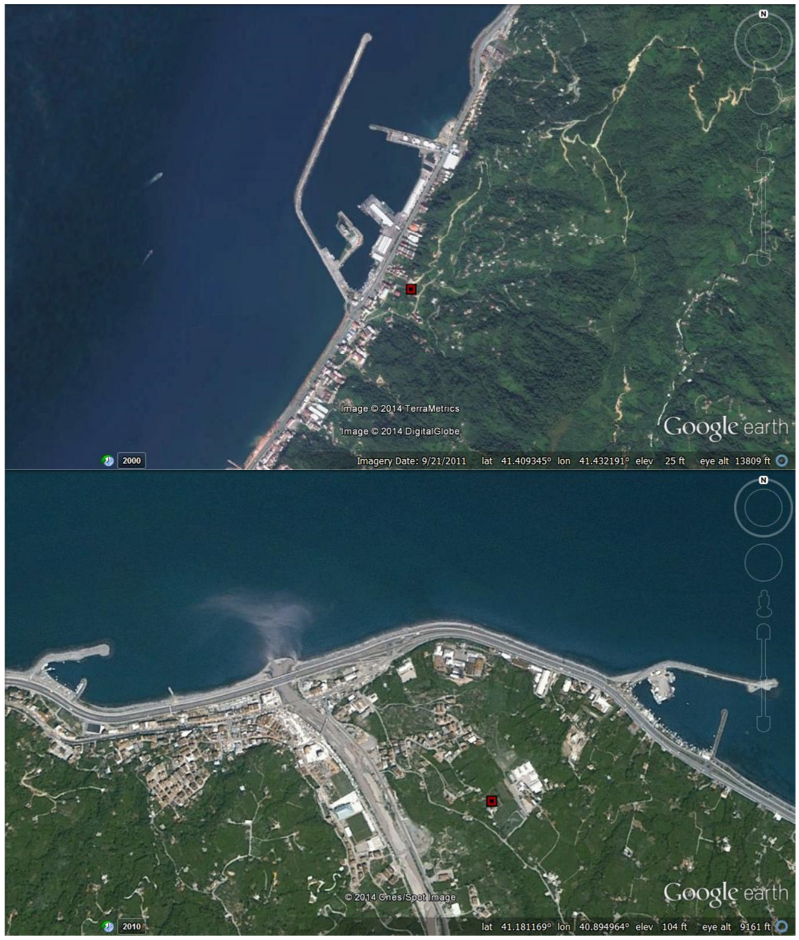

Figure 3.12: Hopa (upper) and Pazar (lower) CMSs (Google Earth, 2014)

As observed in Figure 3.12, Hopa CMS seem to locate in a quite good place and very close to coastline. The only problem may be the existence of coastal highway in between Hopa CMS and marine environment. There may be a possibility that highway traffic may block and affect wind measurements for winds blowing from sea directions. As for Pazar CMS, as it is located at a hill in between a valley of a river and westerly coastline, there is a possibility that the local wind conditions through the valley may influence the wind measurements. In addition, Pazar CMS is located relatively far away from the coastline. Although there is almost no information or indication for vegetation around Pazar CMS, taking into high forestation in the Black Sea coast of Turkey, there is a possibility that forestation may also have an additional impact on wind measurements of Pazar CMS.

Figure 3.13: Rize (upper) and Trabzon Havl. (lower) CMSs (Google Earth, 2014)

It may be said that Rize CMS is located in a good place in terms of representing winds blowing from sea directions. The only visual problem that may trigger as a blocking effect is the highway passing between the coastal zone and a couple of buildings on the western side of the measuring apparatus. Trabzon Havl. CMS is located at the Trabzon Airport and there is a possibility that planes may have blocking effects during landing or taking off. There is no certainty on the exact location of the apparatus within the airport boundaries, thus it is hard to define probable blocking effects.

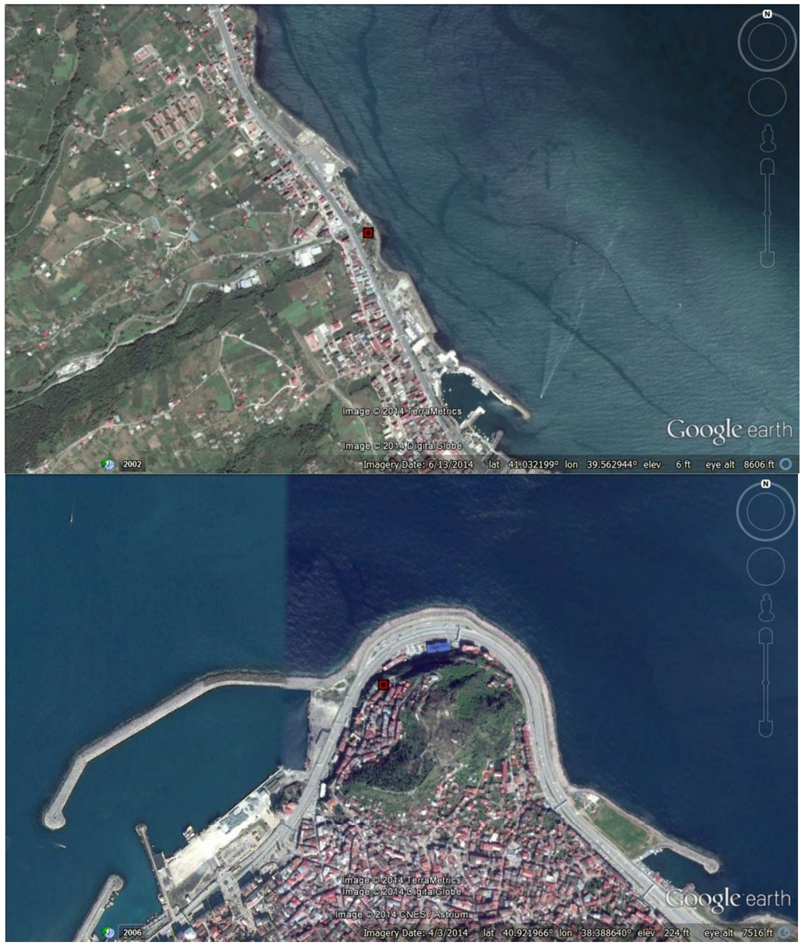

Figure 3.14: Akçaabat (upper) and Giresun (lower) CMSs (Google Earth, 2014)

Akçaabat CMS is located very close to the coastline and unlike Hopa and Rize CMSs as highway passes behind Akçaaabat CMS it is not expected to have any possible problems regarding onshore winds. There are several buildings on the W-NW sector of Akçaabat CMS that may have some blocking effect. As for Giresun CMS, it is located on the left side of a hill very close to coastline. Due to its location at the left side of the hill, there is a strong possibility that winds from ENE-SE sector may not be measured accurate enough or even not at all. Moreover, highway passing between Giresun CMS and the coastline may cause problems for the other sectors.

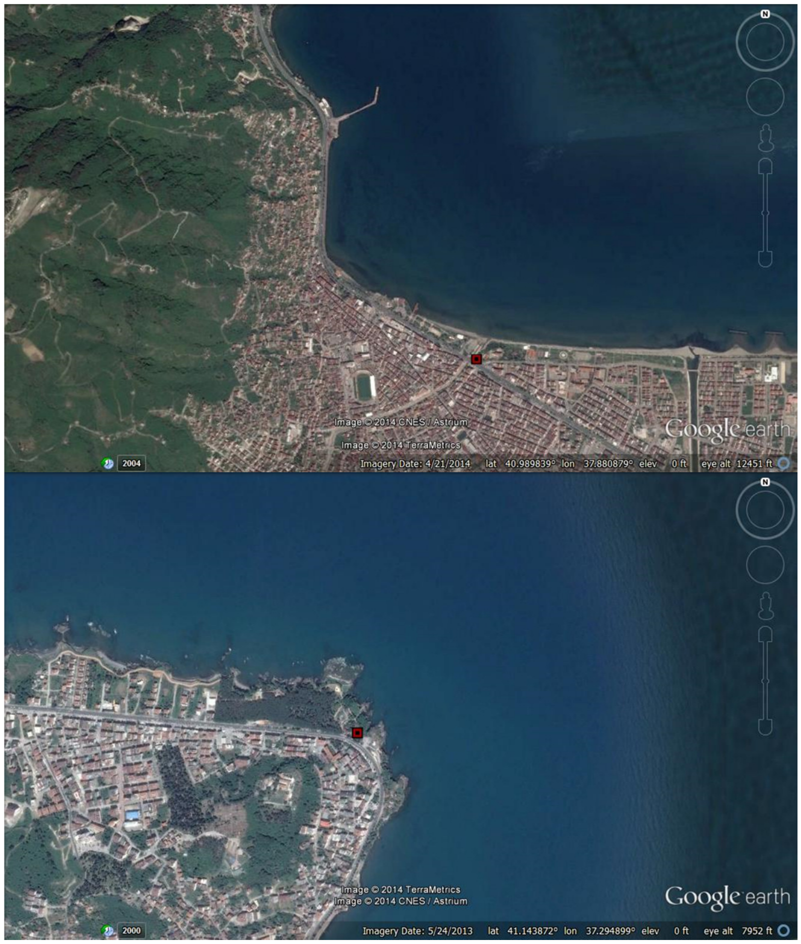

Figure 3.15: Ordu (upper) and Ünye (lower) CMSs (Google Earth, 2014)

Ordu CMS is located at the end of a valley and at the mouth of a river very close to the coastline. Its location is very advantageous as very small obstacles exist nearby. The only possible blocking effect may be the result of the main building of Ordu CMS which is located at the ENE side of the measuring apparatus. Moreover, there is a slight possibility that due to the mountainous areas at W, the measured westerly winds are not accurate enough. As for Ünye CMS, it is located at the tip of a small peninsula which gives an advantage for possible representativeness of all onshore winds. However, the vegetation on the western side of Ünye CMS may cause problems in measuring the westerly winds. Moreover, it is partly blocked by trees on its northern side as well.

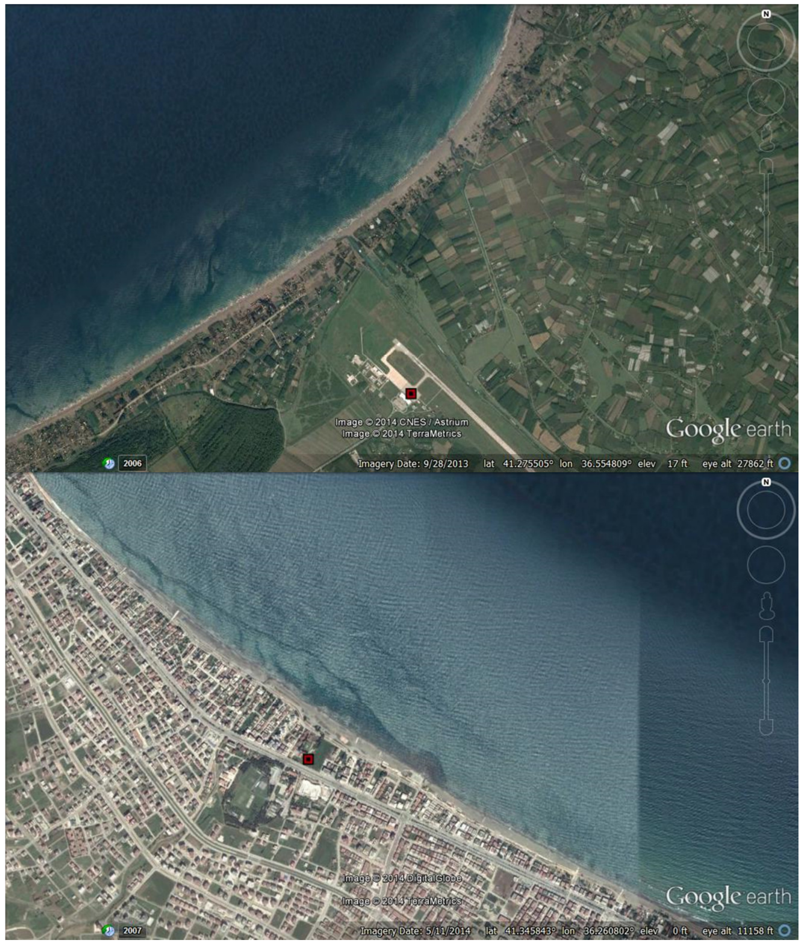

Figure 3.16: Çarşamba Havl. (upper) and Samsun Bölge (lower) CMSs (Google Earth, 2014)

Çarşamba Havl. CMS is located within the boundaries of Çarşamba Airport, and just like the situation for Trabzon Havl CMS, the exact location of the measuring apparatus is not known. It is visually seen that Çarşamba Havl CMS has few blocking effects and except landing and taking off airplanes the impact on measurements is expected to be small. Unlike most of the Black Sea coast CMSs, it is located at a low-lying area which is also advantageous. A disadvantage of Çarşamba Havl CMS may be the distance to the coastline. As for Samsun Bölge CMS, although it is very close to the coastline, it is located at an urbanized area, thus the measuring apparatus are blocked by building on NW-W and E-NNE sectors.

Figure 3.17: Alaçam (upper) and Sinop (lower) CMSs (Google Earth, 2014)

Alaçam CMS is also located at a low-lying area just like Çarşamba Havl CMS which is a positive factor. However, it seems like it is blocked by trees at the W-E sector. Sinop CMS is located at the northern side of Sinop Peninsula. The hilly areas at the NE-E sector may possibly affect the winds blowing from these directions and the buildings on the SW-W sector may do the same for the winds blowing from this sector.

Figure 3.18: Sinop Havl. (upper) and Çatalzeytin (lower) CMSs (Google Earth, 2014)

The exact location of Sinop Havl CMS, just like the previously mentioned CMSs within airport boundaries is not known and again just like the two previously mentioned CMSs in an airport area, planes may influence the measuring wuality an accuracy. On the other hand, its closeness to the coastline and its existence on a low-lying area are good for Sinop Havl CMS measurements. Çatalzeytin CMS is located close to the coastline and almost no visual obstacles exist for measuring apparatus except the highway passing between Çatalzeytin CMS and coastline.

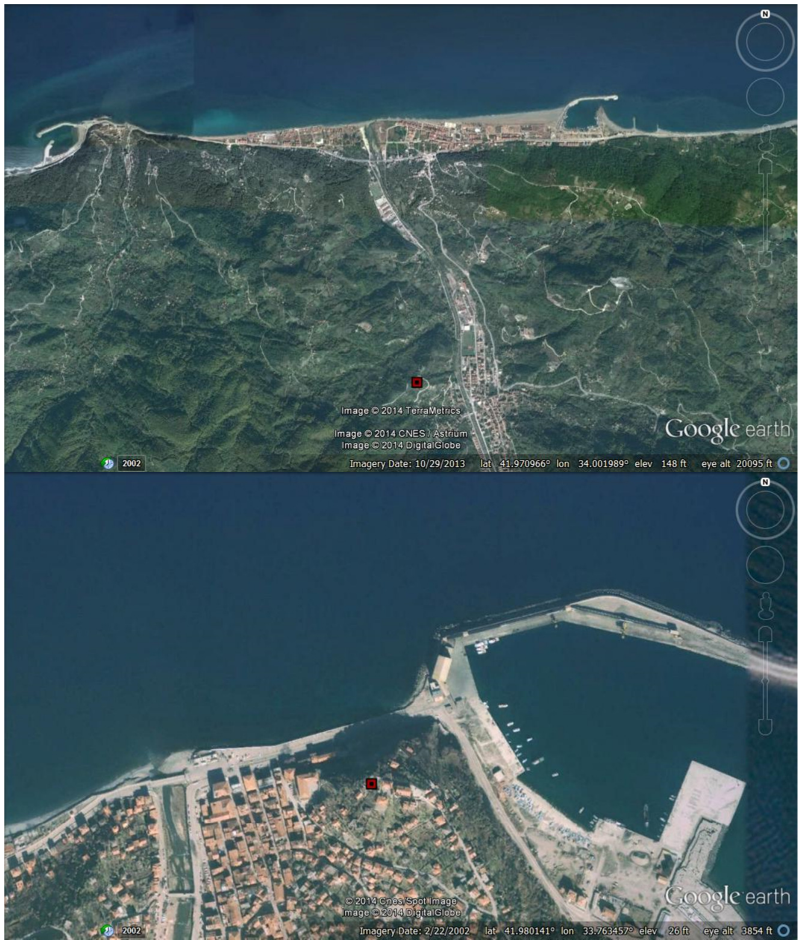

Figure 3.19: Bozkurt (upper) and İnebolu (lower) CMSs (Google Earth, 2014)

Although Bozkurt CMS is located about 2-3 km away from the coastline, which is normally regarded as a common situation for CMSs, for Turkish Black Sea coast, the due to the hilly and mountanious structure nearby the coastal areas, distance of CMS to the coastline play the most important role. Thus, Bozkurt CMS is very poorly situated for a CMS. Moreover, it is located within a river valley through which local winds may be observed and the effect of forestation together with hills mostly on the western side may also cause poor measuring quality. As for İnebolu CMS, just like Giresun CMS, it is located at the western side of a hill which may result in poor measurement of westerly winds.

Figure 3.20: Cide (upper) and Amasra (lower) CMSs (Google Earth, 2014)

Cide CMS is located very close to the coastline and except several trees located in between Cide CMS and coastline on its W-NW side, it has a good location for a CMS. Amasra CMS is located at the top of a high hill (approximately 60 m) at a peninsula which results in almost no obstacles.

Figure 3.21: Zonguldak (upper) and Karadeniz Ereğli (lower) CMSs (Google Earth, 2014)

Zonguldak and Karadeniz Ereğli CMSs are lcoated in highly urbanized areas which is one of the main things that is not wanted in a CMS. Therefore, they are poorly situated. Many possible obstacles exist for these CMSs including buildings and hills.

Figure 3.22: Akçakoca (upper) and Karasu (lower) CMSs (Google Earth, 2014)

Although Akçakoca CMS is very close to the coastline, the measuring apparatus of Akçakoca CMS is blocked by buildings on all sides facing the sea. On the other hand, Karasu CMS which is also very close the coastline, is not blocked by buildings, forestation and etc. The existance of the highway may play some role in measuring quality for each CMS.

Figure 3.23: Şile (upper), Kumköy-Kilyos (middle) and Kıyıköy (lower) CMSs (Google Earth, 2014)

Şile, Kumköy-Kilyos and Kıyıköy CMSs have advantageous locations since they are hardly blocked from sea directions apart from the local vegetation and some minor geographical features.

3.2.2. CMSs around the Marmara Sea Coast

The CMSs around Turkish Marmara Sea coasts are given in Figure 3.24 to 3.36. Following each figure, the conditions around TCMSs are discussed in terms of visual observations and regarding the issues mentioned above.

Figure 3.24: Göztepe (upper) and Göztepe Marmara (lower) CMSs (Google Earth, 2014)

As seen in Figure 3.23, Göztepe and Göztepe Marmara CMSs are located at very high urbanized areas, thus blocking effects of buildings most likely be observed in measuring quality of these CMSs. Among these two CMSs, Göztepe Marmara is locate very far inland which may even result in disclassification of this station as CMS. As a result of the many obstacles around these stations, poor quality wind measurements are naturally expected for these stations.

Figure 3.25: Büyükada (upper) and İstanbul Bölge (lower) CMSs (Google Earth, 2014)

Büyükada CMS is located at the top a hill at Büyükada and have a very high elevation. Although there are very few blocking effect around Büyükada CMS except some forestation around it, its elevation may be the main issue to be discussed in terms of qind measurements. As for İstanbul BölgeCMS, just like Göztepe and Göztepe Marmara CMSs, it is within a highly urbanized area and additionally, there is a hill blocking its SW-W sector. Thus, a poor quality in wind measurements is also expected for Istanbul Bölge CMS.

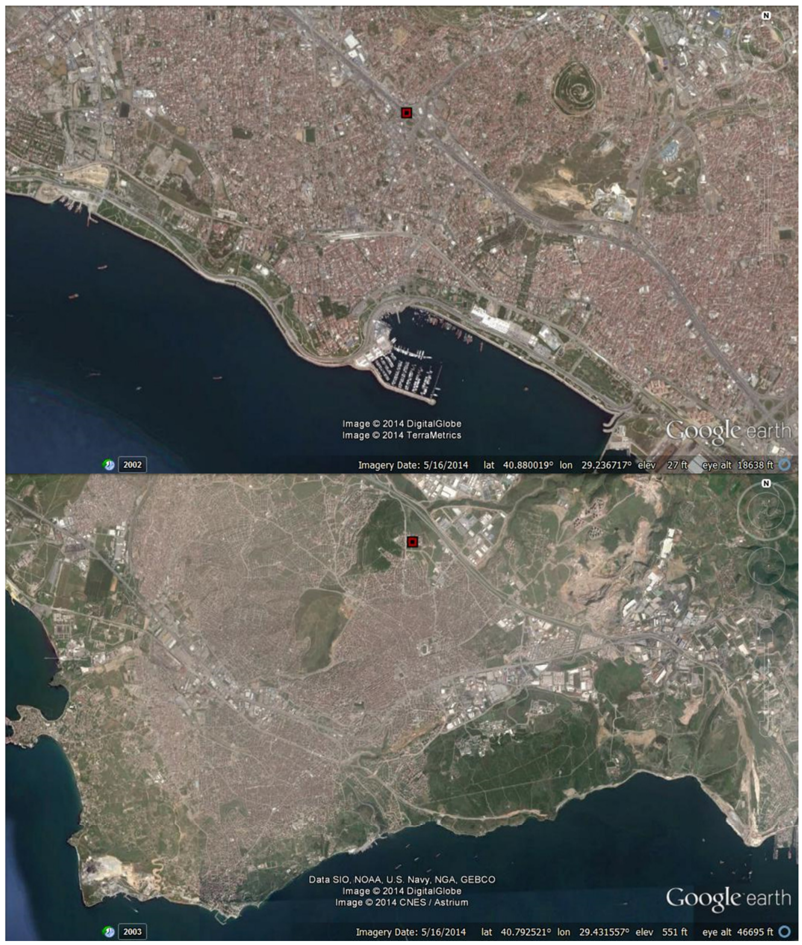

Figure 3.26: Pendik (upper) and Gebze (lower) CMSs (Google Earth, 2014)

Pendik CMS and Gebze CMSs have almost similar situations like Göztepe, Göztepe Marmara and İstanbul BölgeCMSs, therefore poor wind measurements are expected for these CMSs as well.

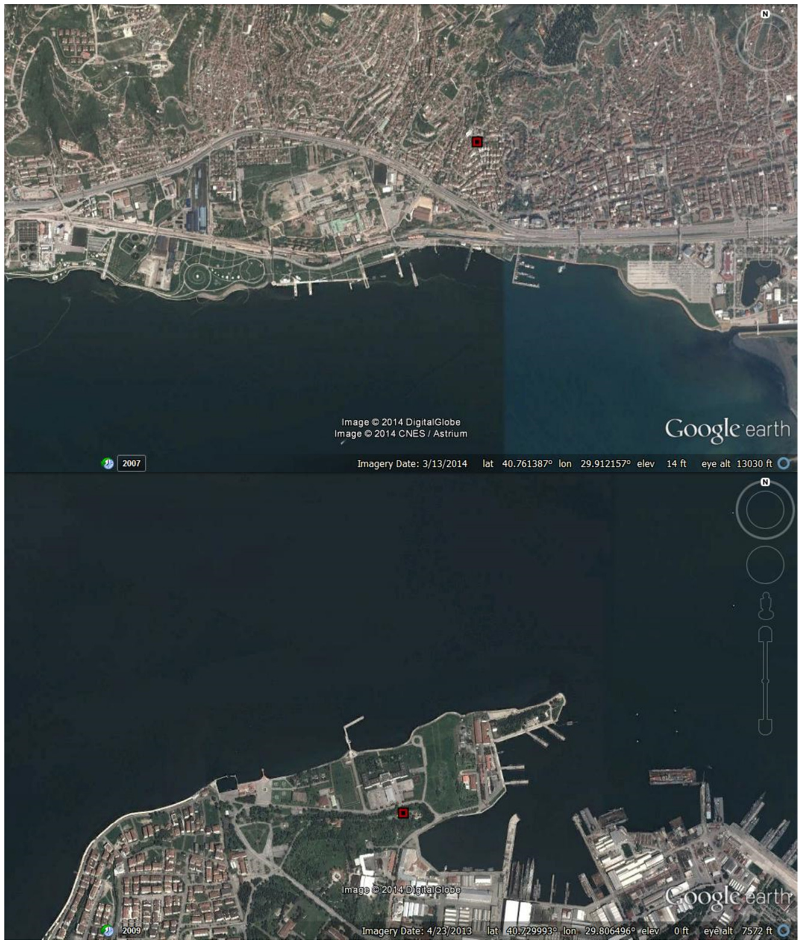

Figure 3.27: Kocaeli (upper) and Gölcük (lower) CMSs (Google Earth, 2014)

Kocaeli CMS is also located in an urbanized area which results in surrounding buildings acting as obstacles for wind measurements. Therefore, poor quality wind measurements are anticipated for Kocaeli CMS. As for Gölcük CMS, although it is situated very close to the coastline, there is a building that may block the winds from NW-N sector.

Figure 3.28: Altınova (upper) and Yalova Havl. (lower) CMSs (Google Earth, 2014)

Altınova CMS is located at some distance to the coast and it is surrounded by buildings which may result in poor quality wind measurements for some directions. Yalova Havl. CMS is a CMS located within Yalova airport and the exact location of it is not known. It is situated at a comparably low-lying area and only blocked by several building situated at the coastal areas on the NW side.

Figure 3.29: Yalova (upper) and Çınarcık (lower) CMSs (Google Earth, 2014)

Yalova CMS is at a good location close to the coastline and only slighlty blocked by several buildings at W. ÇınarcıkCMS which is also very close to the coastal zone, is blocked by buildings on E and W sides and sadly blocked by the main building of Çınarcık CMS on N side.

Figure 3.30: Armutlu (upper) and Gemlik (lower) CMSs (Google Earth, 2014)

Armutlu CMS is at some distance to the coastline and partly blocked by the hilly formation situated at W. Gemlik CMS is located at the northern side of Gemlik Bay at a fairly high elevation. It is only effected by several buildings on the southern side.

Figure 3.31: Bandırma (upper) and Bandırma Havl. (lower) CMSs (Google Earth, 2014)

Bandırma and Bandırma Havl. CMSs are situated at some distance inland and very close to each other. There is an urban area in between the coastline and both CMSs which may have negative influence on wind measurements. However, they are not so much blocked by closeby buildings, especially Bandırma Havl. CMS. Wind measurements at Bandırma CMS may be influenced by several buildings about 200 m north of its location.

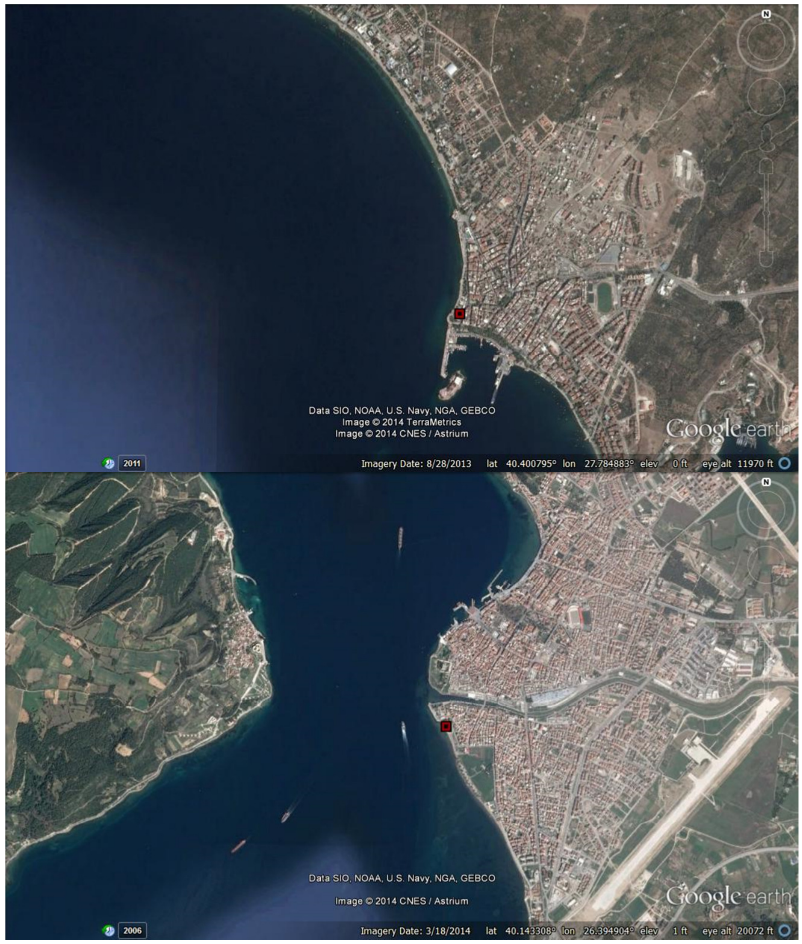

Figure 3.32: Erdek (upper) and Çanakkale (lower) CMSs (Google Earth, 2014)

Erdek CMS is located very close to the coastal zone and very poorly blocked by buildings concerning onshore direction, therefore good quality wind measurements are naturally anticipated for this CMS. As for Çanakkale CMS, it is located at Dardanelles and therefore it is expected that winds blowing through the direction of Dardanelles can be measured quite good at this CMS. Except several buildings on the N-NW sector, very few obstacles exist.

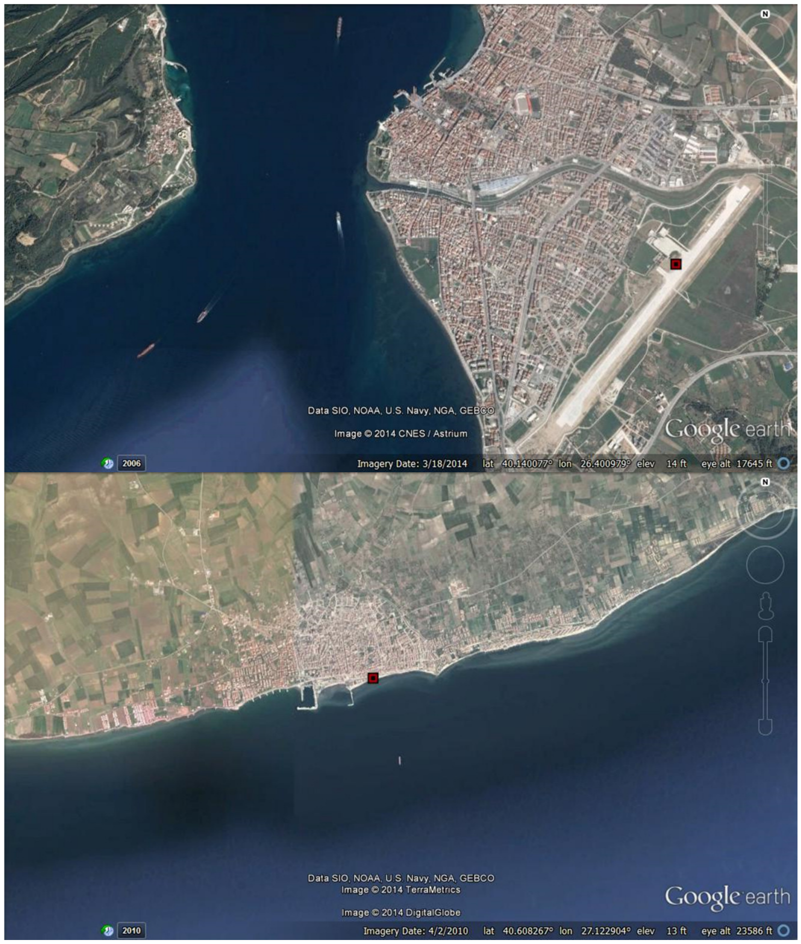

Figure 3.33: Çanakkale Havl. (upper) and Şarköy (lower) CMSs (Google Earth, 2014)

Çanakkale Havl. CMS is located at some distance to the shoreline and Çanakkale city is situated in between Dardanelles and Çanakkale Havl. CMS. Therefore comparably lower quality wind measurements are naturally expected for winds blowing from these directions. Sarkoy CMS, as seen in Figure 3.33, is at a good location, close to the coastal zone and not obstructed concerning sea directions.

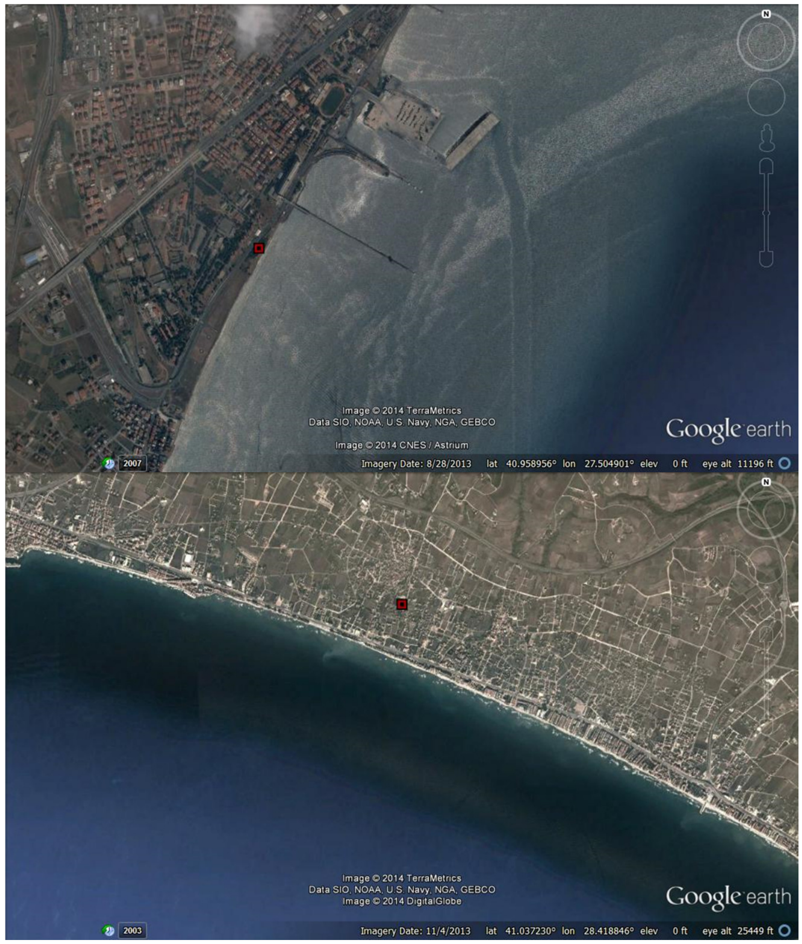

Figure 3.34: Tekirdağ (upper) and Kamiloba (lower) CMSs (Google Earth, 2014)

Tekirdağ CMS is at the southern side of Tekirdağ Harbor, located at a coastal area and there are no visible obstacles in between the sea and Tekirdağ CMS. Kamiloba CMS is at some distance inland and may be blocked by sparsely situated buildings around itself.

Figure 3.35: Büyükçekmece (upper) and Florya (lower) CMSs (Google Earth, 2014)

Büyükçekmece CMS is at the northern side of Büyükçekmece Bay and it is very closely located to the highway that may influence the ulity of wind measurements. Additionally several buildings around the CMS may also have a negative impact. Florya CMS is situated on top of a small hill, partly surrounded by trees, but almost no buildings exist nearby.

Figure 3.36: Atatürk Havl. (upper) and İst. Den. Bil. Enst. (lower) CMSs (Google Earth, 2014)

Atatürk Havl CMS is another CMS located within the boundaries of an airport, theregore the exact location of the CMS is not known. It is expected that several disadvantages such as comparably long distance to the coastal zone, high airport traffic, etc. may be observed concerning wind measurements. İst. Den. Bil. Enst. CMS is located at the historical peninsula which is a very densely populated and settled area, therefore mant many obstacles surround İst. Den. Bil. Enst. CMS.

3.2.3. CMSs around the Aegean Sea Coast

The CMSs around Turkish Aegean Sea coasts are given in Figure 3.37 to 3.49. Following each figure, the conditions around TCMSs will be discussed regarding the issues mentioned above.

Figure 3.37: Enez (upper) and Gökçeada (lower) CMSs (Google Earth, 2014)

Enez CMS is located at the northernmost part of the Turkish Aegean Coast and it is situated very close to the coastal zone with almost no obstacles in between sea and itself. On the other hand, Gökçeada CMS is situated almost in the middle of the island, close to the airport and it is surrounded by hills on three sides, W, NW and partly E.

Figure 3.38: Gökçeada Havl. (upper) and Bozcaada (lower) CMSs (Google Earth, 2014)

Gökçeada Havl. CMS is situated within the boundaries of Gökçeada airport, very close to Gökçeada CMS. Several hills block this station's E-NE and partly NW-W sides. Bozcaada CMS is situated at the eastern side of the island facing the mainland. It is on a small hilltop with almost no blocking effect.

Figure 3.39: Edremit (upper) and Balıkesir Koceseyit Havl. (lower) CMSs (Google Earth, 2014)

Edremit CMS is within the city limits of Edremit and, even though situated at a low-lying plain, it is far away from the coastal zone and surrounded by buildings on all sides. Balıkesir Kocaseyit Havl. CMS is one of the many CMSs within an airport and just like the previously mentioned similar CMSs few obstacles exist in its surroundings.

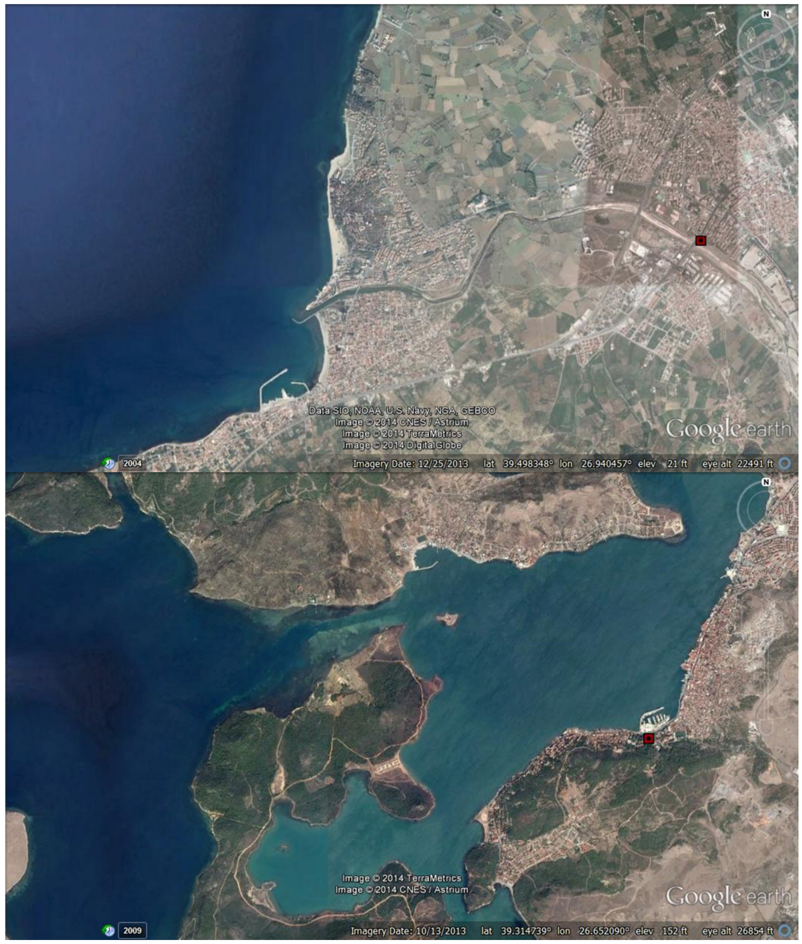

Figure 3.40: Burhaniye (upper) and Ayvalık (lower) CMSs (Google Earth, 2014)

Burhaniye CMS, which have some distance to the surrounding buildings, is located relatively inland but due to the low-lying plain area, there are few geographical features that may act as a blocking effect. Ayvalık CMS is very close to the shoreline and almost no obstacle exists for the NW-NE sector, except for the island relatively far away from the mainland. For the W-NW sector, vegetation and sparsely located buildings may influence the wind measurements.

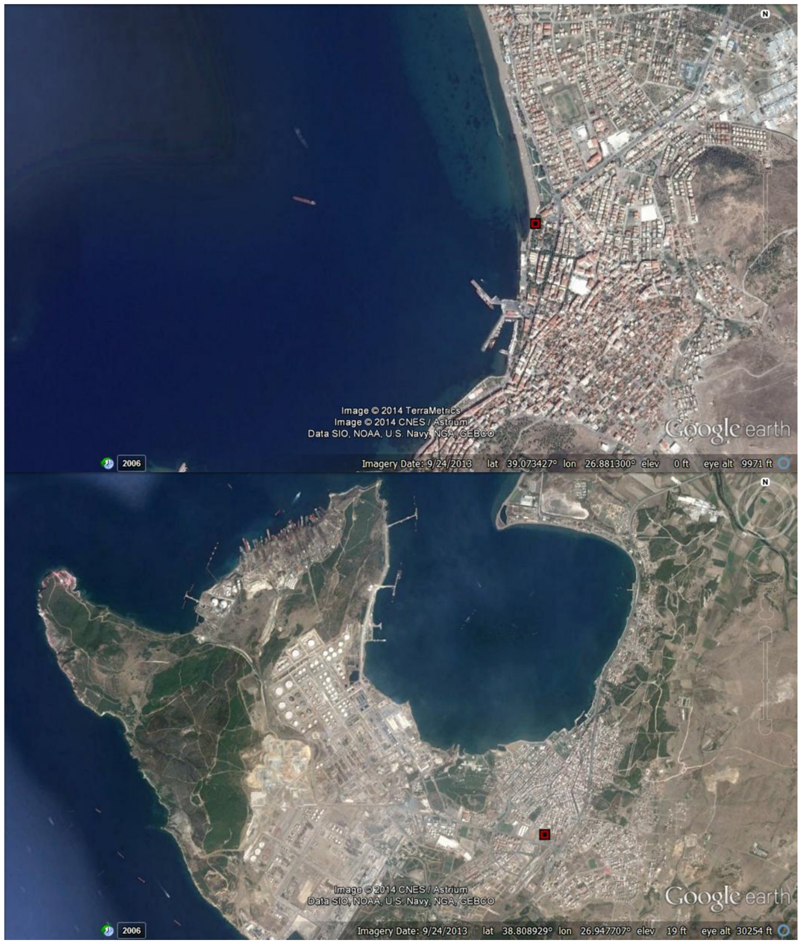

Figure 3.41: Dikili (upper) and Aliağa (lower) CMSs (Google Earth, 2014)

As seen in Figure 3.41, there is no visual obstacle around Dikili CMS, which is located at the shore area. As for Aliağa CMS, due to urbanized surroundings, many buildings may block the winds for certain directions. Moreover, as Aliağa CMS is located facing Aliağa Bay and there is a big hilly area at the far western side of the CMS, there is a possibility that Aliağa CMS have poor quality measurements for certain onshore wind directions.

Figure 3.42: Foça Toprak Su (upper) and Kakliç Havl. (lower) CMSs (Google Earth, 2014)

Foça Toprak Su CMS is located on a small hill on top of which trees exist. The trees may have a obstructive effect and the offshore island at the NW may have a similar impact, too. Kakliç Havl. CMS is one of the two military airports located at the northern side of Izmir Bay. Due to the low-lying plain area and with no surrounding settlements, this station is expected to perform well in terms of wind measurements.

Figure 3.43: Çiğli Havl.(upper) and İzmir Bölge (lower) CMSs (Google Earth, 2014)

The remarks specified for Kakliç Havl. CMS can also be repeated for Çiğli Havl. CMS. On the other hand, İzmir Bölge CMS which is in a densely populated and highly urbanized area have to deal with many obstacles for wind measurements. It is surrounded by buildings on all sides.

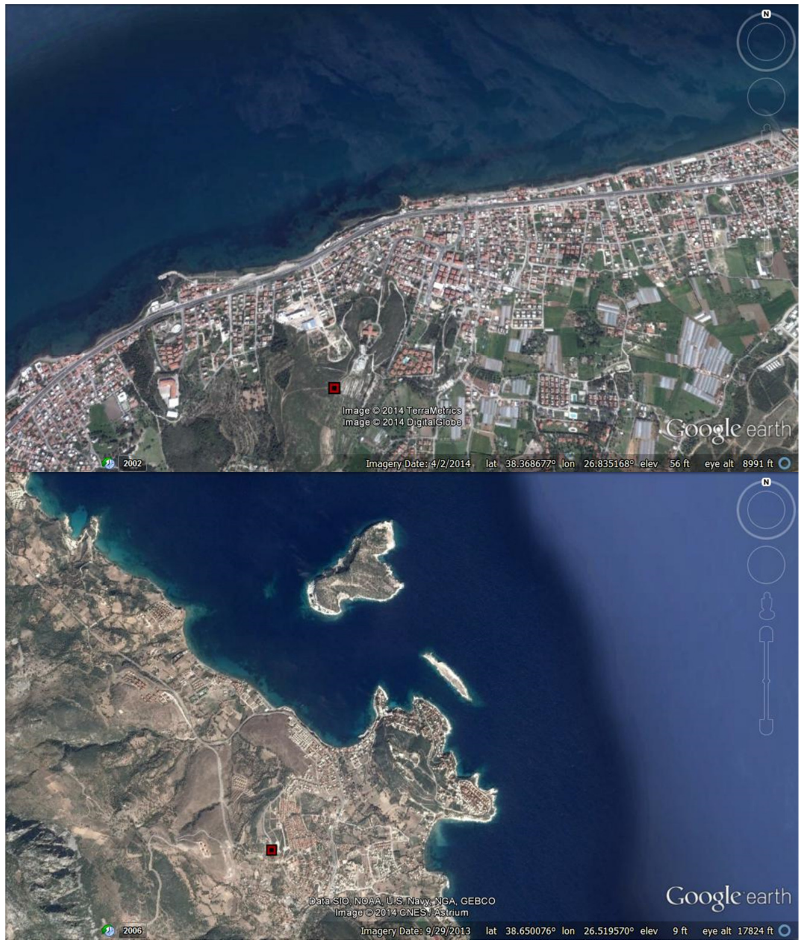

Figure 3.44: Urla (upper) and Karaburun (lower) CMSs (Google Earth, 2014)

Urla CMS is on top of a hill at the southern part of outer Izmir Bay. Not many obstructions exist apart from a few not very close buildings at the NE side. Karaburun CMS which is located on the southern edge of a hill face very few obstructions for easterly winds, whereas due to the hills, the same may not be generalized for northerly winds.

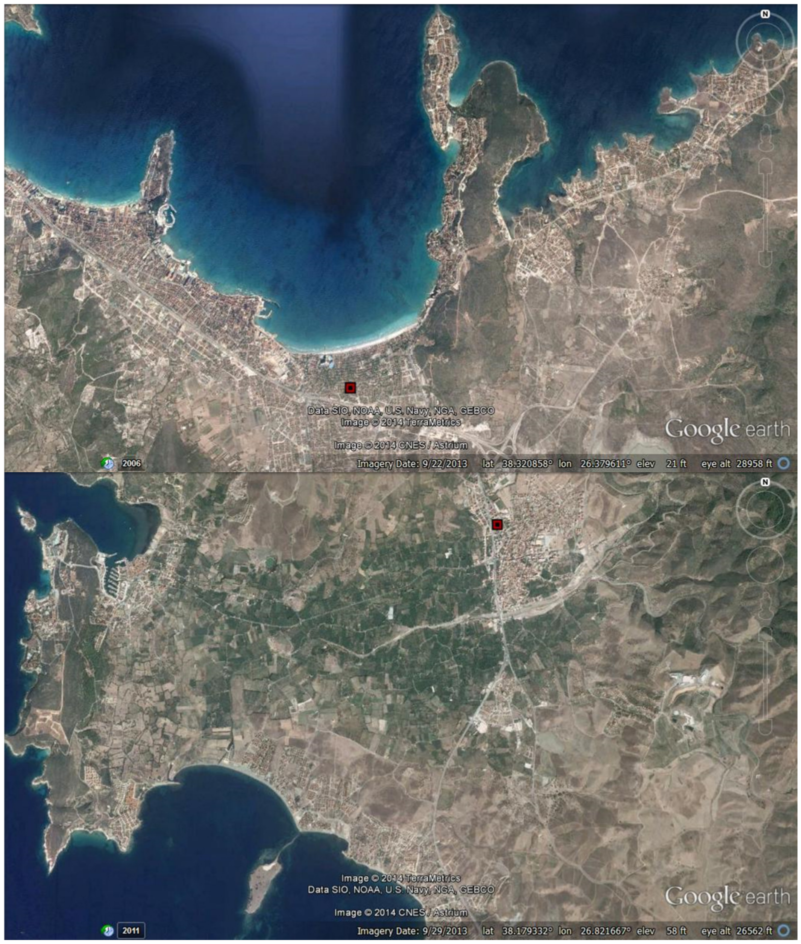

Figure 3.45: Çeşme (upper) and Seferihisar (lower) CMSs (Google Earth, 2014)

Çeşme CMS is facing Çeşme Bay and it is surrounded by many seaside resort and cottages. There is also strong possibility that the onshore winds from westerly directions may not be successfully measured. Seferihisar CMS is situated some distance from coastal zone at a low-lying area at the western part of Seferihisar district. Some amount of buildings as well as hilly formations nearby Sığacık may block the westerly winds blowing from sea directions.

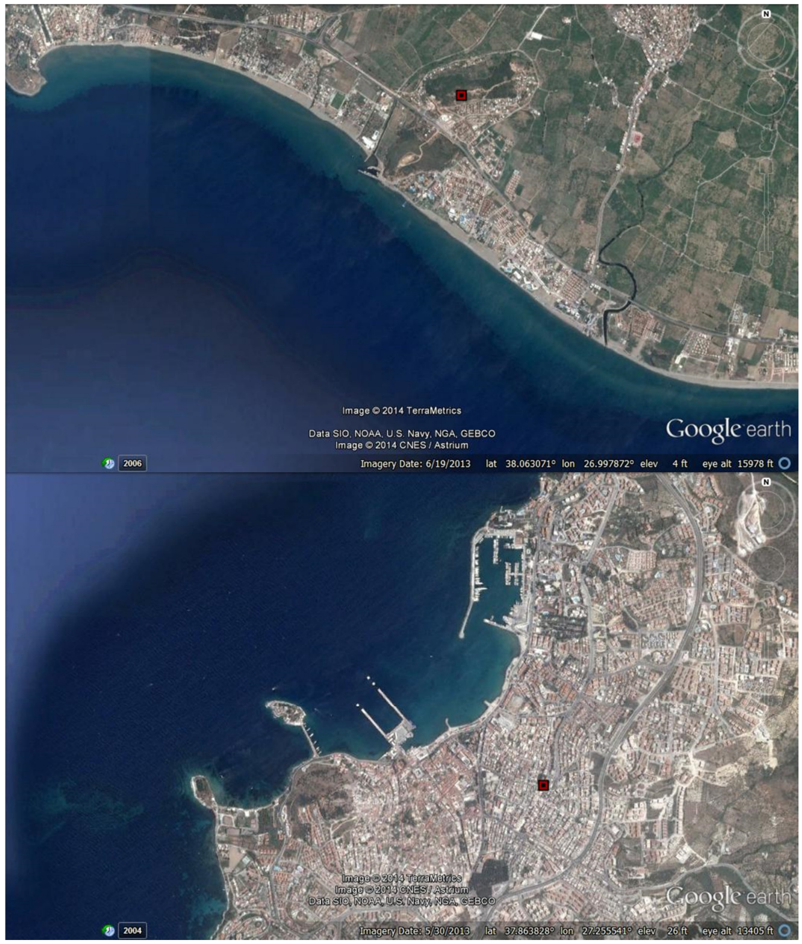

Figure 3.46: Gümüldere (upper) and Kuşadası (lower) CMSs (Google Earth, 2014)

Gümüldere CMS is at a location close to the shore area and except a few buildings not blocked by urbanization, vegetation or any geographical feature. Located in the middle of an urbanized area, wind measurements of Kuşadası CMS may suffer due to blocking effects of surrounding buildings and hilly formations on the west.

Figure 3.47: Didim (upper) and Turgutreis Marina (lower) CMSs (Google Earth, 2014)

Didim CMS, just like KuşadasıCMS, is in the middle of an urban area. Therefore it is naturally anticipated to have poor quality wind measurements for several directions. Turgutreis Marina CMS is at a very favorable location, nearby a yacht harbor and open to offshore winds.

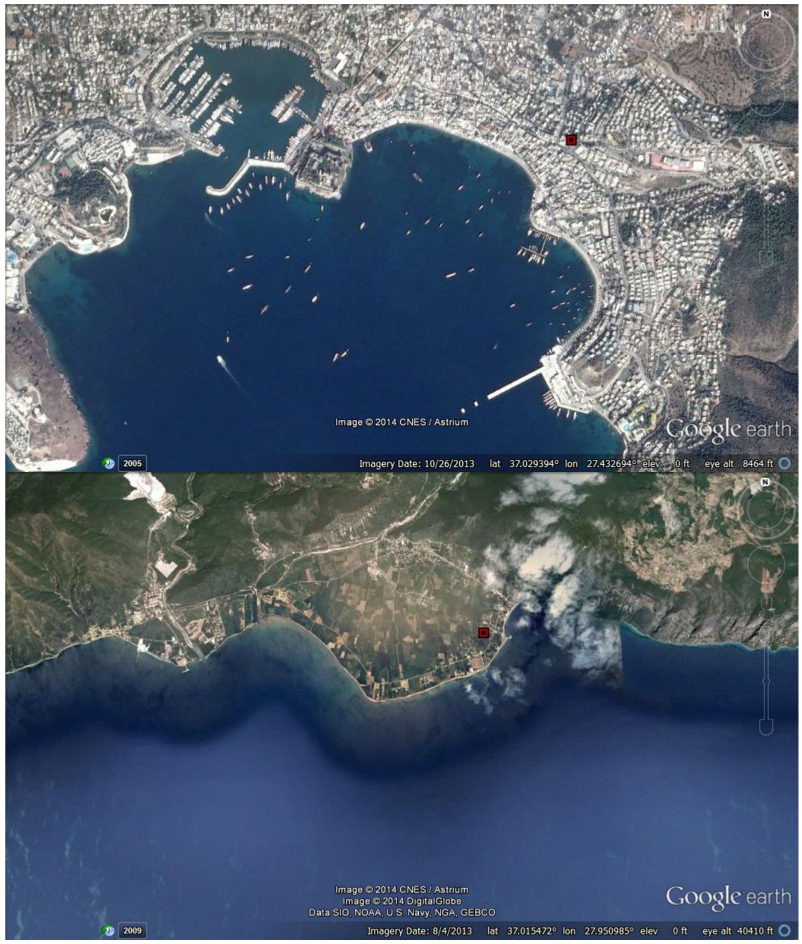

Figure 3.48: Bodrum (upper) and Ören (lower) CMSs (Google Earth, 2014)

Bodrum CMS is another CMS situated within city limits and surrounded by many buildings. Apart from that there are no geographical obstructions between itself and sea. Ören CMS that is closely linked to the shoreline has a very good location with the exception of several not very close seaside cottages.

Figure 3.49: Datça (upper) and Marmaris (lower) CMSs (Google Earth, 2014)

As observed in Figure 3.49, Datça CMS is not obstructed for the NE-S sector. On the other hand, due to the hill, wind blowing from S-SE sector may not be reflected successfully in the wind measurements. Marmaris CMS is located on the southern part of Marmaris facing Marmaris Bay, partly surrounded by buildings and also possibly blocked by the offshore island that may block some of the winds from SSE-ESE sector.

3.2.4. CMSs around the Mediterranean Sea Coast

The CMSs around Turkish Mediterranean Sea coasts are given in Figure 3.50 to 3.61. Following each figure, the conditions around TCMSs will be discussed regarding the issues mentioned above.

Figure 3.50: Dalaman (upper) and Dalaman Havl. (lower) CMSs (Google Earth, 2014)

Dalaman and Dalaman Havl. CMSs are very closely located and both are comparably far away from the coastal area. However, due to the low-lying zone they may be considered as CMS. Since Dalaman Havl. CMS is a CMS within airport boundaries and Dalaman CMS is partly located in an urbanized area, it is expected from Dalaman Havl. CMS to perform better quality wind measurements than Dalaman CMS.

Figure 3.51: Fethiye (upper) and Kaş (lower) CMSs CMSs (Google Earth, 2014)

Fethiye CMS has many disadvantages concerning wind measurements such as its location in highly urbanized area, facing Fethiye Bay which is a closed basin and the existence of hills and mountains in S-W. Kaş CMS is one of the highly elevated CMSs around Turkish coasts. Due to its elevation, almost no obstructions apart from the main building of Kaş CMS, which is at the southern side of measuring apparatus, exist.

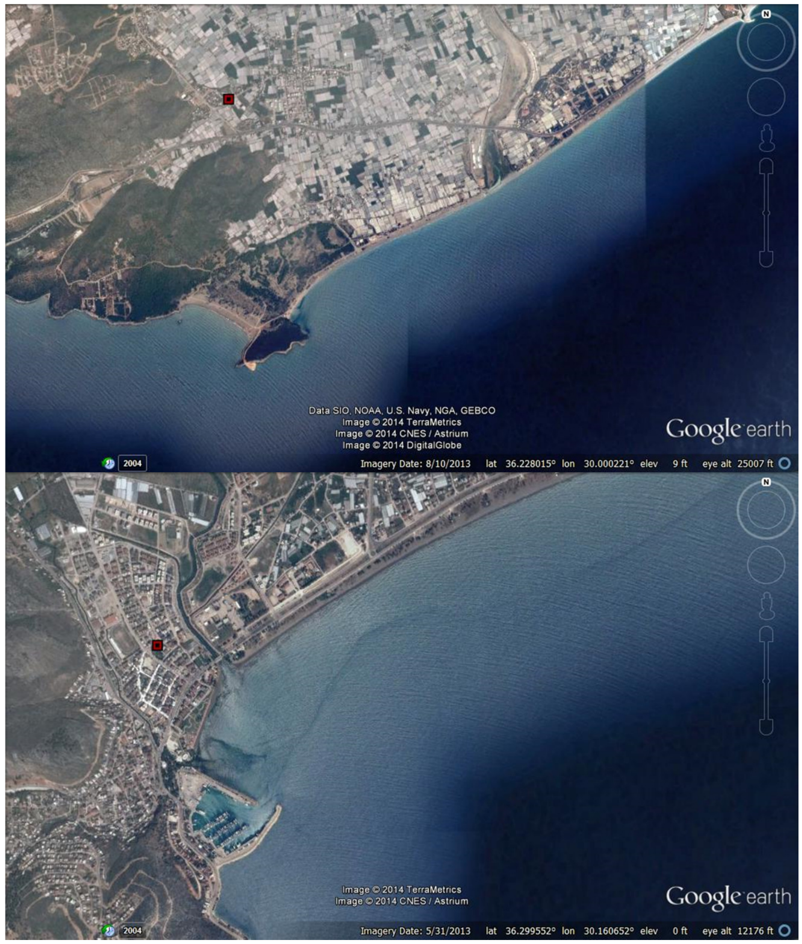

Figure 3.52: Kale (Demre) (upper) and Finike (lower) CMSs (Google Earth, 2014)

As seen in Figure 3.52, the hills most possibly block SW-S winds for both CMSs. Moreover, although their impacts cannot be estimated easily, high number of greenhouses may have some impact on wind measurements, as well. Considering Finike CMS, it is partly blocked by buildings on all sides facing the Mediterranean Sea.

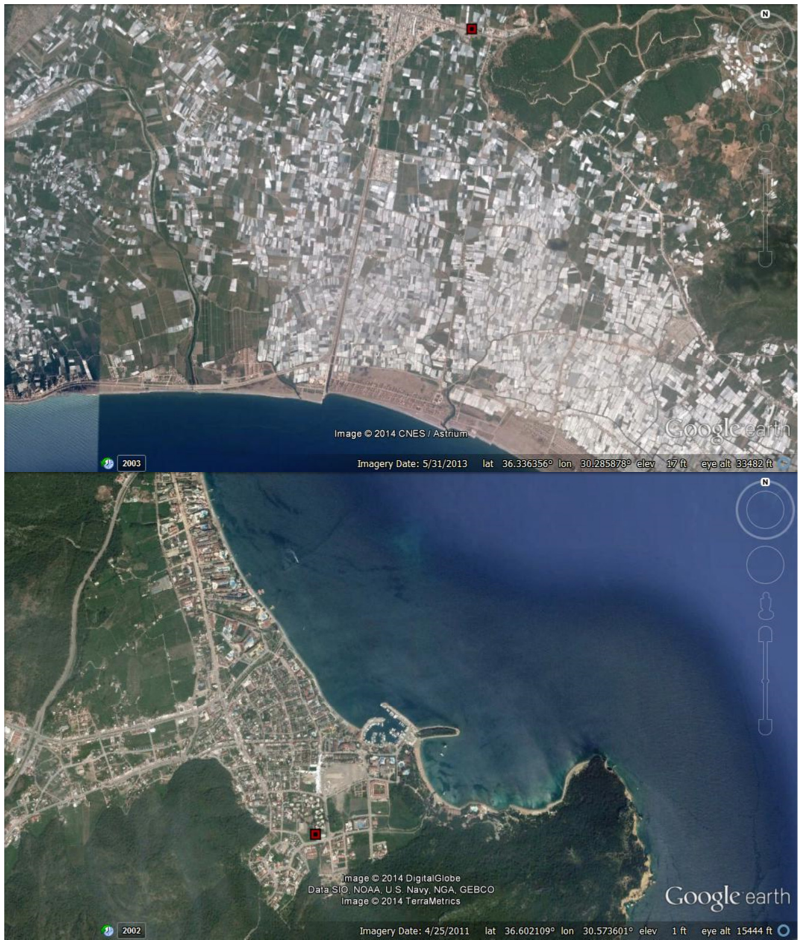

Figure 3.53: Kumluca (upper) and Kemer (lower) CMSs (Google Earth, 2014)

Kumluca CMS is relatively far inland and possibly overshadowed by the hilly formations at W-SW sector. Apart from the greenhouses, there is almost no obstacle between sea and Kumluca CMS. Kemer CMS has several disadvantages such as the hilly formations blocking the W-S sectors, surrounding buildings, thus making it highly expected to result in poor quality wind measurements.

Figure 3.54: Antalya Bölge (upper) and Antalya Havl. (lower) CMSs (Google Earth, 2014)

With the exception of buildings on the west, Antalya Bölge is situated at a favorable location for reflecting onshore winds. On the contrary, Antalya Havl CMS, which is relatively far inland and most probably due to urban areas in between its location and sea, it may have comparably poorer performance.

Figure 3.55: Belek (upper) and Manavgat (lower) CMSs (Google Earth, 2014)

Belek CMS is located relatively inland and blocked by hotels and vegetation concerning sea directions. Just like Belek CMS, Manavgat CMS is also relatively inland, but the only difference is the high rate of buildings surrounding Manavgat CMS.

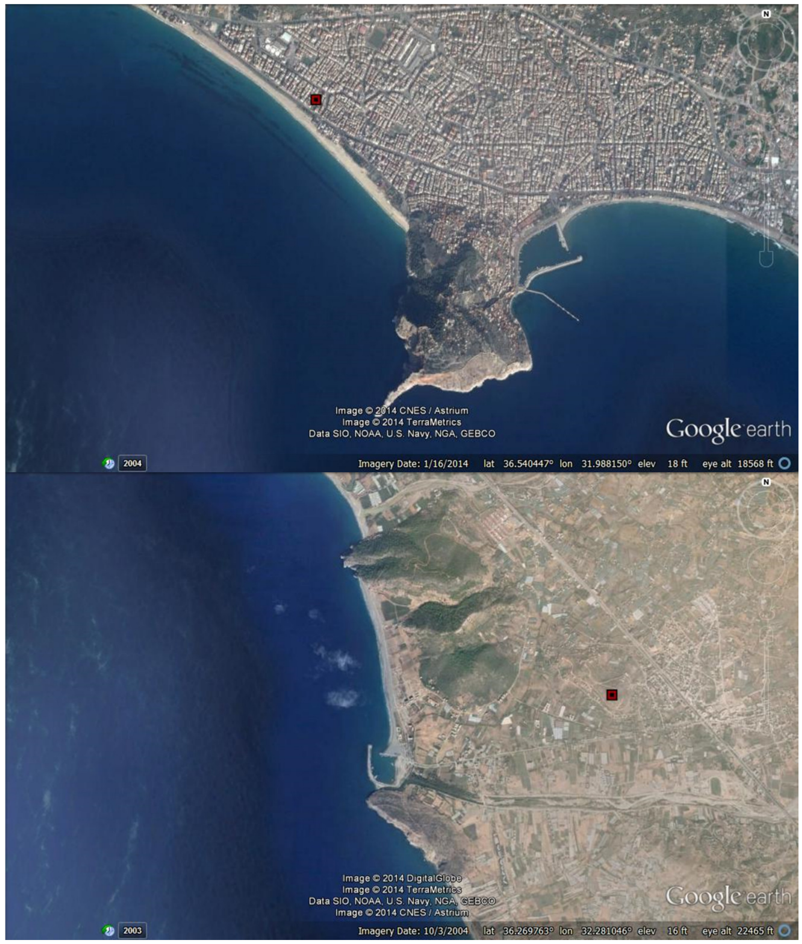

Figure 3.56: Alanya (upper) and Gazipaşa (lower) CMSs (Google Earth, 2014)

SE-W sector is unobstructed for Alanya CMS, whereas almost all other directions are blocked by buildings. There is also a small possibility that the hill, on which Alanya castle is, may be another obstacle although it is partly far away from Alanya CMS. Gazipaşa CMS is located on a small hill relatively inland, therefore it is not expected from buildings to effect wind measurements. On the other hand, the bigger hills in W-NW sector and another hill at SE-SSE sector may cause poor quality wind measurements.

Figure 3.57: Gazipaşa Havl. (upper) and Anamur (lower) CMSs (Google Earth, 2014)

Gazipaşa Havl. CMS is better located that Gazipaşa CMS considering that the aforementioned hills only block SSE-SE sector for Gazipaşa Havl. CMS. Moreover, as it is a CMS within airport boundaries, it is separated from urban areas. As for Anamur CMS, due to its proximity to shoreline and existence of no obstructions, it is expected that wind measurements of Anamur CMS would be of good quality.

Figure 3.58: Aydıncık (upper) and Silifke (lower) CMSs (Google Earth, 2014)

Aydıncık CMS resembles Bozkurt CMS in many aspects. Just like the Black Sea coast, most of the Mediterranean Sea coast of Turkey has hilly and mountainous features in parallel to the sea. Therefore, the proximity of the CMS to sea is very important as well as its possible unobstructed location. Aydıncık is situated in a very high elevation and almost at the top of a small valley. Moreover, the hills at W-S sector most possibly have shadowing effect on Aydıncık CMS. As a result, Aydıncık CMS is anticipated to have poor measuring quality. Considering Silifke CMS, as it is located in Silifke district, which is a densely urbanized area and comparably very far from coastal zone, there may be strong debate whether Silifke CMS should be regarded as CMS or not. As for its measuring quality, poor quality wind measurements are naturally expected.

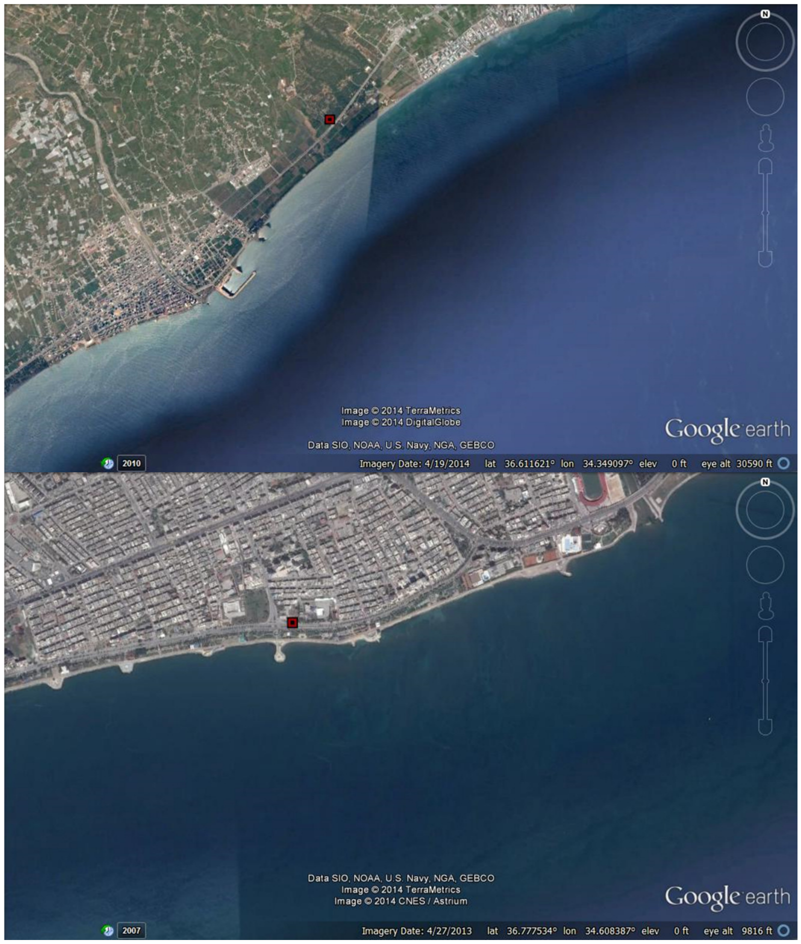

Figure 3.59: Erdemli (upper) and Mersin (lower) CMSs (Google Earth, 2014)

Erdemli CMS, which is only obstructed by vegetation, mainly trees, is expected to measure the onshore winds quite well. A similar conclusion may also be specified for Mersin CMS which is not obstructed by anything concerning sea directions.

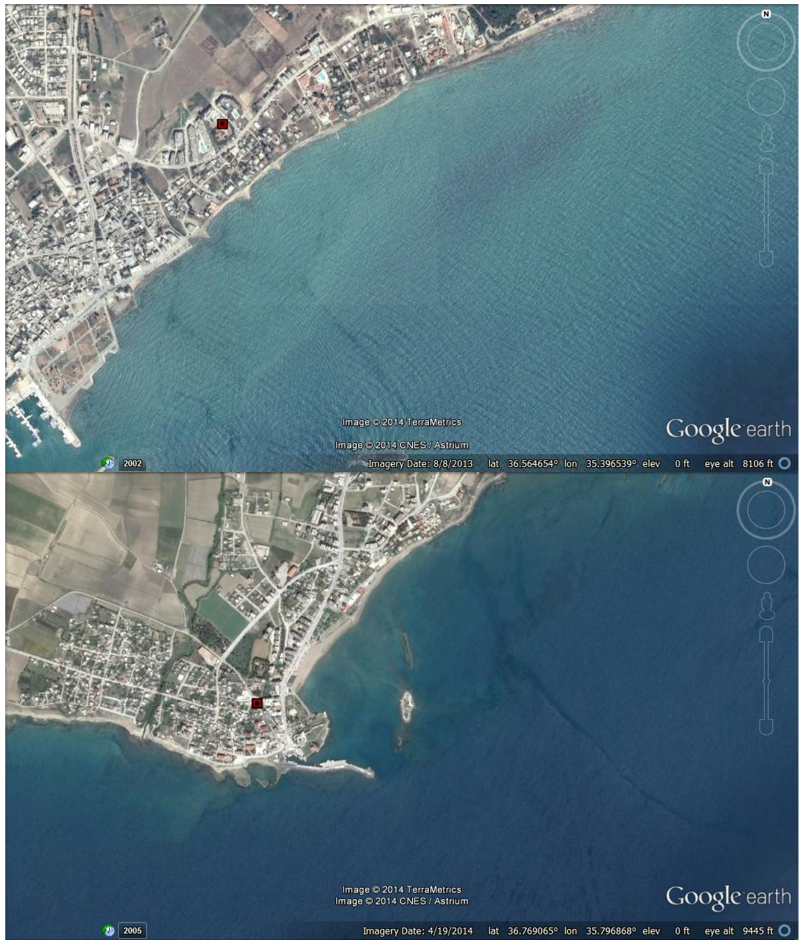

Figure 3.60: Karataş (upper) and Yumurtalık (lower) CMSs (Google Earth, 2014)

Karataş CMS and Yumurtalık CMS are located in similar areas except that Yumurtalık CMS is located on a small peninsula whereas Karataş CMS is on a hill side parallel to shoreline. They are both affected by surrounding buildings, but as observed in Figure 3.58, the intensity of influence is higher for Yumurtalık CMS which is surrounded by more buildings.

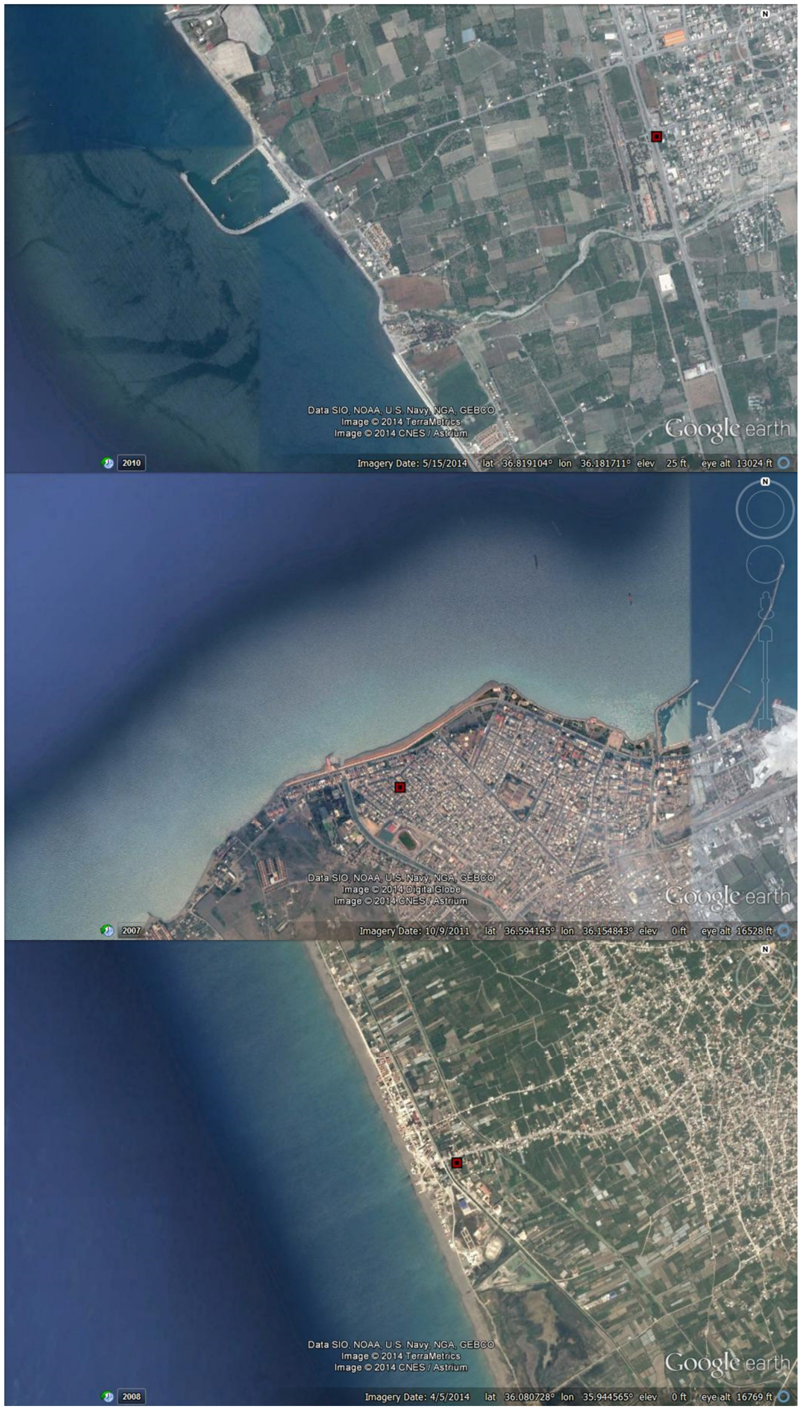

Figure 3.61: Dörtyol (upper), İskenderun (middle) and Samandağ (lower) CMSs (Google Earth, 2014)

Dörtyol CMS is located partly far away from coastal zone but at the western part of Dörtyol county. As it is located in a low-lying area and as seen in Figure 3.61, there is almost no visual obstacle for wind to face while blowing from sea directions. Iskenderun CMS is one of the many CMSs located within an urban area. The surrounding buildings have the main role in possible blocking of winds. As for Samandağ CMS being very close to the shoreline faces several buildings on all directions that may result in poor wind measurements for some wind directions.

3.3. Wind Roses of TCMSs

In this section, based on the general information related to the physical features and conditions around TCMSs given in the previous section, wind roses obtained from hourly and 3 hourly wind measurements of TCMSs. Since, the study area is the Black Sea coast of Turkey and the case study is Sinop region as briefly summarized in Chapter 1, the main focus will be given to the TCMSs around Turkish Black Sea coast. However, several additional wind roses obtained in other coastal regions of Turkey by using hourly wind measurements of TCMSs will also be given in this section to see how good the specified remarks are.

In the following parts, wind roses obtained from hourly wind measurements of TCMSs around Turkish coasts other than the Black Sea coast will be given and the findings will be discussed briefly. The discussion will be on the physical obstructions around TCMSs that may block the winds blowing from sea directions, thus limiting the station's ability to measure onshore winds. This focus on onshore winds is particularly due to the importance of CMS's representability of offshore winds. The aforementioned wind roses are shown in Figure 3.62 to Figure 3.67.It is important to remember that wind roses are prepared considering directions that winds are blowing from.

In addition to the wind roses, wind histograms are obtained to have an idea if the aforementioned obstacles and physical conditions have any impact on wind speeds. The wind histograms are given in Figure 3.68 to Figure 3.73.

The wind roses and wind histograms are prepared by using WRPLOT View Version 7.0.0 (Wind Rose Plot for Meteorological Data), which is a fully operational wind rose program for your meteorological data and provides visual wind rose plots, frequency analysis and plots for several meteorological data formats (www.weblakes.com).

<u>Wind Roses and Wind Histograms of Selected Coastal Meteorological Stations around the Marmara, Aegean and Mediterranean Seas:</u>

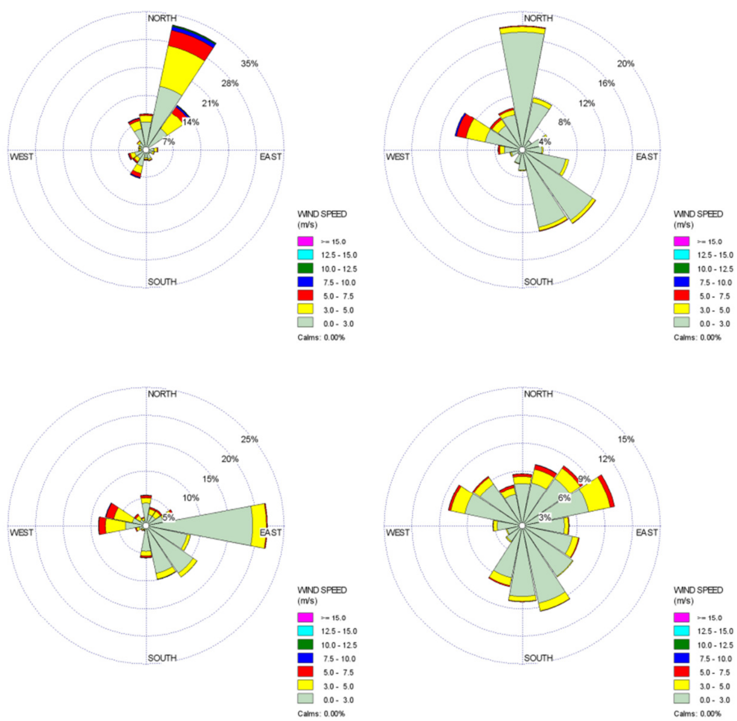

Figure 3.62: Wind Roses for Florya (upper left), Kocaeli (upper right), Gölcük (lower left) and Yalova (lower right) CMSs

As seen in Figure 3.62, the main measured wind directions with highest frequencies are NNW and NW for Florya CMS, N and SE for Kocaeli CMS, E and SE for Gölcük CMS, ENE and WNW for Yalova CMS. Concerning onshore wind directions, Florya and Kocaeli give very small frequency values and Gölcük partly gives bigger values for western directions. It may be concluded that even though the wind speeds are not high, Yalova CMS have the highest frequencies for onshore wind directions. Since there is no major reference to compare these results, a definite conclusion cannot be stated here. However, it is quite good to see that some of the things specified in section 3.2 for these CSMs can be observed here such as the ones specified for Gölcük and Yalova CMSs.

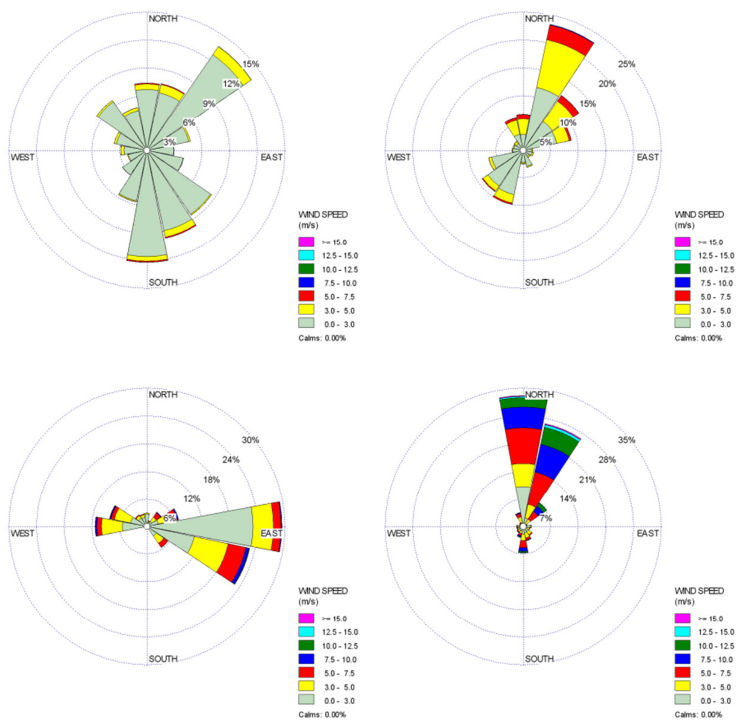

Figure 3.63: Wind Roses for Çınarcık (upper left), İstanbul Bölge (upper right), Gemlik (lower left) and Bandırma (lower right) CMSs

The main measured wind directions with highest frequencies are NW and S for ÇınarcıkCMS, NNE and NE for İstanbul Bölge CMS, W and WSW for Gemlik CMS, N and NNE for Bandirma CMS. Concerning onshore wind directions, Bandırma CMS give the highest wind speeds and frequencies. This is followed by Çınarcık, Gemlik and İstanbul Bölge CMSs. As these results cannot be compared to a reference as stated above, only the accuracy of visual findings stated in Section 3.2 can be discussed here. It is good to see that some of the statements for Bandırma and Gemlik CMSs can be observed in Figure 3.63.

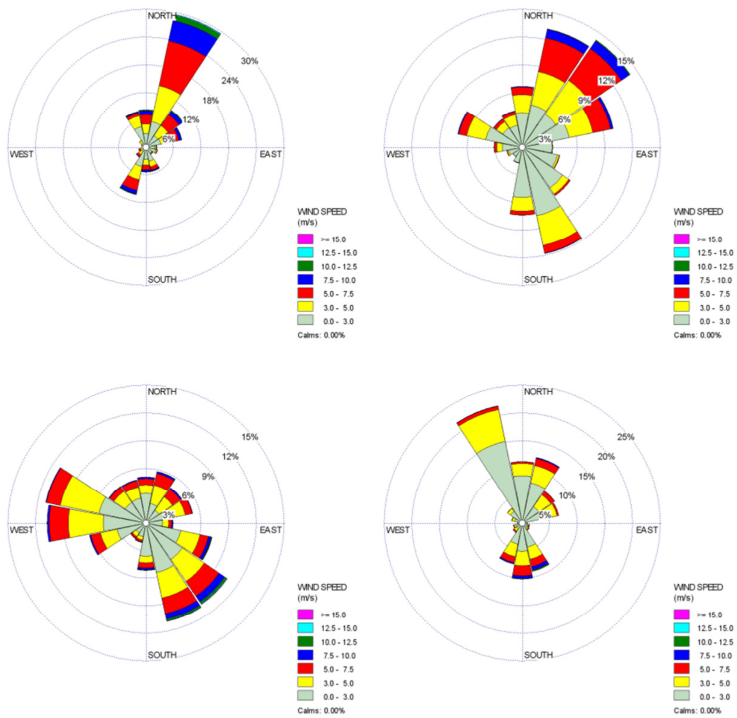

Figure 3.64: Wind Roses for Gökçeada (upper left), Ayvalık (upper right), İzmir Bölge (lower left) and Çeşme (lower right) CMSs

In Figure 3.64, the main measured wind directions with highest frequencies are observed as NNW and SSE for Gökçeada CMS, NE and NNE for Ayvalık CMS, SSW and SW for İzmir Bölge CMS, NNE and NNW for Çeşme CMS. As for onshore wind directions, Gökçeada and Ayvalık CMSs have the highest similar frequencies and directions. Ayvalık lacks good representativeness for directions coinciding with offshore islands as stated in Section 3.2. İzmir Bölge CMS has been able to measure some westerly winds with success, but the poor location of Çeşme CMS results in almost no winds from western sectors as specified in Section 3.2.

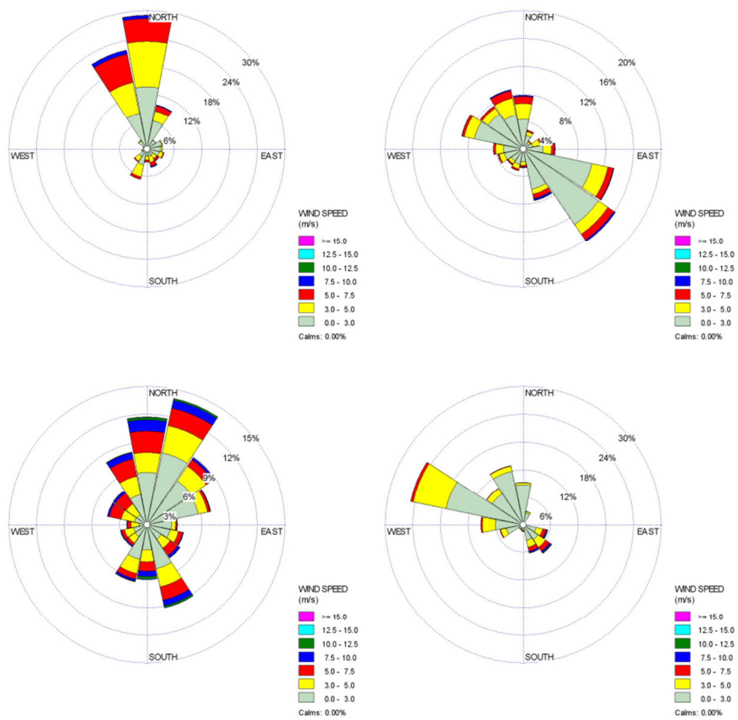

Figure 3.65: Wind Roses for Seferihisar (upper left), Kuşadası (upper right), Bodrum (lower left) and Marmaris (lower right) CMSs

The main measured wind directions with highest frequencies are as follows: N and NNW for Seferihisar CMS, SE and ESE for Kuşadası CMS, NNE and N for Bodrum CMS, ENE and NNE for Marmaris CMS. Bodrum CMS have the highest wind speeds and frequencies for sea directions, followed by Kuşadası CMS. Seferihisar and Marmaris CMSs have poor ability to reflect onshore wind directions due to reasons given in Section 3.2.

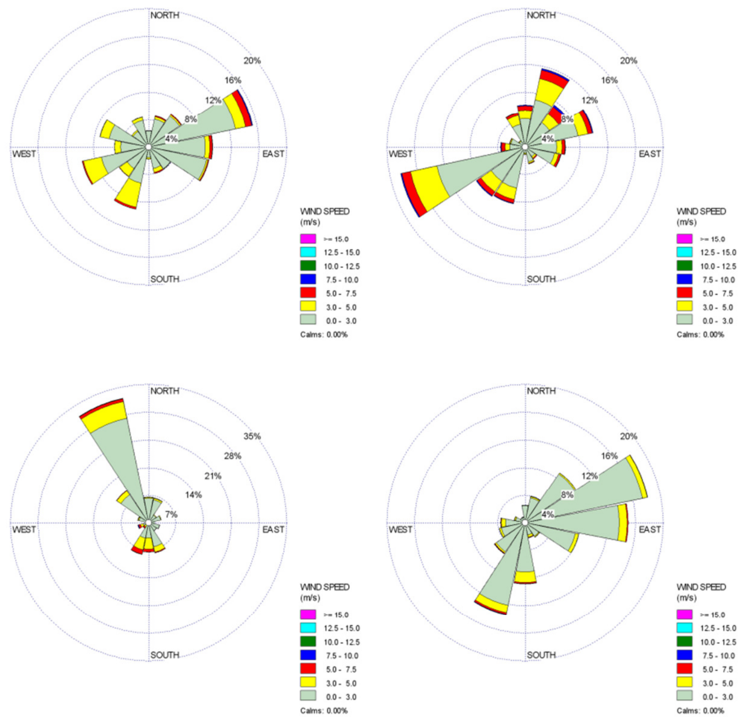

Figure 3.66: Wind Roses for Fethiye (upper left), Kaş (upper right), Finike (lower left) and Alanya (lower right) CMSs

As seen in Figure 3.66, the main measured wind directions with highest frequencies are ENE and WSW for Fethiye CMS, WSW and NNE for Kaş CMS, NNE and NE for Finike CMS, ENE and NNE for Alanya CMS. Among these four coastal stations, wind roses of Kaş CMS have the highest wind speeds and frequencies from sea directions, followed by Alanya, Fethiye and Finike CMSs, respectively. It is good to observe that some of the remarks in Section 3.2, such as blocking effect of hills and buildings for SW-S sector concerning Finike CMS, negative impact of hills and mountains for S-W sector concerning Fethiye CMS are partly accurate.

Figure 3.67: Wind Roses for Gazipaşa (upper left), Erdemli (upper right), Yumurtalık (lower left) and İskenderun (lower right) CMSs

According to Figure 3.67, the main measured wind directions with highest frequencies are WSW and ESE for Gazipaşa CMS, NNW and NNE for Erdemli CMS, SSW and NNE for Yumurtalık CMS and SSE and WSW for İskenderun CMS. Yumurtalık and partly both Gazipaşa and İskenderun CMSs can reflect some of the onshore wind directions. Erdemli can also measure onshore winds for several directions.

To sum up almost all of the CMSs, whose wind roses are prepared have major problems representing onshore wind directions and speeds. The wind speed representativeness can be better understood in below given Figures 3.66-3.71.

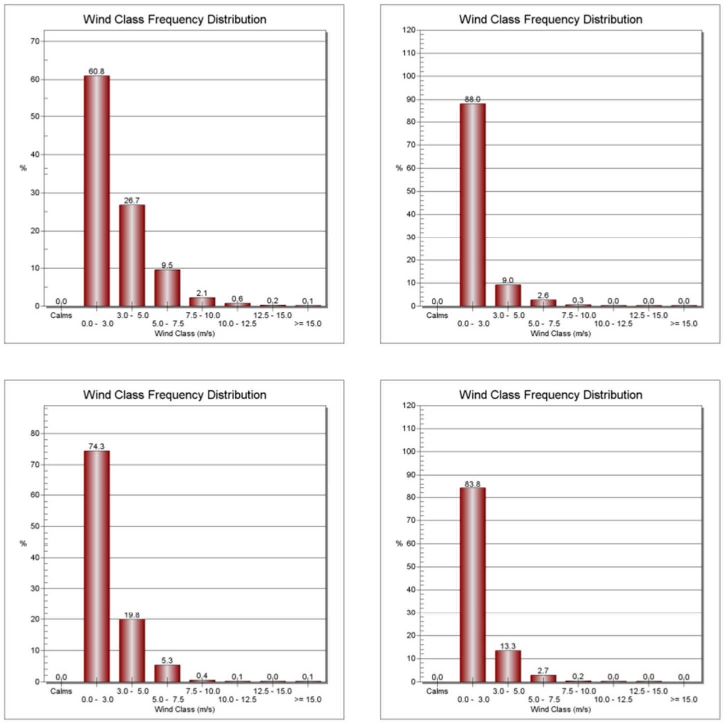

Figure 3.68: Wind Histograms for Florya (upper left), Kocaeli (upper right), Gölcük (lower left) and Yalova (lower right) CMSs

Apart from Florya CMS, other CMSs have similar histograms meaning that the measured wind speeds are mostly within the range of 0-3 m/s as observed in Figure 3.68. In relation with Figure 3.62, more percentages for higher wind speeds than 3m/s for Florya CMS may be addressed to the NNW winds, not onshore winds.

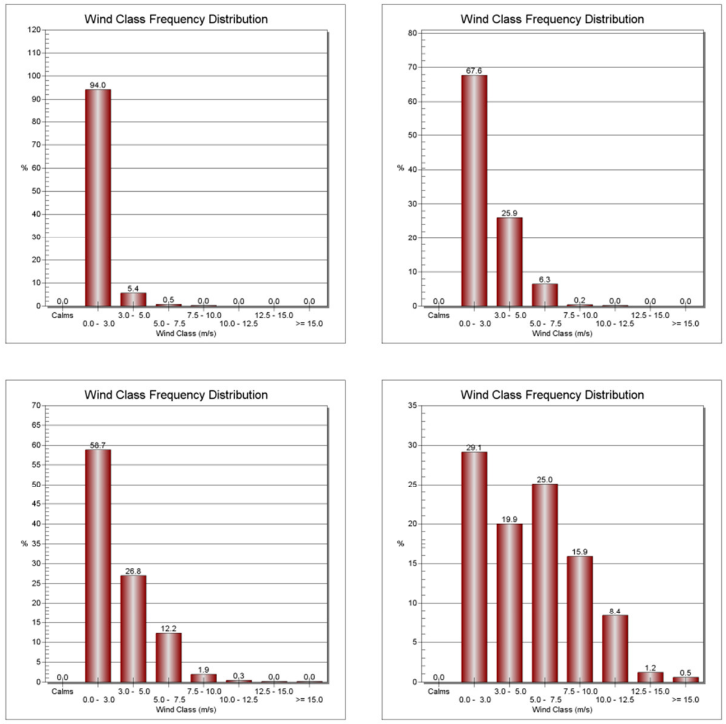

Figure 3.69: Wind Histograms for Çınarcık (upper left), İstanbul Bölge (upper right), Gemlik (lower left) and Bandırma (lower right) CMSs

Çınarcık CMS gives the highest 0-3 m/s wind speed range which may sometimes be regarded as calm condition. İstanbul Bölge and Gemlik CMSs have similar wind histograms with higher percentages for wind speeds of 3-5 m/s and 5-7.5 m/s. Bandırma CMS gives the highest percentages for winds higher than 3m/s for all wind classes which is in parallel with wind rose of Bandırma CMS.

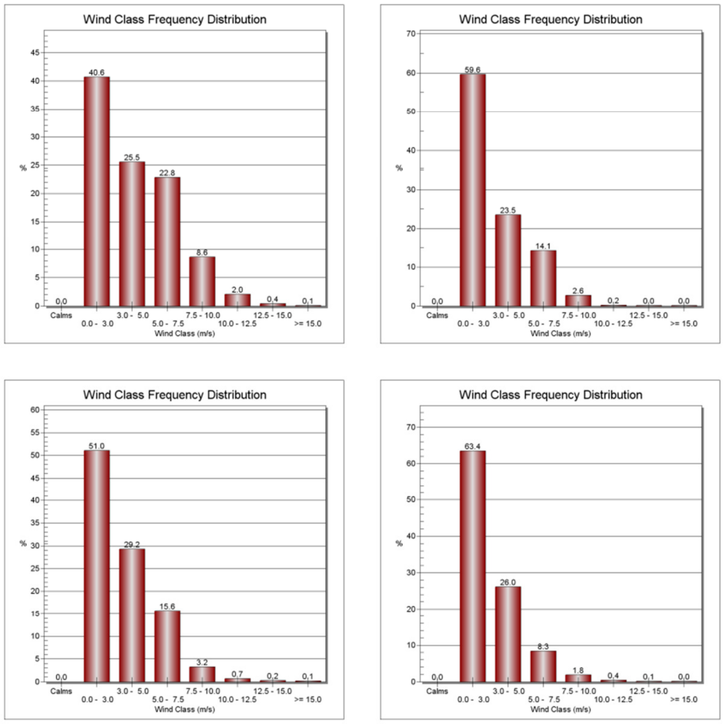

Figure 3.70: Wind Histograms for Gökçeada (upper left), Ayvalık (upper right), İzmir Bölge (lower left) and Çeşme (lower right) CMSs

The wind histograms are in parallel with the findings of Figure 3.62. Gökçeada CMS measures higher wind speeds followed by İzmir Bölge and Ayvalık CMSs with the smallest wind speed measurements obtained by Çeşme CMS.

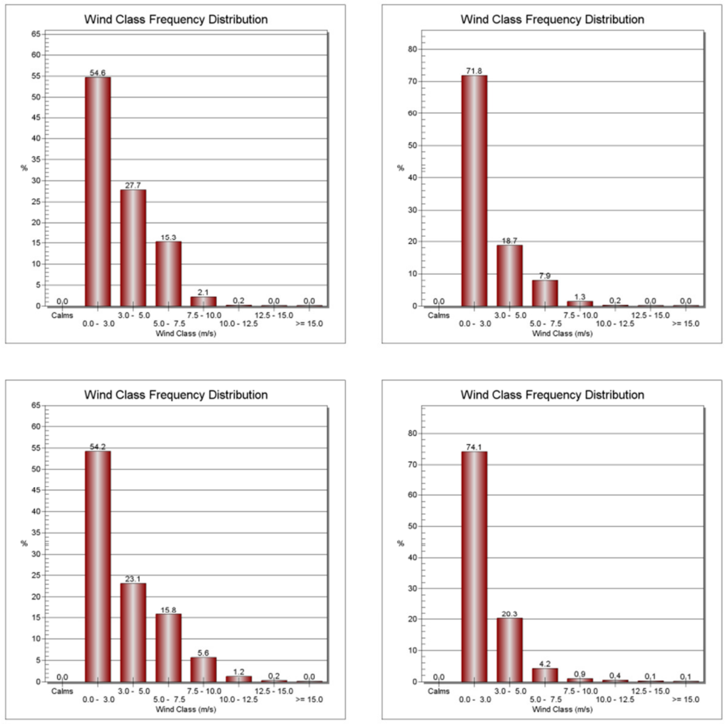

Figure 3.71: Wind Histograms for Seferihisar (upper left), Kuşadası (upper right), Bodrum (lower left) and Marmaris (lower right) CMSs

Seferihisar and Bodrum CMSs have similar wind histograms, but as Bodrum CMS may reflect onshore winds better than Seferihisar this difference may be attributed to the fact that Seferihisar CMS measure higher wind speeds for winds blowing on land while Bodrum CMS is able to measure high onshore winds, as well. Kuşadası and Marmaris CMSs also have similar CMSs and as specified above, both lack good quality onshore wind representation.

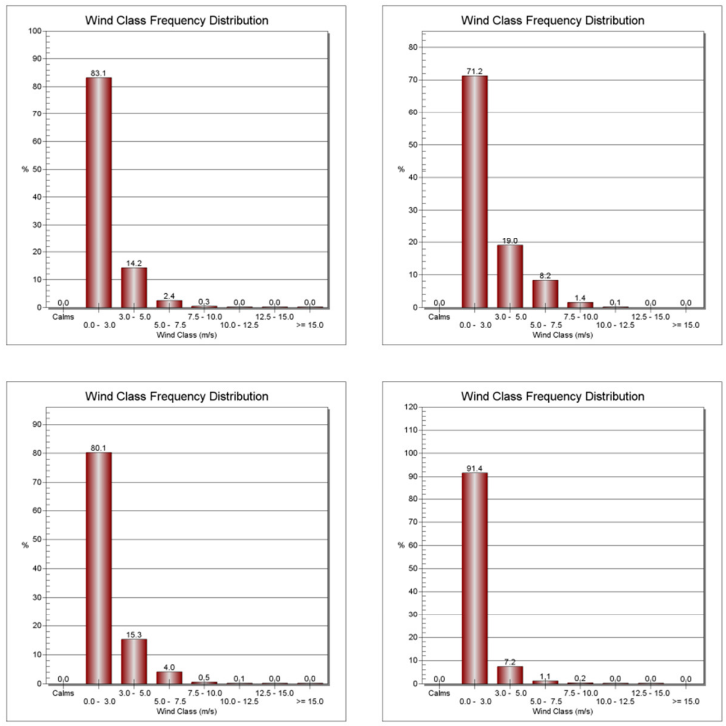

Figure 3.72: Wind Histograms for Fethiye (upper left), Kaş (upper right), Finike (lower left) and Alanya (lower right) CMSs

As seen in Figure 3.72, while Fethiye, Finike and Alanya CMSs have very high percentages for small wind speeds, Kaş CMS is able to measure higher wind speeds resulting in higher percentages for winds bigger than 3m/s.

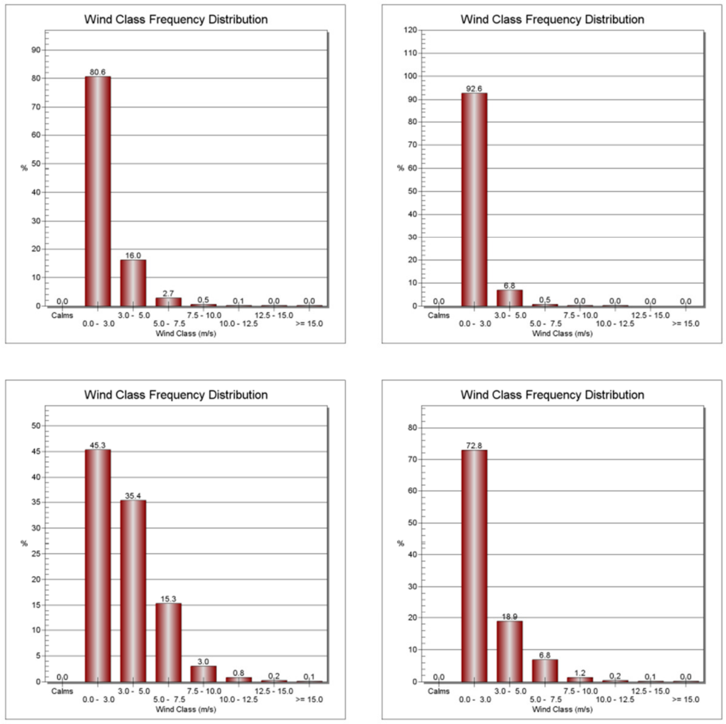

Figure 3.73: Wind Histograms for Gazipaşa (upper left), Erdemli (upper right), Yumurtalık (lower left) and İskenderun (lower right) CMSs

Among these four CMSs, Erdemli, Gazipaşa and İskenderun CMSs have bigger percentages of winds smaller than 3 m/s and Yumurtalık have bigger percentages for winds bigger than 3 m/s.

<u>Wind Roses and Wind Histograms of Selected Coastal Meteorological Stations around the Black Sea:</u>

In addition to the wind roses and wind histograms of chosen CMSs around Marmara, Aegean and Mediterranean Seas, as specifically in this thesis the main focus is given to Black Sea coast of Turkey and therefore CMSs around Black Sea, wind roses and wind histograms of almost all of the coastal meteorological stations are obtained with the exception of a few CMSs whose data could not be obtained from Turkish State Meteorological Service. Wind roses and wind histograms for these stations are given in Figure 3.74 to Figure 3.79 and Figure 3.80 to Figure 3.85, respectively.

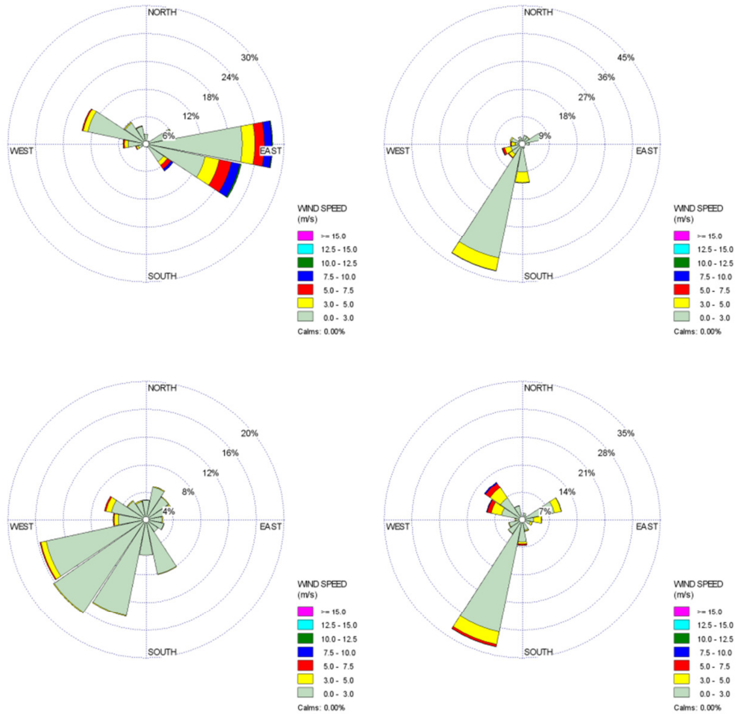

Figure 3.74: Wind Roses for Hopa (upper left), Pazar (upper right), Rize (lower left) and Trabzon Havl. (lower right) CMSs

It is easy to conclude by looking at Figure 3.74 that all of the CMSs (Hopa, Pazar, Rize and Trabzon Havl.) badly represent onshore winds. However, several onshore wind directions for Hopa and Trabzon Havl. CMSs are slightly better measured and thus represented, especially for SSW–SW sector.

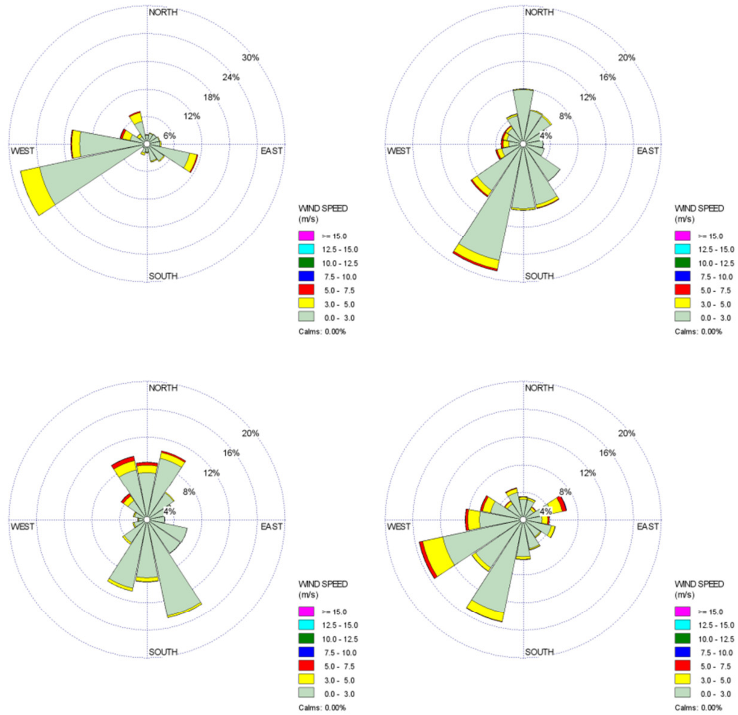

Figure 3.75: Wind Roses for Akçaabat (upper left), Giresun (upper right), Ordu (lower left) and Ünye (lower right) CMSs

The same above given remarks regarding Figure 3.74 may also be applicable for Akçaabat, Giresun, Ordu and Ünye CMSs. Except Ordu CMS, the other three have very bad representative ability for onshore winds for their regions by just visual observation of Figure 3.75. As for Ordu CMS, it seems like it reflects the onshore winds better but whether it is a good enough representation or not is still a question that needs to be answered.

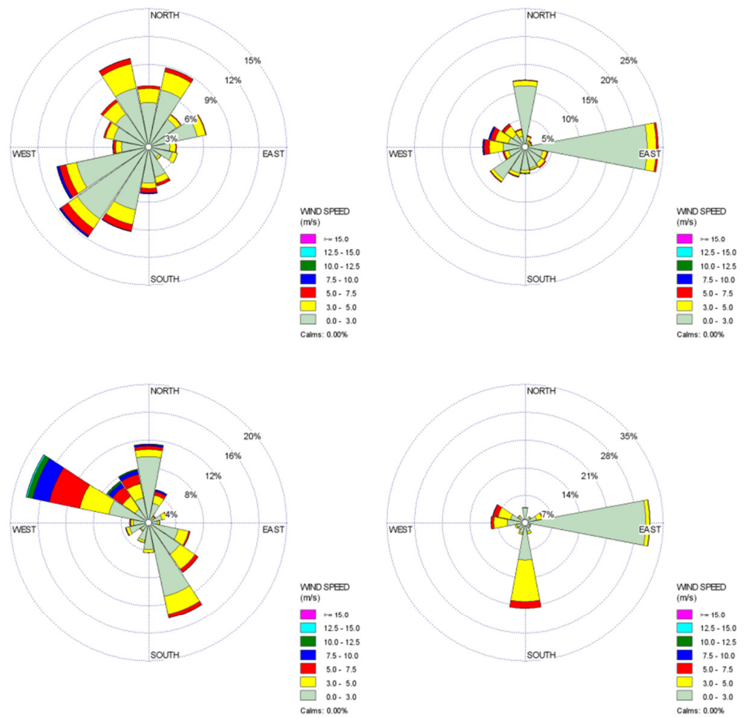

Figure 3.76: Wind Roses for Samsun Bölge (upper left), Alaçam (upper right), Sinop (lower left) and Çatalzeytin (lower right) CMSs

Among the four CMSs whose wind roses are given in Figure 3.74, Çatalzeytin has the worst onshore wind results followed by Alaçam, Samsun Bölge and Sinop. Particularly in terms of wind speeds, Sinop CMS give quite high wind speeds for WNW-N sector. As for Samsun Bölge CMS, overall onshore winds are caught but whether they can be measured well enough is something to be discussed and searched for.

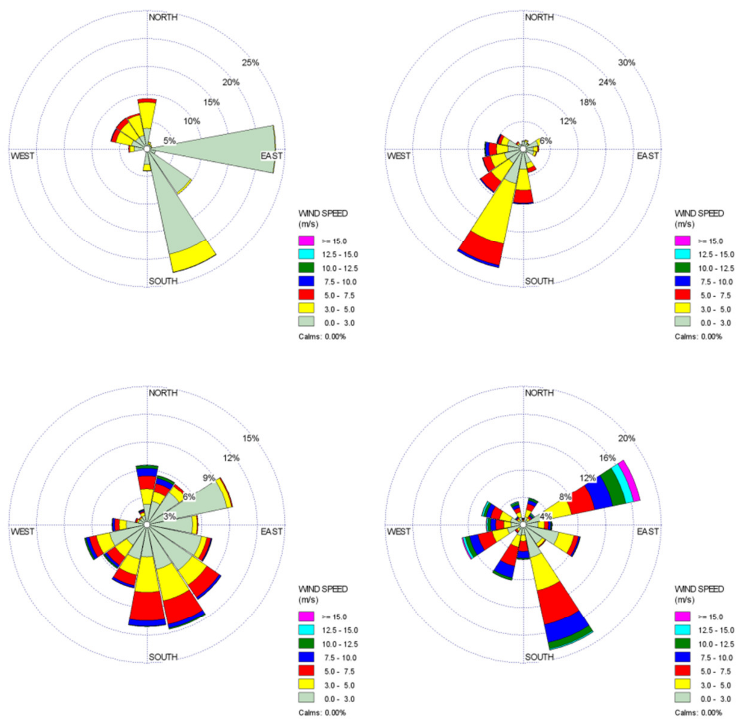

Figure 3.77: Wind Roses for Bozkurt (upper left), İnebolu (upper right), Cide (lower left) and Amasra (lower right) CMSs

As discussed before in Section 3.2, due to its poor location, as seen in Figure 3.77, Bozkurt CMS give small percentages but strangely high wind speeds for onshore winds. If wind rose for Bozkurt CMS may be observed in detail and the location of Bozkurt CMS, a direct relation between onshore wind directions (WNW-N sector) and alignment of the valley (SE-NW) in which Bozkurt CMS is located may be observed. This may be regarded as the main reason of onshore winds in wind rose of Bozkurt CMS. Surprisingly, İnebolu CMS is the poorest of all in terms of reflecting onshore winds which cannot be attributed to any physical feature. However, the lack of easterly winds is in parallel with the remarks in Section 3.2. Wind rose of Cide CMS show some strong onshore winds for N-NW sector and wind rose of Amasra CMS indicate very strong onshore winds from ENE and some moderate wind speeds for E-ENE sector. For all of the CMSs in Figure 3.77, the wind speed percentages are still something to be discussed in detail in the future.

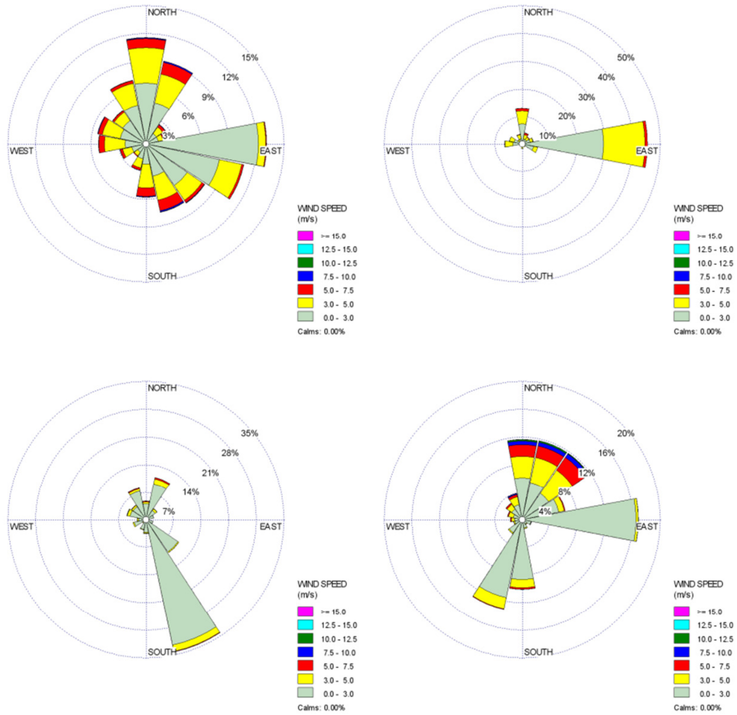

Figure 3.78: Wind Roses for Zonguldak (upper left), Karadeniz Ereğli (upper right), Akçakoca (lower left) and Karasu (lower right) CMSs

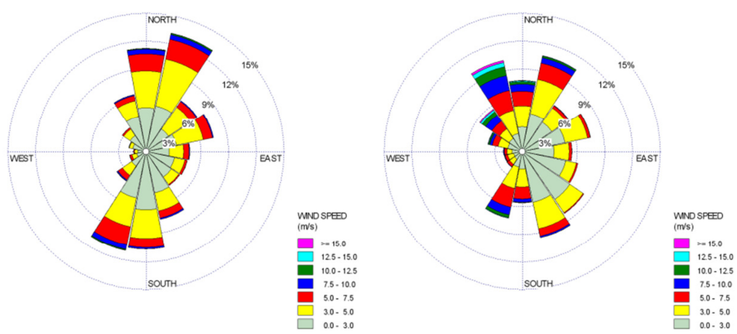

Figure 3.79: Wind Roses for Şile (left), Kumköy-Kilyos (right) CMSs

Observing Figure 3.78 and 3.79, with the exception ofKaradeniz Ereğli and Akçakoca whose wind roses show very few onshore winds, the remaining four CMSs show quite high percentages of onshore winds as well as high onshore wind speeds.

3.4. Discussion on Overall Performance of TCMSs

It should be noted that the remarks stated in Section 3.2 are only based on satellite images of the Earth surface whereas the main focus is given on onshore wind directions. Among many CMSs around Turkey, very few CMSs are visited during a site survey. Therefore, the above stated remarks do not cover the current status of measuring equipment regarding calibration and maintenance that are also expected to play very important role in measuring quality of CMSs. Thus, while discussing above given wind roses, possibility of poor quality measuring equipment should also be considered in the discussions concerning the CMSs.

It is important to mention that various factors affect the accuracy of wind measurements and thus wind roses. For instance, as specified in Chapter 2, Hsu (1986) states that adding up instrumental errors, frictional effects, recorder inaccuracies together with onshore-offshore airflow differences, a directional difference of 45° is expected. If these inaccuracies and errors are higher which may be the case for some CMSs and due to various conditions (i.e. turbulence, forcing the wind through smaller gaps, etc.) created by surrounding geographical features and buildings, as well as the complex topography of Turkish coasts, it is natural to expect non-representative wind roses for most of the cases. Local winds such as sea and land breezes may also play some role in these results.

Based on the conclusions on Turkish Coastal Meteorological Stations (TCMSs), where the accuracy of the data is questionable, in-situ wind measurements become very important, yet there exist few in-situ wind measurements which could be used as reliable sources.

CHAPTER 4

LAND-BASED COASTAL IN-SITU WIND MEASUREMENTS

In Chapter 4, the main focus will be given to the land-based in-situ wind measurements belong to 42.09°N – 34.96°E coordinates near Sinop and were gaged at a land tower installed approximately at 60 m elevation above MSL. Wind measurements are recorded at three different elevations which are 16m, 25m and 60 m with respect to the bottom elevation of the tower specified as 60 m. The local vegetation consists of a small forest which may have some effect on wind measurements at lower elevations, but apart from this, there are no obstacles in between land tower and sea directions. The land tower is placed at a location that may easily measure onshore winds in the sector of WSW-ESE (in clockwise direction). Wind measurements cover a period between February, 2009 and December, 2009 with considerable gaps especially in between July and October while smaller gaps are commonly observed for other periods. Although time interval of most of the wind measurements is 1 hour, due to several reasons gaps exist within the data set.

The wind measurement procedure is guided and controlled by governmental authorities. The type of apparatus and equipment that are used for measurements and the calibration and verification procedures of the wind data are not known, therefore it is necessary to perform comparisons between wind measurements to observe if there is any inconsistency that may arise questions regarding reliability of the wind measurements at these three elevations. From now on, the land-based wind data at 60 m, 25 m and 16 m will be denoted as L60, L25 and L16.

This chapter of the thesis study is divided into two sections. In the first part, the discussions are performed on differences and common points of L60, L25 and L16 wind speed and directions. The second part will be related to the relationship between L60, L25 and L16 wind speeds in vertical plane to obtain a coefficient called Hellman exponent, denoted both as P or α as specified in Chapter 2, to understand if local conditions can be reflected on this exponent, thus whether a common relationship may be applied in vertical plane considering wind speeds.

4.1. Comparison of L60, L25 and L16 Wind Speeds and Wind Directions

As first step, only wind measurements coinciding within the sector of WSW-ESE are considered since the direction within this sector are sea directions that onshore winds are blowing. During this data elimination process only to consider winds blowing from sea directions, an assumption "if one, two or all of L60, L25 and L16 wind directions are within this sector, all of the corresponding L60, L25 and L16 winds are taken into account" is designated. Thus, in this elimination process, it is not important whether only one or two of L60, L25 and L16 wind directions fulfill this condition, even if one of them is in this sector the whole data at that time is incorporated into comparison procedure. After the elimination process, L60, L25 and L16wind measurements are compared in terms of wind speeds and directions to see if there are any unexpected correlations in between and any discrepancies among the data set.

Considering comparison of wind direction differences, they are expressed in sectors rather than in degrees at relevant figures. This choice is to avoid observing high values in y-axis of the graphs which would make it hard to visualize other comparison results with smaller values. Therefore, dividing 360° into 16 sections with 22.5° directional steps as seen in Figure 4.1, directional numbers are denoted to each 16 direction starting with N sector as 1, continuing clockwise and ending up at 16 for NNW sector. In order not to see any problems at direction differences when calculating directions from 1-5and 13-16 sectors, the formulations are arranged accordingly. Moreover, the formulations are also arranged in order not to calculate directional difference more than 180° which corresponds to 8. It is important to remember that wind directions denote that winds directions as `blowing from`.

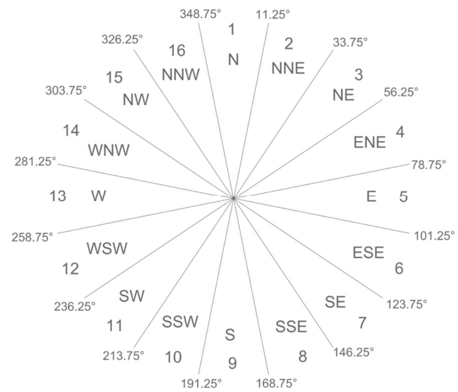

Figure 4.1: Wind Directions and Corresponding Wind Sectors

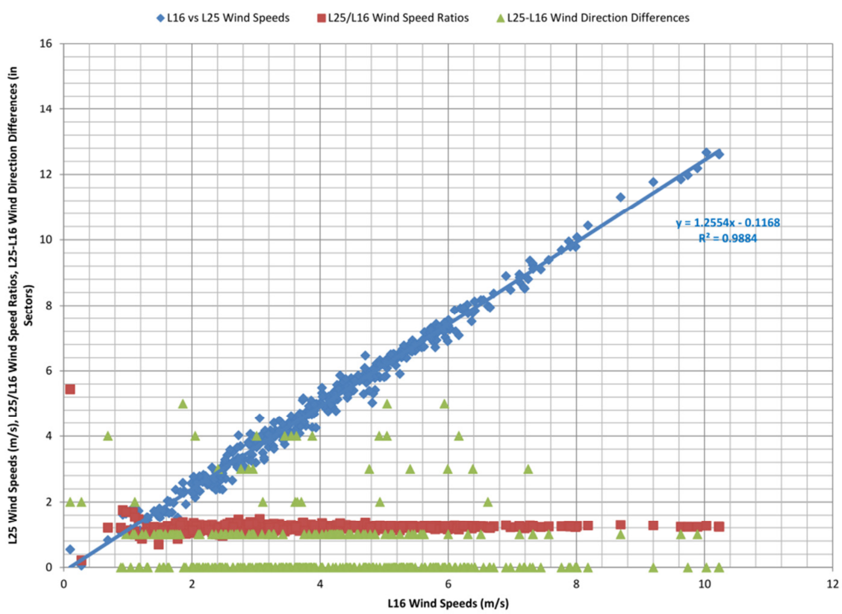

Figure 4.2: Comparison of L25 Wind Speeds, L25/L16 Wind Speed Ratios and L25-L16 Wind Direction Differences with respect to L16 Wind Speeds

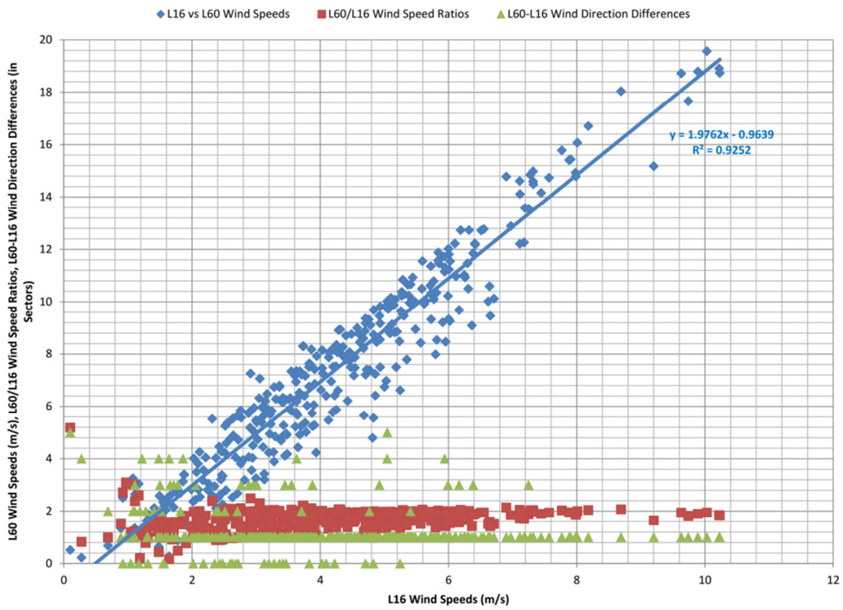

Figure 4.3: Comparison of L60 Wind Speeds, L60/L16 Wind Speed Ratios and L60-L16 Wind Direction Differences with respect to L16 Wind Speeds

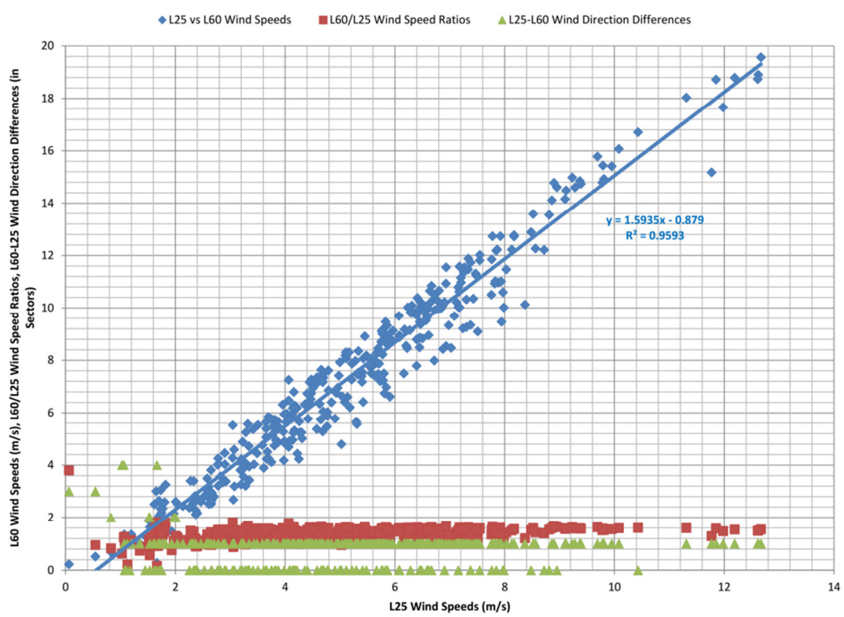

Figure 4.4: Comparison of L60 Wind Speeds, L60/L25 Wind Speed Ratios and L60-L25 Wind Direction Differences with respect to L25 Wind Speeds

Taking into account Figures 4.2-4.4, it is observed that as expected, L60 wind speeds are higher than both and L25 wind speeds are higher than L16 wind speeds in general with few cases which are most probably observed due to several reasons such as different conditions at different heights, different atmospheric conditions changes in vertical plane, etc. L60, L25 and L16 wind speeds have the following correlations between each other:

$$L25 = 1.2554\,L16 - 0.1168 \qquad [4.1]$$

$$L60 = 1.9762\,L16 - 0.9639 \qquad [4.2]$$

$$L60 = 1.5935\,L25 - 0.8790 \qquad [4.3]$$

Considering L25/L16, L60/L16 and L60/L25 wind speed ratios, as wind speeds increase the wind speeds start to converge whereas for lower wind speeds, these values have wider range. This may be influence of Earth's surface and geographic features in terms of surface roughness which has more impact on lower wind speeds. With this information, it may be generalized that going into upper elevations the less effected wind measurements from factors like surface roughness can be obtained.

Looking into L25-L16, L60-L16 and L60-L25 wind direction differences, it is observed that L25 and L60 wind direction differences are in the range of 0 to 1 sectors. This directional difference is higher and with wider range for smaller wind speeds in L25-L16 and L60-L16 comparisons. Therefore, the aforementioned findings related to the effects of surface roughness and etc. have higher impact on wind speeds at lower elevations resulting in more directional difference between L25-L16 and L60-L16 winds. In addition to the graphical representation of the comparisons, mean directional differences with their standard deviations are also calculated for L25-L16, L60-L16 and L60-L25. These values which are are calculated in absolute values are given in Table 4.1. It is seen from Table 4.1 that L60-L25 correlation in terms of wind directions are within the limits of one sector (≤22.5°) with small standard deviation compared to other comparisons.

Table 4.1: Average and Standard Deviation Values of L25-L16, L60-L16 and L60-L25 Wind Comparisons

Comparison Type	Mean Directional Difference ± Standard Deviation (°)
L25-L16	15.59 ± 19.05
L60-L16	25.90 ± 17.32
L60-L25	13.93 ± 9.37

In order to understand if there is any changes in directional differences for winds blowing from different directions and sectors, Figures 4.5-4.7 are prepared. In these figures, the x-axis show L60 wind directions, which is observed to be the least effected wind direction from surface roughness and etc. and y-axis consists of L60-L16 and L60-L25 wind direction differences. All of the data is given in degrees and the directional differences are calculated considering clockwise directional difference as +.

As seen in Figure 4.5, for the sector NW-NE the directional difference between both L60-L16 and L60-L25 are comparably smaller than other sectors with the exception of few results. For the other sectors, the directional differences have wider ranges.

In addition, the easterly onshore winds tend to deflect more inland for lower elevations which can be seen from the positive L60-L25 directional difference for NE-ESE sector. For L60-L16, there is not a certain visual tendency for NE-ESE sector, whereas for ESE-E sector, the directional difference is negative which means that L16 winds slightly turns in clockwise direction.

For westerly onshore winds, a similar but an opposite situation for the directional relation between L60 and L16 winds with the exception of several high negative L60-L16 directional differences.

More important than directional differences, it is observed that all of the L60 wind directions are within WSW-ESE sector which is an indication that L60 do not miss onshore wind directions.

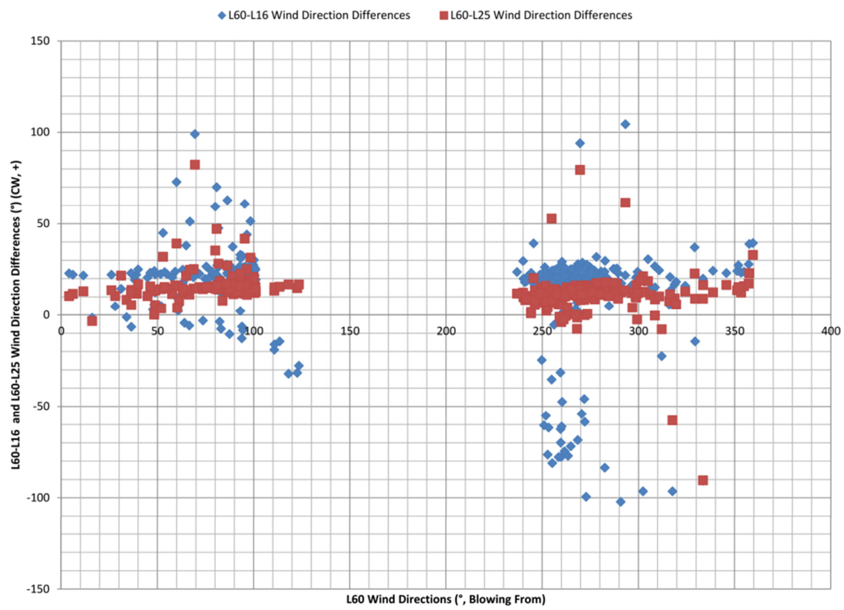

Figure 4.5: L60 Wind Directions vs L60-L16 and L60-L25 Wind Direction Differences

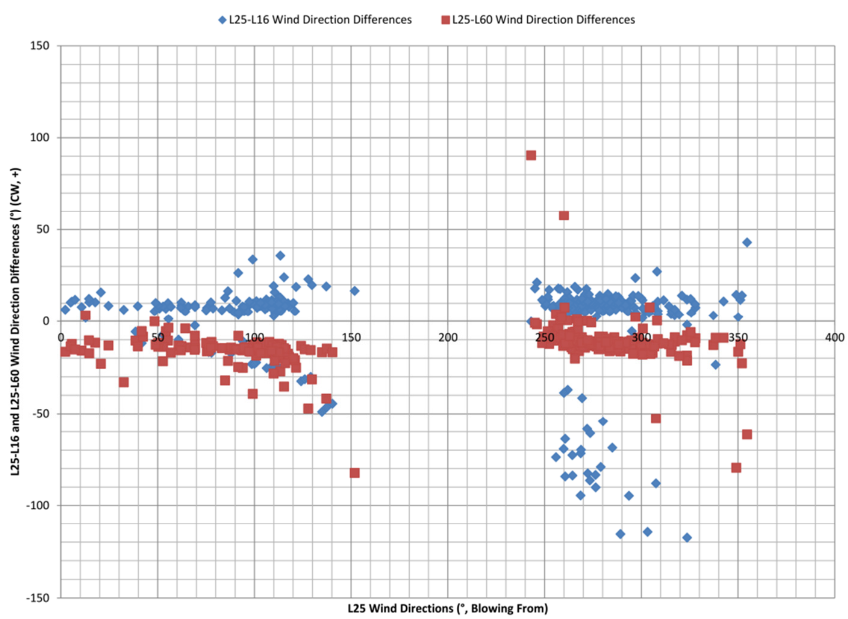

Figure 4.6: L25 Wind Directions vs L25-L16 and L25-L60 Wind Direction Differences

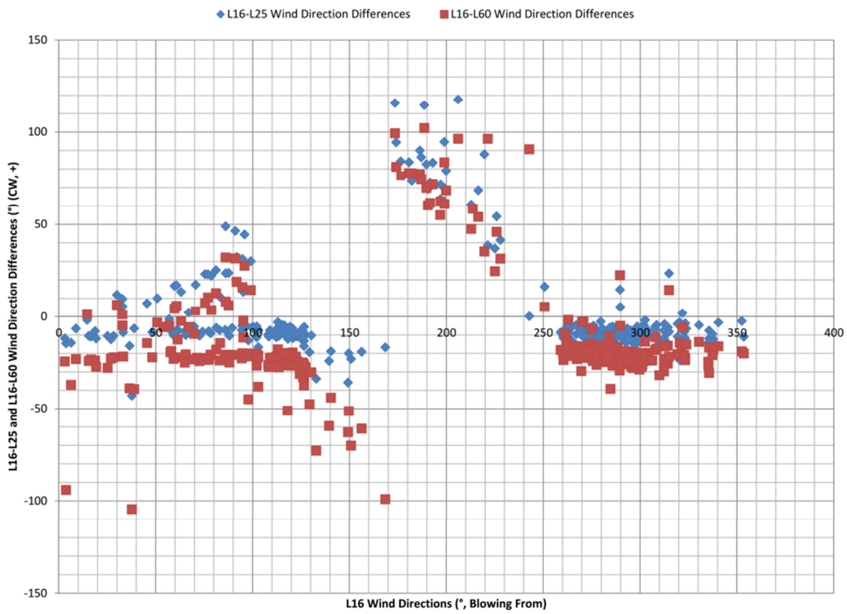

Figure 4.7: L16 Wind Directions vs L16-L25 and L16-L60 Wind Direction Differences

Considering Figure 4.6, although most of the L25 winds are in WSW-ESE sector, some of them are still from SSE-SE sector. This is not applicable for the opposite western side. The directional differences seen in Figure 4.6 indicate that for easterly onshore winds, L25-L16 is generally positive and L25-L60 is generally negative, which shows that winds tend to turn more inland at lower elevations. For westerly onshore winds, L25-L16 is generally positive and L25-L60 is generally negative, which is an indication that winds at lower elevations tend to turn in clockwise direction.

Similar outcomes just like for Figure 4.5 and Figure 4.7 are also observed for Figure 4.7. In addition to these findings, there are a lot more wind directions coming from directions other than the ones within WSW-ESE sector. This shows that lower elevation winds feel the impact of geographic features more resulting in directional changes.

The aforementioned comparisons indicate that L60 winds better represent offshore winds in terms of wind directions. Therefore, from now on the main comparisons will take L60 winds as reference at x-axis. The upcoming two comparisons results of which are plotted in Figure 4.8 and 4.9 focus on to find if there is any relationship between wind directions and speeds as well as wind directions and wind speed ratios. Figure 4.8 is prepared for L60 vs L16 comparisons whereas Figure 4.9 for L60 vs L25 comparisons.

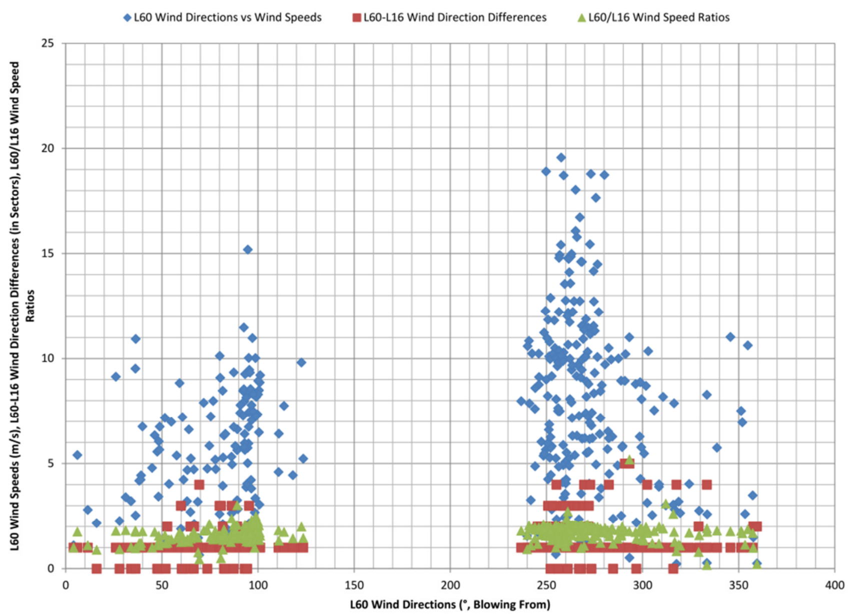

Figure 4.8: L60 Wind Directions vs L60 Wind Speeds, L60-L16 Wind Direction Differences and L60/L16 Wind Speed Ratios

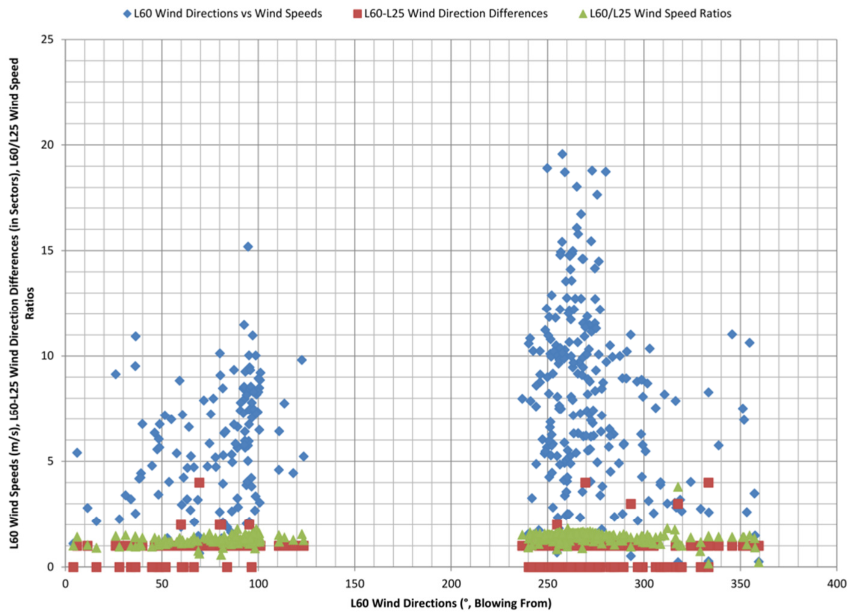

Figure 4.9: L60 Wind Directions vs L60 Wind Speeds, L60-L25 Wind Direction Differences and L60/L25 Wind Speed Ratios

It is observed in Figure 4.8 that for the NW-NE sector, L60-L16 directional difference is comparably smaller than other sea directions, which is also similar with L60-L25 directional differences seen in Figure 4.9. However, L60-L25 directional differences are smaller than L60-L16 directional differences on average. Considering L60/L16 wind speed ratios, for NW-NE sector the range is smaller whereas for other sea directions the range is higher. Therefore, it may be concluded that winds blowing with smaller angles to the shoreline tend to deflect more along vertical plane. The relationship L60 wind directions and wind speeds show that stronger winds mostly blow from WSW-NW sector and partly from NE-ESE sector in terms of wind speed magnitudes. Relatively smaller wind speeds are measured from the other sectors.

4.2. Relationship between L60, L25 and L16 Wind Speeds in Vertical Plane

After concluding that L60 winds represent the onshore winds better than others in terms of wind directions in the first part of this chapter, L60, L25 and L16 wind measurements are planned to put into another study in which wind speeds are compared with each other to observe if it is possible to obtain a vertical profile using simultaneous L60, L25 and L16 wind speeds.

In common usage, wind gradient, or more commonly preferred version, wind velocity/speed gradient, is the vertical gradient of the mean horizontal wind speed in the lower atmosphere. It is the rate of increase of wind strength with unit increase in height above ground level.

Typically, there is a wind gradient in the wind flow just a few hundred meters above the Earth's surface due to aerodynamic drag. Wind speed increases with increasing height above the ground. Near-surface flow encounters obstacles reducing the wind speed, and introducing random vertical and horizontal velocity components at right angles to the main direction of flow (Dalgliesh and Boyd, 1962). This turbulence causes vertical mixing between the air moving horizontally at one level and the air at those levels immediately above and below it.

The reduction in velocity near the surface is a function of surface roughness, so wind velocity profiles vary with different terrain types (Brown, 2001). Rough, irregular ground, and man-made obstructions on the ground, retard near-surface movement of the air, reducing wind velocity (Oke, 1987). Due to low surface roughness on water surface, wind speeds do not increase as much with height above sea level as they do on land (Lubosny, 2003).

For engineering purposes, the wind gradient is generally modeled as a vertical velocity profile based on a power law with a constant exponential coefficient based on surface type. The height above ground where surface friction has a negligible effect on wind speed is called the gradient height and the wind speed above this height is assumed to be a constant called the gradient wind speed (Stoltman, 2005).

For wind turbine engineering, an exponential variation in wind speed with height can be defined relative to wind measured at a reference height, Z as (Harrison, 2001);

$$U_H = U_Z\left(\frac{H}{Z}\right)^{\alpha} \qquad [4.4]$$

In the aforementioned formula, H and Z are the elevations above MSL and U_H and U_Z are the wind speeds at H and Z elevations.

In order to see if there is any relation between L60, L25 and L16 wind speeds that may eventually result in an idealized wind profile for the land-based wind measurement location, firstly Figures 4.10, 4.11 and 4.12 are prepared. In these figures, L60, L25 and L16 wind speeds are plotted against α coefficients that are found using equation 4.4 for L16-L25, L16-L60 and L25-L60 winds. Figure 4.10 is obtained using L16 and L25 wind speeds, whereas Figures 4.11 from L16 and L60 wind speeds followed by Figure 4.12 from L25 and L60 wind speeds.

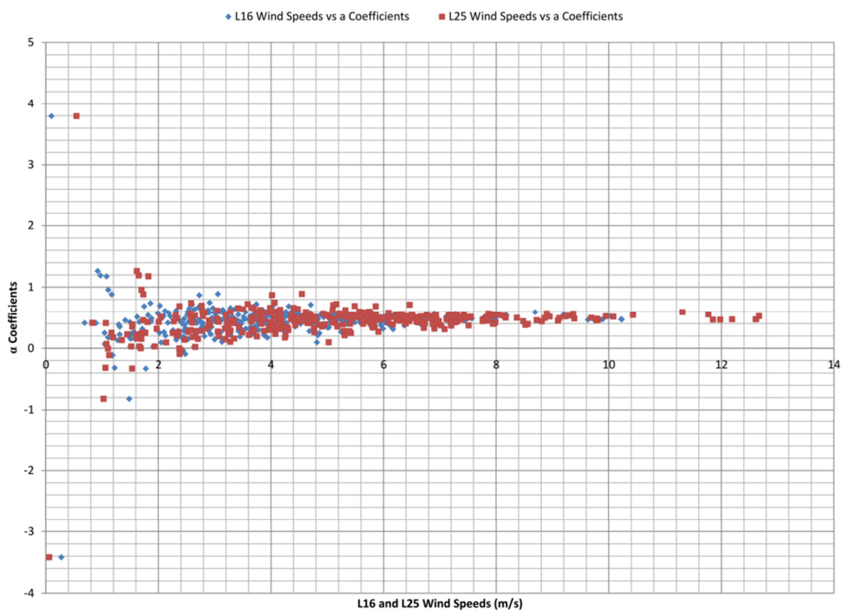

Figure 4.10: L16 and L25 Wind Speeds vs α Coefficients obtained from L16 and L25 Wind Speeds

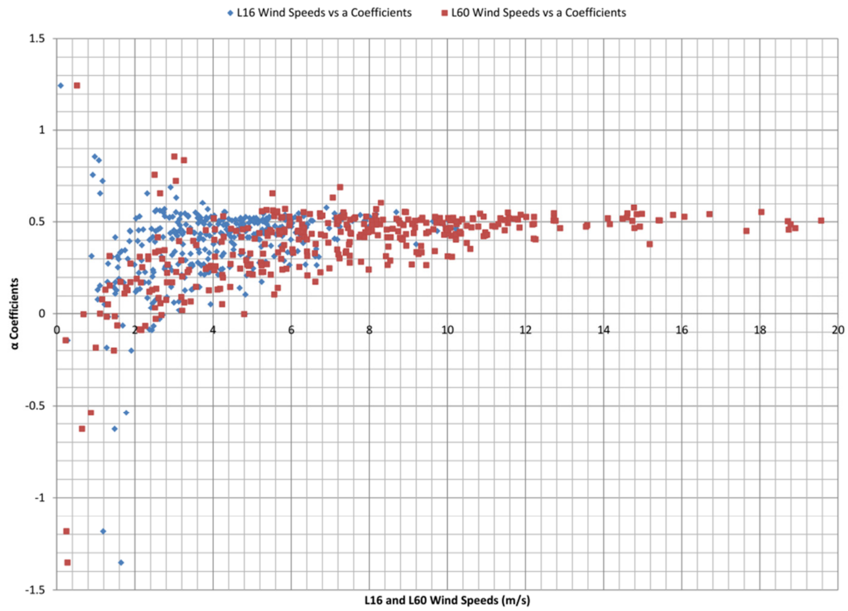

Figure 4.11: L16 and L60 Wind Speeds vs α Coefficients obtained from L16 and L60 Wind Speeds

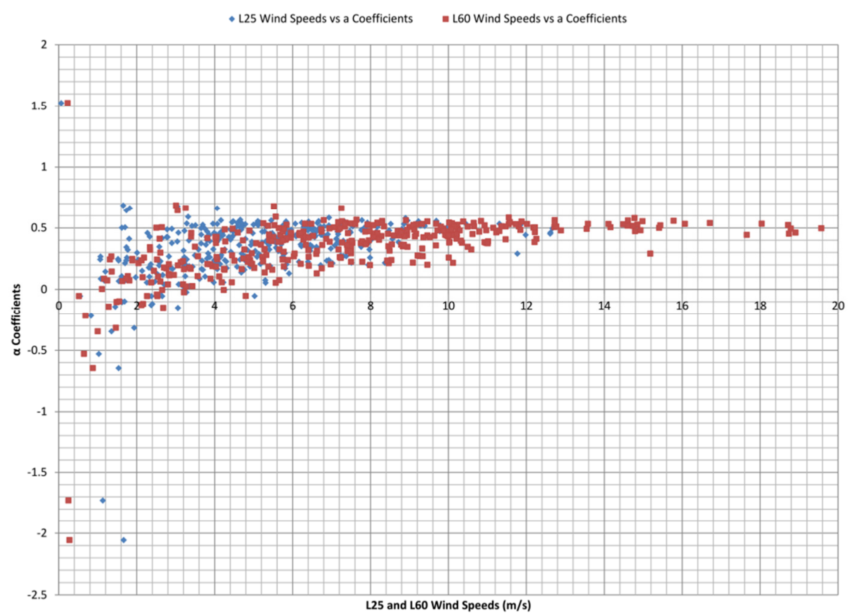

Figure 4.12: L25 and L60 Wind Speeds vs α Coefficients obtained from L25 and L60 Wind Speeds

Figures 4.10-4.12 indicate that the range for α coefficients are smaller for L16-L25 wind speeds, whereas as the elevation between the measurements increase, wider the ranges become. Therefore, α coefficients for L16-L60 wind speeds have wider scatter. Another finding would be that as wind speed decrease the scatter increases for all comparisons, which would be indicated as the more influence of surface roughness on smaller wind speeds. This is also observed better for comparisons between L16-L60 and L25-L60 that have bigger elevation difference. In each figure, after a certain wind speed, α coefficients tend to converge to 0.5 and start to have narrow scatter which is different for each comparison. According to the power law, 0.5 corresponds to a value between 0.4 used for stable air above flat open coast and 0.6 used for stable air human inhabited areas (Kaltschmitt et al, 2007).

Since for relatively smaller wind speeds α coefficients have wider range, it is decided to determine if mean α coefficients for different wind speeds together with their standard deviations. For this study, L16 vs L25, L16 vs L60 and L25 vs L60 comparisons are performed considering the power law relationship between relevant wind speeds. L60 wind speeds are arranged in decreasing order and using power law relationship, α coefficients are determined for each simultaneous wind speeds for L16-L25, L16-L60 and L25-L60 winds. Average values of α coefficients as well as the standard deviations are determined for wind categories of L60 ≥ 10 m/s, 5 m/s ≤ L60 < 10 m/s, 3 m/s ≤ L60 < 5 m/s and L60 < 3 m/s. The reason behind taking L60 wind speeds as reference is that, as specified in previous sections, L60 wind speeds are least effected by the surface and also L60 wind directions give very good results in terms of representing onshore winds. The results are given in Table 4.2.

Table 4.2: Mean and Standard Deviation Values of α Coefficients

α Coefficients	Mean Value ± Standard Deviation		
Wind Speed Categories	L16-L25	L16-L60	L25-L60
L60 ≥ 10 m/s	0.49 ± 0.05	0.48 ± 0.05	0.48 ± 0.07
5 m/s ≤ L60 < 10 m/s	0.49 ± 0.11	0.43 ± 0.11	0.40 ± 0.12
3 m/s ≤ L60 < 5 m/s	0.42 ± 0.22	0.31 ± 0.18	0.26 ± 0.17
L60 < 3 m/s	0.20 ± 0.77	0.08 ± 0.39	0.01 ± 0.48

The values in Table indicate that for L60 ≥ 5 m/s, α coefficients tend to converge between 0.4 and 0.5. This is very similar to the value visually determined and specified above as 0.5. As a result, the measurement location can be regarded as flat open coast and the air conditions as stable even though the value is slightly higher than 0.4. This slight difference may be attributed to the forestation around land tower.

Moreover, this value tend to decrease and different for different elevation relations. For instance, for 3 m/s ≤ L60 < 5 m/s, α coefficients for L25-L60 show that in general the situation is stable air above open water surface, for L60 < 3 m/s, α coefficients for L25-L60 show that in general the situation is somewhere between unstable air above open water surface and neutral air above open water surface.

4.3. Discussion

Land-based coastal in-situ wind measurements that are performed by governmental authorities at 42.09°N – 34.96°E coordinates near Sinop covering a period between February, 2009 and December, 2009 with some gaps are used in this study. The measurements are recorded at three different elevations (16 m; L16, 25 m; L25and 60 m; L60) from the local reference point which is 60 m above MSL.

The studies are performed considering the directional sector WSW-ESE corresponding to onshore winds (sea directions) only. A comparative study on the simultaneous wind measurements at different levels has been carried out and a representative vertical profile is obtained showing that the in-situ measurements are carried out on a flat open coastal area.

Comparisons of L16 and L25 wind measurement with L60 wind measurements show the effect of surface roughness resulting in lower wind speeds and directional changes at lower elevations. Lower wind speeds feel this surface roughness more hence causing larger directional changes.

Coastal in-situ wind measurements may not be reliable enough concerning wind speeds and directions for lower elevations. Therefore, the comparative studies are only performed with in-situ wind measurements at 60 m elevation for the upcoming studies.

CHAPTER 5

SPATIAL VARIABILITY OF ECMWF WIND DATA

In Chapter 3, the findings indicate that, most of the wind roses that represent the overall wind climate of their locations and are obtained from hourly wind measurements of TCMSs, generally give unreliable results due to several reasons discussed within Chapter 3.Therefore, more reliable and more representative wind data is needed for Turkish coasts so that they can be used in coastal engineering applications. For this aim, ECMWF (European Centre for Medium Range Weather Forecasts) is decided to be used for several reasons. These reasons are summarized below;

- Turkey is a member of ECMWF and a key can be provided to every applicant to Turkish State Meteorological Service in return for a certain amount of fee, thus making it easy to obtain ECMWF data from its website (www.ecmwf.int).
- ECMWF provides atmospheric and marine data for various users on its website under several datasets which was discussed in Chapter 2. As discussed in Chapter 2, these datasets cover different time frames and have different grid resolutions.
- A user has the option to choose the grid resolution, time frame and basin dimensions which makes it easy for the user to obtain the exact data he/she needed.

As discussed in Chapter 2, ECMWF have certain grid resolutions for all of the datasets covering forecast, analysis and re-analysis data. For this study, ECMWF Operational Analysis data is chosen. The main reason behind this is that it is becoming more common in Turkey for coastal engineering applications, and there is no possibility for the data set to finish producing analysis data whereas for re-analysis data sets, if a new re-analysis data set will be initiated, just like ERA-40 and ERA-15, the data production process stops. Therefore, there is no certainty whether these data sets including ERA-Interim to stay updated in the future.

Apart from which data set to use for comparisons, it is most probably more important to decide on data of which grid to use for comparisons in this study. In order to understand how data changes with respect to each latitudinal and longitudinal grid change and thus conclude whether ECMWF wind data changes significantly or not. Moreover, it is critical to see if the data close to coastline can be used in these studies since ECMWF uses mean orography in their data assimilations resulting in uncertainty whether the chosen grid point is a land or a sea point.

In order to understand the differences and similarities between wind data for ECMWF grids, a spatial study is performed considering 10 difference ECMWF data points close to the land-based in-situ wind measurement area. The grid resolution is 0.1° which roughly corresponds to 8 km. Figure 5.1 shows the locations of the chosen ECMWF grid points and the initials given to these points starting from A and ends with J. In Figure 5.1, the expression “LAND” is the location of land-based in-situ wind measurement site. Table 5.1 summarizes the coordinates of ECMWF grid points and direct distance between LAND and ECMWF grid points.

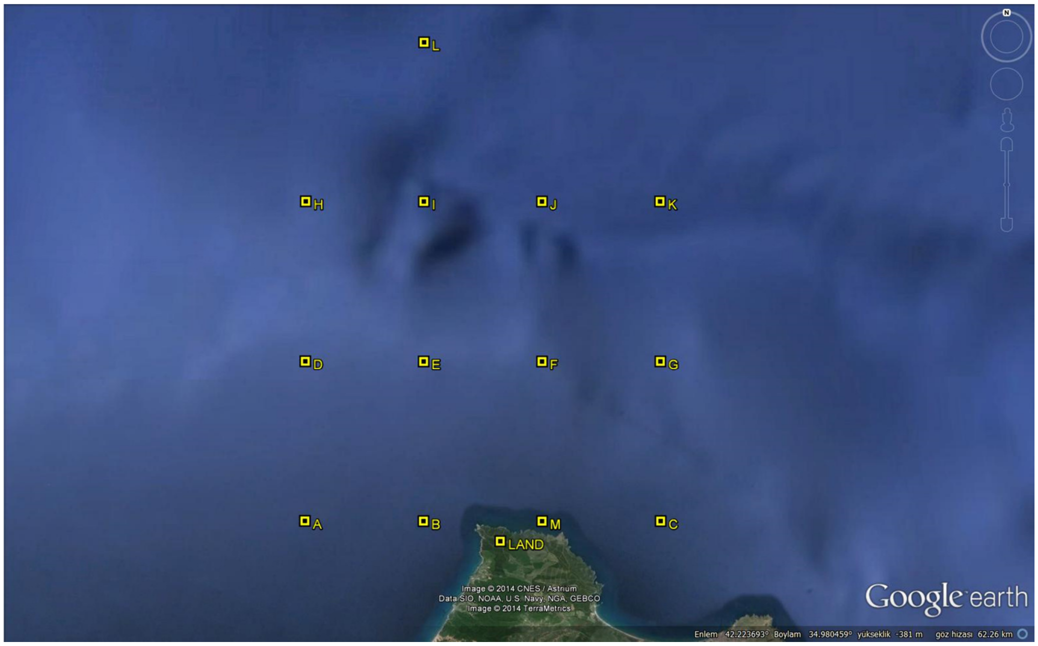

Figure 5.1: Locations of chosen ECMWF grid points for spatial studies (Google Earth, 2014)

Table 5.1: Coordinates of chosen ECMWF grid points and the direct distances between these grid points and LAND site

ECMWF Grid Point	Coordinates	Distance (km)
A	42.10°N – 34.80°E	13.6
B	42.10°N – 34.90°E	5.4
C	42.10°N – 35.10°E	11.4
D	42.20°N – 34.80°E	18.4
E	42.20°N – 34.90°E	18.6
F	42.20°N – 35.00°E	12.8
G	42.20°N – 35.10°E	16.9
H	42.30°N – 34.80°E	27.3
I	42.30°N – 34.90°E	24.3
J	42.30°N – 35.00°E	24.0
K	42.30°N – 35.10°E	26.1
L	42.40°N – 34.90°E	35.2
M	42.10°N – 35.00°E	1.9

Firstly, in order to understand the resemblance of the wind data, wind roses obtained from L60 wind measurements and wind roses obtained from ECMWF wind measurements are compared. All of the wind roses are obtained for the same period of land-based in-situ wind measurements and they are given in Figures 5.2-5.14. Moreover, in order to observe if there is any similarity between wind rose obtained from L60 wind measurements and the closest ECMWF grid point to LAND site that may be regarded as land location, wind rose for M point is given in Figure 5.15. All of the wind roses are prepared for the wind directions `blowing from`.

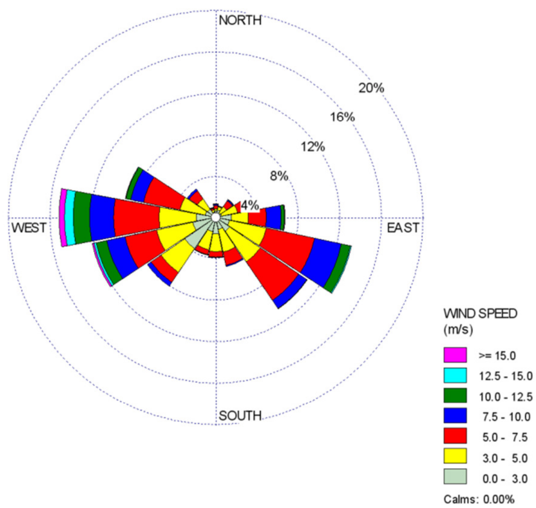

Figure 5.2: Wind Rose Obtained from L60 Wind Measurements

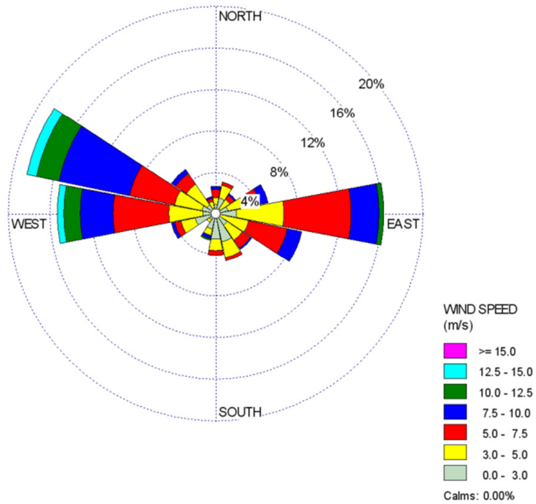

Figure 5.3: Wind Rose of ECMWF Grid Point A (42.10°N – 34.80°E)

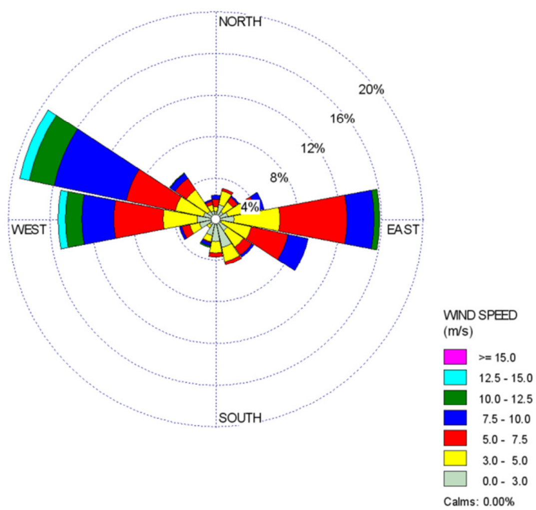

Figure 5.4: Wind Rose of ECMWF Grid Point B (42.10°N – 34.90°E)

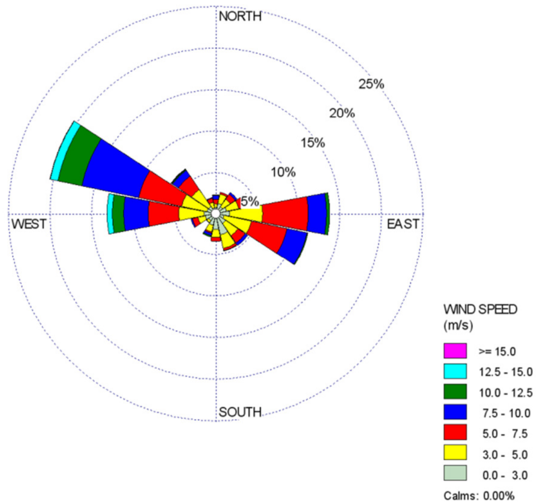

Figure 5.5: Wind Rose of ECMWF Grid Point C (42.10°N – 35.10°E)

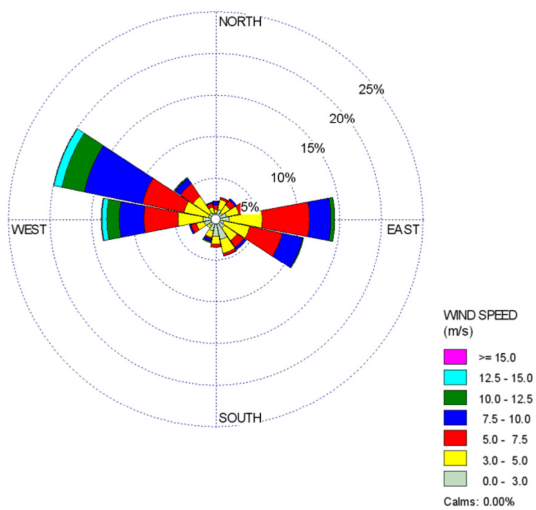

Figure 5.6: Wind Rose of ECMWF Grid Point D (42.20°N – 34.80°E)

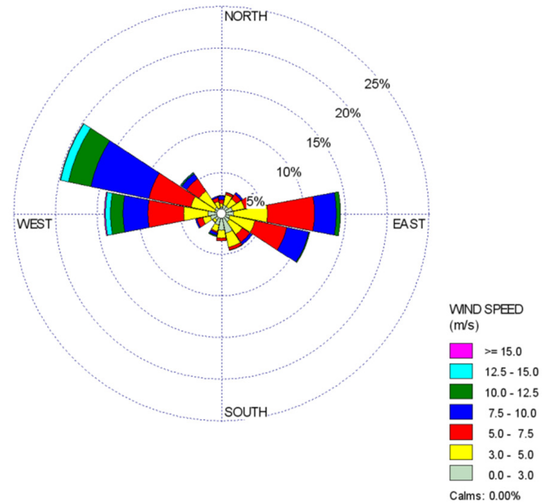

Figure 5.7: Wind Rose of ECMWF Grid Point E (42.20°N – 34.90°E)

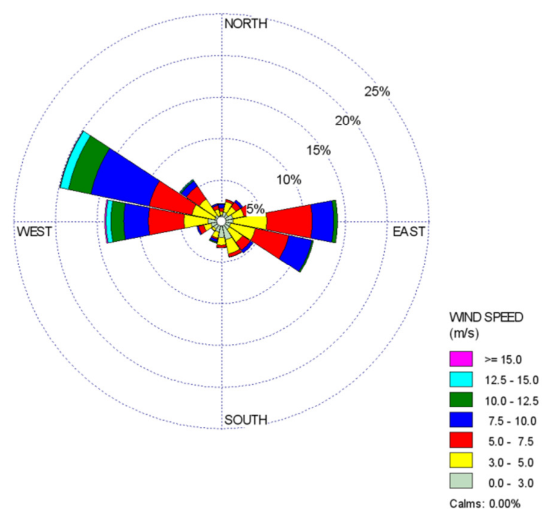

Figure 5.8: Wind Rose of ECMWF Grid Point F (42.20°N – 35.00°E)

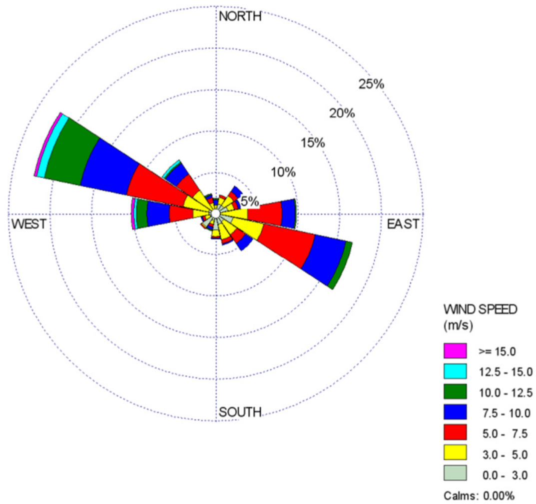

Figure 5.9: Wind Rose of ECMWF Grid Point G (42.20°N – 35.10°E)

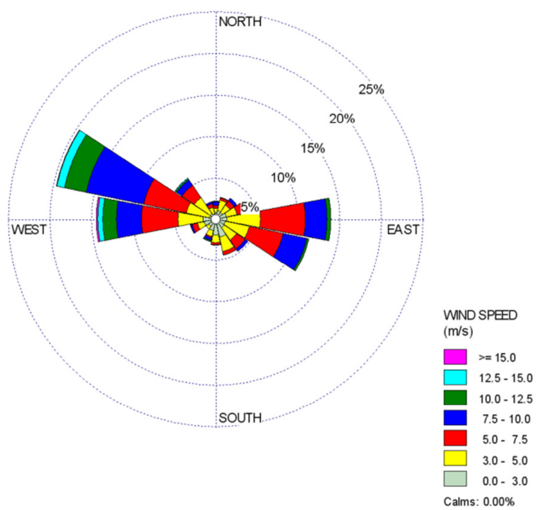

Figure 5.10: Wind Rose of ECMWF Grid Point H (42.30°N – 34.80°E)

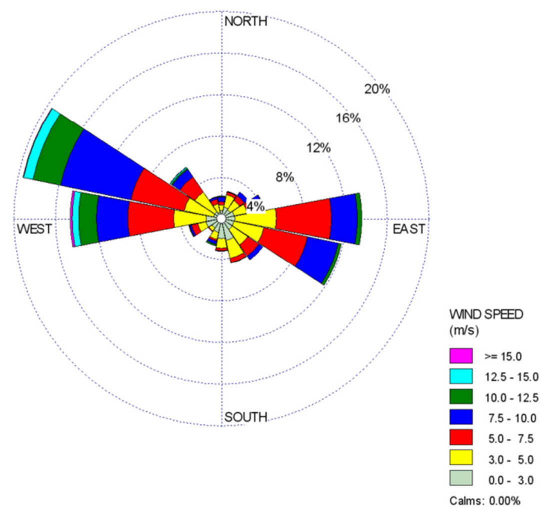

Figure 5.11: Wind Rose of ECMWF Grid Point I (42.30°N – 34.90°E)

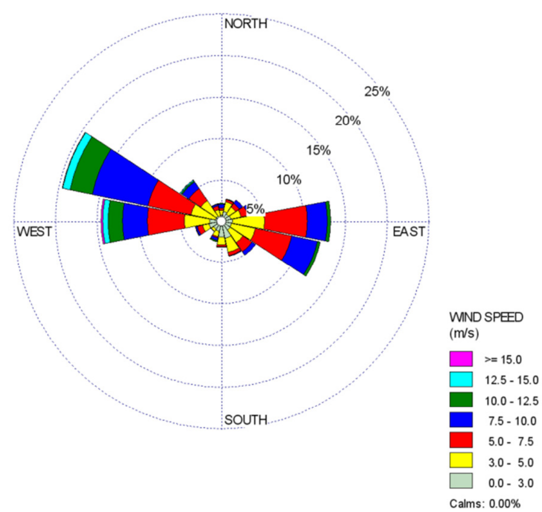

Figure 5.12: Wind Rose of ECMWF Grid Point J (42.30°N – 35.00°E)

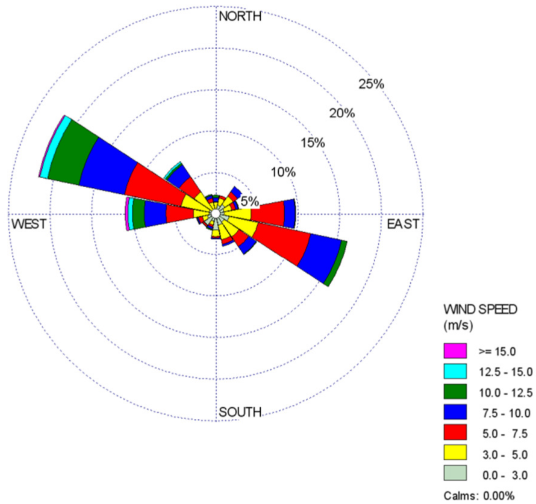

Figure 5.13: Wind Rose of ECMWF Grid Point K (42.30°N – 35.10°E)

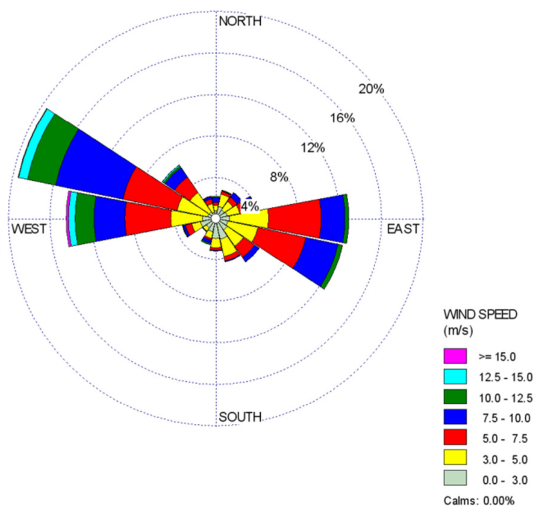

Figure 5.14: Wind Rose of ECMWF Grid Point L (42.40°N – 34.90°E)

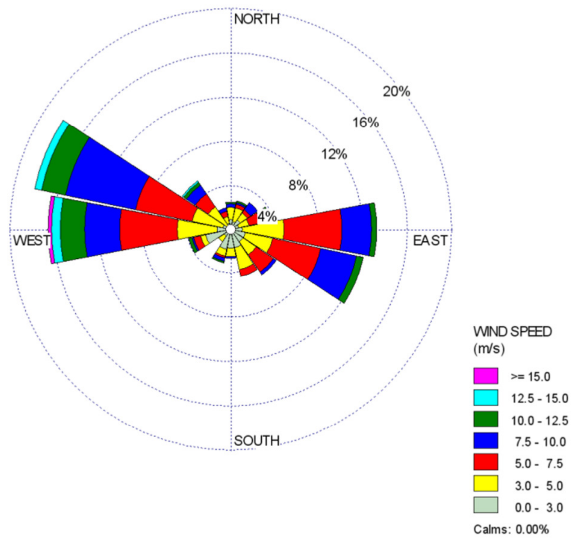

Figure 5.15: Wind Rose of ECMWF Grid Point M (42.10°N – 35.00°E)

It should be noted that wind roses obtained from wind data of ECMWF grid points have some differences with wind rose obtained from L60 wind measurement data. It is expected to observe directional changes between onshore and offshore winds up to 45° according to Hsu (1986). Comparing wind roses obtained from ECMWF data for each grid point with wind rose obtained from L60 wind measurements, it can be concluded that the directional differences are roughly smaller than this value by visual comparison. Therefore, it can be regarded that ECMWF winds give acceptable results in terms of wind directions.

Concerning wind roses for L60 wind measurements and for M point, compared to the resemblance with wind roses of other grid points (Figure 5.3-5.14), the resemblance between Figure 5.2 and Figure 5.15 is higher especially for W and ESE directions. However, it cannot be concluded that the resemblance is high enough.

In order to look deeper into the data, firstly the first three grid points closest to the shoreline (A, B and C) are taken into consideration. It is expected that as points A and B are on the west of LAND, the wind roses for these points reflect similar outcomes. On the other hand, wind rose of point C is expected to have slightly different configuration. Wind roses of points A and B are very similar to each other. On the contrary, winds blowing from WNW and NW directions have higher percentages and easterly winds and winds blowing from W direction have lower percentages for wind rose of point C when compared to wind roses of points A and B.

Considering wind roses of points D, E, F and G which are relatively far away from LAND, the distance being in the order of 12-19 km, wind roses of points D, E and F are very similar to each other whereas wind rose of point G have considerable differences. The wind percentages and speeds for WNW, NW and ESE directions are higher and wind percentages for E and W directions are lower than those of other three points.

As for wind rose of points H, I, J, K and L, at the order of 24 to 35 km distance from the land-based wind measurements, all of the wind roses have similar configurations except the wind rose of point K. The wind percentages and speeds for E, NNW and W directions are lower whereas wind percentages and speeds for ENE, NE and WSW are higher.

In addition to wind roses, wind histograms (wind class frequency distributions) of L60 wind measurements and ECMWF wind grid points are prepared in order to observe if similar outcomes are reached just like the ones from wind roses. The wind histograms are presented in Figure 5.16-5.29.

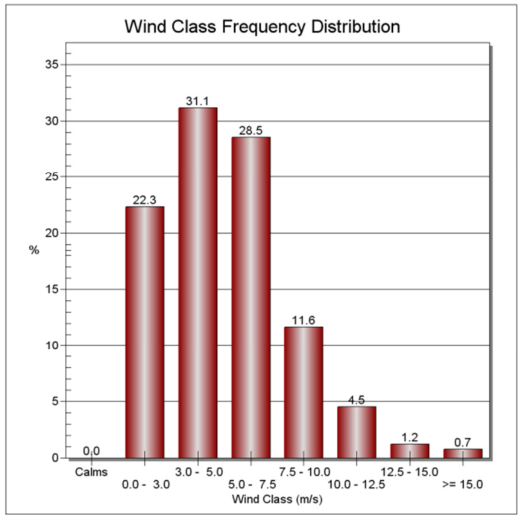

Figure 5.16: Wind Histogram for L60 Wind Measurements

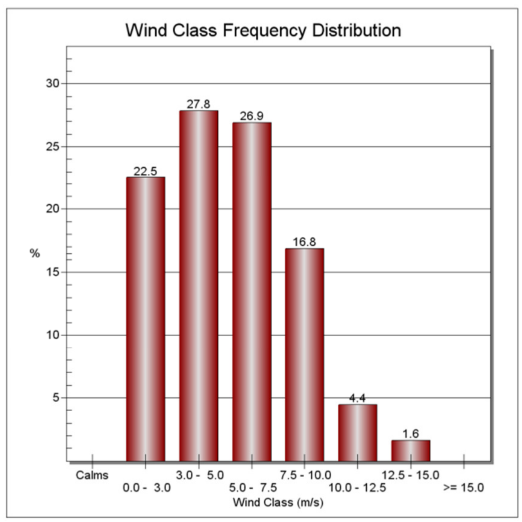

Figure 5.17: Wind Histogram for Point A (42.10°N – 34.80°E)

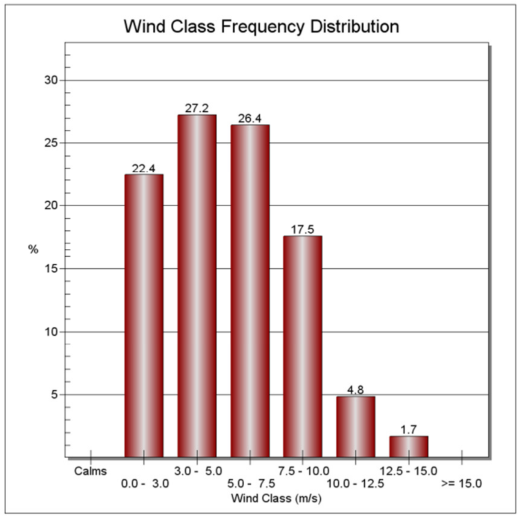

Figure 5.18: Wind Histogram for Point B (42.10°N – 34.90°E)

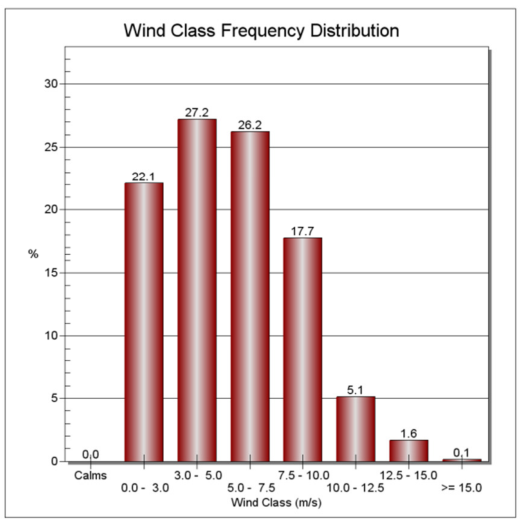

Figure 5.19: Wind Histogram for Point C (42.10°N – 35.10°E)

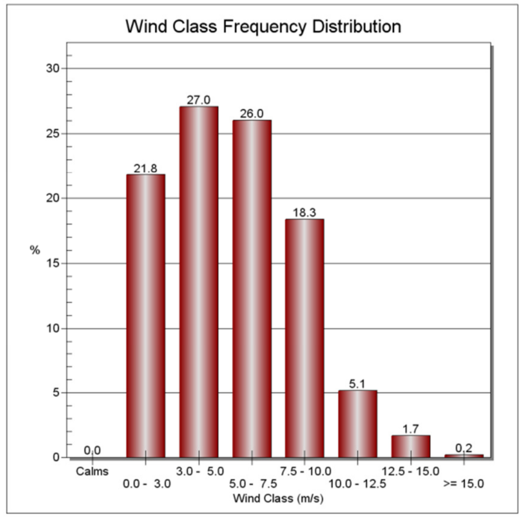

Figure 5.20: Wind Histogram for Point D (42.20°N – 34.80°E)

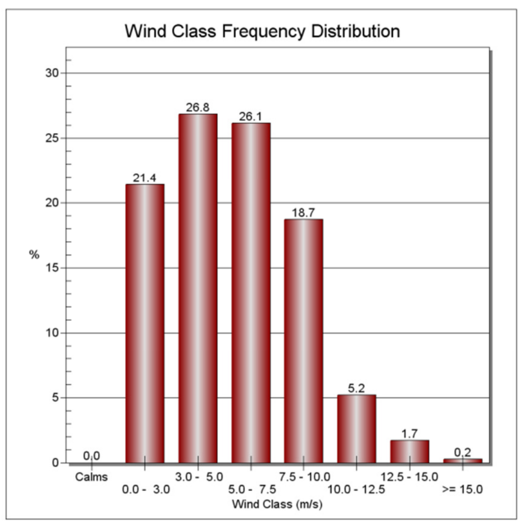

Figure 5.21: Wind Histogram for Point E (42.20°N – 34.90°E)

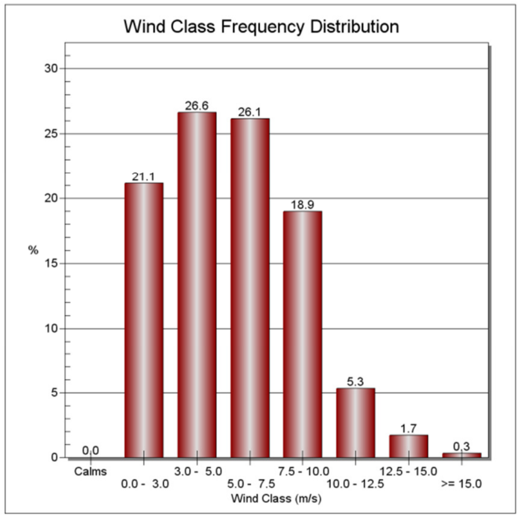

Figure 5.22: Wind Histogram for Point F (42.20°N – 35.00°E)

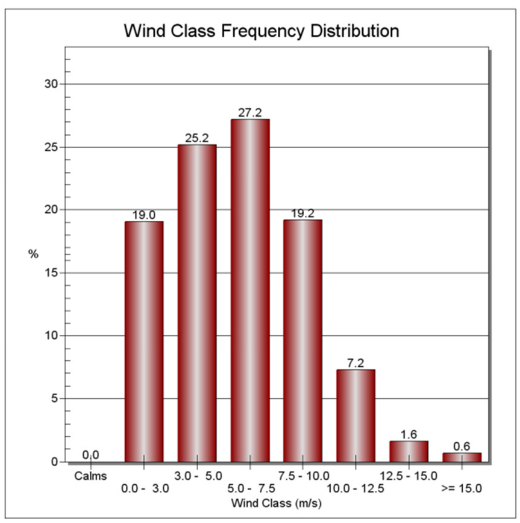

Figure 5.23: Wind Histogram for Point G (42.20°N – 35.10°E)

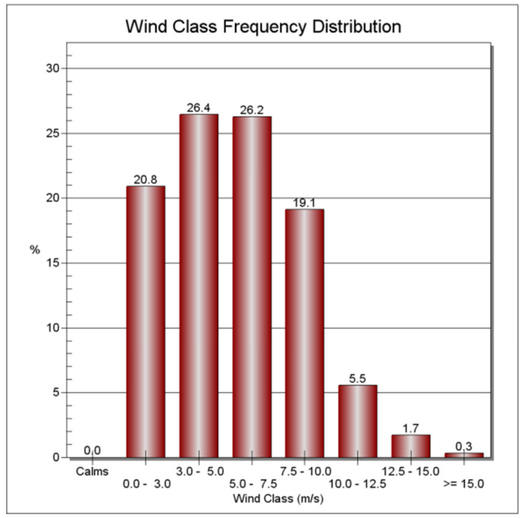

Figure 5.24: Wind Histogram for Point H (42.30°N – 34.80°E)

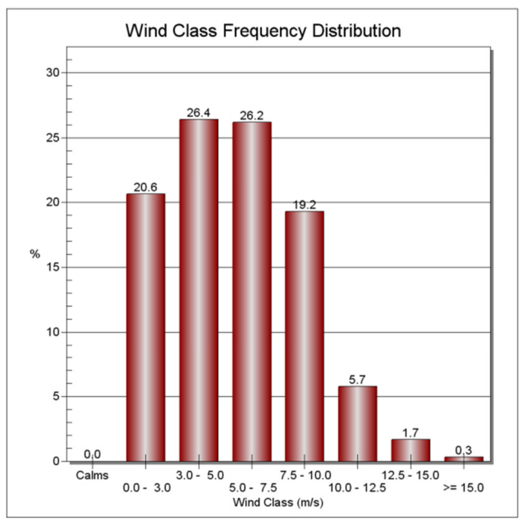

Figure 5.25: Wind Histogram for Point I (42.30°N – 34.90°E)

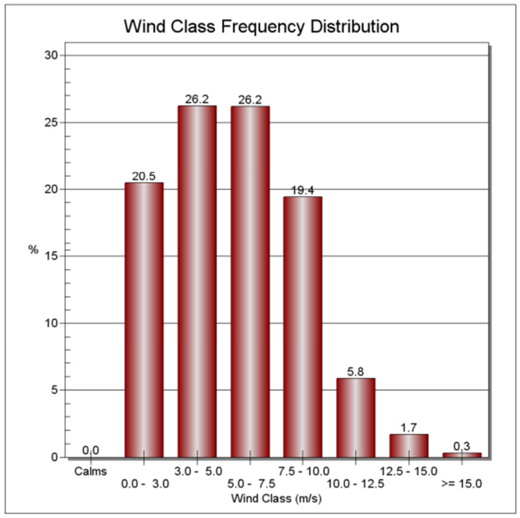

Figure 5.26: Wind Histogram for Point J (42.30°N – 35.00°E)

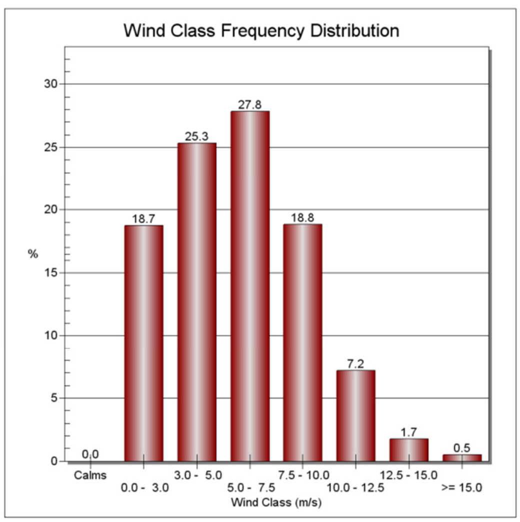

Figure 5.27: Wind Histogram for Point K (42.30°N – 35.10°E)

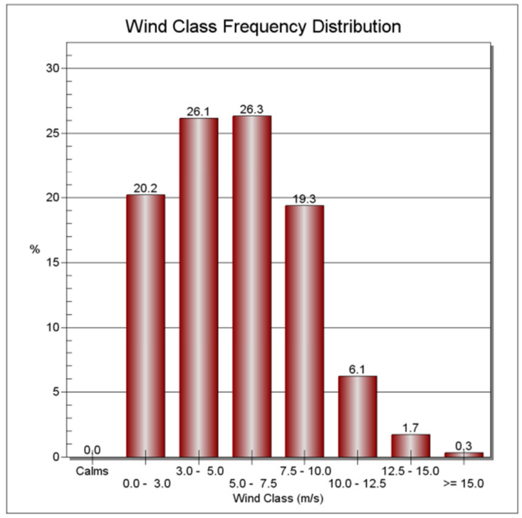

Figure 5.28: Wind Histogram for Point L (42.40°N – 34.90°E)

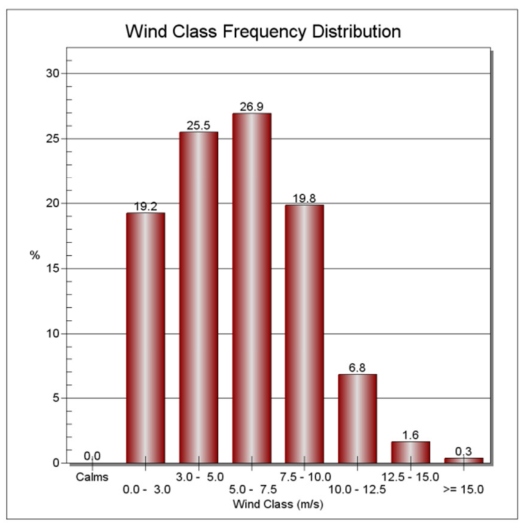

Figure 5.29: Wind Histogram for Point M (42.10°N – 35.00°E)

As wind histograms do not give any hint about wind directions, the comparisons are limited to wind speeds. Looking into wind histograms, it is easily observed that wind histograms other than those of points G and K have similar structures. The wind class frequencies are tabulated into percentages in Appendix A, which would make it easier to numerically realize the aforementioned visual observations and findings concerning wind roses and wind histograms. A summary table is prepared from the information given in tables of Appendix A, considering only the main wind directions E, ENE, NE, NNW, W and WSW to see the wind percentages (Table 5.2). All of the numbers in Table 5.2 denote percentages (%).

Table 5.2: Wind percentages of E, ENE, NE, NNW, W and WSW directions for all ECMWF grid points

ECMWF Grid Point	E	ENE	NE	WNW	W	WSW
A	15.8	4.8	2.8	13.3	15.2	3.6
B	16	5	3	19	15	4
C	13.7	4.4	3.1	20.4	13.1	3.1
D	14.3	4.5	3.1	19.9	13.8	3.3
E	14.3	4.6	3.1	19.8	14.1	3.2
F	14	4.5	3.1	19.9	14	3.1
G	9.7	3.1	4.1	22.3	10.2	1.9
H	13.9	4.4	3.1	19.6	14.4	3.2
I	13.5	4.2	3.1	19.5	14.5	3.2
J	13.2	4.1	3.1	19.5	14.5	3.3
K	16.2	9.7	2.9	21.8	10.9	2.4
L	12.8	4.0	3.1	19.4	14.4	3.3
M	13.2	3.8	3.0	18.1	16.5	3.9

As the wind data that is used for creation of wind roses and histograms are very limited and only covers several periods in 2009, it is believed that the wind roses and histograms are sufficient enough to have an overall idea about how much the wind roses differ in longitudinal and latitudinal directions and how similar are the wind speeds and directions of ECMWF grid points. The grouping of ECMWF grid points performed considering the similarities of wind roses and histograms is shown in Figure 5.27. Based on the similarities between wind roses and histograms of point A and B, they are denoted as Group “1”. As the wind roses and histograms of points G and K are different than those of other points, even though the westerly wind percentages are different, they are denoted as Group “2”. Although wind roses and histograms of points C and L demonstrates small differences from the wind roses and histograms of remained points, all of the remaining eight points (C, D, E, F, H, I, J, L) are categorized into Group "3".

Since Group 3 have more ECMWF grid points, meaning that there is an option of using more than a couple of data points, choosing one of these ECMWF grid points for the following studies would result in the application of the outcomes obtained in those studies to other grid points as well. Thus, it is decided to use wind data of point E in the following studies for this thesis.

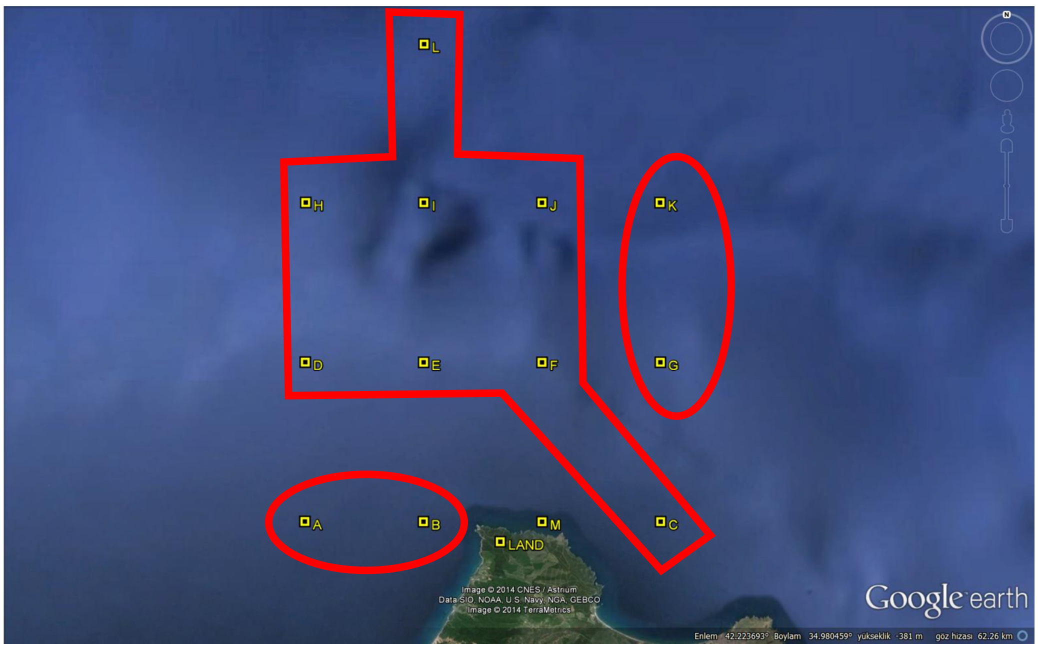

Figure 5.30: Grouping of ECMWF grid points considering wind roses and histograms

<u>Discussion:</u>

For any coastal project, selection of ECMWF wind data points is of great importance since not all of the grid points represent the wind climate accurately due to several reasons such as the distance to shore, orography of the grid and proximity to the site as shown in the above given figure. An example to the topographical reasons can be given as "A and B points" which are found to be altered by the land formations.

CHAPTER 6

COMPARISON BETWEEN IN-SITU WIND MEASUREMENTS AND ECMWF WIND DATA

In Chapter 4, the land-based in-situ wind measurements are checked by performing several simple comparisons in between the wind measurements at three different elevations if any inconsistency exists within the data set. As previously mentioned, this is performed due to the fact that it is not known whether the wind measurements are put through any calibration, verification or quality control processes. The results indicated that among L60, L25 and L16 wind measurements, it would be better to use L60 wind measurements for the rest of the studies and the reason for this choice is attributed to least effected wind measurements performed at 60 m elevation from surface features.

At this stage, a question arises whether L60 wind measurements can be used without making any land-sea conversions for wind speeds and wind directions. Considering wind directions, as mentioned a couple of times within the previous chapters, based on the Hsu's (1986) findings, a directional difference up to 45° between onshore and offshore wind directions can be seen and this value may be accepted as an upper limit. Thus, it would not be necessary to perform any conversions or modifications to the wind directions. However, this will be profoundly discussed in the upcoming sections. The other issue, land-sea wind speed conversions, will definitely be put through as it is not possible to perform any comparisons of two variables measured under completely different environments, which are on land and on sea. Therefore, selected land-sea conversion methods will be applied to the land-based wind measurements so that the land-based winds will be transferred to sea-based winds. For this conversion, Hsu's (1986) approach will be used as it may be used for low-relief areas up to 0.5-1 km and he do not define any criteria for wind speeds and etc.

Thus, Hsu's approach (1986) can be generally used for approximation of sea-based winds. These studies will be covered in Section 6.1.

Following the above given procedures, sea-based wind measurements will be achieved at 60 m above MSL as the conversion in only performed on the horizontal plane at the same elevation with respect to the reference elevations on both environments. As land-based wind measurements are performed at 60 m elevation with respect to the local bottom elevation and as for sea environments the reference level is MSL, the land-sea conversions do not perform any vertical modification in the wind speeds. Consequently, it would be necessary to perform an additional vertical conversion of the sea-based measurements at 60 m elevation which will be denoted as S60 from now on, to obtain sea-based measurements at 10 m elevation which will also be mentioned as S10 in the upcoming studies. The reason behind this vertical conversion is that, as ECMWF wind speeds belong to 10 m elevation above MSL, S60 wind speeds should be carried to S10 wind speeds in order to compare two variables at the same environment and elevation.

The vertical conversion specified above will be performed by applying the power law approach which was discussed in Chapter 4. Just like the procedure for the comparison of land-based wind measurements, a general and applicable α coefficient is needed for the conversion of S60 wind speeds to S10 wind speeds. This can only be achieved by comparing sea-based wind data at two different elevations. ECMWF operational analysis extended their data set by including wind data at 100 m above MSL in 2011. Although, it does not cover the same period with the land-based wind measurements, performing a simple comparison between wind data at 100 m elevation, which will be denoted as E100 in the following studies, and E10 wind data for the chosen period of 2011-2013, covering 3 years of 6 hourly wind data, would be representative enough for the same region.. For this study, E10 and E100 wind data of the same ECMWF grid point E (42.20°N – 34.90°E), that is chosen according to the results of Chapter 5, is used. After finding applicable α coefficients that can be implemented into the power law equation, this value will be used in conversion of

S60 wind speeds to S10 wind speeds. All of the aforementioned studies will be given in Section 6.2.

After achieving S10 wind speeds, it would be possible to perform comparative studies between simultaneous S10 and E10 wind speeds. As previously mentioned in the above sections, the land-based wind measurements cover rather short period between February, 2009 and December, 2009 with considerable long gaps as well as more commonly observed smaller gaps such as 2, 3 hours. Thus, it is really hard to observe continuous data sets especially for onshore winds and storm conditions which may be denoted as wind speeds above 3 m/s. In this study, 29 continuous data sets are extracted from within the data set and not all of them totally consist of storm conditions. Within these data sets, few hours of calm conditions, wind speeds below 3 m/s, are observed, but very high percentage of the wind speeds demonstrates storm conditions. The continuous data sets are chosen so that they would at least last 18 hours, which corresponds to four 6 hourly ECMWF wind data. The details of the extraction process, together with the related graphical representations will be provided in Section 6.3. Moreover, S10 and E10 wind speeds will be compared as well as S10-E10 wind directions and the results will be discussed under the light of previously performed studies in the literature as well as the result of another comparison performed in Aegean Sea between sea-based in-situ wind measurements and ECMWF wind data covering a very short period of time in 2013.

Following the graphical representation of 29 continuous data sets and S10-E10 wind speed and direction differences, an identical approach to obtain similar S10 wind speeds from E10 wind speeds for the times where in-situ wind measurements exist will be introduced in Section 6.4. This approach will be followed by introducing a new method to modify E10 wind speeds for the times when neither sea-based nor land-based in-situ wind measurements are found, which is the generally encountered case in Turkey. The details of this study will profoundly be discussed in Section 6.4 as well.

6.1. Conversion of L60 Wind Speeds to S60 Wind Speeds on Horizontal Plane

In Chapter 4, it is concluded to use L60 wind measurement data for the following comparative studies within the thesis. Since comparisons are planned to be performed considering E10 wind data on sea environment, both horizontal and vertical conversions should be carried out to obtain wind data at the same environment and elevation as E10 wind data. The first stage would be to convert the land-based wind measurement data to wind data over sea environment. This will be performed by application of Hsu's approach which was introduced in 1986 and given with a simple linear formulation as;

$$U_{sea} = 1.62 + 1.17U_{land} \qquad [6.1]$$

In this approach, U_{sea} and U_{land} are the wind speeds at sea and land for the same elevation with respect to their local references, which is the bottom elevation of the land tower or U_{land} and MSL for U_{sea}. The reason behind Hsu's (1986) simple linear approach is based on comparisons between many different simultaneous onshore and offshore wind data as well as the simple condition that while land-based winds are very small or sometimes equal to zero, meaning that calm conditions exist, sea-based winds do not always have calm conditions and most often reflect storm conditions. Moreover, as this is the latest version of series of studies performed by Hsu (1981, 1984 and 1986) and due to its simplicity, not including any atmospheric impacts such as temperature, etc. this approach is chosen for the land-sea conversions.

The details of the 29 continuous data sets are tabulated in Table 6.1 and the results of the land-sea conversions for 29 continuous data sets are given in Appendix B.

Table 6.1: Start and End Date and Time of Continuous Data Sets and Their Durations

Continuous Data No	Start Date	Start Time	End Date	End Time	Duration (hrs)
1	10.02.2009	12:00	11.02.2009	12:00	25
2	15.02.2009	12:00	18.02.2009	00:00	61
3	21.02.2009	12:00	22.02.2009	18:00	37
4	25.02.2009	06:00	03.03.2009	18:00	157
5	12.03.2009	06:00	15.03.2009	00:00	61
6	15.03.2009	12:00	16.03.2009	18:00	31
7	19.03.2009	12:00	21.03.2009	00:00	37
8	22.03.2009	12:00	24.03.2009	00:00	37
9	27.03.2009	00:00	29.03.2009	18:00	67
10	02.04.2009	18:00	04.04.2009	18:00	49
11	04.05.2009	12:00	05.05.2009	12:00	25
12	12.05.2009	06:00	13.05.2009	00:00	19
13	18.05.2009	00:00	21.05.2009	00:00	73
14	01.06.2009	06:00	02.06.2009	00:00	25
15	05.06.2009	00:00	05.06.2009	06:00	19
16	08.06.2009	06:00	09.06.2009	18:00	19
17	13.06.2009	12:00	14.06.2009	06:00	19
18	21.06.2009	06:00	22.06.2009	12:00	37
19	20.07.2009	06:00	21.07.2009	00:00	19
20	31.10.2009	00:00	02.11.2009	12:00	61
21	06.11.2009	00:00	07.11.2009	12:00	37
22	13.11.2009	00:00	14.11.2009	06:00	31
23	17.11.2009	06:00	18.11.2009	12:00	31
24	19.11.2009	12:00	22.11.2009	00:00	61
25	25.11.2009	00:00	26.11.2009	12:00	37
26	29.11.2009	18:00	01.12.2009	18:00	49
27	13.12.2009	18:00	14.12.2009	18:00	25
28	17.12.2009	12:00	18.12.2009	06:00	19
29	21.12.2009	06:00	22.12.2009	00:00	19

6.2. Conversion of S60 Wind Speeds to S10 Wind Speeds on Vertical Plane

As summarized before, there is a need for vertical conversion of S60 wind speeds to obtained S10 wind speed so that S10 vs E10 wind speeds, which will eventually be carried to the same elevation on the same environment, can be compared. This is the first step of trying to determine relationship between S10 and E10 wind speeds.

With this aim, the power law approach given below is used;

$$\left(\frac{U_{10}}{U_{60}}\right) = \left(\frac{10}{60}\right)^{\alpha} \qquad [6.2]$$

In this formula, U_{10} and U_{60} are the wind speeds at heights 10 and 60, respectively. $\alpha$is called Hellman exponent/coefficient depending on the atmospheric stability and surface roughness, Z_o.

For this approach to be applied for vertical conversions at this site, α coefficients representative of this site are needed. These values can be achieved by comparing E100 and E10 wind speeds available for the period of 2011-2013 under the ECMWF operational analysis data set. The details of this study are given in Section 6.2.1.

6.2.1. Comparison of E10 and E100 Wind Data

In this part of the study, firstly E10 and E100 wind speeds and wind directions are obtained from the "Operational Archive" located within the official ECMWF website (www.ecmwf.int). Since ECMWF start to include E100 wind data assimilation after 2011, there is no available E100 wind data within operational analysis data set covering the period of 2009-2010 which coincides with the period of land-based in-situ wind measurements. Thus, it is believed that using a longer period of 2011-2013 covering 3 years for the aim of achieving representative α coefficient applicable for vertical conversions would be convenient. However, since only α coefficient for the sea directions (WSW-ESE sector) are needed, only E10 and E100 wind data of these directions are considered.

At first step, E10 and E100 wind speeds and directions are downloaded for 2011-2013 period, followed by the sorting out the wind directions other than WSW-ESE sector. SimultaneousE10 and E100 wind speeds and directions are plotted in Figure 6.1 and 6.2, respectively to see the general differences and trends.

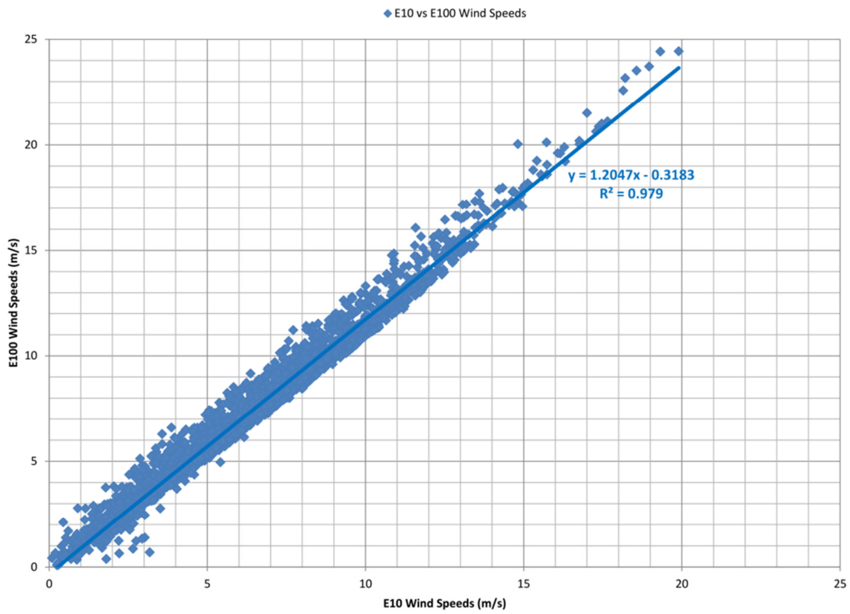

Figure 6.1: E10 Wind Speeds vs E100 Wind Speeds

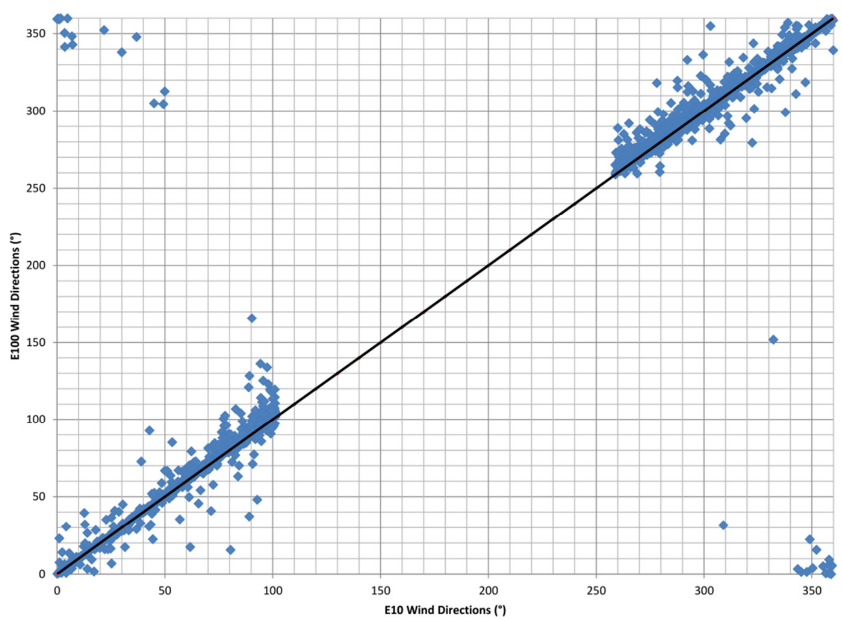

Figure 6.2: E10 Wind Directions vs E100 Wind Directions

The results indicate that E100 wind speeds are slightly higher than E10 wind speeds which are expected. In Figure 6.2, the relation between E10 and E100 wind speeds are presented as best fit with the following equation;

$$E100 = 1.2047E10 - 0.3183 \qquad [6.3]$$

In addition to linear best fit, the mean and standard deviation values for E100/E10 wind speed ratios are also calculated and the relationship between E100 and E10 wind speeds is found as;

$$E100 = (1.14 \pm 0.18)E10 \qquad [6.4]$$

As for Figure 6.2, the plotted simultaneous E100 and E10 wind directions indicate that overall harmony between them is good. The dots situated at upper right corner and lower left corner of Figure 6.2 is the reason attributed to the circular nature of the data that is plotted. Since the reference direction, N, is denoted as 0° and the directional angles increase in clockwise direction up to 360 which also denotes, N direction, the aforementioned dots in upper right and lower left corners represent the winds blowing from northern sector with E100 and E10 winds have slight differences, one blowing from the right side of 0°, other blowing from the left side of 0°.

In order to have a better understanding of the E100-E10 wind directional differences, mean directional difference and its standard deviation is calculated from E100 and E10 wind directions. The directional differences are calculated in absolute values and the formulization is arranged to take into account the northern sector where sudden directional changes between angles due to 0°-360° interface. The results indicate that E100-E10 directional difference 2.7° ± 7.1°, meaning that the difference is almost within -5° - +10° range. This can be assessed as E100 and E10 winds almost blow from the same sector with slight directional changes in between elevations of 10 m and 100 m.

Moreover, in order to understand if wind speeds play some role in these directional differences, E10 wind speeds are plotted against E100-E10 wind direction differences in Figure 6.3. The directional differences are presented in sectoral forms for the relevant figures.

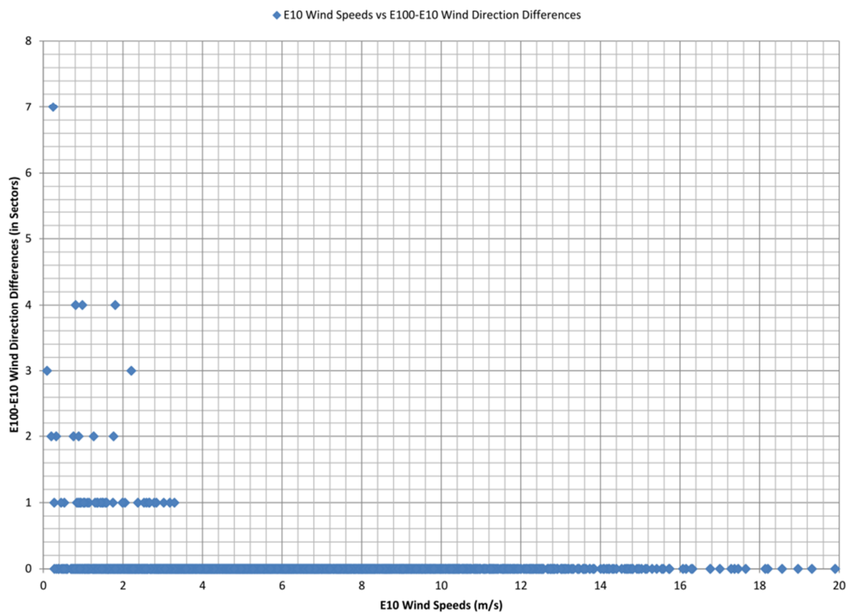

Figure 6.3: E10 Wind Speeds vs E100-E10 Wind Direction Differences

As seen in Figure 6.3, as E10 wind speeds decrease, there is a tendency for directional change for the winds. This may be attributed to the effect of surface roughness on lower wind speeds. However, a definite conclusion is hard to obtain only by looking into Figure 6.3. In addition to this representation, atmospheric stability conditions also need to be searched to reach a precise enough conclusion.

Since it is observed that wind speeds smaller than a certain value is affected more by certain factors, it is thought to perform additional observations if it is the same for wind speed differences. For this aim Figure 6.4 is prepared in which E100-E10 wind speed differences are plotted instead of wind speed differences, which is a different representation of relations between E10 and E100 wind speeds.

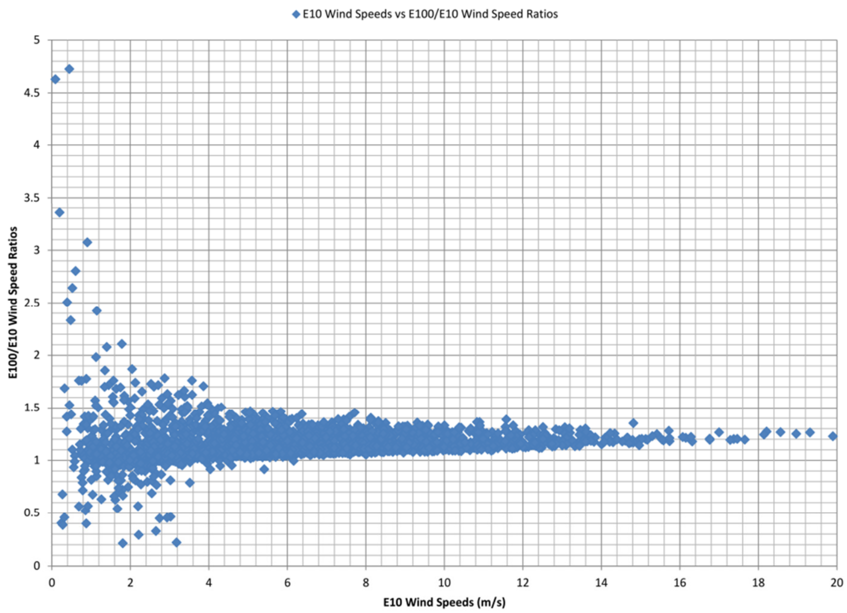

Figure 6.4: E10 Wind Speeds vs E100/E10 Wind Speed Ratios

It is comprehended from Figure 6.4 that as E10 wind speeds increase, E100/E10 wind speed ratios tend to converge to a slightly higher value than 1.14 which was previously specified as the average E100/E10 wind speed ratio. As for smaller wind speeds, the E100/E10 wind speed ratios have wider range, which may be the clue of a similar conclusion reached for E10 wind speeds vs E100-E10 wind direction differences.

Furthermore, in order to see if there is any trend of E100-E10 wind direction differences and E100/E10 wind speed ratios for certain directions Figure 6.5 and Figure 6.6 are prepared.

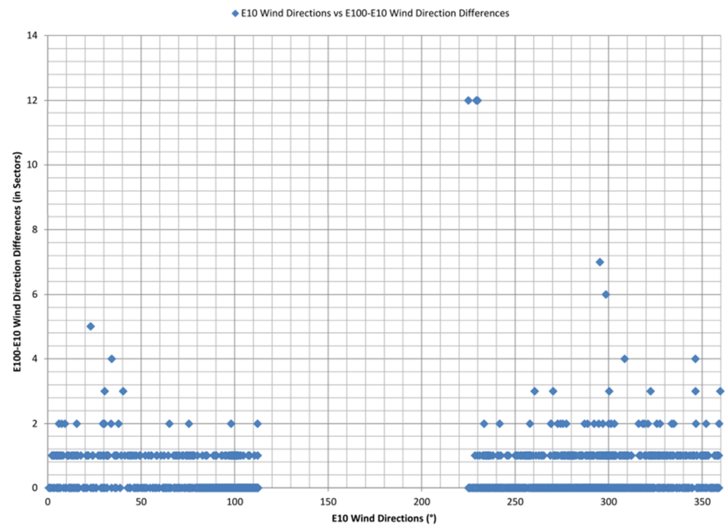

Figure 6.5: E10 Wind Directions vs E100-E10 Wind Direction Differences

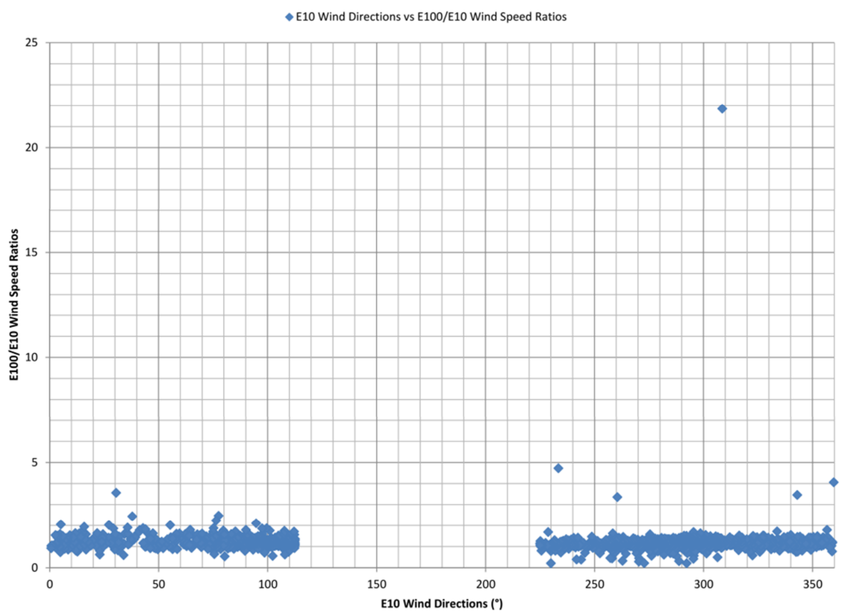

Figure 6.6: E10 Wind Directions vs E100/E10 Wind Speed Ratios

It is observed from both figures (Figure 6.5 and 6.6) that there is not a certain trend neither between E100-E10 wind direction differences and E10 wind directions nor between E100/E10 wind speed ratios and E10 wind directions.

After concluding the comparisons between E10 and E100 wind speeds and directions, in order to achieve a meaningful and representative vertical profile that can be represented as a power law relation between E10 and E100 wind speeds, α coefficients are found using the E10 and E100 wind speeds. In Figure 6.7, general trend of α coefficients with respect to E10 wind speeds are presented. In Figure 6.8, E10 wind directions are plotted against the corresponding α coefficients.

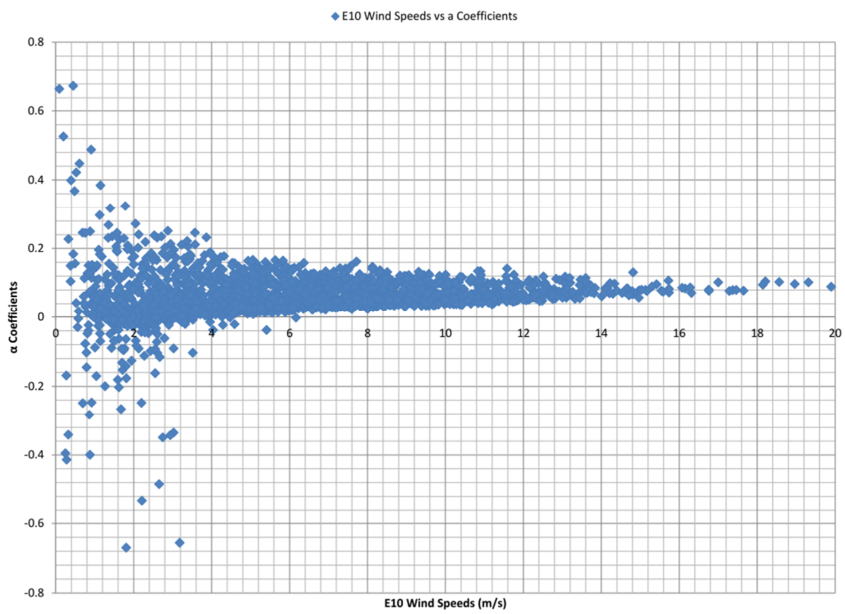

Figure 6.7: E10 Wind Speeds vs α Coefficients

In Figure 6.7, it is seen that α coefficients converge to a slightly higher value for higher E10 wind speeds than the average values observed for smaller E10 wind speeds. This is a similar finding like the one for Figure 6.4 which involves relationships between E10 wind speeds and E100/E10 wind speed ratios. For lower wind speeds, α coefficients show wider range, even negative values are determined which indicates that E100 wind speeds are smaller than E10 wind speeds. Looking into Figure 6.8, there seems to be no direction relation between E10 wind directions and α coefficients.

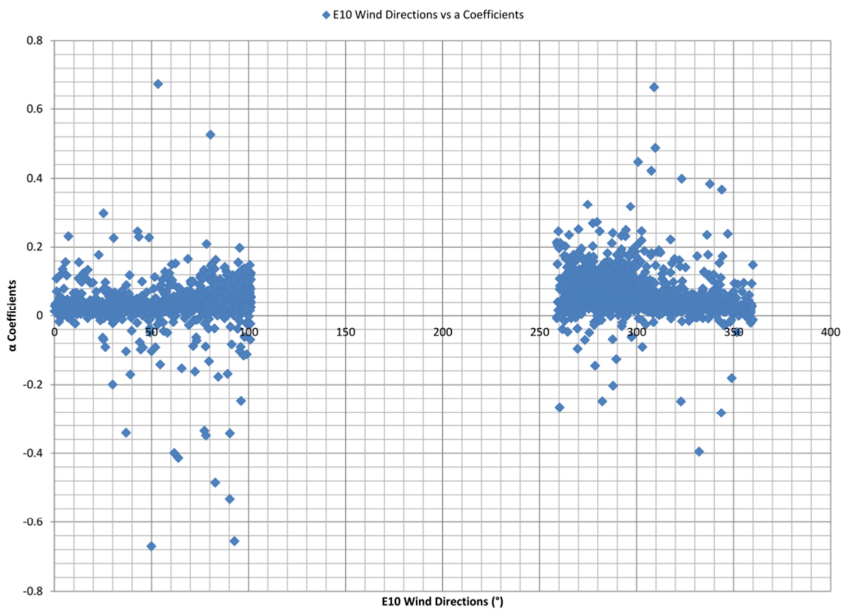

Figure 6.8: E10 Wind Directions vs α Coefficients

Considering that α coefficients and their ranges differ for E10 wind speeds, it is considered to obtain α coefficients for different E10 wind speed classes. The results are shown in Table 6.2 covering mean and standard deviation values.

The results in Table 6.2 show that the average condition at E10 location (42.20°N – 34.90°E) is unstable air above open water surface with occasional neutral air above open water surface conditions and very rarely unstable air above flat open coast. With the rarely observed conditions of unstable air above flat open coast, the location is proofed to be regarded as sea according to ECMWF wind data. The rare unstable air above flat open coast may be the results of its proximity to land, which is around 12 km.

It is also important to decide which α coefficients given in Table 6.2 to use in vertical conversion of wind speeds. In order to have an idea, E100 wind speeds are calculated using E10 wind speeds and mean α coefficients for different E10 wind speed classes and the results are plotted in Figures 6.9 to 6.13. E100 wind speeds calculated by suing the vertical profile and mean α coefficients are regarded as "Calculated E100

Wind Speeds" in the related figures. E10 wind speed classes and corresponding α coefficients that are used are summarized as;

- Mean α coefficients for all E10 wind speeds in Figure 6.9,
- Mean α coefficients for "E10 ≥ 10 m/s", "5 m/s ≤ E10 < 10 m/s", "3 m/s ≤ E10 < 5 m/s" and "E10 < 3 m/s" wind speed classes in Figure 6.10,
- Mean α coefficients for "E10 ≥ 5 m/s", "3 m/s ≤ E10< 5 m/s" and "E10 < 3 m/s" wind speed classes in Figure 6.11,
- Mean α coefficients for "E10 ≥ 3 m/s" and "E10 < 3 m/s" wind speed classes in Figure 6.12,
- Mean α coefficients for "E10 ≥ 15 m/s", "10 m/s ≤ E10 < 15 m/s", "5 m/s ≤ E10 < 10 m/s", "3 m/s ≥ E10 > 5 m/s" and "E10 < 3 m/s" wind speed classes in Figure 6.13,

Table 6.2: α coefficients for different E10 wind speed classes

Wind Speed Classes	α Coefficients
	Mean Value ± Standard Deviation
All	0.053 ± 0.059
E10 ≥ 10 m/s	0.073 ± 0.022
5 m/s ≤ E10 < 10 m/s	0.060 ± 0.032
3 m/s ≤ E10 < 5 m/s	0.047 ± 0.042
E10 < 3 m/s	0.039 ± 0.012
E10 ≥ 5 m/s	0.062 ± 0.030
E10 ≥ 3 m/s	0.057 ± 0.039
E10 ≥ 15 m/s	0.086 ± 0.011
10 m/s ≤ E10 < 15 m/s	0.072 ± 0.022

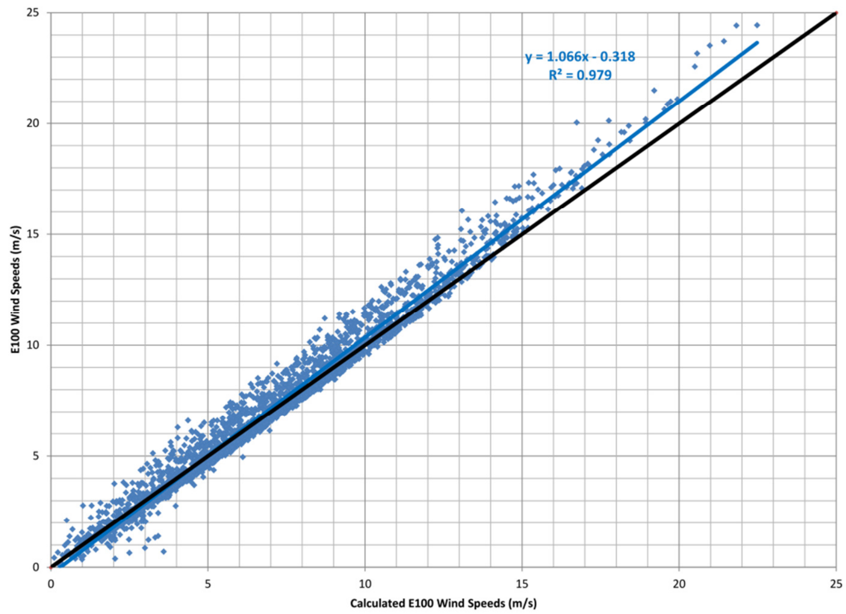

Figure 6.9: Calculated E100 Wind Speeds vs E100 Wind Speeds 1

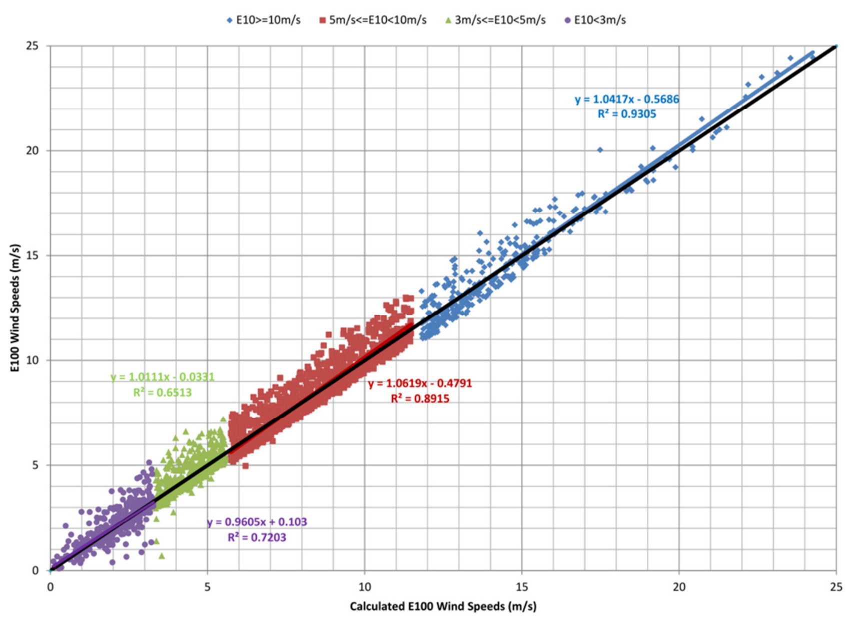

Figure 6.10: Calculated E100 Wind Speeds vs E100 Wind Speeds 2

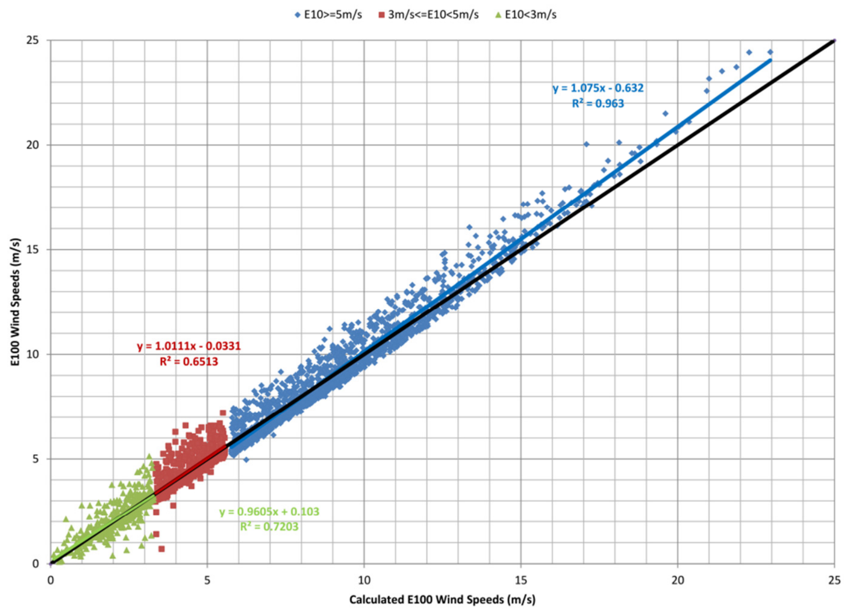

Figure 6.11: Calculated E100 Wind Speeds vs E100 Wind Speeds 3

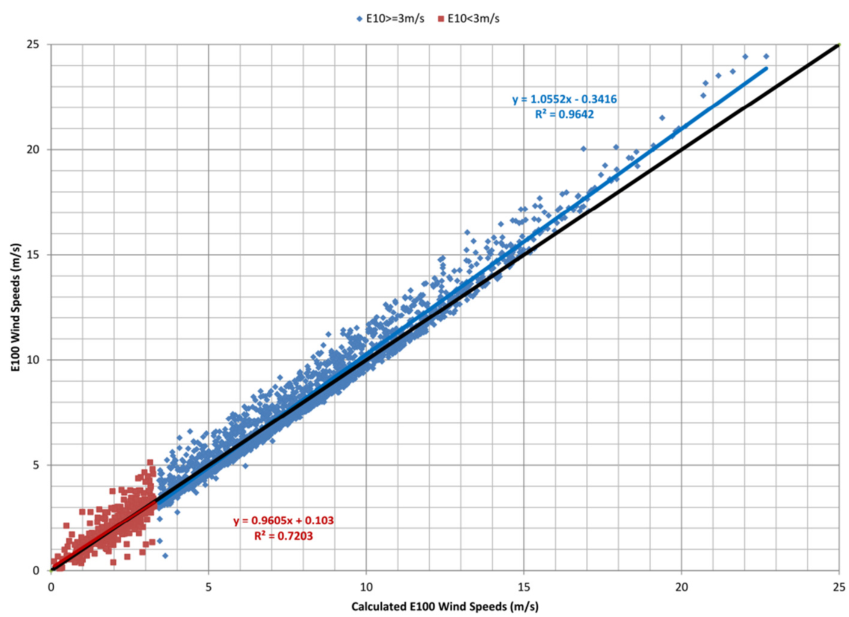

Figure 6.12: Calculated E100 Wind Speeds vs E100 Wind Speeds 4

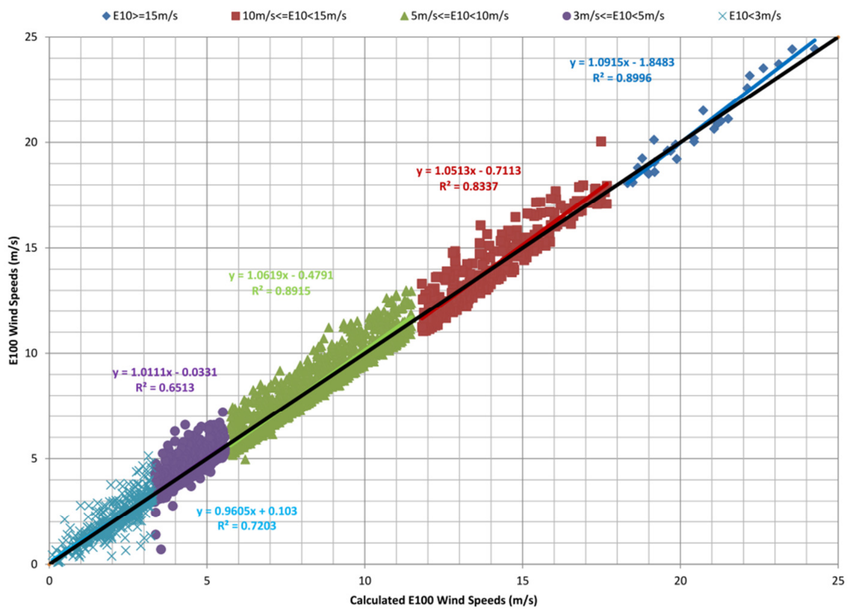

Figure 6.13: Calculated E100 Wind Speeds vs E100 Wind Speeds 5

Analyzing Figure 6.9-6.13, it is observed that as the number of data increases, R^2 increases and the more E10 wind speeds divided into wind speed classes, thesmaller R^2values are, which is also seen in the standard deviation values given in Table 6.2.

On the other hand, it would be slightly advantageous to use mean α coefficient values for various E10 wind speed classes, especially when it is considered that for higher wind speeds, α coefficients increase, thus in case of using mean α coefficients for few E10 wind speed classes or for all E10 wind speeds, there would be an underestimation for higher wind speeds which is very critical in terms of extreme wave studies in coastal engineering applications. Therefore, it is decided to use different mean α coefficients for E10 wind speed classes of "E10 ≥ 15 m/s", "10 m/s ≤ E10 < 15 m/s", "5 m/s ≤ E10 < 10 m/s", "3 m/s ≥ E10 > 5 m/s" and "E10 < 3 m/s" for the upcoming studies.

6.2.2. Comparison of S10 Wind Speeds and E10 Wind Speeds

To start with, using the mean α coefficients for different E10 wind speed classes as mention above, S10 wind speeds are obtained using S60 wind speeds. The results are plotted into figures and arranged in Appendix A. It can be seen from the figures in Appendix A that, while the horizontal conversion of L60 wind speeds cause increase in wind speeds on sea, which are denoted as S60, the vertical conversion of S60 wind speeds to 10 m above MSL cause decrease in wind speeds and the resulting wind speeds 10 m above MSL are regarded as S10 wind speeds.

The second stage is to observe the relationship between S10 and E10 wind speeds and to see if the results are in parallel with the previous studies in the literature for enclosed and semi-enclosed basins such as the Black Sea. It should be noted that the studies mentioned in Chapter 2 are all performed in the Mediterranean Sea which is an enclosed basin, the Adriatic Sea and the Aegean Sea, which are within Mediterranean Sea basin but regarded as semi-enclosed basins. The findings will affirm that the aforementioned studies, assumptions' and calculations are applicable and good choices.

Initially, S10 and E10 wind speeds are plotted as figures for the chosen 29 continuous data set (Appendix B). 6 hourly E10 wind speeds are plotted as single dots for their corresponding hours, whereas hourly S10 wind speeds are plotted with smooth line in order to easily observe changing trends of S10 wind speeds. At this stage, since there is no indication on which representation of 6 hourly E10 wind speeds, in other terms how to combine 6 hourly E10 wind speeds to represent hourly E10 wind speeds, would give better correlations between E10 and S10 wind speeds, 6 hourly E10 wind speeds are not linked to each other.

Although it is hard to have an overall idea of the correlation between 6 hourly E10 and hourly S10 wind speeds due to few number of comparative data attributed to the 6 hour time interval of E10 wind speeds, it can be said that except a few hours of data, S10 wind speeds are higher than E10 wind speeds. Thus, it can be concluded that ECMWF underestimates wind speeds. It is really hard to specify anything related to the underestimation values by visual observation only.

Therefore, in addition to the graphical representation of hourly S10 and 6 hourly E10 wind speed differences, it would be quite good to have a numerical understanding of the situation in terms of S10/E10 wind speed ratios for 6 hour intervals. These values are calculated considering all of the 6 hourly wind speeds of 29 continuous data sets coinciding with E10 wind speed data times. The results are summarized in Table 6.3. Moreover, in order to have a better idea, S10-E10 wind speed differences also calculated and the results are given in Table 6.3.

Table 6.3: S10/E10 wind speed ratios for various S10 wind speed classes considering 6 hourly wind data

Wind Speed Classes	S10/E10 Wind Speed Ratios	S10-E10 Wind Speed Differences
	Mean Value ± Standard Deviation	Mean Value ± Standard Deviation
All	1.65 ± 1.28	2.82 ± 2.10
S10 ≥ 15 m/s	1.46 ± 0.21	5.24 ± 1.86
10 m/s ≤ S10 < 15 m/s	1.50 ± 0.48	3.44 ± 1.69
5 m/s ≤ S10 < 10 m/s	1.65 ± 0.85	2.26 ± 1.88
3 m/s ≤ S10 < 5 m/s	1.76 ± 1.47	0.82 ± 1.55
S10 < 3 m/s	5.19 ± 7.79	0.61 ± 1.69

The values in Table 6.3 makes it possible to observe while 6 hourly E10 wind speeds are underestimated in general, the underestimation is higher for higher wind speeds meaning that peaks in storms are possibly missed, which can also be seen in figures in Appendix C. It may also be said that for atmospheric conditions of S10< 5 m/s, some E10 wind speeds are higher than S10 wind speeds.

Simultaneous 6 hourly S10 and E10 wind speeds are plotted in Figure 6.14 to see if there is a correlation that may describe the aforementioned underestimation. In Figure 6.14, both y=Ax+B type and y=Ax type best fits are drawn and R^2 values are also specified in the figure.

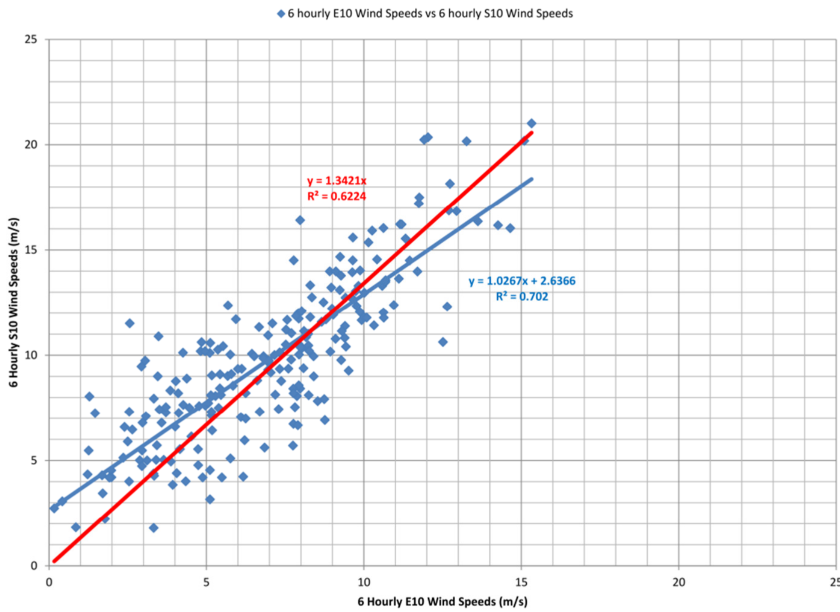

Figure 6.14: 6 Hourly E10 Wind Speeds vs 6 Hourly S10 Wind Speeds

It is seen that a y = Ax + B type best fit between 6 hourly S10 and E10 wind speeds have higher R^2 value. Therefore, instead of using a y=Ax type correlation, a y = Ax + B type correlation may work better for modifying 6 hourly E10 wind speeds.

However, it should be noted that performing comparisons only for 6 hourly wind data would much likely be not enough for obtaining a correlation so that overall representation of S10 wind speed changes by modified E10 wind speeds can be achieved. Moreover, variability of wind measurements performed at coastal areas is significantly higher than that of offshore wind measurements due to several reasons. These reasons some of which are shown in Figure 6.14 can be summarized as;

- Sea breeze
- Land breeze (i.e. mountain slope winds)
- Turbulence

A sea breeze is a gentle wind that develops over water bodies near land due to differences in air pressure created by different heat capacities of land and sea. It is commonly observed along coasts during morning due to the fact that solar radiation heats the land more quickly than water (Ackerman, 1995).

A land breeze is the reverse of sea breeze, caused by more quickly cooling of land compared to water in the evening. The sea breeze dissipates and the wind flows from the land towards the sea (Ackerman, 1995).

Turbulence is defined as the small-scale, irregular air motions characterized by winds that vary in speed and direction. It is important because it mixes and churns the atmosphere and causes water vapor, smoke, and other substances, as well as energy, to become distributed both vertically and horizontally. Turbulence near Earth's surface differs from that at higher levels. At low levels (within a few hundred meters of the surface), turbulence has a marked diurnal variation under partly cloudy and sunny skies, reaching maximum about midday (www.brittanica.com).

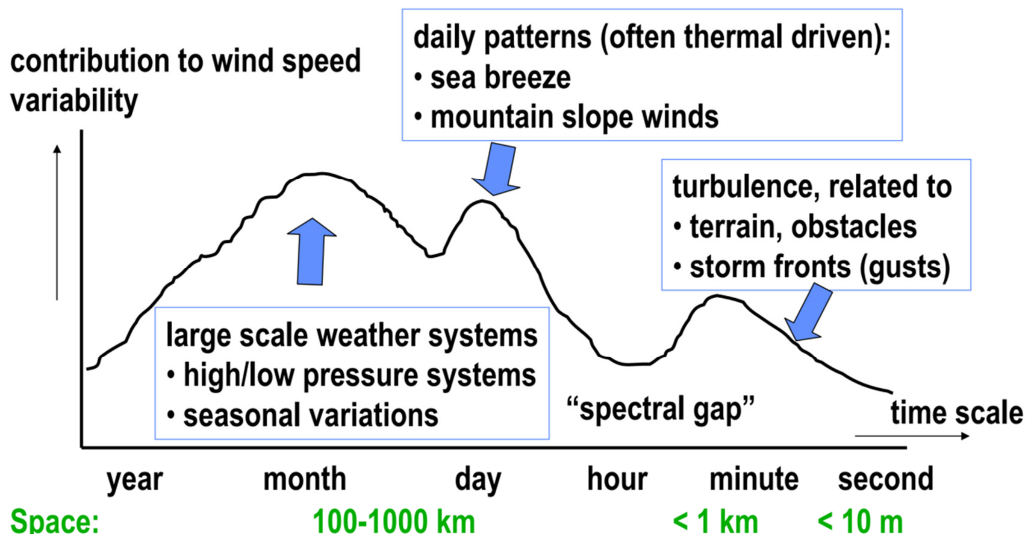

Figure 6.15: Variability of Winds (Bierbooms, 2006)

Figure 6.15 shows possible variability in wind speeds. This variability is very important, since they may influence the wave climate of the region significantly. Especially, sea breezes may have important impacts on wave climate during several months or seasons. Neetu et al (2006) showed that during November-May period where sea breezes dominate the coastal regions of India, a single event indicated that the average fetch distance along which sea breezes are dominant is 77 km with a standard deviation of 43 km. Aboobacker et al (2014) performed a similar study for the same region and found that sea breeze induces wind seas are generated roughly around 210 km off Goa in northwest direction. He also concludes that due to very limited fetch for land breezes, they have no significant effect on wind sea generation. It should be noted that the shortest fetch for the related location that both studies are performed is approximately 1700 km and the longest fetch is around 10000 km. Compared to those distances, 210 km is very small, but on the other hand since sea breezes are active during seasons of weak large scale winds, it is naturally expected that they have influence in wave generation. As for Black Sea coast of Turkey or for the study site, there is no reference information regarding local sea and land breeze patterns.

In addition to the information given above, among several previous studies mentioned in Chapter 2, how the data may be smoothed to overcome these effects are discussed for situations when limited data is available. Cavaleri and Bertotti (1997) mentions that the lack of data can be overcome by locally smoothing the wind fields, meaning smoothing the improperly resolved small-scale features in the wind data.

Depending on the findings of Cavaleri and Bertotti (1997) and taking into account the aforementioned information on factors causing variability of wind speeds, it is decided to overcome high variability in the wind data so that a general and smoothed trend may be obtained. It is natural to expect that it would be easier to resemble this smoothed trend with modified E10 wind speeds.

Even though, the smoothing of S10 wind speeds are performed, it would not be easy to find correlations to modify 6 hourly E10 wind speeds to resemble 6 hourly S10 wind speeds based only on simple comparisons, since the total number of data that can be used is 222. Moreover, there is a possibility that the correlations may vary for different wind conditions such as storm peaks, increasing wind speeds, decreasing wind speeds, downs, and etc. which are also observed in figures in Appendix C. The seasonal and directional variations are not even mentioned here because there is not enough data to perform these studies even though hourly wind speed comparisons may be performed. Especially concerning seasonal comparisons, the data of at least 2 consecutive data of the same season is needed, which roughly means that at least 2 year data is needed.

On the other hand, these new comparisons regarding different wind conditions cannot be performed with only 222 data. There is a need to increase the available 6 hourly E10 wind data. This can only be achieved by obtaining E10 wind speeds at smaller time intervals such as hourly E10 wind speeds.

As mentioned in Chapter 1, one of the aims of this thesis study is to be able to obtain hourly E10 wind speeds and another one is to be able to modify E10 wind speeds to successfully resemble S10 wind speeds or in other terms, to obtain modified E10 wind speeds with good representation of wind speeds during storms.

With application of this new and somehow complicated method to increase E10 wind speed data points, performing comparative studies to find correlations for different wind conditions and modifying obtained hourly E10 wind speeds, all of the stated aims would be achieved.

In this method, the first step would be to obtain hourly E10 wind speeds by adapting and applying a certain approach. In this approach, successive 6 hourly E10 wind speeds would be linked to each other with easily applicable mathematical relations. It is also thought that the simpler the relation is, the easier its application is, and it is imperative that the decided approach would result in good connection between 6 hourly wind speeds so that the general trend of E10 wind speeds resemble the general trend of S10 wind speeds especially for storms.

There are two methods that may be applied in order to connect 6 hourly E10 wind speeds:

- Spline Method
- Linear Connection Method

In the spline method, each successive 3 data points (6 hourly E10 wind speeds) are defined using a different formula and the data in between each 6 hour interval is obtained from these formulations. Since different formulas are applied to each successive 3 data point, this can only be performed with a numerical program such as MatLAB. It should be noted that for this method to be applied, there is a strong need for uninterrupted continuous data set. Since with adding or extracting of even one data at one of the boundaries of the data set, meaning changing the number of data points, almost all of the formulations change.

A simpler way to explain this method is providing a hypothetical example. Provided that only 5 successive 6 hourly wind data of a storm which actually consists of 8 successive 6 hourly wind data exists, the results of the spline method considering 5 data and 8 data would not be the same. It is expected to observe this situation very often for the 29 continuous data sets that are considered in this study, since most of these continuous data sets consist of certain parts of a storm event. Only a few of these data sets cover a storm event in total. Thus, the use of spline method should be considered and evaluated very thoroughly.

In the linear connection method, successive 6 hourly E10 wind speeds are connected to each other with simple linear lines. This means that with application of this method, it is assumed that there won't be any sudden changes within these 6 hour intervals. This assumption would definitely bring some uncertainty to the data set. On the other hand, it would make it simple forward to obtain a certain relationship between the smoothed S10 wind fields and E10 wind speeds. In addition, there won't be any problems for missing storm data as discussed previously for spline method.

Although the application of simple linear connection seems advantageous in terms of simplicity and applicability, it is also important to see which method gives better results in terms of its resemblance with S10 wind speeds. In order to observe this, the results of spline and linear connection methods are plotted in Figures 6.14-6.25 for several of the 29 continuous data sets. The data sets are chosen randomly. Moreover, in order to better understand the general trend similarities, S10 wind speeds are also smoothed. The smoothing process has been performed in the following steps:

- At first, S10 wind speeds are smoothed by designating the average of 5 consecutive hourly S10 wind speeds to the middle point. This is more easily observed in equation 6.5. These average values are denoted as $S10_{ave}$.
- Since enough smoothing cannot be achieved by obtaining $S10_{ave}$ wind speeds, at second stage, 6 hourly $S10_{ave}$ wind speeds with linear line which is very similar to the method used for connecting 6 hourly E10 wind speeds. In several situations where the variability changes significantly, several modifications are performed such as skipping the middle (i) 6 hourly $S10_{ave}$ wind speeds and connecting the 6 hourly wind speeds at i-6 and i+6 times.
- In several continuous data sets, there are no resemblance between the trend of E10 wind speeds and S10 wind speeds, and in some cases there is no possibility for E10 wind speeds to reach the peaks of the storms. There are several possibilities for these situations some of which can be denoted as extremely undulating wind fields, time lack between S10 and E10 wind data, sudden small-scale features resulting in trend changes in either S10 or E10 wind speeds, and etc. During smoothing, since it would not be possible to modify E10 wind speeds for these cases due to limited wind data, these parts of the storms are not included in the smoothing process and sometimes the smoothing has missed these peaks. More data is needed and different methods such as artificial neural network applications should be applied considering seasonal and directional comparisons as specified by Weisberg and Pietrafesa (1983),

$$S10_i = (S10_{i-2} + S10_{i-1} + S10_i + S10_{i+1} + S10_{i+2})/5 \qquad [6.5]$$

The smoothed S10 wind speeds which are denoted as $S10_S$, $S10_{ave}$ wind speeds, hourly E10 wind speeds found by linear connection and spline methods are plotted in figures that are placed in Appendix D. In the related figures, E10 wind speeds that are connected with each other by spline method are denoted as “E10 Spline” and the linearly connected E10 wind speeds are regarded as “E10L”.

With the smoothed S10 wind fields and linearly connected E10 wind speeds, it would be possibly easier to come up with correlations between S10 and E10 wind speeds. The correlation process is given in full detail in the following section.

6.3. Studies on Correlation between S10 Wind Speeds and E10 Wind Speeds

As mentioned in Chapter 1, one of the aims of this study is to be able to obtain a modification method for E10 wind speeds so that E10 wind speeds may also be applied for durations where no in-situ wind measurements exist. Thus, achieving a general site-specific modification is regarded as one of the aims of the study.

Based on the visual observations of the figures in Appendix D for continuous data sets, it is observed that there may be different situations for decreasing and increasing wind speed conditions. In addition, each wind speed located in between 6 hour intervals may also have different modifications during increasing and decreasing wind speed conditions. Thus, for further comparisons, it is decided to divide the increasing wind speeds denoted as "developing winds" and decreasing wind speeds regarded as "calming winds". Developing winds and calming winds are also subdivided depending on the relationship between four successive 6 hourly E10 wind speeds. This situation is explained graphically in Figure 6.16. The dots shown in Figure 6.16 denote the successive 6 hourly E10 wind speeds. Since these wind speeds are linearly connected, it would be best to represent the developing and calming winds by using 6 hourly original E10 wind speeds. The developing and calming wind types specified in Figure 6.16 are for the linear connected line in the middle denoted in dotted red ellipse. It is visually observed that the wind speed change or in other words slope of the previous and the next linear connection tend to change the relationship between E10 and $S10_S$ wind speeds.

Before starting to categorize into 8 different types as given in Figure 6.16, in order to see the impact of smoothing of the wind fields in R^2 values as well as the correlation between hourly E10, $S10_S$, $S10_{ave}$ wind speeds and hourly S10 wind speeds, Figure 6.17 is prepared. As seen in Figure 6.17, the linearized connection between 6 hourly E10 wind speeds do not cause any problems in terms of correlation coefficient whereas R^2 value is slightly bigger than the R^2 value of correlation between 6 hourly E10 and S10 wind speeds. This is a good indication that linear connection method may be implemented for linking 6 hourly E10 wind speeds. It is also seen in Figure 6.16 that R^2 values are 0.96 and 0.85 respectively for $S10_{ave}$ vs S10 and $S10_s$ vs S10 wind speeds. This shows that the smoothing slightly increases the wind speed differences between S10 and $S10_s$ winds. While assessing the R^2 values, the fact that some of the data sets do not show good relationship between S10 and S10s wind speed trends due to the fact that small scale features, seasonal variations, and so on are observed. Therefore, it would be better to evaluate these values for standard storms and example of which can be seen in Figure D24 in Appendix D.

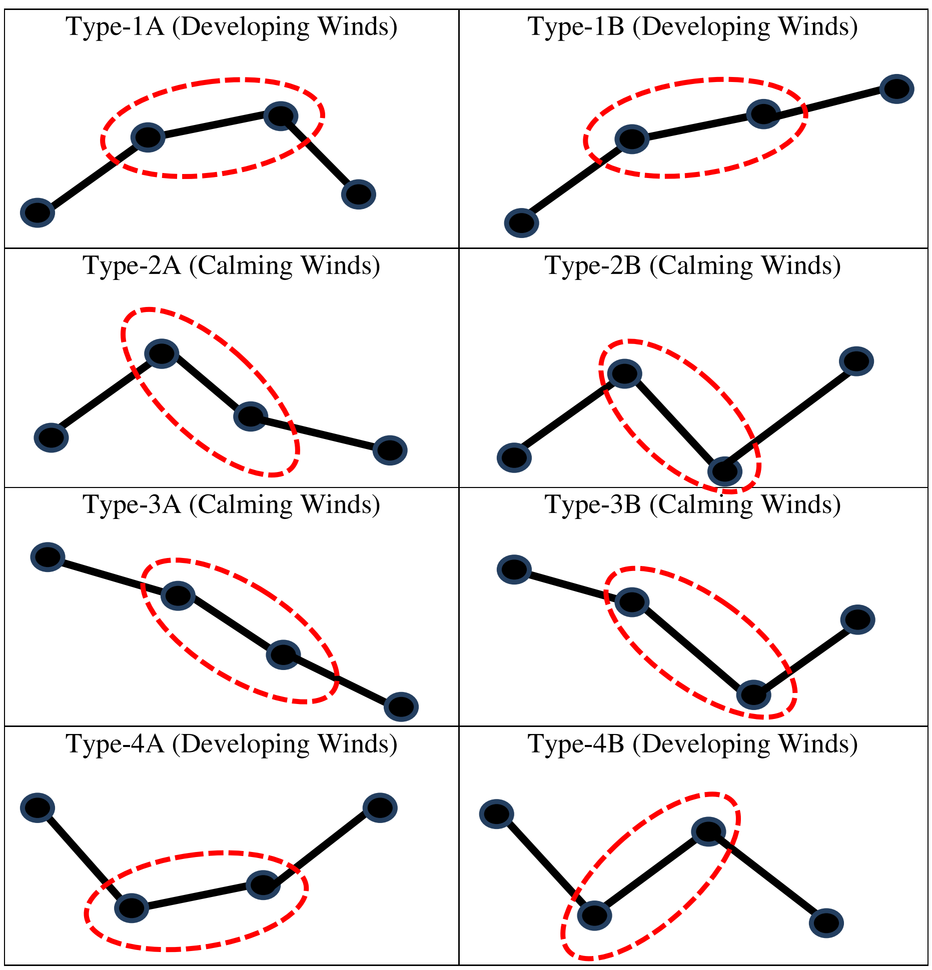

Figure 6.16: Developing and Calming Wind Types

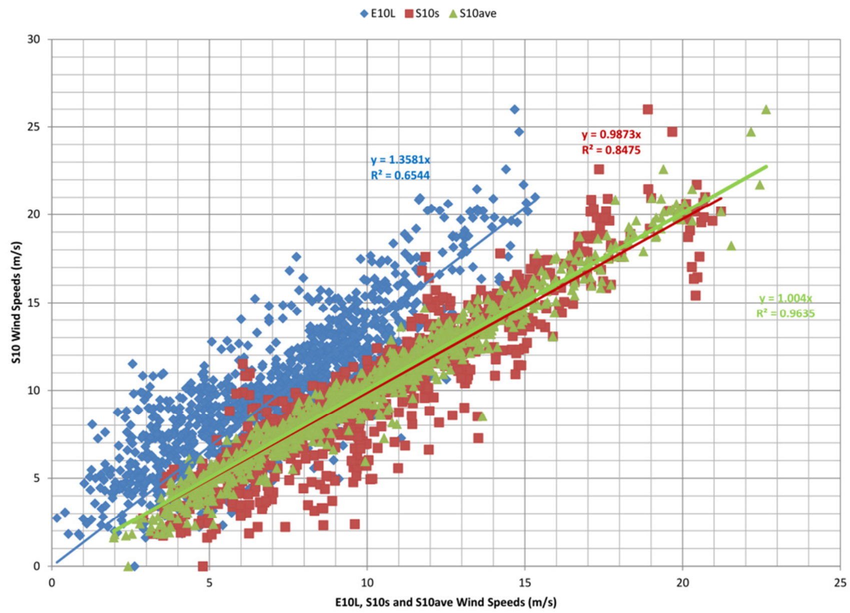

Figure 6.17: Correlations between E10L, $S10_S$, $S10_{ave}$ Wind Speeds and S10 Wind Speeds

The comparative studies have been performed considering that the first two points, the middle two points and the last two points of successive 6 data points on developing and calming winds for all types have different modifications. This assumption is considered to see if the behavior of the developing and calming winds change in time. This is more easily observed in Figure 6.18 giving a schematic view of this explanation.

Four different comparisons are performed and these are described as:

- Method 1: The first two, middle two and the last two points of the calming and developing winds are handled separately for each type and the data sets are arranged in a descending order based on E10 wind speeds. S10s/E10 wind speed ratios are calculated and E10 wind speeds are plotted against their corresponding S10s/E10 wind speed ratios. This is performed in order to see if best fits can be attributed to these graphs so that modifications can be related to E10 wind speeds by formulation. Thus, for different wind speed classes, formulas are obtained to calculate modification coefficients.

- Method 2: Just like in Method 1, the first two, middle two and the last two points are considered together. In this method, the developing and calming winds are categorized according to the wind speed differences between two successive points on the same linear line. This would give an idea if there is any relationship between the speed at which storms develop or calm and the correlations between $S10_s$ and E10 wind speeds. Furthermore, after categorizing according to wind speed change between two consecutive points on a linear line, which will be denoted as "Δ" from now on, a further categorization is performed according to the E10 wind speeds as well. The modification coefficients for each sub-category are found by calculating the mean $S10_s$/E10 wind speed ratios.
- Method 3: This method follows the same steps as Method 2 but at the end for each sub-category, the modification coefficients are related to formulations depending on E10 wind speeds just like in Method 1.
- Method 4: In this method, the same process I followed described in Method 1 except that at the final stage, the correlation between E10 and $S10_s$ wind speeds are calculated as mean $S10_s$/E10 wind speed ratios for different E10 wind speed categories.

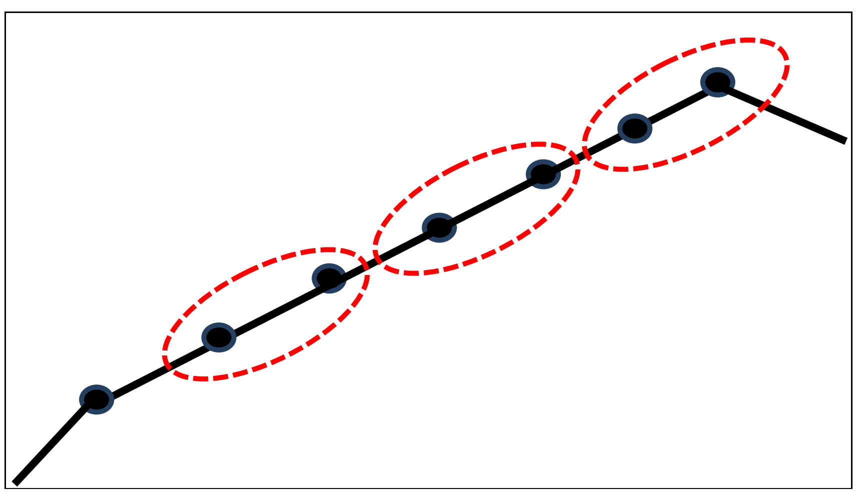

Figure 6.18: Schematic View of Categorization for Modification Studies

The results are given in graphical forms in Appendix E for Methods 1 and 3, whereas the tabulated form of the results are provided in the below tables (Table 6.4-Table

6.35). In these tables, the modification coefficient between $S10_s$ and E10 is denoted as “Mod”. After linear connection of 6 hourly E10 wind speeds, the amount of data that can be used in comparisons are increased 6 times. This provides opportunity to sort the data into several categorizes depending on the wind speed changes and 6 hourly wind speed change trend of a linear line with respect to the previous and next linear lines. Moreover, sorting the wind speeds according to their magnitudes is also considered. As a result, the increased number of data sets is subdivided, resulting in smaller sized data sets for each sub category. Although this brings some disadvantages due to smaller data sets to compare, it is believed that most of the comparisons will provide good and representable enough results in terms of correlations between E10 and $S10_s$. By looking into figures given in Appendix E, it is obviously concluded that for most of the categories, data size is quite good. On the other hand, for some comparisons, the data size is not big enough to get well enough results. However, as there is no additional wind data for this region, it is decided to continue with the results of these comparisons and use the modifications found in each method to estimate modified E10 wind speeds.

Table 6.4: Method 1 Results for Modification Coefficients (Type-1A)

Points	Wind Speed Classes	Modification Coefficient (Mod)
1-2	$E10 \geq 8.75$ m/s	$Mod = 0.0065\ E10 + 1.1898$
	$E10 < 8.75$ m/s	$Mod = 3.0068\ E10^{-0.405}$
3-4	$E10 \geq 9$ m/s	$Mod = 0.0052\ E10 + 1.2196$
	$E10 < 9$ m/s	$Mod = 2.7688\ E10^{-0.353}$
5-6	$E10 \geq 9$ m/s	$Mod = 0.0017\ E10 + 1.2765$
	$E10 < 9$ m/s	$Mod = 2.9109\ E10^{-0.379}$

Table 6.5: Method 2 Results for Modification Coefficients (Type-1A)

Points	Δ Classes	Wind Speed Classes	Mean ± Standard Deviation (Mod)
1-2	Δ ≥ 0.35	E10 ≥ 5 m/s	1.32 ± 0.09
		E10 < 5 m/s	2.16 ± 0.15
	0.35 > Δ ≥ 0.05	All E10's	1.24 ± 0.08
	Δ < 0.05	E10 ≥ 6 m/s	1.35 ± 0.10
		E10 < 6 m/s	1.87 ± 0.01
3-4	Δ ≥ 0.35	E10 ≥ 6 m/s	1.30 ± 0.10
		E10 < 6 m/s	1.82 ± 0.10
	0.35 > Δ ≥ 0.05	All E10's	1.26 ± 0.08
	Δ < 0.05	E10 ≥ 6 m/s	1.37 ± 0.07
		E10 < 6 m/s	1.89 ± 0.01
5-6	Δ ≥ 0.35	E10 ≥ 7 m/s	1.29 ± 0.13
		E10 < 7 m/s	1.57 ± 0.07
	0.35 > Δ ≥ 0.05	All E10's	1.28 ± 0.11
	Δ < 0.05	E10 ≥ 6 m/s	1.40 ± 0.04
		E10 < 6 m/s	1.91 ± 0.01

Table 6.6: Method 3 Results for Modification Coefficients (Type-1A)

Points	Δ Classes	Wind Speed Classes	Modification Coefficient (Mod)
1-2	Δ ≥ 0.35	E10 ≥ 9 m/s	Mod = -0.0294 E10 + 1.5666
		E10 < 9 m/s	Mod= 3.6355 $E10^{-0.479}$
	0.35 > Δ ≥ 0.05	All E10's	Mod= 1.3877 $E10^{-0.055}$
	Δ < 0.05	All E10's	Mod= 3.2804 $E10^{-0.38}$
3-4	Δ ≥ 0.35	All E10's	Mod= 2.8993 $E10^{-0.354}$
	0.35 > Δ ≥ 0.05	All E10's	Mod = 1.509 $E10^{-0.083}$
	Δ < 0.05	All E10's	Mod = 3.0606 $E10^{-0.339}$
5-6	Δ ≥ 0.35	All E10's	Mod = 2.3637 $E10^{-0.259}$
	0.35 > Δ ≥ 0.05	All E10's	Mod = 1.6413 $E10^{-0.112}$
	Δ < 0.05	All E10's	Mod = 2.8813 $E10^{-0.302}$

Table 6.7: Method 4 Results for Modification Coefficients (Type-1A)

Points	Wind Speed Classes	Mean ± Standard Deviation (Mod)
1-2	$E10 \geq 5$ m/s	1.28 ± 0.10
	$E10 < 5$ m/s	1.78 ± 0.39
3-4	$E10 \geq 5.5$ m/s	1.29 ± 0.09
	$E10 < 5.5$ m/s	1.69 ± 0.25
5-6	$E10 \geq 6.5$ m/s	1.30 ± 0.11
	$E10 < 6.5$ m/s	1.63 ± 0.22

Table 6.8: Method 1 Results for Modification Coefficients (Type-1B)

Points	Wind Speed Classes	Modification Coefficient (Mod)
1-2	$E10 \geq 7$ m/s	Mod = -0.0113 E10 + 1.3996
	$E10 < 7$ m/s	$Mod = 2.3208\ E10^{-0.305}$
3-4	$E10 \geq 8$ m/s	Mod= -0.0021 E10 + 1.2991
	$E10 < 8$ m/s	$Mod = 2.2677\ E10^{-0.281}$
5-6	$E10 \geq 8$ m/s	Mod= -0.0016 E10 + 1.2774
	$E10 < 8$ m/s	$Mod = 2.1699\ E10^{-0.261}$

Table 6.9: Method 2 Results for Modification Coefficients (Type-1B)

Points	Δ Classes	Wind Speed Classes	Mean ± Standard Deviation (Mod)
1-2	$\Delta \geq 0.20$	All E10's	1.31 ± 0.09
	$\Delta < 0.20$	$E10 \geq 12$ m/s	1.28 ± 0.00
		4.5 m/s $\leq E10 < 12$ m/s	1.32 ± 0.18
		$E10 < 4.5$ m/s	1.80 ± 0.15
3-4	$\Delta \geq 0.20$	All E10's	1.27 ± 0.06
	$\Delta < 0.20$	$E10 \geq 11.5$ m/s	1.23 ± 0.06
		4.5 m/s $\leq E10 < 11.5$ m/s	1.35 ± 0.15
		$E10 < 4.5$ m/s	1.74 ± 0.07
5-6	$\Delta \geq 0.20$	All E10's	1.24 ± 0.12

Table 6.9 (continued)

	$\Delta < 0.20$	E10 $\geq$ 11.5 m/s	1.29 ± 0.00
		4.5 m/s $\leq$ E10 < 11.5 m/s	1.33 ± 0.14
		E10 < 4.5 m/s	1.69 ± 0.02

Table 6.10: Method 3 Results for Modification Coefficients (Type-1B)

Points	Δ Classes	Wind Speed Classes	Modification Coefficient (Mod)
1-2	$\Delta \geq 0.20$	All E10's	Mod = 1.5628 $E10^{-0.09}$
	$\Delta < 0.20$	E10 $\geq$ 8 m/s	Mod = 0.087 E10 + 1.201
		E10 < 8 m/s	Mod= 2.343 $E10^{-0.294}$
3-4	$\Delta \geq 0.20$	All E10's	Mod = 1.4926 $E10^{-0.078}$
	$\Delta < 0.20$	E10 $\geq$ 8 m/s	Mod = -0.0045 E10 + 1.3515
		E10 < 8 m/s	Mod = 2.2669 $E10^{-0.273}$
5-6	$\Delta \geq 0.20$	All E10's	Mod = 1.4964 $E10^{-0.086}$
	$\Delta < 0.20$	All E10's	Mod = 2.0275 $E10^{-0.196}$

Table 6.11: Method 4 Results for Modification Coefficients (Type-1B)

Points	Wind Speed Classes	Mean ± Standard Deviation (Mod)
1-2	E10 $\geq$ 10 m/s	1.24 ± 0.05
	8 m/s $\leq$ E10 < 10 m/s	1.29 ± 0.13
	4 m/s $\leq$ E10 < 8 m/s	1.34 ± 0.14
	E10 < 4 m/s	1.80 ± 0.15
3-4	E10 $\geq$ 10 m/s	1.24 ± 0.05
	8 m/s $\leq$ E10 < 10 m/s	1.31 ± 0.11
	5 m/s $\leq$ E10 < 8 m/s	1.31 ± 0.12
	E10 < 5 m/s	1.74 ± 0.07
5-6	E10 $\geq$ 10 m/s	1.26 ± 0.11
	8 m/s $\leq$ E10 < 10 m/s	1.26 ± 0.14
	6 m/s $\leq$ E10 < 8 m/s	1.32 ± 0.13
	E10 < 6 m/s	1.69 ± 0.02

Table 6.12: Method 1 Results for Modification Coefficients (Type-2A)

Points	Wind Speed Classes	Modification Coefficient (Mod)
1-2	$E10 \geq 10$ m/s	Mod = 0.0037 E10 + 1.2904
	8 m/s $\leq E10 <$ 10 m/s	Mod= 0.0384 E10 + 0.9161
	$E10 < 8$ m/s	Mod= 2.6803 $E10^{-0.372}$
3-4	$E10 \geq 7$ m/s	Mod = 0.0116 E10 + 1.2252
	$E10 < 7$ m/s	Mod = 3.1364 $E10^{-0.441}$
5-6	$E10 \geq 7$ m/s	Mod= 0.0072 E10 + 1.3151
	$E10 < 7$ m/s	Mod= 3.6245 $E10^{-0.506}$

Table 6.13: Method 2 Results for Modification Coefficients (Type-2A)

Points	Δ Classes	Wind Speed Classes	Mean ± Standard Deviation (Mod)
1-2	$\Delta < -0.35$	$E10 \geq 10$ m/s	1.48 ± 0.04
		$E10 < 10$ m/s	1.26 ± 0.04
	$-0.20 > \Delta \geq -0.35$	$E10 \geq 10$ m/s	1.31 ± 0.13
		7 m/s $\leq E10 <$ 10 m/s	1.31 ± 0.11
		$E10 < 7$ m/s	1.50 ± 0.11
	$0 > \Delta \geq -0.20$	$E10 \geq 8$ m/s	1.18 ± 0.05
		$E10 < 8$ m/s	1.41 ± 0.11
3-4	$\Delta < -0.35$	$E10 \geq 9$ m/s	1.53 ± 0.02
		$E10 < 9$ m/s	1.38 ± 0.05
	$-0.20 > \Delta \geq -0.35$	$E10 \geq 10$ m/s	1.34 ± 0.13
		7 m/s $\leq E10 <$ 10 m/s	1.35 ± 0.10
		6 m/s $\leq E10 <$ 7 m/s	1.43 ± 0.09
		$E10 < 6$ m/s	1.85 ± 0.10
	$0 > \Delta \geq -0.20$	$E10 \geq 8$ m/s	1.20 ± 0.06
		$E10 < 8$ m/s	1.46 ± 0.03
5-6	$\Delta < -0.35$	$E10 \geq 9$ m/s	1.58 ± 0.04
		$E10 < 9$ m/s	1.53 ± 0.10
	$-0.20 > \Delta \geq -0.35$	$E10 \geq 12$ m/s	1.42 ± 0.07

Table 6.13 (continued)

		7 m/s ≤ E10 < 12 m/s	1.39 ± 0.12
		5 m/s ≤ E10 < 7 m/s	1.48 ± 0.12
		E10 < 5 m/s	2.24 ± 0.17
	0 > Δ ≥ -0.20	E10 ≥ 7 m/s	1.21 ± 0.09
		E10 < 7 m/s	1.51 ± 0.07

Table 6.14: Method 3 Results for Modification Coefficients (Type-2A)

Points	Δ Classes	Wind Speed Classes	Modification Coefficient (Mod)
1-2	Δ < -0.35	All E10's	Mod= 0.032 E10 + 1.028
	-0.20 > Δ ≥ -0.35	E10 ≥ 8 m/s	Mod = -0.0038 E10 + 1.3527
		E10 < 8 m/s	Mod= 2.6277 $E10^{-0.351}$
	0 > Δ ≥ -0.20	All E10's	Mod= 2.137 $E10^{-0.25}$
3-4	Δ < -0.35	All E10's	Mod = 0.023 E10 + 1.231
	-0.20 > Δ ≥ -0.35	E10 ≥ 8 m/s	Mod = -0.0066 E10 + 1.421
		E10 < 8 m/s	Mod = 3.2604 $E10^{-0.455}$
	0 > Δ ≥ -0.20	All E10's	Mod = 2.256 $E10^{-0.27}$
5-6	Δ < -0.35	All E10's	Mod = 0.006 E10 + 1.5
	-0.20 > Δ ≥ -0.35	E10 ≥ 7 m/s	Mod= -0.0105 E10 + 1.5023
		E10 < 7 m/s	Mod = 3.9294 $E10^{-0.552}$
	0 > Δ ≥ -0.20	All E10's	Mod = 2.352 $E10^{-0.29}$

Table 6.15: Method 4 Results for Modification Coefficients (Type-2A)

Points	Wind Speed Classes	Mean ± Standard Deviation (Mod)
1-2	E10 ≥ 12 m/s	1.33 ± 0.12
	9 m/s ≤ E10 < 12 m/s	1.32 ± 0.13
	7 m/s ≤ E10 < 9 m/s	1.25 ± 0.10
	E10 < 7 m/s	1.42 ± 0.12
3-4	E10 ≥ 12 m/s	1.42 ± 0.11
	9 m/s ≤ E10 < 12 m/s	1.33 ± 0.13

Table 6.15 (continued)

	7 m/s ≤ E10 < 9 m/s	1.32 ± 0.12
	4 m/s ≤ E10 < 7 m/s	1.43 ± 0.06
	E10 < 4 m/s	1.85 ± 0.11
5-6	E10 ≥ 11.5 m/s	1.49 ± 0.12
	8 m/s ≤ E10 < 11.5 m/s	1.35 ± 0.14
	6 m/s ≤ E10 < 8 m/s	1.40 ± 0.13
	4 m/s ≤ E10 < 6 m/s	1.54 ± 0.08
	E10 < 4 m/s	2.24 ± 0.17

Table 6.16: Method 1 Results for Modification Coefficients (Type-2B)

Points	Wind Speed Classes	Modification Coefficient (Mod)
1-2	E10 ≥ 8 m/s	Mod = -0.0038 E10 + 1.3722
	E10 < 8 m/s	Mod= 3.7783 $E10^{-0.539}$
3-4	E10 ≥ 6 m/s	Mod = 2.504 $E10^{-0.289}$
	E10 < 6 m/s	Mod = 3.6819 $E10^{-0.51}$
5-6	E10 ≥ 6 m/s	Mod= 2.1517 $E10^{-0.229}$
	E10 < 6 m/s	Mod= 4.049 $E10^{-0.566}$

Table 6.17: Method 2 Results for Modification Coefficients (Type-2B)

Points	Δ Classes	Wind Speed Classes	Mean ± Standard Deviation (Mod)
1-2	Δ < -0.35	All E10's	1.42 ± 0.08
	-0.20 > Δ ≥ -0.35	E10 ≥ 7 m/s	1.23 ± 0.05
		3.5 m/s ≤ E10 < 7 m/s	1.57 ± 0.25
		E10 < 3.5 m/s	2.24 ± 0.15
	0 > Δ ≥ -0.20	E10 ≥ 9 m/s	1.13 ± 0.01
		E10 < 9 m/s	1.78 ± 0.10
3-4	Δ < -0.35	E10 ≥ 8 m/s	1.40 ± 0.05
		E10 < 8 m/s	1.75 ± 0.12
	-0.20 > Δ ≥ -0.35	E10 ≥ 6 m/s	1.32 ± 0.11

Table 6.17 (continued)

		4 m/s ≤ E10 < 6 m/s	1.54 ± 0.18
		E10 < 4 m/s	2.29 ± 0.28
	0 > Δ ≥ -0.20	E10 ≥ 9 m/s	1.15 ± 0.01
		E10 < 9 m/s	1.72 ± 0.16
5-6	Δ < -0.35	E10 ≥ 7 m/s	1.41 ± 0.02
		E10 < 7 m/s	2.36 ± 0.35
	-0.20 > Δ ≥ -0.35	E10 ≥ 6 m/s	1.37 ± 0.16
		4 m/s ≤ E10 < 6 m/s	1.57 ± 0.12
		E10 < 4 m/s	2.70 ± 0.38
	0 > Δ ≥ -0.20	E10 ≥8 m/s	1.17 ± 0.01
		E10 < 8 m/s	1.65 ± 0.22

Table 6.18: Method 3 Results for Modification Coefficients (Type-2B)

Points	Δ Classes	Wind Speed Classes	Modification Coefficient (Mod)
1-2	Δ < -0.35	All E10's	Mod = 0.031 E10 + 1.119
	-0.20 > Δ ≥ -0.35	E10 ≥ 7 m/s	Mod= 0.0215 E10 + 1.0235
		E10 < 7 m/s	Mod = 4.2795 $E10^{-0.63}$
	0 > Δ ≥ -0.20	All E10's	Mod= 3.251 $E10^{-0.43}$
3-4	Δ < -0.35	All E10's	Mod= 6.37 E10 – 0.68
	-0.20 > Δ ≥ -0.35	E10 ≥ 6 m/s	Mod = -0.0189 E10 + 1.4702
		E10 < 6 m/s	Mod = 4.9025 $E10^{-0.724}$
	0 > Δ ≥ -0.20	All E10's	Mod = 2.728 $E10^{-0.34}$
5-6	Δ < -0.35	All E10's	Mod = 6.388 E10 – 0.72
	-0.20 > Δ ≥ -0.35	E10 ≥ 6 m/s	Mod = -0.0322 E10 + 1.6152
		E10 < 6 m/s	Mod = 5.031 $E10^{-0.744}$
	0 > Δ ≥ -0.20	All E10's	Mod = 2.249 $E10^{-0.24}$

Table 6.19: Method 4 Results for Modification Coefficients (Type-2B)

Points	Wind Speed Classes	Mean ± Standard Deviation (Mod)
1-2	$E10 \geq 6$ m/s	1.32 ± 0.13
	3.5 m/s $\leq E10 < 6$ m/s	1.70 ± 0.20
	$E10 < 3.5$ m/s	2.24 ± 0.09
3-4	$E10 \geq 11$ m/s	1.27 ± 0.00
	3.5 m/s $\leq E10 < 11$ m/s	1.53 ± 0.25
	$E10 < 3.5$ m/s	2.19 ± 0.38
5-6	$E10 \geq 10$ m/s	1.27 ± 0.00
	3.5 m/s $\leq E10 < 10$ m/s	1.58 ± 0.32
	$E10 < 3.5$ m/s	2.70 ± 0.38

Table 6.20: Method 1 Results for Modification Coefficients (Type-3A)

Points	Wind Speed Classes	Modification Coefficient (Mod)
1-2	$E10 \geq 9$ m/s	$Mod = 0.0365\ E10 + 1.0824$
	$E10 < 9$ m/s	$Mod = 2.862\ E10^{-0.32}$
3-4	$E10 \geq 7.5$ m/s	$Mod = 0.0618\ E10 + 0.8369$
	$E10 < 7.5$ m/s	$Mod = 2.9696\ E10^{-0.345}$
5-6	$E10 \geq 8.5$ m/s	$Mod = 0.0628\ E10 + 0.8613$
	$E10 < 8.5$ m/s	$Mod = 3.2407\ E10^{-0.405}$

Table 6.21: Method 2 Results for Modification Coefficients (Type-3A)

Points	Δ Classes	Wind Speed Classes	Mean ± Standard Deviation (Mod)
1-2	$\Delta < -0.40$	$E10 \geq 9$ m/s	1.33 ± 0.08
		$E10 < 9$ m/s	1.58 ± 0.17
	$-0.20 > \Delta \geq -0.40$	$E10 \geq 11$ m/s	1.63 ± 0.02
		6 m/s $\leq E10 < 11$ m/s	1.46 ± 0.07
		$E10 < 6$ m/s	1.92 ± 0.23
	$0 > \Delta \geq -0.20$	$E10 \geq 8$ m/s	1.44 ± 0.10

Table 6.21 (continued)

		6 m/s ≤ E10 < 8 m/s	1.40 ± 0.11
		E10 < 6 m/s	1.84 ± 0.29
3-4	Δ < -0.40	E10 ≥ 7.5 m/s	1.35± 0.08
		E10 < 7.5 m/s	1.76± 0.22
	-0.20 > Δ ≥ -0.40	E10 ≥ 10 m/s	1.59± 0.06
		5 m/s ≤ E10 < 10 m/s	1.49± 0.10
		E10 < 5 m/s	1.93± 0.20
	0 > Δ ≥ -0.20	E10 ≥ 7.5 m/s	1.38± 0.13
		4.5 m/s ≤ E10 < 7.5 m/s	1.39± 0.14
		E10 < 4.5 m/s	1.99± 0.18
5-6	Δ < -0.40	E10 ≥6.5 m/s	1.35± 0.08
		E10 < 6.5 m/s	2.02 ± 0.33
	-0.20 > Δ ≥ -0.40	E10 ≥ 9 m/s	1.55 ± 0.10
		4.5 m/s ≤ E10 < 9 m/s	1.53 ± 0.14
		E10 < 4.5 m/s	1.95 ± 0.23
	0 > Δ ≥ -0.20	E10 ≥ 9 m/s	1.50 ± 0.01
		5 m/s ≤ E10 < 9 m/s	1.31 ± 0.14
		E10 < 5 m/s	1.90 ± 0.20

Table 6.22: Method 3 Results for Modification Coefficients (Type-3A)

Points	Δ Classes	Wind Speed Classes	Modification Coefficient (Mod)
1-2	Δ < -0.40	All E10's	Mod = 2.7803 $E10^{-0.297}$
	-0.20 > Δ ≥ -0.40	All E10's	Mod= 2.6543 $E10^{-0.253}$
	0 > Δ ≥ -0.20	All E10's	Mod= 2.5193 $E10^{-0.276}$
3-4	Δ < -0.40	All E10's	Mod = 3.5778 $E10^{-0.415}$
	-0.20 > Δ ≥ -0.40	All E10's	Mod = 2.5669 $E10^{-0.244}$
	0 > Δ ≥ -0.20	All E10's	Mod = 2.6842 $E10^{-0.325}$
5-6	Δ < -0.40	All E10's	Mod= 4.3405 $E10^{-0.517}$
	-0.20 > Δ ≥ -0.40	All E10's	Mod= 2.5177 $E10^{-0.243}$
	0 > Δ ≥ -0.20	All E10's	Mod = 2.8503 $E10^{-0.376}$

Table 6.23: Method 4 Results for Modification Coefficients (Type-3A)

Points	Wind Speed Classes	Mean ± Standard Deviation (Mod)
1-2	$E10 \geq 11$ m/s	1.55 ± 0.13
	8 m/s $\leq E10 <$ 11 m/s	1.43 ± 0.11
	6 m/s $\leq E10 <$ 8 m/s	1.50 ± 0.15
	$E10 <$ 6 m/s	1.89 ± 0.24
3-4	$E10 \geq 9.5$ m/s	1.53 ± 0.09
	7 m/s $\leq E10 <$ 9.5 m/s	1.38 ± 0.13
	5 m/s $\leq E10 <$ 7 m/s	1.63 ± 0.19
	$E10 <$ 5 m/s	1.93 ± 0.21
5-6	$E10 \geq 9$ m/s	1.51 ± 0.08
	7 m/s $\leq E10 <$ 9 m/s	1.33 ± 0.14
	4.5 m/s $\leq E10 <$ 7 m/s	1.74 ± 0.25
	$E10 <$ 4.5 m/s	2.05 ± 0.28

Table 6.24: Method 1 Results for Modification Coefficients (Type-3B)

Points	Wind Speed Classes	Modification Coefficient (Mod)
1-2	$E10 \geq 7.5$ m/s	Mod= 0.001 E10 + 1.279
	$E10 <$ 7.5 m/s	Mod = 3.741 $E10^{-0.52}$
3-4	$E10 \geq 6$ m/s	Mod = -0.001 E10 + 1.321
	$E10 <$ 6 m/s	Mod = 3.8853 $E10^{-0.578}$
5-6	$E10 \geq 5$ m/s	Mod = 0.001 E10 + 1.335
	$E10 <$ 5 m/s	Mod= 4.2592 $E10^{-0.703}$

Table 6.25: Method 2 Results for Modification Coefficients (Type-3B)

Points	Δ Classes	Wind Speed Classes	Mean ± Standard Deviation (Mod)
1-2	$\Delta <$ -0.40	$E10 \geq 8$ m/s	1.57 ± 0.01
		7 m/s $\leq E10 <$ 8 m/s	1.25 ± 0.06
		5 m/s $\leq E10 <$ 7 m/s	1.52 ± 0.18

Table 6.25 (continued)

		E10 < 5 m/s	2.03 ± 0.43
	-0.10 > Δ ≥ -0.40	E10 ≥ 5 m/s	1.24 ± 0.08
		2.25 m/s ≤ E10 < 5 m/s	2.09 ± 0.12
		E10 < 2.25 m/s	2.66 ± 0.33
	0 > Δ ≥ -0.10	E10 ≥ 4.5 m/s	1.47 ± 0.07
		E10 < 4.5 m/s	2.06 ± 0.01
3-4	Δ < -0.40	E10 ≥ 4.5 m/s	1.43 ± 0.18
		E10 < 4.5 m/s	2.37 ± 0.54
	-0.10 > Δ ≥ -0.40	E10 ≥ 5 m/s	1.27 ± 0.09
		1.75 m/s ≤ E10 < 5 m/s	2.26 ± 0.21
		E10 < 1.75 m/s	3.39 ± 0.40
	0 > Δ ≥ -0.10	E10 ≥ 4.5 m/s	1.43 ± 0.07
		E10 < 4.5 m/s	2.09 ± 0.01
5-6	Δ < -0.40	E10 ≥ 2.5 m/s	1.50 ± 0.28
		E10 < 2.5 m/s	3.33 ± 0.17
	-0.10 > Δ ≥ -0.40	E10 ≥ 4 m/s	1.30 ± 0.12
		1.5 m/s ≤ E10 < 4 m/s	2.43 ± 0.42
		0.75 m/s ≤ E10 < 1.5 m/s	3.74 ± 0.35
		E10 < 0.75 m/s	11.97 ± 0.8.32
	0 > Δ ≥ -0.10	E10 ≥ 4.5 m/s	1.38 ± 0.07
		E10 < 4.5 m/s	2.13 ± 0.01

Table 6.26: Method 3 Results for Modification Coefficients (Type-3B)

Points	Δ Classes	Wind Speed Classes	Modification Coefficient (Mod)
1-2	Δ < -0.40	All E10's	Mod= $4.0812\ E10^{-0.538}$
	-0.10 > Δ ≥ -0.40	E10 ≥ 7.25 m/s	Mod= 0.022 E10 + 1.026
		3 m/s ≤ E10 < 7.25 m/s	Mod = $4.317\ E10^{-0.68}$
		E10 < 3 m/s	Mod= $3.570\ E10^{-0.50}$
	0 > Δ ≥ -0.10	All E10's	Mod= $8.325\ E10^{-1.03}$
3-4	Δ < -0.40	E10 ≥ 5 m/s	Mod= -0.0409 E10 + 1.665

Table 6.26 (continued)

		E10 < 5 m/s	Mod= 4.9111 $E10^{-0.707}$
	-0.10 > Δ ≥ -0.40	E10 ≥ 7.25 m/s	Mod= 0.024 E10 + 1.039
		E10 < 7.25 m/s	Mod= 3.711 $E10^{-0.57}$
	0 > Δ ≥ -0.10	All E10's	Mod= 12.64 $E10^{-1.32}$
5-6	Δ < -0.40	E10 ≥ 4 m/s	Mod = 0.0501 E10 + 1.1764
		E10 < 4 m/s	Mod = 5.9901 $E10^{-1.17}$
	-0.10 > Δ ≥ -0.40	E10 ≥ 7.5 m/s	Mod = 0.0477 E10 + 0.852
		E10 < 7.5 m/s	Mod = 4.064 $E10^{-0.65}$
	0 > Δ ≥ -0.10	All E10's	Mod = 21.76 $E10^{-1.70}$

Table 6.27: Method 4 Results for Modification Coefficients (Type-3B)

Points	Wind Speed Classes	Mean ± Standard Deviation (Mod)
1-2	E10 ≥ 10 m/s	1.26 ± 0.02
	5 m/s ≤ E10 < 10 m/s	1.36 ± 0.18
	3 m/s ≤ E10 < 5 m/s	1.84 ± 0.32
	E10 < 3 m/s	2.37 ± 0.33
3-4	E10 ≥ 9 m/s	1.29 ± 0.06
	4.25 m/s ≤ E10 < 9 m/s	1.38 ± 0.16
	3 m/s ≤ E10 < 4.25 m/s	2.14 ± 0.33
	1.75 m/s ≤ E10 < 3 m/s	2.36 ± 0.36
	E10 < 1.75 m/s	3.37 ± 0.40
5-6	E10 ≥ 7 m/s	1.27 ± 0.12
	4.5 m/s ≤ E10 < 7 m/s	1.38 ± 0.21
	2.5 m/s ≤ E10 < 4.5 m/s	1.92 ± 0.24
	1.5 m/s ≤ E10 < 2.5 m/s	2.63 ± 0.59
	E10 < 1.5 m/s	6.32 ± 5.16

Table 6.28: Method 1 Results for Modification Coefficients (Type-4A)

Points	Wind Speed Classes	Modification Coefficient (Corr)
1-2	$E10 \geq 5.5$ m/s	Mod = 0.0106 E10 + 1.3103
	$E10 < 5.5$ m/s	Mod= 3.5556 $E10^{-0.567}$
3-4	$E10 \geq 6$ m/s	Mod= 0.0004 E10 + 1.3404
	$E10 < 6$ m/s	Modr = 2.957 $E10^{-0.434}$
5-6	$E10 \geq 6$ m/s	Mod= -0.0352 E10 + 1.5912
	$E10 < 6$ m/s	Mod = 2.4776 $E10^{-0.323}$

Table 6.29: Method 2 Results for Modification Coefficients (Type-4A)

Points	Δ Classes	Wind Speed Classes	Mean ± Standard Deviation (Mod)
1-2	$\Delta \geq 0.30$	$E10 \geq 3.8$ m/s	1.37 ± 0.13
		2.25 m/s ≤ E10 < 3.8 m/s	1.95 ± 0.18
		E10 < 2.25 m/s	2.25 ± 0.68
	$0 \leq \Delta < 0.30$	$E10 \geq 6$ m/s	1.41 ± 0.12
		4 m/s ≤ E10 < 6 m/s	2.06 ± 0.04
		E10 < 4 m/s	3.26 ± 0.32
3-4	$\Delta \geq 0.30$	$E10 \geq 4.25$ m/s	1.32 ± 0.15
		E10 < 4.25 m/s	1.77 ± 0.13
	$0 \leq \Delta < 0.30$	$E10 \geq 6.25$ m/s	1.39 ± 0.12
		4 m/s ≤ E10 < 6.25 m/s	1.96 ± 0.13
		E10 < 4 m/s	2.56 ± 0.18
5-6	$\Delta \geq 0.30$	All E10's	1.33 ± 0.15
	$0 \leq \Delta < 0.30$	$E10 \geq 6$ m/s	1.37 ± 0.12
		4 m/s ≤ E10 < 6 m/s	1.88 ± 0.03
		E10 < 4 m/s	2.14 ± 0.12

Table 6.30: Method 3 Results for Modification Coefficients (Type-4A)

Points	Δ Classes	Wind Speed Classes	Modification Coefficient (Mod)
1-2	$\Delta \geq 0.30$	E10 ≥ 5.5 m/s	Mod = -0.0343 E10 + 1.5002
		E10 < 5.5 m/s	Mod = 3.7437 $E10^{-0.647}$
	$0 \leq \Delta < 0.30$	E10 ≥ 8 m/s	Mod = -0.0712 E10 + 0.7734
		E10 < 8 m/s	Mod = 3.5407 $E10^{-0.472}$
3-4	$\Delta \geq 0.30$	All E10's	Mod= 2.7171 $E10^{-0.405}$
	$0 \leq \Delta < 0.30$	All E10's	Mod = 3.026 $E10^{-0.371}$
5-6	$\Delta \geq 0.30$	E10 ≥ 4 m/s	Mod = 1.7713 $E10^{-0.16}$
	$0 \leq \Delta < 0.30$	All E10's	Mod = 2.6965 $E10^{-0.318}$

Table 6.31: Method 4 Results for Modification Coefficients (Type-4A)

Points	Wind Speed Classes	Mean ± Standard Deviation (Mod)
1-2	E10 ≥ 8 m/s	1.40 ± 0.03
	4 m/s ≤ E10 < 8 m/s	1.47 ± 0.27
	2 m/s ≤ E10 < 4 m/s	1.99 ± 0.39
	E10 < 2 m/s	3.22 ± 0.55
3-4	E10 ≥ 8 m/s	1.36 ± 0.05
	5 m/s ≤ E10 < 8 m/s	1.33 ± 0.15
	2 m/s ≤ E10 < 5 m/s	1.70 ± 0.26
	E10 < 2 m/s	2.10 ± 0.45
5-6	E10 ≥ 9 m/s	1.33 ± 0.07
	6 m/s ≤ E10 < 9 m/s	1.32 ± 0.14
	3 m/s ≤ E10 < 6 m/s	1.51 ± 0.24
	E10 < 3 m/s	2.14 ± 0.12

Table 6.32: Method 1 Results for Correlation Coefficients (Type-4B)

Points	Wind Speed Classes	Correlation Coefficient (Corr)
1-2	$E10 \geq 7$ m/s	Corr = -0.0026 E10 + 1.306
	$E10 < 7$ m/s	Corr = $3.9292\ E10^{-0.581}$
3-4	$E10 \geq 8$ m/s	Corr = 0.0567 E10 + 0.7518
	$E10 < 8$ m/s	Corr = $3.5197\ E10^{-0.53}$
5-6	$E10 \geq 8$ m/s	Corr = 0.042 E10 + 0.8272
	$E10 < 8$ m/s	Corr = $3.0012\ E10^{-0.445}$

Table 6.33: Method 2 Results for Modification Coefficients (Type-4B)

Points	Δ Classes	Wind Speed Classes	Mean ± Standard Deviation (Mod)
1-2	$\Delta \geq 0.30$	$E10 \geq 6.25$ m/s	1.30 ± 0.21
		4 m/s $\leq E10 < 6.25$ m/s	1.32 ± 0.46
		2.5 m/s $\leq E10 < 4$ m/s	2.05 ± 0.32
		$E10 < 2.5$ m/s	3.10 ± 0.73
	$0 \leq \Delta < 0.30$	$E10 \geq 6.75$ m/s	1.28 ± 0.04
		$E10 < 6.75$ m/s	1.62 ± 0.29
3-4	$\Delta \geq 0.30$	$E10 \geq 9.75$ m/s	1.25± 0.07
		6 m/s $\leq E10 < 9.75$ m/s	1.26± 0.14
		4 m/s $\leq E10 < 6$ m/s	1.58± 0.16
		$E10 < 4$ m/s	2.23± 0.39
	$0 \leq \Delta < 0.30$	$E10 \geq 7$ m/s	1.28 ± 0.03
		$E10 < 7$ m/s	1.56± 0.30
5-6	$\Delta \geq 0.30$	$E10 \geq 10$ m/s	1.34 ± 0.05
		5 m/s $\leq E10 < 10$ m/s	1.18 ± 0.13
		$E10 < 5$ m/s	1.70 ± 0.25
	$0 \leq \Delta < 0.30$	$E10 \geq 9.5$ m/s	1.34 ± 0.02
		6 m/s $\leq E10 < 9.5$ m/s	1.25 ± 0.11
		$E10 < 6$ m/s	1.69 ± 0.32

Table 6.34: Method 3 Results for Modification Coefficients (Type-4B)

Points	Δ Classes	Wind Speed Classes	Modification Coefficient (Mod)
1-2	$\Delta \geq 0.30$	$E10 \geq 6.25$ m/s	Mod= 0.0042 E10 + 1.2733
		$E10 < 6.25$ m/s	Mod= 4.621 $E10^{-0.719}$
	$0 \leq \Delta < 0.30$	$E10 \geq 8$ m/s	Mod = 0.0054 E10 + 1.2169
		$E10 < 8$ m/s	Mod = 2.6768 $E10^{-0.345}$
3-4	$\Delta \geq 0.30$	$E10 \geq 8$ m/s	Mod = 0.1107 E10 + 0.2609
		$E10 < 8$ m/s	Mod= 4.2011 $E10^{-0.675}$
	$0 \leq \Delta < 0.30$	$E10 \geq 8.5$ m/s	Mod = 0.0162 E10 + 1.3338
		$E10 < 8.5$ m/s	Modr = 2.905 $E10^{-0.399}$
5-6	$\Delta \geq 0.30$	$E10 \geq 8$ m/s	Mod = 0.0524 E10 + 0.6464
		$E10 < 8$ m/s	Modr = 3.2381 $E10^{-0.52}$
	$0 \leq \Delta < 0.30$	$E10 \geq 8.25$ m/s	Mod= 0.0597 E10 + 0.7022
		$E10 < 8.25$ m/s	Mod = 2.9033 $E10^{-0.404}$

Table 6.35: Method 4 Results for Modification Coefficients (Type-4B)

Points	Wind Speed Classes	Mean ± Standard Deviation (Mod)
1-2	$E10 \geq 8$ m/s	1.27± 0.04
	5 m/s $\leq$ E10 < 8 m/s	1.35± 0.25
	3.5 m/s $\leq$ E10 <5 m/s	1.70± 0.22
	E10 <3.5 m/s	2.46± 0.67
3-4	$E10 \geq 10$ m/s	1.35± 0.05
	7 m/s $\leq$ E10 <10 m/s	1.25± 0.15
	5 m/s $\leq$ E10 <7 m/s	1.33± 0.26
	4 m/s $\leq$ E10 < 5 m/s	1.62 ± 0.45
	E10 < 4 m/s	2.12 ± 0.07
5-6	$E10 \geq 9.5$ m/s	1.34± 0.04
	6 m/s $\leq$ E10 < 9.5 m/s	1.20± 0.13
	5 m/s $\leq$ E10 < 6 m/s	1.43± 0.21
	E10 <5 m/s	1.69± 0.31

In the next stage, hourly E10 wind speeds are modified by using each method mentioned above. The modified hourly E10 wind speeds are regarded as E10m1, E10m2, E10m3 and E10m4 respectively for each method starting from 1 and ending with 4. The results are presented in Appendix F. In addition to E10L, E10m1, E10m2, E10m3, E10m4, $S10_S$, S10 wind speeds, %90 confidence limit boundaries of S10s wind speeds are also drawn in order to see the general scatter of the data and number of modified E10 wind speeds that stay out these boundaries. Moreover, since the data variability is high for several data sets, the confidence limit representation will help covering the most data points within the confidence limits as possible. These upper and lower limits of $S10_S$ wind speeds are denoted as "$S10_S$ Upper" and "$S10_S$ Lower" on top of each figure. Figure F4 in Appendix F consists of 156 hours of data, which is hard to observe the correlations. Thus, Figure F4 is divided into three figures (Figure F5, F6 and F7).

In addition to the figures, to understand if the results (E10m1, E10m2, E10m3 and E10m4 wind speeds are in good agreement with the smoothed and original S10 wind speeds ($S10_S$ and S10) Figure 6.19-6.20 are prepared considering all of the data of 29 continuous data sets. It is easily seen that the previously found R^2 value 0.62 obtained between E10 and S10 wind speeds is increased up to 0.78 and 0.77 by applying methods 2 and 3. Method 1 also gives a similar but slightly smaller increase in R^2 value. Among all methods, method 4 gives the lowest R^2 value. As for the correlation between E10m and S10 wind speeds, each method increases E10 wind speeds substantially so that the best fit of these data give very good fitting almost equal to y=x.

On the other hand, since the main references for E10 wind speeds are the smoothed S10 wind speeds ($S10_S$) while obtaining correlations, it would be]meaningful to look into the relation between E10m and $S10_S$ wind speeds. Just like the outcomes of Figure 6.18, in Figure 6.19, the highest R^2 value is achieved by application of method 2, and this is followed by method 3, 1 and 4, respectively, in the order of descending R^2 value. The highest R^2 is found as 0.92 and the lowest is 0.84.

Although it is important to observe the overall performance of these methods used to modify E10 wind speeds for all continuous data sets, not all of the data sets show a proper storm condition in which starting with a calm duration, winds start to increase, reaches a peak point and starts to calm down. There are few data sets that resemble such storm conditions and these data sets are 2, 5, 7, 9 and 24. The other data sets are either a part of a storm, or do not resemble such storms as described above.

In order to observe the total performance of applying these methods especially for such storms, it would be more important to compare E10m and $S10_S$ wind speeds of these data sets. Since, these types of storms are dominated by high scale atmospheric conditions, in which impact of local conditions such as sea and land breezes are small, better correlation and higher R^2 for these storms would indicate that these methods are working fine, even though the modification methods are developed by using limited wind measurement data and limited continuous onshore wind durations.

The aforementioned correlation between E10m and S10 together with E10m and $S10_S$ wind speeds for the selected continuous data sets can be seen in Figure 6.19 to Figure 6.22.

Additionally, average bias, root mean square error (RMSE) and mean absolute error (MAE) between E10 and S10, E10m and S10, E10 and $S10_s$ and E10m and $S10_s$ wind speeds for each 29 continuous data sets and combined data set regarded as "All" are calculated and tabulated in Table 6.36-6.41. The results show that certain improvements are achieved for most of the continuous data sets as well as for the combined data. Bias, RMSE and MAE are calculated by using formulations given in Appendix G.

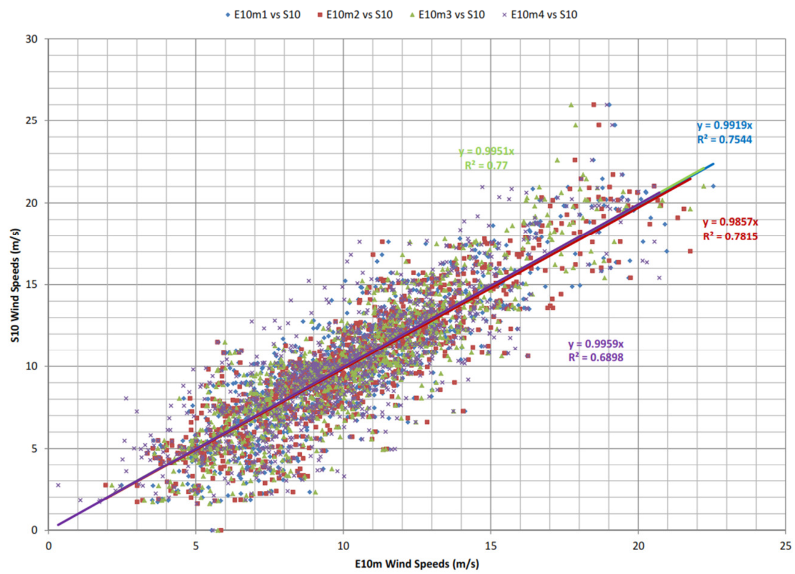

Figure 6.19: E10m1, E10m2, E10m3 and E10m2 Wind Speeds vs S10 Wind Speeds (For All Continuous Data Sets)

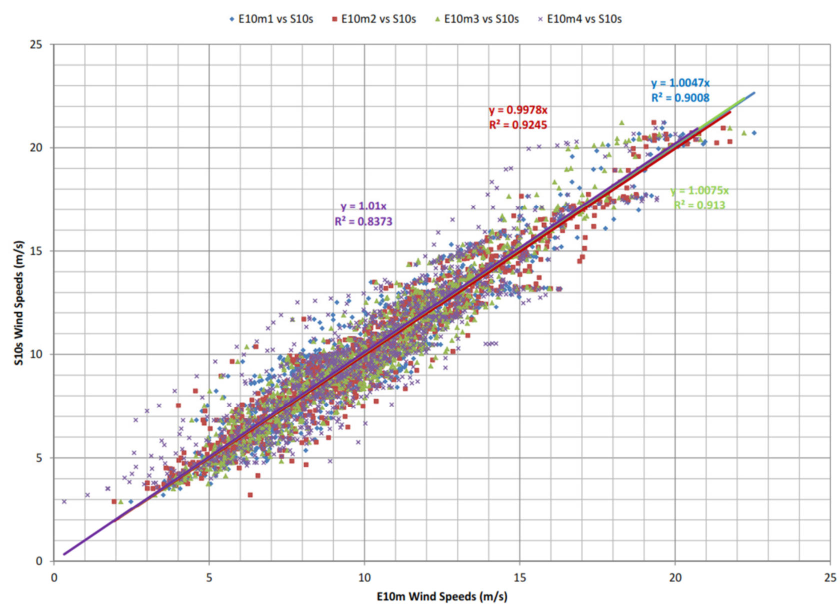

Figure 6.20: E10m1, E10m2, E10m3 and E10m2 Wind Speeds vs S10S Wind Speeds (For All Continuous Data Sets)

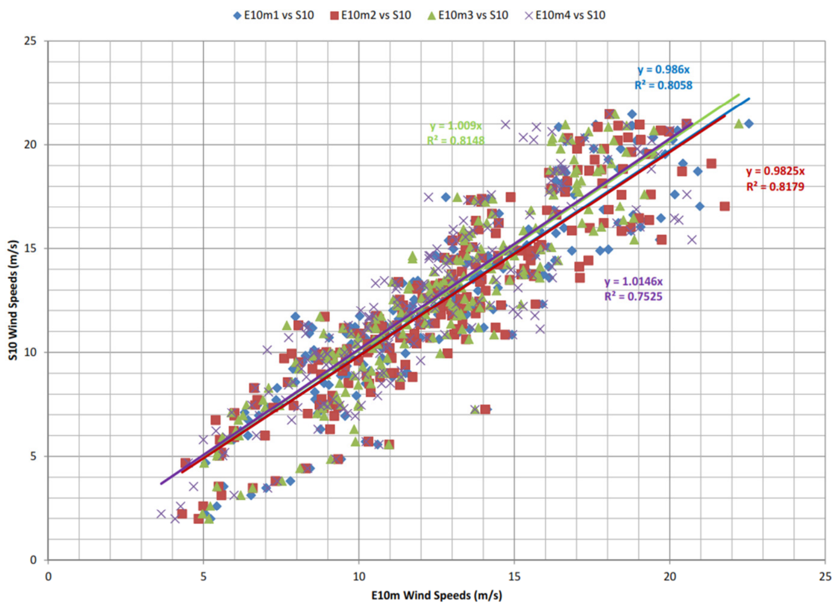

Figure 6.21: E10m1, E10m2, E10m3 and E10m2 Wind Speeds vs S10 Wind Speeds (Selected Data Sets)

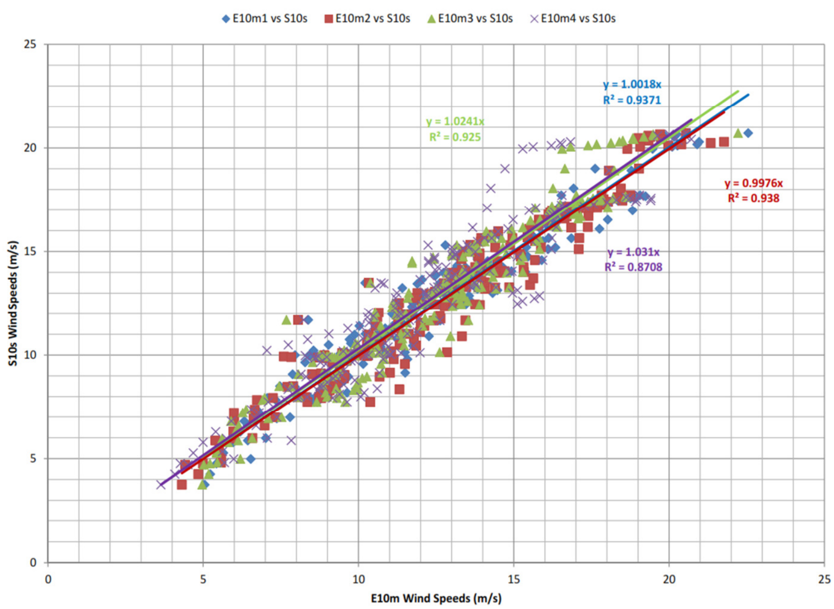

Figure 6.22: E10m1, E10m2, E10m3 and E10m2 Wind Speeds vs $S10_S$ Wind Speeds (Selected Data Sets)

Table 6.36: Calculated Average BIAS between E10, E10m Wind Speeds $S10_s$ Wind Speeds

Continuous Data No	$S10_s$				
	E10	E10m1	E10m2	E10m3	E10m4
1	-3.13	-0.24	0.21	0.34	-0.29
2	-3.11	-0.25	0.02	-0.12	-0.07
3	-3.24	-0.24	-0.15	-0.12	-0.39
4	-2.67	0.27	0.18	0.23	0.27
5	-2.80	0.29	0.40	0.25	0.48
6	-3.89	-1.16	-0.46	-0.85	-0.89
7	-5.30	-0.34	0.09	-0.78	-1.78
8	-2.64	0.11	-0.19	-0.06	-0.31
9	-3.70	-0.51	-0.42	-0.64	-0.92
10	-3.12	-0.46	-0.46	-0.19	-0.57
11	-3.24	-0.68	-0.13	-0.80	-0.36
12	-2.12	0.58	-0.21	0.10	0.46
13	-2.46	0.28	0.25	-0.01	0.35
14	-2.34	0.27	0.22	0.19	0.59
15	-2.89	0.16	0.22	0.13	0.23
16	-3.00	-0.15	-0.29	0.14	-0.61
17	-2.09	0.12	-0.08	-0.07	0.43
18	-2.76	-0.09	-0.26	0.09	-0.54
19	-3.03	0.15	0.60	-0.14	0.26
20	-1.98	0.75	0.36	0.73	0.93
21	-2.63	0.39	0.36	0.34	0.10
22	-2.45	0.20	0.13	-0.01	0.44
23	-2.45	0.80	0.84	0.94	0.26
24	-3.24	0.22	0.04	-0.09	0.01
25	-3.28	-0.47	-0.29	-0.42	-0.65
26	-4.14	-1.20	-0.36	-0.78	-1.03
27	-5.95	-1.42	-0.48	-1.22	-2.12
28	-3.08	-0.43	-0.57	-0.36	-0.21
29	-2.95	0.18	-0.43	-0.05	0.42

Table 6.36 (continued)

All	-3.09	-0.08	-0.01	-0.07	-0.17

Table 6.37: Calculated Average BIAS between E10, E10m Wind Speeds and S10 Wind Speeds

Continuous Data No	S10				
	E10	E10m1	E10m2	E10m3	E10m4
1	-3.51	-0.63	-0.18	-0.05	-0.67
2	-2.55	0.31	0.58	0.44	0.49
3	-3.92	-0.92	-0.83	-0.80	-1.07
4	-2.14	0.80	0.72	0.77	0.80
5	-2.39	0.71	0.81	0.66	0.89
6	-3.71	-0.99	-0.29	-0.67	-0.72
7	-4.77	0.19	0.62	-0.25	-1.25
8	-2.28	0.48	0.18	0.30	0.06
9	-3.24	-0.05	0.03	-0.18	-0.47
10	-3.50	-0.84	-0.84	-0.56	-0.94
11	-3.08	-0.52	0.03	-0.64	-0.20
12	-3.05	-0.35	-1.14	-0.83	-0.47
13	-2.28	0.46	0.42	0.17	0.53
14	-1.90	0.71	0.66	0.63	1.03
15	-2.97	0.09	0.14	0.05	0.15
16	-3.09	-0.25	-0.39	0.05	-0.70
17	-2.26	-0.05	-0.25	-0.23	0.26
18	-1.96	0.72	0.55	0.90	0.26
19	-2.35	0.83	1.27	0.53	0.93
20	-1.88	0.85	0.46	0.83	1.03
21	-1.99	0.91	0.88	0.86	0.62
22	-2.23	0.41	0.34	0.20	0.66
23	-2.31	0.95	0.98	1.08	0.40
24	-3.52	-0.07	-0.25	-0.38	-0.28
25	-4.10	-1.29	-1.10	-1.24	-1.47
26	-3.27	-0.34	0.50	0.08	-0.17

Table 6.37 (continued)

27	-6.84	-2.31	-1.37	-2.11	-3.01
28	-2.79	-0.15	-0.29	-0.08	0.07
29	-3.16	-0.04	-0.64	-0.26	0.20
All	-2.90	0.11	0.18	0.11	0.01

Table 6.38: Calculated RMSE between E10, E10m Wind Speeds and $S10_s$ Wind Speeds

Continuous Data No	$S10_s$				
	E10	E10m1	E10m2	E10m3	E10m4
1	3.49	1.26	0.52	0.87	1.35
2	3.30	1.19	1.13	0.99	1.19
3	3.51	1.18	0.87	0.98	1.44
4	3.06	1.36	1.13	1.17	1.78
5	2.96	0.90	0.85	0.74	1.18
6	4.06	1.40	0.94	1.19	1.29
7	5.52	1.10	1.35	1.78	2.31
8	3.38	1.80	1.73	1.75	2.18
9	3.92	0.98	0.82	1.09	1.42
10	3.15	0.69	0.87	0.67	0.91
11	3.33	0.98	1.55	1.01	1.15
12	2.24	0.85	0.46	0.27	0.96
13	2.73	1.04	0.88	1.12	1.12
14	2.46	0.71	0.47	0.61	1.32
15	3.20	1.15	0.98	1.15	1.02
16	3.03	0.53	0.66	0.71	0.87
17	2.13	0.50	0.38	0.45	0.93
18	2.86	0.41	0.56	0.43	0.96
19	3.07	0.43	0.99	0.66	0.36
20	2.17	1.16	0.68	0.96	1.45
21	0.46	0.09	0.14	0.09	0.15
22	2.50	0.80	0.80	0.98	0.86
23	2.50	0.98	1.18	1.28	1.24

Table 6.38 (continued)

24	3.34	0.94	0.93	0.86	0.96
25	3.64	1.21	0.73	0.90	1.65
26	4.20	1.46	0.86	1.14	1.33
27	6.07	1.68	0.75	1.56	2.58
28	3.13	0.80	0.68	0.65	0.85
29	2.98	0.33	0.95	0.99	1.04
All	3.38	1.11	0.97	1.04	1.42

Table 6.39: Calculated RMSE between E10, E10m Wind Speeds and S10 Wind Speeds

Continuous Data No	S10				
	E10	E10m1	E10m2	E10m3	E10m4
1	4.24	2.17	1.22	1.60	2.29
2	3.07	1.81	1.96	1.75	1.88
3	4.78	2.60	2.23	2.08	3.04
4	3.04	2.08	2.00	1.97	2.48
5	3.04	1.93	1.84	1.79	2.13
6	4.25	1.88	1.46	1.89	1.97
7	5.24	2.02	2.05	2.08	2.88
8	3.42	2.29	2.08	2.22	2.56
9	4.01	2.01	1.91	1.97	2.16
10	3.72	1.39	1.56	1.46	1.66
11	3.52	1.60	1.71	1.57	1.59
12	4.18	2.77	2.52	2.42	2.84
13	2.90	1.75	1.55	1.76	1.77
14	2.69	2.09	1.68	2.00	2.59
15	3.67	1.89	1.67	1.87	1.92
16	3.17	0.84	0.88	0.91	1.06
17	2.45	0.86	0.74	0.90	1.21
18	2.68	2.12	1.91	2.16	1.85
19	3.45	2.52	2.83	2.72	2.52
20	2.29	1.47	1.06	1.35	1.80

Table 6.39 (continued)

21	0.52	0.37	0.37	0.36	0.39
22	2.64	1.61	1.64	1.79	1.56
23	2.53	1.38	1.57	1.56	1.40
24	3.92	1.69	1.67	1.64	1.57
25	4.70	2.29	1.94	2.05	2.74
26	3.94	2.13	2.13	2.14	2.31
27	7.06	2.91	2.61	3.21	3.60
28	3.39	1.87	1.66	1.64	1.87
29	3.44	1.07	1.42	1.28	1.82
All	3.64	1.97	1.86	1.91	2.22

Table 6.40: Calculated Average MAE between E10, E10m Wind Speeds and $S10_s$ Wind Speeds (in %)

Continuous Data No	$S10_s$				
	E10	E10m1	E10m2	E10m3	E10m4
1	29.0	12.3	4.4	8.2	11.4
2	31.8	10.2	10.2	7.6	9.8
3	30.9	10.7	7.1	7.9	11.6
4	27.3	11.5	9.5	9.9	15.5
5	22.5	6.8	5.9	5.6	8.1
6	31.5	9.7	5.7	6.7	8.6
7	33.3	5.5	8.1	10.0	11.2
8	35.5	22.2	17.1	19.3	22.9
9	34.9	8.6	6.3	8.0	10.7
10	38.9	5.8	8.9	6.5	9.8
11	34.2	7.2	15.6	8.8	11.1
12	39.6	12.6	8.2	4.1	15.0
13	32.4	11.9	9.5	12.0	10.9
14	31.3	8.6	5.1	6.5	14.5
15	39.1	14.5	12.5	14.4	13.2
16	29.2	4.0	5.1	5.6	7.4
17	23.2	3.7	3.1	3.8	6.6

Table 6.40 (continued)

18	50.6	5.1	6.4	4.6	12.6
19	21.5	2.6	5.2	3.2	2.2
20	18.5	10.0	5.8	8.1	11.1
21	43.7	8.0	11.3	7.9	12.5
22	22.3	6.4	6.3	7.4	6.7
23	42.4	13.1	15.8	13.0	21.9
24	26.3	6.5	6.1	5.9	6.0
25	31.5	9.1	5.8	6.8	10.9
26	42.1	13.4	5.8	9.1	11.9
27	35.9	9.8	3.8	8.0	14.4
28	30.6	7.1	6.4	6.2	8.0
29	28.5	2.5	6.7	8.6	8.5
All	31.6	9.3	8.0	8.2	11.6

Table 6.41: Calculated Average MAE between E10, E10m Wind Speeds S10 Wind Speeds (in %)

Continuous Data No	S10				
	E10	E10m1	E10m2	E10m3	E10m4
1	33.1	21.6	12.8	17.7	24.0
2	26.8	21.9	24.2	20.7	22.0
3	33.6	17.1	13.2	13.1	19.8
4	28.8	21.2	20.3	19.8	26.3
5	20.7	15.2	14.0	14.3	16.7
6	30.0	14.3	10.4	14.0	15.6
7	30.5	9.5	12.1	11.2	14.0
8	38.4	33.7	28.6	30.9	35.6
9	34.7	24.5	22.4	23.5	24.5
10	40.5	11.6	12.9	11.9	14.0
11	30.7	15.5	17.4	15.7	15.7
12	40.8	34.6	23.1	23.4	36.4
13	32.0	22.5	18.3	21.0	21.8
14	29.2	31.4	25.2	30.1	38.5

Table 6.41 (continued)

15	38.0	27.2	25.5	27.1	28.3
16	29.7	6.5	5.8	6.6	8.6
17	24.1	7.3	6.4	7.2	10.3
18	49.6	43.8	39.6	43.3	36.9
19	23.9	19.5	24.9	21.0	19.2
20	17.9	13.2	9.0	11.4	14.5
21	50.3	51.1	51.3	50.2	53.5
22	20.7	12.7	13.1	14.5	11.9
23	39.8	24.8	29.1	25.3	21.2
24	26.9	10.4	10.7	9.9	9.5
25	35.5	13.6	11.7	12.4	15.6
26	36.4	27.2	29.1	28.1	30.4
27	38.7	13.7	9.7	12.3	17.4
28	29.9	19.8	15.4	16.2	19.9
29	28.6	8.5	11.7	12.0	15.7
All	31.6	20.5	19.2	19.5	22.2

The findings of the figures in Appendix F, Figures 6.19-6.22 and Tables 6.36-6.41 are summarized below:

- In general, especially for a regular storm condition where small scale features such as sea and land breezes are rarely effective, the application of all modification methods inceases the correlation between E10m and S10s wind speeds as well as E10m and S10 wind speeds.
- For cases, where small scale features are more effective and observed commonly, which increases the variability in wind measurements, the results obtained after applying modification methods indicate an increase in correlationbetween E10m and S10s wind speeds. Similarly, same is applicable for E10m and S10 wind speeds. However, compared to the previous outcome, the correlation is less.

- As discussed previously, even though the modification methods increase the correlation for a certain amount, considering certain seasons or periods, where instead of offshore wind conditions, local weather conditions are dominant such as sea breezes, there may be a need to perform slightly different method to obtain better correlation. This can not be performed with limited data, but only possible with longer periods of wind measurements covering these seasons. It is understood from the data set that these small scale feature are commonly observed for the period of May-July.
- Since there are certain gaps within the data set, it is hard to obtain a storm from its beginning to its end. Thus, most of the data cover a certain part of a storm or completely different weather conditions where the wind speeds are constantly changing to create an ondulating storm which as can be seen from the results in Appendix F are hardly demonstrated by ECMWF wind data. Therefore, it would be better and logical to look into continuous data sets where almost all parts of complete storms are covered such as 2, 5, 7, 9 and 24.
- Since, ECMWF does not always successfully show the trends in wind speed changes due to the variability in data sets (wind speeds) are higher due to several factors observed within 6 hour intervals, it would be much practical and easier to obtain an applicable modification by obtaining a smoothed wind field so that the trends of ECMWF and in-situ wind measurements are more like in terms of its shape and trend. This does not mean that while smoothing the wind measurement data, the structure is changed completely, but it is rather a way to better modify E10 wind speeds for situation where it is possible to have good E10m wind speeds. As for cases where it is not possible to come up with good E10m wind speeds due to significant changes between E10 and S10 wind speeds, the smoothing are arranged so that the underestimation of E10m wind speeds would be as low as possible. Examples of these situations are observed in several of the figures in Appendix F.

- Average BIAS, RMSE and Average MAE results indicate that certain improvements are achieved with each modification method. Modification methods 2 and 3 give better improvements compared to the other modification methods. As expected, the correlations between E10m and $S10_S$ wind speeds are better than correlations betweenE10m and S10 wind speeds due to smoothing of the wind fields.

6.4. Discussion

In this study, the data the reliability of which is studied in Chapter 4, is first carried to 60 m elevation above MSL (S60) on the sea and then carried to 10 m elevation above MSL (S10) with the representative velocity profile obtained from ECMWF wind data at 10 m (E10) and 100 m (E100) elevations.

Study carried on the comparison of S10 and E10 wind data show that ECMWF gives lower wind speeds compared to in-situ wind measurements. This has been already reported in several studies as given in Chapter 2.

In order to obtain wind speeds that may better represent S10 winds, it is decided that E10 wind speeds should be modified based on the correlations between simultaneous S10 and E10 wind speeds. Significant improvements in the correlation between two data sources are achieved with the developed modification methods which are based on the wind speeds and trends of wind speed changes.

CHAPTER 7

COMPARISON BETWEEN IN-SITU WAVE MEASUREMENTS AND WAVE ESTIMATIONS

In this last part of the study, using modified E10 wind speeds (E10m wind speeds) wave climate studies will be performed for the case study area. Since, it is not enough only to achieve E10m wind speeds that have good correlation with S10 and S10S wind speeds, it is even more important to see how these E10m wind speeds work in terms of the waves that they create.

It is highly critical in coastal engineering studies to have both good wind and wave data so that the accurate enough design wave parameters can be obtained. Since wave data is obtained from wind data for most of the cases, especially commonly used in coastal engineering applications in Turkey, it is of paramount importance that the aforementioned modifications methods would lead good E10m wind data which would eventually result in realistic wave data.

In this part of the study, firstly, E10, E10m and S10 wind data for several continuous data sets are chosen to create wave data sets for these periods and the results will be discussed within each other by comparing the results. Since, there is no simultaneous wave measurements for the period of land-based in-situ wid measurements, comparisons with real time wave data can not be performed at this stage. However, these comparisons would give quite good idea on the wave height and period differentiates between the results of waves obtained from several wind data sets. Moreover, since not all of the continuous data sets cover storm totally, the data sets which cover a whole storm event or most of it, are chosen so that the whole series of waves can be created from the beginning of a storm. Another consideration for this choice is that since the numerical model to be used in estimation of wave parameters depend on energy-based equations, it is paramount to have most of the storm wind data. The details of the numerical model and its bases will be discussed in detail in the upcoming sections.

After comparisons of the results of the aforementioned studies, the chosen modification methods will also be implemented for certain storms in the past during which in-situ wave measurements are available for the same region. This part of the study will be ciritcal to show that the plus sides in using the modification methods in obtaining wave data and the accuracy of the obtained results are valid. For wave data estimations in certain storms, two different models are used in order to see the differences in between model results to see if the used numerical model brings some uncertainty in the wave estimations.

Finally, several storms in another stie in the eastern coast of Turkey, Hopa are chosen to see that the applications of the same methods would also be applicable for other regions as well as if they perform similarly for other regions as well.

7.1. Comparison of Wave Results for the Chosen Continuous Data Sets for Sinop Region

The storms used in this section are some of whole part of the data sets with the given numbers 2, 6, 7, 9, 24 and 25. The reason behing the choice of these data sets is that they almost include a complete storm in which after a certain period of calmness at the beginning wind starts to increase and at the end they dissipate and calm conditions are reached. Although the definition of calm duration or calm condition changes, in general weather conditions when wind speeds are below 3 m/s are regarded as calm.

In the wave estimations, the numerical model for hindcasting wind-waves, W61 numerical model was used. W61 was developed by Middle East Technical University, Department of Civil Engineering, Ocean Engineering Research Center (Koca, 1979; Ozhan, 1981; Ergin and Ozhan, 1986). The model is based on the Pierson-Moskovitz wave hindcasting method (1964), in which spectral form for fully developed wind waves was proposed in terms of wind speed averaged over a time period. As the total energy of the sea state changes during a storm event with changing wind speed and direction, the computed spectrum of sea waves, modified by the added energies at every time step of the storm event, is used to determine the deep water significant wave parameters at the respective time step of the storm. The numerical model requires three types of input data, hourly average wind speed and directions and the effective fetch distances computed for the study area. In return, the program gives the hourly significant deep water wave heights and periods computed for the respective duration of the wind data. One might refer to the above given references for further details of the program.

Since W61 uses effective fetch distances computed for the study area, fetch distances are calculated for the site. The fetch distances as shown in Figure 7.1 is calculated at every 7.5° interval and each consecutive 5 fetch distances is used to calculate the effective fetch for the middle direction. This is fomulazied as;

$$F_E = \frac{\Sigma([F(cos\beta)^2]}{\Sigma cos\beta} \quad [7.1]$$

In this formula, F_E is the effective fetch for the middle direction, F is the calculated fetch at each 7.5° interval and β is the angle between the middle direction and the corresponding fetch direction.

The fetch distances considered in this study is shown in Figure 7.1, whereas the tabulated form of the calculated effective fetch distances for the case study site, Sinop, is given in Table 7.1.

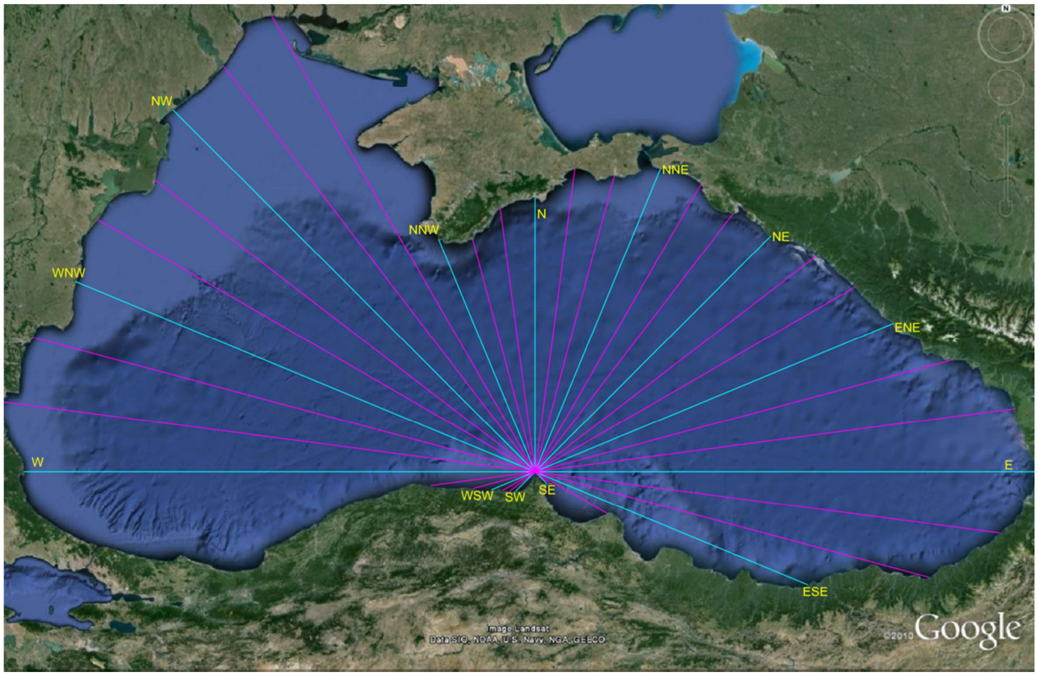

Figure 7.1: Considered Fetch Distances for the Case Study Site, Sinop (Google Earth, 2014)

Table 7.1: Effective Fetch Distances for the Case Study Site, Sinop

Direction	Effective Fetch (km)
WSW	119
W	349
WNW	539
NW	500
NNW	389
N	298
NNE	334
NE	367
ENE	433
E	454
ESE	271

The results of wave estimations performed with W61 considering hourly S10, $S10_S$, E10, E10m2 and E10m3 wind speeds are given in Figures 7.2-7.13 in terms of wave heights and directions. As it is observed from these figures, although the storms end due to longer period needed for the added energy to dissipate compared to storm duration, waves are still observed.

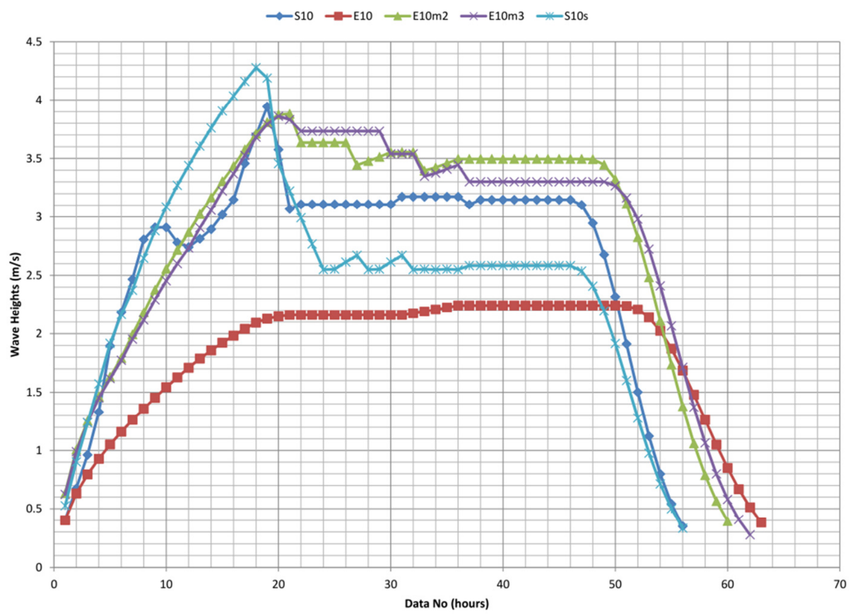

Figure 7.2: Wave Heights Obtained from S10, $S10_S$, E10, E10m2 and E10m3 Wind Speeds for Continuous Data Set 2 with W61 Numerical Model

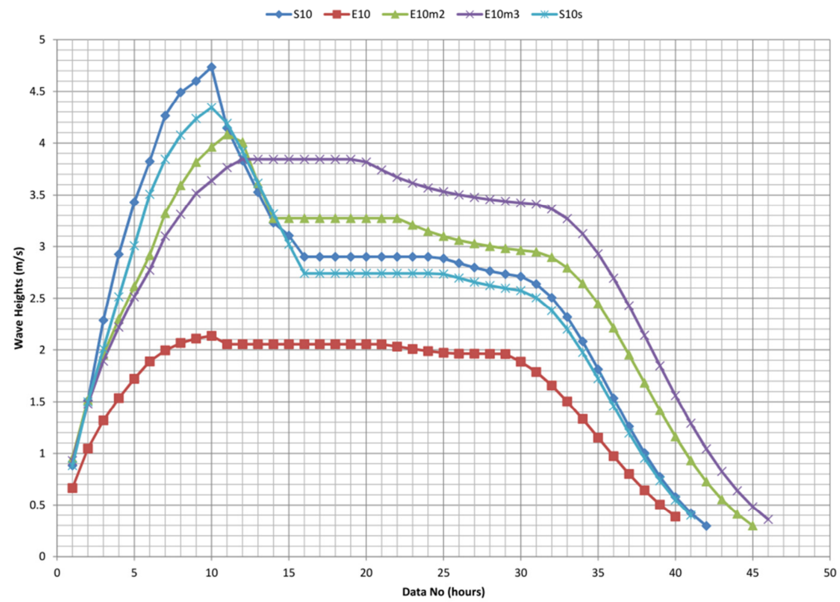

Figure 7.3: Wave Heights Obtained from S10, S10$_S$, E10, E10m2 and E10m3 Wind Speeds for Continuous Data Set 6 with W61 Numerical Model

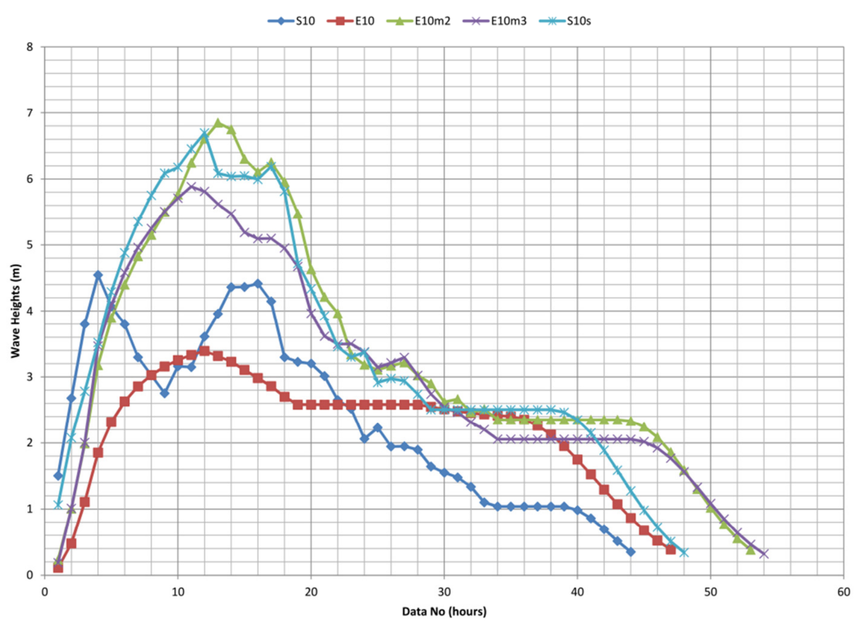

Figure 7.4: Wave Heights Obtained from S10, S10$_S$, E10, E10m2 and E10m3 Wind Speeds for Continuous Data Set 7 with W61 Numerical Model

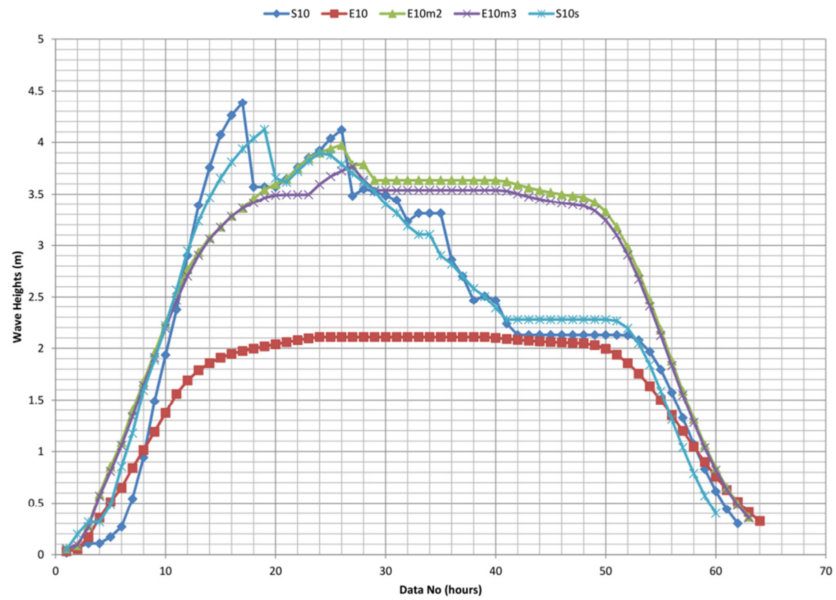

Figure 7.5: Wave Heights Obtained from S10, $S10_S$, E10, E10m2 and E10m3 Wind Speeds for Continuous Data Set 9 with W61 Numerical Model

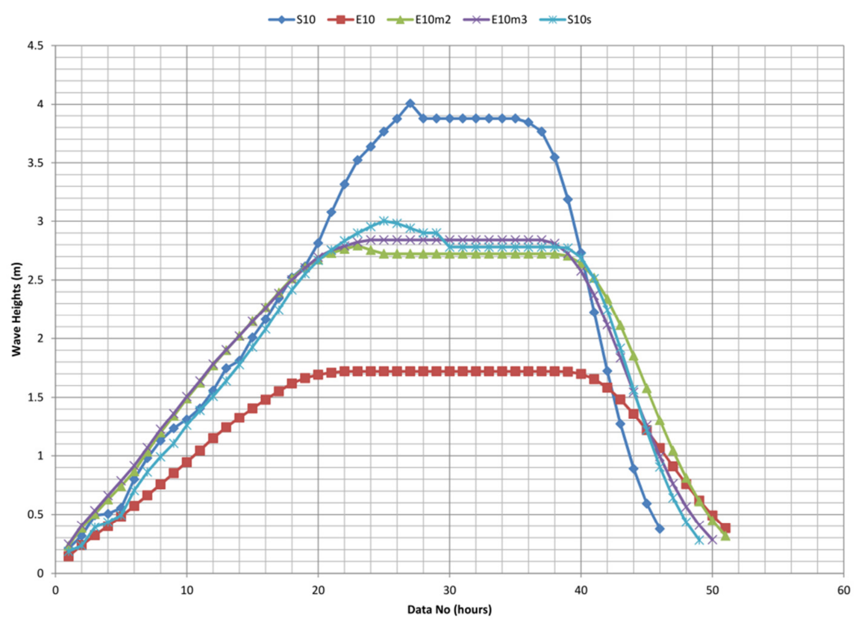

Figure 7.6: Wave Heights Obtained from S10, $S10_S$, E10, E10m2 and E10m3 Wind Speeds for Continuous Data Set 24 with W61 Numerical Model

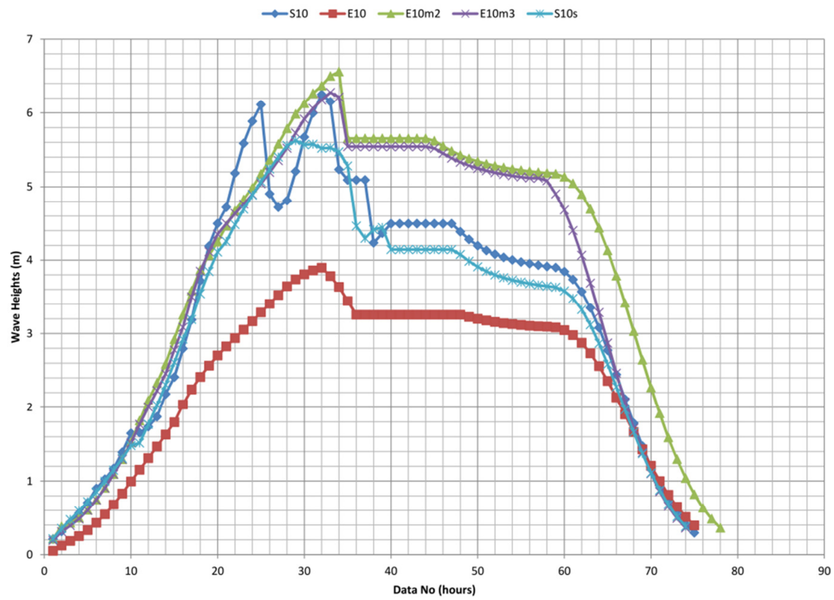

Figure 7.7: Wave Heights Obtained from S10, S10$_S$, E10, E10m2 and E10m3 Wind Speeds for Continuous Data Set 25 with W61 Numerical Model

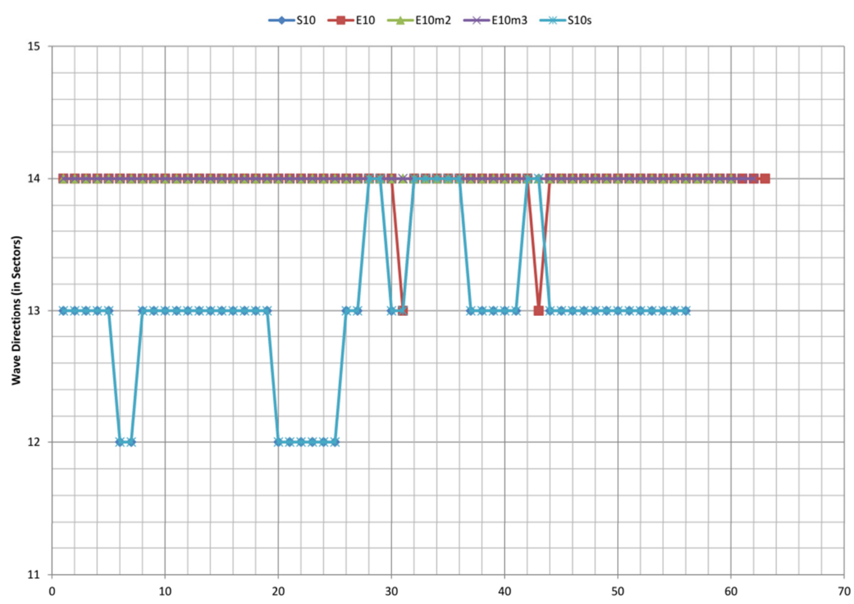

Figure 7.8: Wave Directions Obtained from S10, S10$_S$, E10, E10m2 and E10m3 Wind Speeds for Continuous Data Set 2 with W61 Numerical Model

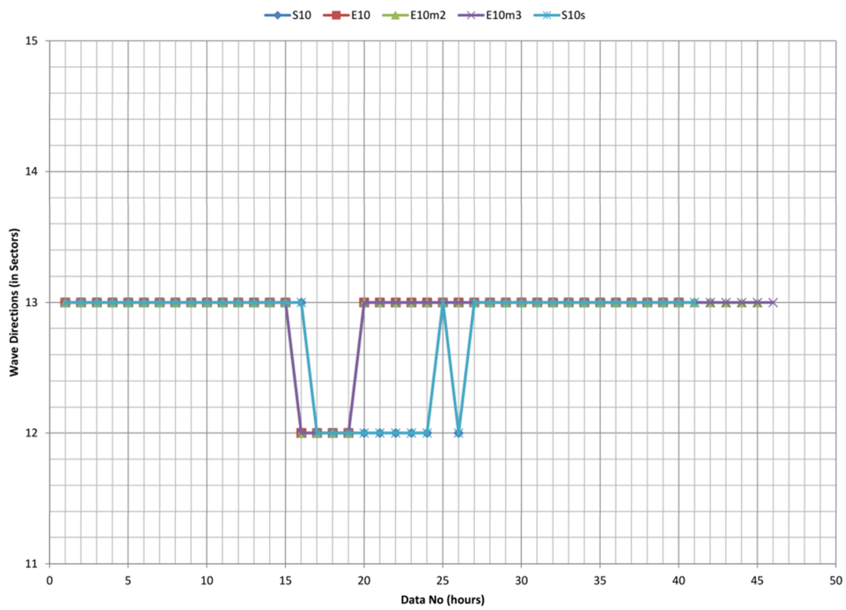

Figure 7.9: Wave Directions Obtained from S10, $S10_S$, E10, E10m2 and E10m3 Wind Speeds for Continuous Data Set 6 with W61 Numerical Model

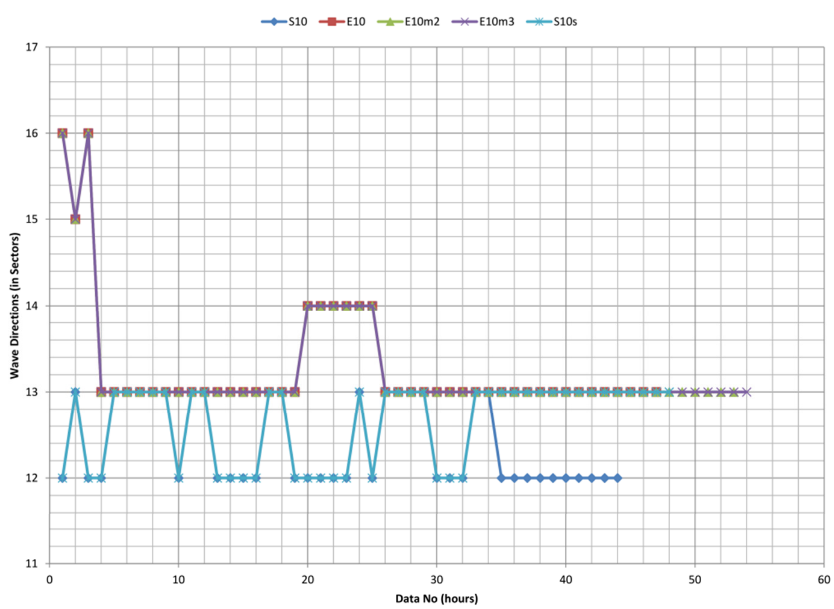

Figure 7.10: Wave Directions Obtained from S10, $S10_S$, E10, E10m2 and E10m3 Wind Speeds for Continuous Data Set 7 with W61 Numerical Model

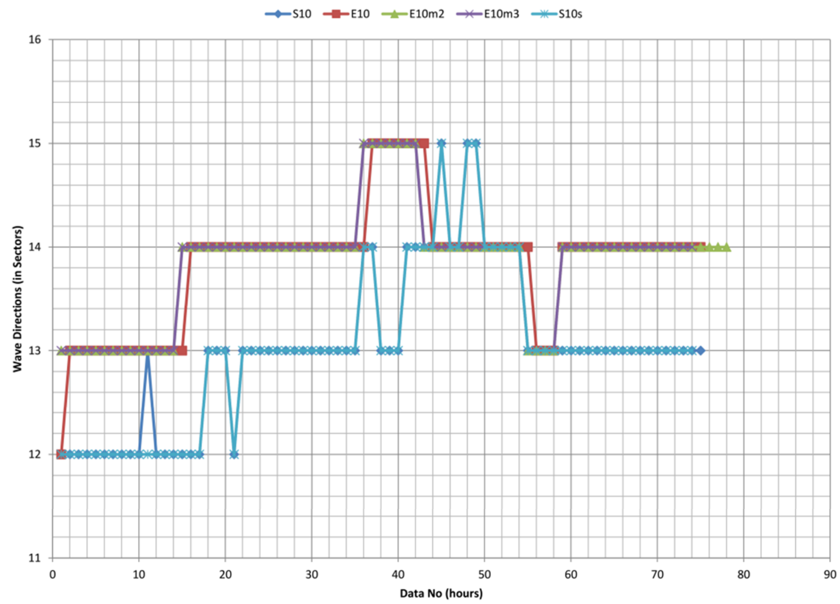

Figure 7.11: Wave Directions Obtained from S10, $S10_S$, E10, E10m2 and E10m3 Wind Speeds for Continuous Data Set 9 with W61 Numerical Model

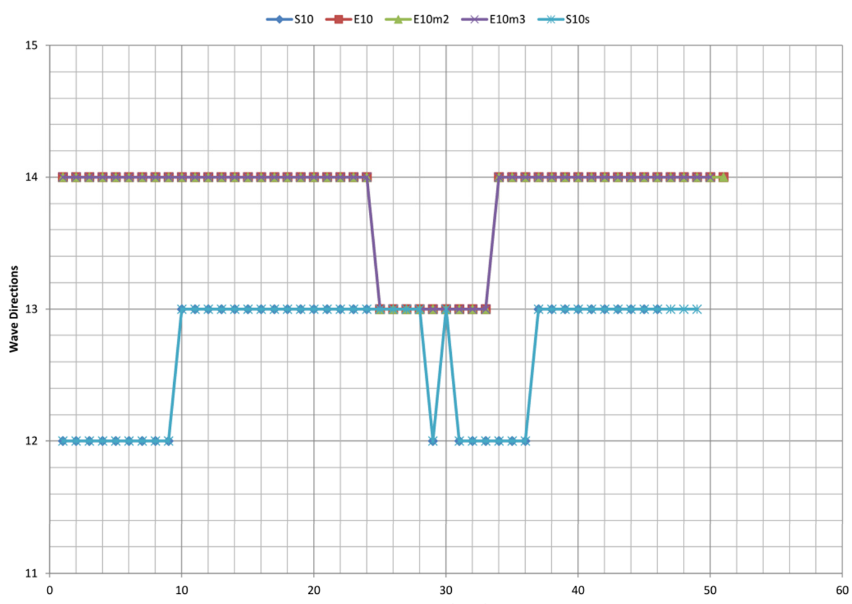

Figure 7.12: Wave Directions Obtained from S10, $S10_S$, E10, E10m2 and E10m3 Wind Speeds for Continuous Data Set 24 with W61 Numerical Model

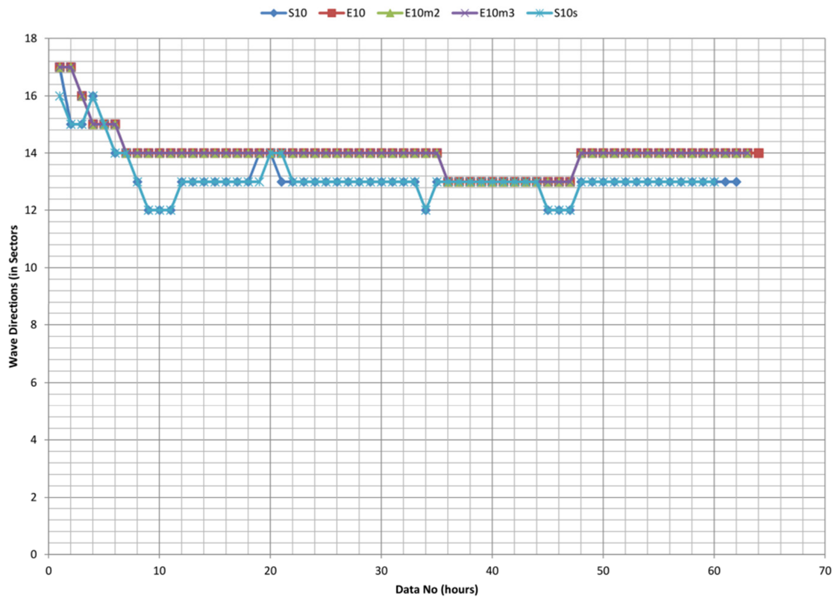

Figure 7.13: Wave Directions Obtained from S10, S10$_S$, E10, E10m2 and E10m3 Wind Speeds for Continuous Data Set 25 with W61 Numerical Model

The findings derivated from Figures 7.2-7.13 can be summarized as;

- For all of the cases, the direct use of E10 winds for wave estimations result in significant underestimation.
- For most of the cases, E10m2 and E10m3 waves give quite good correlation with S10 waves and comparably better correlation with S10$_S$ waves.
- Considering the maximum wave heights observed during storms, except two cases, the wave estimations for E10m2 and E10m3 winds are good.
- The underestimation and overestimation observed for the storm peaks in the above given figures may be related to the double peak structure of the storms and the implemented smoothing method. The smoothing would possibly bring some additional inaccuracy to the results which are more critical at the storm peaks.
- The wave estimations for developing storm conditions are better than the wave estimations for dissipating (calming) storm conditions, resulting in overestimation of waves while storms start to dissipate.

- As for the wind directions, the estimations are quite good for most of the cases with directional differences generally at most 2 sectors (45°) except for the first couple of hours in continuous data set 7 in which this difference reaches 4 sectors (90°).
- The directional differences between obtained S10, S10S winds and E10, E10m2, E10m3 winds may also have some role in the directional differences of wave estimations.

In the the above given figures, wind directions of S10 wind speeds, thus land-based in-situ wind measurements are used for the estimation of wind-waves. However, as stated several times in the previous sections, a directional difference between land and sea wind measurements up to 45° is often observed and regarded acceptable. Since, the average directional difference between land-based in-situ wind measurements and E10 wind data is under this value, it can also be said that directional information for E10 wind data may also be used for wave estimations considering S10 and $S10_S$ winds. Taking into account this situation, several runs have been performed for the same cases given above to obtain wave heights and the results are given in Figures 7.14-7.19.

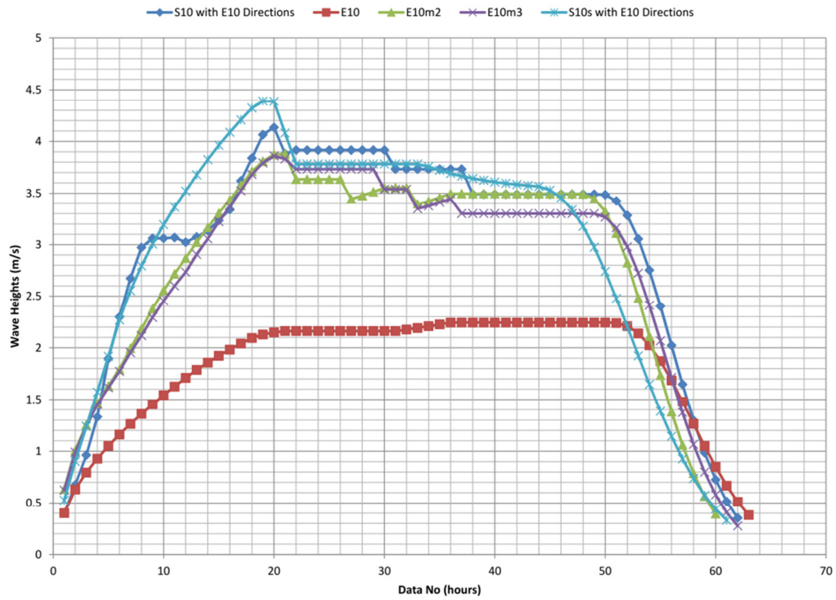

Figure 7.14: Wave Heights Obtained from S10, $S10_S$, E10, E10m2 and E10m3 Wind Speeds for Continuous Data Set 2 with W61 Numerical Model (Using E10 Wind Directions for S10 and $S10_S$ Wind Speeds)

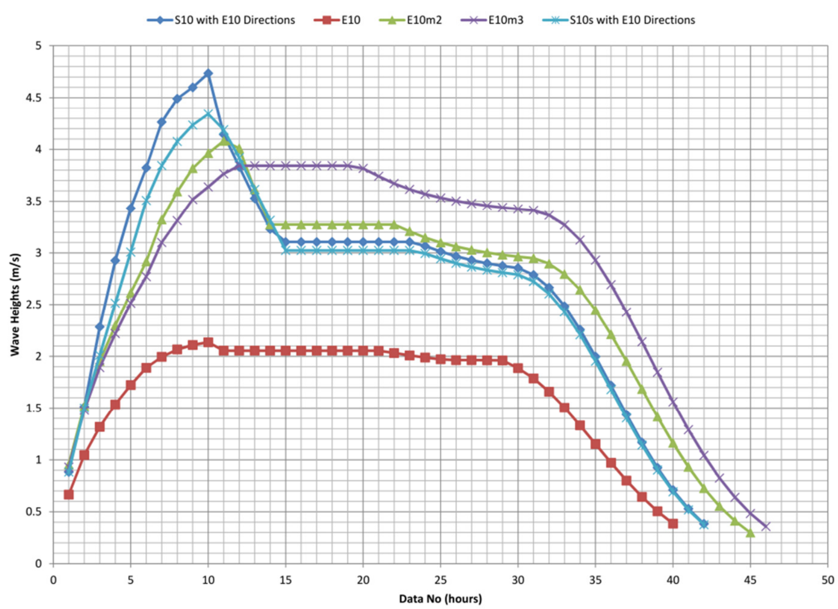

Figure 7.15: Wave Heights Obtained from S10, $S10_S$, E10, E10m2 and E10m3 Wind Speeds for Continuous Data Set 6 with W61 Numerical Model (Using ECMWF Wind Directions for S10 and $S10_S$ Wind Speeds)

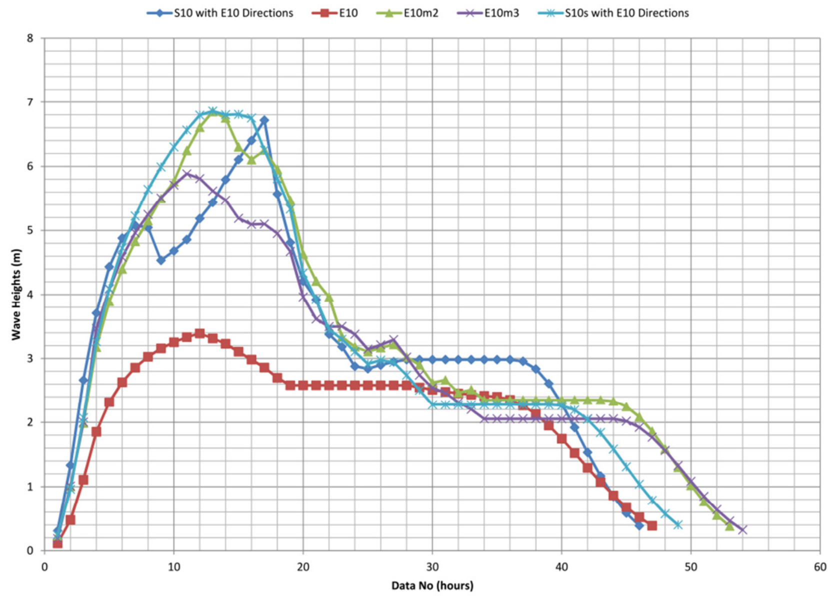

Figure 7.16: Wave Heights Obtained from S10, $S10_S$, E10, E10m2 and E10m3 Wind Speeds for Continuous Data Set 7 with W61 Numerical Model (Using E10 Wind Directions for S10 and $S10_S$ Wind Speeds)

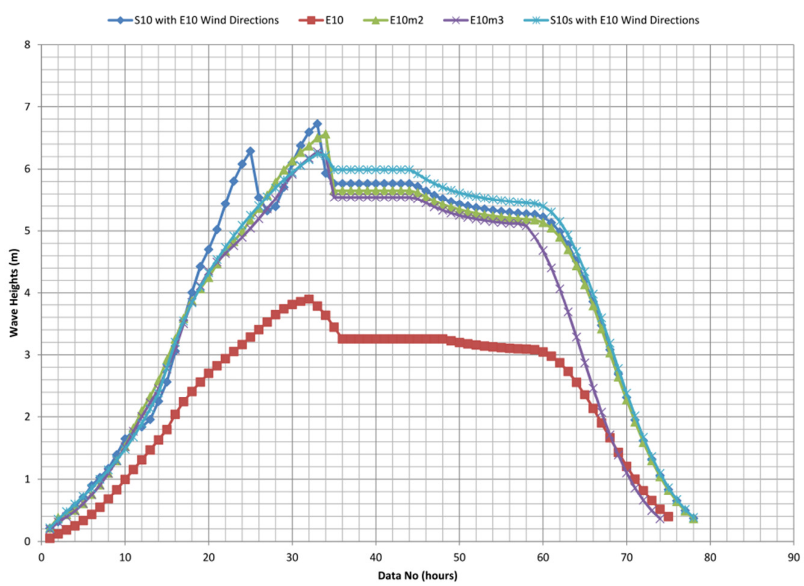

Figure 7.17: Wave Heights Obtained from S10, $S10_S$, E10, E10m2 and E10m3 Wind Speeds for Continuous Data Set 9 with W61 Numerical Model (Using E10 Wind Directions for S10 and $S10_S$ Wind Speeds)

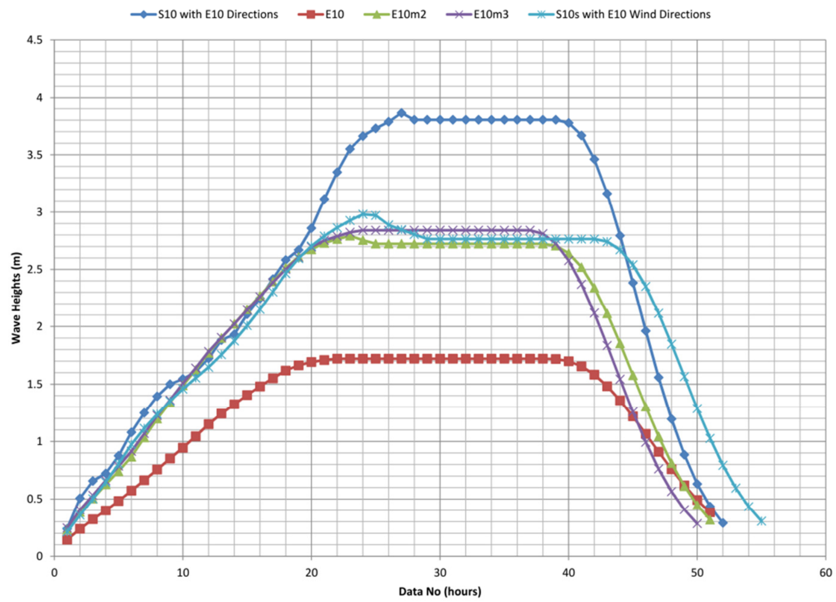

Figure 7.18: Wave Heights Obtained from S10, $S10_S$, E10, E10m2 and E10m3 Wind Speeds for Continuous Data Set 24 with W61 Numerical Model (Using E10 Wind Directions for S10 and $S10_S$ Wind Speeds)

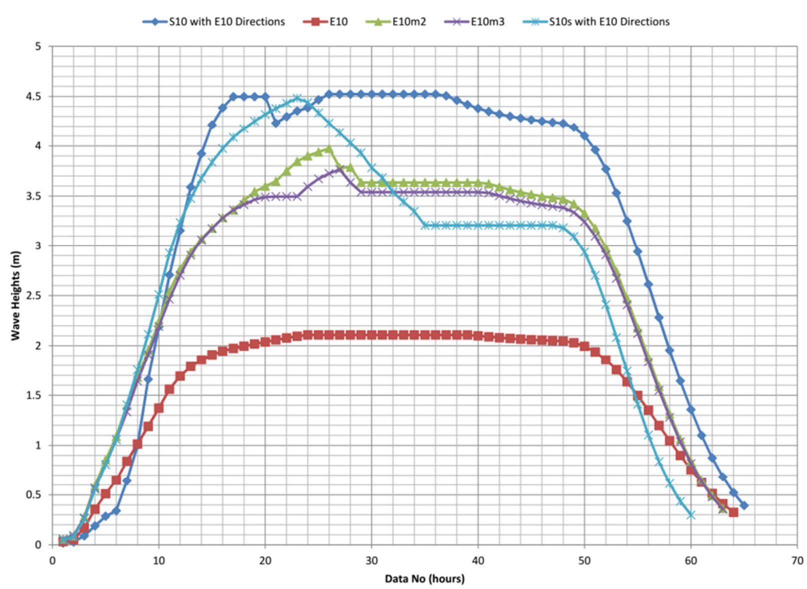

Figure 7.19: Wave Heights Obtained from S10, $S10_S$, E10, E10m2 and E10m3 Wind Speeds for Continuous Data Set 25 with W61 Numerical Model (Using E10 Wind Directions for S10 and $S10_S$ Wind Speeds)

The outcomes derived from Figures 7.14-7.19 are given below;

- Several of the findings stated above for Figures 7.2-7.6 are not seen anymore due to adaptation of E10 wind directions instead of S10 and $S10_S$ wind directions for all continuous data sets for the wave estimations.
- Especially for the duration after the storm peaks (dissipating storm conditions), the previously mentioned overestimation is partly overcame.
- Considering the overestimation and underestimation at storm peaks, even though several improvements in wave heights are achieved for these periods, all of the overestimations are not eliminated such as the case for continuous data set 24.

All of the above given comparisons give quite good overall idea about the differences in wave estimations performed by different wind data and also summarize the overall performance of the modification methods 2 and 3. In addition, the differences between wave estimations when two different wind directions (E10 and S10) are used are also observed. It can be concluded that smoothing and choice of which wind directions to be used play important role in the accuracy of the wave estimations. As for wind direction choice, since, for most of the cases, several of the differences in wave heights are not observed while adapting E10 wind directions for wave estimations from S10 ans $S10_S$ wind speeds, the use of ECMWF wind directions in wave estimations is preferrable for wave estimations for the case study site, Sinop.

In the above given comparisons performed for Sinop, only land-based in-situ wind measurement periods are covered during which simultaneous in-situ wave measurements do not exist. In order to see the performance of these methods for the other periods especially during which in-situ wave measurements are available, several storms are chosen in the past between 1994 and 1996, a period in which in-situ wave measurements are performed. This will provide additional information about wave estimations for the period when in-situ wind measurements are not available and direct use of modification methods 2 and 3 at times where neither in-situ wind nor in-situ wave measurements are available.

7.2. Comparison of In-Situ Wave Measurements and Wave Estimations for the Chosen Storms in the Past for Sinop Region

The in-situ wave measurements are performed within the scope of NATO TU-WAVES project in which a national wave gauge network is set up with deploying six directional buoys around Turkish coasts one of which is in Sinop. In-situ wave measurements cover certain periods between 1994 and 1996 with considerable gaps.

Sinop wave buoy is set up at coordinates 42°07´24´´ N - 35°05´12´´ E at water depth of 100 m and at a distance of 11.6 m km from the shore.For in-situ wave measurements spherically shaped directional waverider buoys, which measures the directional wave spectra, are used. It includes a heave-pitch sensor, a compass, fixed accelerometers in x and y directions and a mico-processor. Calculating the accelerations for north and west axes and performing FFT at every 30 minute time step, significant wave heights, H_S and mean wave periods, T_m are eventually computed together with several other additional outputs.The graphical forms of these in-situ wave measurements are available in official MEDCOAST website, "www.medcoast.org.tr".

The periods considered in comparisons are;

- 01:00 20.12.1995 – 20:00 22.12.1995 (68 hours) (P01)
- 19:00 12.11.1994 – 07:00 16.11.1994 (85 hours) (P02)
- 18:00 04.06.1996 – 01:00 08.06.1996 (80 hours) (P03)
- 17:00 04.11.1994 – 12:00 09.11.1994 (116 hours) (P04)
- 00:00 08.04.1996 – 00:00 11.04.1996 (73 hours) (P05)
- 00:00 12.04.1996 – 15:00 14.04.1996 (64 hours) (P06)
- 13:00 23.05.1996 – 10:00 26.05.1996 (70 hours) (P07)
- 19:00 30.01.1996 – 17:00 02.02.1996 (71 hours) (P08)
- 09:00 30.11.1995 – 05:00 03.12.1995 (69 hours) (P09)
- 00:00 14.12.1995 – 21:00 17.12.1995 (94 hours) (P10)
- 15:00 24.11.1994 – 00:00 29.11.1994 (106 hours) (P11)

The wave estimations are performed with S10, E10, E10m2 and E10m wind speeds and for wind directions E10 wind directions are used. Moreover, in order to see the influence of numerical model on wave estimations SWAN is used in addition to W61. The wave estimations with SWAN are performed with unmodified original wind fields over the whole Black Sea basin as well as with modified E10 wind speeds (E10m2) over the whole Black Sea basin. Since modification methods 2 and 3 give similar improvements and results in the previous studies, it is thought that using one of these modification methods would be enough. The unmodified and modified SWAN wave estimations are regarded as "SWAN" and "SWANm", respectively. SWAN runs are performed with unmodified and modified 6 hourly ECMWF wind data, thus wave estimations are obtained in 6 hour intervals unlike hourly wind data for other runs. Both numerical models are run longer than the above given periods (cases) since it takes time for waves to develop, thus it is aimed to avoid possible overestimation and underestimation at the beginning and ending of these periods. As a result, the starting point of x-axis in the below given figures do not coincide with 0. The results of wave estimations in terms of significant wave heights, significant wave periods and wave directions are given in Figure 7.21-7.53. The wave directions are given in accordance with Figure 7.20 in which except for the SW and SE directions, sea directions are covered. The wave directions are described in terms of sectors so that it would be easy to observe the directional differences as well as to overcome the complication of spherical representation of directions, especially at N where 0° and 360° meets where it would be hard to observe the directional changes in a graphical representation.

In addition to Figures 7.21-7.53, Tables 7.2-7.12, which summarize the results in terms of H_{max}, T_{max}, H_{ave}, T_{ave}, representative wave direction (REP), are prepared for each period (P). Moreover, average bias, RMSE and average MAE are also given in Tables 7.13-7.15 (for significant wave heights) and Tables 7.19-7.21 (for significant wave periods) for each case. In these tables, only W61 wave estimations performed with modified wind measurements are considered since W61 wave estimations are obtained hourly whereas SWAN wave estimations are obtained 6 hourly, thus W61 wave estimations are more appropriate such comparisons. In Tables 7.16-7.18 and

Tables 7.22-7.24, average bias, RMSE and average MAE obtained only for the peak consecutive 9 wave estimations at the storm peaks are given in terms of significant wave heights and periods. The peak (maximum) points are chosen according to in-situ wave measurements and the peak (maximum) in-situ wave height forms the mid point of these 9 consecutive points. This comparison is performed to understand if wave estimations are different for the storm peaks other than the developing and calming parts of the storm.

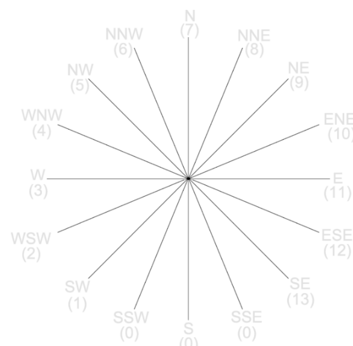

Figure 7.20: Wave Directions and Their Designation in Terms of Sectorel Numbers Considered in Figures 7.21-7.53

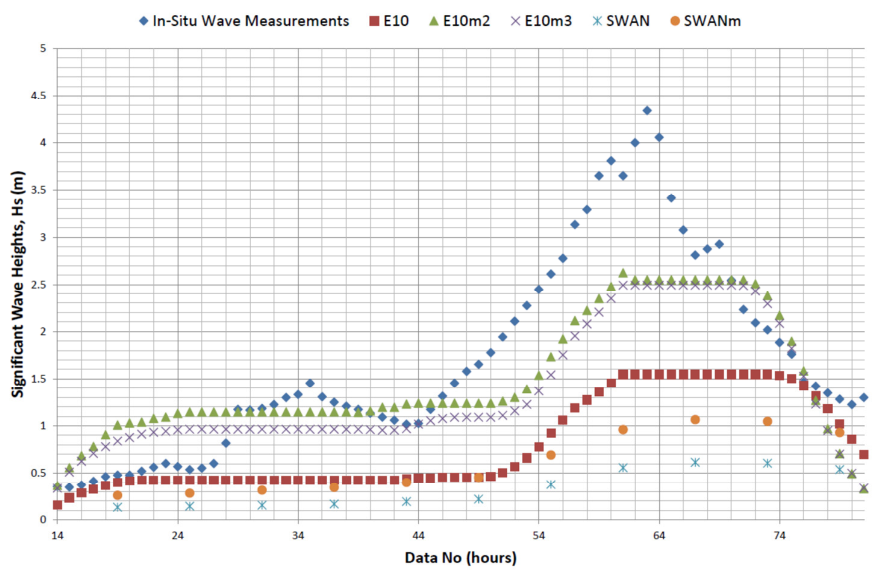

Figure 7.21: Significant Wave Heights Obtained from S10, E10, E10m2, E10m3, SWAN and SWANm Wind Speeds for P01

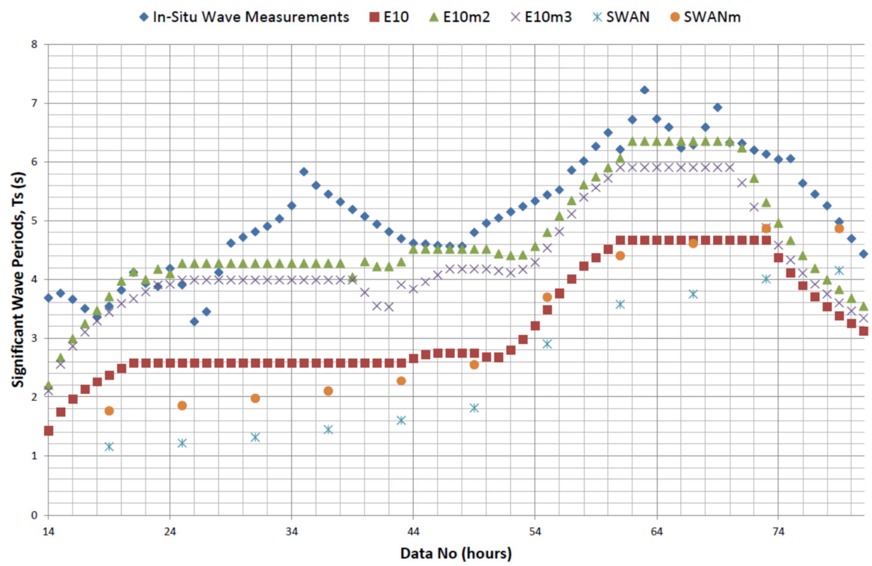

Figure 7.22: Significant Wave Periods Obtained from S10, E10, E10m2, E10m3, SWAN and SWANm Wind Speeds for P01

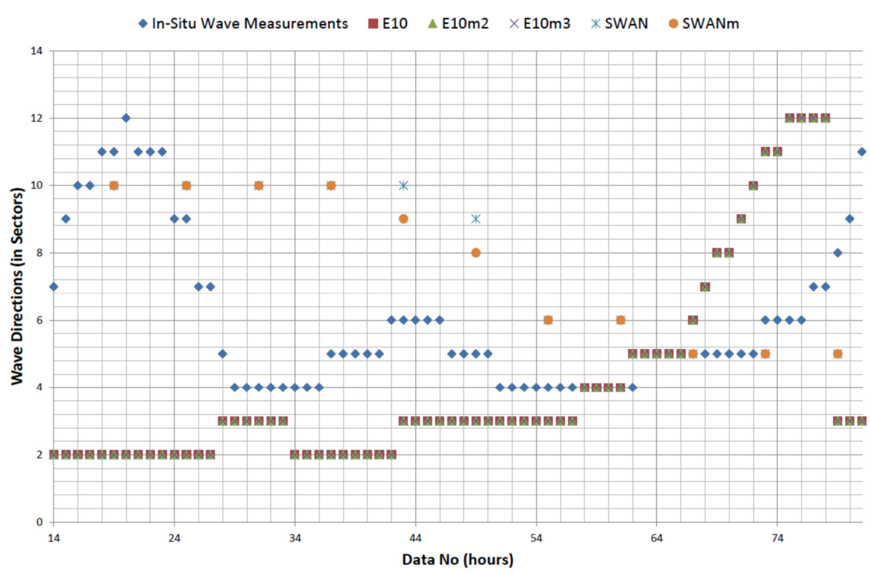

Figure 7.23: Wave Directions Obtained from S10, E10, E10m2, E10m3, SWAN and SWANm Wind Speeds for P01

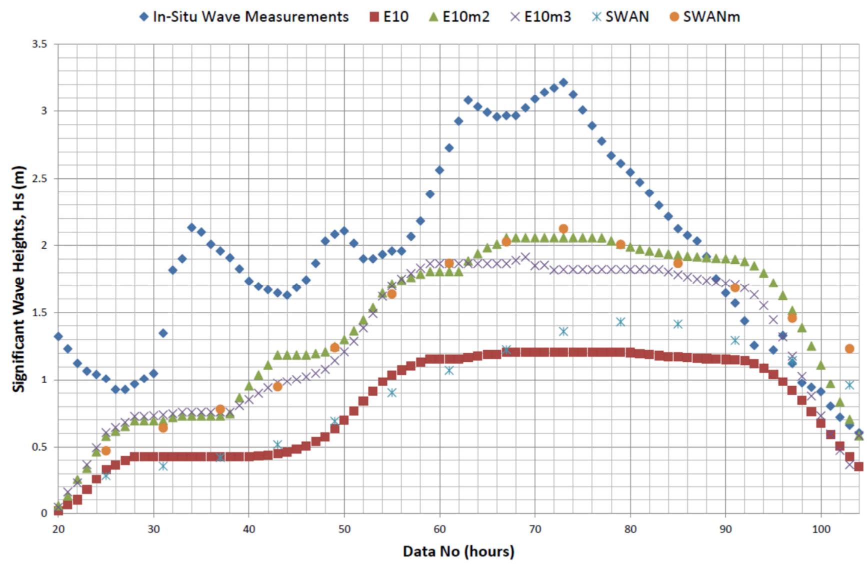

Figure 7.24: Significant Wave Heights Obtained from S10, E10, E10m2, E10m3, SWAN and SWANm Wind Speeds for P02

Figure 7.25: Significant Wave Periods Obtained from S10, E10, E10m2, E10m3, SWAN and SWANm Wind Speeds for P02

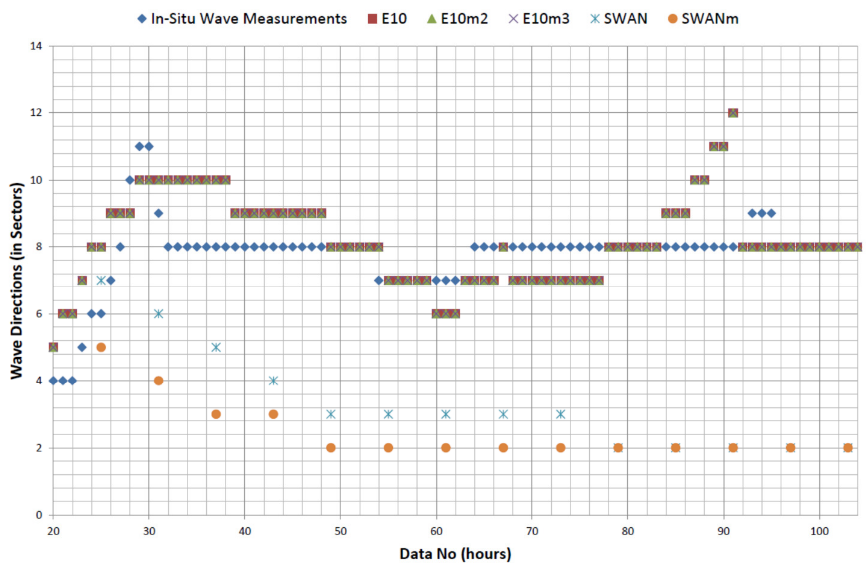

Figure 7.26: Wave Directions Obtained from S10, E10, E10m2, E10m3, SWAN and SWANm Wind Speeds for P02

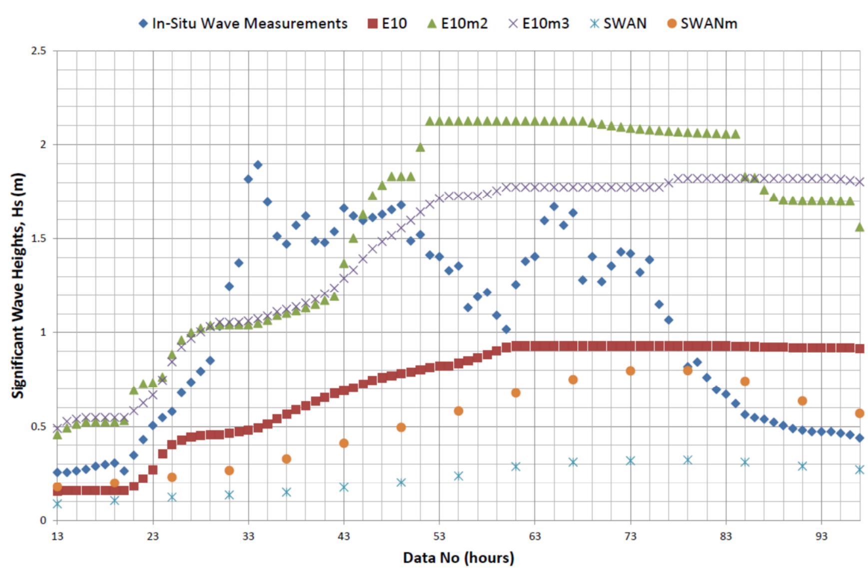

Figure 7.27: Significant Wave Heights Obtained from S10, E10, E10m2, E10m3, SWAN and SWANm Wind Speeds for P03

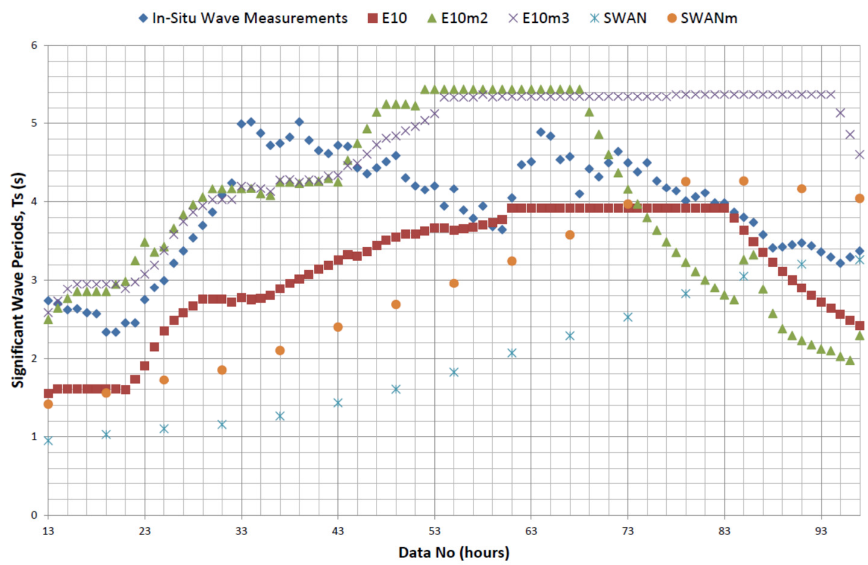

Figure 7.28: Significant Wave Periods Obtained from S10, E10, E10m2, E10m3, SWAN and SWANm Wind Speeds for P03

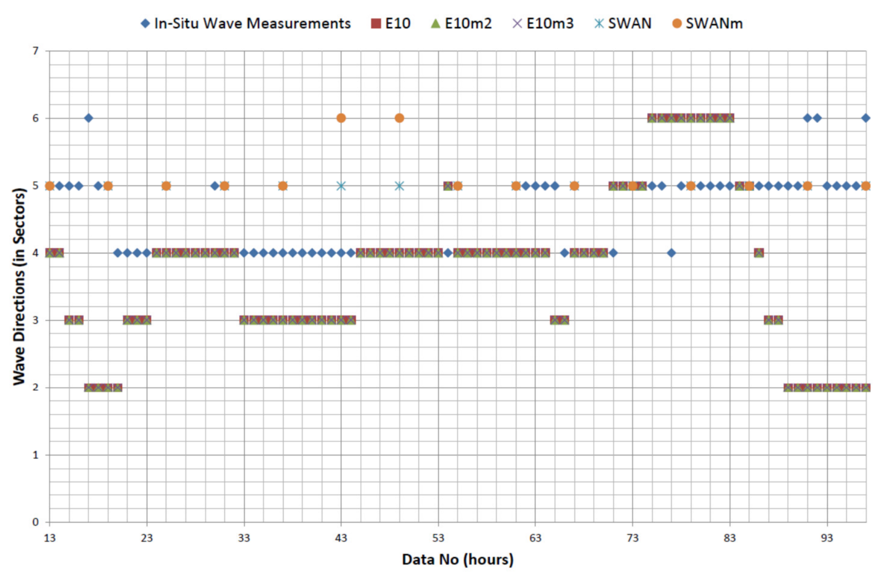

Figure 7.29: Wave Directions Obtained from S10, E10, E10m2, E10m3, SWAN and SWANm Wind Speeds for P03

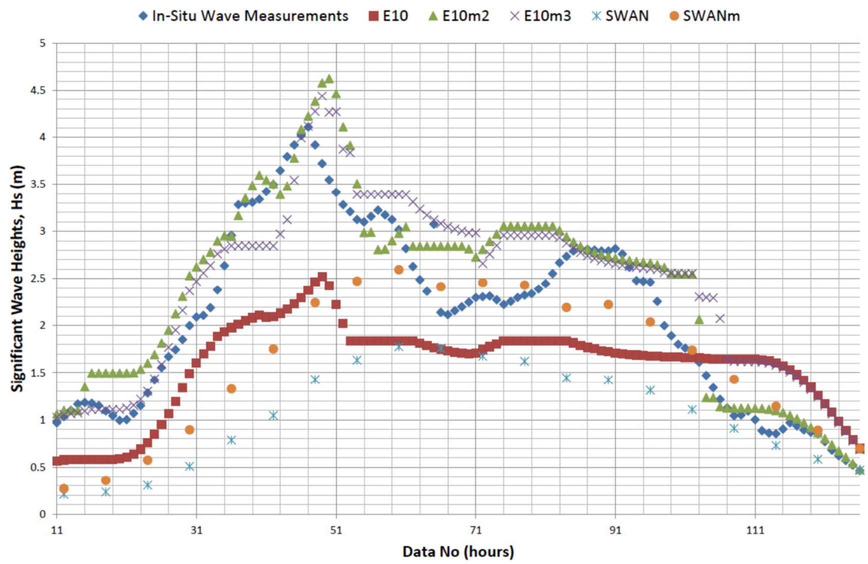

Figure 7.30: Significant Wave Heights Obtained from S10, E10, E10m2, E10m3, SWAN and SWANm Wind Speeds for P04

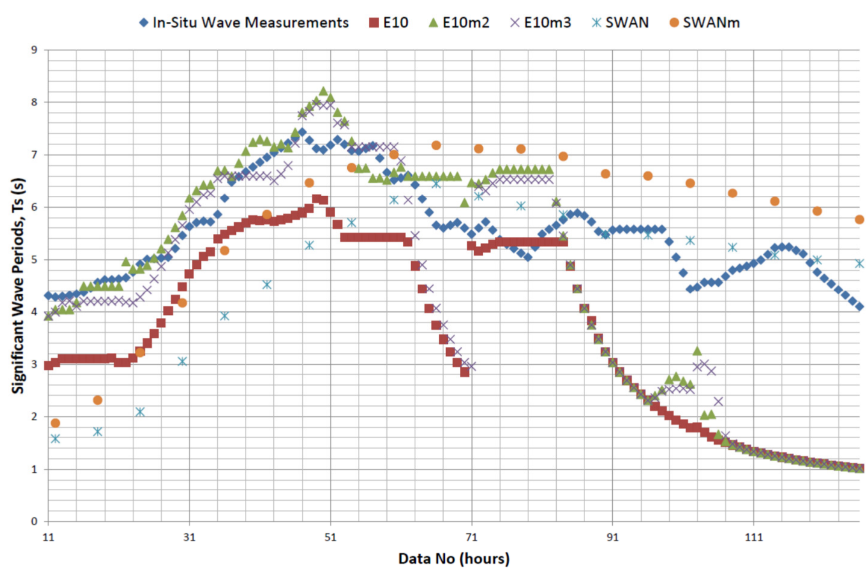

Figure 7.31: Significant Wave Periods Obtained from S10, E10, E10m2, E10m3, SWAN and SWANm Wind Speeds for P04

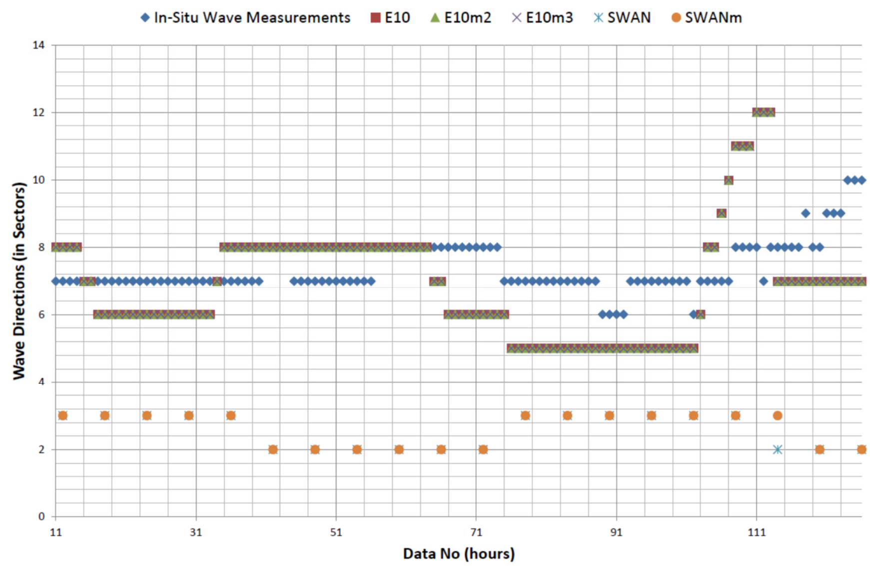

Figure 7.32: Wave Directions Obtained from S10, E10, E10m2, E10m3, SWAN and SWANm Wind Speeds for P04

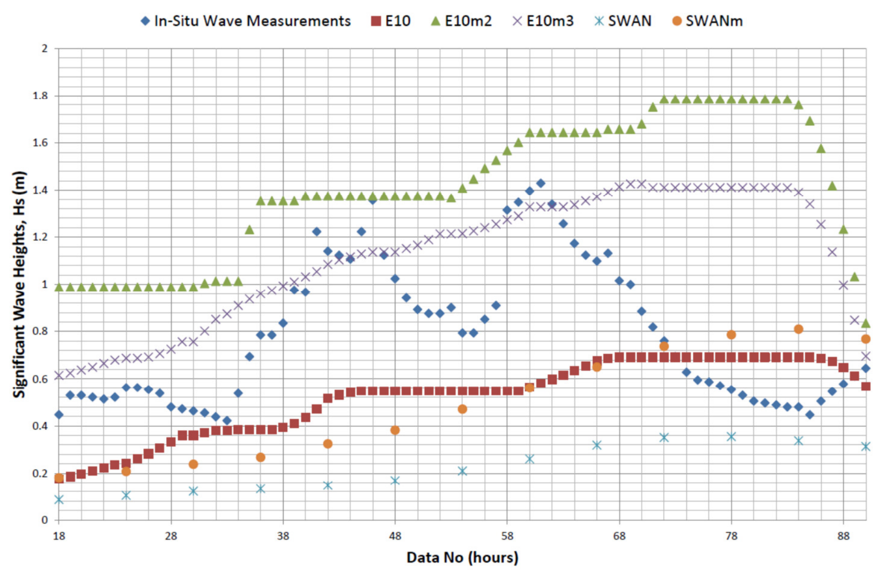

Figure 7.33: Significant Wave Heights Obtained from S10, E10, E10m2, E10m3, SWAN and SWANm Wind Speeds for P05

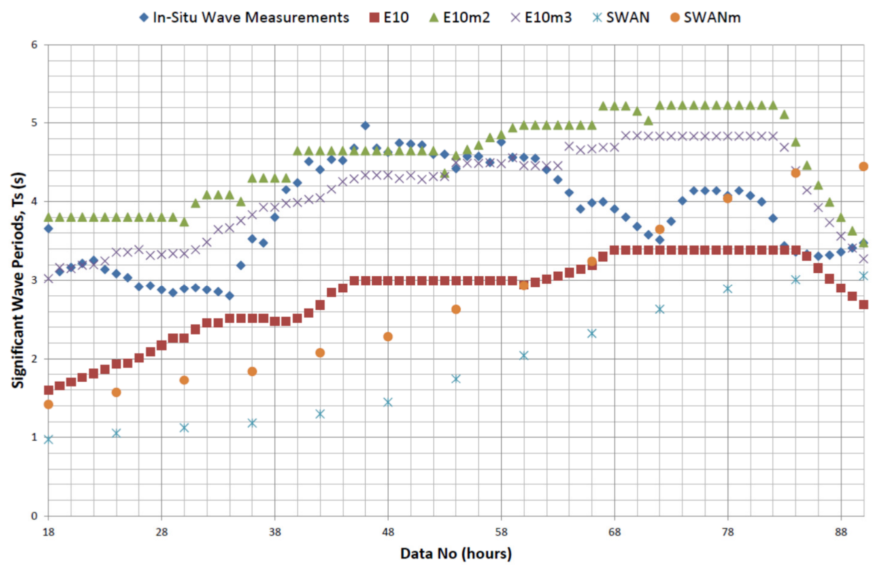

Figure 7.34: Significant Wave Periods Obtained from S10, E10, E10m2, E10m3, SWAN and SWANm Wind Speeds for P05

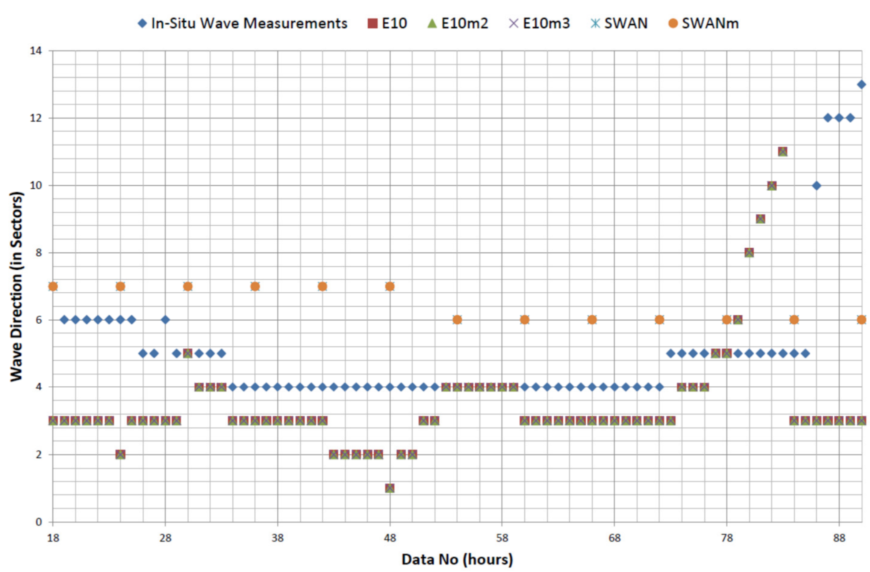

Figure 7.35: Wave Directions Obtained from S10, E10, E10m2, E10m3, SWAN and SWANm Wind Speeds for P05

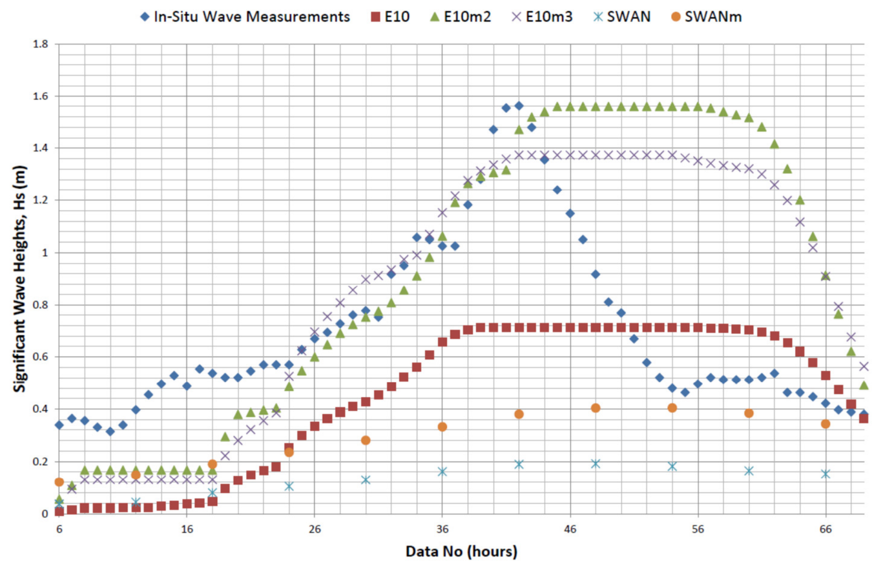

Figure 7.36: Significant Wave Heights Obtained from S10, E10, E10m2, E10m3, SWAN and SWANm Wind Speeds for P06

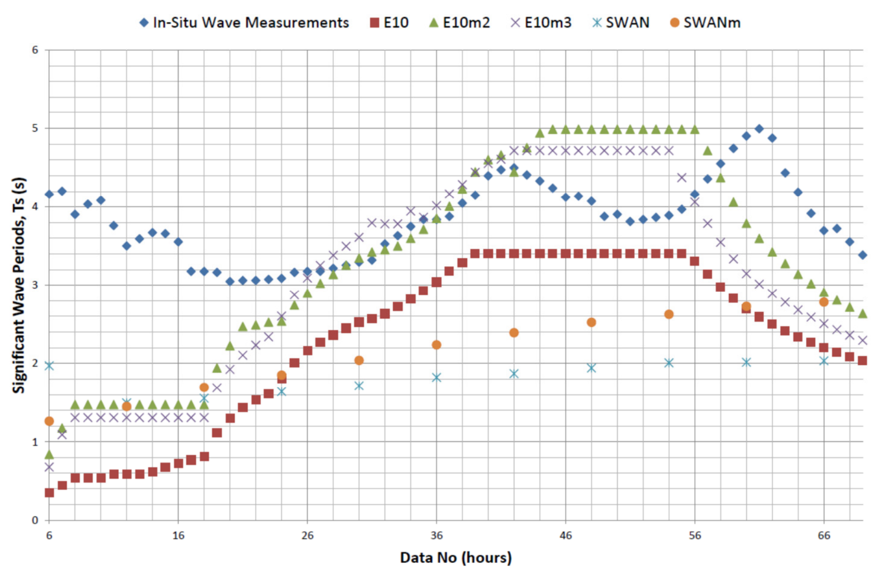

Figure 7.37: Significant Wave Periods Obtained from S10, E10, E10m2, E10m3, SWAN and SWANm Wind Speeds for P06

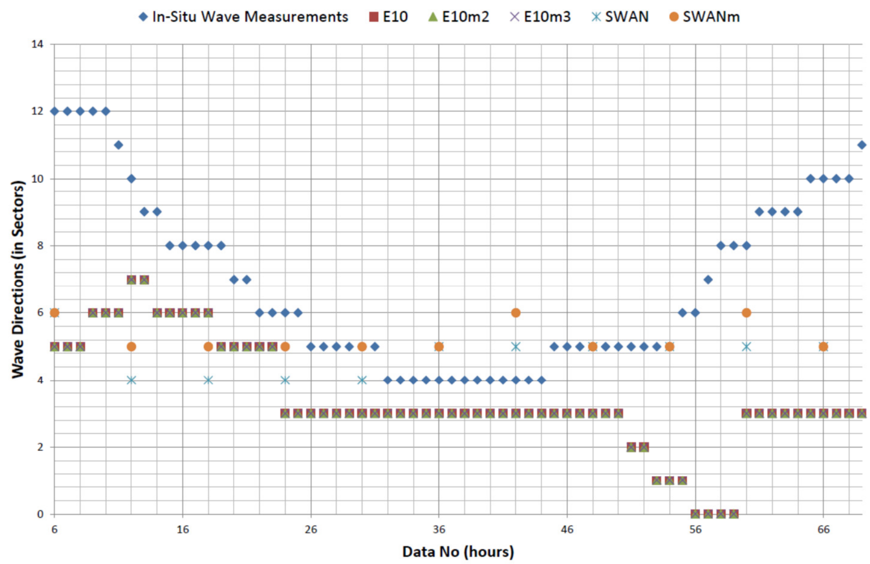

Figure 7.38: Wave Directions Obtained from S10, E10, E10m2, E10m3, SWAN and SWANm Wind Speeds for P06

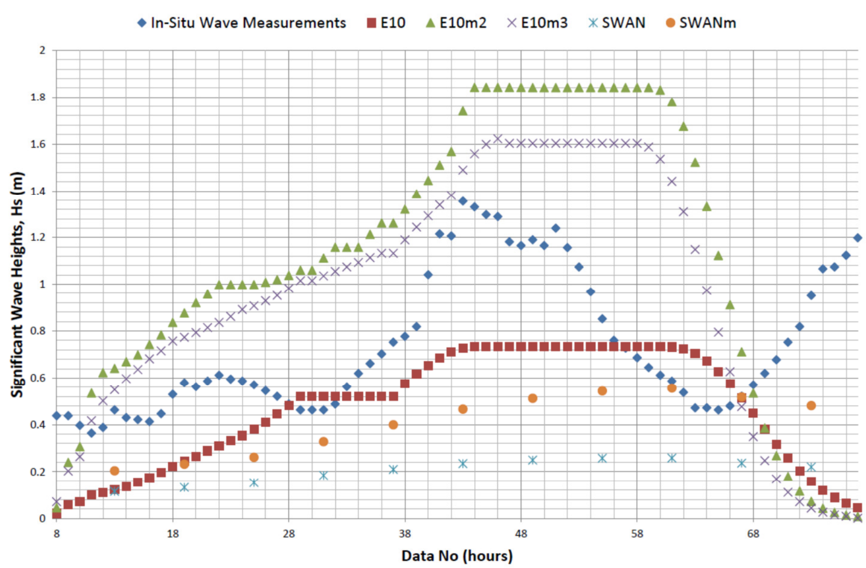

Figure 7.39: Significant Wave Heights Obtained from S10, E10, E10m2, E10m3, SWAN and SWANm Wind Speeds for P07

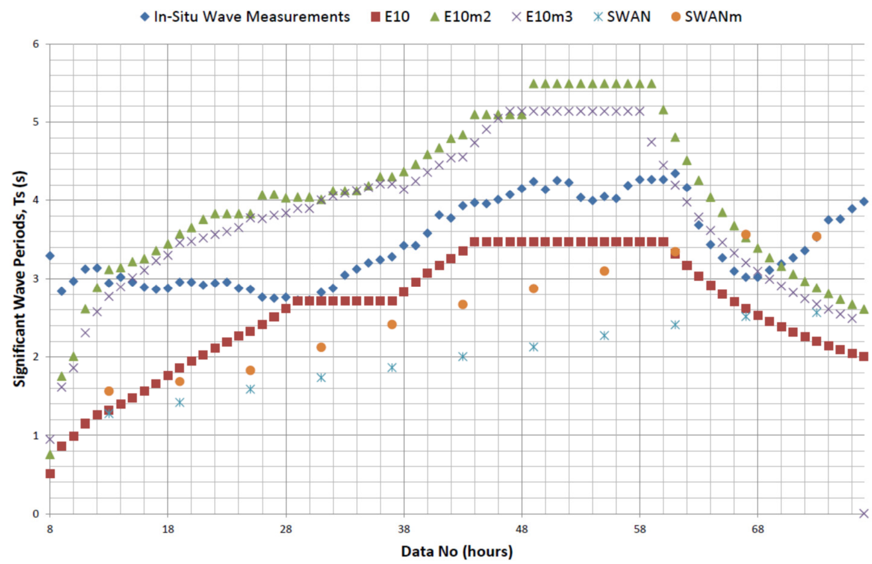

Figure 7.40: Significant Wave Periods Obtained from S10, E10, E10m2, E10m3, SWAN and SWANm Wind Speeds for P07

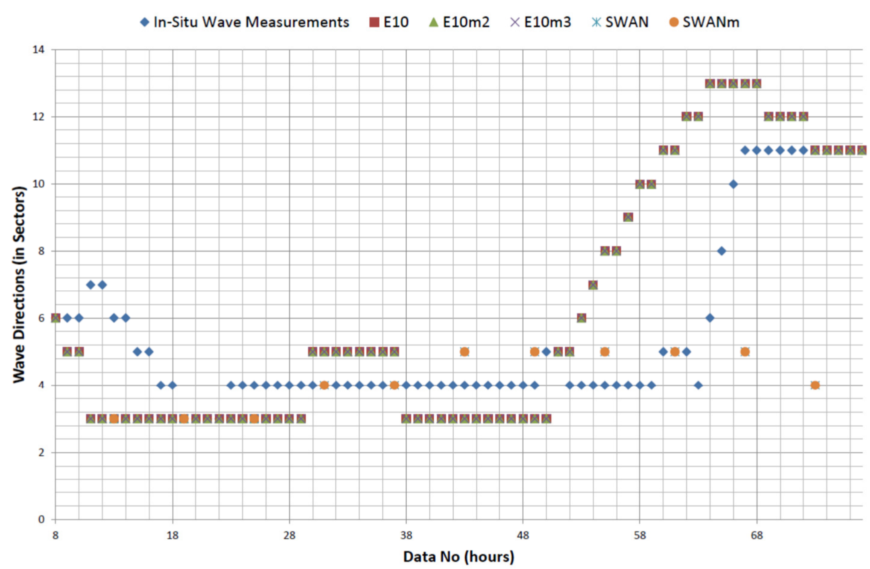

Figure 7.41: Wave Directions Obtained from S10, E10, E10m2, E10m3, SWAN and SWANm Wind Speeds for P07

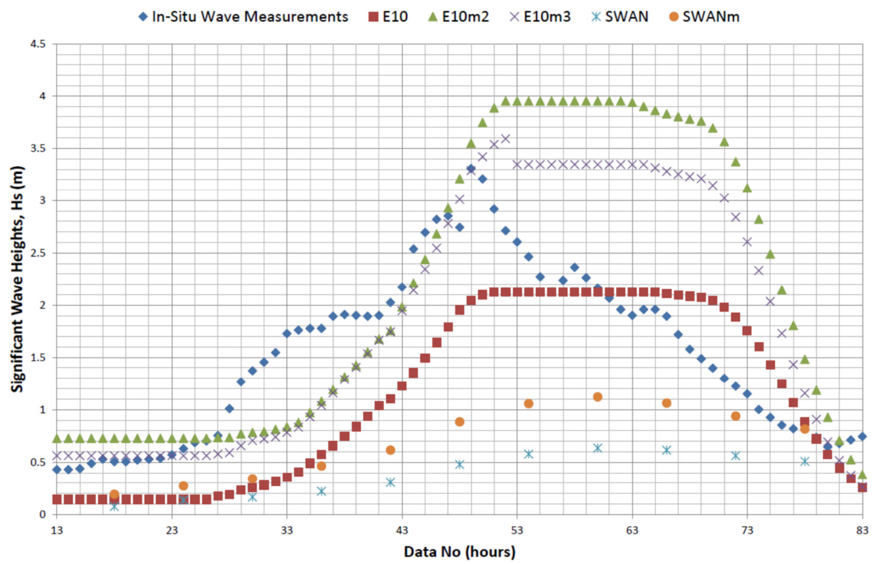

Figure 7.42: Significant Wave Heights Obtained from S10, E10, E10m2, E10m3, SWAN and SWANm Wind Speeds for P08

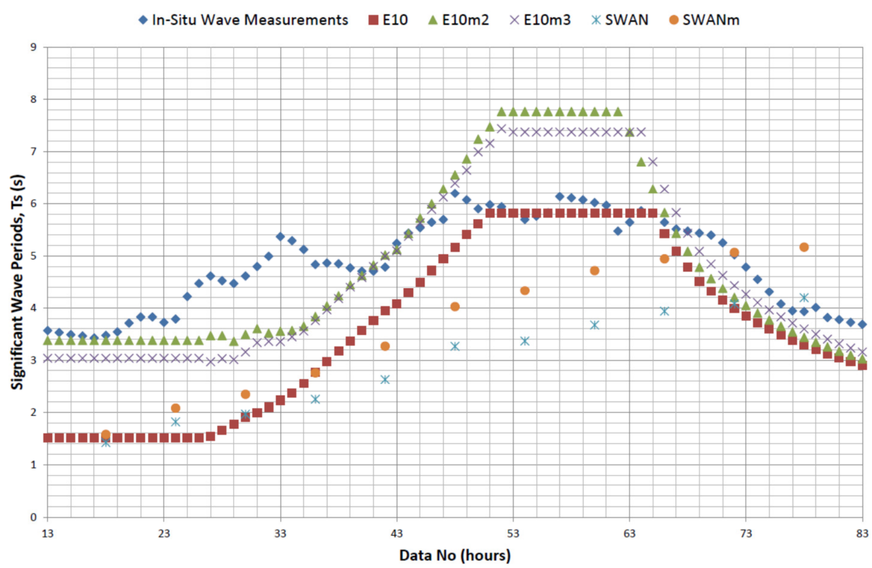

Figure 7.43: Significant Wave Periods Obtained from S10, E10, E10m2, E10m3, SWAN and SWANm Wind Speeds for P08

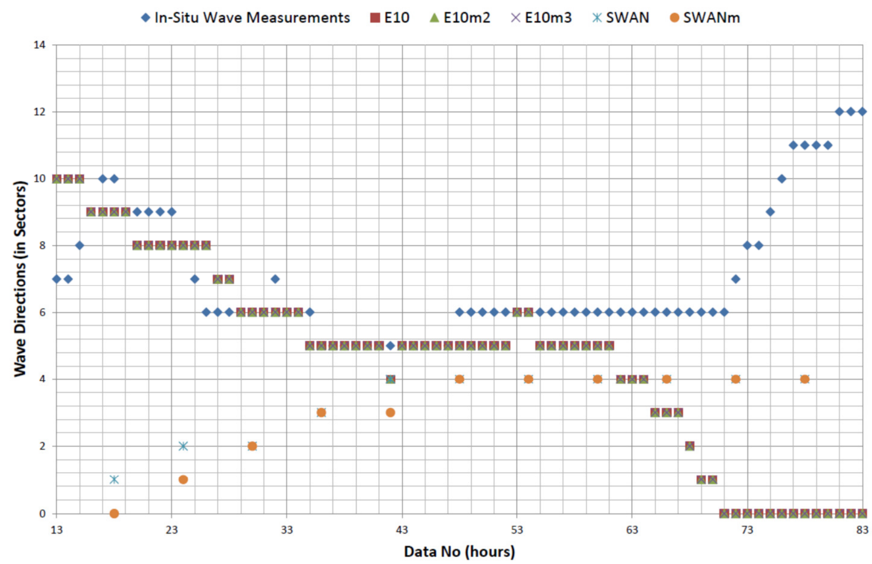

Figure 7.44: Wave Directions Obtained from S10, E10, E10m2, E10m3, SWAN and SWANm Wind Speeds for P08

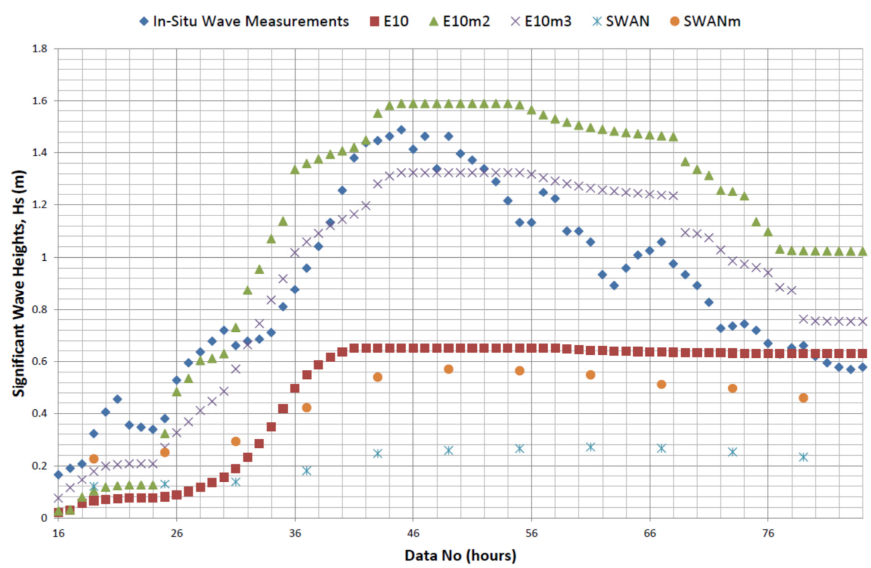

Figure 7.45: Significant Wave Heights Obtained from S10, E10, E10m2, E10m3, SWAN and SWANm Wind Speeds for P09

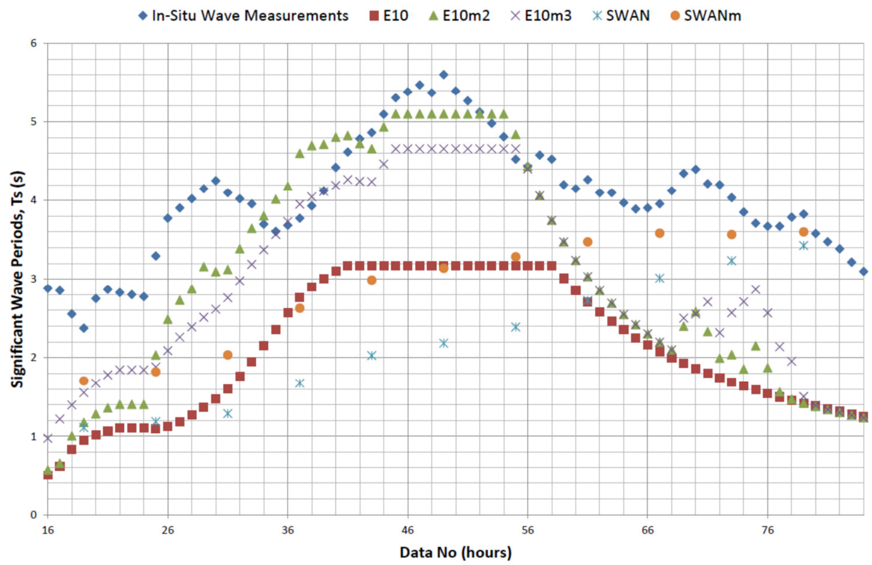

Figure 7.46: Significant Wave Periods Obtained from S10, E10, E10m2, E10m3, SWAN and SWANm Wind Speeds for P09

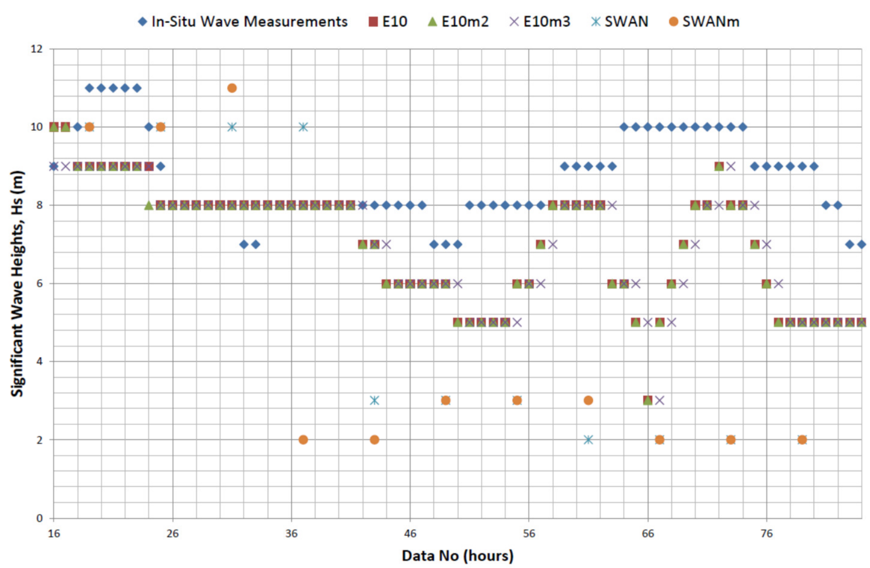

Figure 7.47: Wave Directions Obtained from S10, E10, E10m2, E10m3, SWAN and SWANm Wind Speeds for P09

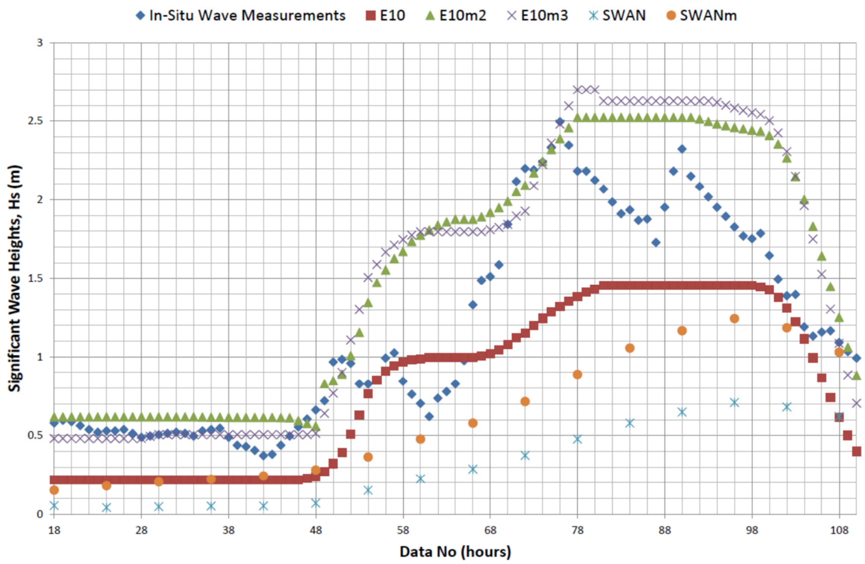

Figure 7.48: Significant Wave Heights Obtained from S10, E10, E10m2, E10m3, SWAN and SWANm Wind Speeds for P10

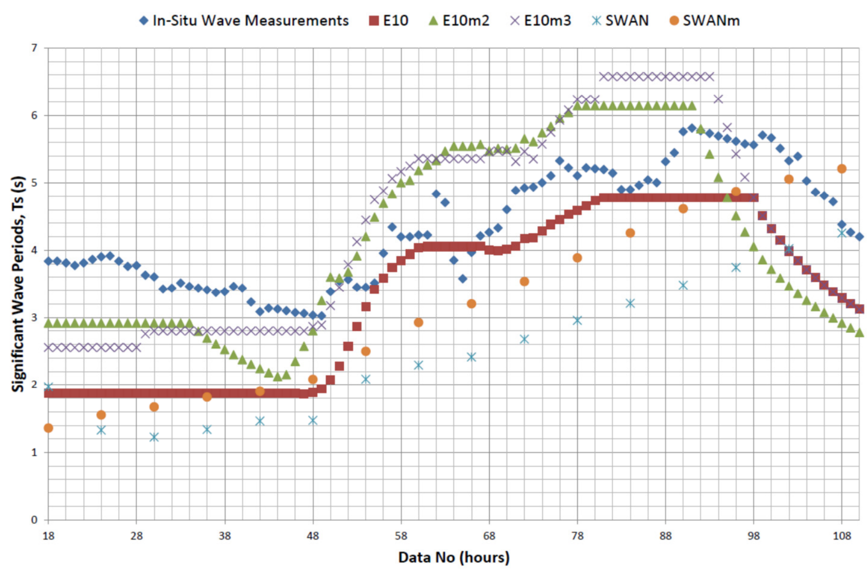

Figure 7.49: Significant Wave Periods Obtained from S10, E10, E10m2, E10m3, SWAN and SWANm Wind Speeds for P10

Figure 7.50: Wave Directions Obtained from S10, E10, E10m2, E10m3, SWAN and SWANm Wind Speeds for P10

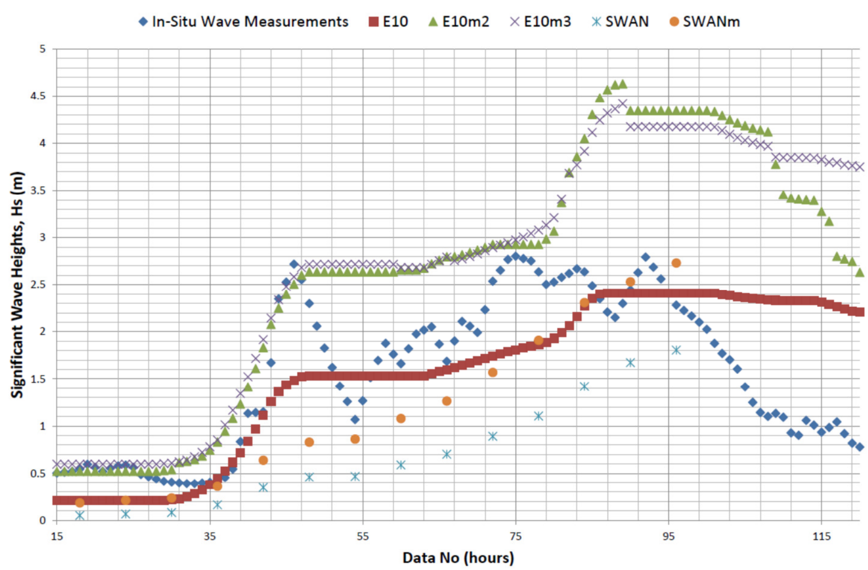

Figure 7.51: Significant Wave Heights Obtained from S10, E10, E10m2, E10m3, SWAN and SWANm Wind Speeds for P11

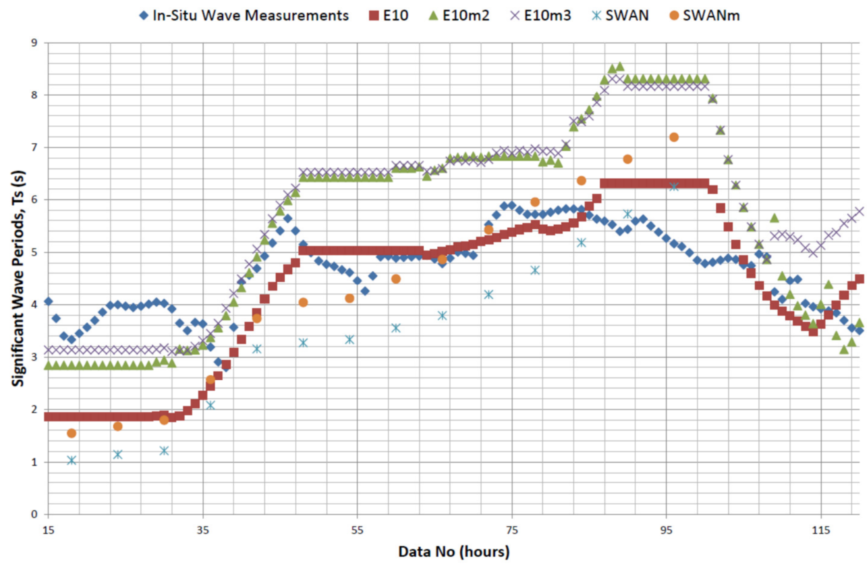

Figure 7.52: Significant Wave Periods Obtained from S10, E10, E10m2, E10m3, SWAN and SWANm Wind Speeds for P11

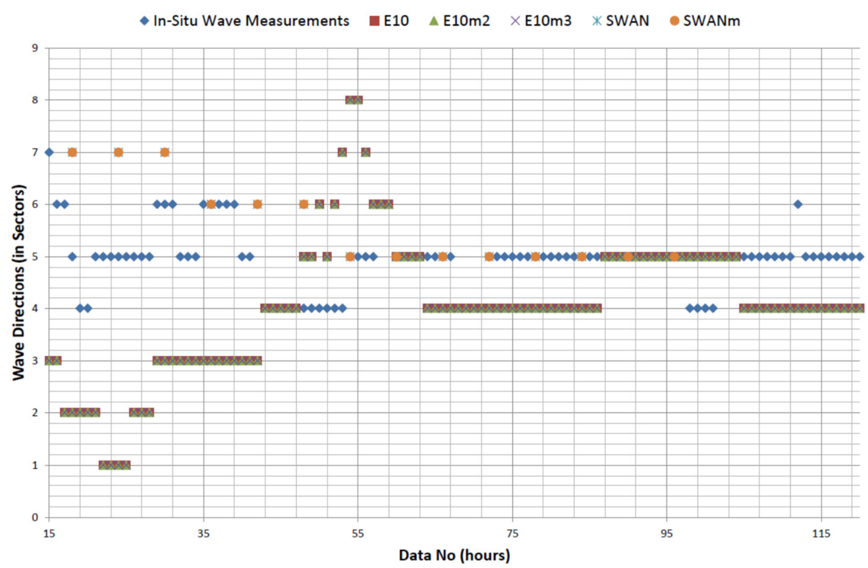

Figure 7.53: Wave Directions Obtained from S10, E10, E10m2, E10m3, SWAN and SWANm Wind Speeds for P11

Table 7.2: H_{max}, T_{max}, H_{ave}, T_{ave} and REP regarding In-Situ Wave Measurements (In-Situ), E10, E10m2, E10m3, SWAN and SWANm for P01

P01	H_{max} (m)	T_{max} (s)	H_{ave} (m)	T_{ave} (s)	REP
In-Situ	4.34	7.22	1.70	5.12	6
E10	1.55	4.66	0.80	3.22	4
E10m2	2.62	6.35	1.49	4.64	4
E10m3	2.49	5.91	1.36	4.31	4
SWAN	0.61	4.20	0.31	2.51	8
SWANm	1.07	4.87	0.57	3.14	8

Table 7.3: H_{max}, T_{max}, H_{ave}, T_{ave} and REP regarding In-Situ Wave Measurements (In-Situ), E10, E10m2, E10m3, SWAN and SWANm for P02

P02	H_{max} (m)	T_{max} (s)	H_{ave} (m)	T_{ave} (s)	REP
In-Situ	3.21	6.74	1.93	5.66	8
E10	1.21	4.43	0.82	2.99	8
E10m2	2.06	5.64	1.41	3.72	8
E10m3	1.91	5.51	1.29	3.96	8
SWAN	1.43	7.08	0.75	4.51	4
SWANm	2.12	7.38	1.13	5.28	3

Table 7.4: H_{max}, T_{max}, H_{ave}, T_{ave} and REP regarding In-Situ Wave Measurements (In-Situ), E10, E10m2, E10m3, SWAN and SWANm for P03

P03	H_{max} (m)	T_{max} (s)	H_{ave} (m)	T_{ave} (s)	REP
In-Situ	1.89	5.02	1.04	3.91	5
E10	0.93	3.92	0.71	3.14	4
E10m2	2.12	5.44	1.57	3.96	4
E10m3	1.82	5.37	1.43	4.64	4
SWAN	0.33	3.26	0.22	1.97	5
SWANm	0.80	4.27	0.51	2.95	5

Table 7.5: H_{max}, T_{max}, H_{ave}, T_{ave} and REP regarding In-Situ Wave Measurements (In-Situ), E10, E10m2, E10m3, SWAN and SWANm for P04

P04	H_{max} (m)	T_{max} (s)	H_{ave} (m)	T_{ave} (s)	REP
In-Situ	4.11	7.43	2.13	5.57	7
E10	2.52	6.17	1.59	3.72	7
E10m2	4.62	8.22	2.40	4.76	7
E10m3	4.44	7.96	2.43	4.47	7
SWAN	1.77	6.45	1.01	4.59	3
SWANm	2.59	7.18	1.54	5.55	3

Table 7.6: H_{max}, T_{max}, H_{ave}, T_{ave} and REP regarding In-Situ Wave Measurements (In-Situ), E10, E10m2, E10m3, SWAN and SWANm for P05

P05	H_{max} (m)	T_{max} (s)	H_{ave} (m)	T_{ave} (s)	REP
In-Situ	1.43	4.97	0.79	3.85	5
E10	0.69	3.39	0.52	2.82	4
E10m2	1.79	5.23	1.41	4.54	4
E10m3	1.43	4.84	1.12	4.14	4
SWAN	0.35	3.06	0.22	1.90	6
SWANm	0.81	4.45	0.49	2.78	6

Table 7.7: H_{max}, T_{max}, H_{ave}, T_{ave} and REP regarding In-Situ Wave Measurements (In-Situ), E10, E10m2, E10m3, SWAN and SWANm for P06

P06	H_{max} (m)	T_{max} (s)	H_{ave} (m)	T_{ave} (s)	REP
In-Situ	1.56	4.99	0.70	3.84	7
E10	0.71	3.41	0.45	2.30	3
E10m2	1.56	4.99	0.92	3.32	3
E10m3	1.37	4.72	0.87	3.14	3
SWAN	0.19	2.04	0.13	1.85	5
SWANm	0.40	2.79	0.30	2.24	5

Table 7.8: H_{max}, T_{max}, H_{ave}, T_{ave} and REP regarding In-Situ Wave Measurements (In-Situ), E10, E10m2, E10m3, SWAN and SWANm for P07

P07	H_{max} (m)	T_{max} (s)	H_{ave} (m)	T_{ave} (s)	REP
In-Situ	1.36	4.34	0.74	3.44	6
E10	0.73	3.47	0.47	2.59	6
E10m2	1.84	5.50	1.10	4.03	6
E10m3	1.62	5.14	0.95	3.76	6
SWAN	0.26	2.84	0.21	2.11	4
SWANm	0.56	3.74	0.42	2.78	4

Table 7.9: H_{max}, T_{max}, H_{ave}, T_{ave} and REP regarding In-Situ Wave Measurements (In-Situ), E10, E10m2, E10m3, SWAN and SWANm for P08

P08	H_{max} (m)	T_{max} (s)	H_{ave} (m)	T_{ave} (s)	REP
In-Situ	3.31	6.20	1.54	4.86	7
E10	2.12	5.82	1.13	3.63	5
E10m2	3.95	7.76	2.15	4.86	5
E10m3	3.59	7.43	1.86	4.75	5
SWAN	0.63	4.26	0.36	3.18	4
SWANm	1.12	5.17	0.61	3.69	4

Table 7.10: H_{max}, T_{max}, H_{ave}, T_{ave} and REP regarding In-Situ Wave Measurements (In-Situ), E10, E10m2, E10m3, SWAN and SWANm for P09

P09	H_{max} (m)	T_{max} (s)	H_{ave} (m)	T_{ave} (s)	REP
In-Situ	1.49	5.60	0.88	4.04	9
E10	0.65	3.17	0.49	2.12	7
E10m2	1.59	5.10	1.11	3.04	7
E10m3	1.32	4.66	0.92	2.98	7
SWAN	0.27	3.54	0.19	2.30	5
SWANm	0.57	3.65	0.41	2.85	5

Table 7.11: H_{max}, T_{max}, H_{ave}, T_{ave} and REP regarding In-Situ Wave Measurements (In-Situ), E10, E10m2, E10m3, SWAN and SWANm for P10

P10	H_{max} (m)	T_{max} (s)	H_{ave} (m)	T_{ave} (s)	REP
In-Situ	2.50	5.81	1.20	4.34	7
E10	1.45	4.79	0.82	3.34	6
E10m2	2.52	6.14	1.55	4.18	6
E10m3	2.70	6.58	1.52	4.37	6
SWAN	0.71	4.42	0.33	2.61	6
SWANm	1.24	5.37	0.64	3.28	6

Table 7.12: H_{max}, T_{max}, H_{ave}, T_{ave} and REP regarding In-Situ Wave Measurements (In-Situ), E10, E10m2, E10m3, SWAN and SWANm for P11

P11	H_{max} (m)	T_{max} (s)	H_{ave} (m)	T_{ave} (s)	REP
In-Situ	2.81	5.89	1.57	4.67	5
E10	2.41	6.32	1.55	4.37	4
E10m2	4.63	8.55	2.65	5.62	4
E10m3	4.42	8.31	2.72	5.83	4
SWAN	1.80	6.25	0.66	3.30	6
SWANm	2.73	7.19	1.12	4.13	6

Table 7.13: Average BIAS, RMSE and Average MAE (%) between In-Situ and E10, E10m2, E10m3 Significant Wave Heights (P01, P02, P03 and P04)

	P01			P02		
	BIAS	RMSE	MAE	BIAS	RMSE	MAE
In-Situ vs E10	-0.90	1.15	48	-1.11	1.44	56
In-Situ vs E10m2	-0.21	0.62	35	-0.52	0.86	34
In-Situ vs E10m3	-0.34	0.67	34	-0.64	0.92	34
In-Situ vs SWAN	-0.90	1.21	68	-0.72	1.01	63
In-Situ vs SWANm	-0.65	0.99	46	-0.34	0.67	62
	P03			P04		
	BIAS	RMSE	MAE	BIAS	RMSE	MAE
In-Situ vs E10	-0.33	0.33	49	-0.54	0.84	37

Table 7.13 (continued)

In-Situ vs E10m2	0.62	0.92	90	0.27	0.42	17
In-Situ vs E10m3	0.39	0.87	82	0.30	0.49	24
In-Situ vs SWAN	-0.79	0.94	71	-1.03	1.26	46
In-Situ vs SWANm	-0.50	0.71	48	-0.47	0.81	32

Table 7.14: Average BIAS, RMSE and Average MAE (%) between In-Situ and E10, E10m2, E10m3 Significant Wave Heights (P05, P06, P07 and P08)

	P05			P06		
	BIAS	RMSE	MAE	BIAS	RMSE	MAE
In-Situ vs E10	-0.27	0.40	39	-0.25	0.39	52
In-Situ vs E10m2	0.62	0.70	98	0.22	0.53	72
In-Situ vs E10m3	0.33	0.45	58	0.17	0.44	66
In-Situ vs SWAN	-0.56	0.66	68	-0.53	0.38	78
In-Situ vs SWANm	-0.29	0.48	50	-0.37	0.23	50
	P07			P08		
	BIAS	RMSE	MAE	BIAS	RMSE	MAE
In-Situ vs E10	-0.27	0.72	42	-0.41	0.72	46
In-Situ vs E10m2	0.37	1.66	86	0.61	1.66	62
In-Situ vs E10m3	0.21	0.86	67	0.32	0.86	45
In-Situ vs SWAN	-0.55	0.37	70	-0.92	1.26	66
In-Situ vs SWANm	-0.34	0.18	41	-0.65	0.74	44

\

Table 7.15: Average BIAS, RMSE and Average MAE (%) between In-Situ and E10, E10m2, E10m3 Significant Wave Heights (P09, P10 and P11)

	P09			P10		
	BIAS	RMSE	MAE	BIAS	RMSE	MAE
In-Situ vs E10	-0.39	0.46	47	-0.37	0.48	39
In-Situ vs E10m2	0.23	0.34	41	0.35	0.49	36
In-Situ vs E10m3	0.04	0.18	23	0.33	0.52	34
In-Situ vs SWAN	-0.54	0.40	68	-0.84	0.95	74
In-Situ vs SWANm	-0.32	0.18	38	-0.53	0.46	46

Table 7.15 (continued)

	P11					
	BIAS	RMSE	MAE			
In-Situ vs E10	-0.02	0.66	42			
In-Situ vs E10m2	1.08	1.43	79			
In-Situ vs E10m3	1.15	1.15	87			
In-Situ vs SWAN	-0.89	1.04	62			
In-Situ vs SWANm	-0.40	0.36	34			

Table 7.16: Average BIAS, RMSE and Average MAE (%) between In-Situ and E10, E10m2, E10m3 Significant Wave Heights for Storm Peaks (P01, P02, P03 and P04)

	P01			P02		
	BIAS	RMSE	MAE	BIAS	RMSE	MAE
In-Situ vs E10	-2.13	2.18	58	-1.84	3.41	60
In-Situ vs E10m2	-1.12	1.21	29	-0.99	1.00	32
In-Situ vs E10m3	-1.20	1.29	32	-1.21	1.48	40
In-Situ vs SWAN	-2.51	2.54	83	-1.59	1.62	54
In-Situ vs SWANm	-2.12	2.16	70	-0.88	0.90	30
	P03			P04		
	BIAS	RMSE	MAE	BIAS	RMSE	MAE
In-Situ vs E10	-1.01	1.04	66	-1.47	2.22	39
In-Situ vs E10m2	0.45	0.51	28	0.33	0.38	13
In-Situ vs E10m3	0.43	0.50	27	0.11	0.33	13
In-Situ vs SWAN	-1.36	1.37	87	-2.14	2.19	60
In-Situ vs SWANm	-1.07	1.09	68	-1.36	1.45	38

Table 7.17: Average BIAS, RMSE and Average MAE (%) between In-Situ and E10, E10m2, E10m3 Significant Wave Heights for Storm Peaks (P05, P06, P07 and P08)

	P05			P06		
	BIAS	RMSE	MAE	BIAS	RMSE	MAE

Table 7.17 (continued)

In-Situ vs E10	-0.67	0.47	52	-0.65	0.45	47
In-Situ vs E10m2	0.36	0.14	31	0.06	0.04	13
In-Situ vs E10m3	0.06	0.02	11	-0.01	0.02	9
In-Situ vs SWAN	-0.83	0.86	75	-0.99	1.03	84
In-Situ vs SWANm	-0.54	0.58	47	-0.80	0.84	66
	P07			P08		
	BIAS	RMSE	MAE	BIAS	RMSE	MAE
In-Situ vs E10	-0.49	0.25	40	-0.94	0.96	32
In-Situ vs E10m2	0.48	0.24	41	0.50	0.55	21
In-Situ vs E10m3	0.27	0.08	24	0.22	0.23	14
In-Situ vs SWAN	-0.87	0.90	78	-1.96	1.97	81
In-Situ vs SWANm	-0.64	0.68	57	-1.56	1.57	65

Table 7.18: Average BIAS, RMSE and Average MAE (%) between In-Situ and E10, E10m2, E10m3 Significant Wave Heights for Storm Peaks (P09, P10 and P11)

	P09			P10		
	BIAS	RMSE	MAE	BIAS	RMSE	MAE
In-Situ vs E10	-0.78	0.61	55	-0.95	0.92	42
In-Situ vs E10m2	0.12	0.02	8	0.11	0.05	7
In-Situ vs E10m3	-0.15	0.02	10	0.17	0.11	12
In-Situ vs SWAN	-1.09	1.10	81	-1.38	1.40	68
In-Situ vs SWANm	-0.79	0.80	58	-0.87	0.90	42
	P11					
	BIAS	RMSE	MAE			
In-Situ vs E10	-0.83	0.71	31			
In-Situ vs E10m2	0.30	0.15	12			
In-Situ vs E10m3	0.35	0.15	14			
In-Situ vs SWAN	-1.08	1.21	69			
In-Situ vs SWANm	-0.73	0.91	43			

Table 7.19: Average BIAS, RMSE and Average MAE (%) between In-Situ and E10, E10m2, E10m3 Significant Wave Periods (P01, P02, P03 and P04)

	P01			P02		
	BIAS	RMSE	MAE	BIAS	RMSE	MAE
In-Situ vs E10	-1.91	1.97	38	-2.67	2.75	48
In-Situ vs E10m2	-0.49	0.72	12	-1.95	2.20	35
In-Situ vs E10m3	-0.81	0.96	17	-1.70	1.89	31
In-Situ vs SWAN	-2.18	2.39	48	-0.64	2.04	39
In-Situ vs SWANm	-1.55	1.80	35	0.13	1.94	36
	P03			P04		
	BIAS	RMSE	MAE	BIAS	RMSE	MAE
In-Situ vs E10	-0.77	1.11	20	-1.85	2.18	35
In-Situ vs E10m2	0.05	1.02	20	-0.81	1.92	27
In-Situ vs E10m3	0.73	1.24	24	-1.09	1.96	28
In-Situ vs SWAN	-1.90	2.15	48	-1.53	2.10	25
In-Situ vs SWANm	-0.93	1.40	31	-0.53	1.55	21

Table 7.20: Average BIAS, RMSE and Average MAE (%) between In-Situ and E10, E10m2, E10m3 Significant Wave Periods (P05, P06, P07 and P08)

	P05			P06		
	BIAS	RMSE	MAE	BIAS	RMSE	MAE
In-Situ vs E10	-1.03	1.18	26	-1.54	1.81	41
In-Situ vs E10m2	0.69	0.86	20	-0.51	1.26	25
In-Situ vs E10m3	0.29	0.59	13	-0.69	1.38	28
In-Situ vs SWAN	-2.46	2.76	56	-2.47	6.41	57
In-Situ vs SWANm	-1.58	2.06	39	-2.11	4.97	48
	P07			P08		
	BIAS	RMSE	MAE	BIAS	RMSE	MAE
In-Situ vs E10	-0.54	0.29	14	-1.24	1.58	29
In-Situ vs E10m2	1.02	1.06	27	-0.01	1.04	16
In-Situ vs E10m3	0.83	0.71	22	-0.12	1.01	17
In-Situ vs SWAN	-1.95	4.08	49	-2.14	5.87	38

Table 7.20 (continued)

In-Situ vs SWANm	-1.30	2.10	33	-1.60	4.04	33

Table 7.21: Average BIAS, RMSE and Average MAE (%) between In-Situ and E10, E10m2, E10m3 Significant Wave Periods (P09, P10 and P11)

	P09			P10		
	BIAS	RMSE	MAE	BIAS	RMSE	MAE
In-Situ vs E10	-1.92	1.97	49	-1.00	1.17	25
In-Situ vs E10m2	-1.00	1.34	31	-0.16	1.05	22
In-Situ vs E10m3	-1.08	1.26	29	0.02	1.01	21
In-Situ vs SWAN	-2.07	5.57	47	-2.29	5.79	48
In-Situ vs SWANm	-1.52	3.06	35	-1.61	3.43	37
	P11					
	BIAS	RMSE	MAE			
In-Situ vs E10	-0.30	1.02	18			
In-Situ vs E10m2	0.95	1.62	28			
In-Situ vs E10m3	1.16	1.63	30			
In-Situ vs SWAN	-1.96	4.78	40			
In-Situ vs SWANm	-1.10	2.50	28			

Table 7.22: Average BIAS, RMSE and Average MAE (%) between In-Situ and E10, E10m2, E10m3 Significant Wave Periods for Storm Peaks (P01, P02, P03 and P04)

	P01			P02		
	BIAS	RMSE	MAE	BIAS	RMSE	MAE
In-Situ vs E10	-1.92	1.94	29	-2.28	5.19	34
In-Situ vs E10m2	-0.32	0.44	5	-1.08	1.18	16
In-Situ vs E10m3	-0.68	0.74	10	-1.16	1.34	17
In-Situ vs SWAN	-2.57	2.57	43	-0.61	0.76	10
In-Situ vs SWANm	-1.74	1.74	29	0.45	0.54	7
	P03			P04		
	BIAS	RMSE	MAE	BIAS	RMSE	MAE

Table 7.22 (continued)

In-Situ vs E10	-1.80	1.84	39	-1.29	1.71	18
In-Situ vs E10m2	-0.43	0.59	11	0.46	0.39	7
In-Situ vs E10m3	-0.45	0.55	10	0.19	0.34	8
In-Situ vs SWAN	-2.87	2.90	64	-2.97	3.00	37
In-Situ vs SWANm	-1.81	1.87	40	-1.77	1.80	22

Table 7.23: Average BIAS, RMSE and Average MAE (%) between In-Situ and E10, E10m2, E10m3 Significant Wave Periods for Storm Peaks (P05, P06, P07 and P08)

	P05			P06		
	BIAS	RMSE	MAE	BIAS	RMSE	MAE
In-Situ vs E10	-1.38	2.00	31	-0.90	0.83	21
In-Situ vs E10m2	0.53	0.36	13	0.38	0.22	9
In-Situ vs E10m3	0.12	0.12	5	0.31	0.12	7
In-Situ vs SWAN	-2.92	2.96	59	-2.86	2.88	60
In-Situ vs SWANm	-2.02	2.08	40	-2.36	2.37	50
	P07			P08		
	BIAS	RMSE	MAE	BIAS	RMSE	MAE
In-Situ vs E10	-0.54	0.29	14	-0.55	0.45	9
In-Situ vs E10m2	1.02	1.06	27	0.99	1.38	17
In-Situ vs E10m3	0.83	0.71	24	0.76	0.88	13
In-Situ vs SWAN	-2.37	2.40	54	-3.28	3.31	51
In-Situ vs SWANm	-1.72	1.74	39	-2.49	2.53	39

Table 7.24: Average BIAS, RMSE and Average MAE (%) between In-Situ and E10, E10m2, E10m3 Significant Wave Periods for Storm Peaks (P09, P10 and P11)

	P09			P10		
	BIAS	RMSE	MAE	BIAS	RMSE	MAE
In-Situ vs E10	-1.99	4.07	38	-0.68	0.47	13
In-Situ vs E10m2	-0.21	0.08	5	0.80	0.65	16
In-Situ vs E10m3	-0.66	0.47	13	0.75	0.62	15

Table 7.24 (continued)

In-Situ vs SWAN	-3.52	3.57	61	-2.73	2.75	44
In-Situ vs SWANm	-2.59	2.65	45	-1.63	1.65	26
	P11					
	BIAS	RMSE	MAE			
In-Situ vs E10	-0.31	0.12	5			
In-Situ vs E10m2	1.14	1.33	20			
In-Situ vs E10m3	1.20	1.46	21			
In-Situ vs SWAN	-2.27	2.28	41			
In-Situ vs SWANm	-1.56	1.58	28			

The findings from Figures 7.21-7.53 and Tables 7.2-7.18 can be summarized as;

- In general, significant wave heights, H_s, obtained from E10 wind speeds are underestimated considering both W61 and SWAN applications.
- Using modified E10 wind speeds (E10m2 and E10m3) for wave estimations result in certain improvements in H_s, H_{max}, T_{max}, H_{ave} and T_{ave} values for most of the cases considering both W61 and SWAN applications.
- Considering average bias, root mean square error (RMSE) and average mean absolute error (MAE) values for each case, certain improvements are achieved in P01, P02, P04, P09 and P10 in terms of significant wave heights, whereas for other cases, although certain improvements are achieved especially for the storm peaks, in general these values indicate an opposite situation in terms of significant wave heights.
- As for storm peaks, calculated average bias, root mean square error (RMSE) and average mean absolute error (MAE) values indicate that for all of the cases substantial improvements are achieved in terms of significant wave heights.
- The aforementioned two outcomes are indications that modified E10 wind speeds result in better representation at storm peaks in terms of significant wave heights.

- As for the significant wave periods, when average bias, root mean square error (RMSE) and average mean absolute error (MAE) values are considered, certain improvements are achieved in all cases except P03, P07 and P11.
- As for storm peaks, average bias, root mean square error (RMSE) and average mean absolute error (MAE) values indicate that with the exception of P07, P08, P10 and P11, improvements are observed in terms of significant wave periods.
- The aforementioned two outcomes are indications that modified E10 wind speeds (E10m2 and E10m3) give better results in presenting storm peaks in terms of significant wave periods.
- In-situ significant wave heights are generally higher than significant wave heights estimated from W61 and SWAN applications for storm peaks. It is observed that the significant wave heights obtained from W61 applications covering the storm peaks are presented with 7%-41% mean absolute error, whereas, significant wave heights obtained from SWAN applications corresponding to the same storm peaks are all underestimated with 54%-87% mean absolute error. Overall significant wave height estimations during the storm do not give a consistent trend for both W61 and SWAN applications. The mean absolute error fluctuates between 17%-98% and 32%-62% for W61 and SWAN applications respectively. This conclusion shows that studies have to be carried to have reliable wave height estimations from modified wind speeds using W61 and SWAN models covering the directional effects.
- The results of W61 applications show that significant wave heights for the storm durations following the storm peaks are generally overestimated.
- As for significant wave periods, W61 gives results with mean absolute error in the range of 5%-27% at storm peaks, whereas SWAN results have mean absolute error in the range of 7%-50% at storm peaks. As for overall significant wave period estimations during the storm, the mean absolute error fluctuates between 12%-35% and 21%-48% for W61 and SWAN applications respectively.

- Except for P06, directional differences between representative wave directions of in-situ waves and of W61 wave estimations (E10, E10m2 and E10m3) are at most 2 sectors corresponding to 45°. The directional differences between representative wave directions of in-situ waves and of SWAN wave estimations (E10, E10m2 and E10m3) are at most 2 sectors corresponding to 45° for all cases except for P02, P04, P08 and P09. These directional differences might be the source of the mean absolute error in the estimation of wave heights in both W61 and SWAN models.

7.3. Comparison of In-Situ Wave Measurements and Wave Estimations for the Chosen Storms in the Past for Hopa Region

Based on the chosen storms, the previous comparisons for the case study site, Sinop, show the applicability of the proposed wind speed modifications, even though it is preferred to update these methods with more comparisons for this region. In order to understand the applicability of these methods for other regions, another study area, Hopa, is chosen. Just like Sinop, Hopa is another site where in-situ wave measurements are performed within NATO-TU WAVES project.

Firstly, effective fetch distances are calculated using the same approach given for Sinop case study. The fetch distances and the effective fetch distances are given in Figure 7.54 and Table 7.25.

Using the effective fetch distances, wave estimations for the below given periods (cases) are obtained with S10, E10, E10m2 and E10m3 wind speeds.

- 12:00 29.10.1995 – 15:00 31.10.1995 (52 hours) (H01)
- 21:00 22.11.1995 – 00:00 28.11.1995 (124 hours) (H02)
- 10:00 15.12.1995 – 18:00 18.12.1995 (81 hours) (H03)
- 10:00 12.04.1996 – 15:00 14.04.1996 (54 hours) (H04)
- 00:00 18.02.1998 – 05:00 20.02.1998 (54 hours) (H05)
- 12:00 14.03.1999 – 00:00 18.03.1999 (85 hours) (H06)
- 08:00 27.12.1996 – 23:00 30.12.1996 (88 hours) (H07)

- 12:00 21.12.1995 – 21:00 23.12.1995 (58 hours) (H08)
- 00:00 14.12.1995 – 21:00 17.12.1995 (94 hours) (H09)

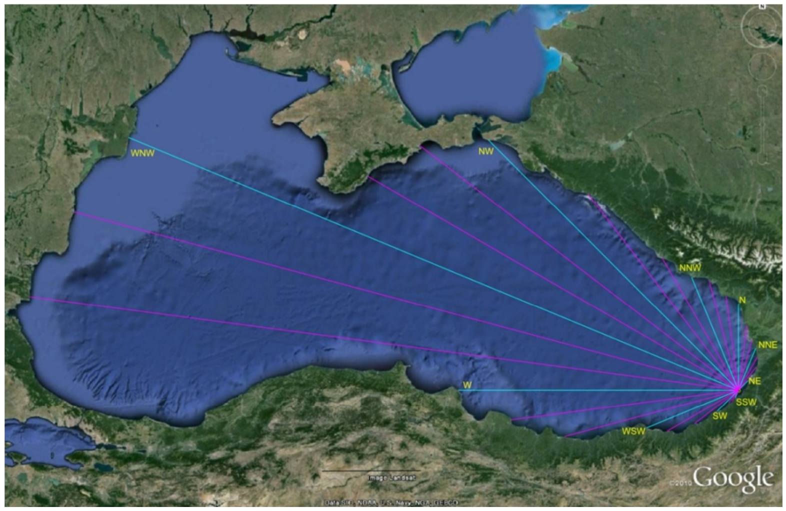

Figure 7.54: Considered Fetch Distances for the Case Study Site, Hopa (Google Earth, 2014)

Table 7.25: Effective Fetch Distances for the Case Study Site, Hopa

Direction	Effective Fetch (km)
SW	63
WSW	200
W	603
WNW	755
NW	498
NNW	244
N	122
NNE	69

The wave estimations are performed with S10, E10, E10m2 and E10m wind speeds and for wind directions E10 wind directions are used. Moreover, in order to see the influence of numerical model on wave estimations SWAN is used in addition to W61. The wave estimations with SWAN are performed with unmodified original wind fields over the Black Sea basin as well as with modified E10 wind speeds

(E10m2) over the Black Sea basin. Since modification methods 2 and 3 give similar improvements and results in the previous studies, it is thought that using one of these modification methods would be enough. The unmodified and modified SWAN wave estimations are regarded as “SWAN” and “SWANm”, respectively. SWAN runs are performed with unmodified and modified 6 hourly ECMWF wind data, thus wave estimations are obtained in 6 hour intervals unlike hourly wind data for other runs. Both numerical models are run longer than the above given periods (cases) since it takes time for waves to develop, thus it is aimed to avoid possible overestimation and underestimation at the beginning and ending of these periods. As a result, the starting point of x-axis in the below given figures do not coincide with 0. The results of wave estimations in terms of significant wave heights, significant wave periods and wave directions are given in Figure 7.56-7.82. The wave directions are given in accordance with Figure 7.55 in which except for the SSW and NE directions, sea directions are covered. The wave directions are described in terms of sectors so that it would be easy to observe the directional differences as well as to overcome the complication of spherical representation of directions, especially at N where 0° and 360° meets where it would be hard to observe the directional changes in a graphical representation.

In addition to Figures 7.56-7.82, Tables 7.26-7.34, which summarize the results in terms of H_{max}, T_{max}, H_{ave}, T_{ave}, represerntative wave direction (REP), are prepared for each period (H). Moreover, average bias, RMSE and average MAE are also given in Tables 7.35-7.36 (for significant wave heights) and Tables 7.39-7.40 (for significant wave periods) for each case. In these tables, only W61 wave estimations performed with modified wind measurements are considered since W61 wave estimations are obtained hourly whereas SWAN wave estimations are obtained 6 hourly, thus W61 wave estimations are more appropriate such comparisons. In Tables 7.37-7.38 and Tables 7.41-7.42, average bias, RMSE and average MAE obtained only for the peak consecutive 9 wave estimations at the storm peaks are given in terms of significant wave heights and periods. The peak (maximum) points are chosen according to in-situ wave measurements and the peak (maximum) in-situ wave height forms the mid point of these 9 consecutive points. This comparison is performed to understand if wave estimations are different for the storm peaks other than the developing and calming parts of the storm.

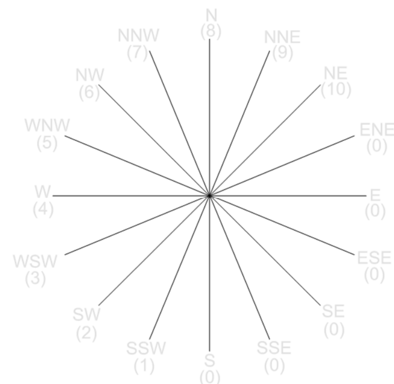

Figure 7.55: Wave Directions and Their Designation in Terms of Sectorel Numbers Considered in Figures 7.21-7.53

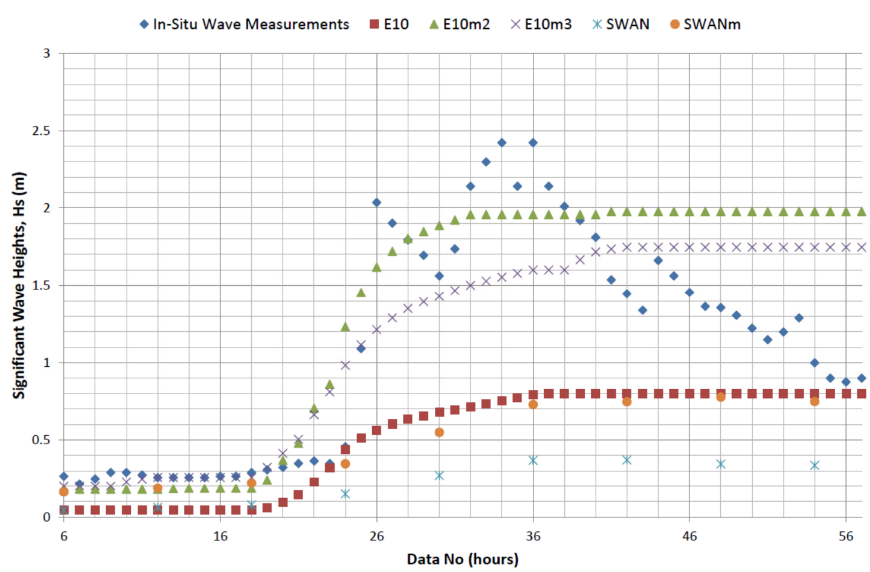

Figure 7.56: Significant Wave Heights Obtained from S10, E10, E10m2, E10m3, SWAN and SWANm Wind Speeds for H01

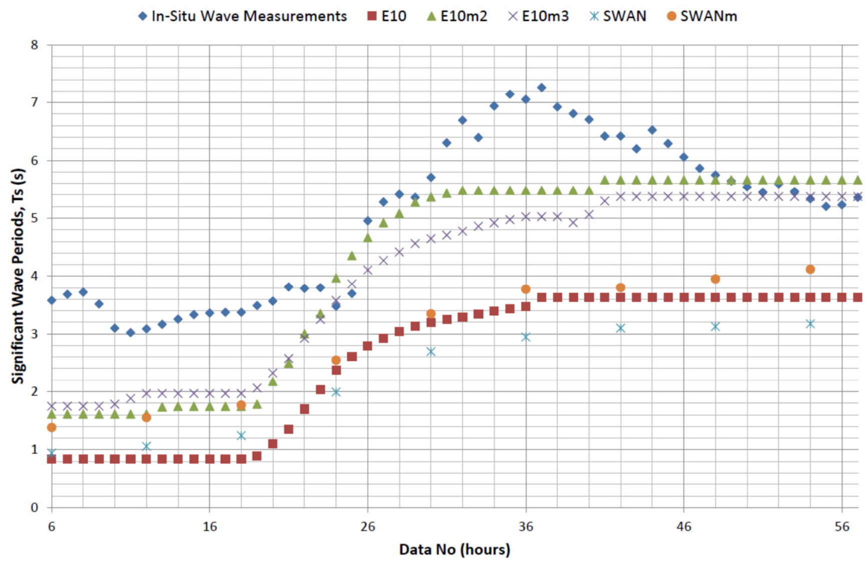

Figure 7.57: Significant Wave Periods Obtained from S10, E10, E10m2, E10m3, SWAN and SWANm Wind Speeds for H01

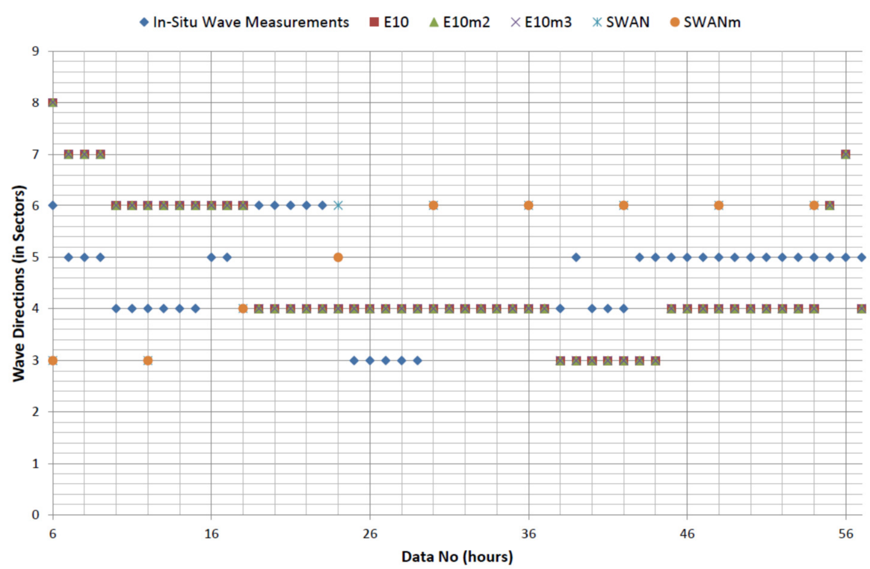

Figure 7.58: Wave Directions Obtained from S10, E10, E10m2, E10m3, SWAN and SWANm Wind Speeds for H01

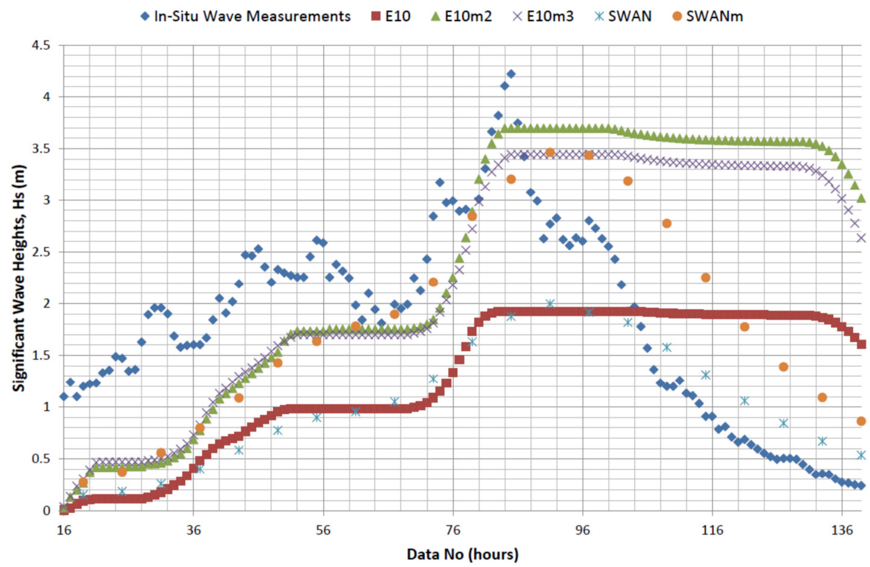

Figure 7.59: Significant Wave Heights Obtained from S10, E10, E10m2, E10m3, SWAN and SWANm Wind Speeds for H02

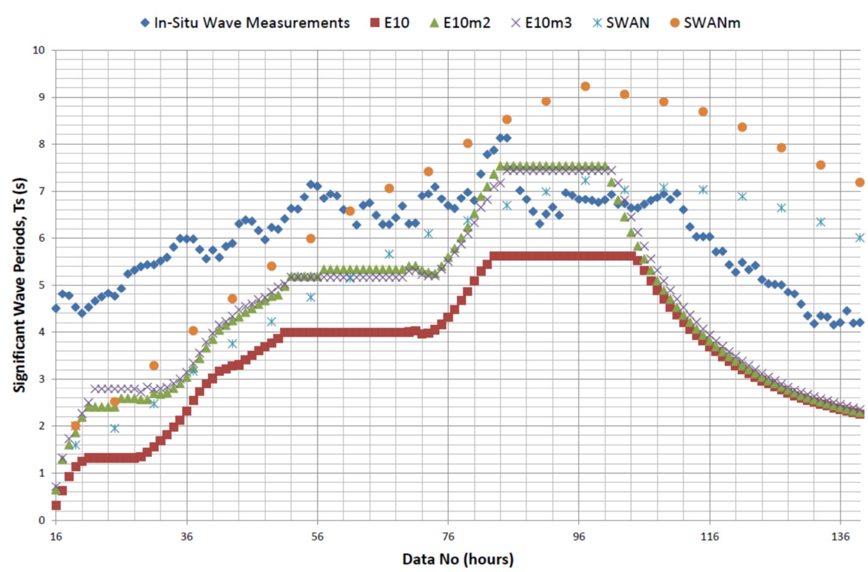

Figure 7.60: Significant Wave Periods Obtained from S10, E10, E10m2, E10m3, SWAN and SWANm Wind Speeds for H02

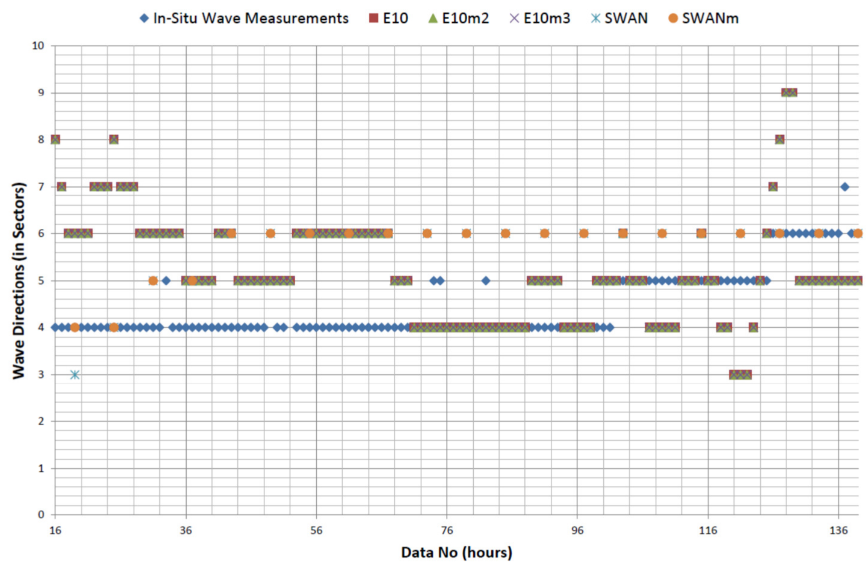

Figure 7.61: Wave Directions Obtained from S10, E10, E10m2, E10m3, SWAN and SWANm Wind Speeds for H02

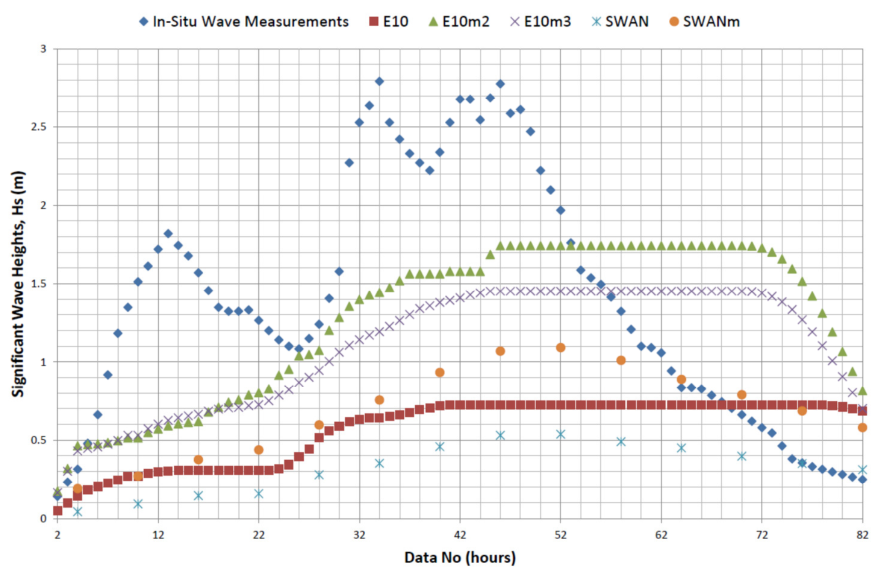

Figure 7.62: Significant Wave Heights Obtained from S10, E10, E10m2, E10m3, SWAN and SWANm Wind Speeds for H03

Figure 7.63: Significant Wave Periods Obtained from S10, E10, E10m2, E10m3, SWAN and SWANm Wind Speeds for H03

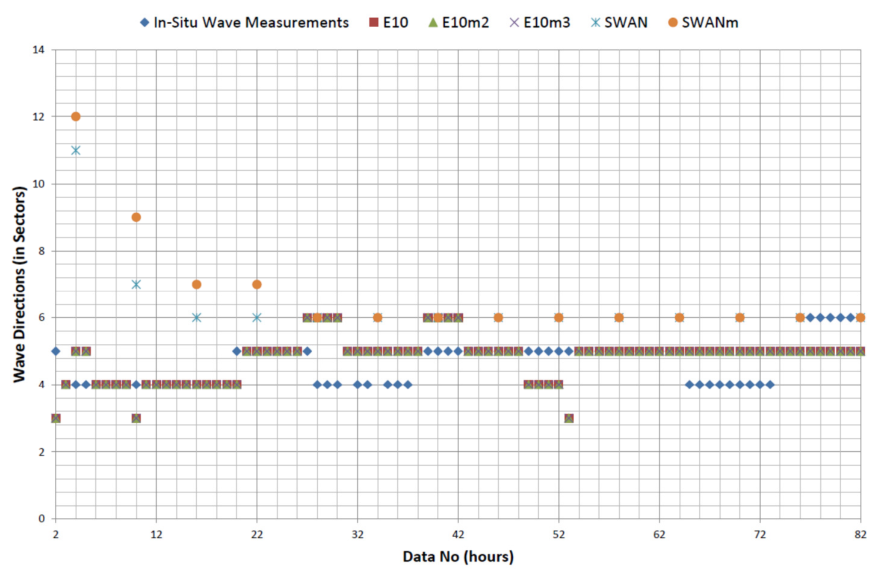

Figure 7.64: Wave Directions Obtained from S10, E10, E10m2, E10m3, SWAN and SWANm Wind Speeds for H03

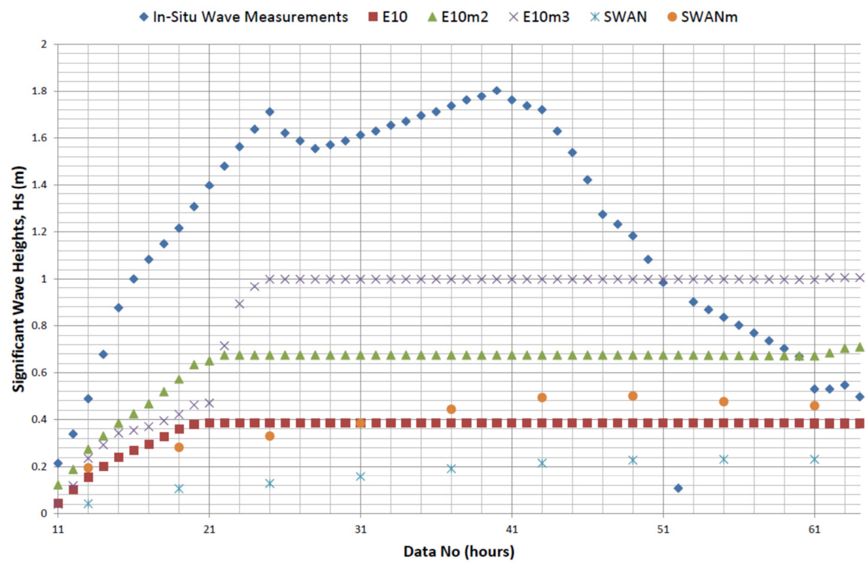

Figure 7.65: Significant Wave Heights Obtained from S10, E10, E10m2, E10m3, SWAN and SWANm Wind Speeds for H04

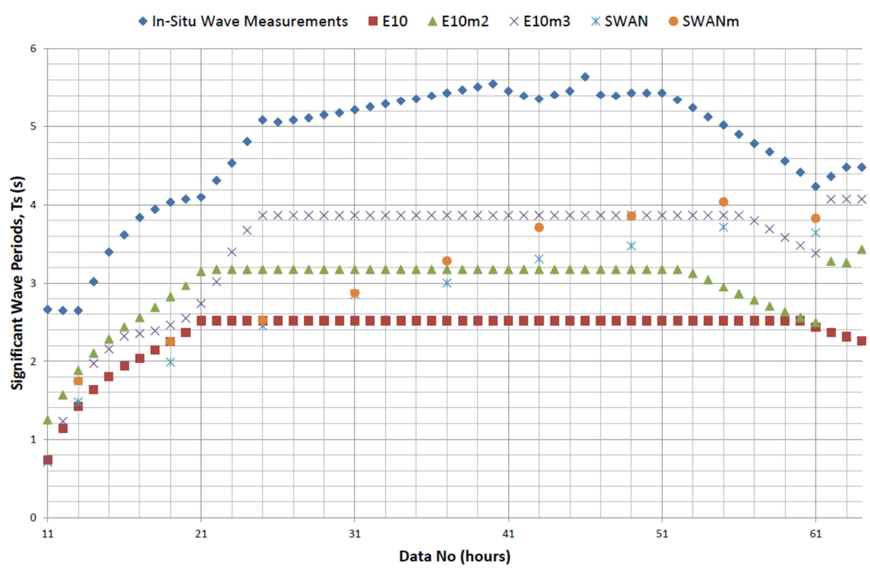

Figure 7.66: Significant Wave Periods Obtained from S10, E10, E10m2, E10m3, SWAN and SWANm Wind Speeds for H04

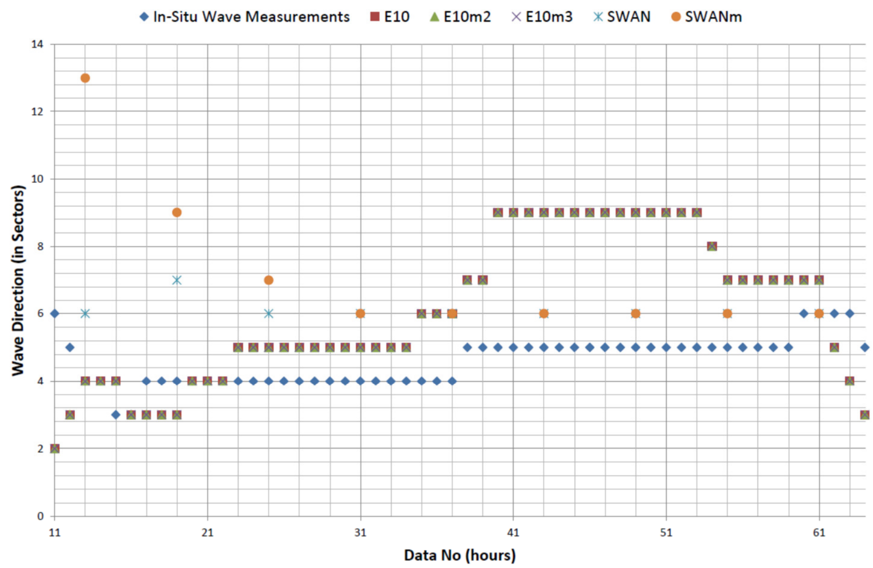

Figure 7.67: Wave Directions Obtained from S10, E10, E10m2, E10m3, SWAN and SWANm Wind Speeds for H04

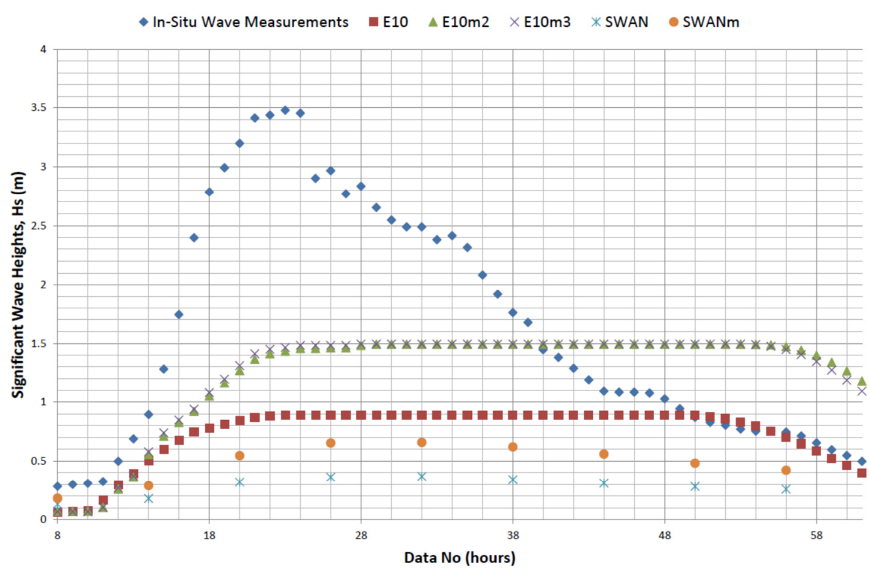

Figure 7.68: Significant Wave Heights Obtained from S10, E10, E10m2, E10m3, SWAN and SWANm Wind Speeds for H05

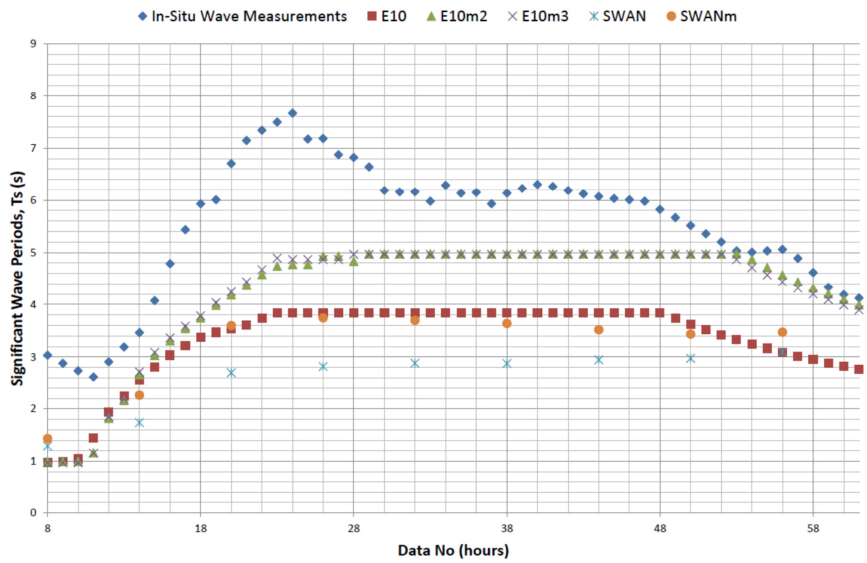

Figure 7.69: Significant Wave Periods Obtained from S10, E10, E10m2, E10m3, SWAN and SWANm Wind Speeds for H05

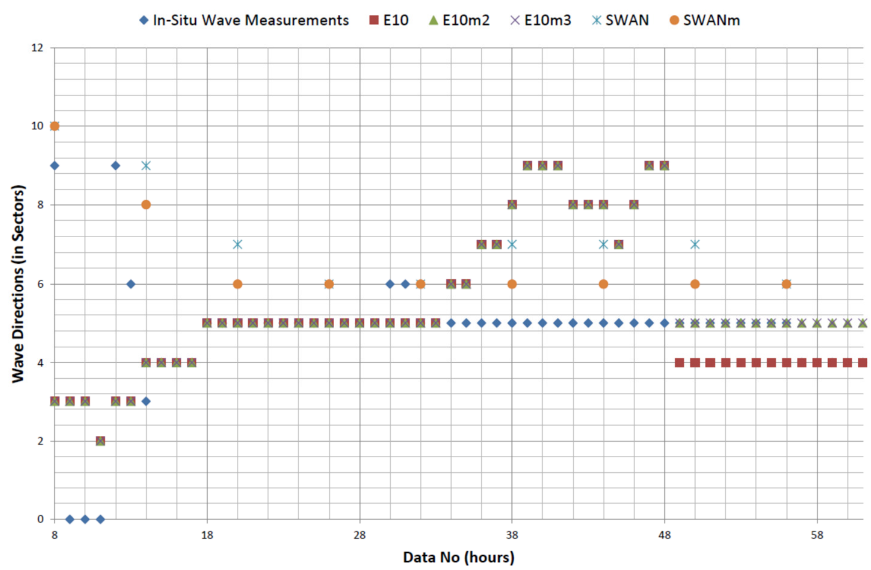

Figure 7.70: Wave Directions Obtained from S10, E10, E10m2, E10m3, SWAN and SWANm Wind Speeds for H05

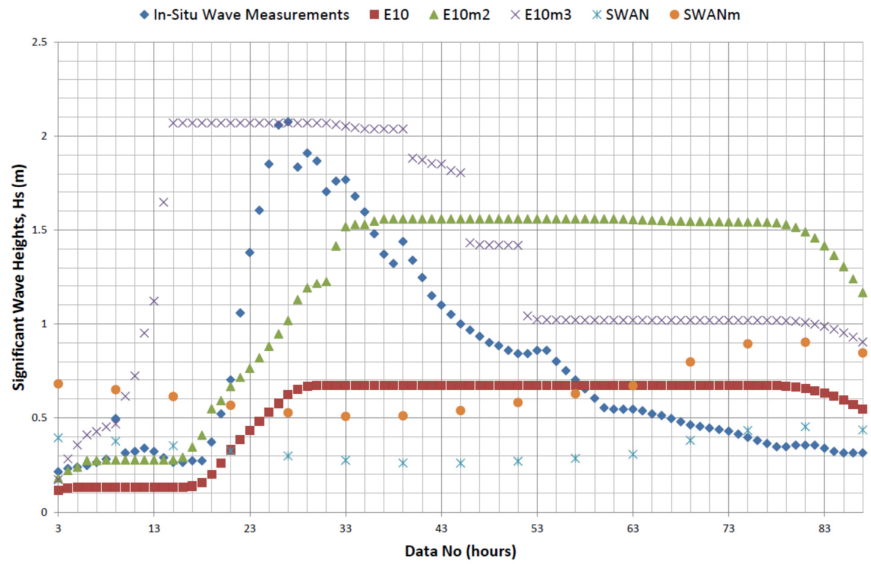

Figure 7.71: Significant Wave Heights Obtained from S10, E10, E10m2, E10m3, SWAN and SWANm Wind Speeds for H06

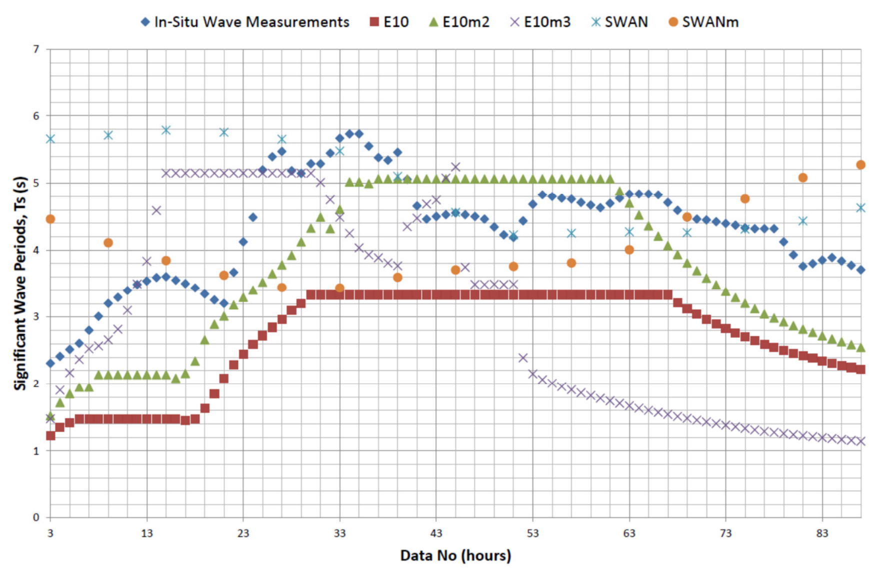

Figure 7.72: Significant Wave Periods Obtained from S10, E10, E10m2, E10m3, SWAN and SWANm Wind Speeds for H06

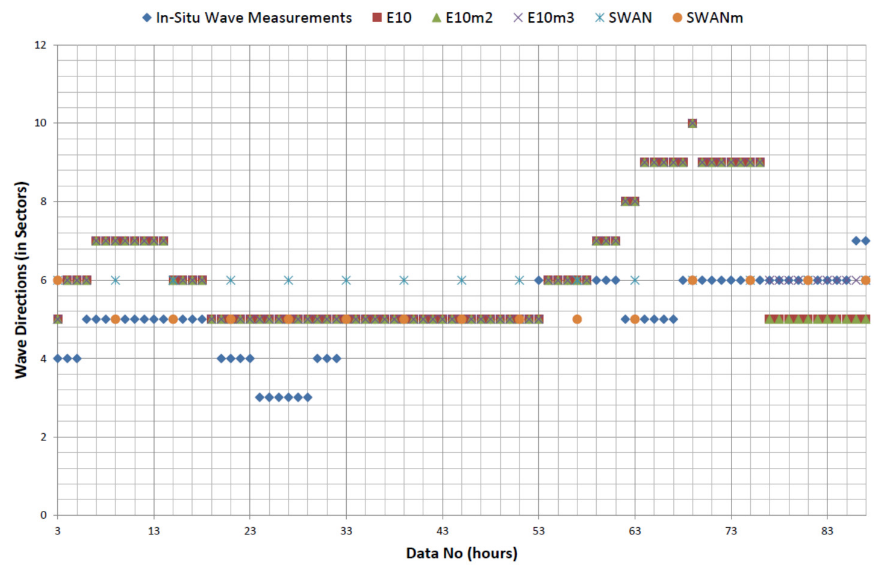

Figure 7.73: Wave Directions Obtained from S10, E10, E10m2, E10m3, SWAN and SWANm Wind Speeds for H06

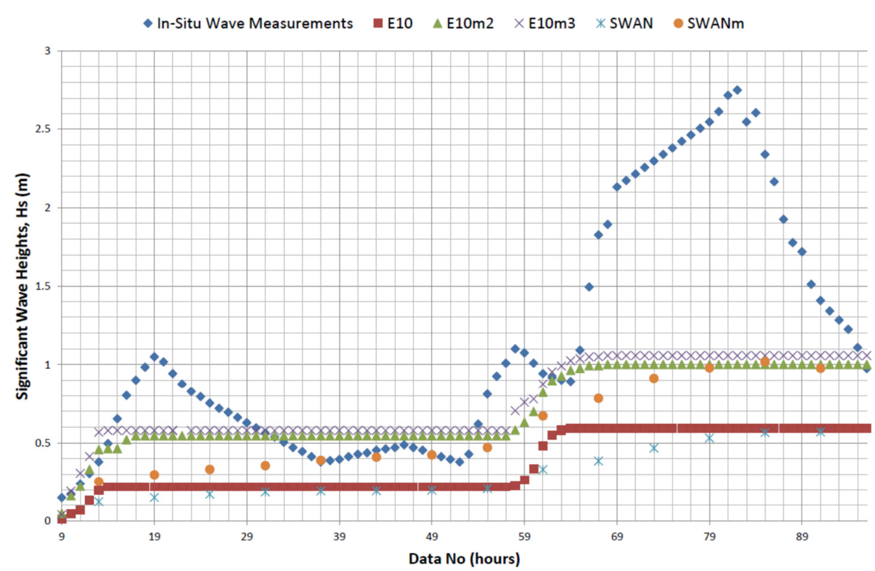

Figure 7.74: Significant Wave Heights Obtained from S10, E10, E10m2, E10m3, SWAN and SWANm Wind Speeds for H07

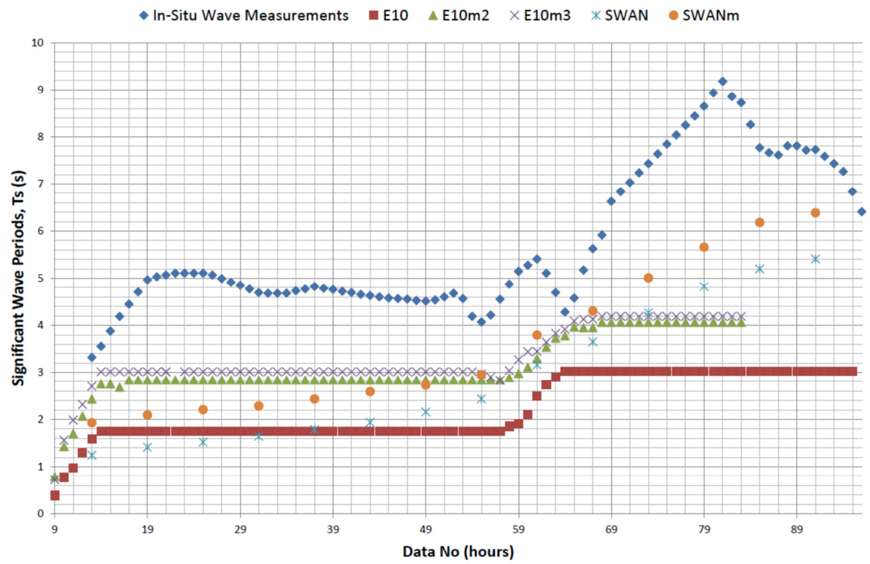

Figure 7.75: Significant Wave Periods Obtained from S10, E10, E10m2, E10m3, SWAN and SWANm Wind Speeds for H07

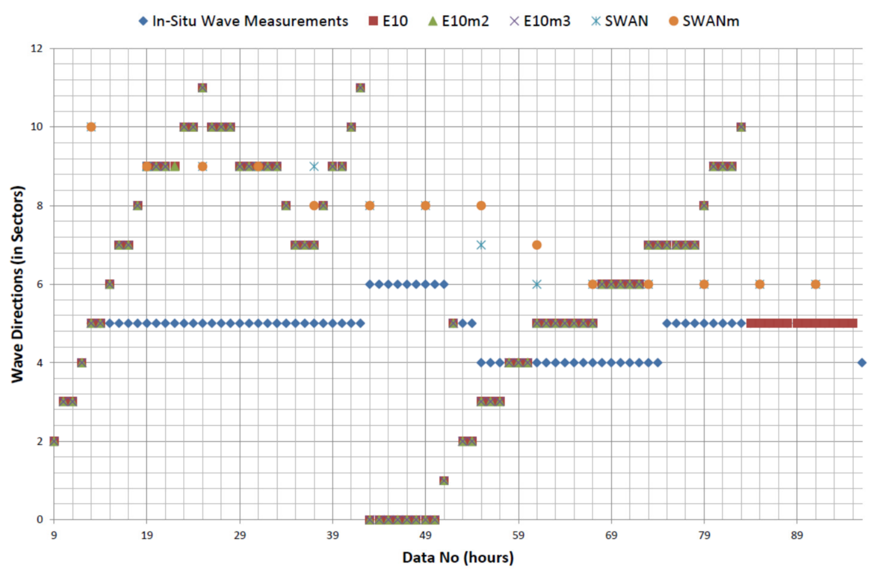

Figure 7.76: Wave Directions Obtained from S10, E10, E10m2, E10m3, SWAN and SWANm Wind Speeds for H07

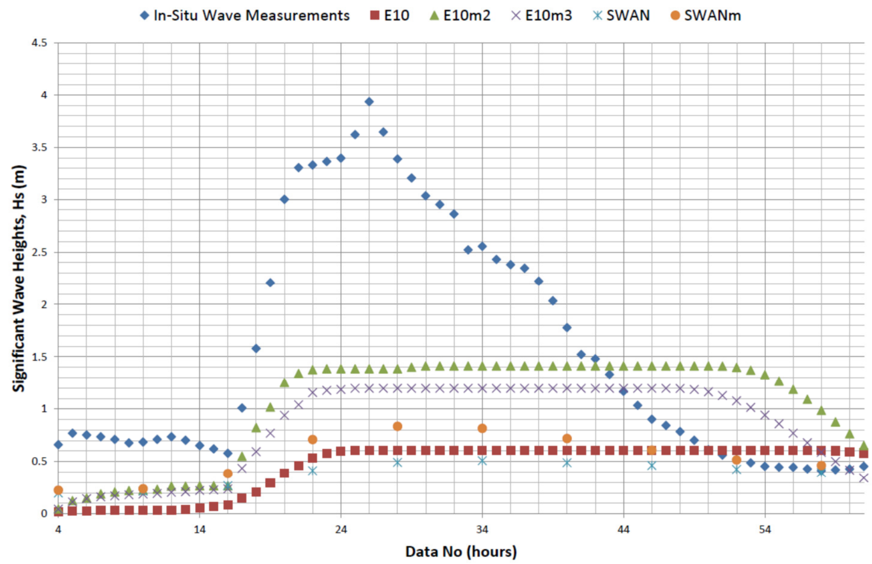

Figure 7.77: Significant Wave Heights Obtained from S10, E10, E10m2, E10m3, SWAN and SWANm Wind Speeds for H08

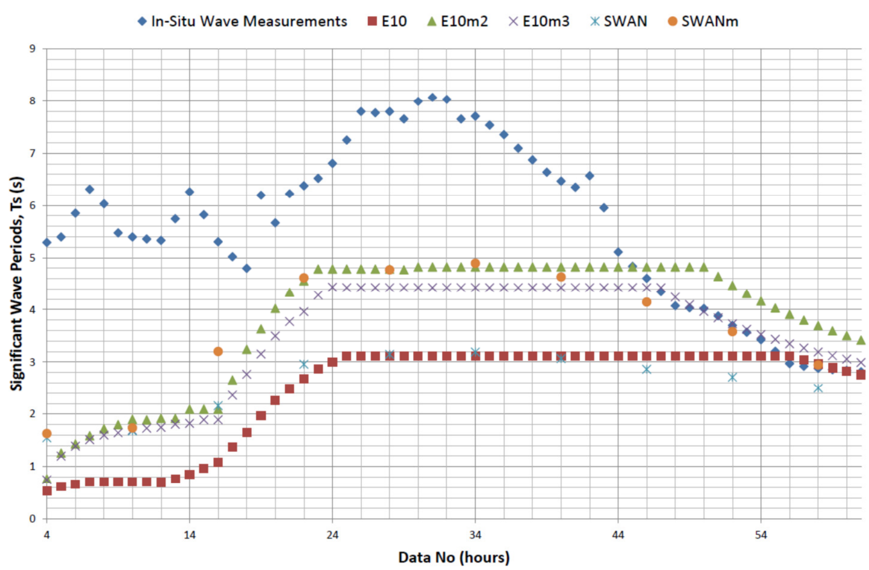

Figure 7.78: Significant Wave Periods Obtained from S10, E10, E10m2, E10m3, SWAN and SWANm Wind Speeds for H08

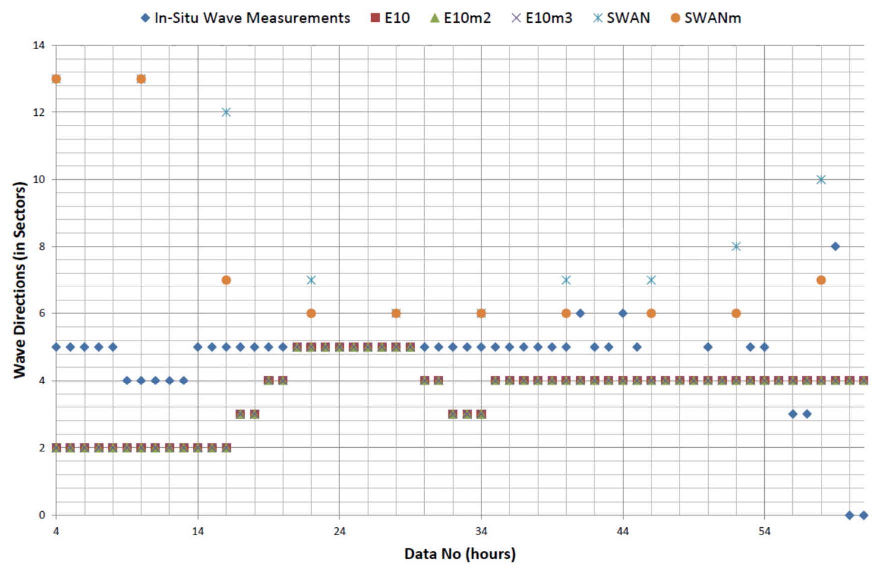

Figure 7.79: Wave Directions Obtained from S10, E10, E10m2, E10m3, SWAN and SWANm Wind Speeds for H08

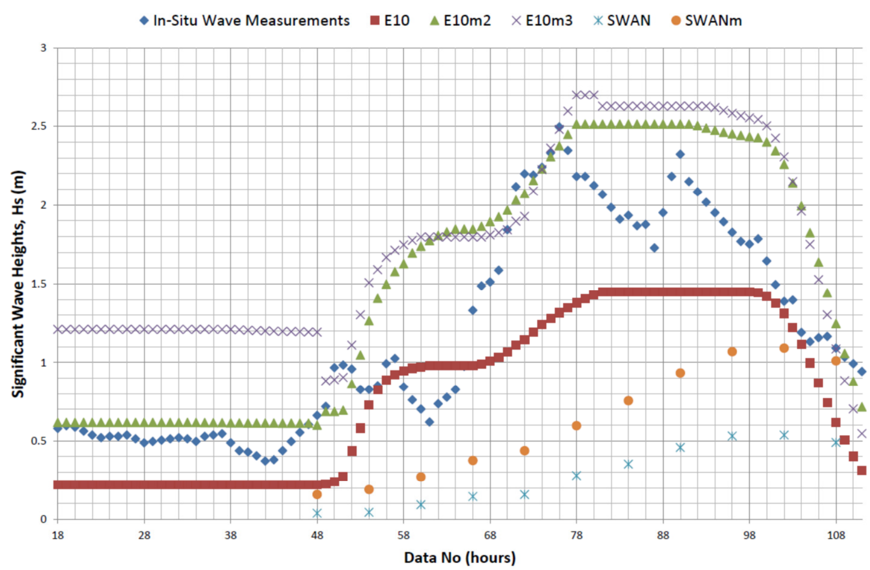

Figure 7.80: Significant Wave Heights Obtained from S10, E10, E10m2, E10m3, SWAN and SWANm Wind Speeds for H09

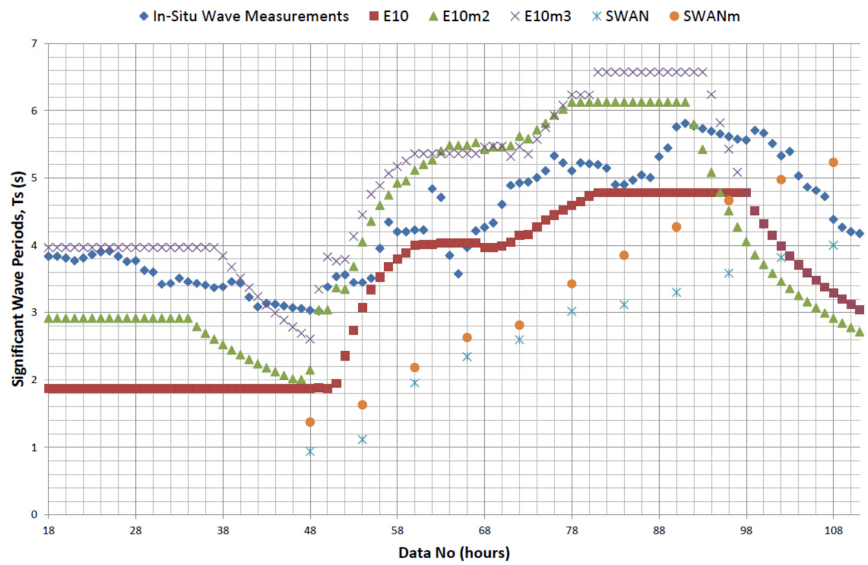

Figure 7.81: Significant Wave Periods Obtained from S10, E10, E10m2, E10m3, SWAN and SWANm Wind Speeds for H09

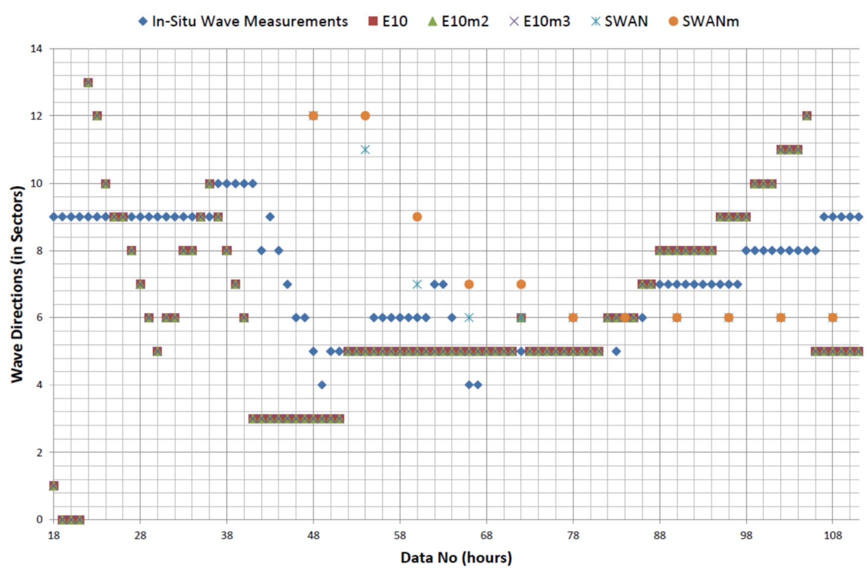

Figure 7.82: Wave Directions Obtained from S10, E10, E10m2, E10m3, SWAN and SWANm Wind Speeds for H09

Table 7.26: H_{max}, T_{max}, H_{ave}, T_{ave} and REP regarding In-Situ Wave Measurements (In-Situ), E10, E10m2, E10m3, SWAN and SWANm for H01

H01	H_{max} (m)	T_{max} (s)	H_{ave} (m)	T_{ave} (s)	REP
In-Situ	2.42	7.26	1.12	5.05	5
E10	0.80	3.63	0.51	2.58	5
E10m2	1.98	5.66	1.34	4.21	5
E10m3	1.75	5.37	1.15	3.99	5
SWAN	0.37	3.25	0.23	2.59	6
SWANm	0.78	4.18	0.49	3.26	6

Table 7.27: H_{max}, T_{max}, H_{ave}, T_{ave} and REP regarding In-Situ Wave Measurements (In-Situ), E10, E10m2, E10m3, SWAN and SWANm for H02

H02	H_{max} (m)	T_{max} (s)	H_{ave} (m)	T_{ave} (s)	REP
In-Situ	4.22	8.13	1.84	6.05	5
E10	1.92	5.62	1.28	3.64	5
E10m2	3.69	7.54	2.38	4.58	5
E10m3	3.44	7.44	2.26	4.62	5
SWAN	2.00	7.23	0.95	5.02	6
SWANm	3.46	9.23	1.68	6.28	6

Table 7.28: H_{max}, T_{max}, H_{ave}, T_{ave} and REP regarding In-Situ Wave Measurements (In-Situ), E10, E10m2, E10m3, SWAN and SWANm for H03

H03	H_{max} (m)	T_{max} (s)	H_{ave} (m)	T_{ave} (s)	REP
In-Situ	2.79	6.22	1.40	4.89	5
E10	0.73	3.45	0.57	2.92	5
E10m2	1.74	5.08	1.28	4.22	5
E10m3	1.45	4.89	1.10	4.05	5
SWAN	0.45	4.29	0.31	3.11	7
SWANm	1.09	5.50	0.66	3.91	7

Table 7.29: H_{max}, T_{max}, H_{ave}, T_{ave} and REP regarding In-Situ Wave Measurements (In-Situ), E10, E10m2, E10m3, SWAN and SWANm for H04

H04	H_{max} (m)	T_{max} (s)	H_{ave} (m)	T_{ave} (s)	REP
In-Situ	1.81	5.64	1.21	4.77	5
E10	0.38	2.52	0.36	2.36	6
E10m2	0.71	3.43	0.62	2.95	6
E10m3	1.01	4.07	0.85	3.45	6
SWAN	0.23	3.79	0.16	2.88	7
SWANm	0.50	4.04	0.34	2.88	7

Table 7.30: H_{max}, T_{max}, H_{ave}, T_{ave} and REP regarding In-Situ Wave Measurements (In-Situ), E10, E10m2, E10m3, SWAN and SWANm for H05

H05	H_{max} (m)	T_{max} (s)	H_{ave} (m)	T_{ave} (s)	REP
In-Situ	3.48	7.66	1.63	5.52	5
E10	0.89	3.84	0.74	3.32	5
E10m2	1.49	4.97	1.25	4.26	5
E10m3	1.49	4.96	1.25	4.25	5
SWAN	0.37	4.31	0.27	2.97	8
SWANm	0.66	4.20	0.46	3.43	7

Table 7.31: H_{max}, T_{max}, H_{ave}, T_{ave} and REP regarding In-Situ Wave Measurements (In-Situ), E10, E10m2, E10m3, SWAN and SWANm for H06

H06	H_{max} (m)	T_{max} (s)	H_{ave} (m)	T_{ave} (s)	REP
In-Situ	2.07	5.73	0.78	4.31	5
E10	0.67	3.33	0.54	2.70	6
E10m2	1.56	5.06	1.19	3.74	6
E10m3	2.07	5.24	1.35	3.05	6
SWAN	0.45	5.79	0.34	4.94	7
SWANm	0.90	5.27	0.66	4.09	6

Table 7.32: H_{max}, T_{max}, H_{ave}, T_{ave} and REP regarding In-Situ Wave Measurements (In-Situ), E10, E10m2, E10m3, SWAN and SWANm for H07

H07	H_{max} (m)	T_{max} (s)	H_{ave} (m)	T_{ave} (s)	REP
In-Situ	2.75	9.18	1.13	5.72	5
E10	0.59	3.02	0.37	2.23	6
E10m2	1.00	4.06	0.71	3.25	6
E10m3	1.06	4.19	0.76	3.41	6
SWAN	0.57	5.55	0.32	3.34	8
SWANm	1.02	6.38	0.57	3.86	8

Table 7.33: H_{max}, T_{max}, H_{ave}, T_{ave} and REP regarding In-Situ Wave Measurements (In-Situ), E10, E10m2, E10m3, SWAN and SWANm for H08

H08	H_{max} (m)	T_{max} (s)	H_{ave} (m)	T_{ave} (s)	REP
In-Situ	3.31	6.20	1.54	4.86	7
E10	2.12	5.82	1.13	3.63	5
E10m2	3.95	7.76	2.15	4.86	5
E10m3	3.59	7.43	1.86	4.75	5
SWAN	0.63	4.26	0.36	3.18	4
SWANm	1.12	5.17	0.61	3.69	4

Table 7.34: H_{max}, T_{max}, H_{ave}, T_{ave} and REP regarding In-Situ Wave Measurements (In-Situ), E10, E10m2, E10m3, SWAN and SWANm for H09

H09	H_{max} (m)	T_{max} (s)	H_{ave} (m)	T_{ave} (s)	REP
In-Situ	2.50	5.81	1.19	4.34	5
E10	1.45	4.78	0.81	3.32	4
E10m2	2.51	6.13	1.52	4.12	4
E10m3	2.70	6.58	1.75	4.69	4
SWAN	0.54	4.29	0.31	3.11	8
SWANm	1.09	5.50	0.66	3.91	7

Table 7.35: Average BIAS, RMSE and Average MAE (%) between In-Situ and E10, E10m2, E10m3 Significant Wave Heights (H01, H02, H03 and H04)

	H01			H02		
	BIAS	RMSE	MAE	BIAS	RMSE	MAE
In-Situ vs E10	-0.61	0.78	56	-0.57	1.27	109
In-Situ vs E10m2	0.22	0.47	41	0.54	1.67	180
In-Situ vs E10m3	0.03	0.44	31	0.41	1.53	164
In-Situ vs SWAN	-0.54	0.78	59	-0.78	1.14	61
In-Situ vs SWANm	-0.28	0.57	43	-0.03	0.93	78
	H03			H04		
	BIAS	RMSE	MAE	BIAS	RMSE	MAE
In-Situ vs E10	-0.84	1.13	67	-0.85	0.96	71
In-Situ vs E10m2	-0.13	0.80	79	-0.58	0.73	56
In-Situ vs E10m3	-0.31	0.81	69	-0.35	0.57	59
In-Situ vs SWAN	-1.04	1.30	67	-0.68	0.90	67
In-Situ vs SWANm	-0.68	1.01	59	-0.49	0.74	49

Table 7.36: Average BIAS, RMSE and Average MAE (%) between In-Situ and E10, E10m2, E10m3 Significant Wave Heights (H05, H06, H07, H08 and H09)

	H05			H06		
	BIAS	RMSE	MAE	BIAS	RMSE	MAE
In-Situ vs E10	-0.88	1.24	44	-0.24	0.54	50
In-Situ vs E10m2	-0.38	0.99	57	0.41	0.75	114
In-Situ vs E10m3	-0.38	0.97	56	0.57	0.71	125
In-Situ vs SWAN	-1.01	1.40	64	-0.43	0.73	52
In-Situ vs SWANm	-0.81	1.22	51	-0.11	0.66	83
	H07			H08		
	BIAS	RMSE	MAE	BIAS	RMSE	MAE
In-Situ vs E10	-0.76	0.97	63	-1.11	1.53	66
In-Situ vs E10m2	-0.42	0.71	33	-0.51	1.09	72
In-Situ vs E10m3	-0.37	0.67	34	-0.72	1.18	60
In-Situ vs SWAN	-0.61	0.89	62	-0.87	1.35	51

Table 7.36 (continued)

In-Situ vs SWANm	-0.35	0.66	49	-0.72	1.18	44
	H09					
	BIAS	RMSE	MAE			
In-Situ vs E10	-0.38	0.49	40			
In-Situ vs E10m2	0.33	0.47	35			
In-Situ vs E10m3	0.56	0.65	76			
In-Situ vs SWAN	-1.14	1.27	78			
In-Situ vs SWANm	-0.79	0.97	53			

Table 7.37: Average BIAS, RMSE and Average MAE (%) between In-Situ and E10, E10m2, E10m3 Significant Wave Heights for Storm Peaks (H01, H02, H03 and H04)

	H01			H02		
	BIAS	RMSE	MAE	BIAS	RMSE	MAE
In-Situ vs E10	-1.34	1.39	64	-1.39	1.40	58
In-Situ vs E10m2	-0.19	0.27	10	-0.64	0.65	27
In-Situ vs E10m3	-0.55	0.60	25	-0.68	0.69	28
In-Situ vs SWAN	-1.47	1.53	81	-1.45	1.59	42
In-Situ vs SWANm	-1.14	1.21	61	-0.11	0.71	17
	H03			H04		
	BIAS	RMSE	MAE	BIAS	RMSE	MAE
In-Situ vs E10	-1.73	1.76	72	-1.35	1.35	78
In-Situ vs E10m2	-0.92	0.97	38	-1.06	1.06	61
In-Situ vs E10m3	-1.18	1.21	48	-0.74	0.74	42
In-Situ vs SWAN	-2.19	2.20	83	-1.50	1.50	89
In-Situ vs SWANm	-1.72	1.74	65	-1.25	1.25	74

Table 7.38: Average BIAS, RMSE and Average MAE (%) between In-Situ and E10, E10m2, E10m3 Significant Wave Heights for Storm Peaks (H05, H06, H07, H08 and H09)

	H05	H06

Table 7.38 (continued)

	BIAS	RMSE	MAE	BIAS	RMSE	MAE
In-Situ vs E10	-2.31	2.32	72	-1.22	1.23	67
In-Situ vs E10m2	-1.79	1.81	56	-0.79	0.81	43
In-Situ vs E10m3	-1.76	1.78	55	0.26	0.33	16
In-Situ vs SWAN	-2.54	2.56	88	-1.22	1.36	75
In-Situ vs SWANm	-2.22	2.29	78	-0.98	1.15	55
	H07			H08		
	BIAS	RMSE	MAE	BIAS	RMSE	MAE
In-Situ vs E10	-1.94	1.94	76	-2.84	2.85	83
In-Situ vs E10m2	-1.53	1.54	60	-2.05	2.06	59
In-Situ vs E10m3	-1.47	1.48	58	-2.25	2.26	65
In-Situ vs SWAN	-1.87	1.88	78	-2.62	2.65	84
In-Situ vs SWANm	-1.42	1.42	59	-2.30	2.34	74
	H09					
	BIAS	RMSE	MAE			
In-Situ vs E10	-0.95	0.96	42			
In-Situ vs E10m2	0.09	0.21	7			
In-Situ vs E10m3	0.17	0.34	12			
In-Situ vs SWAN	-1.58	1.60	78			
In-Situ vs SWANm	-1.11	1.14	54			

Table 7.39: Average BIAS, RMSE and Average MAE (%) between In-Situ and E10, E10m2, E10m3 Significant Wave Periods (H01, H02, H03 and H04)

	H01			H02		
	BIAS	RMSE	MAE	BIAS	RMSE	MAE
In-Situ vs E10	-2.46	2.53	52	-2.41	2.54	42
In-Situ vs E10m2	-0.83	1.15	22	-1.46	1.82	29
In-Situ vs E10m3	-1.06	1.26	23	-1.43	1.75	28
In-Situ vs SWAN	-2.76	2.96	51	-1.65	2.39	31
In-Situ vs SWANm	-2.11	2.33	39	-0.35	2.07	30
	H03			H04		
	BIAS	RMSE	MAE	BIAS	RMSE	MAE

Table 7.39 (continued)

In-Situ vs E10	-1.97	2.12	40	-2.41	2.46	50
In-Situ vs E10m2	-0.67	1.04	18	-1.82	1.88	38
In-Situ vs E10m3	-0.84	1.14	20	-1.32	1.35	28
In-Situ vs SWAN	-2.20	2.54	40	-2.01	2.28	39
In-Situ vs SWANm	-3.51	3.53	51	-1.99	2.22	39

Table 7.40: Average BIAS, RMSE and Average MAE (%) between In-Situ and E10, E10m2, E10m3 Significant Wave Periods (H05, H06, H07, H08 and H09)

	H05			H06		
	BIAS	RMSE	MAE	BIAS	RMSE	MAE
In-Situ vs E10	-2.20	2.30	40	-1.61	1.66	38
In-Situ vs E10m2	-1.26	1.47	24	-0.57	0.91	20
In-Situ vs E10m3	-1.27	1.46	24	-1.27	2.03	40
In-Situ vs SWAN	-3.24	3.47	52	0.09	1.37	28
In-Situ vs SWANm	-2.73	2.90	44	-0.76	1.60	26
	H07			H08		
	BIAS	RMSE	MAE	BIAS	RMSE	MAE
In-Situ vs E10	-3.49	3.65	61	-3.17	3.66	52
In-Situ vs E10m2	-2.47	2.70	42	-1.77	2.52	37
In-Situ vs E10m3	-2.31	2.57	39	-2.17	2.72	36
In-Situ vs SWAN	-2.89	3.19	50	-3.40	3.61	50
In-Situ vs SWANm	-2.29	2.59	41	-2.25	2.75	36
	H09					
	BIAS	RMSE	MAE			
In-Situ vs E10	-1.02	1.18	26			
In-Situ vs E10m2	-0.22	1.05	22			
In-Situ vs E10m3	0.34	0.90	17			
In-Situ vs SWAN	-2.41	2.53	47			
In-Situ vs SWANm	-1.69	2.00	37			

Table 7.41: Average BIAS, RMSE and Average MAE (%) between In-Situ and E10, E10m2, E10m3 Significant Wave Periods for Storm Peaks (H01, H02, H03 and H04)

	H01			H02		
	BIAS	RMSE	MAE	BIAS	RMSE	MAE
In-Situ vs E10	-3.39	3.39	49	-2.84	2.85	41
In-Situ vs E10m2	-1.40	1.42	20	-1.61	1.62	24
In-Situ vs E10m3	-1.93	1.94	28	-1.68	1.69	24
In-Situ vs SWAN	-4.41	4.44	60	-1.57	1.80	18
In-Situ vs SWANm	-3.68	3.71	50	0.23	0.96	9
	H03			H04		
	BIAS	RMSE	MAE	BIAS	RMSE	MAE
In-Situ vs E10	-2.40	2.43	43	-2.93	2.93	54
In-Situ vs E10m2	-0.92	0.97	16	-2.26	2.26	42
In-Situ vs E10m3	-1.34	1.39	24	-1.58	1.58	29
In-Situ vs SWAN	-1.37	2.01	32	-3.05	3.06	50
In-Situ vs SWANm	-2.58	2.63	37	-2.82	2.83	46

Table 7.42: Average BIAS, RMSE and Average MAE (%) between In-Situ and E10, E10m2, E10m3 Significant Wave Periods for Storm Peaks (H05, H06, H07, H08 and H09)

	H05			H06		
	BIAS	RMSE	MAE	BIAS	RMSE	MAE
In-Situ vs E10	-3.33	3.35	47	-2.12	2.14	42
In-Situ vs E10m2	-2.48	2.50	35	-1.23	1.28	24
In-Situ vs E10m3	-2.43	2.44	34	0.07	0.44	7
In-Situ vs SWAN	-4.85	4.88	63	0.15	1.39	27
In-Situ vs SWANm	-3.98	4.00	52	-1.97	2.40	31
	H07			H08		
	BIAS	RMSE	MAE	BIAS	RMSE	MAE
In-Situ vs E10	-5.47	5.50	64	-4.30	4.33	59
In-Situ vs E10m2	-4.44	4.46	52	-2.57	2.62	35

Table 7.42 (continued)

In-Situ vs E10m3	-4.31	4.34	51	-2.97	3.01	40
In-Situ vs SWAN	-2.89	3.19	50	-3.10	3.61	50
In-Situ vs SWANm	-2.29	2.59	41	-2.25	2.75	36
	H09					
	BIAS	RMSE	MAE			
In-Situ vs E10	-0.69	0.70	13			
In-Situ vs E10m2	0.78	0.79	15			
In-Situ vs E10m3	0.75	0.79	15			
In-Situ vs SWAN	-2.88	2.90	46			
In-Situ vs SWANm	-1.95	1.97	31			

The findings from Figures 7.56-7.62 and Tables 7.26-7.42 can be summarized as;

- In general, significant wave heights, H_s, obtained from E10 wind speeds are underestimated considering both W61 and SWAN applications.
- Using modified E10 wind speeds (E10m2 and E10m3) for wave estimations result in certain improvements in H_s, H_{max}, T_{max}, H_{ave} and T_{ave} values for most of the cases considering both W61 and SWAN wave estimations.
- As for average bias, root mean square error (RMSE) and average mean absolute error (MAE) values for each case, certain improvements are achieved in all of the cases in terms of significant wave heights and significant wave periods.
- As for storm peaks, average bias, root mean square error (RMSE) and average mean absolute error (MAE) values indicate that for all of the cases substantial improvements are achieved in terms of significant wave heights and significant wave periods.
- Although improvements are observed for significant wave heights and wave periods, the underestimation is not overcame for most of the cases.
- Considering average bias, root mean square error (RMSE) and average mean absolute error (MAE) values for each case, certain improvements are

achieved in all cases except P03, P07 and P11 in terms of significant wave periods.

- As for storm peaks, average bias, root mean square error (RMSE) and average mean absolute error (MAE) values indicate that with the exception of P07, P08, P10 and P11, improvements are achieved in terms of significant wave periods.
- The aforementioned two outcomes are an indication that modified E10 wind speeds (E10m2 and E10m3) result in better representation at storm peaks in terms of significant wave periods.
- In-situ significant wave heights are generally higher than significant wave heights estimated from W61 and SWAN applications for storm peaks. It is observed that the significant wave heights obtained from W61 applications covering the storm peaks are generally presented with 7%-65% mean absolute error, whereas, wave heights obtained by SWAN applications corresponding to the same storm peaks are all underestimated with 17%-78% mean absolute error. Overall significant wave height estimations during the storm do not give a consistent trend for both W61 and SWAN applications. The mean absolute error fluctuates between 31%-180% and 43%-83% for W61 and SWAN applications respectively. This conclusion shows that studies have to be carried to have reliable wave height estimations using W61 and SWAN models covering the directional effects.
- Concerning W61 applications, significant wave heights are generally overestimated at the tail of the storms. This overestimation is also observed for the storm durations following the storm peaks.
- As for significant wave periods, W61 gives results with mean absolute error in the range of 7%-52% at storm peaks, whereas SWAN results have mean absolute error in the range of 9%-52%. As for overall significant wave period estimations during the storm, the mean absolute error fluctuates between 17%-42% and 26%-51% for W61 and SWAN applications respectively.
- Directional difference between representative wave directions of in-situ waves and of W61 wave estimations (E10, E10m2 and E10m3) are at most 2

sectors corresponding to 45° for all of the cases. The directional difference between representative wave directions of in-situ waves and of SWAN wave estimations (SWANm) are at most 2 sectors corresponding to 45° for half of the cases. These directional differences might be the source of the mean absolute error in the estimation of wave heights in both W61 and SWAN models.

- Compared to Sinop cases in Section 7.2, even though improvements are achieved with the modified wind data (E10m2 and E10m3), significant wave heights and periods are still underestimated. In Sinop cases, the underestimations are partly overcame with the use of modified wind data. On the other hand, whereas in Hopa cases, the underestimations are not overcame for most of the cases even though wave estimations are improved. This may be an indication of site-specific characteristics of wind modifications. Thus, if possible, for each region, site-specific comparisons should be performed between in-situ wind measurements and ECMWF wind data to improve the wave estimations.

7.4. Discussion

Case Studies for Sinop:

Wave estimations performed with E10, modified E10 (E10m2 and E10m3), S10 wind speeds for the selected storms among the data set show that E10 wave estimations are underestimated whereas underestimation decreases for E10m2, E10m3 and S10 wave estimations. Wave heights obtained from E10 wind speeds are underestimated in the order of 37%-56% compared to wave heights estimated from S10 winds.

Additionally, wave estimations carried out with ECMWF wind speeds instead of S10 wind directions become more compatible with wave estimations carried out with E10m2 and E10m3 wind directions.

At second stage of the study, wave estimations are performed for the selected durations when in-situ wave measurements are available. The results indicate that compared to in-situ significant wave heights, significant wave heights obtained from E10m2 and E10m3 winds have mean absolute error (MAE) is in the range of 7%-41% and 17%-98% respectively for storm peaks and for overall significant wave height estimations during the storm. As for significant wave period estimations with W61 applications from E10m2 and E10m3 winds, the mean absolute error (MAE) is observed in the range of 5%-27% and 12%-35% respectively for storm peaks and for overall significant wave height estimations during the storm.

Concerning SWAN applications with modified wind speeds, compared to in-situ wave heights and periods, significant wave heights and significant wave periods have absolute mean error in the range of 30%-70% and 7%-50% respectively at storm peaks. As for overall significant wave height and period estimations during the storm, the mean absolute errors are in the range of 32%-62% and 21%-48% for SWAN wave height and period estimations respectively.

<u>Case Studies for Hopa:</u>

Wave estimations are also applied to several durations when in-situ wind measurements are available for another site, Hopa, at Black Sea coast of Turkey in order to observe the applicability of the selected modification methods for another site. The wave underestimations specified in the above given paragraphs, are also observed for this region. Wave estimations (significant wave heights and wave periods) are improved both with W61 and SWAN numerical models in cases where E10m2 and E10m3 winds are used. However, improvements are more remarkable for W61 results that SWAN results for both parameters in all of the cases.

As for representative wave directions, most of the representative wave directions of wave estimations are more than 45° for half of the cases. This may be another implication of the site-specific characteristics of wind and wave comparisons. Thus, it would be better to check the impact of differences in wind directions, in order to observe their influence in wave estimations with more comparative studies if additional in-situ wind measurements will be available in the future.

In addition, the results indicate that compared to in-situ significant wave heights, significant wave heights obtained from E10m2 and E10m3 winds have mean absolute error (MAE) is in the range of 7%-65% and 31%-180% for storm peaks and for overall significant wave height estimations during the storm respectively. As for significant wave period estimations with W61 applications from E10m2 and E10m3 winds, the mean absolute error (MAE) is observed in the range of 7%-52% and 17%-42% for storm peaks and for overall significant wave height estimations during the storm respectively.

Concerning SWAN applications with modified wind speeds, compared to in-situ wave heights and periods, significant wave heights and significant wave periods have absolute mean error in the range of 17%-78% and 9%-52% respectively at storm peaks. As for overall significant wave height and period estimations during the storm, the mean absolute errors are in the range of 43%-83% and 26%-51% for significant wave height and period estimations respectively.

CHAPTER 8

CONCLUSION

Over the years, after each application to obtain design significant wave data for different Turkish coasts, it is found that there is a big reliability and representability problem for the hourly wind measurements of coastal meteorological stations (CMSs). This problem, although being site specific, commonly observed for many coastal stations.

At the first stage of the study, an overall review of Turkish Coastal Meteorological Stations (TCMSs) are carried out. The results show that the accuracy of the data for TCMSs is questionable. Therefore, in-situ wind measurements become very important to be used as reliable data for comparative studies and wave estimations.

At the second stage, it is aimed to understand the reliability of the selected ECMWF wind data which forms the bases for wave estimations for coastal projects by performing a comparative study for the selected site, Sinop at Black Sea coast of Turkey where land-based coastal in-situ wind measurements are acquired by governmental agencies. The in-situ wind measurements cover a duration between February, 2009 and December, 2009 with several gaps and thewind measurements are performed at elevations of 16 m, 25 m and 60 m above the local reference elevation (60m above MSL). The studies are performed only considering the directional sector WSW-ESE corresponding to onshore winds and a representative vertical profile is obtained showing that the in-situ measurements are carried out on a flat open coastal area.

As a result of comparative studies between wind measurements at three different elevations, it is found that coastal in-situ wind measurements may not be reliable enough concerning wind speeds and directions for lower elevations for coastal engineering applications, since lower wind speeds and directions are effected more by the surface roughness. Therefore, in-situ wind measurements at 60 m elevation are considered for the following comparative studies.

The above given in-situ wind measurements are used to understand the applicability of ECMWF wind data as a continuous wind data source to be used in coastal engineering practical applications. Firstly, special care is given to the selection of ECMWF wind data points, since not all of the grid points represent the wind climate accurately due to several reasons such as the distance to the shore, orography of the grid point and proximity to the site. Considering these factors, an ECMWF grid point is selected to be used for the upcoming comparative wind and wave studies.

In order to compare ECMWF wind data and in-situ wind measurements, in-situ wind measurements at 60 m above the local reference point on land is carried to 10 m elevation above MSL (S10). Comparisons of S10 and E10 wind data show that ECMWF give lower wind speeds compared to in-situ wind speeds. Therefore, it is decided that E10 wind speeds should be modified based on the correlations between simultaneous S10 and E10 wind speeds. During this study, modification methods are developed based on the wind speeds and trends of wind speed changes. Average BIAS, root mean square errors (RMSE) and average mean absolute errors (MAE) are also computed for each continuous data set as well as for all data of continuous data sets, in order to understand the general performance of modifications. The results indicate that improvements are observed with modified wind speeds for almost all of the cases. The mean absolute errors (MAE) are improved from 18.5%-42.4% to 2.5-22.9% with modification methods concerning $S10_S$ wind speeds.

At the third stage of the study, waves are estimated from S10, E10, selected modified E10 (E10m2 and E10m3) and $S10_S$ wind speeds by using W61 numerical model for the selected continuous data sets. The results show that the direct use of E10 winds for wave estimations result in significant underestimation, whereas estimated E10m2 and E10m3 waves give quite good correlation with S10 waves and comparably better correlation with $S10_S$ waves. Moreover, the maximum wave height estimations from E10m2 and E10m3 winds are generally good at storm peaks. On the other hand, wave estimations for durations before storm peaks are generally better than the wave estimations for durations after the storm peaks, resulting in overestimation of waves while storms are dissipating.

At the fourth stage, wave estimations are performed at Sinop region for the selected durations (cases) when in-situ wave measurements are available. The significant wave heights and periods are estimated with mean absolute errors in the range of 17%-98% and 12%-35% by using W61 model. These mean absolute errors are in the range of 7%-41% and 5%-27% respectively for significant wave heights and periods at storm peaks. As for wave estimations with SWAN model, the mean absolute errors are in the range of 32%-62% and 21%-48% respectively for significant wave heights and periods, whereas concerning storm peaks, significant wave heights and periods are estimated with mean absolute errors in the range of 30%-70% and 7%-50% respectively.

The aforementioned values and results indicate that improvements are observed with modified wind speeds for several cases in W61 applications in terms of significant wave heights and periods. As for SWAN applications, the improvements are still under the in-situ wave measurements both for significant wave heights and periods for most of the cases.

For most of the cases at Sinop studies, representative wave directions are within 45° of representative in-situ wave direction for W61 applications, whereas this directional difference is more than 45° for SWAN applications.

This study is also applied to several durations (cases) for another site, Hopa, at Black Sea coast of Turkey. Although improvements are observed concerning significant wave heights and periods, the underestimations are not overcame for most of the cases. For Hopa case, significant wave heights and periods estimated with W61 model have mean absolute errors in the range of 31%-180% and 17%-42% respectively. As for storm peaks, mean absolute errors are in the range of 7%-65% and 7%-52% respectively for significant wave heights and periods. Concerning wave estimations by using SWAN model, the mean absolute errors are in the range of

43%-83% and 26%-51% respectively for significant wave heights and periods, whereas for storm peaks, significant wave heights and periods are estimated with mean absolute errors in the range of 17%-78% and 9%-52% respectively.

As for the representative wave directions, W61 performs better than SWAN, meaning that for most of the cases the representative wave directions obtained from W61 applications remain within 45° of representative in-situ wave directions.

In the end, results of this study can be summarized as following:

- The wind data available at TCMSs is found to be not reliable enough and thus they are questionable. As a result, it is not recommended to be used as the only data source for the coastal engineering applications.
- As an alternative wind data source to the TCMSs, ECMWF wind data source is found to be a continuous wind data source for Turkish coasts that has to be used with modifications.
- The modifications developed throughout this study are site-specific therefore these comparative studies should be carried out for other sites along the Turkish coasts and for various fetch distances as well.
- To carry out these comparative studies, simultaneous offshore wind and wave measurements are strongly recommended for coastal engineering projects.

As for the future studies;

- It is necessary to update the developed modification methods by performing additional comparative studies with continuous data sets with longer periods for different sites.
- Application of various methods such as artificial neural network may be considered in developing different modification methods. However, in order to apply such a method, simultaneous in-situ wind and wave measurements covering longer durations with sufficient data are required.
- The smoothing of in-situ wind measurements should be reconsidered thoroughly by performing additional studies on the impact of hourly

variations of wind speeds and local effects like sea breezes along Turkish coasts.

- The effects of filtering out the hourly variations of wind speeds on wave estimations has to be also considered in terms of long term and extreme wave statistics.
- The wave estimations carried out in this thesis study might be extended with the use of other wave estimation methods.

REFERENCES

Abdalla, S., and Cavaleri, L., (2002), *"Effect of Wind Variability and Variable Air Density on Wave Modelling",* Journal of Geophysical Research, No. C7, 17-1/17-17

Aboobacker, V. M., Seemanth, M., Samiksha, S. V., Sudheesh, K., Kerkar, J., and Vethamony, P., (2014), *"Sea Breeze-Induced Wind Sea Growth in the Central West Coast of India",* Ocean Engineering, Vol. 84, pp. 20-28

Ackerman, S., (1995), *"Sea and Land Breezes",* University of Wisconsin

Aspliden, C. I., Lynn, A., Desouza, R. L., and Rudder, G., (1977), *"Diurnal and Semi-diurnal Low Level Wind Cycles over a Tropical Island",* Boundary-Layer Meteorology, Vol. 12, pp. 187-199

Berrisford, P., Dee, D., Poli, P., Brugge, R., Fielding, K., Fuentes, M., Kallberg, P., Kobayashi, S., Uppala, S., and Simmons, A., (2011), *"ERA Report Series: The ERA-Interim Archive Version 2.0",* European Centre for Medium Range Weather Forecasts, Reading, UK

Bierbooms, W., (2006), "*Course OE5662 Offshore Wind Farm Design",* Delft University Wind Energy Research Institue, DUWIND

Brown, G., (2001), *"Sun, Wind & Light",*ISBN 0-471-34877-5, New York: Wiley. pp. 18. .

Cavaleri, L., (2002), *"ECMWF Progress Report 2002 of the Special Project Testing and Application of a Third Generation Model in the Mediterranean Sea",* ECMWF web page, www.ecmwf.int

Cavaleri, L., and Bertotti, L., (1997), *"In Search of the Correct Wind and Wave Fields in a Minor Basin",* Monthly Weather Review, Vol. 125, 8, pp. 1964-1975

Cavaleri, L., and Bertotti, L., (2004), *“Accuracy of the Modelled Wind and Wave Fields in Enclosed Seas”,* Tellus A, Vol. 56, Issue 2, pp.161-175

Cavaleri, L., Bertotti, L., Sclavo, M., and Ramieri, E., (2002), *“Calibration of Wind and Wave Model Data in the Mediterranean Sea”,* ISDGM Report WW-MEDATLAS Project, 2002-1, pp.11

Coastal Engineering Manual, CEM, 1998

Dalgliesh, W. A., and Boyd, D. W., (1962), *"CBD-28. Wind on Buildings"*, Canadian Building Digest

Dando, P., (2013), *“Interpolation introduction and Basic Concepts”,* Computer User Training Course 2013,

Davenport, A. G., (1965), *“The Relationship of Wind Structure to Wind Loading”,* National Physical Laboratory Symposium No. 16, Wind Effects on Buildings and Structures, pp. 54-102, Her Majesty’s Stationery Office, London

Demirbilek Z., Bratos S. M. and Thompson E. F., (1993), *“Wind Products for Use in Coastal Wave and Surge Models”,* USACE Waterways Experiment Station Coastal Engineering Research Center

Ergin A., Özhan E., (1986), *“15 Bölge Yöresi için Dalga Tahminleri ve Tasarım Dalgası Özelliklerinin Belirlenmesi”,* Sonuç Raporu, Orta Doğu Teknik Üniversitesi, İnşaat Mühendisliği Bölümü, Şubat 1986, Ankara, (in Turkish)

European Centre for Medium Range Weather Forecasts, ECMWF, www.ecmwf.int

Google Earth, 2014

Harrison, R., (2001), *“Large Wind Turbines”,*ISBN 0-471-49456-9, Chichester: John Wiley & Sons, pp. 30

Hsu, S. A., (1981), *“On the Correction of Land-Based Wind Measurements for Oceanographic Applications”,* Boundary-Layer Meteorology, Vol. 17, pp. 485-495

Hsu, S. A., (1984), *"Improved Formulas for Estimating Offshore Winds",* Estimating Offshore Winds, Ch. 149, pp. 2220-2231

Hsu, S. A., (1986), *"Correction of Land-Based Wind Data for Offshore Applications: A Further Evaluation",* Journal of Physical Oceanography, Vol. 16, pp. 390-394

Kallberg, P., Simmons, A., Uppala, S., and Fuentes, M., (2007), *"ERA-40 Project Report Series 17.The ERA-40 Archive",* European Centre for Medium Range Weather Forecasts, Reading, UK

Kaltschmitt, M., Streicher, W., and Wiese, A., (2007), *"Renewable Energy: Technology, Economics, and Environment",* Springer, 2007, ISBN 3-540-70947-9, ISBN 978-3-540-70947-3, pp. 55

Koca, C. (1979), *"A Computer Program for Wave Hindcasting and Wave Statistics,"* M.Sc. Thesis, Middle East Technical University, Department of Civil Engineering, Ankara, Turkey

Komen, G. J., Cavaleri, L., Donelan, M., Hasselmann, K., Hasselmann, and S., Janssen, (1994), *"Dynamics and Modelling of Ocean Waves",* Cambridge University Press, pp. 532

Liu, P. C., Schwab, D. J., and Bennett, J. R., (1984), *"Comparison of a Two-Dimensional Wave Prediction Model with Synoptic Measurements in Lake Michigan",* Journal of Physical Oceanography, Vol. 14, pp. 1514-1518

Liu, P. C., and Ross, D. B., (1980), *"Airborne Measurements of Wave Growth for Stable and Unstable Atmosphere in Lake Michigan",* Journal of Physical Oceanography, Vol. 10, pp. 1842-1853

Lubosny, Z. (2003), *"Wind Turbine Operation in Electric Power Systems: Advanced Modeling",*Journal of Earth System Science, Vol 115, No. 2, pp. 229-234

Mazzarella, D. A., (1985), *"Measurements Today, Handbook of Applied Meteorology",* D.D. Houghton Ed., Wiley and Sons, pp. 283-328

Mediterranean Coastal Foudnation, MEDCOAST, www.medcoast.org.tr

Neetu, S., Shetye, S. and Chandramohan, P., (2006), *"Impact of Sea Breeze on Wind-Sead off Goa, West Coast of India",* Journal of Great Lakes Research, Vol. 10, pp. 68-72

Oke, T. (1987), *"Boundary Layer Climates",*ISBN 0-415-04319-0, London: Methuen, pp. 54.

Ozhan, E. (1981), *"Rüzgar Dalgalarının Kısa Dönem Istatistiksel Ozellikleri, Enerji Spektrumu ve Dalga Tahminleri",* Rapor No. 25, Orta Doğu Teknik Üniversitesi, İnşaat Mühendisliği Bölümü, Ankara, (in Turkish)

Pierson, W.J. and Moskovitz, L. (1964) *"A Proposed Spectral Form for Fully Developed Wind Seas Based on the Similarity Theory of S.A. Kitaigorodskii,"* Journal of Geophysical Research. 69: 5181-5190.

Resio, P. T., and Vincent, C. L., (1977), *"Estimation of Winds over the Great Lakes",* Journal of Waterways Harbors Coastal Division, ASCE, Vol. 102, pp. 265-283

Schwab, D. J., (1978), *"Simulation and Forecasting of Lake Erie Storm Surges",* Monthly Weather Review, Vol. 106, pp. 1842-1853

Schwab, D. J., and Morton, J. A., (1984), *"Estimation of Overlake Wind Speed from Overland Wind Speed: A Comparison of Three Methods",* Journal of Great Lakes Research, Vol. 10, pp. 68-72

Schwing, F. B., and Blanton, J. O., (1984), *"The Use of Land and Sea Based Wind Data in a Simple Circulation Model",* Journal of Physical Oceanography, Vol. 14, pp. 193-197

SethuRaman, S., and Raynor, G. S., (1980), *"Comparison of Mean Wind Speeds and Turbulence at a Coastal Site and Offshore Location",* Journal of Applied Meteorology, ASCE, Vol. 110, pp. 1912-1932

Signell, R. P., Carniel, S., Cavaleri, L., Chiggiato J., Doyle, J. D., Pullen J., and Sclavo, M., (2005), *"Assessment of Wind Quality for Oceanographic Modelling in Semi-Enclosed Basins",* Journal of Marine Systems, Vol. 53, pp. 217-233

Soukassian, T., and Vouvakalas, E., (2013), *"CoCoNet Project M25 Atmospheric Model Results for the Mediterranean and Black Seas",* CoCoNet Project: FP7 – OCEAN.2011-4-GA, Seventh Framework Programme

Stoltman, J. (2005), *"International Perspectives on Natural Disasters: Occurrence, Mitigation, and Consequences",*ISBN 1-4020-2850-4, Berlin: Springer, pp. 73

Thomas, B.R., Kent, E.C., and Swail, V.R. (2005), *"Methods to Homogenize Wind Speeds from Ships and Buoys",* International Journal of Climatology, Vol. 25, pp. 979-995

Turkish State Meteorological Service, www.dmi.gov.tr

Wakelin, S. L., and Proctor, R., (2002), *"The Impact of Meteorology on Modeling Storm Surges in the Adriatic Sea",* Global and Planetary Change, Vol. 34, pp. 97-119

Weisberg, R. H., and Pietrafesa, L. J., (1983), *"Kinematics and Correlation of the Surface Wind Field in the South Atlantic Bight",* Journal of Geophyical Research, Vol. 88, pp. 4593-4610

Wieringa, J., (1980), *"Representativeness of Wind Observations at Airports",* Bulletin of the American Meteorological Society, Vol. 61, pp. 962-971

WRPLOT View Version 7.0.0, Lakes Environmental, www.weblakes.com

APPENDIX A

WIND SPEED CLASSIFICATIONS

Wind speed classifications for the selected ECMWF grid points as well as LAND loation (in-situ wind measurements) are given in the figures below.

Table A.1: Classification of Winds in Terms of Directions and Speeds (Point A, 42.10°N – 34.80°E)

Wind Directions (in °)	Wind Classes (m/s)							
	0.0 – 3.0	3.0 – 5.0	5.0 – 7.5	7.5 – 10.0	10.0 – 12.5	12.5 – 15.0	>= 15.0	Total
348.75 - 11.25	0.8%	0.5%	0.7%	0.4%	0.0%	0.0%	0.0%	2.4%
11.25 - 33.75	1.5%	1.3%	0.2%	0.0%	0.0%	0.0%	0.0%	3.1%
33.75 - 56.25	0.9%	1.1%	0.6%	0.2%	0.0%	0.0%	0.0%	2.8%
56.25 - 78.75	1.3%	1.6%	1.2%	0.8%	0.0%	0.0%	0.0%	4.8%
78.75 - 101.25	1.8%	4.4%	6.4%	2.6%	0.6%	0.0%	0.0%	15.8%
101.25 - 123.75	0.6%	2.9%	3.6%	2.0%	0.0%	0.0%	0.0%	9.1%
Sub-Total	6.9%	11.8%	12.7%	6.0%	0.6%	0.0%	0.0%	38.0%
123.75 - 146.25	1.4%	1.9%	0.9%	0.2%	0.0%	0.0%	0.0%	4.5%
146.25 - 168.75	2.8%	1.4%	0.3%	0.0%	0.0%	0.0%	0.0%	4.6%
168.75 - 191.25	2.2%	1.1%	0.4%	0.0%	0.0%	0.0%	0.0%	3.7%
191.25 - 213.75	1.7%	0.6%	0.1%	0.3%	0.2%	0.0%	0.0%	2.8%
213.75 - 236.25	0.8%	0.3%	0.0%	0.0%	0.0%	0.0%	0.0%	1.1%
Sub-Total	8.9%	5.3%	1.7%	0.5%	0.2%	0.0%	0.0%	16.7%
236.25 - 258.75	1.7%	0.9%	0.8%	0.2%	0.0%	0.0%	0.0%	3.6%
258.75 - 281.25	1.8%	3.3%	4.7%	3.1%	1.6%	0.7%	0.0%	15.2%
281.25 - 303.75	1.3%	2.8%	4.8%	7.1%	2.4%	0.9%	0.0%	19.3%
303.75 - 326.25	1.0%	2.4%	1.3%	0.6%	0.1%	0.0%	0.0%	5.4%
326.25 - 348.75	0.9%	0.6%	0.3%	0.2%	0.0%	0.0%	0.0%	2.0%
Sub-Total	6.7%	10.0%	11.9%	11.2%	4.1%	1.6%	0.0%	45.5%
Total	22.4%	27.2%	26.4%	17.5%	4.8%	1.7%	0.0%	100.0%

Table A.2: Classification of Winds in Terms of Directions and Speeds (Point A, 42.10°N – 34.80°E)

Wind Directions (in °)	Wind Classes (m/s)							
	0.0 – 3.0	3.0 – 5.0	5.0 – 7.5	7.5 – 10.0	10.0 – 12.5	12.5 – 15.0	>= 15.0	Total
348.75 - 11.25	0.8%	0.5%	0.7%	0.4%	0.0%	0.0%	0.0%	2.4%
11.25 - 33.75	1.5%	1.3%	0.2%	0.0%	0.0%	0.0%	0.0%	3.1%
33.75 - 56.25	0.9%	1.1%	0.6%	0.2%	0.0%	0.0%	0.0%	2.8%
56.25 - 78.75	1.3%	1.6%	1.2%	0.8%	0.0%	0.0%	0.0%	4.8%
78.75 - 101.25	1.8%	4.4%	6.4%	2.6%	0.6%	0.0%	0.0%	15.8%
101.25 - 123.75	0.6%	2.9%	3.6%	2.0%	0.0%	0.0%	0.0%	9.1%
Sub-Total	6.9%	11.8%	12.7%	6.0%	0.6%	0.0%	0.0%	38.0%
123.75 - 146.25	1.4%	1.9%	0.9%	0.2%	0.0%	0.0%	0.0%	4.5%
146.25 - 168.75	2.8%	1.4%	0.3%	0.0%	0.0%	0.0%	0.0%	4.6%
168.75 - 191.25	2.2%	1.1%	0.4%	0.0%	0.0%	0.0%	0.0%	3.7%
191.25 - 213.75	1.7%	0.6%	0.1%	0.3%	0.2%	0.0%	0.0%	2.8%
213.75 - 236.25	0.8%	0.3%	0.0%	0.0%	0.0%	0.0%	0.0%	1.1%
Sub-Total	8.9%	5.3%	1.7%	0.5%	0.2%	0.0%	0.0%	16.7%
236.25 - 258.75	1.7%	0.9%	0.8%	0.2%	0.0%	0.0%	0.0%	3.6%
258.75 - 281.25	1.8%	3.3%	4.7%	3.1%	1.6%	0.7%	0.0%	15.2%
281.25 - 303.75	1.3%	2.8%	4.8%	7.1%	2.4%	0.9%	0.0%	19.3%
303.75 - 326.25	1.0%	2.4%	1.3%	0.6%	0.1%	0.0%	0.0%	5.4%
326.25 - 348.75	0.9%	0.6%	0.3%	0.2%	0.0%	0.0%	0.0%	2.0%
Sub-Total	6.7%	10.0%	11.9%	11.2%	4.1%	1.6%	0.0%	45.5%
Total	22.4%	27.2%	26.4%	17.5%	4.8%	1.7%	0.0%	100.0%

Table A.3: Classification of Winds in Terms of Directions and Speeds (Point B, 42.10°N – 34.90°E)

Wind Directions (in °)	Wind Classes (m/s)							
	0.0 – 3.0	3.0 – 5.0	5.0 – 7.5	7.5 – 10.0	10.0 – 12.5	12.5 – 15.0	>= 15.0	Total
348.75 - 11.25	1.0%	0.0%	1.0%	0.0%	0.0%	0.0%	0.0%	2.0%
11.25 - 33.75	1.0%	1.0%	0.0%	0.0%	0.0%	0.0%	0.0%	3.0%
33.75 - 56.25	1.0%	1.0%	1.0%	0.0%	0.0%	0.0%	0.0%	3.0%
56.25 - 78.75	1.0%	2.0%	1.0%	1.0%	0.0%	0.0%	0.0%	5.0%
78.75 - 101.25	2.0%	4.0%	6.0%	3.0%	1.0%	0.0%	0.0%	16.0%
101.25 - 123.75	1.0%	3.0%	4.0%	2.0%	0.0%	0.0%	0.0%	9.0%
Sub-Total	7.0%	11.0%	13.0%	6.0%	1.0%	0.0%	0.0%	38.0%
123.75 - 146.25	1.0%	2.0%	1.0%	0.0%	0.0%	0.0%	0.0%	4.0%
146.25 - 168.75	3.0%	1.0%	0.0%	0.0%	0.0%	0.0%	0.0%	5.0%
168.75 - 191.25	2.0%	1.0%	0.0%	0.0%	0.0%	0.0%	0.0%	4.0%
191.25 - 213.75	2.0%	1.0%	0.0%	0.0%	0.0%	0.0%	0.0%	3.0%
213.75 - 236.25	1.0%	0.0%	0.0%	0.0%	0.0%	0.0%	0.0%	1.0%
Sub-Total	9.0%	5.0%	1.0%	0.0%	0.0%	0.0%	0.0%	17.0%
236.25 - 258.75	2.0%	1.0%	1.0%	0.0%	0.0%	0.0%	0.0%	4.0%
258.75 - 281.25	2.0%	3.0%	5.0%	3.0%	2.0%	1.0%	0.0%	15.0%
281.25 - 303.75	1.0%	3.0%	5.0%	7.0%	2.0%	1.0%	0.0%	19.0%
303.75 - 326.25	1.0%	2.0%	1.0%	1.0%	0.0%	0.0%	0.0%	5.0%
326.25 - 348.75	1.0%	1.0%	0.0%	0.0%	0.0%	0.0%	0.0%	2.0%
Sub-Total	7.0%	10.0%	12.0%	11.0%	4.0%	2.0%	0.0%	45.0%
Total	22.4%	27.2%	26.4%	17.5%	4.8%	1.7%	0.0%	100.0%

Table A.4: Classification of Winds in Terms of Directions and Speeds (Point C, 42.10°N – 35.10°E) (in %)

Wind Directions (in °)	Wind Classes (m/s)							
	0.0 – 3.0	3.0 – 5.0	5.0 – 7.5	7.5 – 10.0	10.0 – 12.5	12.5 – 15.0	>= 15.0	Total
348.75 - 11.25	0.8%	0.4%	0.6%	0.5%	0.1%	0.0%	0.0%	2.3%
11.25 - 33.75	1.3%	1.2%	0.2%	0.0%	0.0%	0.0%	0.0%	2.7%
33.75 - 56.25	1.0%	1.2%	0.7%	0.3%	0.0%	0.0%	0.0%	3.1%
56.25 - 78.75	1.4%	1.5%	0.9%	0.6%	0.0%	0.0%	0.0%	4.4%
78.75 - 101.25	1.7%	4.0%	5.5%	2.2%	0.4%	0.0%	0.0%	13.7%
101.25 - 123.75	1.1%	3.4%	4.4%	2.5%	0.1%	0.0%	0.0%	11.4%
Sub-Total	7.3%	11.7%	12.3%	6.1%	0.6%	0.0%	0.0%	37.6%
123.75 - 146.25	1.5%	1.8%	1.0%	0.4%	0.0%	0.0%	0.0%	4.7%
146.25 - 168.75	2.7%	1.7%	0.3%	0.1%	0.0%	0.0%	0.0%	4.7%
168.75 - 191.25	2.0%	0.9%	0.5%	0.0%	0.0%	0.0%	0.0%	3.4%
191.25 - 213.75	1.5%	0.8%	0.2%	0.3%	0.2%	0.0%	0.0%	2.9%
213.75 - 236.25	1.1%	0.3%	0.1%	0.0%	0.0%	0.0%	0.0%	1.5%
Sub-Total	8.8%	5.5%	2.1%	0.8%	0.2%	0.0%	0.0%	17.2%
236.25 - 258.75	1.4%	0.9%	0.7%	0.2%	0.0%	0.0%	0.0%	3.1%
258.75 - 281.25	1.5%	3.0%	3.7%	2.9%	1.4%	0.6%	0.0%	13.1%
281.25 - 303.75	1.2%	3.1%	5.2%	7.0%	2.9%	0.9%	0.1%	20.4%
303.75 - 326.25	1.1%	2.5%	1.9%	0.8%	0.1%	0.1%	0.1%	6.6%
326.25 - 348.75	0.8%	0.7%	0.5%	0.1%	0.0%	0.0%	0.0%	2.0%
Sub-Total	6.0%	10.2%	12.0%	11.0%	4.4%	1.6%	0.2%	45.2%
Total	22.1%	27.2%	26.2%	17.7%	5.1%	1.6%	0.1%	100.0%

Table A.5: Classification of Winds in Terms of Directions and Speeds (Point D, 42.20°N – 34.80°E)

Wind Directions (in °)	Wind Classes (m/s)							
	0.0 – 3.0	3.0 – 5.0	5.0 – 7.5	7.5 – 10.0	10.0 – 12.5	12.5 – 15.0	>= 15.0	Total
348.75 - 11.25	0.8%	0.4%	0.6%	0.4%	0.0%	0.0%	0.0%	2.2%
11.25 - 33.75	1.3%	1.2%	0.2%	0.0%	0.0%	0.0%	0.0%	2.8%
33.75 - 56.25	1.0%	1.1%	0.7%	0.2%	0.0%	0.0%	0.0%	3.1%
56.25 - 78.75	1.4%	1.5%	0.9%	0.7%	0.0%	0.0%	0.0%	4.5%
78.75 - 101.25	1.7%	4.0%	5.7%	2.6%	0.5%	0.0%	0.0%	14.3%
101.25 - 123.75	1.1%	3.1%	4.0%	2.5%	0.1%	0.0%	0.0%	10.8%
Sub-Total	7.3%	11.3%	12.1%	6.4%	0.6%	0.0%	0.0%	37.7%
123.75 - 146.25	1.4%	1.8%	1.0%	0.4%	0.0%	0.0%	0.0%	4.5%
146.25 - 168.75	2.6%	1.7%	0.3%	0.0%	0.0%	0.0%	0.0%	4.6%
168.75 - 191.25	2.1%	0.9%	0.4%	0.0%	0.0%	0.0%	0.0%	3.5%
191.25 - 213.75	1.5%	0.8%	0.2%	0.3%	0.2%	0.0%	0.0%	2.9%
213.75 - 236.25	1.0%	0.3%	0.0%	0.0%	0.0%	0.0%	0.0%	1.4%
Sub-Total	8.6%	5.5%	1.9%	0.7%	0.2%	0.0%	0.0%	16.9%
236.25 - 258.75	1.5%	0.9%	0.7%	0.2%	0.0%	0.0%	0.0%	3.3%
258.75 - 281.25	1.6%	3.0%	4.1%	2.9%	1.5%	0.6%	0.1%	13.8%
281.25 - 303.75	1.0%	3.0%	5.1%	7.1%	2.8%	1.0%	0.0%	19.9%
303.75 - 326.25	1.0%	2.4%	1.8%	0.7%	0.1%	0.1%	0.0%	6.1%
326.25 - 348.75	0.8%	0.7%	0.4%	0.2%	0.0%	0.0%	0.0%	2.2%
Sub-Total	5.9%	10.0%	12.1%	11.1%	4.4%	1.7%	0.1%	45.3%
Total	21.8%	27.0%	26.0%	18.3%	5.1%	1.7%	0.2%	100.0%

Table A.6: Classification of Winds in Terms of Directions and Speeds (Point E, 42.20°N – 34.90°E)

Wind Directions (in °)	Wind Classes (m/s)							
	0.0 – 3.0	3.0 – 5.0	5.0 – 7.5	7.5 – 10.0	10.0 – 12.5	12.5 – 15.0	>= 15.0	Total
348.75 - 11.25	0.8%	0.4%	0.5%	0.5%	0.0%	0.0%	0.0%	2.2%
11.25 - 33.75	1.1%	1.3%	0.3%	0.0%	0.0%	0.0%	0.0%	2.7%
33.75 - 56.25	1.1%	1.1%	0.7%	0.3%	0.0%	0.0%	0.0%	3.1%
56.25 - 78.75	1.4%	1.4%	0.9%	0.8%	0.0%	0.0%	0.0%	4.6%
78.75 - 101.25	1.5%	4.1%	5.6%	2.6%	0.5%	0.0%	0.0%	14.3%
101.25 - 123.75	1.1%	3.1%	3.9%	2.7%	0.1%	0.0%	0.0%	10.9%
Sub-Total	7.0%	11.4%	11.9%	6.9%	0.6%	0.0%	0.0%	37.8%
123.75 - 146.25	1.3%	1.8%	1.1%	0.3%	0.0%	0.0%	0.0%	4.6%
146.25 - 168.75	2.5%	1.7%	0.3%	0.0%	0.0%	0.0%	0.0%	4.6%
168.75 - 191.25	2.1%	0.9%	0.3%	0.0%	0.0%	0.0%	0.0%	3.4%
191.25 - 213.75	1.5%	0.8%	0.2%	0.3%	0.2%	0.0%	0.0%	2.9%
213.75 - 236.25	1.0%	0.3%	0.0%	0.0%	0.0%	0.0%	0.0%	1.4%
Sub-Total	8.4%	5.5%	1.9%	0.6%	0.2%	0.0%	0.0%	16.9%
236.25 - 258.75	1.4%	0.9%	0.7%	0.2%	0.0%	0.0%	0.0%	3.2%
258.75 - 281.25	1.7%	2.9%	4.3%	3.0%	1.5%	0.6%	0.1%	14.1%
281.25 - 303.75	0.9%	2.9%	5.1%	7.1%	2.7%	1.0%	0.1%	19.8%
303.75 - 326.25	1.0%	2.3%	1.8%	0.7%	0.1%	0.1%	0.0%	6.0%
326.25 - 348.75	0.8%	0.8%	0.4%	0.2%	0.0%	0.0%	0.0%	2.2%
Sub-Total	5.8%	9.8%	12.3%	11.2%	4.3%	1.7%	0.2%	45.3%
Total	21.4%	26.8%	26.1%	18.7%	5.2%	1.7%	0.2%	100.0%

Table A.7: Classification of Winds in Terms of Directions and Speeds (Point F, 42.20°N – 35.00°E)

Wind Directions (in °)	Wind Classes (m/s)							
	0.0 – 3.0	3.0 – 5.0	5.0 – 7.5	7.5 – 10.0	10.0 – 12.5	12.5 – 15.0	>= 15.0	Total
348.75 - 11.25	0.8%	0.4%	0.4%	0.5%	0.1%	0.0%	0.0%	2.2%
11.25 - 33.75	1.2%	1.3%	0.3%	0.0%	0.0%	0.0%	0.0%	2.8%
33.75 - 56.25	1.0%	1.2%	0.6%	0.3%	0.0%	0.0%	0.0%	3.1%
56.25 - 78.75	1.5%	1.3%	0.9%	0.8%	0.0%	0.0%	0.0%	4.5%
78.75 - 101.25	1.5%	4.1%	5.4%	2.6%	0.5%	0.0%	0.0%	14.0%
101.25 - 123.75	1.2%	3.0%	4.1%	2.8%	0.2%	0.0%	0.0%	11.3%
Sub-Total	7.2%	11.3%	11.7%	7.0%	0.8%	0.0%	0.0%	37.9%
123.75 - 146.25	1.3%	1.9%	1.2%	0.4%	0.0%	0.0%	0.0%	4.7%
146.25 - 168.75	2.4%	1.7%	0.4%	0.0%	0.0%	0.0%	0.0%	4.5%
168.75 - 191.25	2.0%	0.9%	0.3%	0.0%	0.0%	0.0%	0.0%	3.3%
191.25 - 213.75	1.4%	0.7%	0.2%	0.3%	0.2%	0.0%	0.0%	2.8%
213.75 - 236.25	1.2%	0.3%	0.1%	0.0%	0.0%	0.0%	0.0%	1.5%
Sub-Total	8.3%	5.5%	2.2%	0.7%	0.2%	0.0%	0.0%	16.8%
236.25 - 258.75	1.4%	0.9%	0.7%	0.2%	0.0%	0.0%	0.0%	3.1%
258.75 - 281.25	1.7%	2.9%	4.2%	3.0%	1.5%	0.6%	0.2%	14.0%
281.25 - 303.75	0.9%	2.8%	5.2%	7.1%	2.8%	1.0%	0.1%	19.9%
303.75 - 326.25	1.0%	2.3%	1.9%	0.7%	0.1%	0.1%	0.0%	6.1%
326.25 - 348.75	0.7%	0.9%	0.4%	0.2%	0.0%	0.0%	0.0%	2.2%
Sub-Total	5.7%	9.8%	12.4%	11.2%	4.4%	1.7%	0.3%	45.3%
Total	21.1%	26.6%	26.1%	18.9%	5.3%	1.7%	0.3%	100.0%

Table A.8: Classification of Winds in Terms of Directions and Speeds (Point G, 42.20°N – 35.10°E)

Wind Directions (in °)	Wind Classes (m/s)							
	0.0 – 3.0	3.0 – 5.0	5.0 – 7.5	7.5 – 10.0	10.0 – 12.5	12.5 – 15.0	>= 15.0	Total
348.75 - 11.25	0.5%	0.6%	0.0%	0.6%	0.2%	0.0%	0.0%	1.9%
11.25 - 33.75	1.3%	0.8%	0.3%	0.0%	0.0%	0.0%	0.0%	2.4%
33.75 - 56.25	1.3%	1.4%	0.6%	0.8%	0.0%	0.0%	0.0%	4.1%
56.25 - 78.75	1.6%	0.8%	0.5%	0.3%	0.0%	0.0%	0.0%	3.1%
78.75 - 101.25	0.6%	3.3%	4.1%	1.6%	0.2%	0.0%	0.0%	9.7%
101.25 - 123.75	2.2%	3.8%	6.3%	3.8%	0.8%	0.0%	0.0%	16.8%
Sub-Total	7.5%	10.7%	11.8%	7.1%	1.2%	0.0%	0.0%	38.0%
123.75 - 146.25	1.3%	1.9%	1.3%	1.1%	0.0%	0.0%	0.0%	5.5%
146.25 - 168.75	1.4%	1.9%	0.5%	0.2%	0.0%	0.0%	0.0%	3.9%
168.75 - 191.25	2.0%	0.8%	0.2%	0.2%	0.0%	0.0%	0.0%	3.1%
191.25 - 213.75	0.9%	0.5%	0.3%	0.3%	0.2%	0.0%	0.0%	2.2%
213.75 - 236.25	2.0%	0.2%	0.2%	0.0%	0.0%	0.0%	0.0%	2.4%
Sub-Total	7.6%	5.3%	2.5%	1.8%	0.2%	0.0%	0.0%	17.1%
236.25 - 258.75	0.8%	0.6%	0.3%	0.2%	0.0%	0.0%	0.0%	1.9%
258.75 - 281.25	0.9%	1.9%	2.8%	2.7%	1.3%	0.3%	0.3%	10.2%
281.25 - 303.75	0.9%	3.1%	6.9%	5.7%	4.4%	0.9%	0.3%	22.3%
303.75 - 326.25	0.6%	2.8%	2.4%	1.6%	0.2%	0.3%	0.0%	7.9%
326.25 - 348.75	0.6%	0.8%	0.6%	0.3%	0.2%	0.0%	0.0%	2.5%
Sub-Total	3.8%	9.2%	13.0%	10.5%	6.1%	1.5%	0.6%	44.8%
Total	19.0%	25.2%	27.2%	19.2%	7.2%	1.6%	0.6%	100.0%

Table A.9: Classification of Winds in Terms of Directions and Speeds (Point H, 42.30°N – 34.80°E)

Wind Directions (in °)	Wind Classes (m/s)							
	0.0 – 3.0	3.0 – 5.0	5.0 – 7.5	7.5 – 10.0	10.0 – 12.5	12.5 – 15.0	>= 15.0	Total
348.75 - 11.25	0.9%	0.5%	0.3%	0.5%	0.1%	0.0%	0.0%	2.2%
11.25 - 33.75	1.1%	1.3%	0.3%	0.0%	0.0%	0.0%	0.0%	2.7%
33.75 - 56.25	1.1%	1.1%	0.6%	0.4%	0.0%	0.0%	0.0%	3.1%
56.25 - 78.75	1.4%	1.3%	0.9%	0.8%	0.0%	0.0%	0.0%	4.4%
78.75 - 101.25	1.4%	4.0%	5.4%	2.6%	0.5%	0.0%	0.0%	13.9%
101.25 - 123.75	1.3%	2.9%	4.1%	2.9%	0.2%	0.0%	0.0%	11.5%
Sub-Total	7.2%	11.1%	11.6%	7.2%	0.8%	0.0%	0.0%	37.8%
123.75 - 146.25	1.3%	1.8%	1.3%	0.4%	0.0%	0.0%	0.0%	4.7%
146.25 - 168.75	2.3%	1.8%	0.4%	0.0%	0.0%	0.0%	0.0%	4.5%
168.75 - 191.25	2.0%	0.9%	0.2%	0.0%	0.0%	0.0%	0.0%	3.2%
191.25 - 213.75	1.5%	0.7%	0.2%	0.3%	0.2%	0.0%	0.0%	2.8%
213.75 - 236.25	1.1%	0.3%	0.0%	0.0%	0.0%	0.0%	0.0%	1.5%
Sub-Total	8.2%	5.5%	2.1%	0.7%	0.2%	0.0%	0.0%	16.7%
236.25 - 258.75	1.5%	0.8%	0.7%	0.2%	0.0%	0.0%	0.0%	3.2%
258.75 - 281.25	1.6%	3.0%	4.4%	3.0%	1.6%	0.6%	0.2%	14.4%
281.25 - 303.75	0.9%	2.8%	5.2%	7.0%	2.7%	0.9%	0.1%	19.6%
303.75 - 326.25	0.9%	2.3%	1.8%	0.8%	0.1%	0.1%	0.0%	6.0%
326.25 - 348.75	0.7%	0.8%	0.4%	0.2%	0.0%	0.0%	0.0%	2.2%
Sub-Total	5.6%	9.7%	12.5%	11.2%	4.4%	1.6%	0.3%	45.4%
Total	20.8%	26.4%	26.2%	19.1%	5.5%	1.7%	0.3%	100.0%

Table A.10: Classification of Winds in Terms of Directions and Speeds (Point I, 42.30°N – 34.90°E)

Wind Directions (in °)	Wind Classes (m/s)							
	0.0 – 3.0	3.0 – 5.0	5.0 – 7.5	7.5 – 10.0	10.0 – 12.5	12.5 – 15.0	>= 15.0	Total
348.75 - 11.25	0.8%	0.5%	0.3%	0.5%	0.1%	0.0%	0.0%	2.2%
11.25 - 33.75	1.2%	1.2%	0.3%	0.0%	0.0%	0.0%	0.0%	2.7%
33.75 - 56.25	1.1%	1.1%	0.6%	0.4%	0.0%	0.0%	0.0%	3.1%
56.25 - 78.75	1.3%	1.3%	0.9%	0.8%	0.0%	0.0%	0.0%	4.2%
78.75 - 101.25	1.4%	4.0%	5.3%	2.5%	0.4%	0.0%	0.0%	13.5%
101.25 - 123.75	1.3%	2.9%	4.3%	3.0%	0.3%	0.0%	0.0%	11.8%
Sub-Total	7.1%	11.0%	11.7%	7.2%	0.8%	0.0%	0.0%	37.5%
123.75 - 146.25	1.3%	1.8%	1.3%	0.5%	0.0%	0.0%	0.0%	4.9%
146.25 - 168.75	2.2%	1.8%	0.4%	0.0%	0.0%	0.0%	0.0%	4.4%
168.75 - 191.25	2.0%	0.9%	0.2%	0.1%	0.0%	0.0%	0.0%	3.2%
191.25 - 213.75	1.4%	0.7%	0.2%	0.3%	0.2%	0.0%	0.0%	2.7%
213.75 - 236.25	1.2%	0.3%	0.1%	0.0%	0.0%	0.0%	0.0%	1.6%
Sub-Total	8.1%	5.5%	2.2%	0.9%	0.2%	0.0%	0.0%	16.8%
236.25 - 258.75	1.6%	0.8%	0.6%	0.2%	0.1%	0.0%	0.0%	3.2%
258.75 - 281.25	1.5%	3.1%	4.4%	3.0%	1.7%	0.6%	0.2%	14.5%
281.25 - 303.75	0.8%	2.9%	5.2%	6.9%	2.7%	0.9%	0.1%	19.5%
303.75 - 326.25	0.9%	2.3%	1.8%	0.9%	0.1%	0.1%	0.0%	6.0%
326.25 - 348.75	0.7%	0.8%	0.5%	0.2%	0.0%	0.0%	0.0%	2.2%
Sub-Total	5.5%	9.9%	12.5%	11.2%	4.6%	1.6%	0.3%	45.4%
Total	20.6%	26.4%	26.2%	19.2%	5.7%	1.7%	0.3%	100.0%

Table A.11: Classification of Winds in Terms of Directions and Speeds (Point J, 42.30°N – 35.00°E)

Wind Directions (in °)	Wind Classes (m/s)							
	0.0 – 3.0	3.0 – 5.0	5.0 – 7.5	7.5 – 10.0	10.0 – 12.5	12.5 – 15.0	>= 15.0	Total
348.75 - 11.25	0.8%	0.5%	0.3%	0.5%	0.1%	0.0%	0.0%	2.2%
11.25 - 33.75	1.3%	1.2%	0.3%	0.0%	0.0%	0.0%	0.0%	2.8%
33.75 - 56.25	1.1%	1.0%	0.5%	0.5%	0.0%	0.0%	0.0%	3.1%
56.25 - 78.75	1.2%	1.2%	0.8%	0.8%	0.1%	0.0%	0.0%	4.1%
78.75 - 101.25	1.4%	3.9%	5.1%	2.4%	0.4%	0.0%	0.0%	13.2%
101.25 - 123.75	1.3%	2.9%	4.4%	3.1%	0.3%	0.0%	0.0%	12.2%
Sub-Total	7.1%	10.7%	11.4%	7.3%	0.9%	0.0%	0.0%	37.6%
123.75 - 146.25	1.3%	1.9%	1.3%	0.5%	0.0%	0.0%	0.0%	5.0%
146.25 - 168.75	2.2%	1.7%	0.4%	0.1%	0.0%	0.0%	0.0%	4.4%
168.75 - 191.25	2.0%	0.9%	0.2%	0.1%	0.0%	0.0%	0.0%	3.2%
191.25 - 213.75	1.3%	0.7%	0.2%	0.3%	0.2%	0.0%	0.0%	2.6%
213.75 - 236.25	1.2%	0.3%	0.1%	0.0%	0.0%	0.0%	0.0%	1.6%
Sub-Total	8.0%	5.5%	2.2%	1.0%	0.2%	0.0%	0.0%	16.8%
236.25 - 258.75	1.6%	0.8%	0.6%	0.2%	0.1%	0.0%	0.0%	3.3%
258.75 - 281.25	1.5%	3.1%	4.4%	3.0%	1.7%	0.6%	0.2%	14.5%
281.25 - 303.75	0.8%	3.0%	5.3%	6.8%	2.7%	0.9%	0.1%	19.5%
303.75 - 326.25	0.8%	2.2%	1.7%	1.0%	0.2%	0.1%	0.0%	6.1%
326.25 - 348.75	0.6%	0.9%	0.4%	0.2%	0.1%	0.0%	0.0%	2.2%
Sub-Total	5.3%	10.0%	12.4%	11.2%	4.8%	1.6%	0.3%	45.6%
Total	20.5%	26.2%	26.2%	19.4%	5.8%	1.7%	0.3%	100.0%

Table A.12: Classification of Winds in Terms of Directions and Speeds (Point K, 42.30°N – 35.10°E)

Wind Directions (in °)	Wind Classes (m/s)							
	0.0 – 3.0	3.0 – 5.0	5.0 – 7.5	7.5 – 10.0	10.0 – 12.5	12.5 – 15.0	>= 15.0	Total
348.75 - 11.25	0.6%	0.8%	0.1%	0.5%	0.3%	0.0%	0.0%	2.3%
11.25 - 33.75	1.1%	0.9%	0.3%	0.0%	0.0%	0.0%	0.0%	2.3%
33.75 - 56.25	1.4%	1.2%	0.6%	0.8%	0.0%	0.0%	0.0%	4.0%
56.25 - 78.75	1.1%	0.9%	0.5%	0.3%	0.1%	0.0%	0.0%	2.9%
78.75 - 101.25	1.1%	3.2%	4.0%	1.3%	0.1%	0.0%	0.0%	9.7%
101.25 - 123.75	1.7%	3.5%	6.4%	3.8%	0.7%	0.0%	0.0%	16.2%
Sub-Total	7.0%	10.5%	11.9%	6.7%	1.2%	0.0%	0.0%	37.4%
123.75 - 146.25	1.3%	2.1%	1.4%	1.1%	0.1%	0.0%	0.0%	6.1%
146.25 - 168.75	1.5%	1.8%	0.6%	0.2%	0.0%	0.0%	0.0%	4.1%
168.75 - 191.25	2.0%	0.8%	0.2%	0.2%	0.0%	0.0%	0.0%	3.1%
191.25 - 213.75	1.0%	0.5%	0.2%	0.2%	0.2%	0.0%	0.0%	2.1%
213.75 - 236.25	1.7%	0.1%	0.2%	0.1%	0.0%	0.0%	0.0%	2.0%
Sub-Total	7.5%	5.3%	2.6%	1.8%	0.3%	0.0%	0.0%	17.4%
236.25 - 258.75	1.1%	0.6%	0.5%	0.2%	0.1%	0.0%	0.0%	2.4%
258.75 - 281.25	0.9%	1.9%	3.3%	2.6%	1.4%	0.6%	0.3%	10.9%
281.25 - 303.75	0.9%	3.5%	6.9%	5.6%	3.9%	0.9%	0.2%	21.8%
303.75 - 326.25	0.6%	2.6%	2.2%	1.7%	0.2%	0.2%	0.0%	7.6%
326.25 - 348.75	0.6%	0.9%	0.5%	0.3%	0.2%	0.0%	0.0%	2.4%
Sub-Total	4.1%	9.5%	13.4%	10.4%	5.8%	1.7%	0.5%	45.1%
Total	18.7%	25.3%	27.8%	18.8%	7.2%	1.7%	0.5%	100.0%

Table A.13: Classification of Winds in Terms of Directions and Speeds (Point L, 42.40°N – 34.90°E)

Wind Directions (in °)	Wind Classes (m/s)							
	0.0 – 3.0	3.0 – 5.0	5.0 – 7.5	7.5 – 10.0	10.0 – 12.5	12.5 – 15.0	>= 15.0	Total
348.75 - 11.25	0.8%	0.6%	0.3%	0.5%	0.1%	0.0%	0.0%	2.2%
11.25 - 33.75	1.3%	1.2%	0.3%	0.0%	0.1%	0.0%	0.0%	2.8%
33.75 - 56.25	1.0%	1.0%	0.5%	0.5%	0.0%	0.0%	0.0%	3.1%
56.25 - 78.75	1.2%	1.2%	0.8%	0.7%	0.1%	0.0%	0.0%	4.0%
78.75 - 101.25	1.4%	3.7%	5.0%	2.3%	0.4%	0.0%	0.0%	12.8%
101.25 - 123.75	1.3%	2.9%	4.7%	3.2%	0.5%	0.0%	0.0%	12.5%
Sub-Total	7.0%	10.6%	11.6%	7.2%	1.2%	0.0%	0.0%	37.4%
123.75 - 146.25	1.4%	1.9%	1.3%	0.5%	0.0%	0.0%	0.0%	5.1%
146.25 - 168.75	2.1%	1.7%	0.4%	0.1%	0.0%	0.0%	0.0%	4.3%
168.75 - 191.25	2.0%	0.9%	0.2%	0.1%	0.0%	0.0%	0.0%	3.2%
191.25 - 213.75	1.4%	0.6%	0.2%	0.3%	0.2%	0.0%	0.0%	2.6%
213.75 - 236.25	1.2%	0.4%	0.1%	0.0%	0.0%	0.0%	0.0%	1.6%
Sub-Total	8.1%	5.5%	2.2%	1.0%	0.2%	0.0%	0.0%	16.8%
236.25 - 258.75	1.6%	0.9%	0.6%	0.2%	0.1%	0.0%	0.0%	3.3%
258.75 - 281.25	1.4%	3.0%	4.4%	3.0%	1.8%	0.6%	0.2%	14.4%
281.25 - 303.75	0.8%	3.0%	5.3%	6.6%	2.8%	0.9%	0.0%	19.4%
303.75 - 326.25	0.8%	2.2%	1.8%	1.1%	0.2%	0.1%	0.0%	6.3%
326.25 - 348.75	0.7%	0.8%	0.4%	0.2%	0.1%	0.0%	0.0%	2.2%
Sub-Total	5.3%	9.9%	12.5%	11.1%	5.0%	1.6%	0.2%	45.6%
Total	20.2%	26.1%	26.3%	19.3%	6.1%	1.7%	0.3%	100.0%

Table A.14: Classification of Winds in Terms of Directions and Speeds (Point M, 42.10°N – 35.00°E)

Wind Directions (in °)	Wind Classes (m/s)							
	0.0 – 3.0	3.0 – 5.0	5.0 – 7.5	7.5 – 10.0	10.0 – 12.5	12.5 – 15.0	>= 15.0	Total
348.75 - 11.25	0.9%	1.1%	0.0%	0.3%	0.2%	0.0%	0.0%	2.5%
11.25 - 33.75	0.8%	1.3%	0.3%	0.2%	0.2%	0.0%	0.0%	2.7%
33.75 - 56.25	1.1%	0.8%	0.3%	0.8%	0.0%	0.0%	0.0%	3.0%
56.25 - 78.75	0.8%	0.9%	1.1%	0.8%	0.2%	0.0%	0.0%	3.8%
78.75 - 101.25	1.1%	3.8%	5.2%	2.7%	0.5%	0.0%	0.0%	13.2%
101.25 - 123.75	1.4%	2.5%	4.4%	3.3%	0.6%	0.0%	0.0%	12.3%
Sub-Total	6.1%	10.4%	11.3%	8.1%	1.7%	0.0%	0.0%	37.5%
123.75 - 146.25	1.4%	1.4%	1.9%	0.3%	0.0%	0.0%	0.0%	5.0%
146.25 - 168.75	1.7%	2.0%	0.6%	0.0%	0.0%	0.0%	0.0%	4.4%
168.75 - 191.25	1.7%	0.8%	0.0%	0.2%	0.0%	0.0%	0.0%	2.7%
191.25 - 213.75	1.9%	0.6%	0.2%	0.3%	0.2%	0.0%	0.0%	3.1%
213.75 - 236.25	0.8%	0.6%	0.0%	0.0%	0.0%	0.0%	0.0%	1.4%
Sub-Total	7.5%	5.4%	2.7%	0.8%	0.2%	0.0%	0.0%	16.6%
236.25 - 258.75	2.4%	0.5%	0.6%	0.2%	0.3%	0.0%	0.0%	3.9%
258.75 - 281.25	1.3%	3.7%	5.2%	3.1%	2.2%	0.8%	0.3%	16.5%
281.25 - 303.75	0.8%	2.8%	5.2%	6.4%	2.2%	0.6%	0.0%	18.1%
303.75 - 326.25	0.5%	2.0%	1.4%	0.9%	0.3%	0.2%	0.0%	5.3%
326.25 - 348.75	0.6%	0.6%	0.5%	0.3%	0.0%	0.0%	0.0%	2.0%
Sub-Total	5.6%	9.6%	12.9%	10.9%	5.0%	1.6%	0.3%	45.8%
Total	19.2%	25.4%	26.9%	19.8%	6.8%	1.6%	0.3%	100.0%

APPENDIX B

L60, S60 AND S10 WIND SPEEDS FOR CONTINUOUS DATA SETS

L60, S60 and S10 wind speeds for continuous data sets are given in this section.

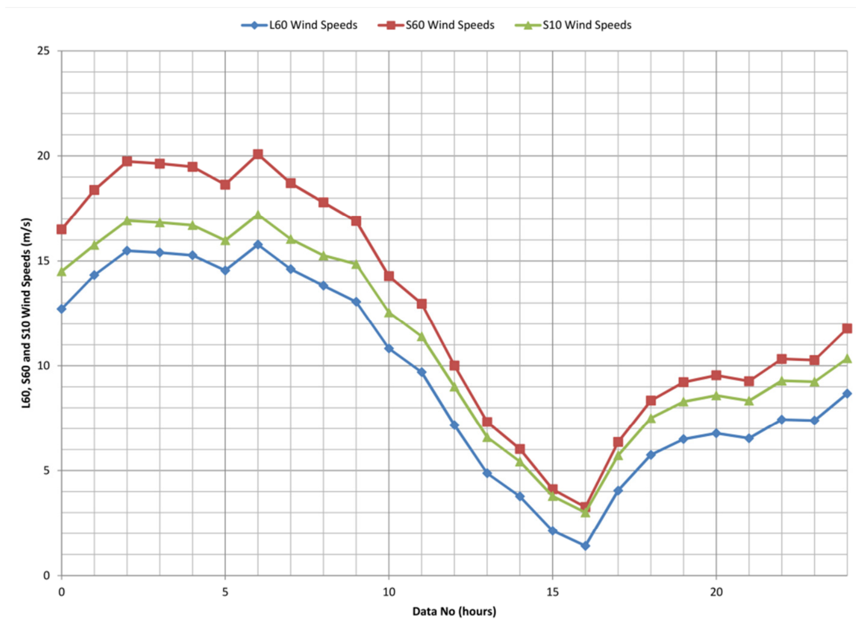

Figure B.1: L60, S60 and S10 Wind Speeds for Continuous Data Set 1

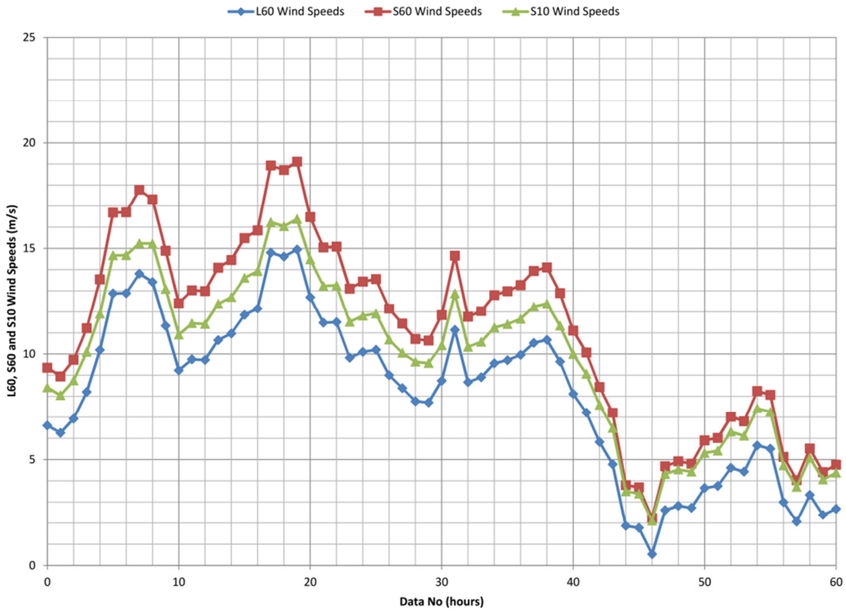

Figure B.2: L60, S60 and S10 Wind Speeds for Continuous Data Set 2

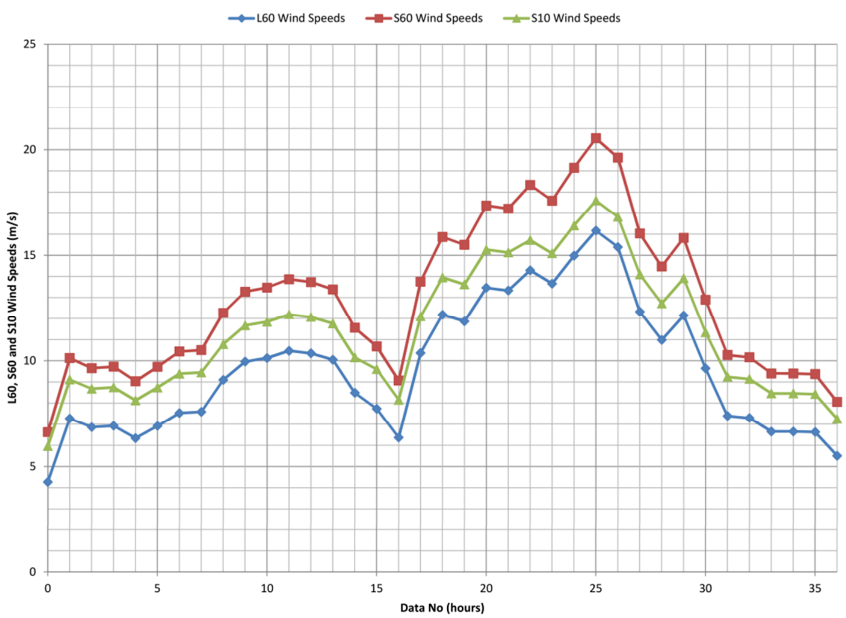

Figure B.3: L60, S60 and S10 Wind Speeds for Continuous Data Set 3

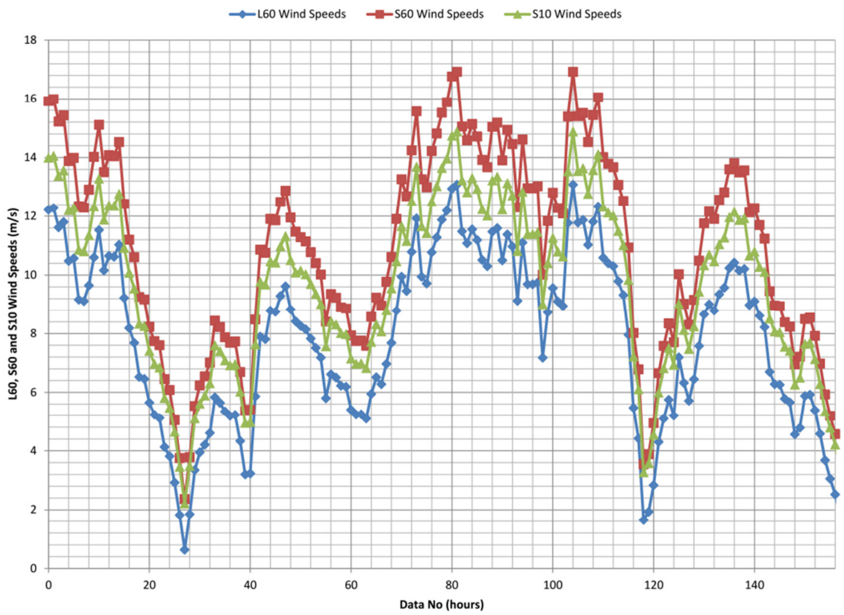

Figure B.4: L60, S60 and S10 Wind Speeds for Continuous Data Set 4

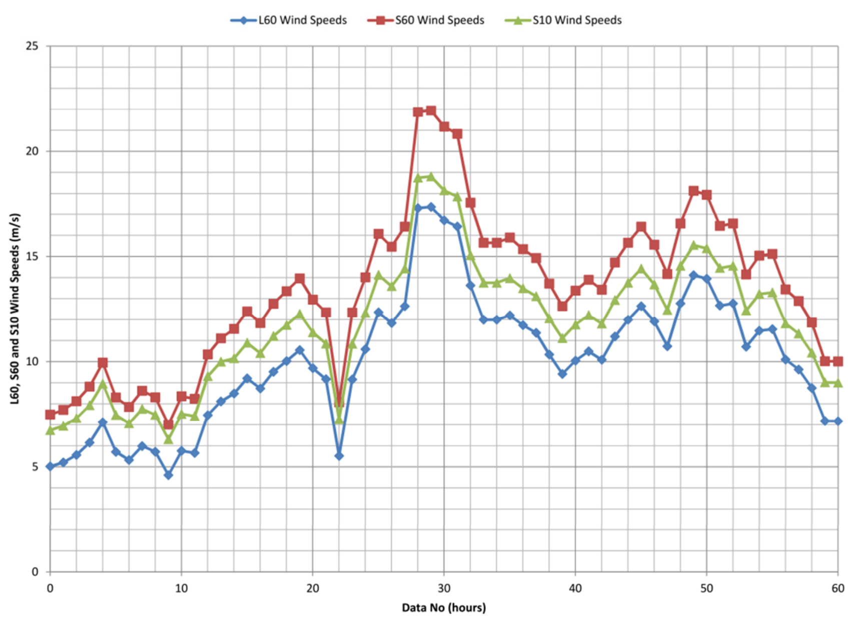

Figure B.5: L60, S60 and S10 Wind Speeds for Continuous Data Set 5

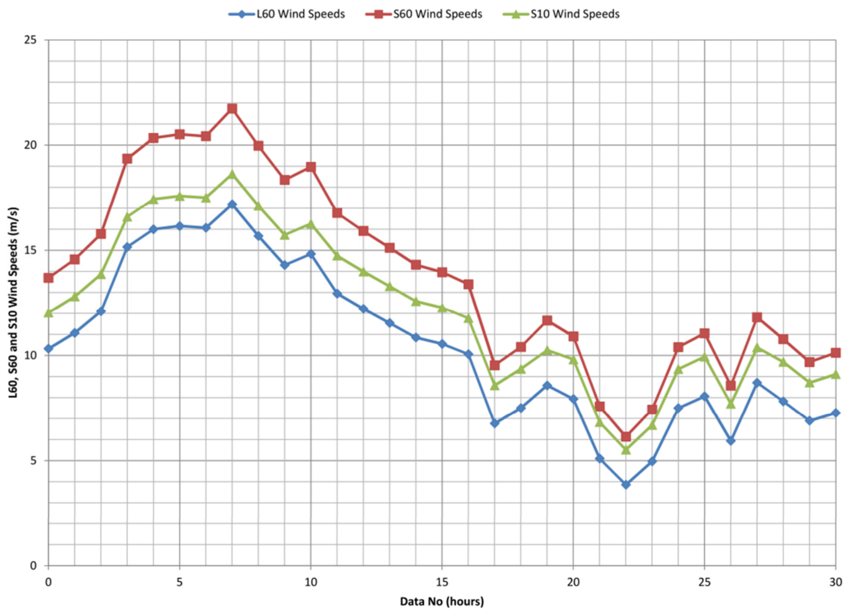

Figure B.6: L60, S60 and S10 Wind Speeds for Continuous Data Set 6

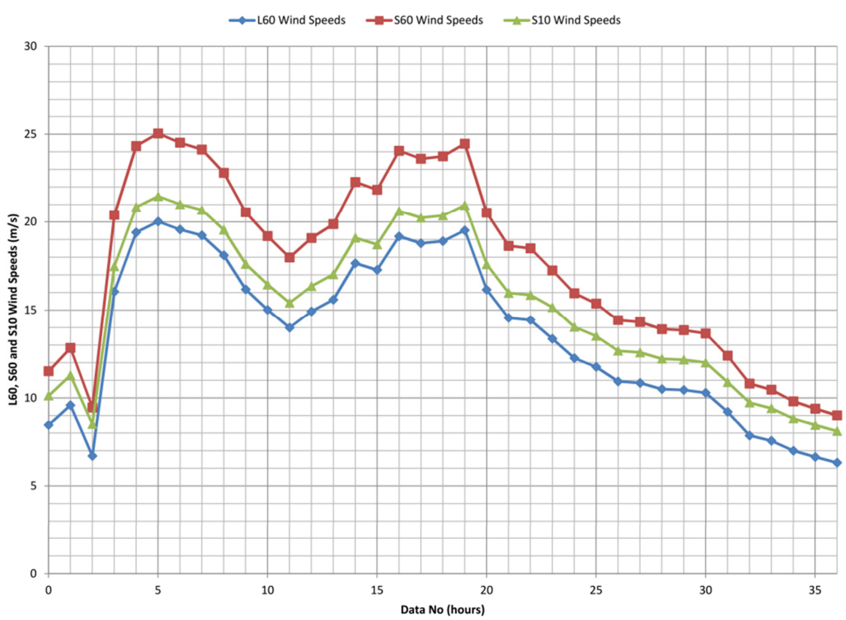

Figure B.7: L60, S60 and S10 Wind Speeds for Continuous Data Set 7

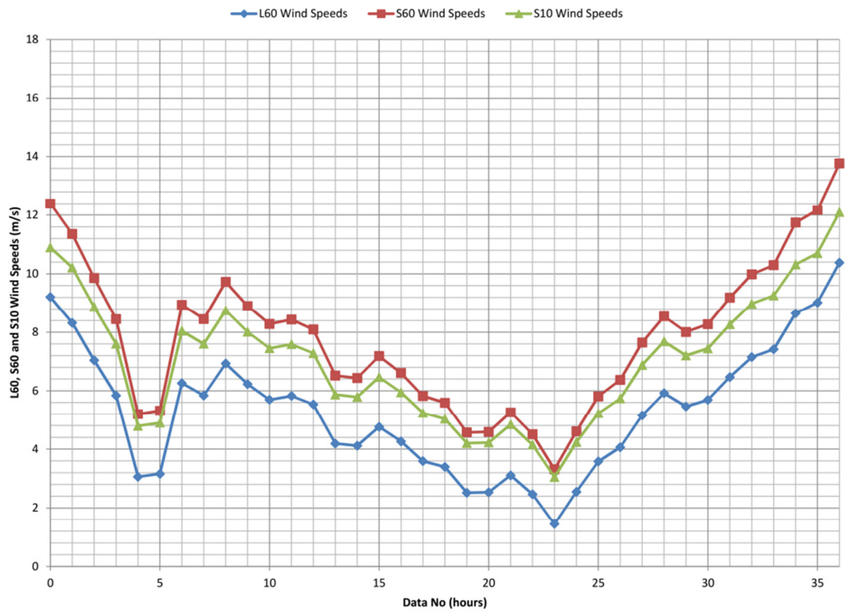

Figure B.8: L60, S60 and S10 Wind Speeds for Continuous Data Set 8

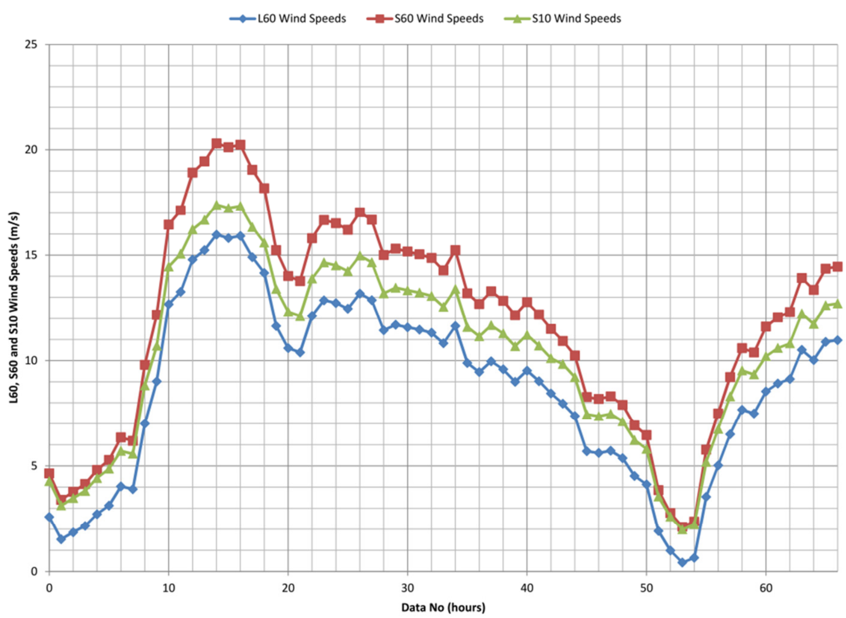

Figure B.9: L60, S60 and S10 Wind Speeds for Continuous Data Set 9

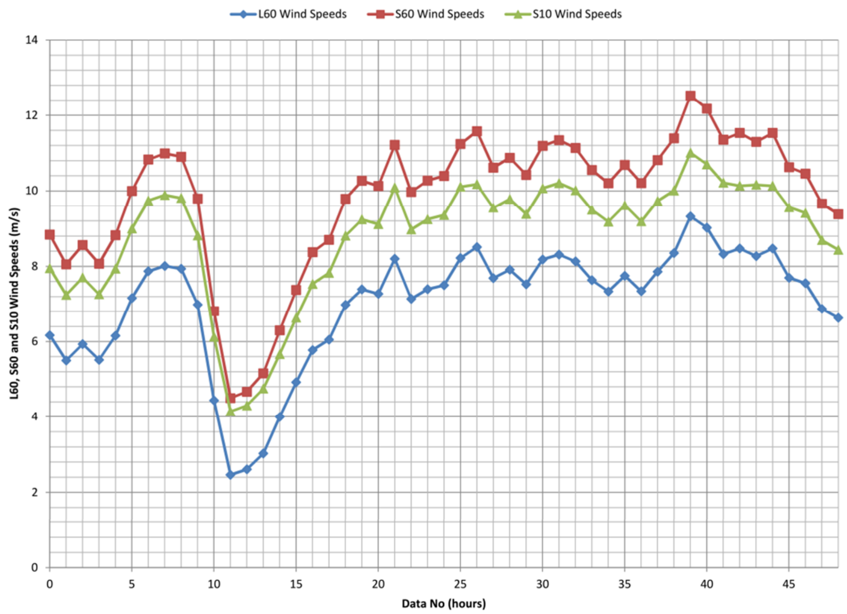

Figure B.10: L60, S60 and S10 Wind Speeds for Continuous Data Set 10

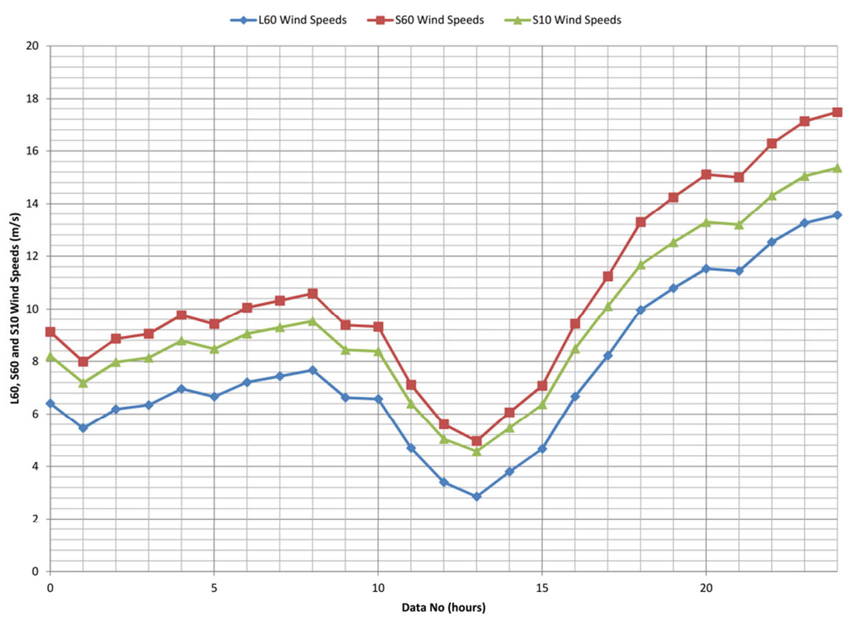

Figure B.11: L60, S60 and S10 Wind Speeds for Continuous Data Set 11

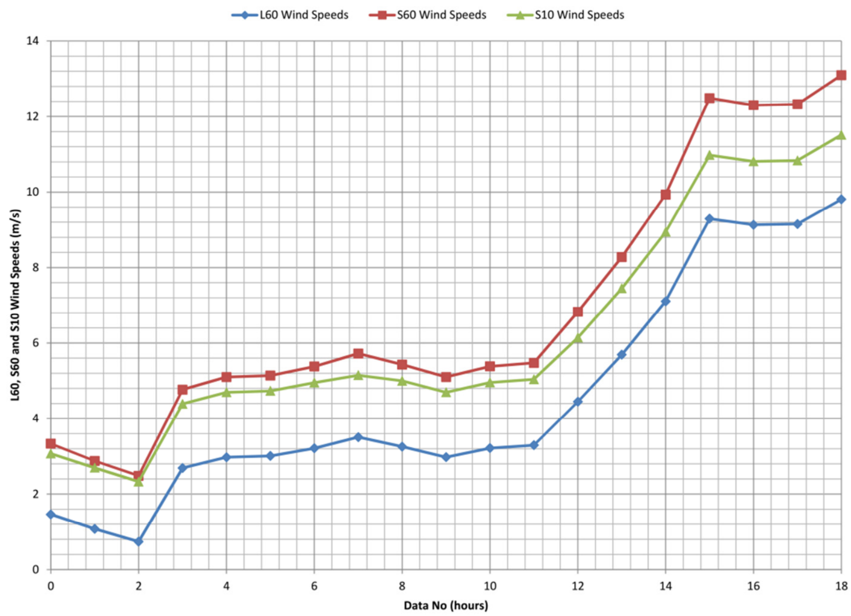

Figure B.12: L60, S60 and S10 Wind Speeds for Continuous Data Set 12

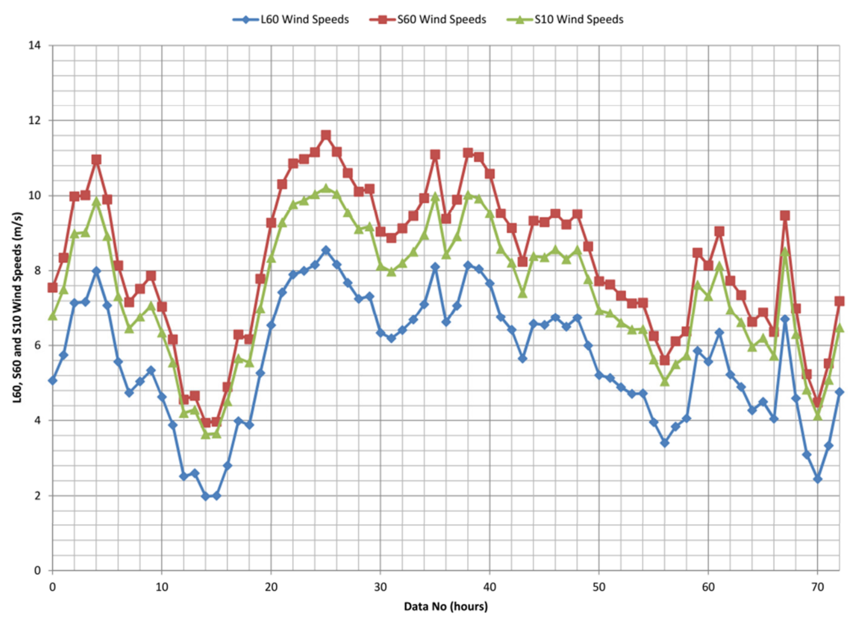

Figure B.13: L60, S60 and S10 Wind Speeds for Continuous Data Set 13

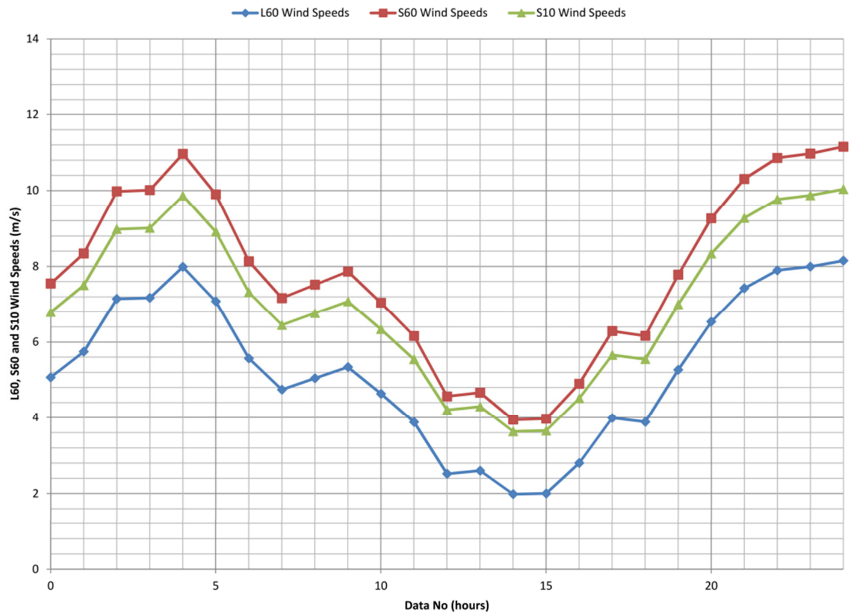

Figure B.14: L60, S60 and S10 Wind Speeds for Continuous Data Set 14

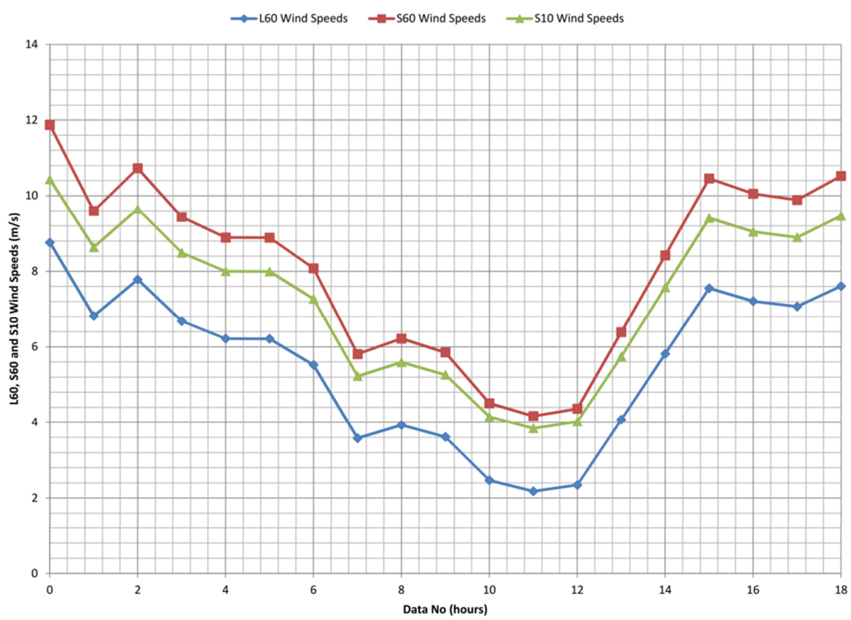

Figure B.15: L60, S60 and S10 Wind Speeds for Continuous Data Set 15

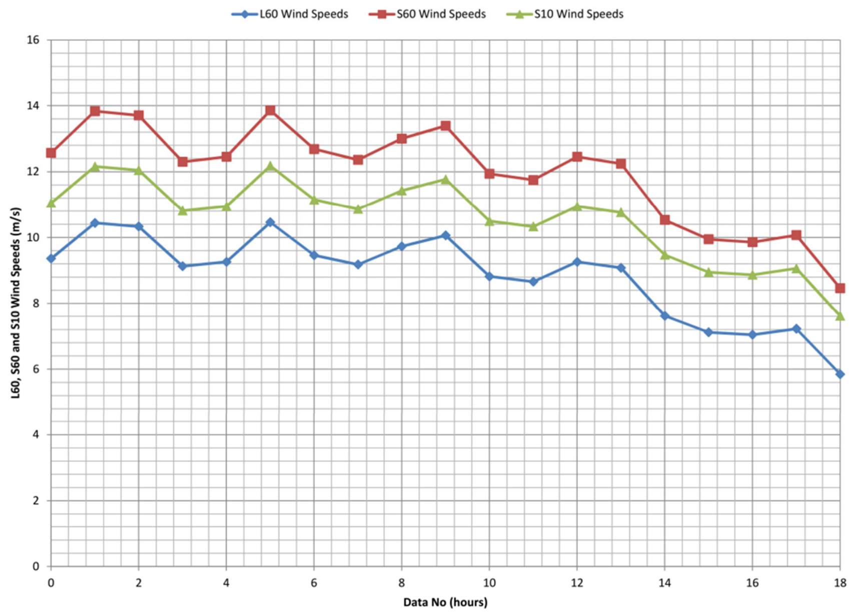

Figure B.16: L60, S60 and S10 Wind Speeds for Continuous Data Set 16

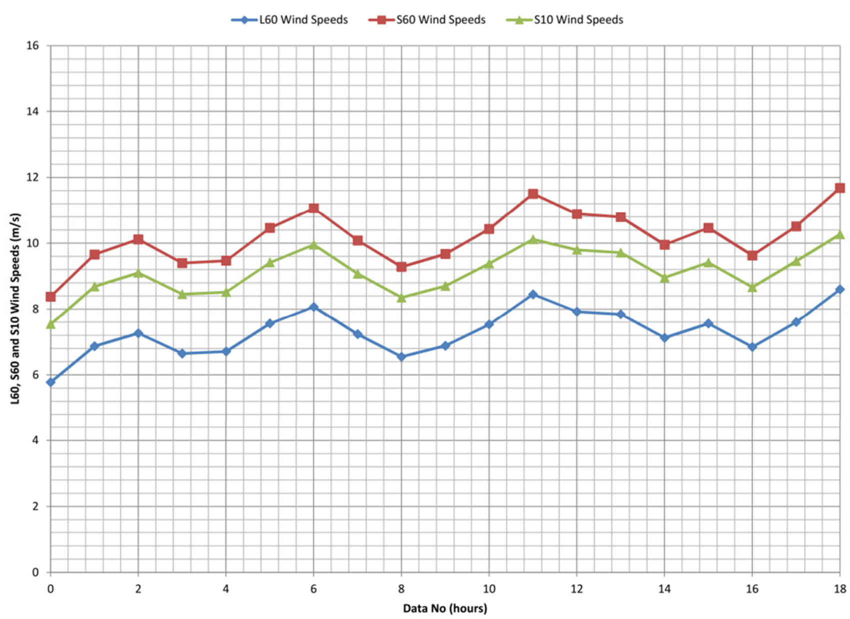

Figure B.17: L60, S60 and S10 Wind Speeds for Continuous Data Set 17

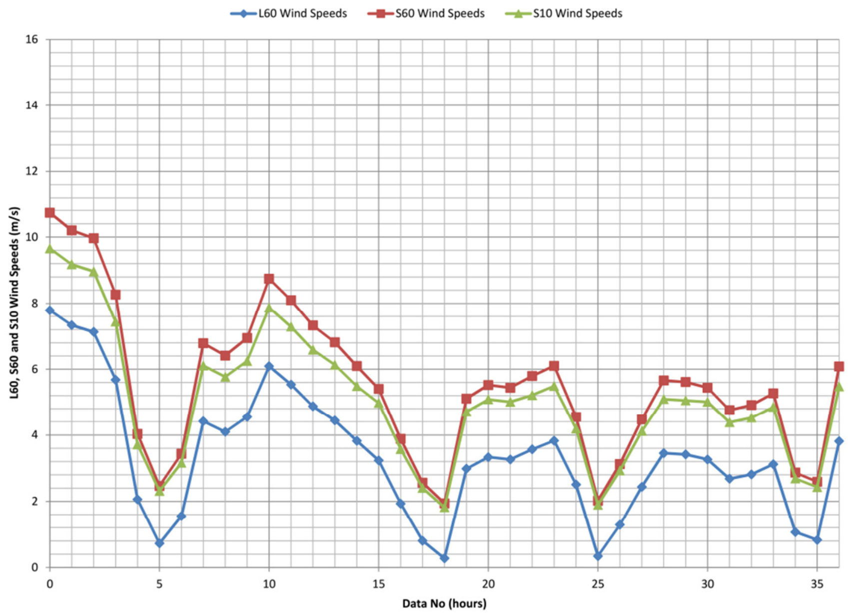

Figure B.18: L60, S60 and S10 Wind Speeds for Continuous Data Set 18

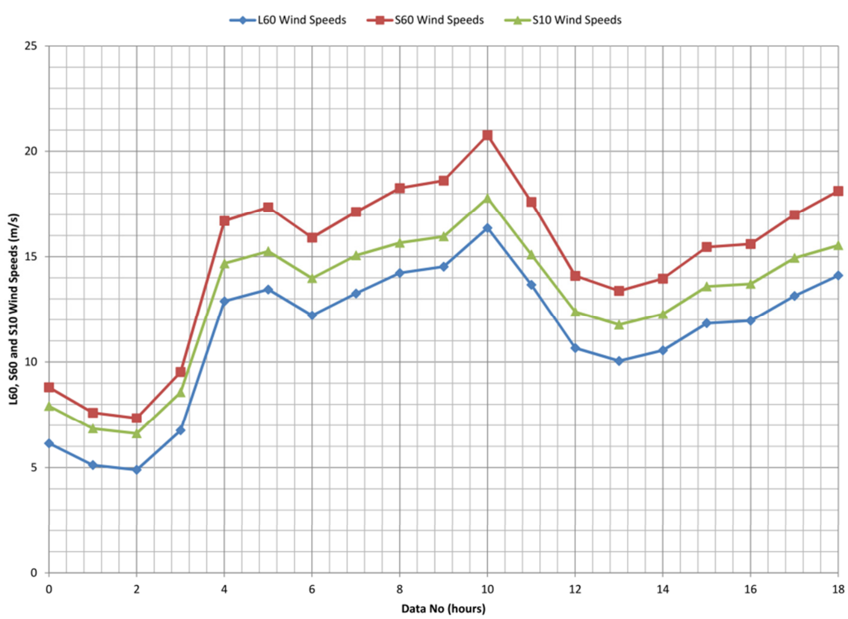

Figure B.19: L60, S60 and S10 Wind Speeds for Continuous Data Set 19

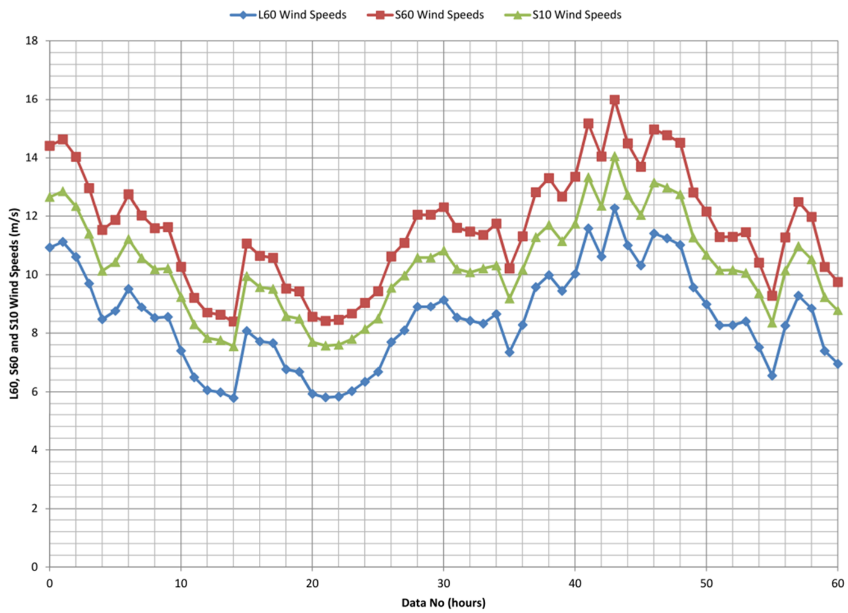

Figure B.20: L60, S60 and S10 Wind Speeds for Continuous Data Set 20

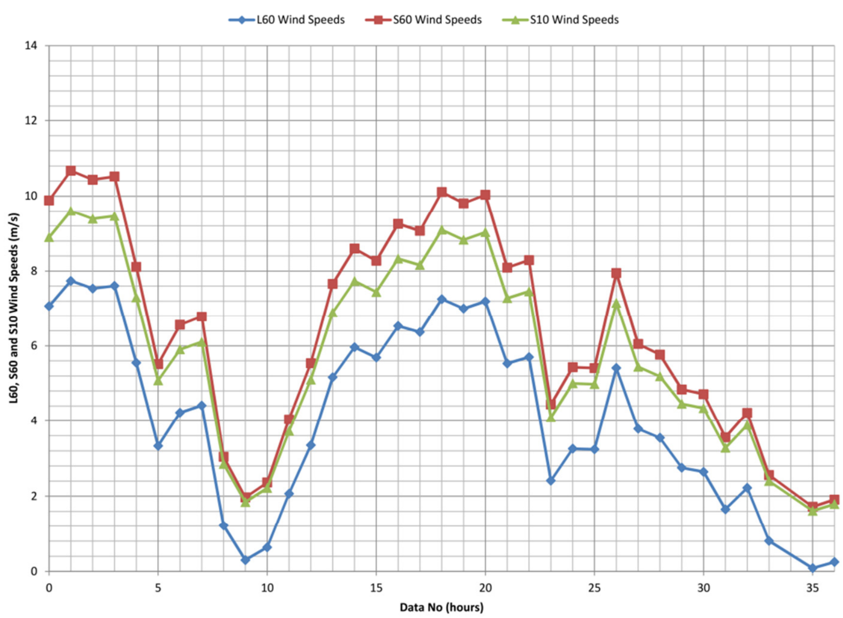

Figure B.21: L60, S60 and S10 Wind Speeds for Continuous Data Set 21

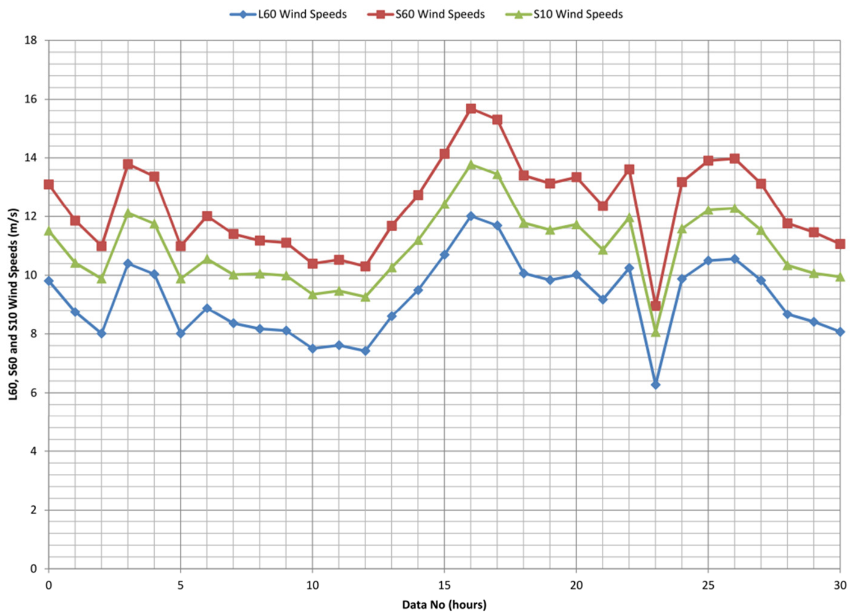

Figure B.22: L60, S60 and S10 Wind Speeds for Continuous Data Set 22

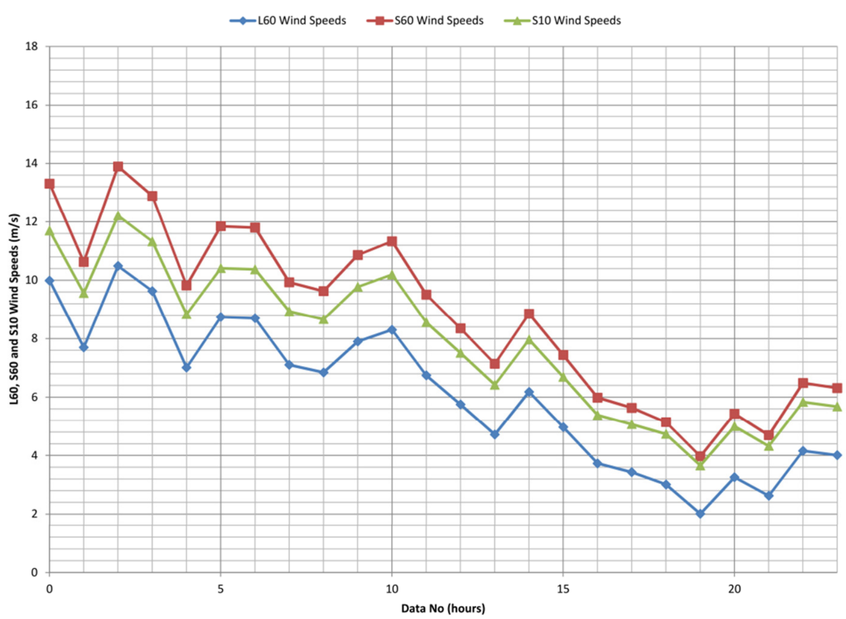

Figure B.23: L60, S60 and S10 Wind Speeds for Continuous Data Set 23

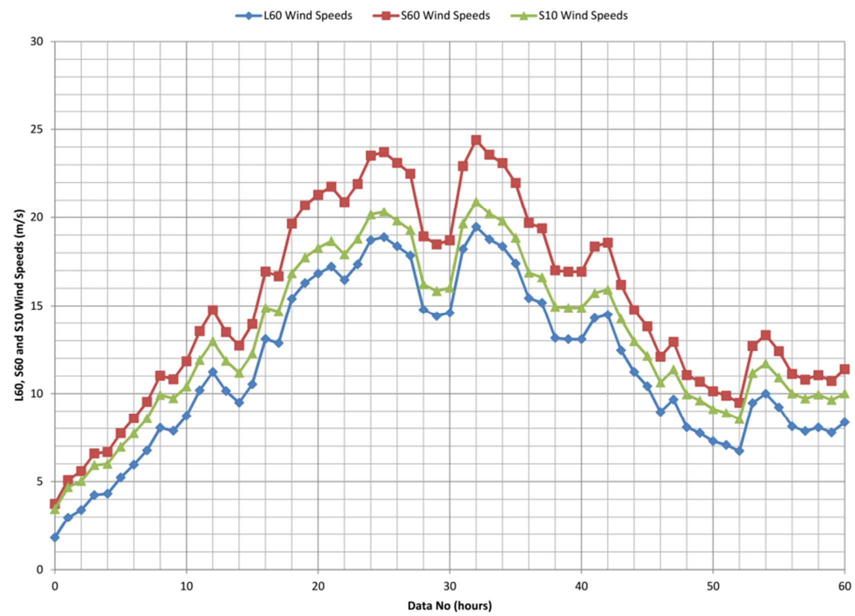

Figure B.24: L60, S60 and S10 Wind Speeds for Continuous Data Set 24

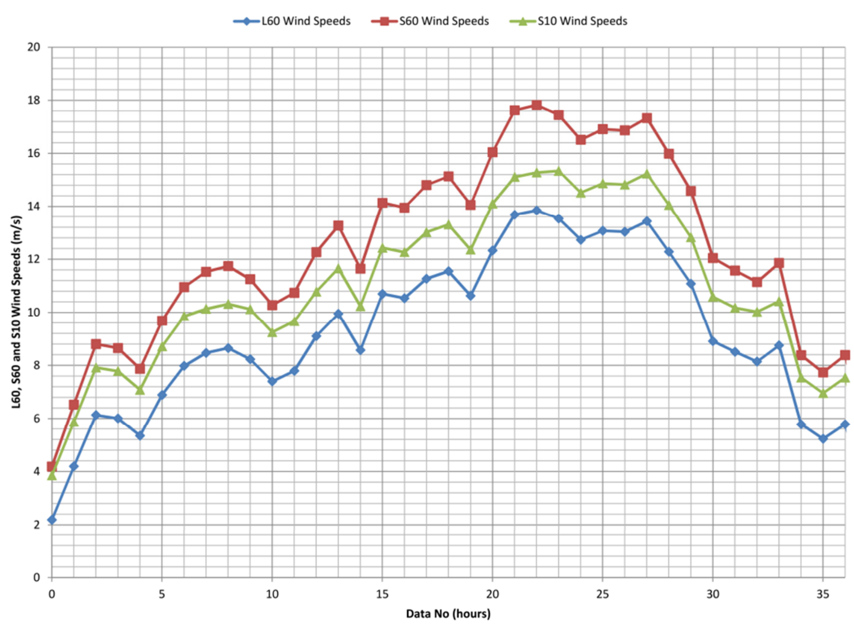

Figure B.25: L60, S60 and S10 Wind Speeds for Continuous Data Set 25

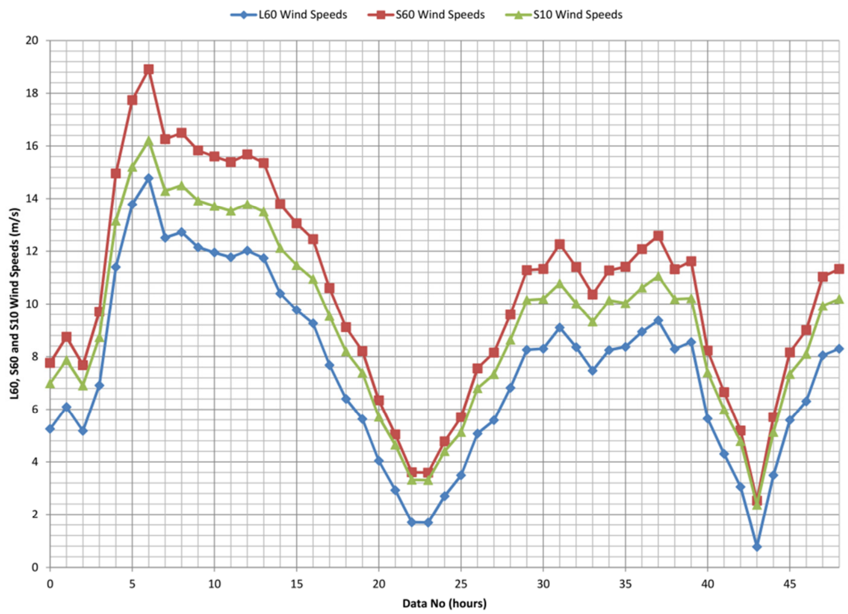

Figure B.26: L60, S60 and S10 Wind Speeds for Continuous Data Set 26

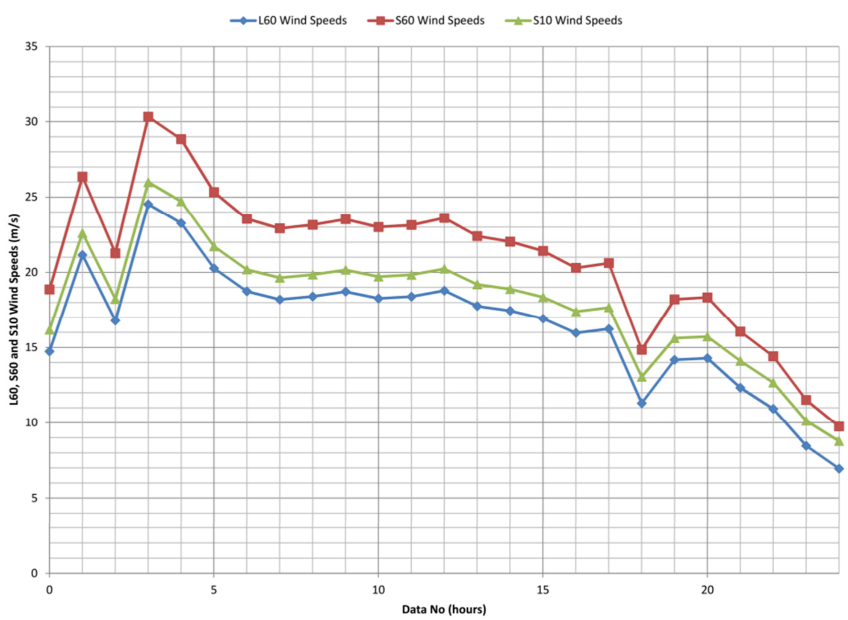

Figure B.27: L60, S60 and S10 Wind Speeds for Continuous Data Set 27

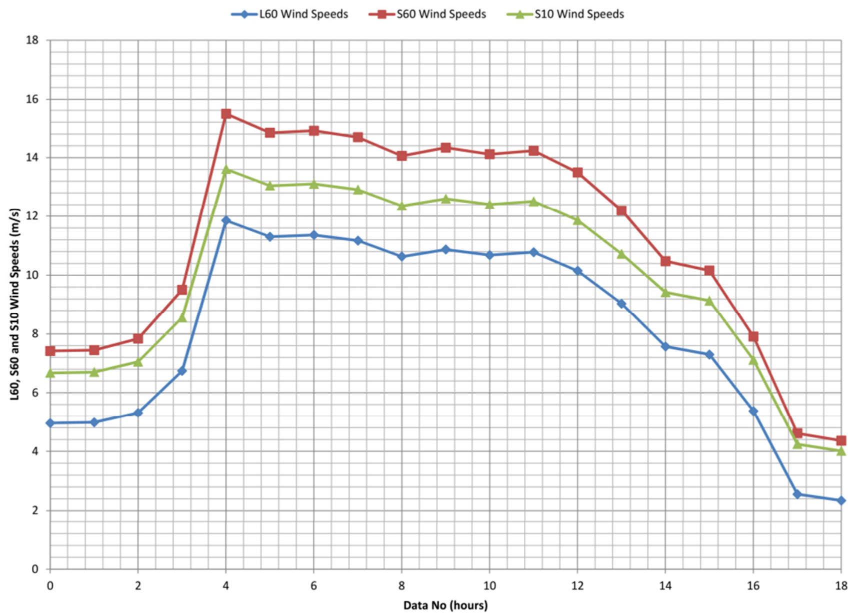

Figure B.28: L60, S60 and S10 Wind Speeds for Continuous Data Set 28

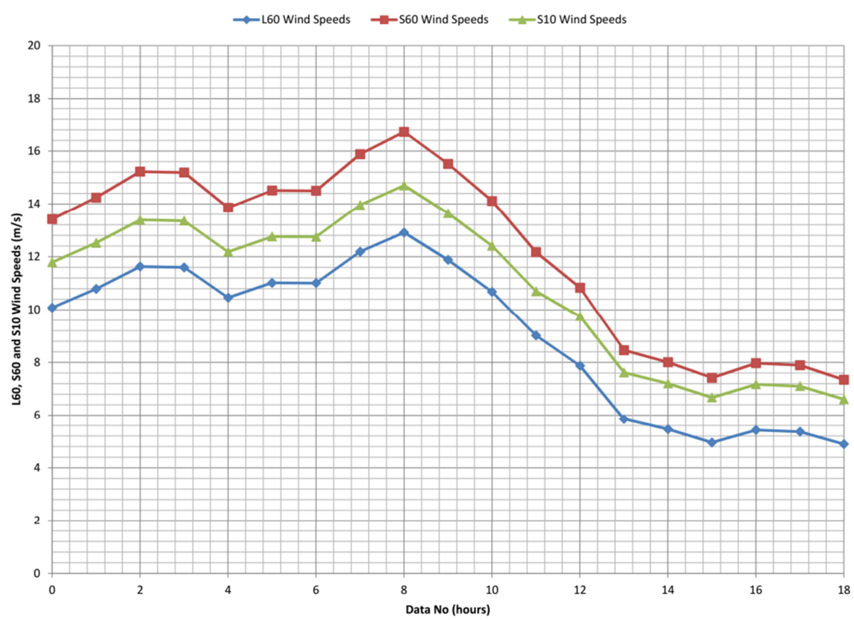

Figure B.29: L60, S60 and S10 Wind Speeds for Continuous Data Set 29

APPENDIX C

S10 AND E10 WIND SPEEDS FOR CONTINUOUS DATA SETS

S10 and E10 wind speeds for continuous data sets are given in this section.

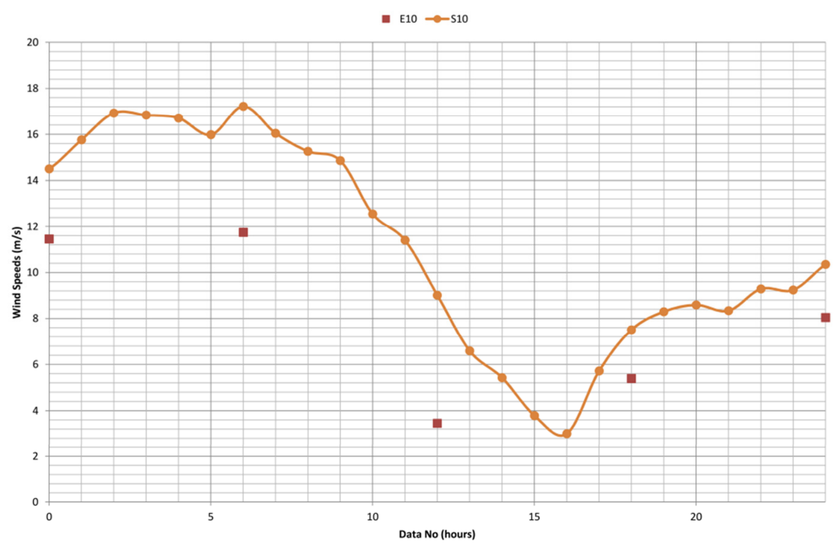

Figure C.1: E10 and S10 Wind Speeds for Continuous Data Set 1

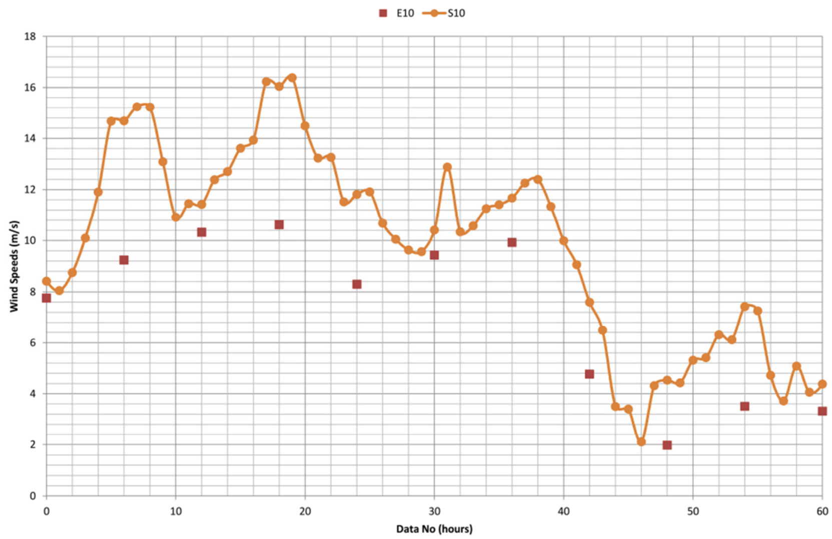

Figure C.2: E10 and S10 Wind Speeds for Continuous Data Set 2

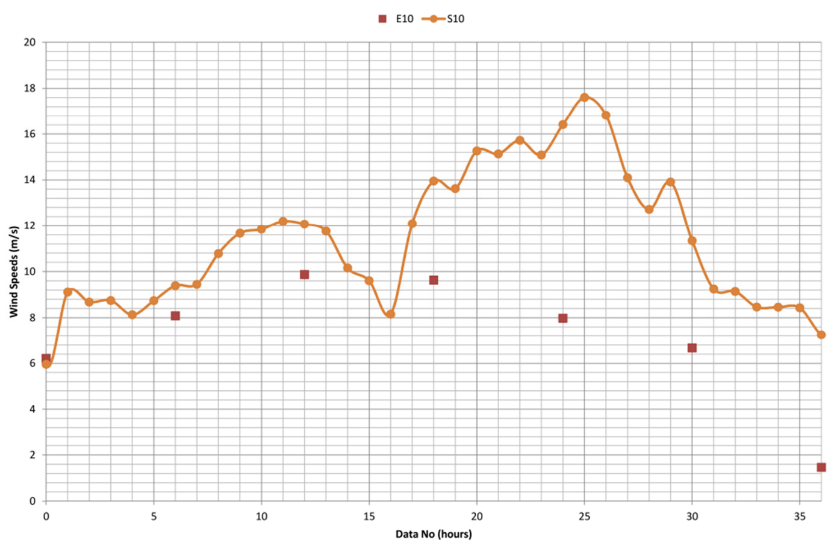

Figure C.3: E10 and S10 Wind Speeds for Continuous Data Set 3

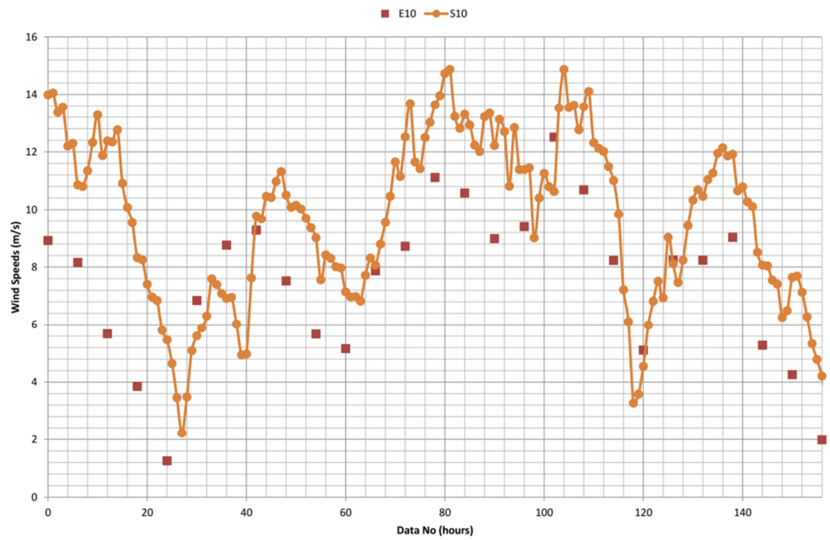

Figure C.4: E10 and S10 Wind Speeds for Continuous Data Set 4

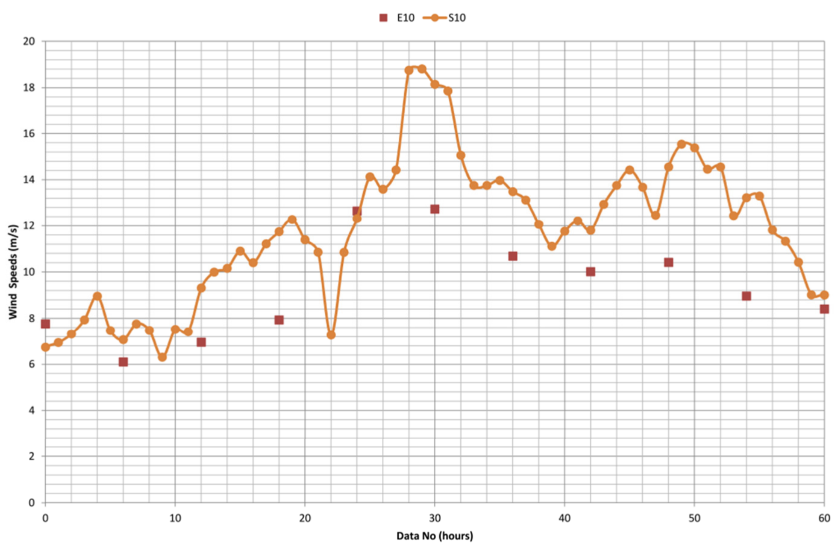

Figure C.5: E10 and S10 Wind Speeds for Continuous Data Set 5

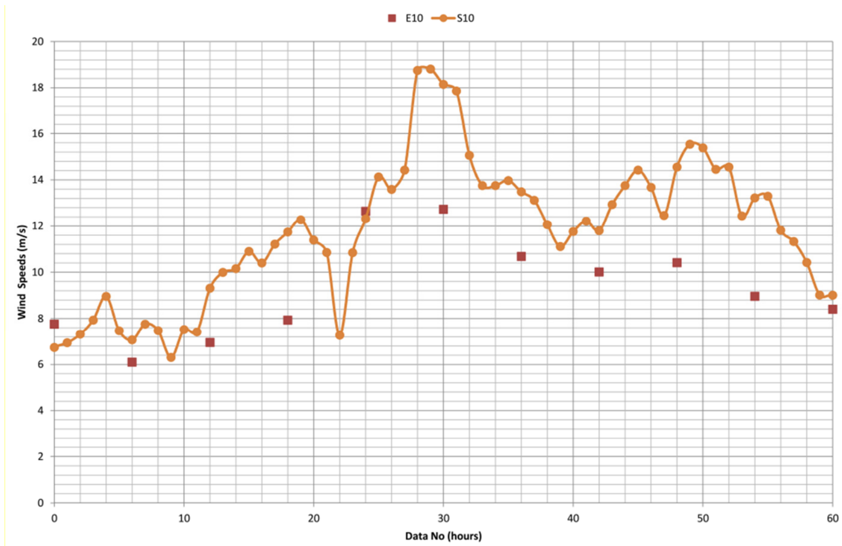

Figure C.6: E10 and S10 Wind Speeds for Continuous Data Set 6

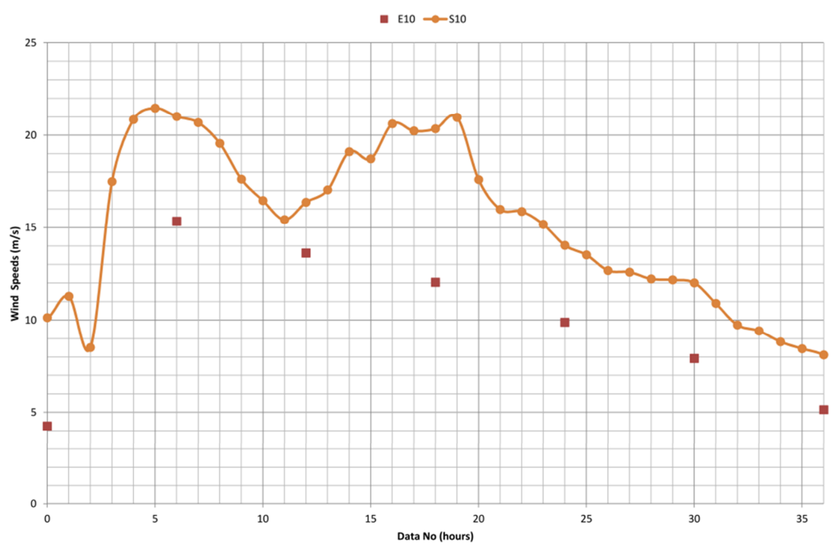

Figure C.7: E10 and S10 Wind Speeds for Continuous Data Set 7

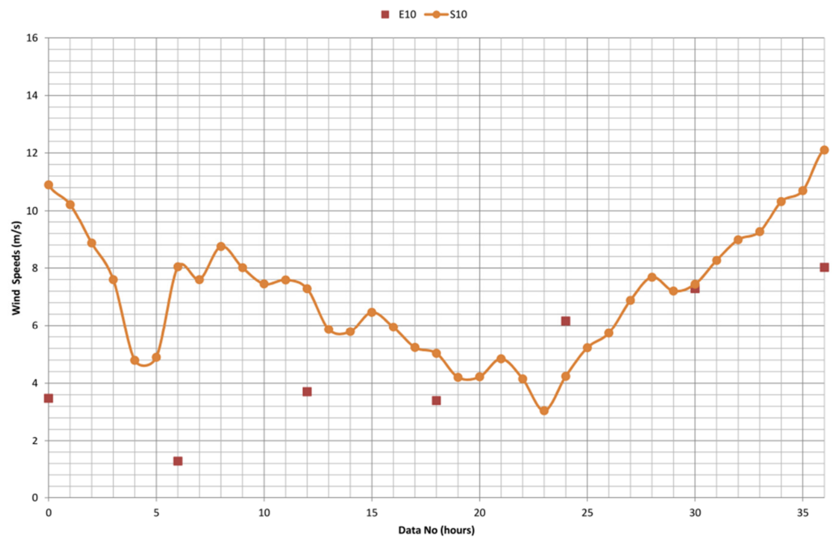

Figure C.8: E10 and S10 Wind Speeds for Continuous Data Set 8

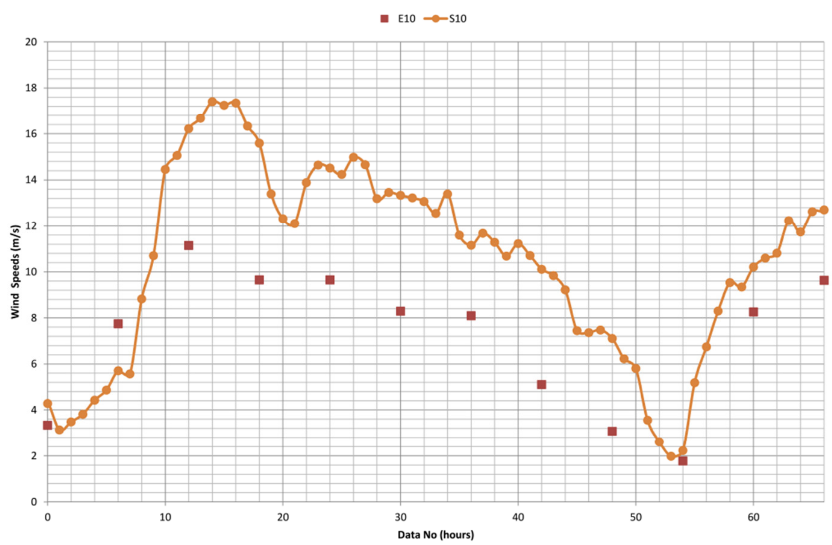

Figure C.9: E10 and S10 Wind Speeds for Continuous Data Set 9

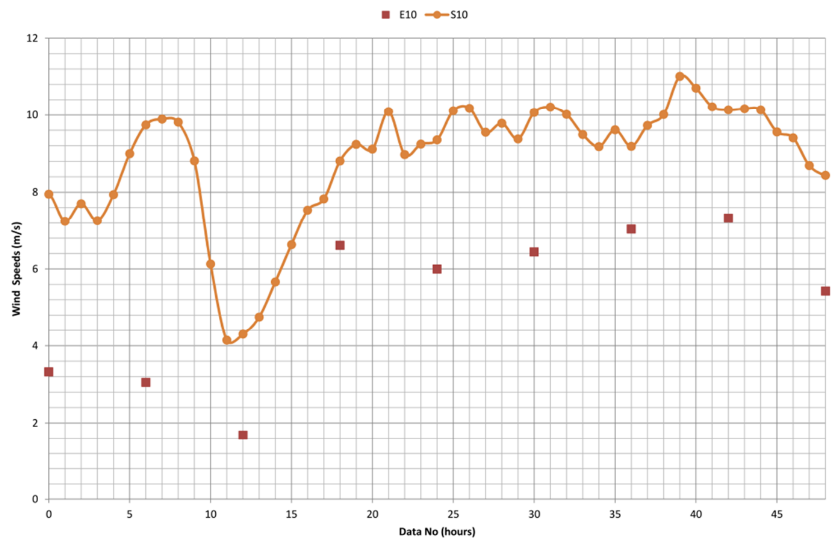

Figure C.10: E10 and S10 Wind Speeds for Continuous Data Set 10

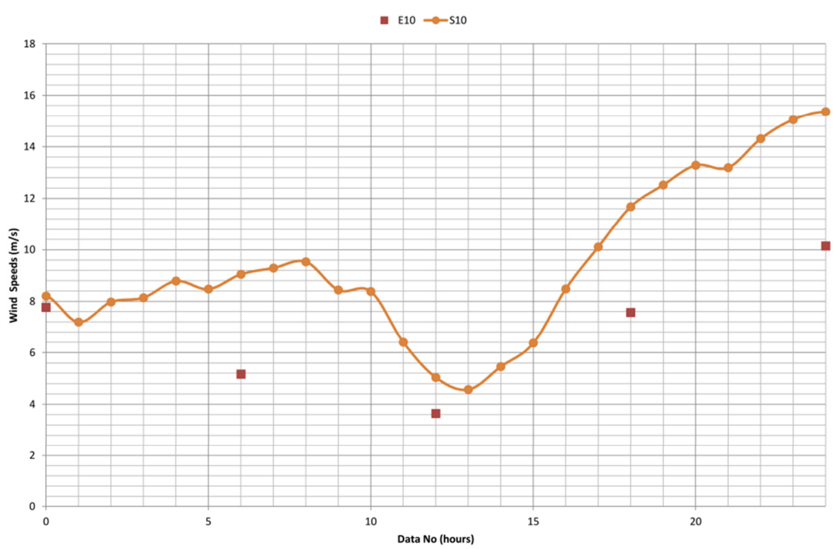

Figure C.11: E10 and S10 Wind Speeds for Continuous Data Set 11

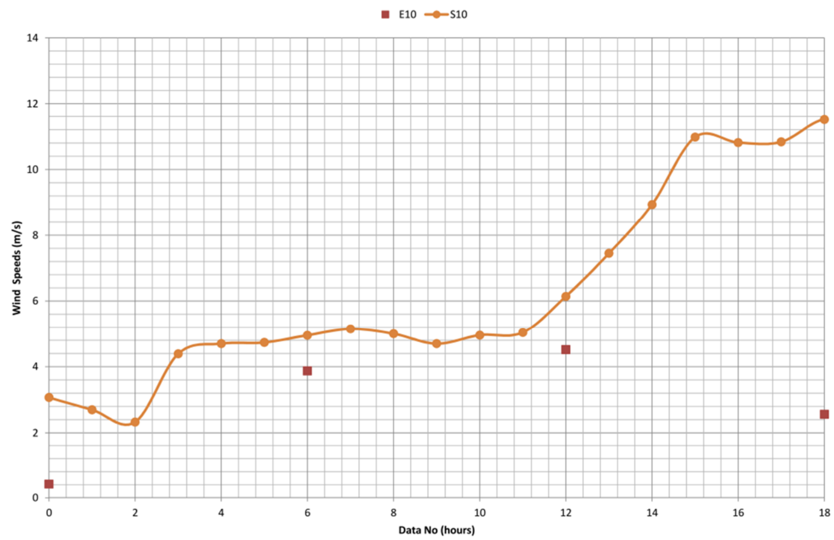

Figure C.12: E10 and S10 Wind Speeds for Continuous Data Set 12

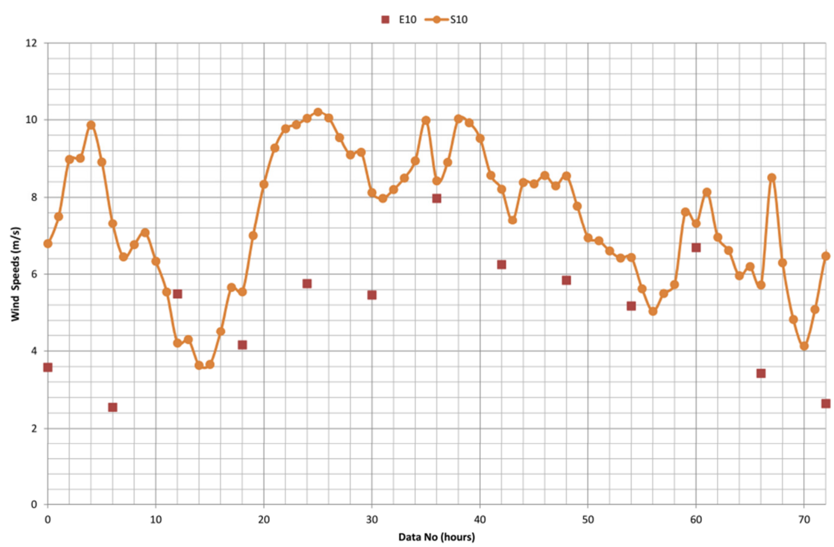

Figure C.13: E10 and S10 Wind Speeds for Continuous Data Set 13

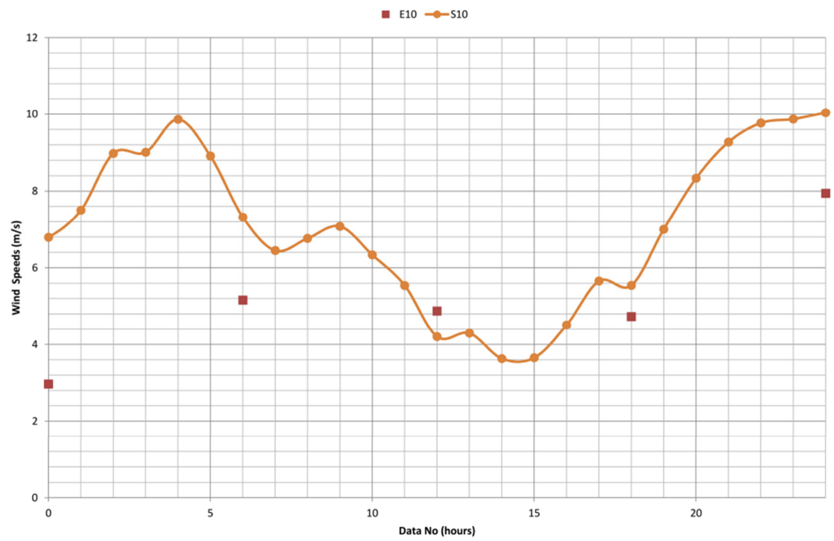

Figure C.14: E10 and S10 Wind Speeds for Continuous Data Set 14

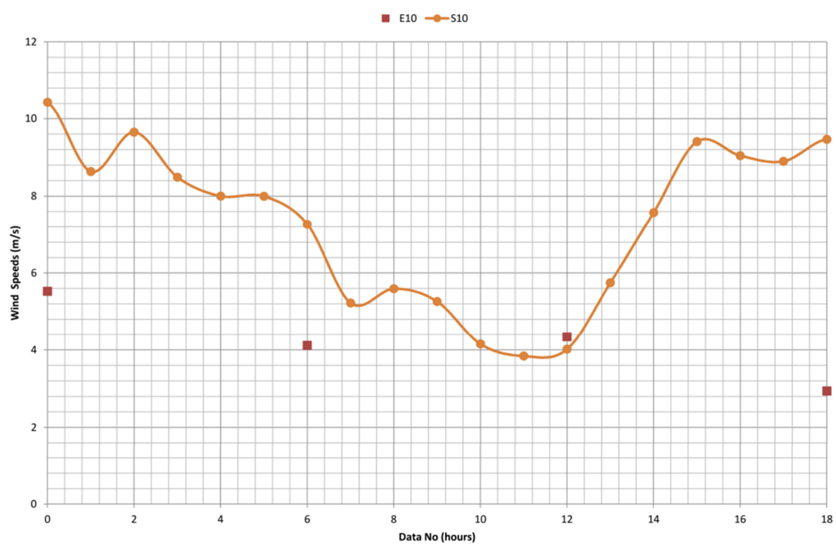

Figure C.15: E10 and S10 Wind Speeds for Continuous Data Set 15

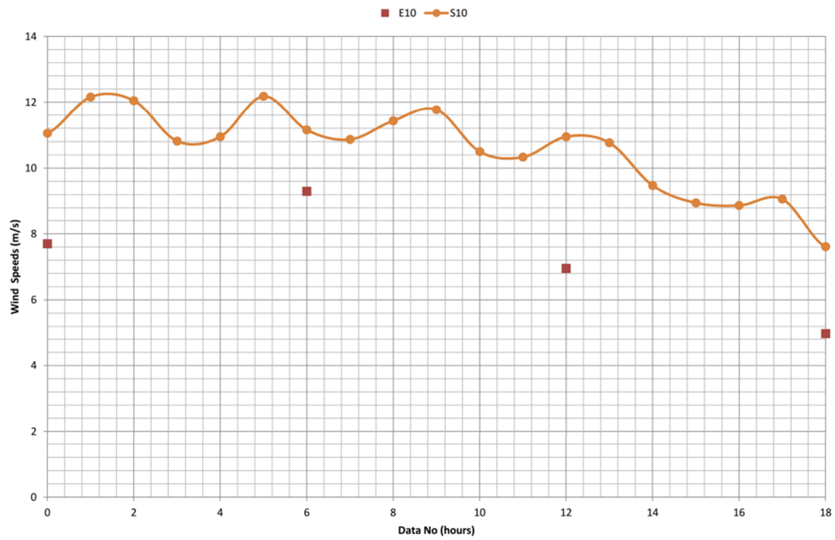

Figure C.16: E10 and S10 Wind Speeds for Continuous Data Set 16

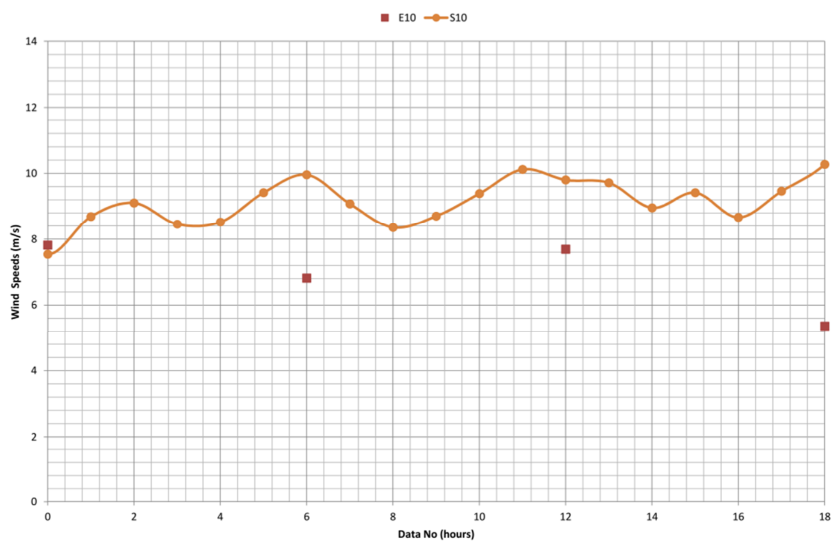

Figure C.17: E10 and S10 Wind Speeds for Continuous Data Set 17

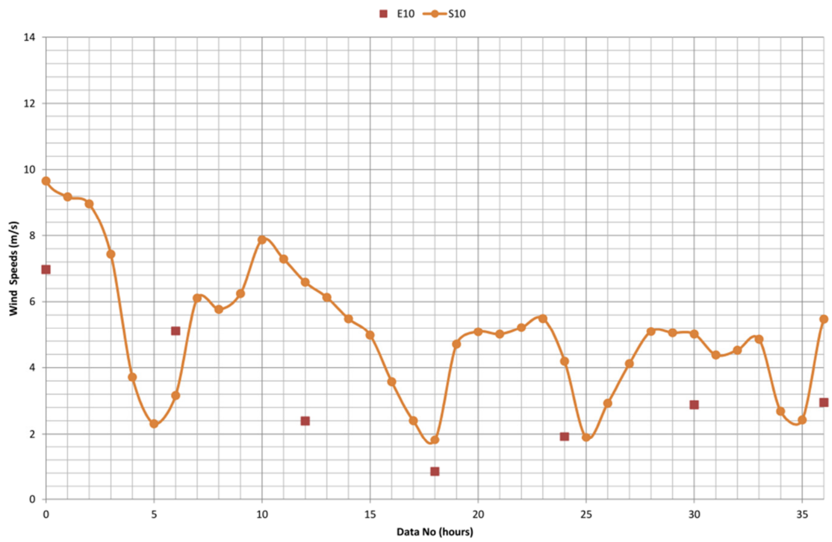

Figure C.18: E10 and S10 Wind Speeds for Continuous Data Set 18

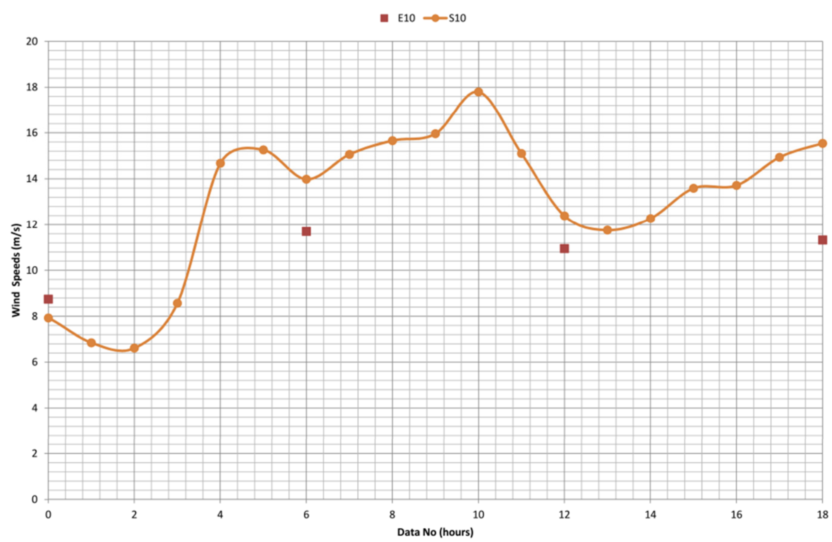

Figure C.19: E10 and S10 Wind Speeds for Continuous Data Set 19

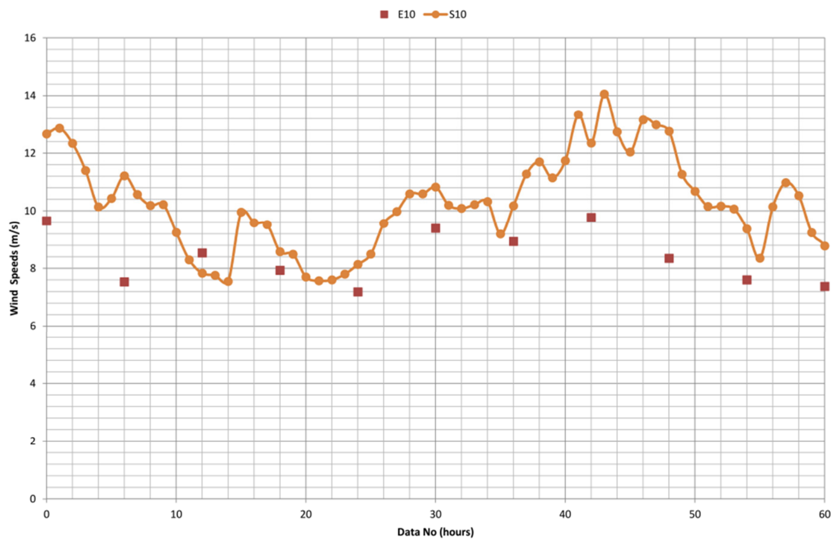

Figure C.20: E10 and S10 Wind Speeds for Continuous Data Set 20

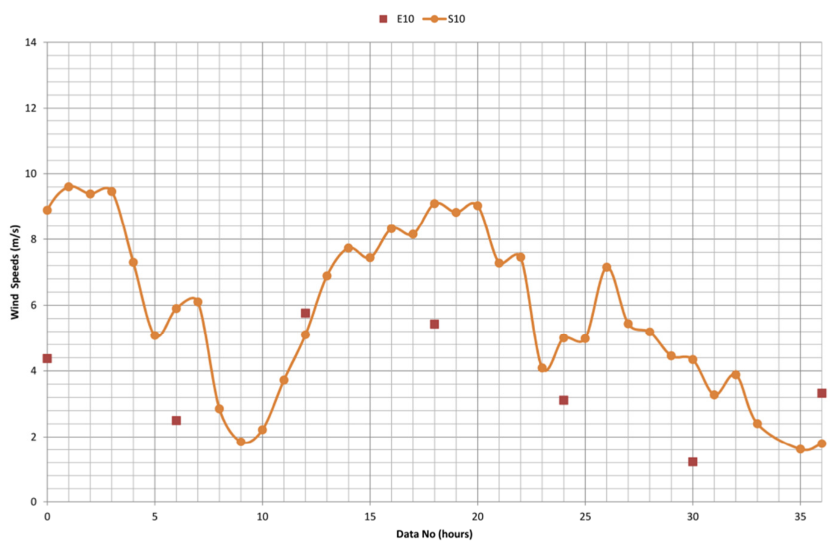

Figure C.21: E10 and S10 Wind Speeds for Continuous Data Set 21

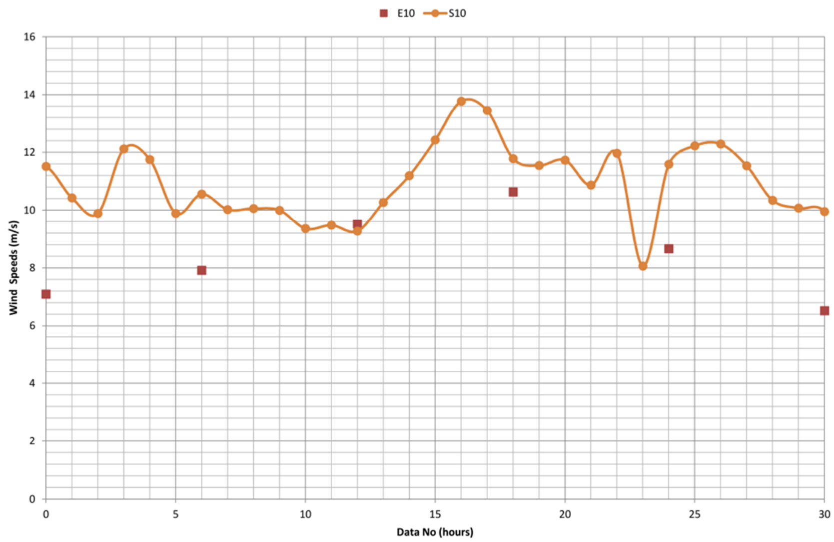

Figure C.22: E10 and S10 Wind Speeds for Continuous Data Set 22

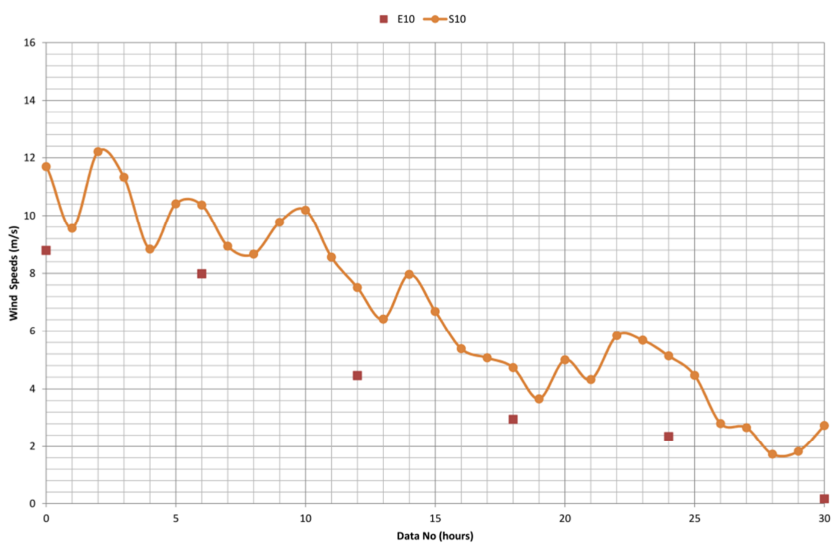

Figure C.23: E10 and S10 Wind Speeds for Continuous Data Set 23

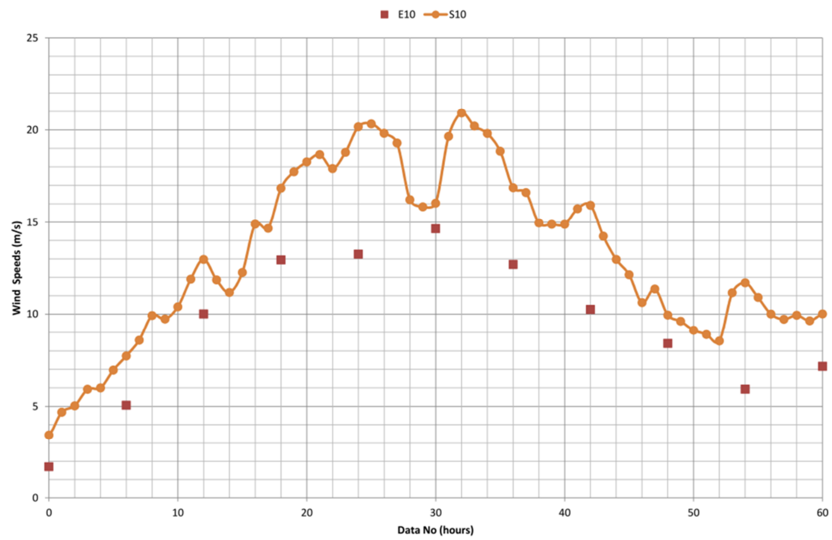

Figure C.24: E10 and S10 Wind Speeds for Continuous Data Set 24

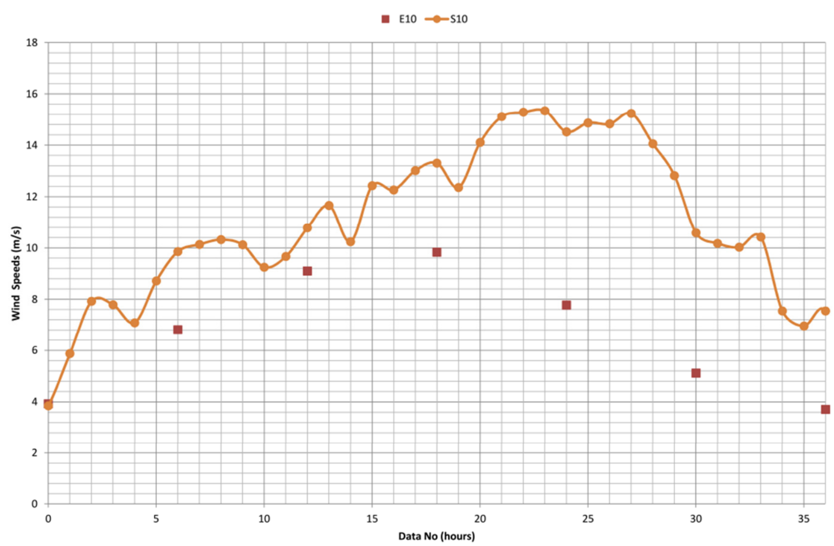

Figure C.25: E10 and S10 Wind Speeds for Continuous Data Set 25

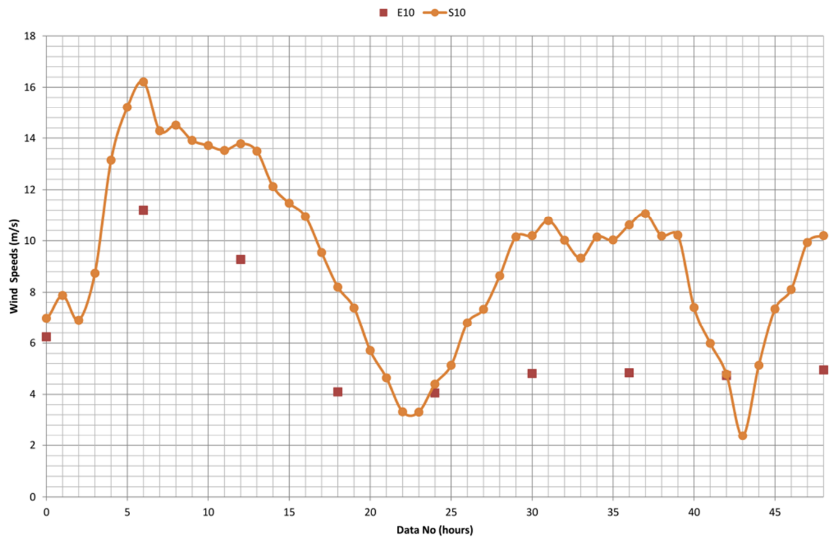

Figure C.26: E10 and S10 Wind Speeds for Continuous Data Set 26

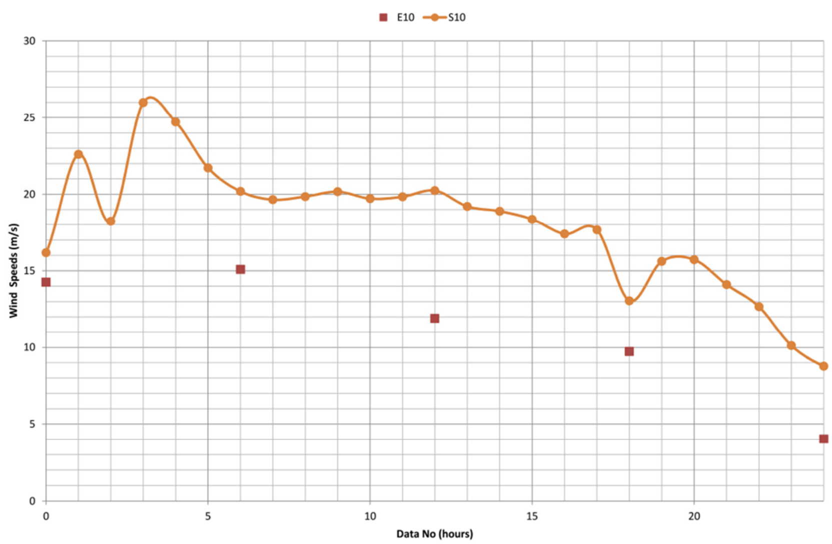

Figure C.27: E10 and S10 Wind Speeds for Continuous Data Set 27

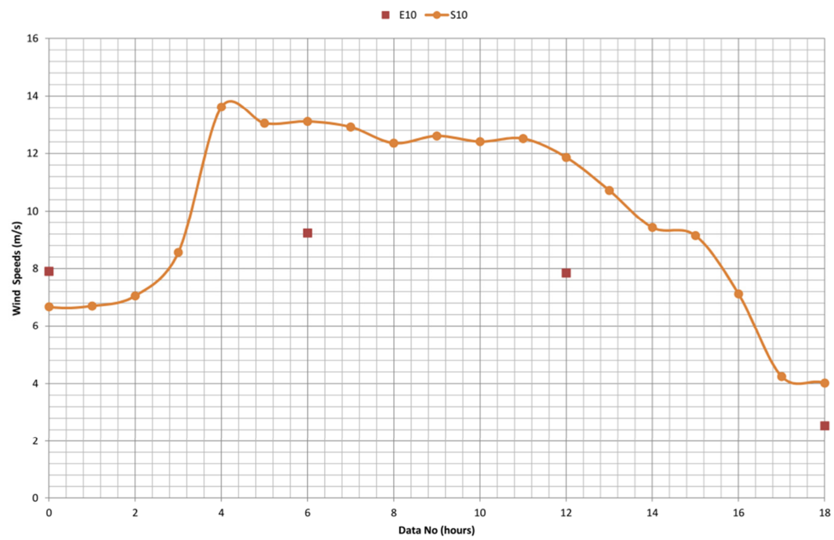

Figure C.28: E10 and S10 Wind Speeds for Continuous Data Set 28

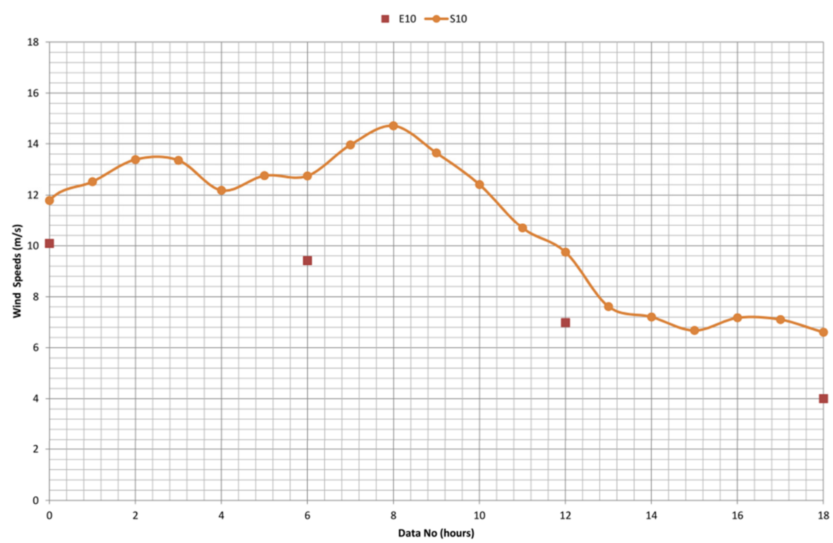

Figure C.29: E10 and S10 Wind Speeds for Continuous Data Set 29

APPENDIX D

S10, $S10_S$, $S10_{ave}$, E10 SPLINE AND E10L WIND SPEEDS FOR CONTINUOUS DATA SETS

S10 and $S10_S$, $S10_{ave}$, E10 Spline and E10L wind speeds for continuous data sets are given in this section.

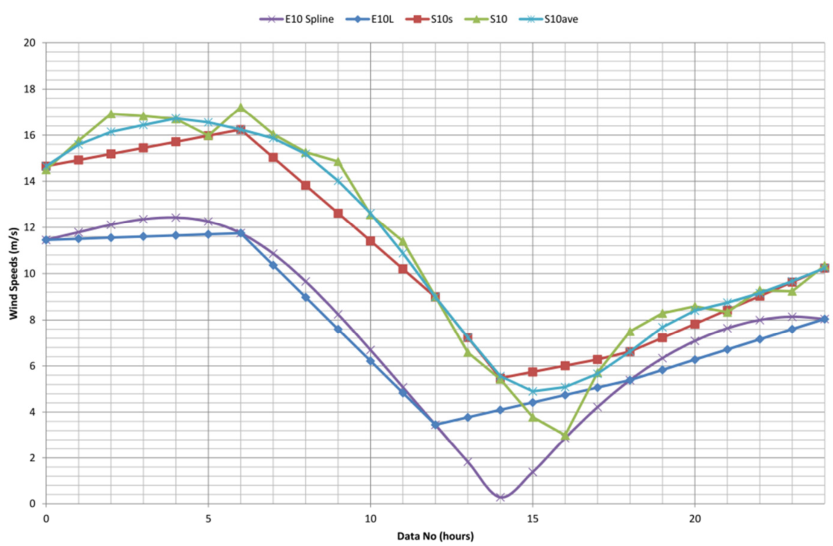

Figure D.1: $E10_L$, E10 Spline, S10, $S10_{ave}$ and $S10_S$ Wind Speeds for Continuous Data Set 1

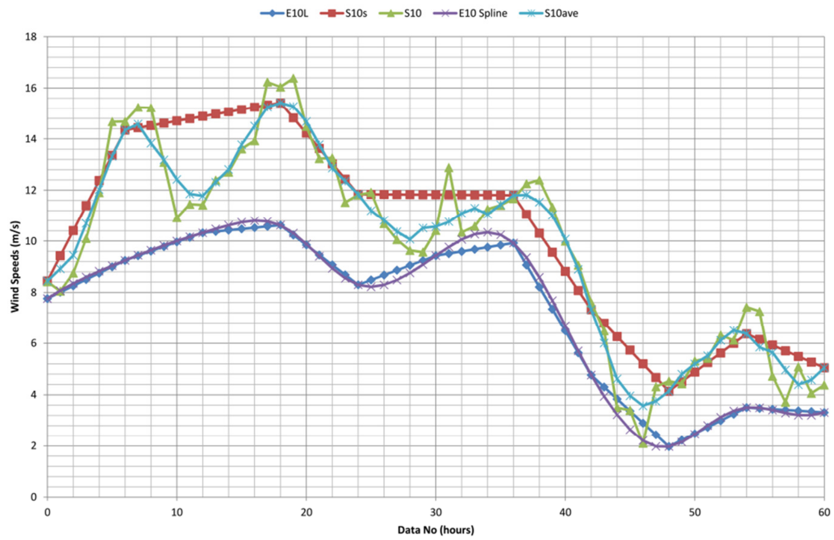

Figure D.2: $E10_L$, E10 Spline, S10, $S10_{ave}$ and $S10_S$ Wind Speeds for Continuous Data Set 2

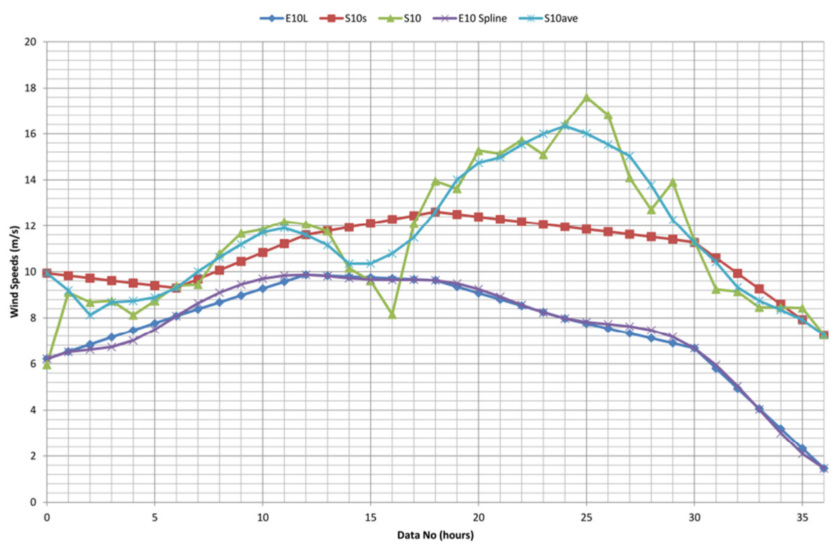

Figure D.3: $E10_L$, E10 Spline, S10, $S10_{ave}$ and $S10_S$ Wind Speeds for Continuous Data Set 3

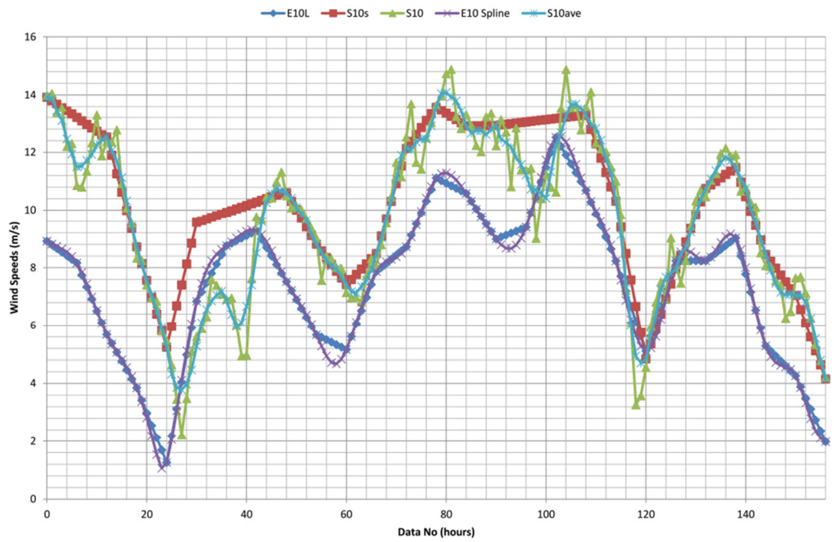

Figure D.4: $E10_L$, E10 Spline, S10, $S10_{ave}$ and $S10_S$ Wind Speeds for Continuous Data Set 4

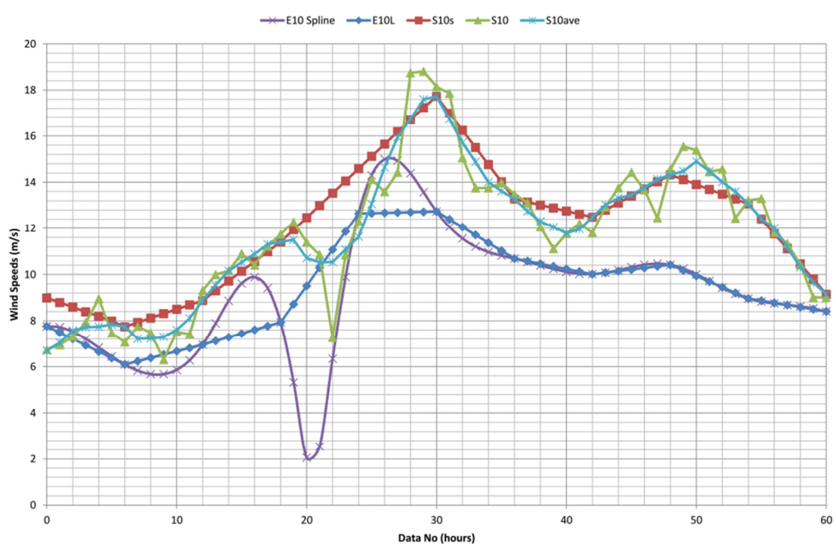

Figure D.5: $E10_L$, E10 Spline, S10, $S10_{ave}$ and $S10_S$ Wind Speeds for Continuous Data Set 5

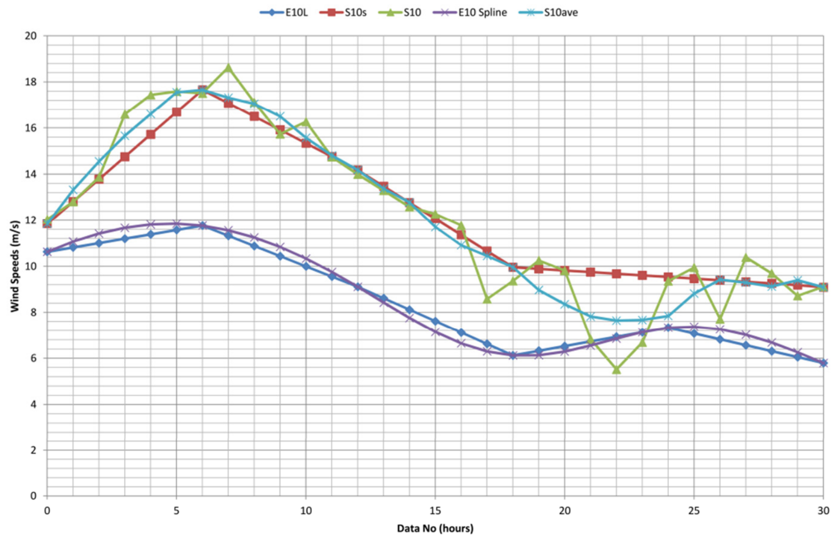

Figure D.6: E10$_L$, E10 Spline, S10, S10$_{ave}$ and S10$_S$ Wind Speeds for Continuous Data Set 6

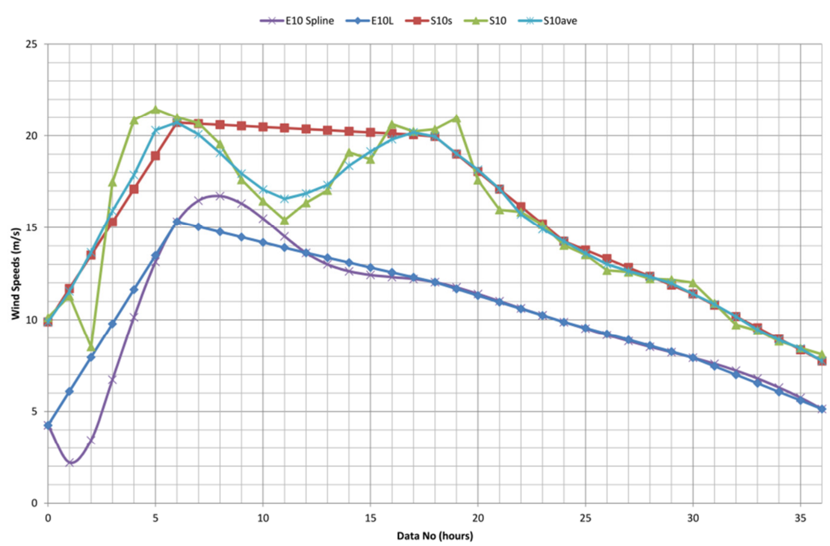

Figure D.7: E10$_L$, E10 Spline, S10, S10$_{ave}$ and S10$_S$ Wind Speeds for Continuous Data Set 7

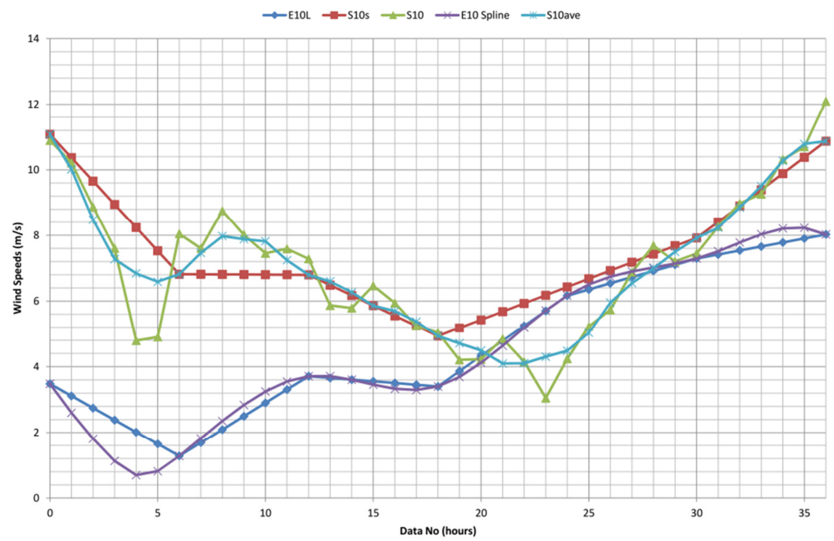

Figure D.8: $E10_L$, E10 Spline, S10, $S10_{ave}$ and $S10_S$ Wind Speeds for Continuous Data Set 8

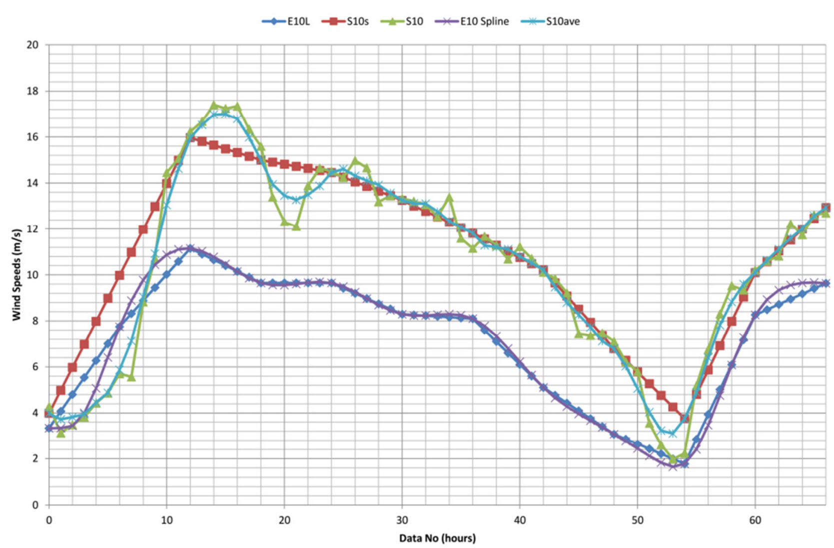

Figure D.9: $E10_L$, E10 Spline, S10, $S10_{ave}$ and $S10_S$ Wind Speeds for Continuous Data Set 9

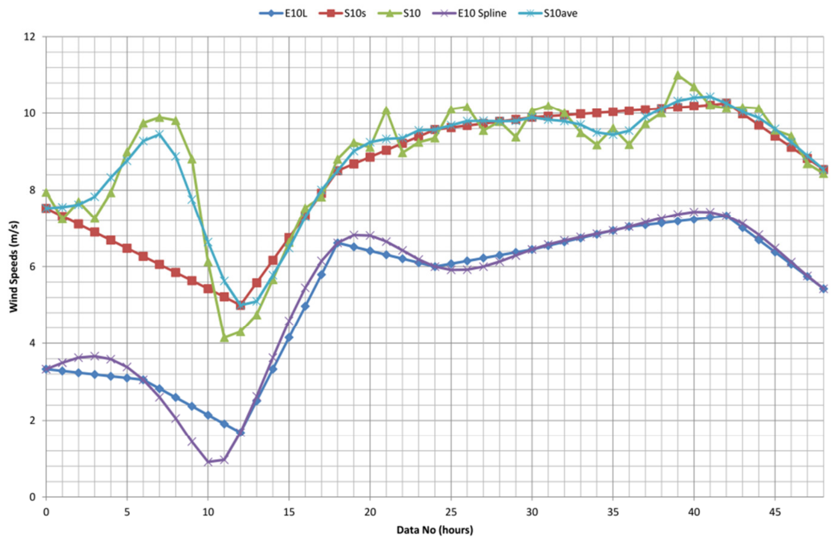

Figure D.10: $E10_L$, E10 Spline, S10, $S10_{ave}$ and $S10_S$ Wind Speeds for Continuous Data Set 10

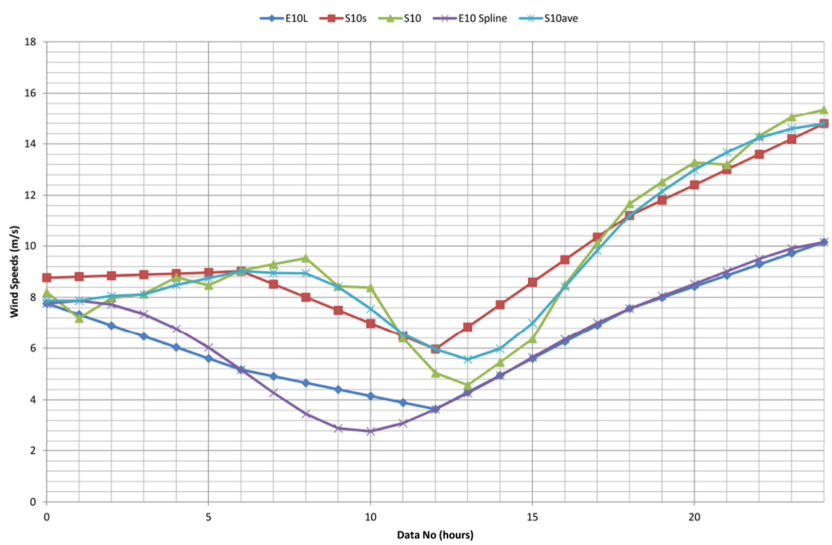

Figure D.11: $E10_L$, E10 Spline, S10, $S10_{ave}$ and $S10_S$ Wind Speeds for Continuous Data Set 11

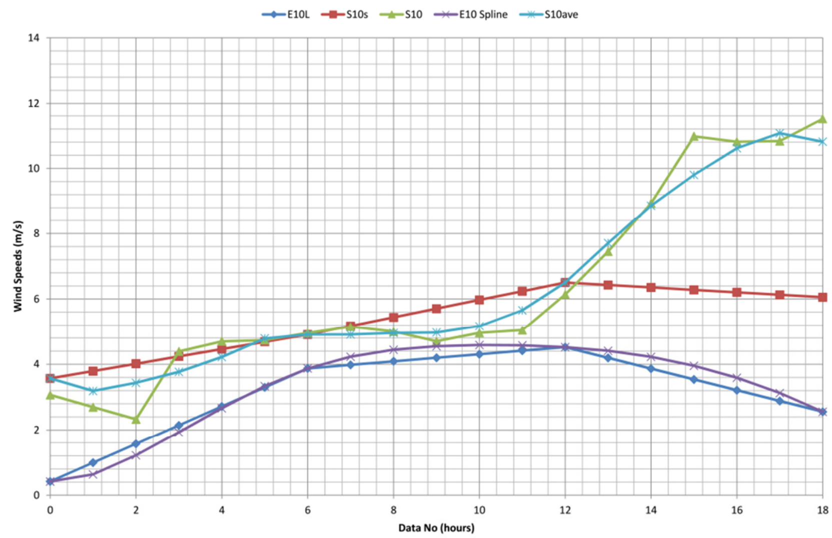

Figure D.12: $E10_L$, E10 Spline, S10, $S10_{ave}$ and $S10_S$ Wind Speeds for Continuous Data Set 12

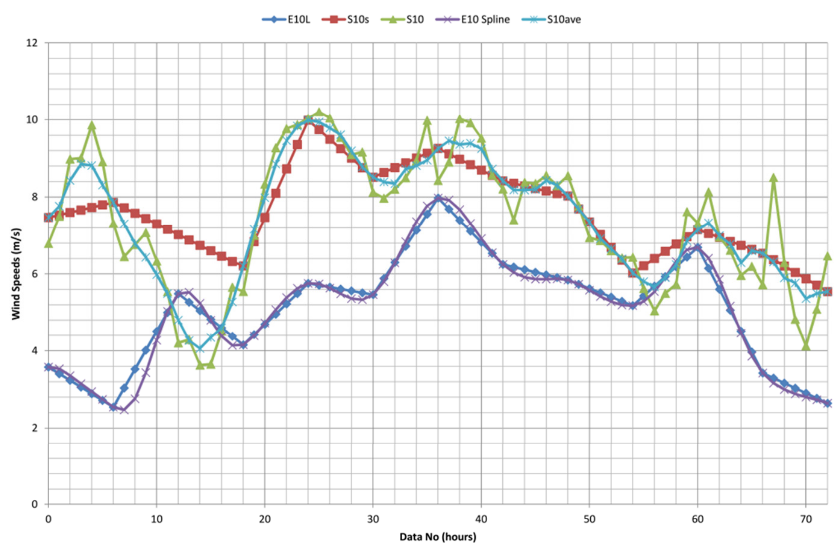

Figure D.13: $E10_L$, E10 Spline, S10, $S10_{ave}$ and $S10_S$ Wind Speeds for Continuous Data Set 13

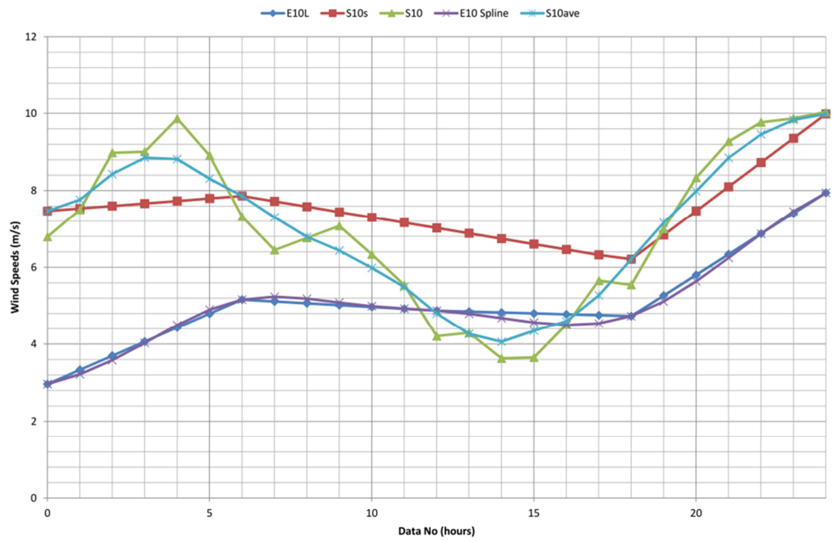

Figure D.14: $E10_L$, E10 Spline, S10, $S10_{ave}$ and $S10_S$ Wind Speeds for Continuous Data Set 14

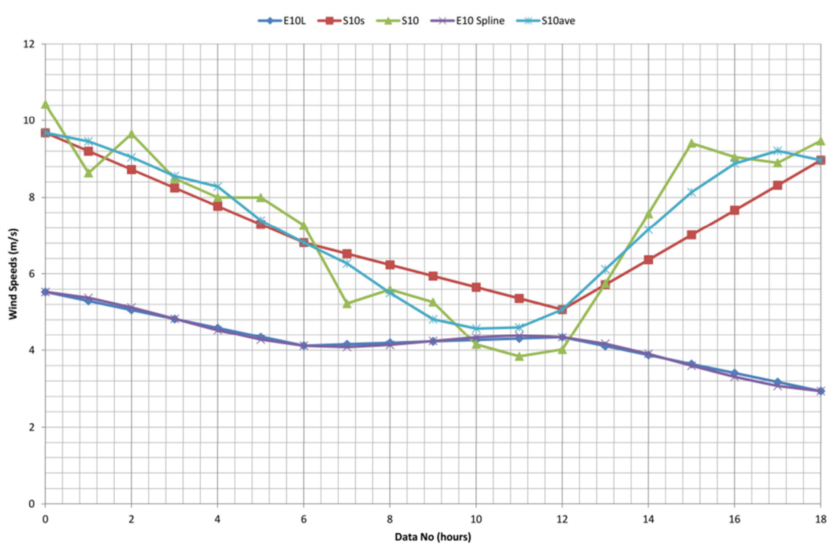

Figure D.15: $E10_L$, E10 Spline, S10, $S10_{ave}$ and $S10_S$ Wind Speeds for Continuous Data Set 15

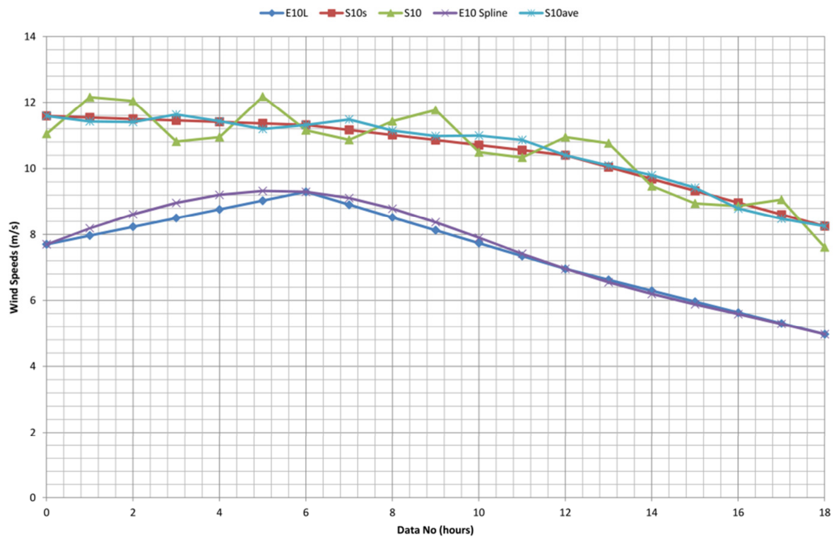

Figure D.16: $E10_L$, E10 Spline, S10, $S10_{ave}$ and $S10_S$ Wind Speeds for Continuous Data Set 16

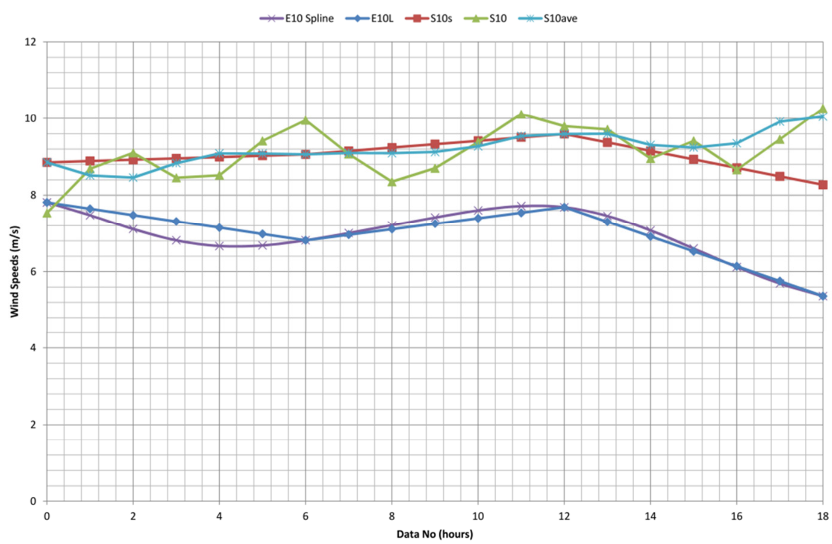

Figure D.17: $E10_L$, E10 Spline, S10, $S10_{ave}$ and $S10_S$ Wind Speeds for Continuous Data Set 17

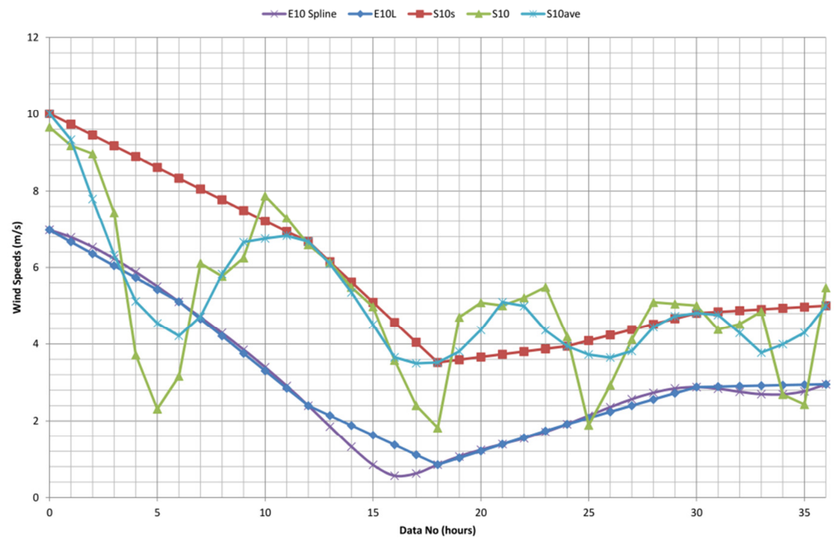

Figure D.18: $E10_L$, E10 Spline, S10, $S10_{ave}$ and $S10_S$ Wind Speeds for Continuous Data Set 18

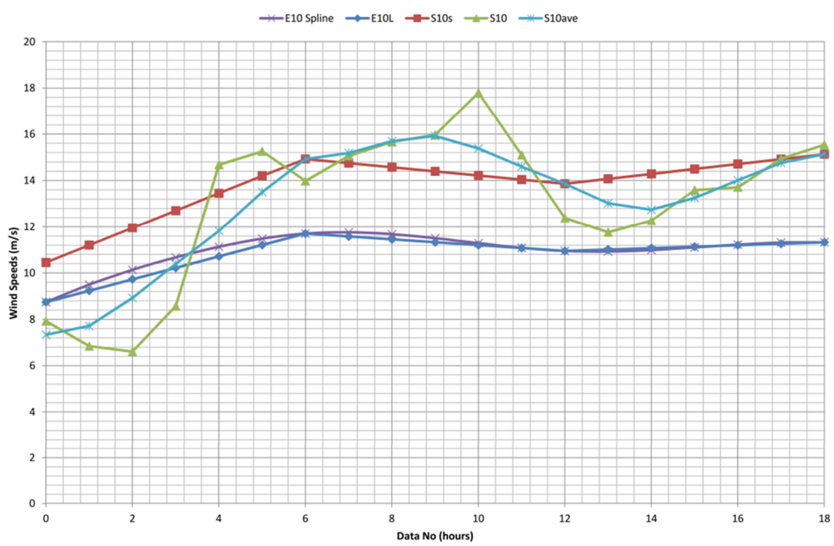

Figure D.19: $E10_L$, E10 Spline, S10, $S10_{ave}$ and $S10_S$ Wind Speeds for Continuous Data Set 19

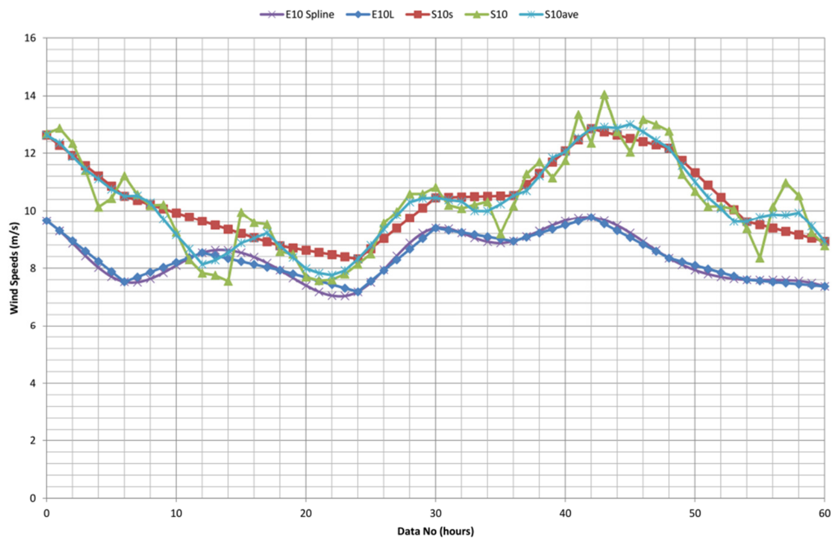

Figure D.20: $E10_L$, E10 Spline, S10, $S10_{ave}$ and $S10_S$ Wind Speeds for Continuous Data Set 20

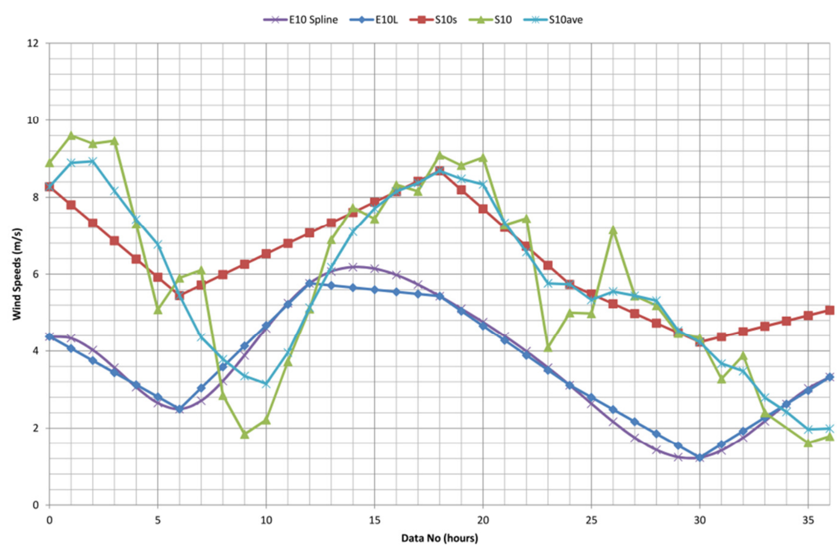

Figure D.21: $E10_L$, E10 Spline, S10, $S10_{ave}$ and $S10_S$ Wind Speeds for Continuous Data Set 21

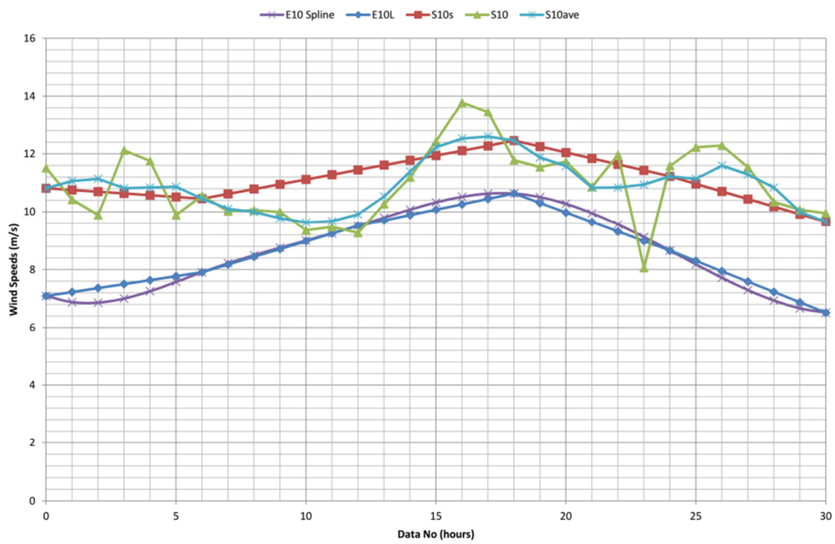

Figure D.22: $E10_L$, E10 Spline, S10, $S10_{ave}$ and $S10_S$ Wind Speeds for Continuous Data Set 22

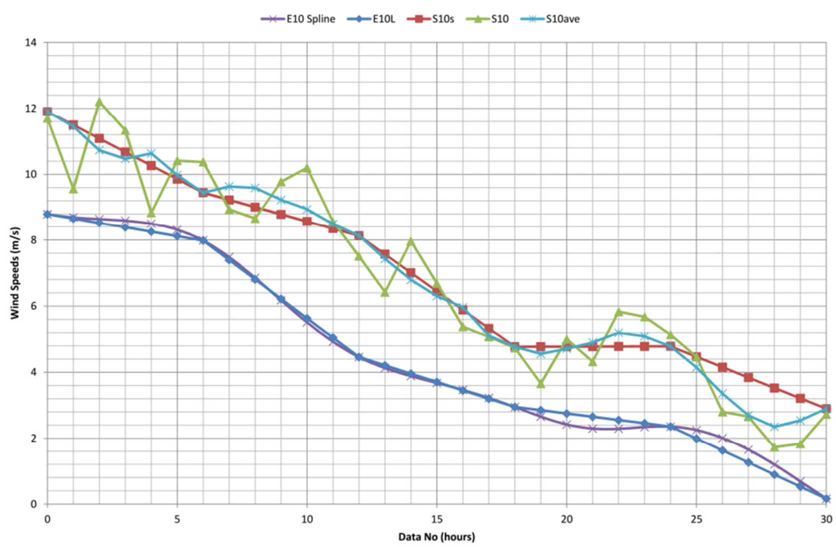

Figure D.23: $E10_L$, E10 Spline, S10, $S10_{ave}$ and $S10_S$ Wind Speeds for Continuous Data Set 23

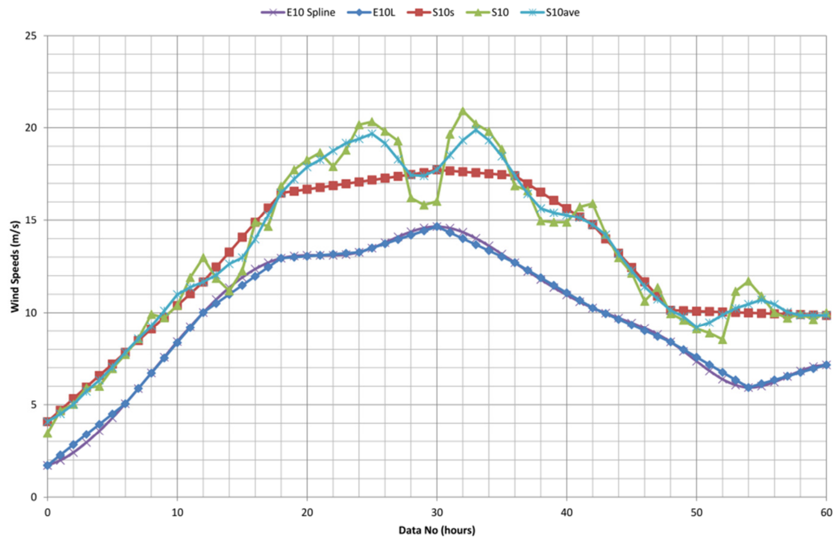

Figure D.24: $E10_L$, E10 Spline, S10, $S10_{ave}$ and $S10_S$ Wind Speeds for Continuous Data Set 24

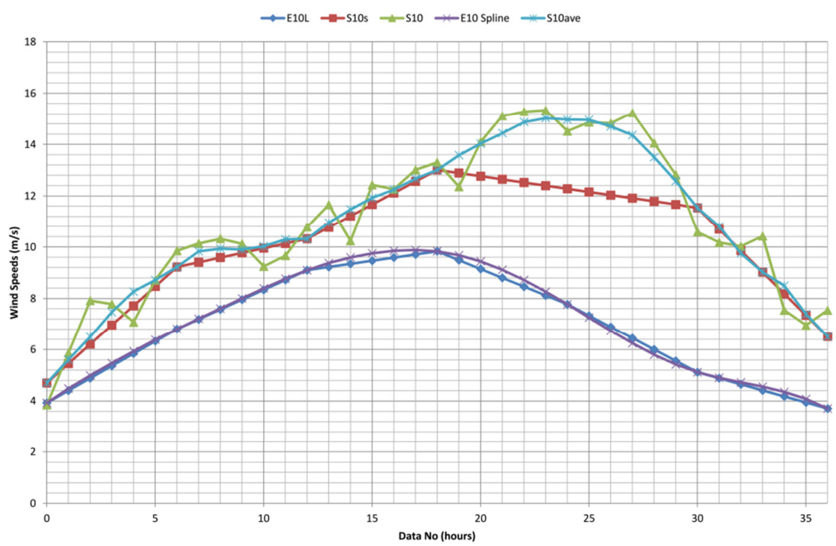

Figure D.25: $E10_L$, E10 Spline, S10, $S10_{ave}$ and $S10_S$ Wind Speeds for Continuous Data Set 25

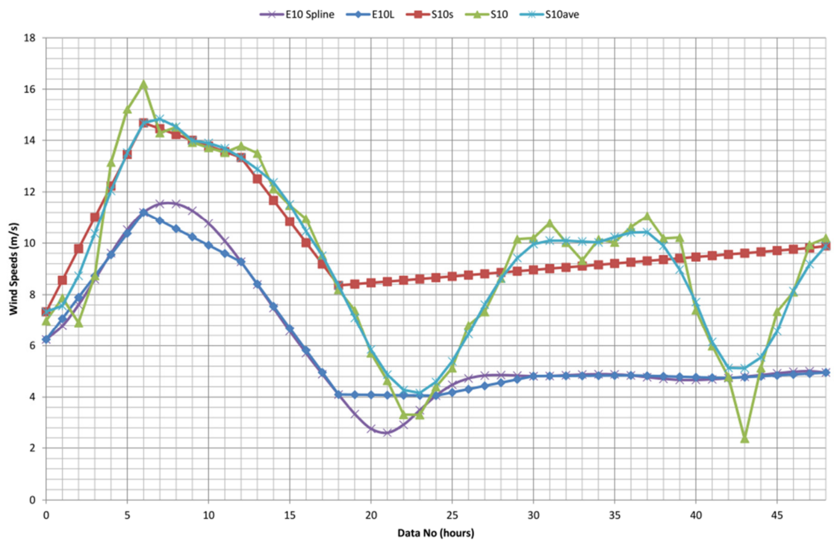

Figure D.26: $E10_L$, E10 Spline, S10, $S10_{ave}$ and $S10_S$ Wind Speeds for Continuous Data Set 26

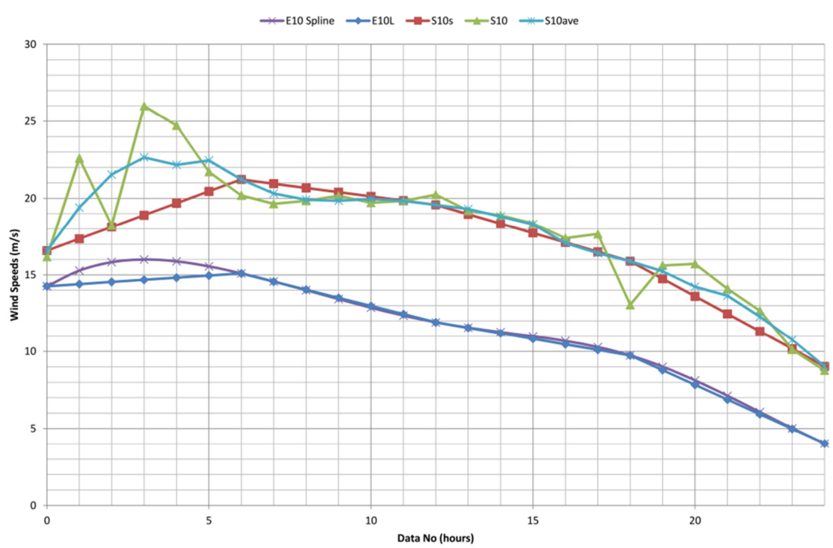

Figure D.27: $E10_L$, E10 Spline, S10, $S10_{ave}$ and $S10_S$ Wind Speeds for Continuous Data Set 27

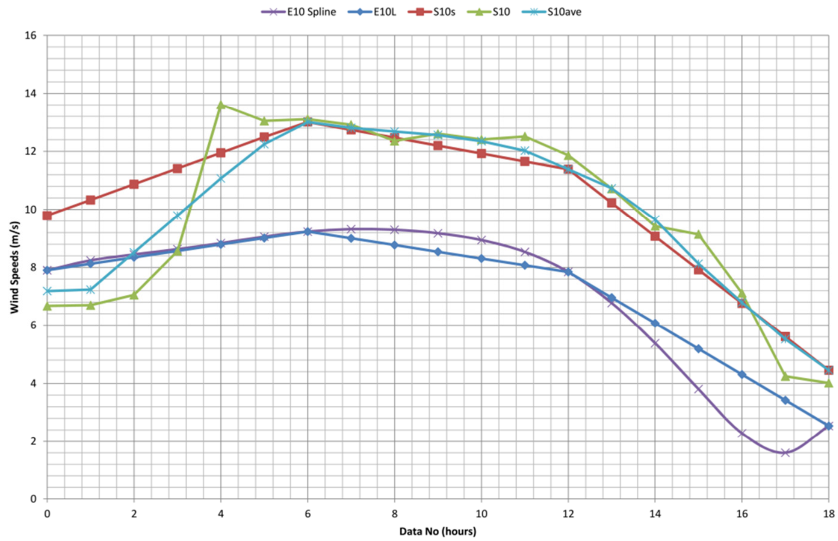

Figure D.28: $E10_L$, E10 Spline, S10, $S10_{ave}$ and $S10_S$ Wind Speeds for Continuous Data Set 28

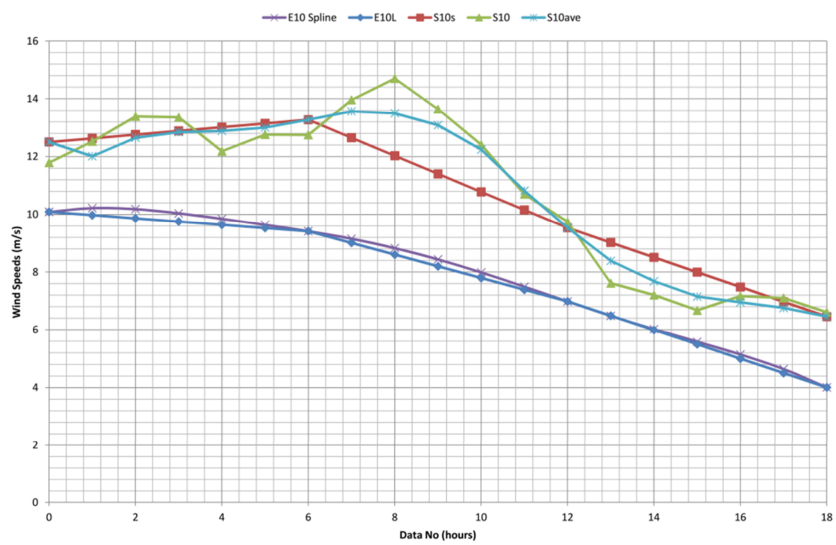

Figure D.29: $E10_L$, E10 Spline, S10, $S10_{ave}$ and $S10_S$ Wind Speeds for Continuous Data Set 29

APPENDIX E

CORRELATION FIGURES BETWEEN E10 WIND SPEEDS AND S10$_S$/E10 WIND SPEED RATIOS

Correlation figures between E10 wind speeds and S10$_S$/E10 wind speed ratios are given in this section.

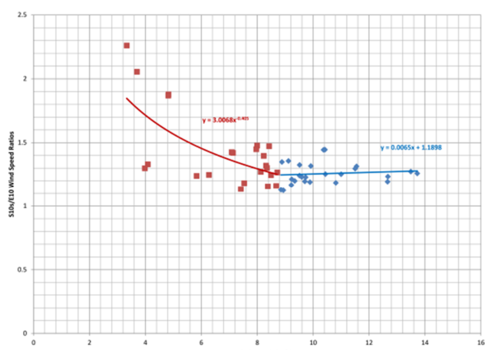

Figure E.1: E10 Wind Speeds vs S10s/E10 Wind Speed Ratios for the First Two Points (1 and 2) of Type-1A (Developing Winds) by Method 1

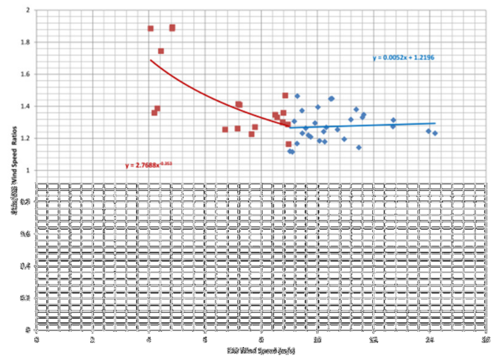

Figure E.2: E10 Wind Speeds vs S10s/E10 Wind Speed Ratios for the Middle Two Points (3 and 4) of Type-1A (Developing Winds) by Method 1

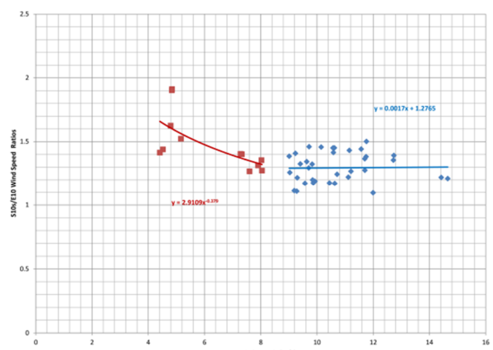

Figure E.3: E10 Wind Speeds vs S10s/E10 Wind Speed Ratios for the Last Two Points (5 and 6) of Type-1A (Developing Winds) by Method 1

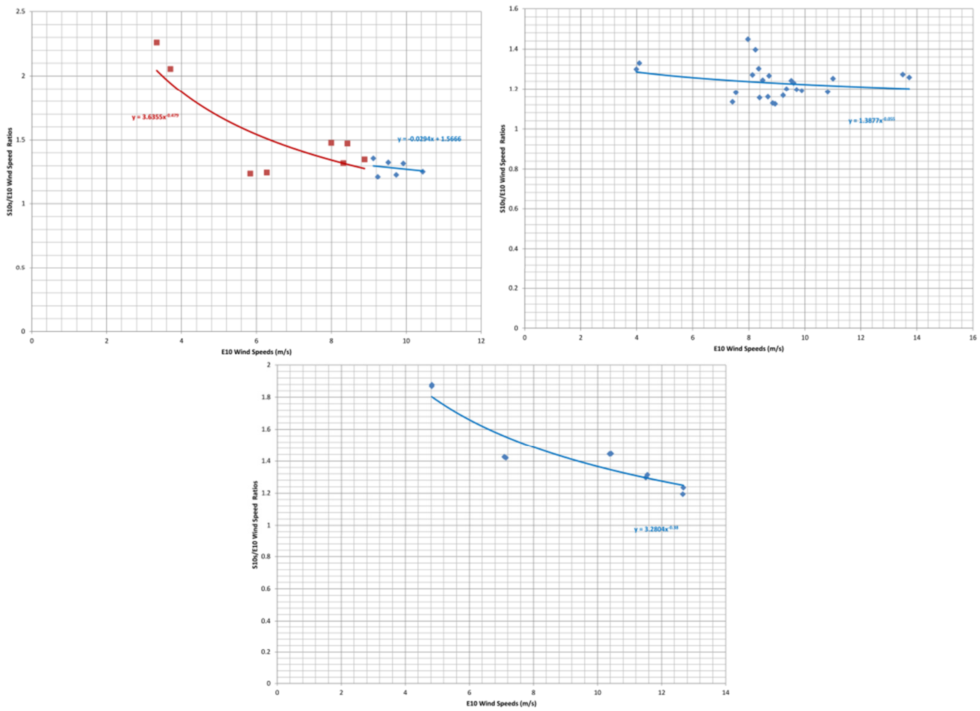

Figure E.4: E10 Wind Speeds vs $S10_s$/E10 Wind Speed Ratios for the First Two Points (1 and 2) of Type-1A (Developing Winds) by Method 3 ($\Delta \geq 0.35$ Upper Left Graph; $0.35 > \Delta \geq 0.05$ Upper Right Graph; $0.05 > \Delta \geq 0$ Lower Graph)

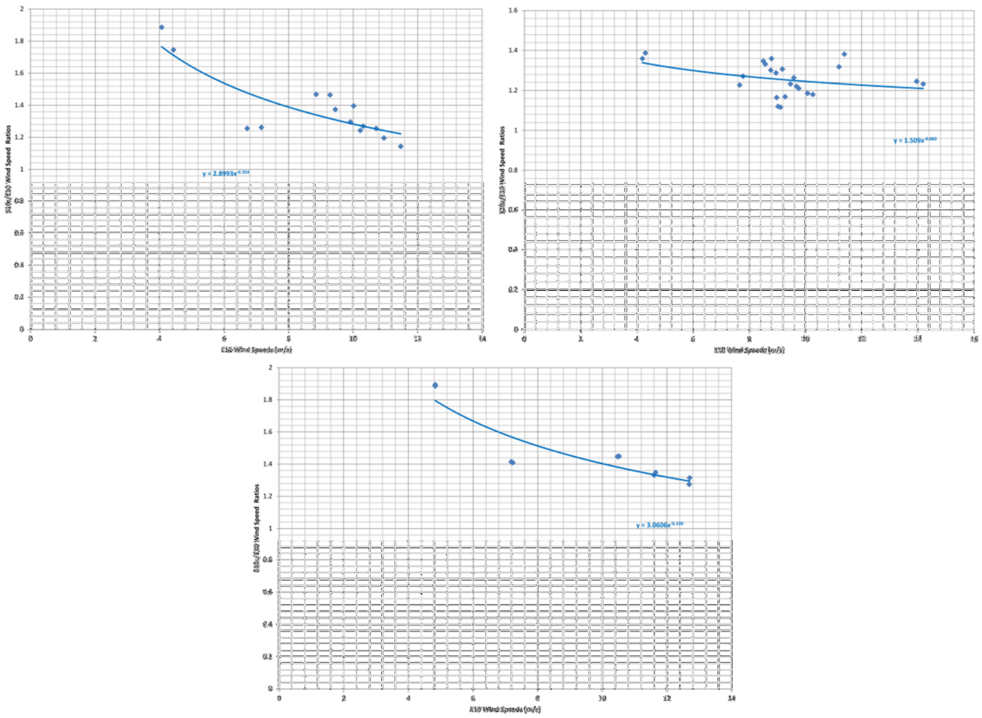

Figure E.5: E10 Wind Speeds vs S10s/E10 Wind Speed Ratios for the Middle Two Points (3 and 4) of Type-1A (Developing Winds) by Method 3 (Δ ≥ 0.35 Upper Left Graph; 0.35 > Δ ≥ 0.05 Upper Right Graph; 0.05 > Δ ≥ 0 Lower Graph)

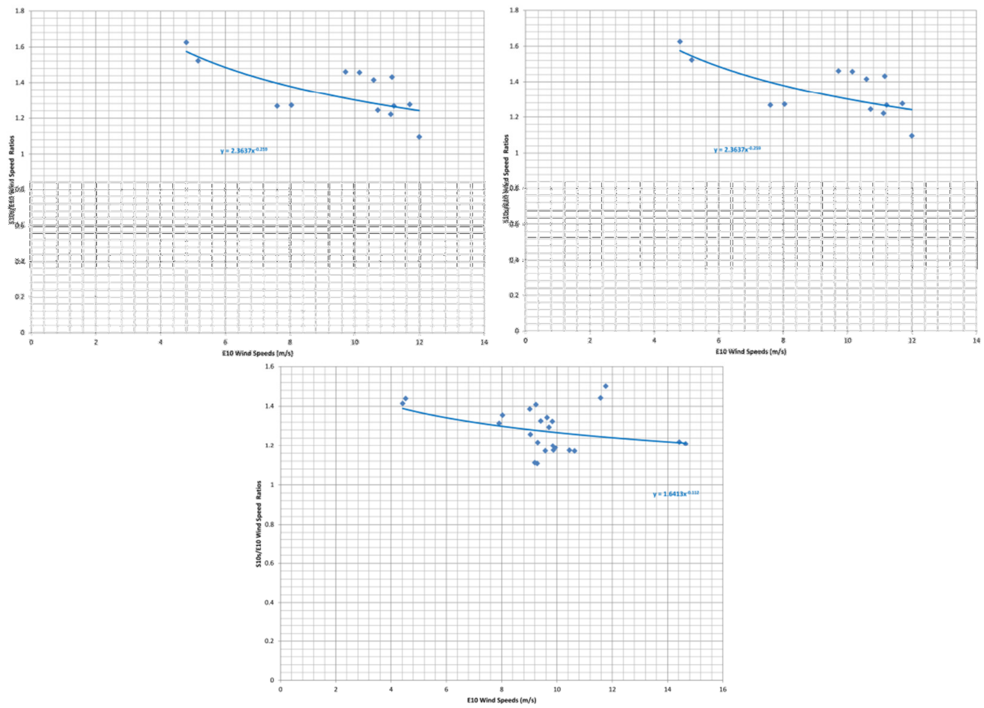

Figure E.6: E10 Wind Speeds vs S10s/E10 Wind Speed Ratios for the Last Two Points (5 and 6) of Type-1A (Developing Winds) by Method 3 (Δ ≥ 0.35 Upper Left Graph; 0.35 > Δ ≥ 0.05 Upper Right Graph; 0.05 > Δ ≥ 0 Lower Graph)

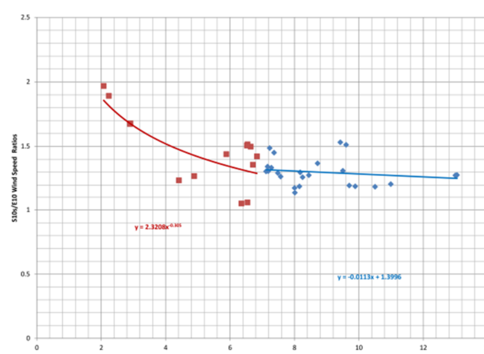

Figure E.7: E10 Wind Speeds vs S10s/E10 Wind Speed Ratios for the First Two Points (1 and 2) of Type-1B (Developing Winds) by Method 1

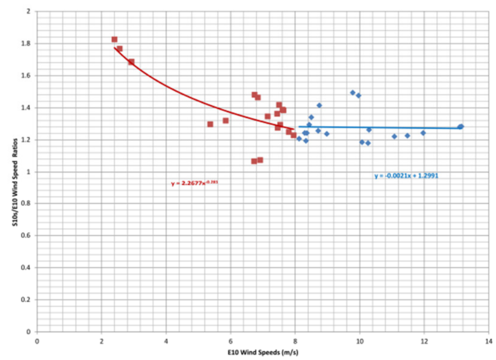

Figure E.8: E10 Wind Speeds vs S10s/E10 Wind Speed Ratios for the Middle Two Points (3 and 4) of Type-1B (Developing Winds) by Method 1

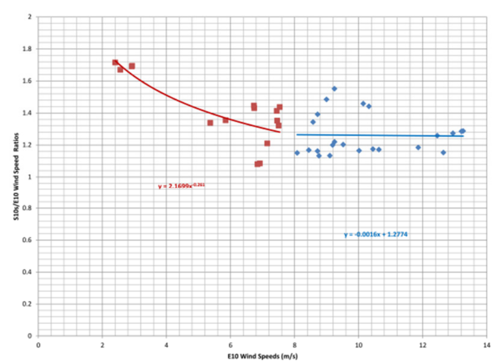

Figure E.9: E10 Wind Speeds vs S10s/E10 Wind Speed Ratios for the Last Two Points (5 and 6) of Type-1B (Developing Winds) by Method 1

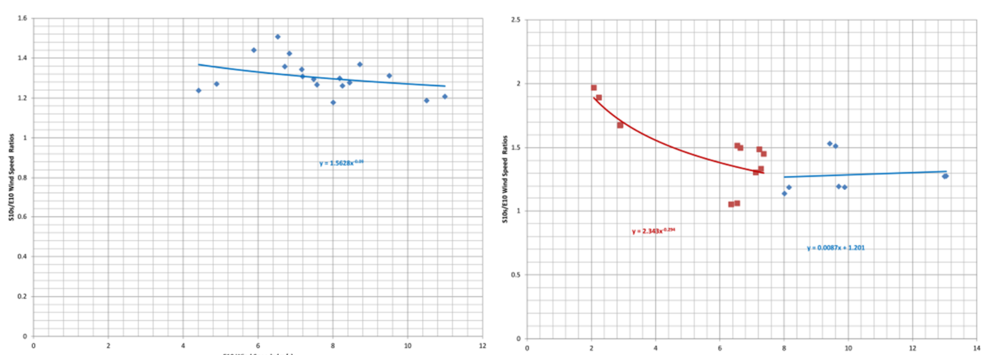

Figure E.10: E10 Wind Speeds vs S10s/E10 Wind Speed Ratios for the First Two Points (1 and 2) of Type-1B (Developing Winds) by Method 3 ($\Delta \geq 0.20$ Right Graph; $0.20 > \Delta \geq 0$ Left Graph)

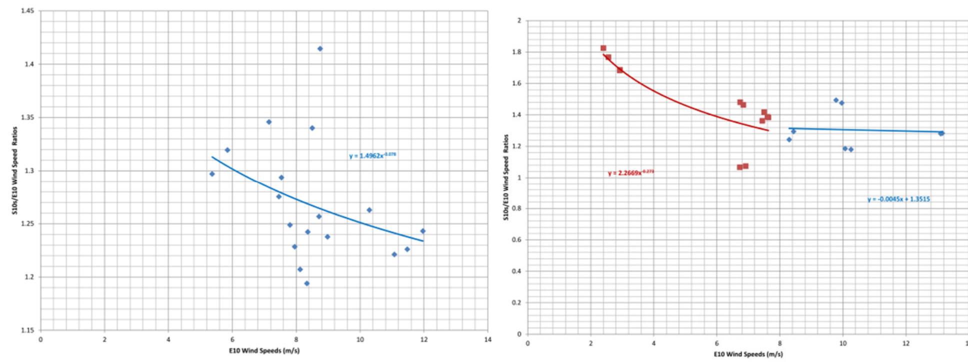

Figure E.11: E10 Wind Speeds vs S10s/E10 Wind Speed Ratios for the Middle Two Points (3 and 4) of Type-1B (Developing Winds) by Method 3 ($\Delta \geq 0.20$ Right Graph; $0.20 > \Delta \geq 0$ Left Graph)

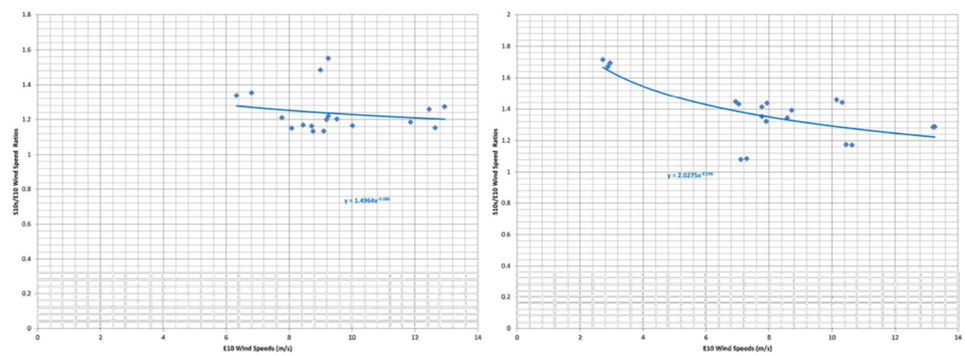

Figure E.12: E10 Wind Speeds vs S10s/E10 Wind Speed Ratios for the Last Two Points (5 and 6) of Type-1B (Developing Winds) by Method 3 ($\Delta \geq 0.20$ Right Graph; $0.20 > \Delta \geq 0$ Left Graph)

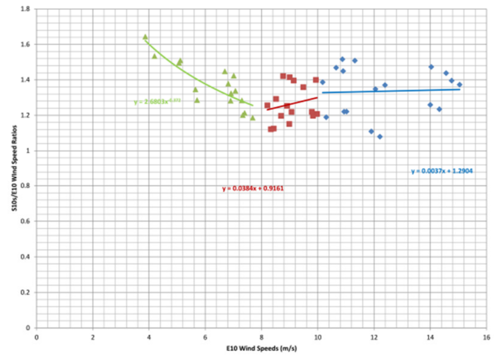

Figure E.13: E10 Wind Speeds vs S10s/E10 Wind Speed Ratios for the First Two Points (1 and 2) of Type-2A (Calming Winds) by Method 1

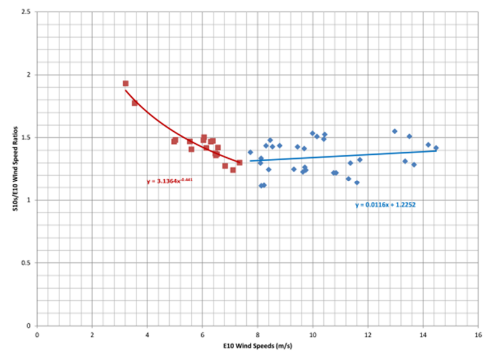

Figure E.14: E10 Wind Speeds vs S10s/E10 Wind Speed Ratios for the Middle Two Points (3 and 4) of Type-2A (Calming Winds) by Method 1

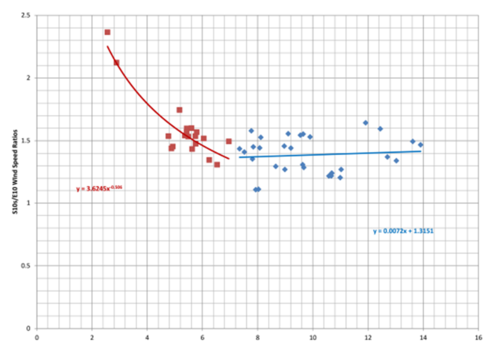

Figure E.15: E10 Wind Speeds vs S10s/E10 Wind Speed Ratios for the Last Two Points (5 and 6) of Type-2A (Calming Winds) by Method 1

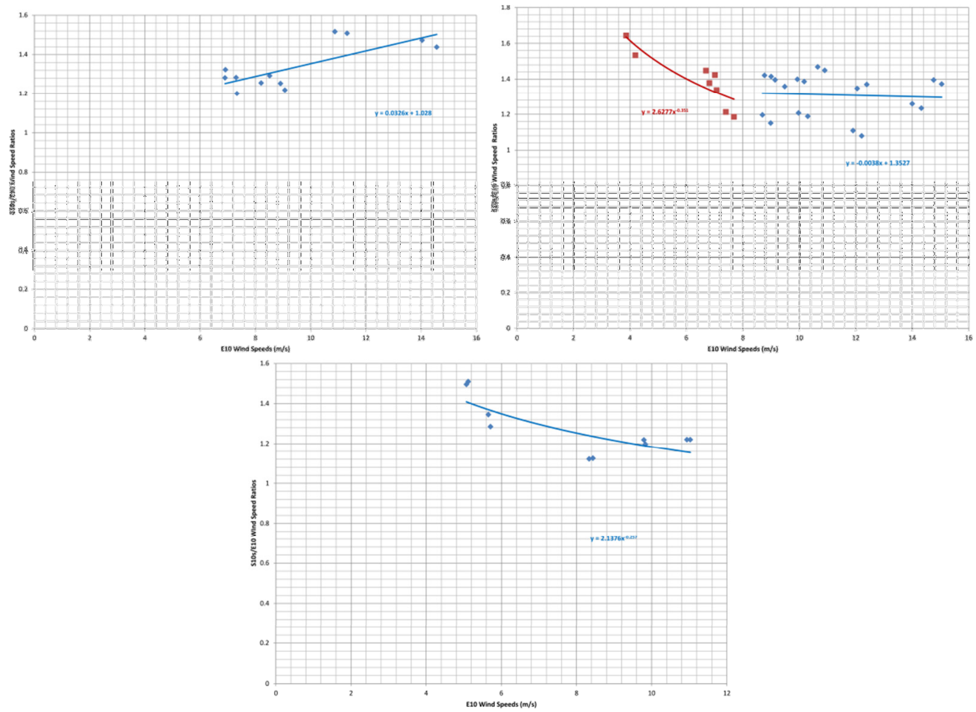

Figure E.16: E10 Wind Speeds vs S10s/E10 Wind Speed Ratios for the First Two Points (1 and 2) of Type-2A (Calming Winds) by Method 3 (Δ < -0.35 Upper Right Graph; -0.35 ≤ Δ < -0.20 Upper Left Graph; -0.20 ≤ Δ < 0 Lower Graph)

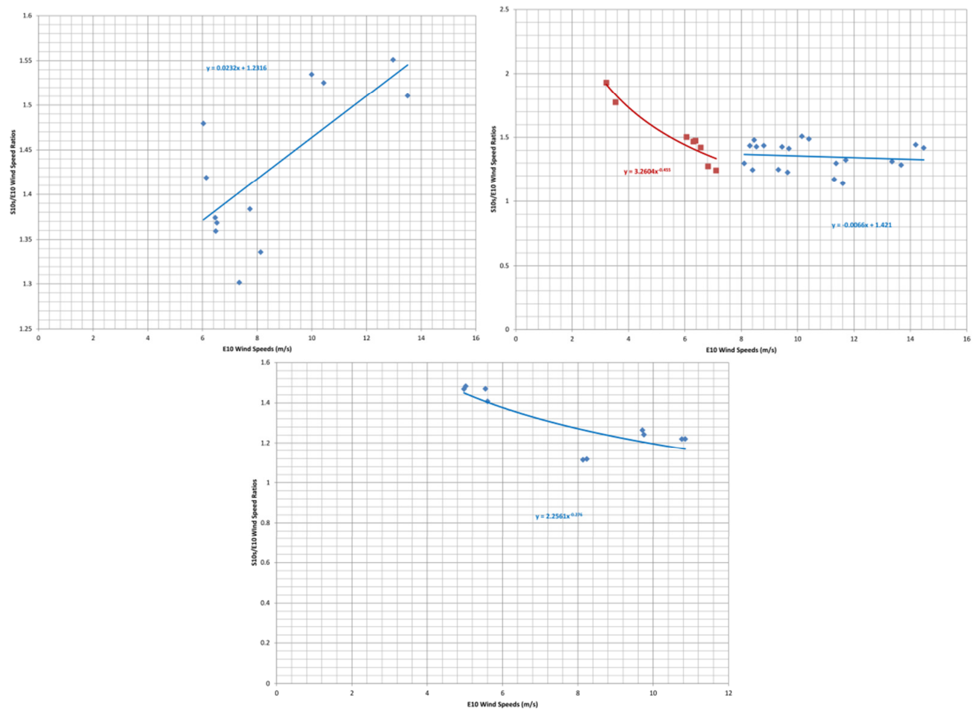

Figure E.17: E10 Wind Speeds vs S10s/E10 Wind Speed Ratios for the Middle Two Points (3 and 4) of Type-2A (Calming Winds) by Method 3 (Δ < -0.35 Upper Right Graph; -0.35 ≤ Δ < -0.20 Upper Left Graph; -0.20 ≤ Δ < 0 Lower Graph)

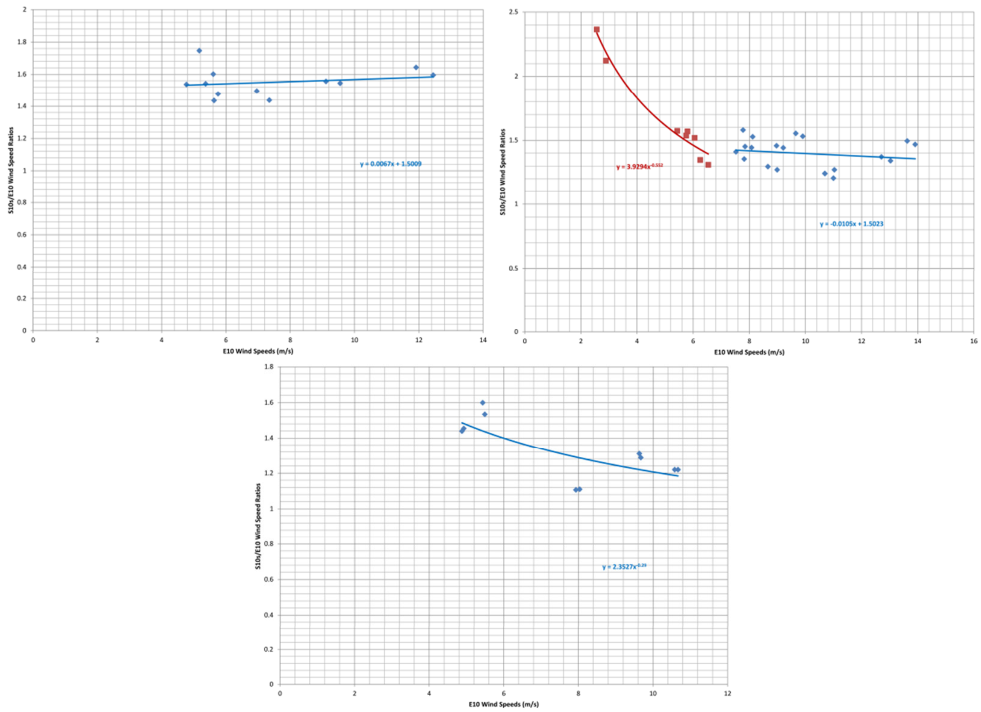

Figure E.18: E10 Wind Speeds vs S10s/E10 Wind Speed Ratios for the Last Two Points (5 and 6) of Type-2A (Calming Winds) by Method 3 (Δ < -0.35 Upper Right Graph; -0.35 ≤ Δ < -0.20 Upper Left Graph; -0.20 ≤ Δ < 0 Lower Graph)

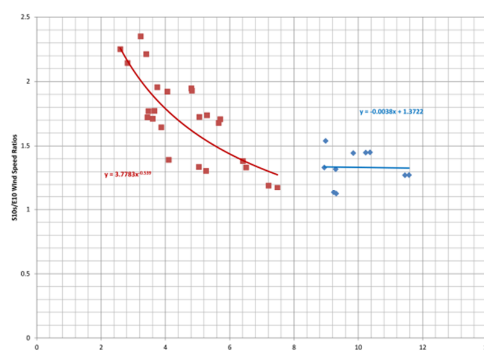

Figure E.19: E10 Wind Speeds vs S10s/E10 Wind Speed Ratios for the First Two Points (1 and 2) of Type-2B (Calming Winds) by Method 1

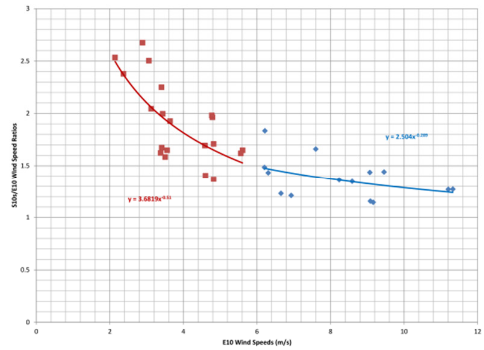

Figure E.20: E10 Wind Speeds vs S10s/E10 Wind Speed Ratios for the Middle Two Points (3 and 4) of Type-2B (Calming Winds) by Method 1

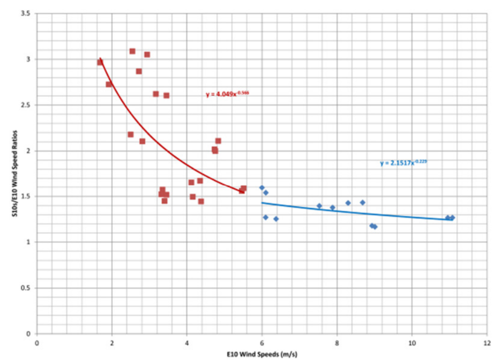

Figure E.21: E10 Wind Speeds vs S10s/E10 Wind Speed Ratios for the Last Two Points (5 and 6) of Type-2B (Calming Winds) by Method 1

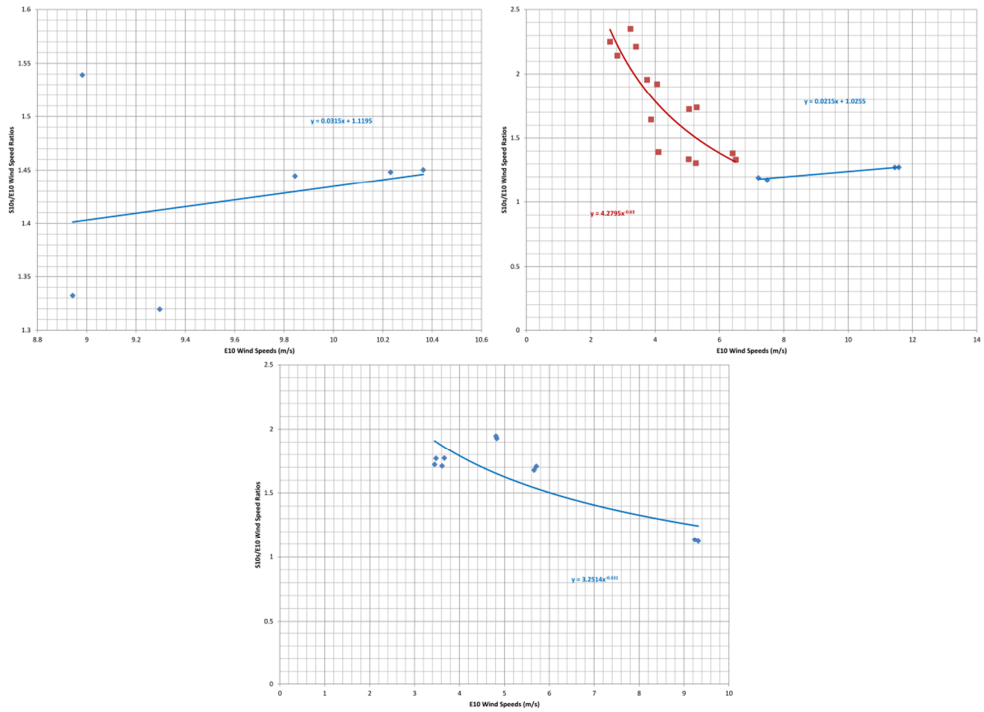

Figure E.22: E10 Wind Speeds vs S10s/E10 Wind Speed Ratios for the First Two Points (1 and 2) of Type-2B (Calming Winds) by Method 3 (Δ < -0.35 Upper Right Graph; -0.35 ≤ Δ < -0.10 Upper Left Graph; -0.10 ≤ Δ < 0 Lower Graph)

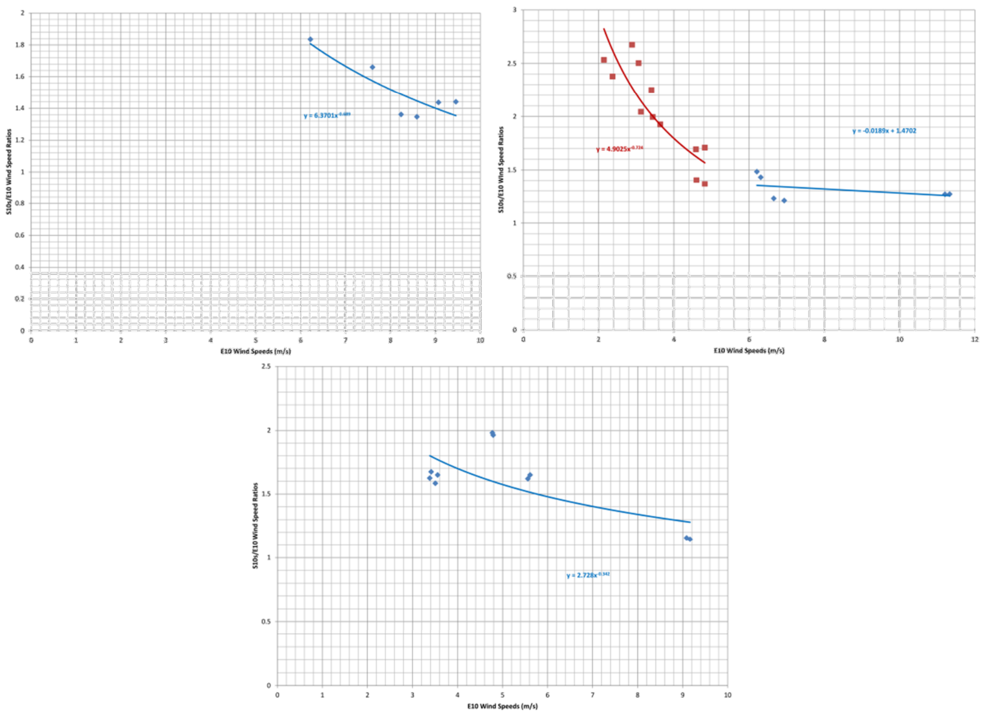

Figure E.23: E10 Wind Speeds vs S10s/E10 Wind Speed Ratios for the Middle Two Points (3 and 4) of Type-2B (Calming Winds) by Method 3 (Δ < -0.35 Upper Right Graph; -0.35 ≤ Δ < -0.10 Upper Left Graph; -0.10 ≤ Δ < 0 Lower Graph)

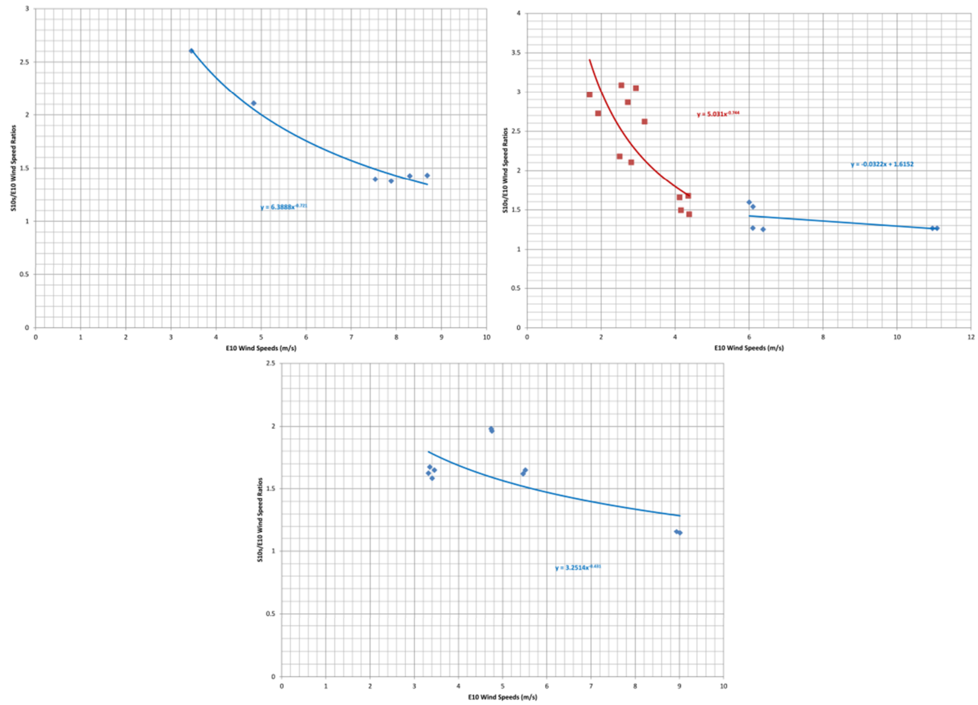

Figure E.24: E10 Wind Speeds vs S10s/E10 Wind Speed Ratios for the Last Two Points (5 and 6) of Type-2B (Calming Winds) by Method 3 (Δ < -0.35 Upper Right Graph; -0.35 ≤ Δ < -0.10 Upper Left Graph; -0.10 ≤ Δ < 0 Lower Graph)

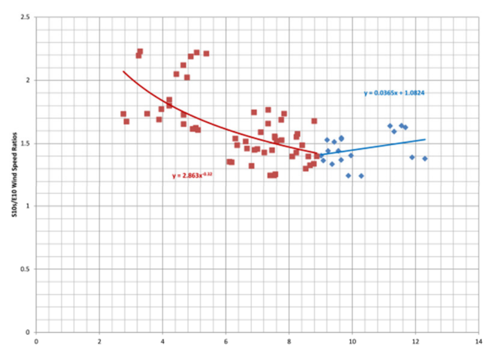

Figure E.25: E10 Wind Speeds vs S10s/E10 Wind Speed Ratios for the First Two Points (1 and 2) of Type-3A (Calming Winds) by Method 1

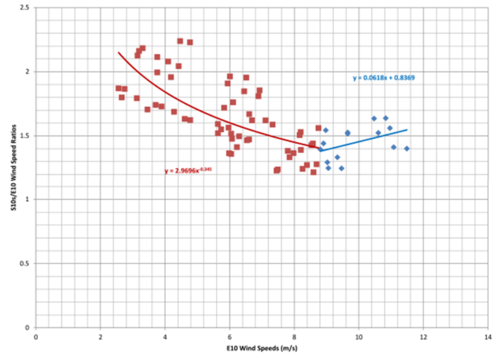

Figure E.26: E10 Wind Speeds vs S10s/E10 Wind Speed Ratios for the Middle Two Points (3 and 4) of Type-3A (Calming Winds) by Method 1

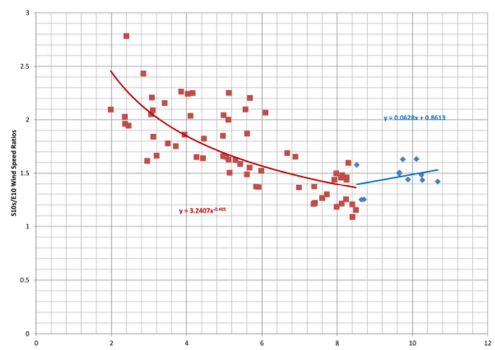

Figure E.27: E10 Wind Speeds vs S10s/E10 Wind Speed Ratios for the Last Two Points (5 and 6) of Type-3A (Calming Winds) by Method 1

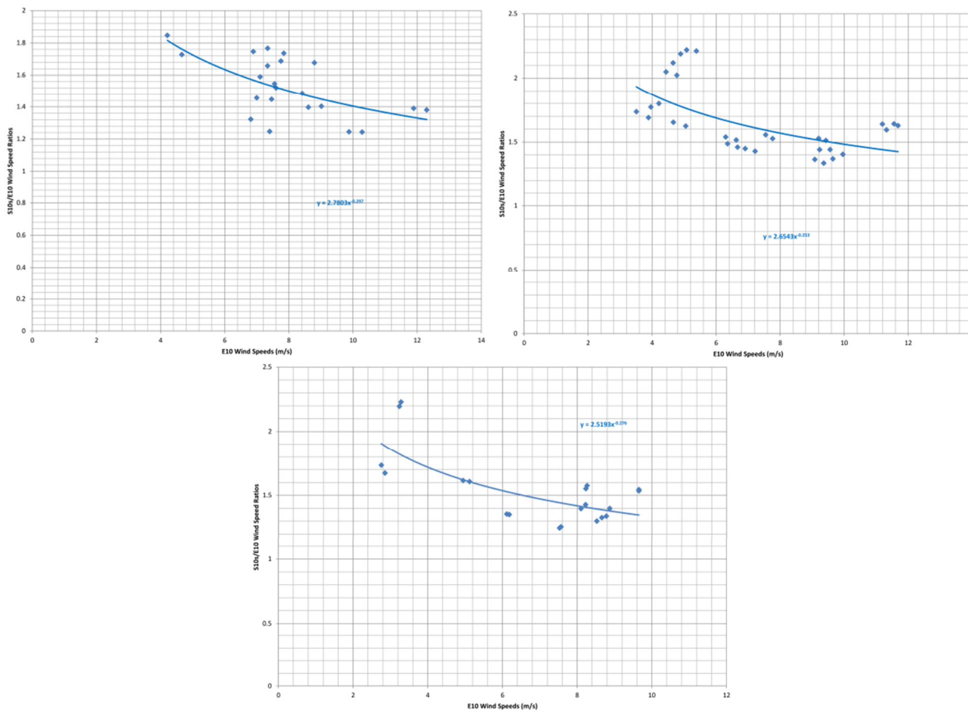

Figure E.28: E10 Wind Speeds vs S10s/E10 Wind Speed Ratios for the First Two Points (1 and 2) of Type-3A (Calming Winds) by Method 3 (Δ < -0.40 Upper Right Graph; -0.40 ≤ Δ < -0.20 Upper Left Graph; -0.20 ≤ Δ < 0 Lower Graph)

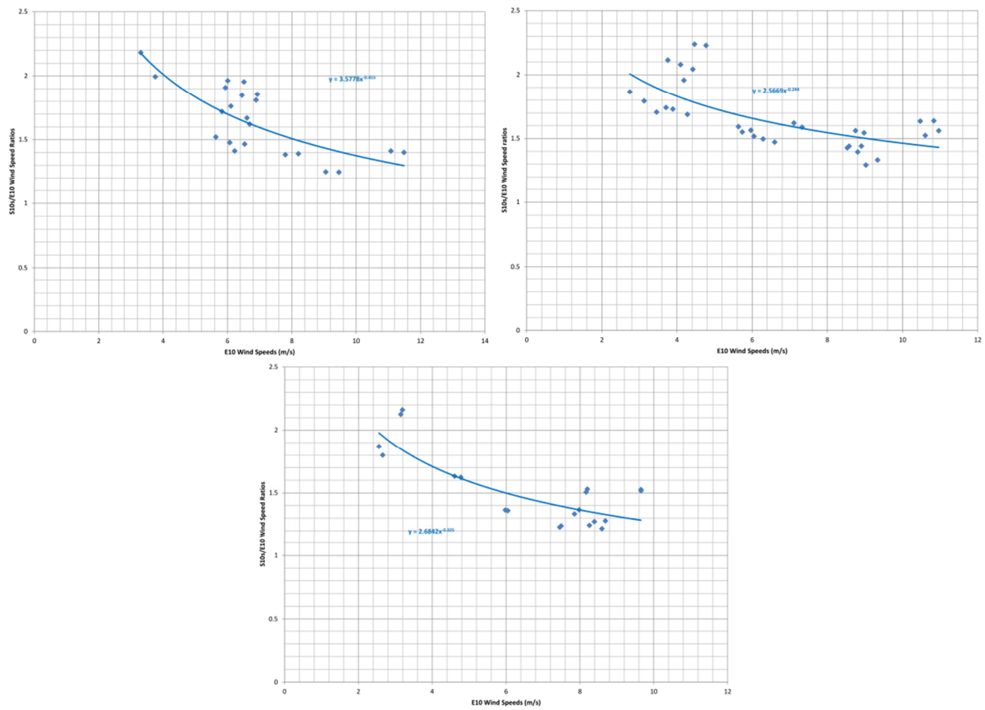

Figure E.29: E10 Wind Speeds vs S10s/E10 Wind Speed Ratios for the Middle Two Points (3 and 4) of Type-3A (Calming Winds) by Method 3 ($\Delta < -0.40$ Upper Right Graph; $-0.40 \leq \Delta < -0.20$ Upper Left Graph; $-0.20 \leq \Delta < 0$ Lower Graph)

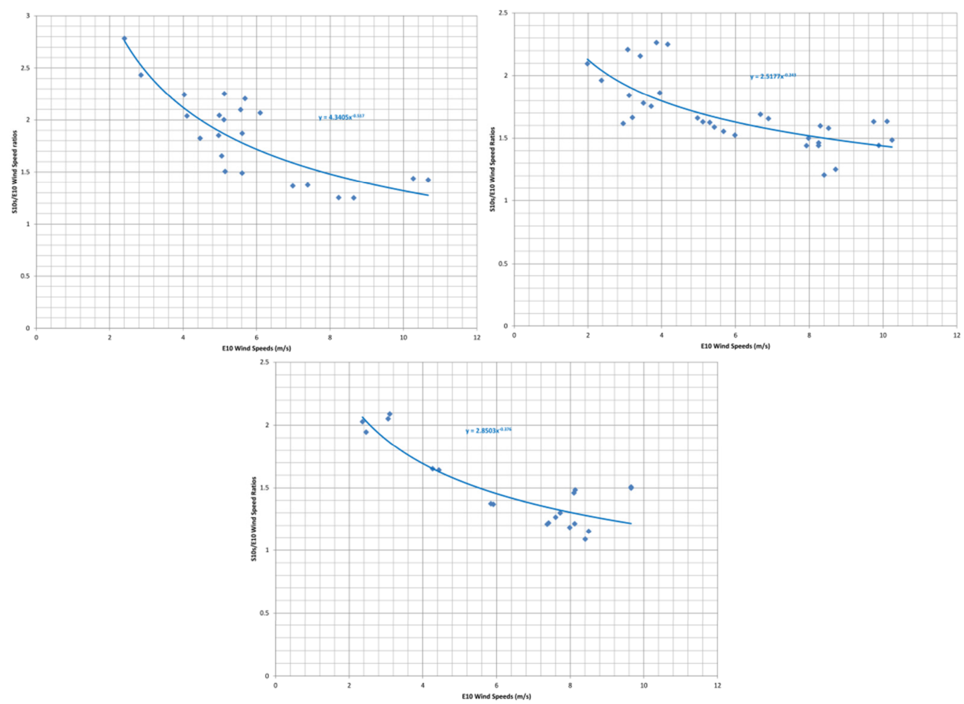

Figure E.30: E10 Wind Speeds vs S10s/E10 Wind Speed Ratios for the Last Two Points (5 and 6) of Type-3A (Calming Winds) by Method 3 ($\Delta < -0.40$ Upper Right Graph; $-0.40 \leq \Delta < -0.20$ Upper Left Graph; $-0.20 \leq \Delta < 0$ Lower Graph)

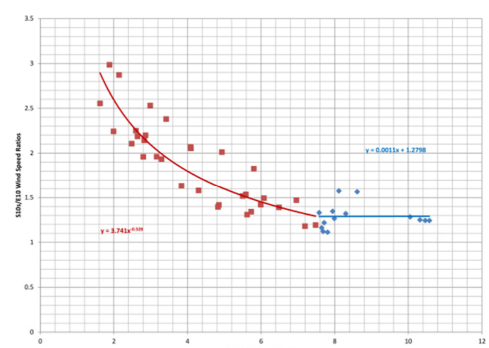

Figure E.31: E10 Wind Speeds vs S10s/E10 Wind Speed Ratios for the First Two Points (1 and 2) of Type-3B (Calming Winds) by Method 1

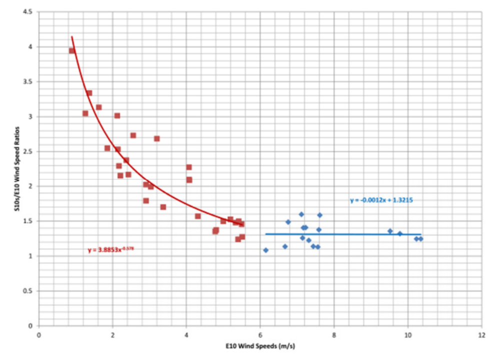

Figure E.32: E10 Wind Speeds vs S10s/E10 Wind Speed Ratios for the Middle Two Points (3 and 4) of Type-3B (Calming Winds) by Method 1

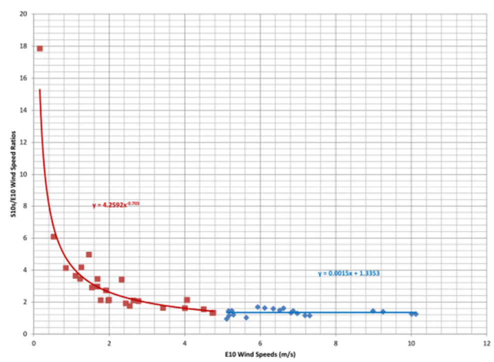

Figure E.33: E10 Wind Speeds vs S10s/E10 Wind Speed Ratios for the Last Two Points (5 and 6) of Type-3B (Calming Winds) by Method 1

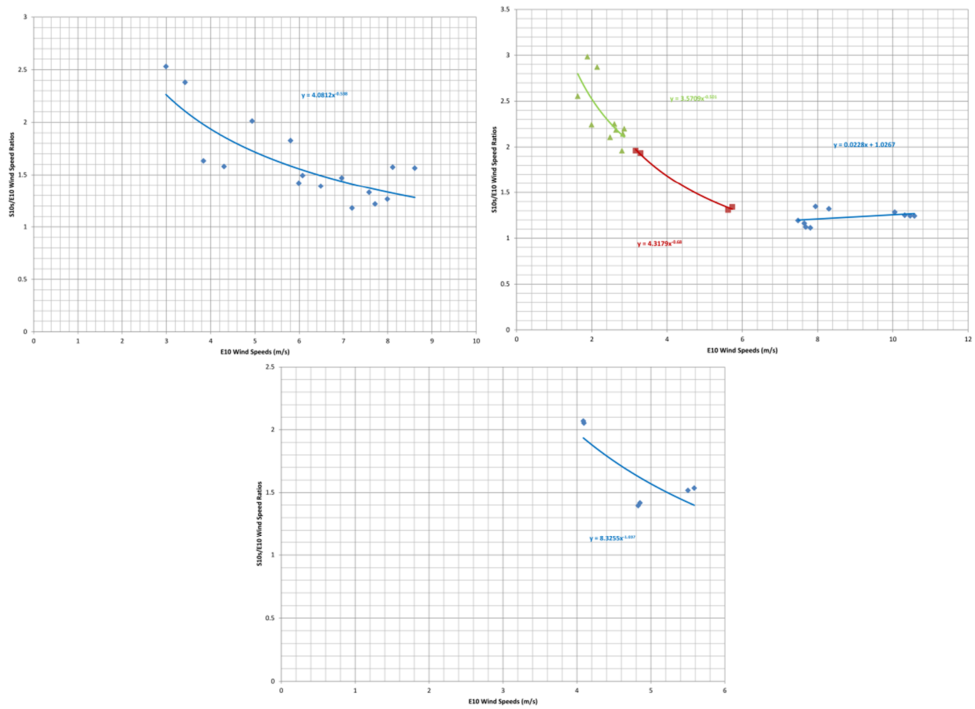

Figure E.34: E10 Wind Speeds vs S10s/E10 Wind Speed Ratios for the First Two Points (1 and 2) of Type-3B (Calming Winds) by Method 3 (Δ < -0.40 Upper Right Graph; -0.40 ≤ Δ < -0.10 Upper Left Graph; -0.10 ≤ Δ < 0 Lower Graph)

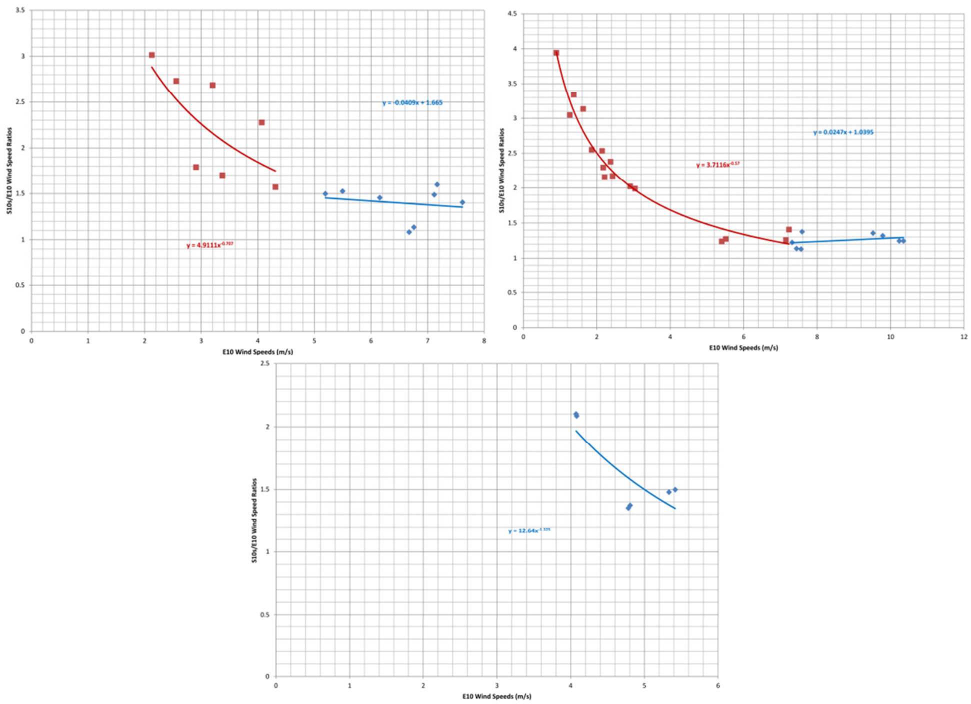

Figure E.35: E10 Wind Speeds vs S10s/E10 Wind Speed Ratios for the Middle Two Points (3 and 4) of Type-3B (Calming Winds) by Method 3 (Δ < -0.40 Upper Right Graph; -0.40 ≤ Δ < -0.10 Upper Left Graph; -0.10 ≤ Δ < 0 Lower Graph)

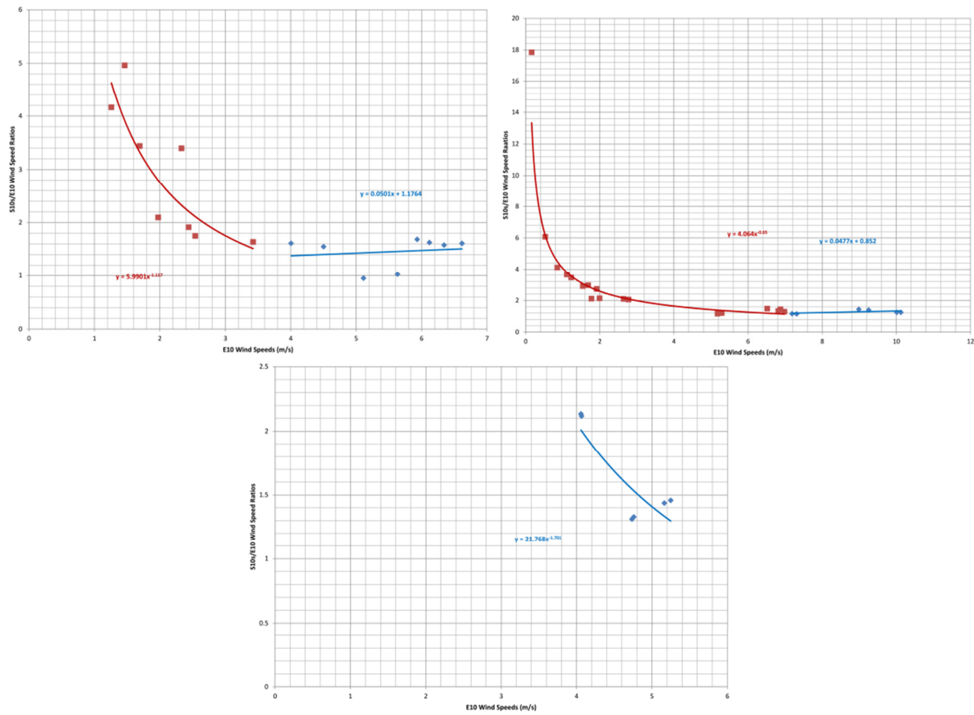

Figure E.36: E10 Wind Speeds vs S10s/E10 Wind Speed Ratios for the Last Two Points (5 and 6) of Type-3B (Calming Winds) by Method 3 (Δ < -0.40 Upper Right Graph; -0.40 ≤ Δ < -0.10 Upper Left Graph; -0.10 ≤ Δ < 0 Lower Graph)

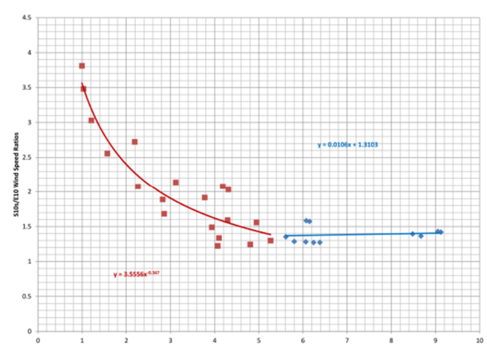

Figure E.37: E10 Wind Speeds vs S10s/E10 Wind Speed Ratios for the First Two Points (1 and 2) of Type-4A (Developing Winds) by Method 1

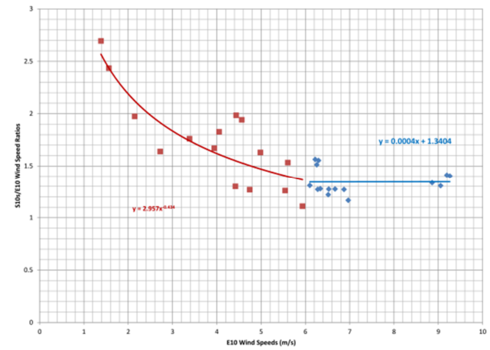

Figure E.38: E10 Wind Speeds vs S10s/E10 Wind Speed Ratios for the Middle Two Points (3 and 4) of Type-4A (Developing Winds) by Method 1

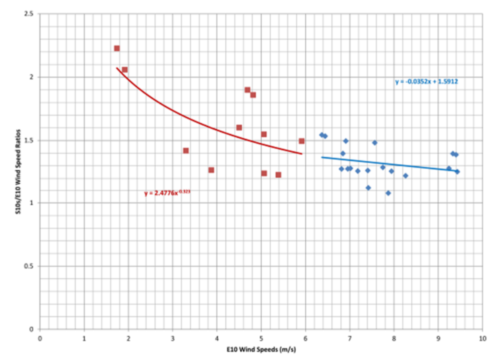

Figure E.39: E10 Wind Speeds vs S10s/E10 Wind Speed Ratios for the Last Two Points (5 and 6) of Type-4A (Developing Winds) by Method 1

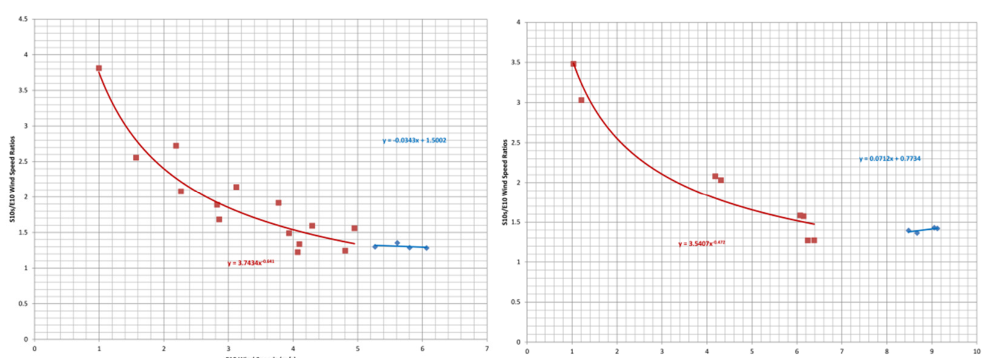

Figure E.40: E10 Wind Speeds vs S10s/E10 Wind Speed Ratios for the First Two Points (1 and 2) of Type-4A (Developing Winds) by Method 3 ($\Delta \geq 0.30$ Right Graph; $0 \leq \Delta < 0.30$ Left Graph)

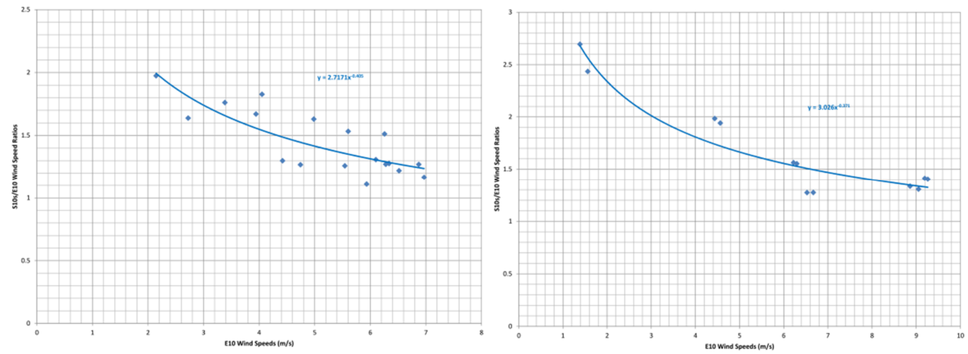

Figure E.41: E10 Wind Speeds vs S10s/E10 Wind Speed Ratios for the Middle Two Points (3 and 4) of Type-4A (Developing Winds) by Method 3 ($\Delta \geq 0.30$ Right Graph; $0 \leq \Delta < 0.30$ Left Graph)

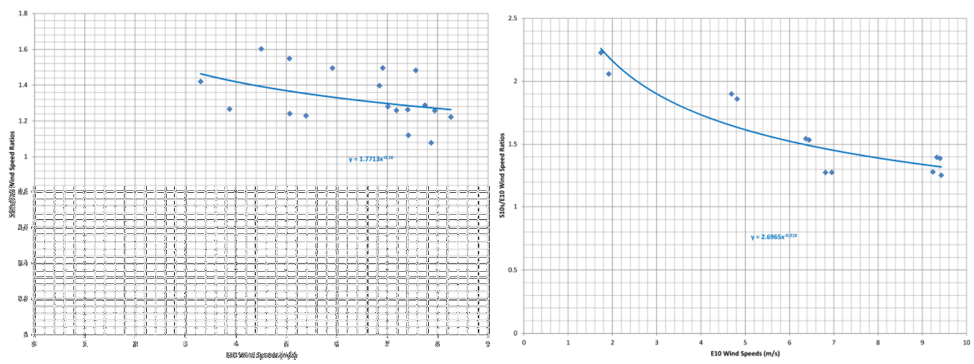

Figure E.42: E10 Wind Speeds vs S10s/E10 Wind Speed Ratios for the Last Two Points (5 and 6) of Type-4A (Developing Winds) by Method 3 ($\Delta \geq 0.30$ Right Graph; $0 \leq \Delta < 0.30$ Left Graph)

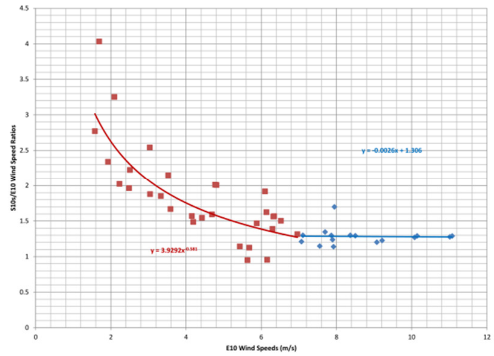

Figure E.43: E10 Wind Speeds vs S10s/E10 Wind Speed Ratios for the First Two Points (1 and 2) of Type-4B (Developing Winds) by Method 1

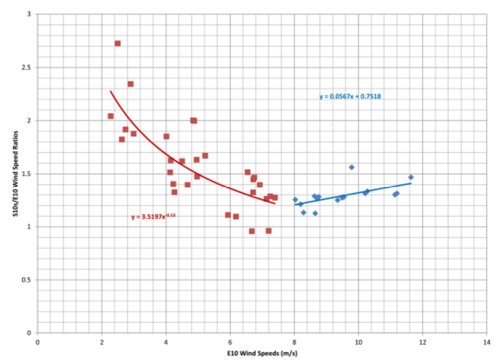

Figure E.44: E10 Wind Speeds vs S10s/E10 Wind Speed Ratios for the Middle Two Points (3 and 4) of Type-4B (Developing Winds) by Method 1

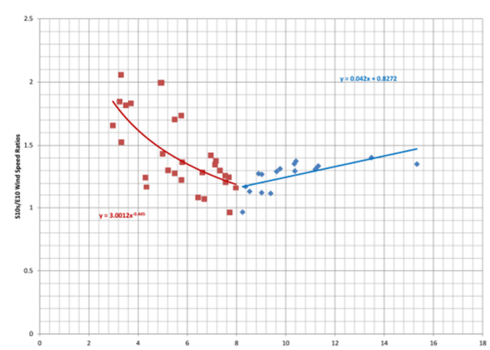

Figure E.45: E10 Wind Speeds vs S10s/E10 Wind Speed Ratios for the Last Two Points (5 and 6) of Type-4B (Developing Winds) by Method 1

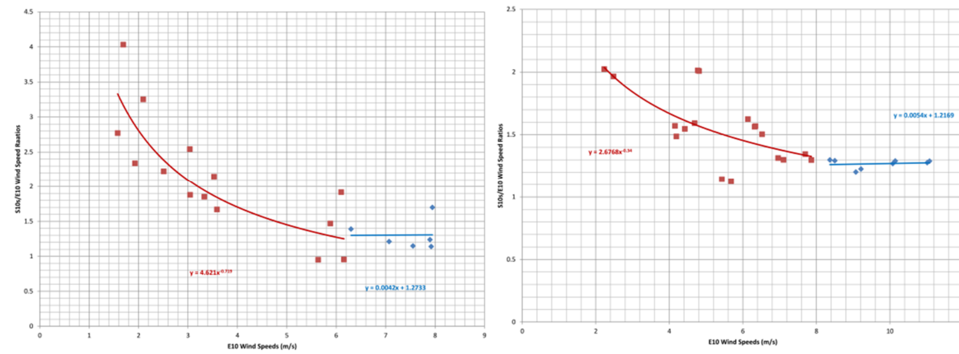

Figure E.46: E10 Wind Speeds vs S10s/E10 Wind Speed Ratios for the First Two Points (1 and 2) of Type-4B (Developing Winds) by Method 3 ($\Delta \geq 0.30$ Right Graph; $0 \leq \Delta < 0.30$ Left Graph)

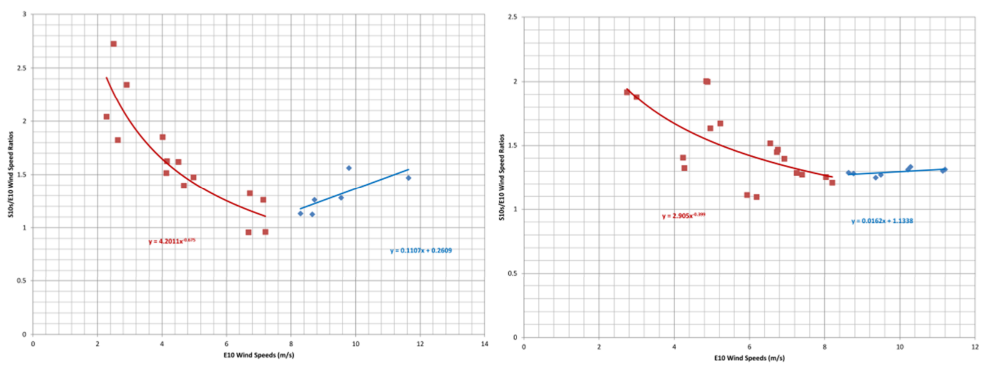

Figure E.47: E10 Wind Speeds vs S10s/E10 Wind Speed Ratios for the Middle Two Points (3 and 4) of Type-4B (Developing Winds) by Method 3 ($\Delta \geq 0.30$ Right Graph; $0 \leq \Delta < 0.30$ Left Graph)

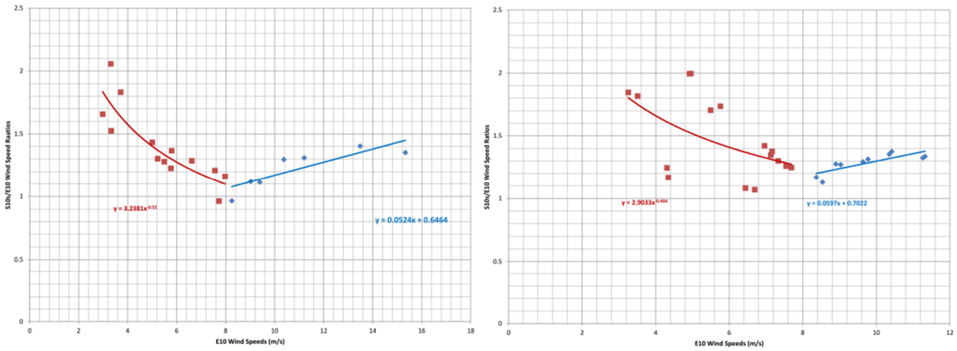

Figure E.48: E10 Wind Speeds vs S10s/E10 Wind Speed Ratios for the Last Two Points (5 and 6) of Type-4B (Developing Winds) by Method 3 (Δ ≥ 0.30 Right Graph; 0 ≤ Δ < 0.30 Left Graph)

APPENDIX F

GRAPHICAL PRESENTATION OF SIMULTANEOUS E10L, E10m1, E10m2, E10m3, E10m4, S10, S10$_S$, S10$_S$ Upper and S10$_S$ Lower WIND SPEEDS

Simultaneous E10L, E10m1, E10m2, E10m3, E10m4, S10, S10$_S$, S10$_S$ Upper, S10$_S$ Lower wind speed are presented in the below given figures.

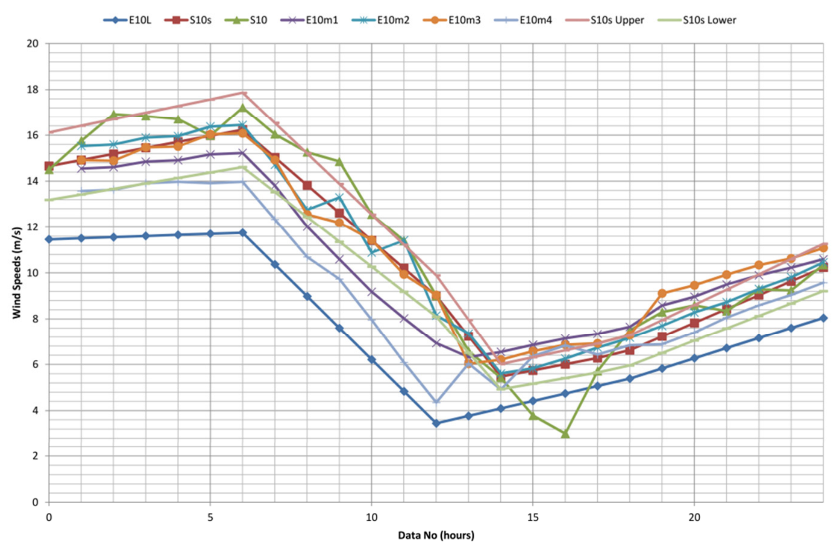

Figure F.1: E10L, E10m1, E10m2, E10m3, E10m4, S10, S10$_S$, S10$_S$ Upper and S10$_S$ Lower Wind Speeds for Continuous Data Set 1

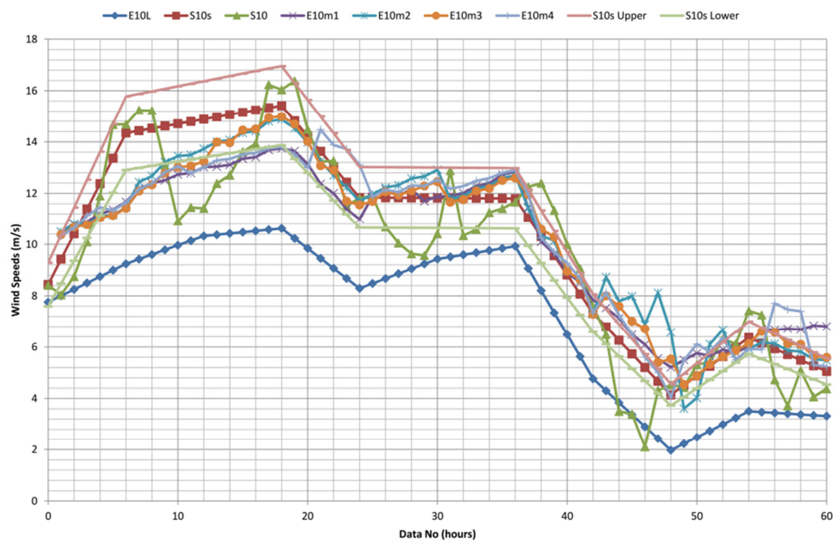

Figure F.2: E10L, E10m1, E10m2, E10m3, E10m4, S10, $S10_S$, $S10_S$ Upper and $S10_S$ Lower Wind Speeds for Continuous Data Set 2

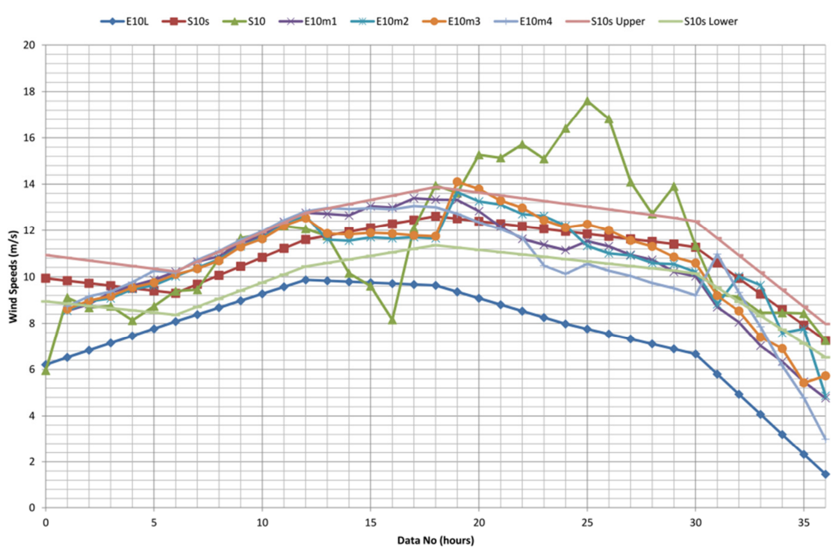

Figure F.3: E10L, E10m1, E10m2, E10m3, E10m4, S10, $S10_S$, $S10_S$ Upper and $S10_S$ Lower Wind Speeds for Continuous Data Set 3

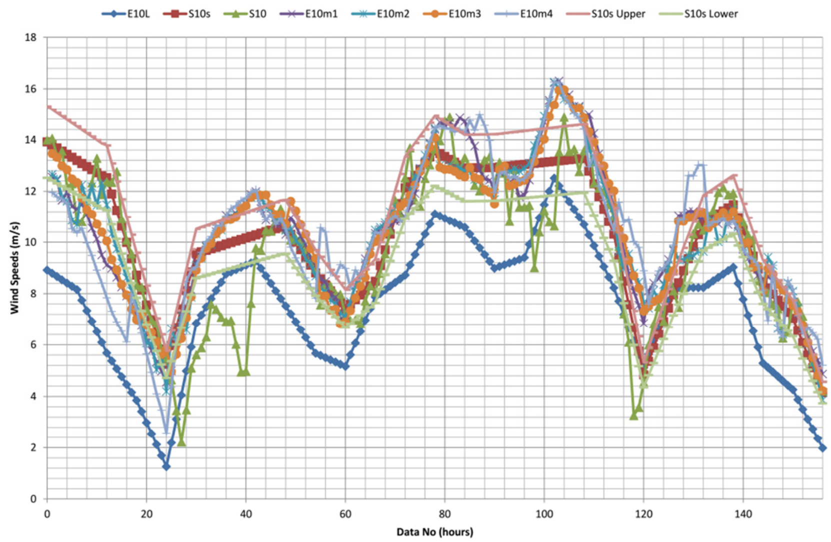

Figure F.4: E10L, E10m1, E10m2, E10m3, E10m4, S10, S10$_S$, S10$_S$ Upper and S10$_S$ Lower Wind Speeds for Continuous Data Set 4

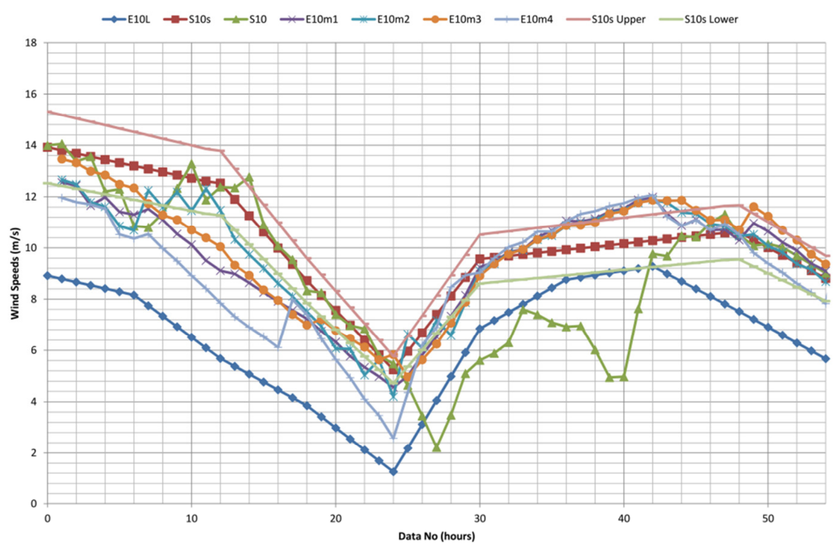

Figure F.5: E10L, E10m1, E10m2, E10m3, E10m4, S10, S10$_S$, S10$_S$ Upper and S10$_S$ Lower Wind Speeds for Continuous Data Set 4 (Part 1)

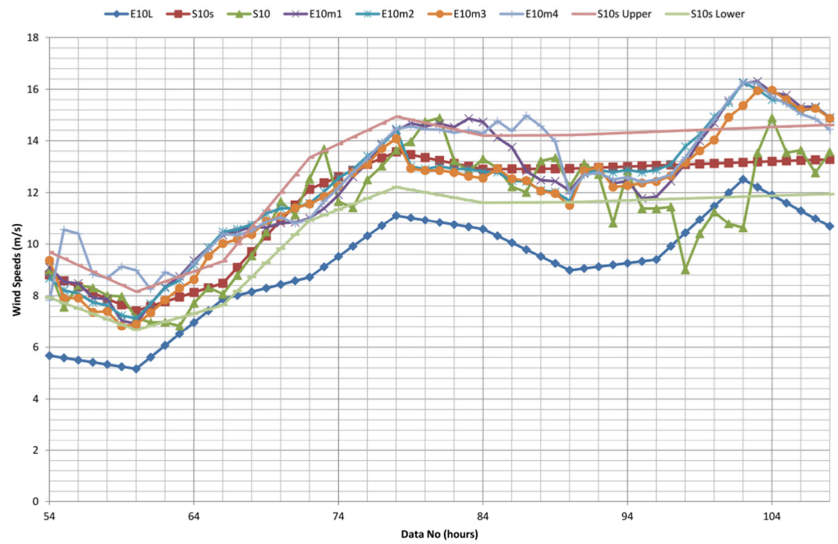

Figure F.6: E10L, E10m1, E10m2, E10m3, E10m4, S10, $S10_S$, $S10_S$ Upper and $S10_S$ Lower Wind Speeds for Continuous Data Set 4 (Part 2)

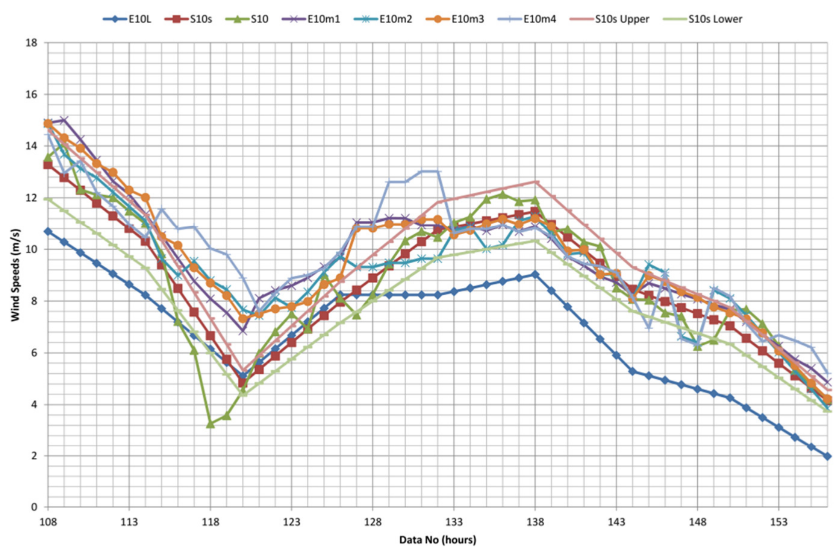

Figure F.7: E10L, E10m1, E10m2, E10m3, E10m4, S10, $S10_S$, $S10_S$ Upper and $S10_S$ Lower Wind Speeds for Continuous Data Set 4 (Part 3)

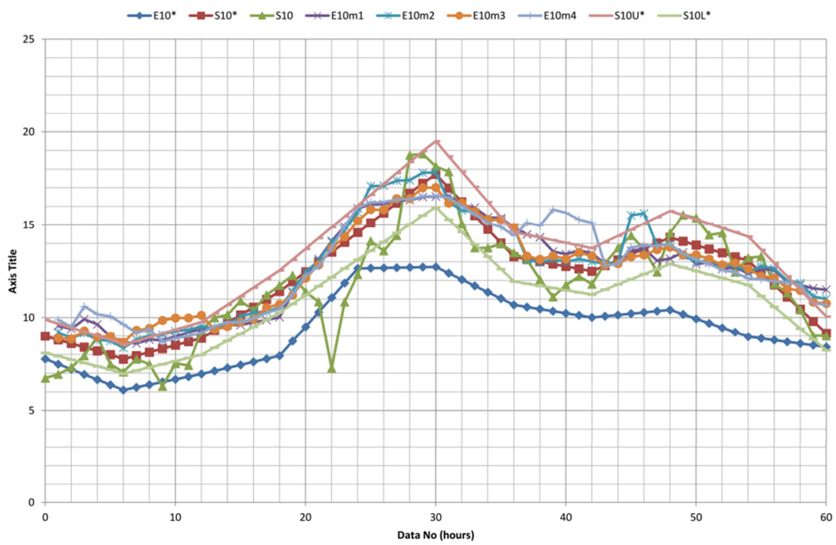

Figure F.8: E10L, E10m1, E10m2, E10m3, E10m4, S10, $S10_S$, $S10_S$ Upper and $S10_S$ Lower Wind Speeds for Continuous Data Set 5

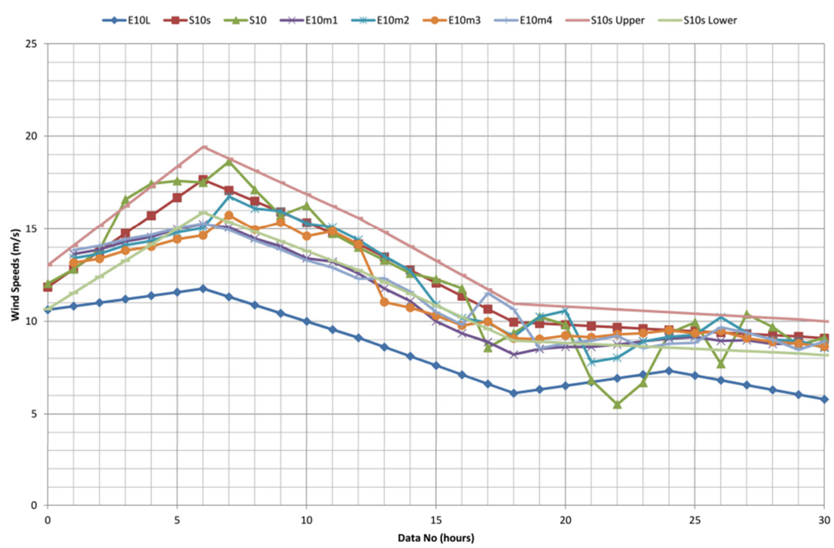

Figure F.9: E10L, E10m1, E10m2, E10m3, E10m4, S10, $S10_S$, $S10_S$ Upper and $S10_S$ Lower Wind Speeds for Continuous Data Set 6

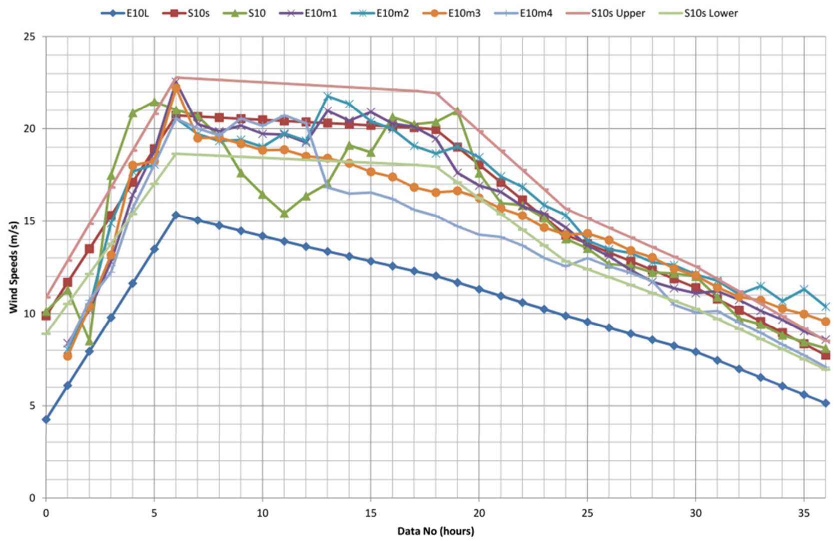

Figure F.10: E10L, E10m1, E10m2, E10m3, E10m4, S10, $S10_S$, $S10_S$ Upper and $S10_S$ Lower Wind Speeds for Continuous Data Set 7

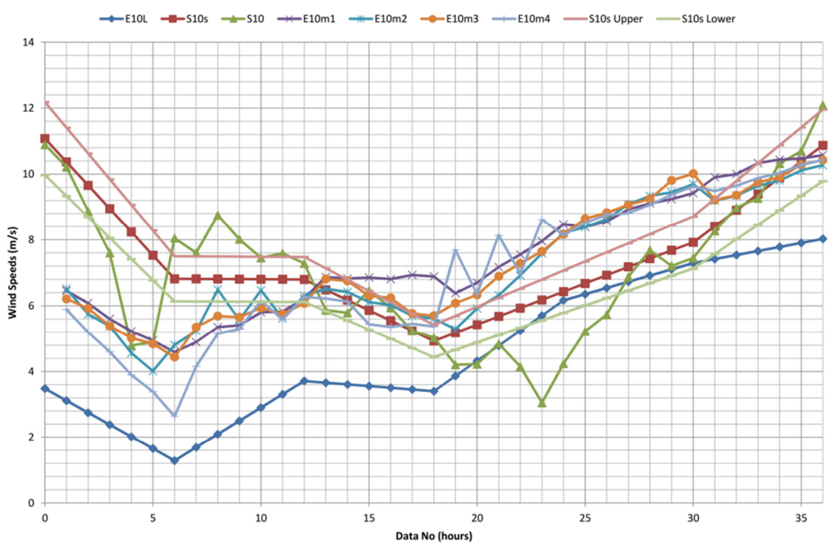

Figure F.11: E10L, E10m1, E10m2, E10m3, E10m4, S10, $S10_S$, $S10_S$ Upper and $S10_S$ Lower Wind Speeds for Continuous Data Set 8

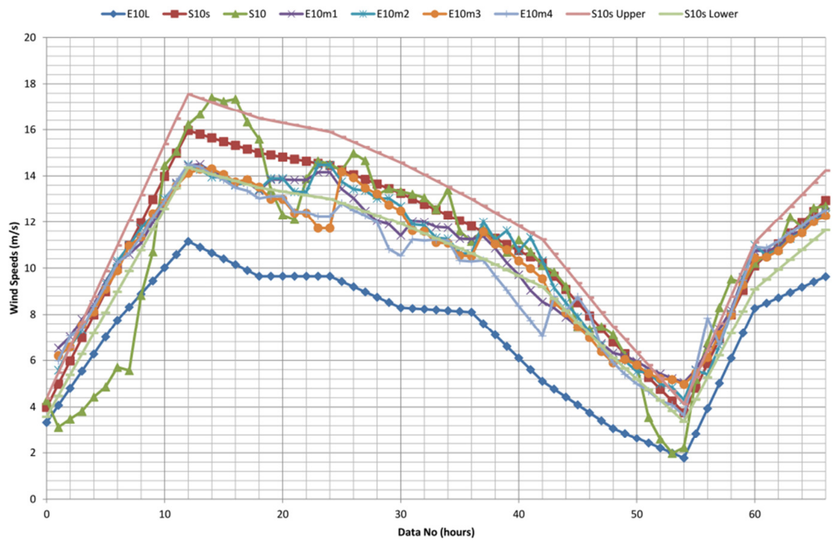

Figure F.12: E10L, E10m1, E10m2, E10m3, E10m4, S10, $S10_S$, $S10_S$ Upper and $S10_S$ Lower Wind Speeds for Continuous Data Set 9

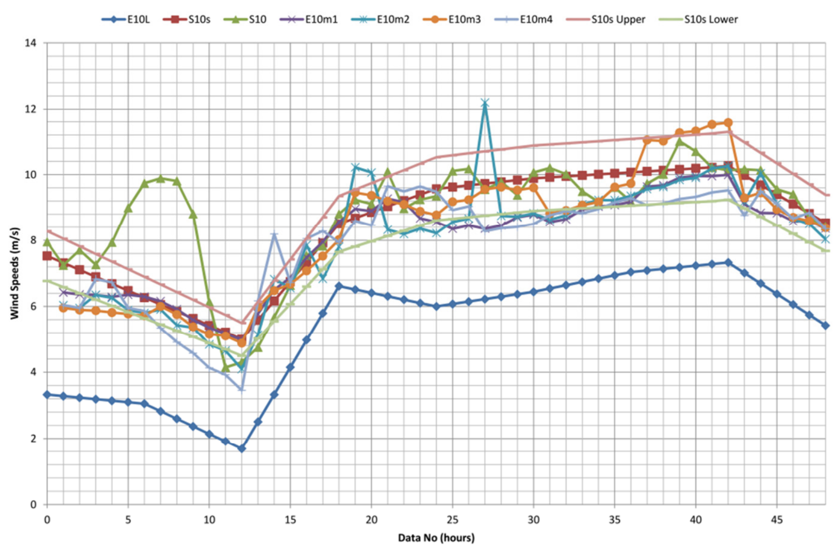

Figure F.13: E10L, E10m1, E10m2, E10m3, E10m4, S10, $S10_S$, $S10_S$ Upper and $S10_S$ Lower Wind Speeds for Continuous Data Set 10

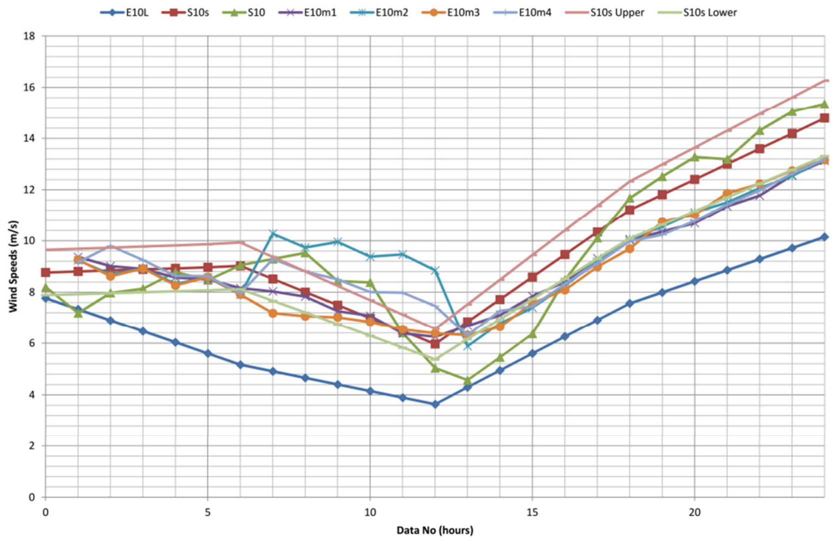

Figure F.14: E10L, E10m1, E10m2, E10m3, E10m4, S10, $S10_S$, $S10_S$ Upper and $S10_S$ Lower Wind Speeds for Continuous Data Set 11

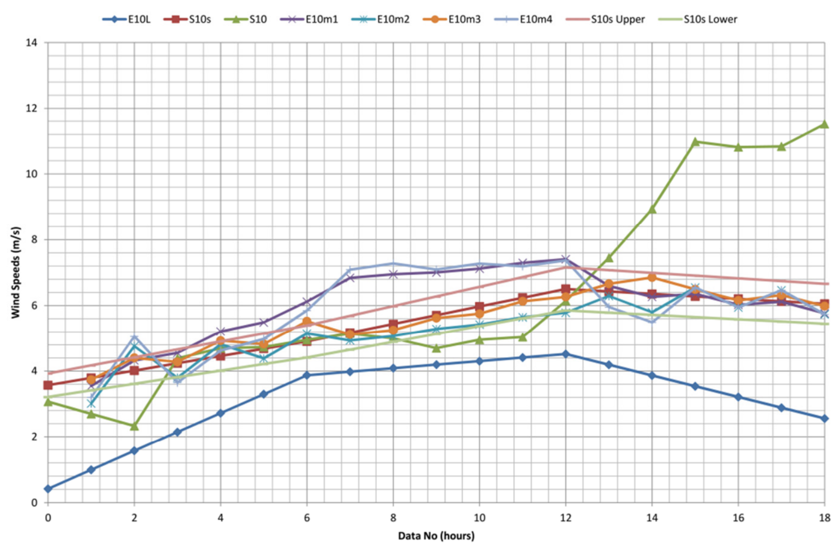

Figure F.15: E10L, E10m1, E10m2, E10m3, E10m4, S10, $S10_S$, $S10_S$ Upper and $S10_S$ Lower Wind Speeds for Continuous Data Set 12

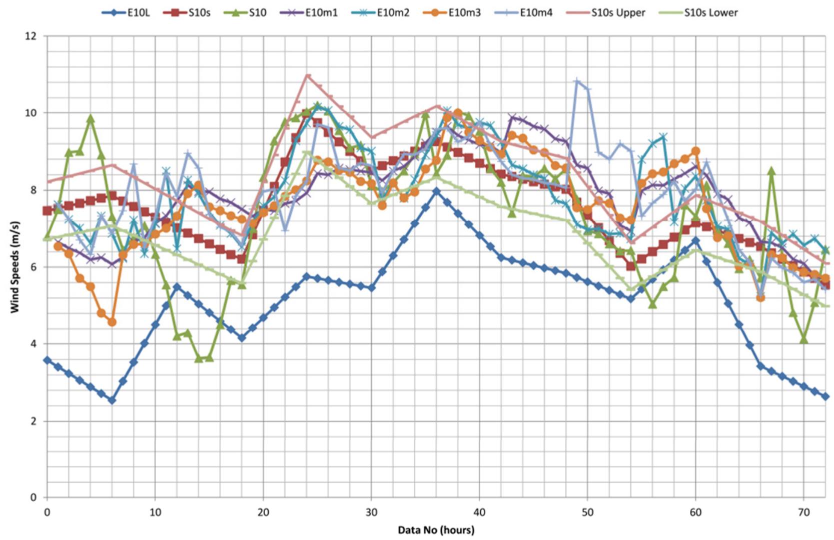

Figure F.16: E10L, E10m1, E10m2, E10m3, E10m4, S10, S10$_S$, S10$_S$ Upper and S10$_S$ Lower Wind Speeds for Continuous Data Set 13

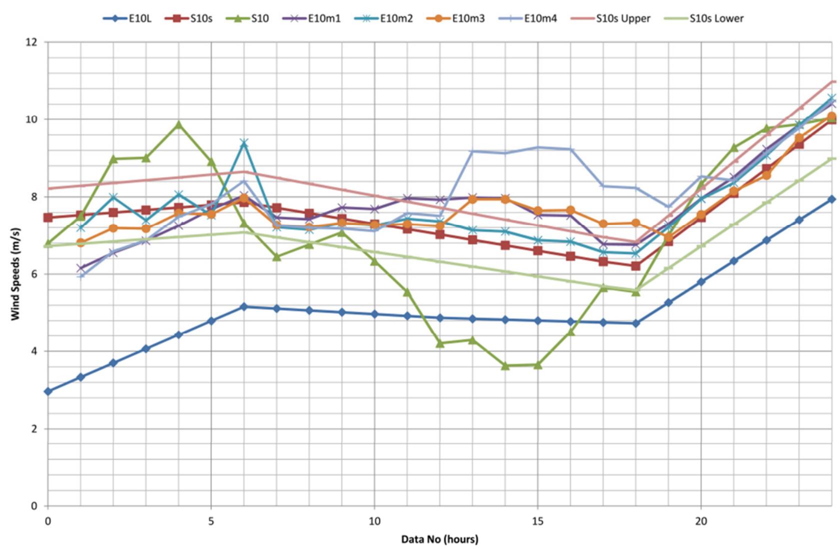

Figure F.17: E10L, E10m1, E10m2, E10m3, E10m4, S10, S10$_S$, S10$_S$ Upper and S10$_S$ Lower Wind Speeds for Continuous Data Set 14

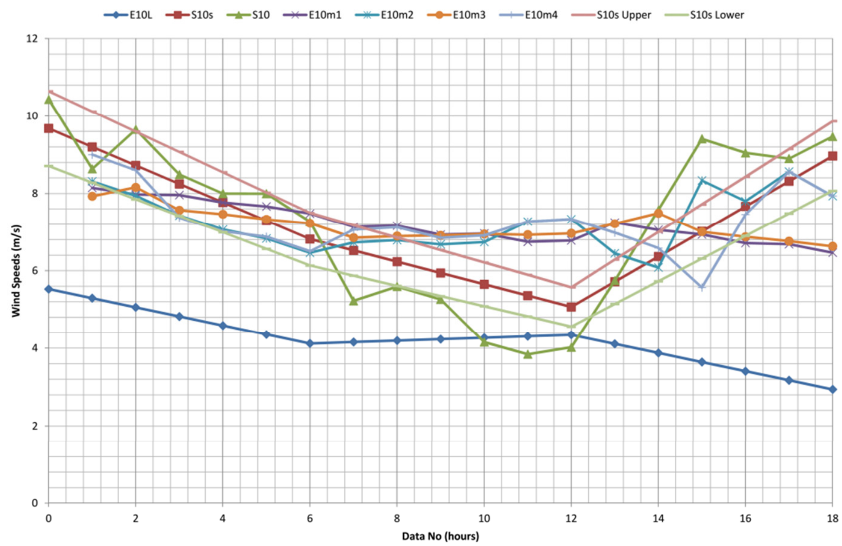

Figure F.18: E10L, E10m1, E10m2, E10m3, E10m4, S10, $S10_S$, $S10_S$ Upper and $S10_S$ Lower Wind Speeds for Continuous Data Set 15

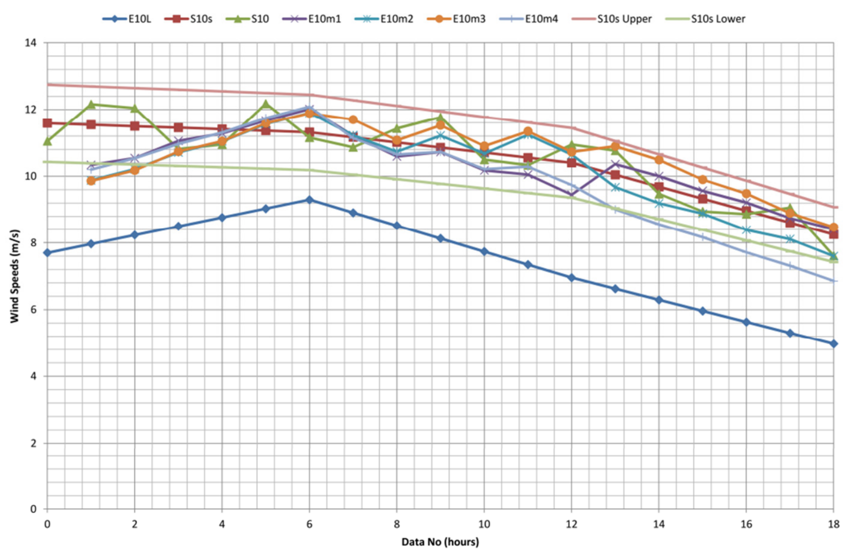

Figure F.19: E10L, E10m1, E10m2, E10m3, E10m4, S10, $S10_S$, $S10_S$ Upper and $S10_S$ Lower Wind Speeds for Continuous Data Set 16

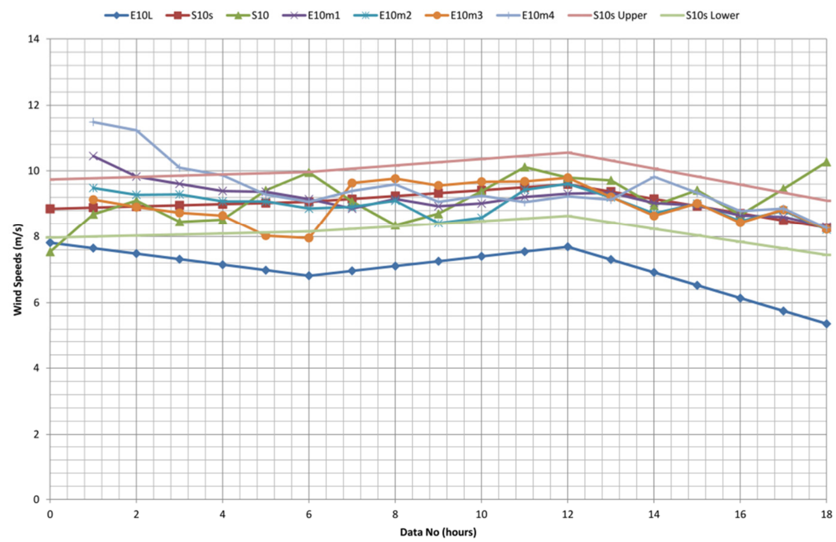

Figure F.20: E10L, E10m1, E10m2, E10m3, E10m4, S10, $S10_S$, $S10_S$ Upper and $S10_S$ Lower Wind Speeds for Continuous Data Set 17

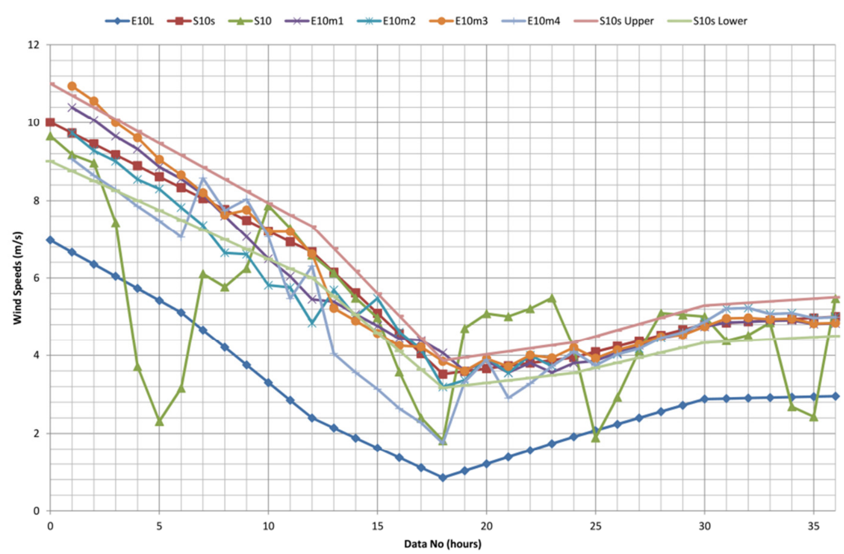

Figure F.21: E10L, E10m1, E10m2, E10m3, E10m4, S10, $S10_S$, $S10_S$ Upper and $S10_S$ Lower Wind Speeds for Continuous Data Set 18

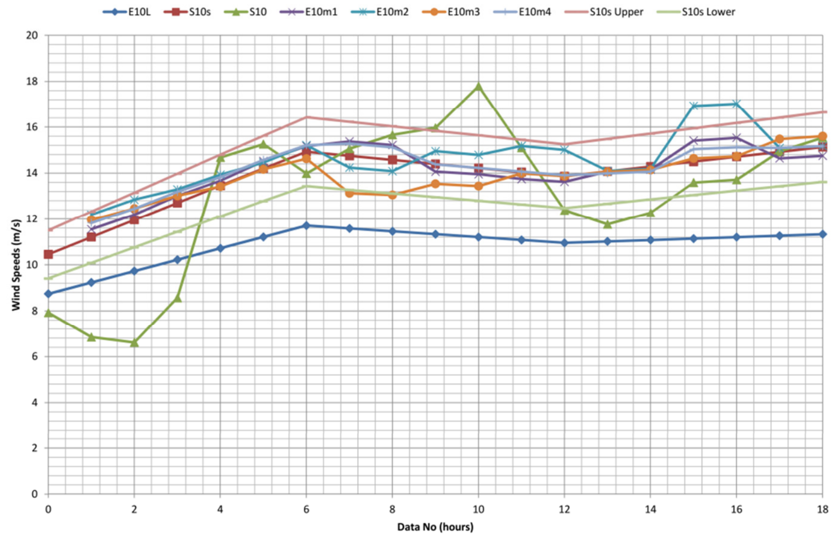

Figure F.22: E10L, E10m1, E10m2, E10m3, E10m4, S10, $S10_S$, $S10_S$ Upper and $S10_S$ Lower Wind Speeds for Continuous Data Set 19

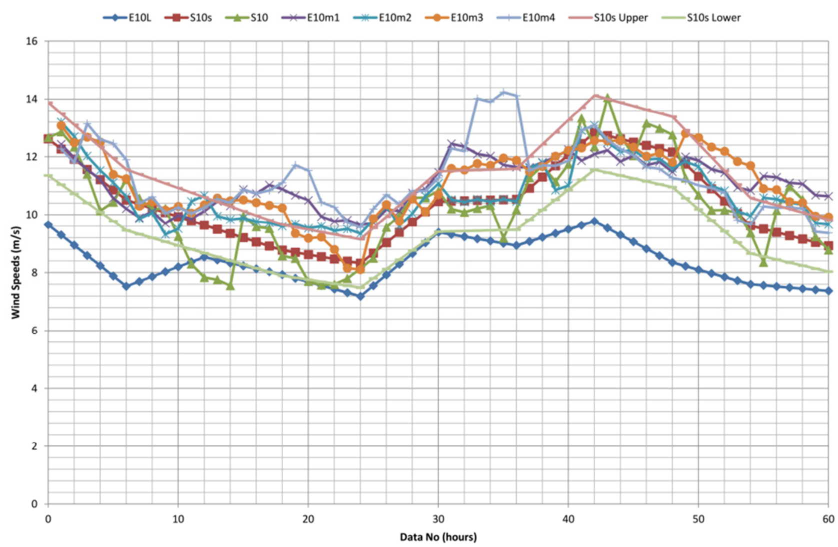

Figure F.23: E10L, E10m1, E10m2, E10m3, E10m4, S10, $S10_S$, $S10_S$ Upper and $S10_S$ Lower Wind Speeds for Continuous Data Set 20

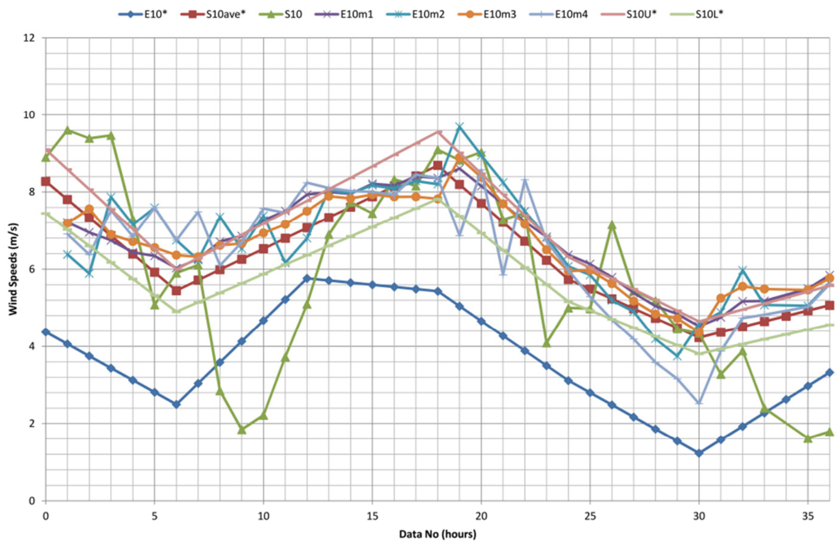

Figure F.24: E10L, E10m1, E10m2, E10m3, E10m4, S10, $S10_S$, $S10_S$ Upper and $S10_S$ Lower Wind Speeds for Continuous Data Set 21

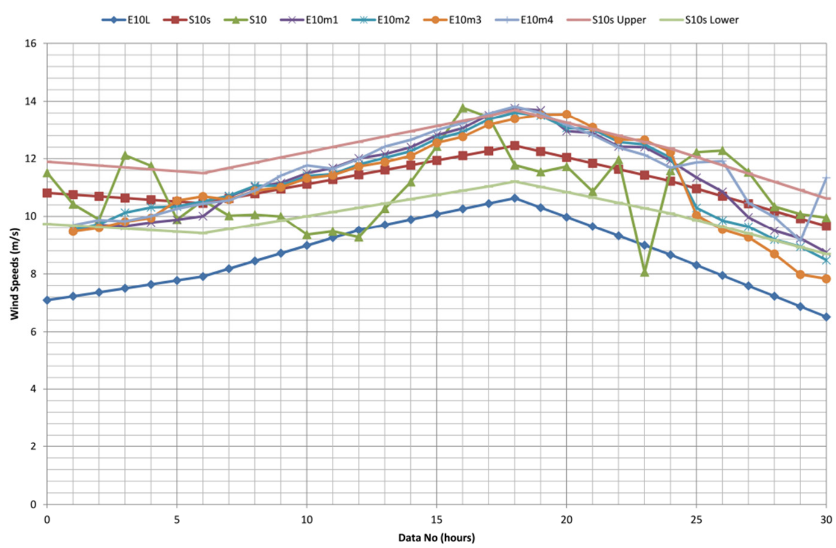

Figure F.25: E10L, E10m1, E10m2, E10m3, E10m4, S10, $S10_S$, $S10_S$ Upper and $S10_S$ Lower Wind Speeds for Continuous Data Set 22

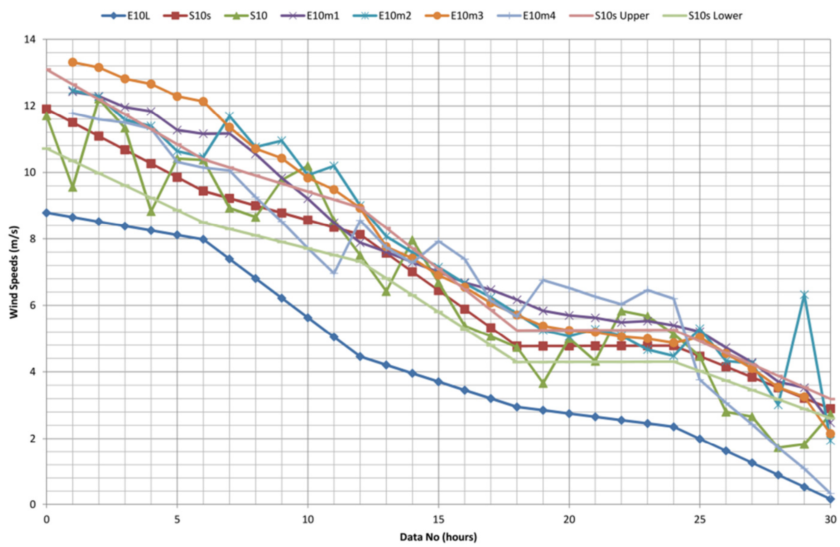

Figure F.26: E10L, E10m1, E10m2, E10m3, E10m4, S10, S10$_S$, S10$_S$ Upper and S10$_S$ Lower Wind Speeds for Continuous Data Set 23

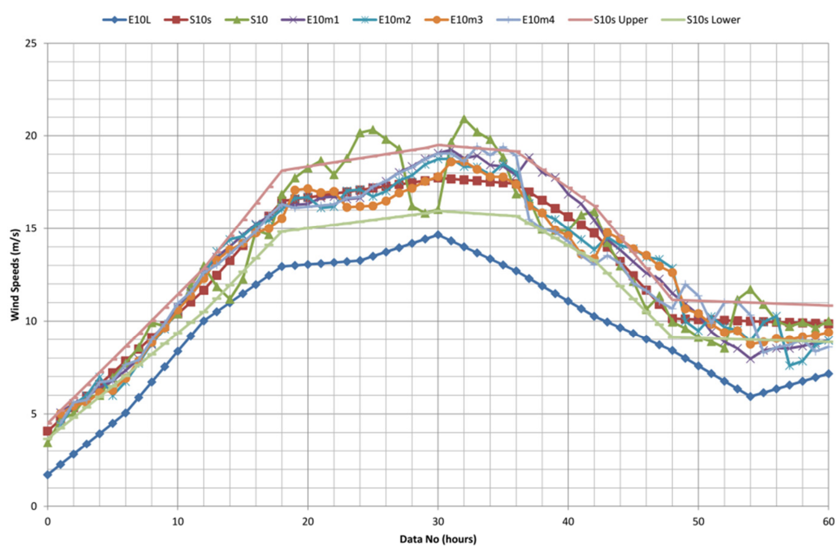

Figure F.27: E10L, E10m1, E10m2, E10m3, E10m4, S10, S10$_S$, S10$_S$ Upper and S10$_S$ Lower Wind Speeds for Continuous Data Set 24

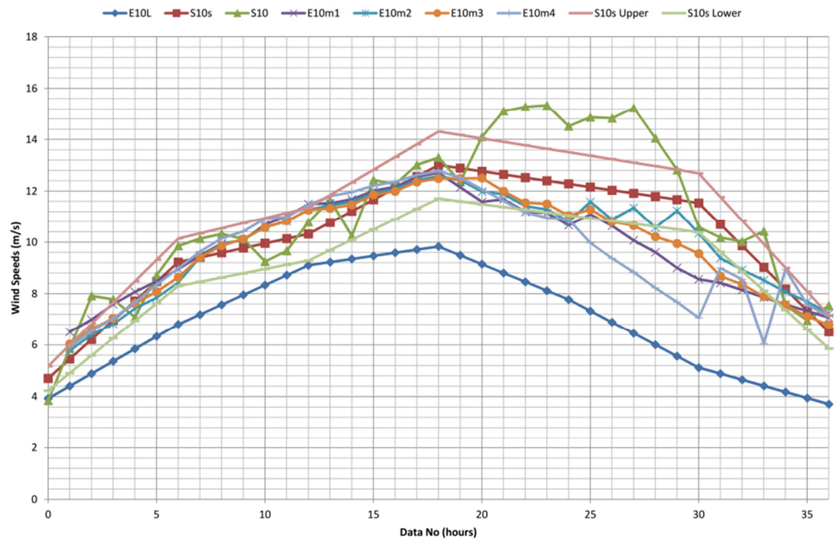

Figure F.28: E10L, E10m1, E10m2, E10m3, E10m4, S10, $S10_S$, $S10_S$ Upper and $S10_S$ Lower Wind Speeds for Continuous Data Set 25

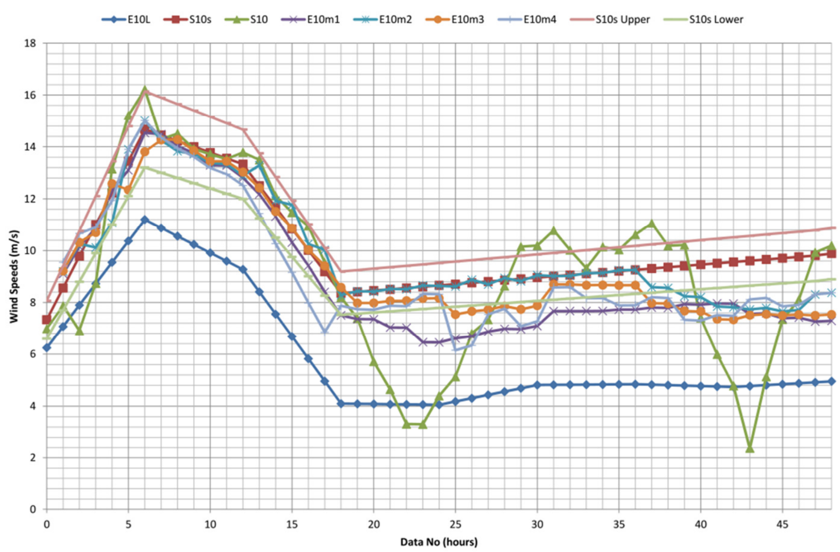

Figure F.29: E10L, E10m1, E10m2, E10m3, E10m4, S10, $S10_S$, $S10_S$ Upper and $S10_S$ Lower Wind Speeds for Continuous Data Set 26

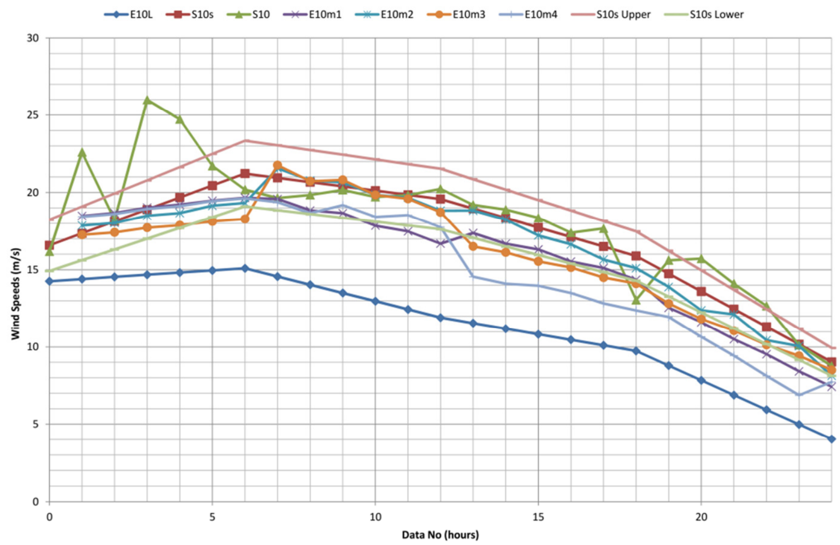

Figure F.30: E10L, E10m1, E10m2, E10m3, E10m4, S10, $S10_S$, $S10_S$ Upper and $S10_S$ Lower Wind Speeds for Continuous Data Set 27

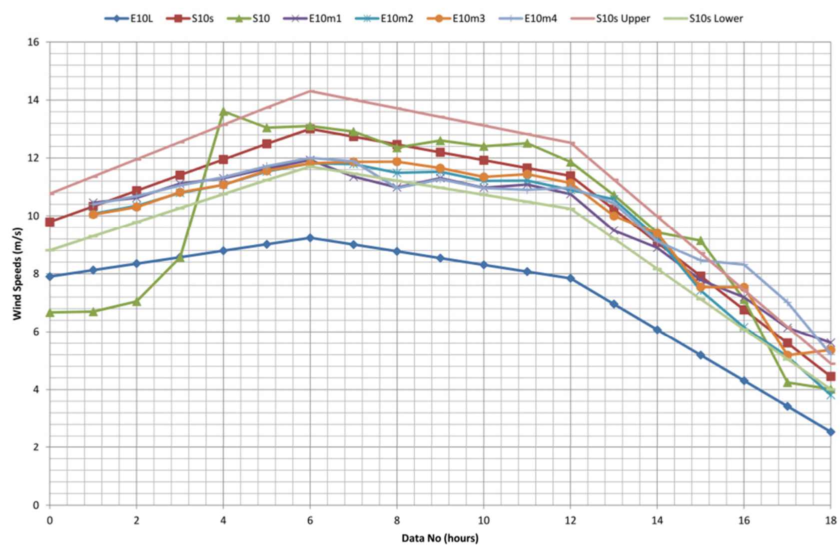

Figure F.31: E10L, E10m1, E10m2, E10m3, E10m4, S10, $S10_S$, $S10_S$ Upper and $S10_S$ Lower Wind Speeds for Continuous Data Set 28

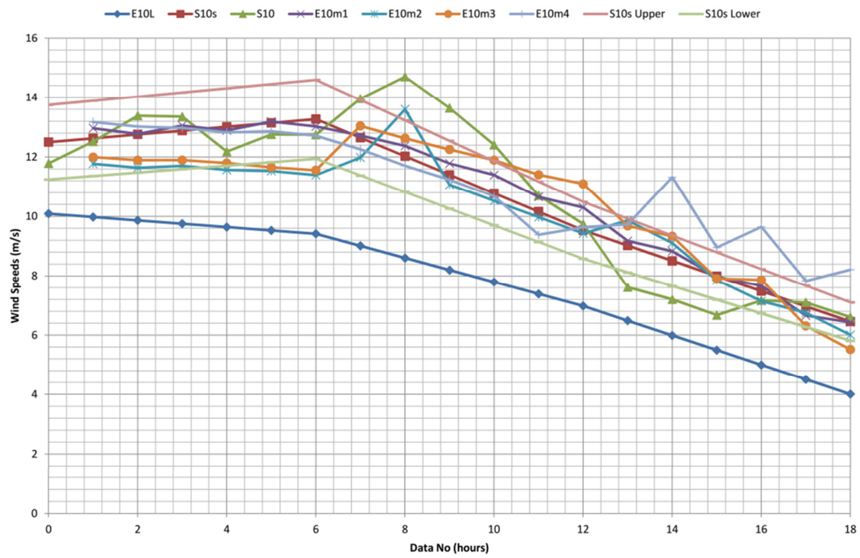

Figure F.32: E10L, E10m1, E10m2, E10m3, E10m4, S10, $S10_S$, $S10_S$ Upper and $S10_S$ Lower Wind Speeds for Continuous Data Set 29

APPENDIX G

BIAS, RMSE AND MAE FORMULATIONS

BIAS of an estimator (BIAS):

$$BIAS[\hat{\theta}] = \hat{\theta} - \theta \qquad [G.1]$$

where;

$\mathrm{BIAS}[\hat{\theta}]$	bias of the estimator
$\hat{\theta}$	estimated value
θ	expected value

Root-Mean-Square Error (RMSE):

$$RMSE = \sqrt{\frac{\sum_{i=1}^{n}\left(\hat{\theta}-\theta\right)^2}{n}} \qquad [G.2]$$

where;

n	number of values

Mean Absolute Error (MAE):

$$MAE = \left|\frac{\hat{\theta}-\theta}{\theta}\right| \qquad [G.3]$$

CURRICULUM VITAE

PERSONAL INFORMATION

Name:	MUSTAFA ESEN
Address:	Ceyhun Atıf Kansu Cad. 1220 Sok. 3/2 Çankaya/Ankara
Telephone:	05373175909
E-mail:	esenmustafaesen@gmail.com
Nationality:	Republic of Turkey
Date of Birth:	08.06.1980
Marital Status:	Single

EDUCATION AND TRAINING

PhD (2007-2014):	Middle East Technical University, Civil Engineering Department
M.S. (2004-2007):	Middle East Technical University, Civil Engineering Department
B.S. (1998-2004):	Middle East Technical University, Civil Engineering Department

WORK EXPERIENCE

Design Engineer (2011-present)	Yüksel Proje Uluslararası A. Ş.
Part Time Research Assistant (2007-2011)	Middle East Technical University, Civil Engineering Department
Design Engineer (2006-2007)	Yüksel Proje Uluslararası A. Ş.
Control Engineer (2006-2006)	Prokon
Design Engineer (2005-2006)	Bupim

FOREIGN LANGUAGES

English (Advanced)

RESEARCH TOPICS

Numerical Modelling of Coastal Sedimentation and Wave Generation, Shore Protection Structures, Wind and Wave Statistics

SELECTED WORKS AND PROJECTS

DEFRA Project on Climate Change, Göksu Delta

Methodology and Modeling Study for Tsunami Risk in the Sea of Marmara

Side Perissia Hotel Beach Protection Project

TRANSFER (Tsunami Risk Assessment and Strategies for European Region)

Bodrum-Gümbet Yacht Harbor Design and Physical Model Works

Determination of Yacht Capacity of Göcek-Fethiye Region

Beach Regulation and Structural Measures for Fugla Beach, Alanya

Tsunami and Storm Surge Evaluation for Yenikapı and Üsküdar Stations at Marmaray Project

İskenderun İsdemir Harbor Sedimentation Report

PUBLICATIONS AND PRESENTATIONS

Esen, M., (2007), "An Implicit One-Line Numerical Model on Longshore Sediment Transport", M.S. Thesis, Middle East Technical University, Turkey

Esen, M., Ergin, A., Güler, I. and Baykal, C. (2007), "Yapay Besleme ile Kıyı Dengelenmesi, Örnek Uygulama: Bir Kıyı Aşınımı Sorunu, Side, Türkiye", 6th National Coastal Engineering Symposium, Izmir, Turkey

Özyurt,G., Ergin, A., and Esen, M. (2008) "Indicator Based Coastal Vulnerability Assessment Model to Sea Level Rise", COPEDEC, Dubai, UAE

Esen, M., Güler, I., Karakuş Cihan, H., Özaslan, H. and Tunçay, H. T., (2014) "Izmir Bay Dredging", PIANC World Congress, San Francisco, USA

Esen, M., Ergin, A., Güler, I. and Özyurt Tarakçıoğlu, G., (2014) "A Comparative Study on Wind and Wave Sources for Turkish Black Sea Coast", ICCE 2014 Congress, Seoul, Korea